Ella Been · Asier Gómez-Olivencia
Patricia Ann Kramer *Editors*

Spinal Evolution

Morphology, Function, and Pathology of the Spine in Hominoid Evolution

Springer

Spinal Evolution

Ella Been • Asier Gómez-Olivencia
Patricia Ann Kramer
Editors

Spinal Evolution

Morphology, Function, and Pathology of the Spine in Hominoid Evolution

Springer

Editors
Ella Been
Department of Sports Therapy
Faculty of Health Professions
Ono Academic College
Kiryat Ono, Israel

Department of Anatomy and Anthropology
Sackler Faculty of Medicine
Tel Aviv University
Tel Aviv, Israel

Patricia Ann Kramer
Departments of Anthropology and
Orthopaedics and Sports Medicine
University of Washington
Seattle, WA, USA

Asier Gómez-Olivencia
Departamento de Estratigrafía y
Paleontología
Facultad de Ciencia y Tecnología
Universidad del País Vasco/Euskal Herriko
Unibertsitatea (UPV/EHU)
Leioa, Spain

IKERBASQUE
Basque Foundation for Science
Bilbao, Spain

Centro Mixto UCM-ISCIII de Evolución y
Comportamiento Humanos
Avda. Monforte de Lemos
Madrid, Spain

ISBN 978-3-030-19348-5 ISBN 978-3-030-19349-2 (eBook)
https://doi.org/10.1007/978-3-030-19349-2

This Springer imprint is published by the registered company Springer Nature Switzerland AG
The registered company address is: Gewerbestrasse 11, 6330 Cham, Switzerland

Foreword

Since the publication of J. T. Robinson's *Early Hominid Posture and Locomotion* in 1972, there hasn't been such a comprehensive, detailed analysis of the hominid vertebral column as in this splendid volume. True, this topic has attracted much attention in highly regarded publications (see, e.g., Aiello and Dean's *An Introduction to Human Evolutionary Anatomy* [1990] and Cartmill and Smith's *The Human Lineage* [2009]), but in most cases, the discussion either constitutes part of a broad treatment of human anatomy and its evolution, is focused on a specific structure, or simply reports on the inventory of recently discovered fossil vertebrae, giving a basic list of their metric characteristics. Here comes Been, Gómez-Olivencia, and Kramer's *Spinal Evolution: Morphology, Function, and Pathology of the Spine in Hominoid Evolution*, whose 17 chapters are dedicated to elucidating diverse biological and evolutionary aspects of the vertebral column.

During the decades that have elapsed since Robinson published his book, we have witnessed an unprecedented expansion of our inventory of fossil remains relevant to locomotion and posture. This rich assemblage affords us a view of anatomical elements that for many years were terra incognita in the human fossil record, such as the pelvis of *Australopithecus afarensis* and that of the more primitive *Ardipithecus*; vertebrae of various hominid species, including a complete Neandertal vertebral column accompanied by an entire pelvis; structures that indicate body proportions; hand and foot bones, including two medial navicular bones, one resembling a modern human big toe and the other indicating a medially divergent big toe; and even a rare tiny pisiform bone that appears to represent an intermediate stage between the morphology of modern humans and that of chimpanzees. All of these elements have no doubt influenced the vertebral column, both as a single anatomical unit and a collection of individual components.

The increase in the number of available fossils has not only added new links in our own evolutionary chain, making the fossil record denser, but also provided evidence of numerous species that we have reassigned to side branches of the hominin clade. These species have been placed in different clades because their skulls, mandibles, and teeth are incompatible with the morphocline leading to modern humans, even though these cranial elements represent bipedal species. Nevertheless, it is

both interesting and surprising that most researchers continue to arrange the postcranial remains of the side branches in a single morphocline, as if the only possible mode of bipedality is that of humans.

On the contrary, I see bipedality as manifested in many forms, just as animal flight takes many forms. Consider, for example, the hummingbird, which flaps its wings hundreds of times a minute, can hover in midair and can even fly backwards, as opposed to the albatross, which glides for days without flapping its wings even once. Sure, the substantially longer evolutionary history of birds is expressed in much richer and more dramatic anatomical differentiation than what we would expect of the hominin clade. Nevertheless, the principle is what counts: we cannot assume a priori that the locomotion system in the hominin clade falls into a single morphocline and that each specimen (or even each postcranial fragment) represents a character state in that morphocline. In other words, we should not be content with the hypothesis that all hominids walked "upright" and that there is no difference between the mode of locomotion found in various hominids and that of modern humans. Accepting such a hypothesis would be a blatant repetition of the historical mistake of arranging all fossil hominid skulls into a single lineage that is based on a morphocline of brain capacity, even when specimens clearly did not fit into the evolutionary sequence.

Take, for example, the remains of hominid pelvises and their accompanying vertebral column. One configuration is seen in *Homo sapiens*, a different one in Neandertals, a still different one in Lucy (and maybe also in *Au. africanus*), and a much different one in *Ardipithecus*. Still, we have only a vague idea of the pelvic anatomy of other hominids, such as *Au. robustus*, *Au. boisei*, *H. heidelbergensis*, and even the well-known Peking assemblage. Do all these pelvises and vertebral columns fall into a single morphocline (in which every pelvis represents a different character state), and does that morphocline lead to the anatomy of modern humans? I seriously doubt it. If we happen to find a robust australopith pelvis and vertebral column, would they fit into a morphocline that leads to modern humans, or would their degree of specialization force us to remove them from our lineage, just as the unique robust australopith masticatory system has?

Furthermore, when anagenesis was still the dominant theme, Franz Weidenreich had the insight to declare that "the humanlike features of the Australopithecinae are signs of their past rather than of their 'future.' In other words, the features they share with man are those retained from an original stock" (1948, p. 158). What he is actually saying is that not every element that resembles the corresponding element in the modern human skeleton signifies a derived anatomy just because the element is found in modern humans today. The "future," according to Weidenreich, can certainly include morphologies that do not lead to modern humans, morphologies whose character states do not fit into our morphocline, as indeed we have learned from the robust australopith anatomy.

Let us not forget the frequency of parallelism: the fact that extreme orthognathism characterizes some australopithecine faces does not render them "super humans" (a term often applied to describe such faces), nor does the extremely wide birth canal of Lucy render her "wonder woman." These two traits are manifestations

of unique specializations that bear no relationship to the homologous characters in modern humans.

No doubt that the hominin clade is rich in branches, some of which have brought us to *H. sapiens* and others that are completely unrelated to that journey. The contributions in the present volume clearly observe the cautious, meticulous approach and tight adherence to the common rules of the game (parsimony and the proper identification of outgroups) that are required for recruiting postcranial elements, including the vertebral column and its many components, to arrive at a deeper understanding thereof and an accurate phylogenetic reconstruction. Indeed, *Spinal Evolution* offers a welcome deliverance from the many preconceptions about the vertebral column that have held us captive in recent years.

Tel Aviv, Israel Yoel Rak

Contents

Chapter 1
The Study of the Human Spine and Its Evolution: State of the Art and Future Perspectives

Ella Been, Asier Gómez-Olivencia, and Patricia Ann Kramer

1.1 Introduction

The vertebral spine is a key element of the vertebrate anatomy. Its two main roles are related to protection of the spinal cord and the main blood vessels and to provision of a structural foundation that is of paramount importance for posture and locomotion. The vertebral column is the axis of the body where the limbs attach; it enables the mobility required for breathing and for locomotion and, at the same time, it provides stability for the attachment of the sensory organs of the head. Despite its great importance, in evolution the human vertebral spine is often overlooked by researchers because (1) vertebrae are fragile in nature, which makes their fossilization a rare event; (2) they are metameric (seriated and repeated elements) which makes their anatomical determination and, thus, their subsequent study difficult

E. Been (✉)
Department of Sports Therapy, Faculty of Health Professions, Ono Academic College, Kiryat Ono, Israel

Department of Anatomy and Anthropology, Sackler Faculty of Medicine, Tel Aviv University, Tel Aviv, Israel

A. Gómez-Olivencia (✉)
Departamento de Estratigrafía y Paleontología, Facultad de Ciencia y Tecnología, Universidad del País Vasco/Euskal Herriko Unibertsitatea (UPV/EHU), Leioa, Spain

IKERBASQUE, Basque Foundation for Science, Bilbao, Spain

Centro Mixto UCM-ISCIII de Evolución y Comportamiento Humanos, Avda. Monforte de Lemos, 5, Madrid, Spain
e-mail: asier.gomezo@ehu.eus

P. A. Kramer (✉)
Departments of Anthropology and Orthopaedics and Sports Medicine, University of Washington, Seattle, WA, USA
e-mail: pakramer@uw.edu

E. Been et al. (eds.), *Spinal Evolution*,
https://doi.org/10.1007/978-3-030-19349-2_1

(Franciscus and Churchill 2002); and (3) the plethora of bones and joints involved in every movement or function of the axial skeleton makes the reconstruction of posture, breathing mechanics, and locomotion extraordinarily difficult (Been et al. 2017; Gómez-Olivencia et al. 2018). Nonetheless, it is well established that the spine has changed dramatically during human evolution. Spinal curvatures, spinal load transmission, and thoracic shape of modern humans are unique among primates. Yet, there are many debates regarding how and when these changes occurred and about their phylogenetic, functional, and pathological implications.

In recent years, renewed interest in the axial skeleton, and more precisely in the vertebral column, has arisen. New and exciting finds, mostly from Europe and Africa, as well as new methods for reconstructing the spine, have been introduced to the research community (e.g., Carretero et al. 1999; Meyer 2005, 2016; Gómez-Olivencia et al. 2007; Bonmatí et al. 2010; Williams et al. 2013, 2017; Bastir et al. 2017). Additionally, the revisions of previously found specimens has provided new information about important aspects of spine evolution (Haeusler et al. 2002, 2011; Been et al. 2010; Gómez-Olivencia et al. 2013, 2017). Methodologies such as finite element analysis, trabecular bone analysis, geometric morphometrics, the study of patterns of integration, and gait analysis that have been applied to the spines of primates and humans (Bastir et al. 2014; Nalley and Grider-Potter 2015; Arlegi et al. 2018) and have become common in parallel with the study of the numbers of vertebrae in primates, including active debates with regard to the vertebral formula of the last common ancestor between chimpanzees and modern humans (Pilbeam 2004; McCollum et al. 2010; Lovejoy and McCollum 2010; Williams 2012a, b; Williams and Russo 2015; Gómez-Olivencia and Gómez-Robles 2016; Williams et al. 2016; Thompson and Almécija 2017). Additionally, advanced biomechanical research regarding posture, range of motion, stability, and shock attenuation of the human spine has interesting evolutionary implications (Castillo and Lieberman 2018). All these new avenues provide novel perspective on the evolution of the spine.

The objective of this book is to explore both these new methodologies and the new data, including recent fossil, morphological, biomechanical, and theoretical advances regarding vertebral column evolution, and to provide "state-of-the-art" information on the evolution of the human spine. The book was born after a session at the 2017 AAPA meeting entitled "The Axial Skeleton: Morphology, Function, and Pathology of the Spine and Thorax in Hominoid Evolution" that was organized by one of us (EB) and Alon Barash.

The book is divided into four main sections: the hominoid spine; the vertebral spine of extinct hominins; ontogeny, biomechanics, and pathology of the modern human spine; and new methodologies of spinal research. Each of these sections is composed of several chapters that complement each other and together provide a wide-ranging and comprehensive examination of different themes of importance to understanding spinal evolution.

1.2 Part One: The Vertebral Spine of Nonhuman Hominoids

The first part of the book focuses on the vertebral spine of nonhuman hominoids. It describes the morphology and biomechanics of the cranial base and the cervical, thoracic, and lumbar areas of extant nonhuman hominoid species and explores the relationships of morphology and biomechanics with posture and locomotion. The last two chapters of this first section deal with the important question of vertebral formulae in hominoid evolution, the early stages of spinal evolution in Miocene apes and the appearance of recent spinal morphology in extant apes.

In Chap. 2, Russo and Kirk (2019) describe the cranial base in hominoids and its relation to posture and locomotion. They find that at the "cranio-cervical interface," the morphology of the hominoid cranial base offers a wealth of information regarding posture and locomotion. In particular, compared to the other great apes, modern humans exhibit more anteriorly positioned and anteroinferiorly oriented foramina magna, more anteriorly positioned and flatter occipital condyles, and a reduction and reorganization of the nuchal musculature. Anteriorly positioned foramina magna and occipital condyles confer a mechanical advantage for balancing the head above an upright (orthograde) torso in humans rather than in front of a horizontal torso as in great apes. Differences in the head equilibrium are related to the development of neck musculature. In fact, more balanced heads (such as those present in modern humans) require less neck musculature (Aiello and Dean 1990). Extinct hominin taxa resemble modern humans in some (e.g., forward migration of the foramen magnum) but not all (e.g., nuchal plane architecture) aspects of cranial base morphology. They suggest that research on the "cranio-cervical interface" will continue to inform our understanding of how hominoid cranial anatomy relates to posture and locomotion and, in particular, how the modern human cranium evolved in relation to our unique reliance on bipedalism.

In Chap. 3, Nalley and Grider-Potter (2019) review the current knowledge regarding cervical vertebral morphology in relation to head posture and locomotion in nonhuman hominoids. They provide compelling evidence for function-form relationships between cervical bony morphology and behavior, as well as new data detailing the relationship between head shape and cervical variation. They suggest that future efforts should focus on expanding skeletal samples to include more orthograde and antipronograde taxa (e.g., strepsirrhines), as well as on documenting internal bony architecture to further test these proposed functional explanations.

Shapiro and Russo (2019) explore in Chap. 4 the lumbar spine of nonhuman hominoids. Hominoids show a distinct suite of characteristics in their lumbar region. The authors conclude that the evolution of hominoids was accompanied by a transformation of the primate body plan from a monkey-like ancestral condition to one characterized by a distinct suite of postcranial features functionally associated with orthograde posture and/or forelimb-dominated locomotor behaviors. While diagnostic hominoid features can be found throughout the postcranial skeleton, the trunk, and especially the lumbar region, can be considered one of the most functionally important and immediately noticeable aspects of the hominoid body plan. The

most important features of the hominoid body plan include the vertebral formula, relative lumbar spine length, vertebral body shape, and vertebral arch morphology, including the shape of the transverse and spinal processes.

In Chap. 5, Nakatsukasa (2019) provides a thorough review of the study of orthogrady in Miocene ape spinal morphology. This chapter links with previous chapters of this book presenting the derived features present in the vertebral column of extant hominoids, attributable to the frequent forelimb-dominated orthograde positional behavior such as suspension or vertical climbing. These specializations include a cranial shift in the lumbosacral border (decreased number of lumbar vertebrae and increased number of sacral vertebrae), loss of an external tail, spinal invagination into the thoracic and abdominal cavities, and craniocaudally short and dorsoventrally deep lumbar vertebral centra. Despite the large number of Miocene ape genera, only a few preserve sufficiently complete vertebrae to examine these features. Fossil apes (*Ekembo* and *Nacholapithecus*) from the beginning and mid-part of the Miocene in Africa (~19–15 Mya, Kenya) were essentially deliberate arboreal pronograde quadrupeds and retained primitive catarrhine axial skeletal morphology: long and dorsomobile lumbar spine, short sacrum, absence of spinal invagination (although *Nacholapithecus* shows a hint of an early transition to orthograde positional behavior). The penultimate lumbar vertebra of *Morotopithecus* (20.6 Mya, Uganda) exhibits craniocaudally short and dorsoventrally deep centrum and dorsal position of the transverse process, similar to that of extant apes, which seems to be the result of parallel evolution, based on the dentognathic evidence. European ape fossil record (*Pierolapithecus* and *Hispanopithecus*) illustrates a progressive evolution toward orthogrady. Nakatsukasa (2019) also provides insights regarding the current debates on the evolution of orthogrady: whether it evolved in European and African ape lineages (and Asian as well) independently or not; whether the dorsostable spine in the extant African apes is homologous or homoplastic; and whether the last common ancestor of the extant African apes and humans had an intermediate body plan between pronogrady and orthogrady ("multigrady").

In Chap. 6, Williams et al. (2019) provide an overview of the numbers of vertebrae in extant hominoids, presenting a summary of the largest database of hominoid vertebral numbers. In fact, this database provides, for the first time, data of previously unstudied species and subspecies. They conclude that vertebral formulae, the combination of regional numbers of vertebrae making up the bony spine, vary across vertebrates and within hominoid primates. They found more variation within and between species than expected, particularly in gibbons and in the gorilla and chimpanzee subspecies. Williams et al. (2019) suggest that combined thoracic and lumbar numbers of vertebrae are somewhat phylogenetically structured: while outgroup taxa (two species of cercopithecoids) retain the primitive number of 19 thoracolumbar vertebrae, hylobatids generally possess 18 thoracolumbar vertebrae, and hominids (great apes and humans) have 17 or 16 thoracolumbar vertebrae. When compared to cercopithecoids, and to putative stem hominoids, extant hominoids show evidence for homeotic change at both the lumbosacral (e.g., decrease in lumbar vertebrae; increase in sacral segments) and in the position of the transitional vertebrae. Homeotic changes are probably also responsible for the differences

between African apes and modern humans, with differences in the number of thoracic and lumbar within a 17-segment thoracolumbar framework.

Interesting and promising areas for future research of the vertebral spine of non-human hominoids include, among others, studying the interaction between spinal posture, motion, and mode of locomotion using new methodologies such as digital motion X-rays (Nalley and Grider-Potter 2019). Additionally, more information on how the spine covaries with other anatomical region is necessary, as well as an expanded fossil record that can answer to the current questions regarding hominoid spine evolution.

1.3 Part Two: The Vertebral Spines of Extinct Hominins

The second part of the book gives the most current description of the spines of extinct hominins, from *Australopithecus* to fossil *H. sapiens*.

In Chap. 7, Williams and Meyer (2019) discuss the spinal remains of *Australopithecus* from five sites in East and South Africa: Aramis, Asa Issie, and Hadar from the Afar Depression of Ethiopia and Sterkfontein and Malapa in the Cradle of Humankind, South Africa (Robinson 1972; Lovejoy et al. 1982; Cook et al. 1983; Sanders 1998; Haeusler et al. 2002; Williams et al. 2013, 2018). They indicate that australopith cervical vertebrae are intermediate in morphology (and potentially in function) between chimpanzees and modern humans; their thoracic vertebrae tend to show Scheuermann's hyperkyphosis deformity; and the lumbar vertebrae show human-like lumbar lordosis.

In Chap. 8, Meyer and Williams (2019) summarize vertebral remains from early *Homo*, including *H. erectus* as well as the Middle Pleistocene *H. naledi*. Two partial immature *H. erectus* skeletons preserve vertebrae: KNM-WT 15000 ("Turkana boy"; Latimer and Ward 1993) and the D2700 individual from Dmanisi (Meyer 2005; Lordkipanidze et al. 2007). Vertebrae from *H. naledi* include those from the Dinaledi Chamber (Williams et al. 2017) as well as those from LES1 partial skeleton ("Neo") found in the Lesedi Chamber (Hawks et al. 2017; Williams et al. 2017). Based on the current evidence, the vertebral column of *H. erectus* possessed a modal number of 12 thoracic and 5 lumbar segments, as is the case in australopiths and modern humans. Nonetheless, the spine of *H. erectus* reveals key changes relative to earlier hominins, with an expanded thoracolumbar spinal canal offering increased neurovascular capacities and a ventral pillar (formed by the vertebral bodies) better equipped to mitigate compressive loads and provide energy return (Meyer and Haeusler 2015). These biological developments are germane to understanding the advent of derived human behaviors, including efficient long-range locomotion and the first hominin expansion out of Africa.

In Chap. 9, Gómez-Olivencia and Been (2019) summarize the vertebral fossil record for "late" *Homo*, including *H. antecessor*, Middle Pleistocene *Homo* (except *H. naledi*), Neandertals, and fossil *H. sapiens*. The fossil record of the *H. antecessor* is currently restricted to the fossil remains from Gran Dolina-TD6 (Sierra de

Atapuerca, Spain), the Middle Pleistocene vertebral fossil record is sparse both geographically and chronologically, and the Late Pleistocene fossil record is more abundant. Based on the current evidence, these authors recognize the presence of at least two distinct morphologies arising from the more primitive *H. erectus* spine morphology: that of the Neandertal lineage and that of *H. sapiens*. Neandertals and their Middle Pleistocene ancestors show differences in all the anatomical regions when compared to modern humans related to a more stable spine with less accentuated curvatures (Gómez-Olivencia et al. 2007, 2013, 2017; Been et al. 2010, 2012, 2014, 2017). The Sima de los Huesos (SH) paleodeme does not, however, display the full suite of derived Neandertal features, a pattern also present in the cranium and the rest of the postcranium (Arsuaga et al. 2014, 2015). This implies that the distinctive Neandertal morphology did not arise all at once, but rather in a mosaic fashion. The Neandertal spinal morphology seems to be more stable in both sagittal and mediolateral directions. According to this review, the evolution of the modern human spine is less well known compared to Neandertals due to the scarce Middle Pleistocene fossil record ancestral to *H. sapiens* and the poor preservation of *H. sapiens* remains during the first half of the Late Pleistocene.

In Chap. 10, Haeusler (2019) provides an overview of the spinal disorders found in the hominin fossil record and alternative etiologies for several of them. The spinal disorders present in the hominin fossil record include one case of a benign primary bone tumor in MH2 (*A. sediba*), one case of developmental aplasia of the lumbar spinous processes in the Kebara 2 Neandertal, and many cases of degenerative osteoarthritis and pathologies related to the biomechanical failure of the growing spine. These include spondylolisthesis in the Middle Pleistocene Pelvis 1 individual from Sima de los Huesos (Sierra de Atapuerca; Bonmatí et al. 2010), traumatic juvenile disc herniation in KNM-WT 15000 (*H. erectus*; Schiess et al. 2014), anterior disc herniation (limbus vertebra) in Stw 431 (*A. africanus*; contra D'Anastasio et al. 2009), and Scheuermann's disease in several *Australopithecus* specimens. Haeusler (2019) argued that juvenile disc herniation, traumatic anterior disc herniation, and Scheuermann's disease all result from displacement of disc material and have a higher incidence following strains and trauma to the spine during the increased vulnerability phase of the pubertal growth spurt. He concluded that the remarkably high prevalence of this kind of disorders in our ancestors might suggest that our spine has become less vulnerable during the course of human evolution.

Summarizing the data and knowledge of the spine of extinct hominins made us realize that there are major lacunae in current research. For example, data regarding the spine of early *H. sapiens* (the hominins from Skhul and Qafzeh for example) is based mostly on the original publications (McCown and Keith 1939; Vandermeersch 1981), and it has not been thoroughly reexamined since their discovery. Reinvestigating these remains with modern technologies and methods is of paramount importance in order to understand spinal evolution in hominins. Additionally, this section emphasizes the presence of a significant fossil record that has not published in detail yet, either from old excavations or from recent discoveries, including the thoracic vertebrae of the hominins from Sima de Los Huesos, the cervical vertebrae of El Sidrón, the recently discovered vertebrae from the Little foot individual

(Stw 573), and the spine of immature individuals (e.g., Amud 7). New publications describing and documenting these remains and comparing them to modern humans and to other hominins will broaden our knowledge and understanding of the evolution of the spinal column in hominins. Another important question emerging from this part of the book is the taxonomic value of vertebrae for species recognition. In other words, can a hominin species be defined or recognized based on vertebral morphology?

Of note, this section is also tightly connected with two chapters from the fourth section that describe the reconstruction of the complete spinal columns of fossil hominins based on their vertebral morphology (Bastir et al. 2019; Been et al. 2019b). These reconstructions enable us to measure and understand the relationship between body parts in a way we could not establish before reconstruction and constitute the basis for future biomechanical analysis of the thorax/spine/pelvis in extinct hominins.

1.4 Part Three: The Vertebral Spine of Modern Humans

The third part of the book explores the spine of modern humans. Spinal ontogeny, biomechanics, posture, and pathology are discussed in relation to human evolution.

Chapter 11, by Martelli (2019), presents an overview of the pre- and postnatal ontogeny of the modern human and modern great and lesser ape vertebral column. In this chapter, Martelli introduces the key events in the prenatal development of the human vertebral column and sums up the postnatal development of the size and shape of the different elements—vertebrae, discs—and of the vertebral spine as a whole. At the end of this chapter, Martelli provides a summary of what is known about the pre- and postnatal ontogeny of the modern ape vertebral column. This is followed by an overview on the postnatal growth of various fossil specimens/species, including *A. afarensis* (Dikika 1-1), *A. sediba* (MH1), *H. erectus* (KNM-WT 15000), and Neandertals, compared to both extant nonhuman ape and modern human patterns. Martelli (2019) concludes that the patterns of postnatal development of the vertebral column are roughly similar for all hominoids, but given the overall variation in life history and growth period duration, variation of these patterns is observed. The shift from a great ape-like pattern of postnatal ontogeny happens late in the hominin evolution, and recent data from Neandertal fossils indicate further diversity in those patterns in late hominin evolution.

In Chap. 12, Been and Bailey (2019) describe the association between spinal posture and spinal biomechanics in modern humans and discuss the implications for extinct hominins. They determine the interactions between spinal posture and biomechanics within modern humans and translate those results to extinct hominins. Their main findings indicate that each group/lineage of hominins had special biomechanical characteristics. Early (Mousterian) *H. sapiens* and *H. erectus*, with moderate to high spinal curvatures, similar to the posture of modern humans,

probably had similar spinal biomechanical characteristics as modern humans do. Neandertal lineage hominins (NLH) with small spinal curvatures, reduced from their *H. erectus* ancestors, might have had somewhat different spinal biomechanics characterized by more stability and with reduced shock attenuation abilities compared to modern humans. NLH probably also preferred to squat rather than stoop and had better overhead throwing kinematics compared to modern humans. *Australopithecus* probably had lumbar biomechanical characteristics within the range of modern humans together with very stable cervical spine and a small cervical range of motion (ROM).

In Chap. 13, Been et al. (2019a) review the interaction between spinal posture and pathology in modern humans. They explore the relationship between sagittal spinal posture and spinal pathologies, back pain, and health-related quality of life. Their major findings indicate that spinal posture closely correlates with spinal pathology. Individuals with a well-aligned spine—within the neutral zone defined as moderate spinal curvatures and the line of gravity close to the acetabulum—have a better quality of life, less back pain, and less spinal pathology. Individuals out of the neutral zone, with accentuated or with decreased pelvic incidence and spinal curvatures, are at a higher risk for developing spinal pathology, back pain, and reduced quality of life. In fact, some of the unique spinal pathological lesions in modern humans are related to our distinct locomotion mode and are not present in other primates. This implicates that the emergence of an erect posture and bipedal locomotion was paralleled with the appearance of new pathological lesions.

In Chap. 14, Ezra et al. (2019) discuss the cervical lordosis of modern humans. They explore the ontogeny of the cervical lordosis, its association with pathology, ergonomics, and the evolution of cervical lordosis in hominins. They conclude that many factors influence the amount of cervical lordosis and its internal architecture, including age, sex, and the morphology of the thorax, head, pelvis, and spine. The leading morphologies that associate with cervical lordosis are those of the cervicothoracic junction (C7 or T1 slope), craniofacial features, mandibular morphology, the orientation of the foramen magnum, and pelvic and lumbar posture. They report that certain working groups suffer from neck pain more than others. Neck pain seems typical for sitting occupations and is researched mostly in office workers. Forward head posture and sustained sitting, which are associated with computer use, are typical risk factors, because they produce a prolonged static trunk and neck postures that create the need for excessive nuchal muscle stabilization which causes neck pain. They report cervical pathologies in the spine of extinct hominins and in the spine of pre- and post-agricultural societies, as well as in modern humans. The authors conclude that the possible contribution of the evolution of cervical lordosis in hominins to neck pain and dysfunction is far from being resolved and that future studies should explore the prevalence and nature of cervical pathology in extinct and extant hominoids and in pre- and post-agricultural societies. This might shed light on the different contributors to cervical pain and pathology—evolutionary components and postural and/or functional mechanisms.

Several questions stem from this part. Although it has been shown that back and neck pain/pathology are associated with spinal posture, not enough research has

been done to conclude that changing one's posture will lead to better outcome. Little research suggests that we can create permanent postural change without using surgical intervention, but is that due to the dearth of appropriate research? What kind of impact on spinal posture does the early stages of ontogeny have? Can we influence the development of spinal posture in children? Can we prevent the development of spinal pathologies by intervening early with postural changes? All of these questions are relevant in order to develop preventive medicine to reduce spinal pain and pathology. Enhancing our understanding of spinal biomechanics will provide us with the knowledge to produce better ergonomics solutions in order to ensure better working environments and reduce spinal pain and pathology.

Another major issue that is not well understood yet is the interaction among the morphology of the different body regions, which also has an evolutionary element. For example, how does pelvic morphology influence spinal and thorax morphology (and vice versa)? How does spinal morphology relate to the body bauplan? Given the ubiquity of spinal pain and the consequences of it to quality of life and economic activity, connecting spinal evolution, morphology, and biomechanics to pathology remains a critical research area.

1.5 Part Four: Current Methodologies for the Study of the Vertebral Spine

While the first three parts of the book summarize current knowledge regarding different aspects of spinal evolution in hominoids, hominins, and modern humans, the last part explores some of the current methodologies for the study of the spine, mainly with an evolutionary objective.

In Chap. 15 Been et al. (2019b) describe the methods to reconstruct spinal posture based solely on osseous material and its application to fossil hominins. Despite its importance, researchers face many difficulties in reconstructing spinal posture based solely on osseous material due to the absence of soft tissues. In this chapter, the authors provide information on how to overcome the absence of the intervertebral discs and to align two consecutive vertebrae, and they summarize the methods for measuring/calculating spinal posture based on osseous material. These methods include (1) pelvic incidence (PI) and sacral anatomical angle (SAA) to describe sacral orientation, when the pelvis is relatively complete; (2) lumbar vertebral body wedging (LVBW), inferior articular process angle (IAPA), and lumbar lordosis based on PI (LLPI) to estimate lumbar lordosis; (3) thoracic vertebral body wedging (TVBW) and thoracic vertebral body height difference (TVBHD) to estimate thoracic kyphosis; and (4) the foramen magnum orientation (FMO) for the reconstruction of cervical lordosis. Using these methods, the authors calculate the curvatures of the spine of Kebara 2, and based on these calculations, they have presented a complete 3D virtual reconstruction of the spine of Kebara 2 from the atlas to the sacrum. This is the first reconstruction of a complete vertebral spine that has been

performed for a fossil hominin specimen. The authors recommend utilizing a combination of methods for reconstructing the posture of extinct hominins in order to provide a more robust estimate of spinal curvature.

Bastir et al. (2019) in Chap. 16 provide a brief introduction to geometric morphometrics (GMM) and detail several examples of its application to the spine. GMM is based on the multivariate statistical analysis of Cartesian 2D or 3D landmark coordinates and has seen an exponential increase in its use since its recent development. Bastir et al. (2019) provide an overview of the recent applications of GMM to the human spine anatomy. This overview includes works of general (e.g., Arlegi et al. 2017) and specific aspects (Meyer et al. 2008) of spine anatomy, of how GMM can aid in the reconstruction of fragmentary specimens (Palancar 2017), and of quantitative analysis of sexual dimorphism (Bastir et al. 2014).

Kramer et al. (2019) in Chap. 17 explain the basics of finite element analysis (FEA) and the important considerations and cautions of modeling the spine using this methodology. They conclude that, as with all analysis techniques, the results will only be as good as the assumptions used to create it, so great care and a strong grounding in the first principles of the theory are required to implement an FEA. Of particular importance with the spine is the question of interest. For example, the approach to understand "how do osteophytes form?" will be substantively different from "how does the lumbar curve change when loaded?" The interface of vertebra and soft tissues (such as the intervertebral discs and ligaments) make modeling the spine challenging. Nonetheless, the spine is a 3D structure whose substantial complexity in its morphology and boundary conditions make it worth the effort required to create an FEM to analyze it.

The methods presented in this section have the potential, when applied to both the individual elements (i.e., the vertebrae) and the complete spines of both extinct and extant species, to open new horizons for our understanding of the vertebral spine and its role as the fundamental part of human motion. Using FEM models will enhance our understanding of spinal motion and the development of spinal pathology. It will also enable researchers to simulate the influence of different spinal surgeries.

1.6 Conclusion

The last 20 years has seen substantial improvement in our understanding of the evolution of the spine in hominoids in general and in hominins in particular. New fossils, new approaches, and new methodological applications have multiplied the number of studies published and have drastically changed our perception of how the spine evolved. Moreover, this new information has provided an expansive framework against which new fossil findings can be compared. This book is born from the necessity to provide an overview of the state of the art in the field in a single volume, in order to detect areas in which additional research should be performed. The reviews of the authors of this book do not only provide evidence for substantial

improvement in the understanding of this anatomical region but also demonstrate that the years ahead of us will be exciting: many fossils already excavated have not been published in detail (e.g., Sima de los Huesos, Dinaledi, Little foot), some "classical fossils" need to be restudied using the current methodological frameworks, and the application of new technologies and statistical approaches to new areas of the study of the spine all promise many changes in our understanding of the spine in coming years.

Additionally, much work remains to be done, not only in the field to recover new fossils but also to develop and implement new conceptual and analytical tools that can be useful in the study of the hominoid fossil record. For instance, tackling the always difficult question of homology vs homoplasy requires new perspectives. In fact, the studies of the patterns of integration in extant hominoids, combined with studies of covariation across vertebrae and analyses of the patterns of allometry, may well shed light on this issue. In another example of the work left to be done, we also need more information regarding extant locomotion and its relationship to the morphology (shape, orientation, trabecular organization) of the vertebral bodies in extant hominoids compared to cercopithecoids, in order to infer locomotion patterns in fossil hominoids. Another promising and important area is the implication of erect posture and bipedalism to paleopathology of the spine and to modern human spinal disease and back pain. Our hope is that this volume will serve as a foundation upon which all of these new studies—and many others—will be designed.

Acknowledgments We would like to thank the participants in the session entitled "The Axial Skeleton: Morphology, Function, and Pathology of the Spine and Thorax in Hominoid Evolution" of the 86th AAPA annual meeting, held in 2017 in New Orleans, LA, as well as to all the participants, authors, and reviewers of this book for very fruitful discussions and for all their work in this volume.

AGO is supported by the Spanish Ministerio de Ciencia y Tecnología (Project: CGL-2015-65387-C3-2-P, MINECO/FEDER), by the Spanish Ministerio de Ciencia, Innovación y Universidades (project PGC2018-093925-B-C33) and is part of the Research Group IT1418-19 from the Eusko Jaurlaritza-Gobierno Vasco.

References

Aiello LC, Dean C (1990) An Introduction to Human Evolutionary Anatomy. Academic Press, London

Arlegi M, Gómez-Olivencia A, Albessard L, Martínez I, Balzeau A, Arsuaga JL, Been E (2017) The role of allometry and posture in the evolution of the hominin subaxial cervical spine. J Hum Evol 104:80–99

Arlegi M, Gómez-Robles A, Gómez-Olivencia A (2018) Morphological integration in the gorilla, chimpanzee, and human neck. Am J Phys Anthropol 166:408–416

Arsuaga JL, Martínez I, Arnold LJ, Aranburu A, Gracia-Téllez A, Sharp WD, Quam RM, Falguères C, Pantoja-Pérez A, Bischoff J, Poza-Rey E, Parés JM, Carretero JM, Demuro M, Lorenzo C, Sala N, Martinón-Torres M, García N, Alcázar De Velasco A, Cuenca-Bescós G, Gómez-Olivencia A, Moreno D, Pablos A, Shen C-C, Rodríguez L, Ortega AI, García R, Bonmatí A, Bermúdez De Castro JM, Carbonell E (2014) Neandertal roots: Cranial and chronological evidence from Sima de los Huesos. Science 344:1358–1363

Arsuaga JL, Carretero J-M, Lorenzo C, Gómez-Olivencia A, Pablos A, Rodríguez L, García-González R, Bonmatí A, Quam RM, Pantoja-Pérez A, Martínez I, Aranburu A, Gracia-Téllez A, Poza-Rey E, Sala N, García N, Alcázar De Velasco A, Cuenca-Bescós G, Bermúdez De Castro JM, Carbonell E (2015) Postcranial morphology of the middle Pleistocene humans from Sima de los Huesos, Spain. Proc Natl Acad Sci U S A 112:11524–11529

Bastir M, Higuero A, Ríos L, García Martínez D (2014) Three-dimensional analysis of sexual dimorphism in human thoracic vertebrae: implications for the respiratory system and spine morphology. Am J Phys Anthropol 155:513–521

Bastir M, García Martínez D, Rios L, Higuero A, Barash A, Martelli S, García Tabernero A, Estalrrich A, Huguet R, De La Rasilla M, Rosas A (2017) Three-dimensional morphometrics of thoracic vertebrae in Neandertals and the fossil evidence from El Sidrón (Asturias, Northern Spain). J Hum Evol 108:47–61

Bastir M, Torres-Tamayo N, Palancar CA, Zlolniski SL, García-Martínez D, Riesco-López A, Vidal D, Blanco-Pérez E, Barash A, Nalla S, Martelli S, Sanchis-Gimeno JL, Schlager S (2019) Geometric morphometric studies in the human spine. In: Been E, Gómez-Olivencia A, Kramer PA (eds) Spinal evolution: morphology, function, and pathology of the spine in hominoid evolution. Springer, New York, pp 360–386

Been E, Bailey JF (2019) The association between spinal posture and spinal biomechanics in modern humans: implications for extinct hominins. In: Been E, Gómez-Olivencia A, Kramer PA (eds) Spinal evolution: morphology, function, and pathology of the spine in hominoid evolution. Springer, New York, pp 283–300

Been E, Peleg S, Marom A, Barash A (2010) Morphology and function of the lumbar spine of the Kebara 2 Neandertal. Am J Phys Anthropol 142:549–557

Been E, Simonovich A, Kalichman L (2019a) Spinal posture and pathology in modern humans. In: Been E, Gómez-Olivencia A, Kramer PA (eds) Spinal evolution: morphology, function, and pathology of the spine in hominoid evolution. Springer, New York, pp 301–320

Been E, Weintraub T, Gómez-Olivencia A, Kalichman L, Kramer P, Shefi S, Soudack M, Barash A (2019b) How to build a model of a fossil hominin vertebral spine based on osseous material? In: Been E, Gómez-Olivencia A, Kramer PA (eds) Spinal evolution: morphology, function, and pathology of the spine in hominoid evolution. Springer, New York, pp 341–360

Been E, Gómez-Olivencia A, Kramer PA (2014) Brief Communication: Lumbar lordosis in extinct hominins: Implications of the pelvic incidence. Am J Phys Anthropol 154:307–314

Been E, Gómez-Olivencia A, Shefi S, Soudack M, Bastir M, Barash A (2017) Evolution of Spinopelvic Alignment in Hominins. The Anatomical Record 300:900–911

Bonmatí A, Gómez-Olivencia A, Arsuaga JL, Carretero JM, Gracia A, Martínez I, Lorenzo C, Bermúdez De Castro JM, Carbonell E (2010) Middle Pleistocene lower back and pelvis from an aged human individual from the Sima de los Huesos site, Spain. Proc Natl Acad Sci USA 107:18386–18391

Carretero JM, Lorenzo C, Arsuaga JL (1999) Axial and appendicular skeleton of *Homo antecessor*. J Hum Evol 37:459–499

Castillo ER, Lieberman DE (2018) Shock attenuation in the human lumbar spine during walking and running. J Exp Biol. https://doi.org/10.1242/jeb.177949

Cook DC, Buikstra JE, DeRousseau CJ, Johanson DC (1983) Vertebral pathology in the Afar australopithecines. Am J Phys Anthropol 60:83–102

D'Anastasio R, Zipfel B, Moggi-Cecchi J, Stanyon R, Capasso L (2009) Possible brucellosis in an early hominin skeleton from Sterkfontein, South Africa. PLoS ONE 4:e6439

Ezra D, Been E, Alperovitch-Najenson D, Kalichman L (2019) Cervical posture, pain, and pathology: developmental, evolutionary and occupational perspective. In: Been E, Gómez-Olivencia A, Kramer PA (eds) Spinal evolution: morphology, function, and pathology of the spine in hominoid evolution. Springer, New York, pp 321–340

Franciscus RG, Churchill SE (2002) The costal skeleton of Shanidar 3 and a reappraisal of Neandertal thoracic morphology. J Hum Evol 42(3):303–356

Gómez-Olivencia A, Been E (2019) The spine of late *Homo*. In: Been E, Gómez-Olivencia A, Kramer PA (eds) Spinal evolution: morphology, function, and pathology of the spine in hominoid evolution. Springer, New York, pp 185–212

Gómez-Olivencia A, Barash A, García-Martínez D, Arlegi M, Kramer P, Bastir M, Been E (2018) 3D virtual reconstruction of the Kebara 2 Neandertal thorax. Nature Communications 9:4387

Gómez-Olivencia A, Carretero JM, Arsuaga JL, Rodríguez-García L, García-González R, Martínez I (2007) Metric and morphological study of the upper cervical spine from the Sima de los Huesos site (Sierra de Atapuerca, Burgos, Spain). J Hum Evol 53:6–25

Gómez-Olivencia A, Been E, Arsuaga JL, Stock JT (2013) The Neandertal vertebral column 1: the cervical spine. J Hum Evol 64:608–630

Gómez-Olivencia A, Arlegi M, Barash A, Stock JT, Been E (2017) The Neandertal vertebral column 2: the lumbar spine. J Hum Evol 106:84–101

Gómez-Olivencia A, Gómez-Robles A (2016) Evolution of the vertebral formula in hominoids: insights from ancestral state reconstruction approaches. Proc Eur Soc study of Hum Evol 5:109

Haeusler M (2019) Spinal pathologies in fossil hominins. In: Been E, Gómez-Olivencia A, Kramer PA (eds) Spinal evolution: morphology, function, and pathology of the spine in hominoid evolution. Springer, New York, pp 213–246

Haeusler M, Martelli S, Boeni T (2002) Vertebrae numbers of the early hominid lumbar spine. J Hum Evol 43:621–643

Haeusler M, Schiess R, Boeni T (2011) New vertebral and rib material point to modern bauplan of the Nariokotome *Homo erectus* skeleton. J Hum Evol 61:575–582

Hawks J, Elliott M, Schmid P, Churchill SE, Ruiter DJd, Roberts EM, Hilbert-Wolf H, Garvin HM, Williams SA, Delezene LK, Feuerriegel EM, Randolph-Quinney P, Kivell TL, Laird MF, Tawane G, DeSilva JM, Bailey SE, Brophy JK, Meyer MR, Skinner MM, Tocheri MW, VanSickle C, Walker CS, Campbell TL, Kuhn B, Kruger A, Tucker S, Gurtov A, Hlophe N, Hunter R, Morris H, Peixotto B, Ramalepa M, Rooyen Dv, Tsikoane M, Boshoff P, Dirks P, Berger LR (2017) New fossil remains of *Homo naledi* from the Lesedi Chamber, South Africa. eLife 6:e24232

Kramer PA, Hammerberg AG, Sylvester AD (2019) Modeling the spine using finite element models: considerations and cautions. In: Been E, Gómez-Olivencia A, Kramer PA (eds) Spinal evolution: morphology, function, and pathology of the spine in hominoid evolution. Springer, New York, pp 387–400

Latimer B, Ward CV (1993) The thoracic and lumbar vertebrae. In: Walker A, Leakey R (eds) The Nariokotome *Homo erectus* Skeleton. Harvard University Press, Cambridge, 266–293

Lordkipanidze D, Jashashvili T, Vekua A, Ponce de Leon MS., Zollikofer CP, Rightmire GP, Pontzer H, Ferring R, Oms O, Tappen M, Bukhsianidze M, Agusti J, Kahlke R, Kiladze G, Martinez-Navarro B, Mouskhelishvili A, Nioradze M, Rook L (2007)Postcranial evidence from early *Homo* from Dmanisi, Georgia. Nature 449:305–10

Lovejoy CO, Johanson DC, Coppens Y (1982) Elements of the axial skeleton recovered from the Hadar formation: 1974–1977 Collections. Am J Phys Anthropol 57:631–635

Lovejoy CO, McCollum MA (2010) Spinopelvic pathways to bipedality: why no hominids ever relied on a bent-hip–bent-knee gait. Philos Trans R Soc Lond B Biol Sci 365:3289–3299

Martelli S (2019) The modern and fossil hominoid spinal ontogeny. In: Been E, Gómez-Olivencia A, Kramer PA (eds) Spinal evolution: morphology, function, and pathology of the spine in hominoid evolution. Springer, New York, pp 246–282

McCollum M, Rosenman BA, Suwa G, Meindl RS, Lovejoy CO (2010) The vertebral formula of the last common ancestor of African apes and humans. J Exp Zool (Mol Dev Evol) 314B:123–134

McCown TD, Keith A (1939) The stone age of Mount Carmel. The fossil human remains from the Levalloiso-Mousterian. Clarendon Press, Oxford

Meyer MR (2005) Functional Biology of the *Homo erectus* Axial Skeleton from Dmanisi, Georgia. Ph.D. Dissertation, University of Pennsylvania

Meyer MR (2008) Skeletal Indications for distance locomotion in early *Homo* erectus. Am J Phys Anthropol 135(S46):155

Meyer MR, Haeusler M (2015) Spinal cord evolution in early *Homo*. J Hum Evol 88:43–53

Meyer MR (2016) The cervical vertebrae of KSD-VP-1/1. In: Haile-Selassie Y, Su D (eds) The postcranial anatomy of *Australopithecus afarensis*: new insights from KSD-VP-1/1. Springer, New York, pp 63–111

Meyer MR, Williams SA (2019) The spine of early Pleistocene *Homo*. In: Been E, Gómez-Olivencia A, Kramer PA (eds) Spinal evolution: morphology, function, and pathology of the spine in hominoid evolution. Springer, New York, pp 153–184

Nakatsukasa M (2019) Miocene ape spinal morphology: the evolution of orthogrady. In: Been E, Gómez-Olivencia A, Kramer PA (eds) Spinal evolution: morphology, function, and pathology of the spine in hominoid evolution. Springer, New York, pp 73–96

Nalley TK, Grider-Potter N (2015) Functional morphology of the primate head and neck. Am J Phys Anthropol 156:531–542

Nalley TK, Grider-Potter N (2019) Vertebral morphology in relation to head posture and locomotion: the cervical spine. In: Been E, Gómez-Olivencia A, Kramer PA (eds) Spinal evolution: morphology, function, and pathology of the spine in hominoid evolution. Springer, New York, pp 35–50

Palancar CA, García-Martínez D, Barash A, Radovčić D, Antonio Rosas, Bastir M (2018) Reconstruction of the atlas (C1) of the La Chapelle-aux-Saints Neanderthal through geometric morphometric techniques. Proceedings of the European Society for the Study of Human Evolution, 7:152

Pilbeam D (2004) The anthropoid postcranial axial skeleton: comments on development, variation, and evolution. J Exp Zool 302B:241–267

Robinson JT (1972) Early hominid posture and locomotion. The University of Chicago Press, Chicago

Russo GA, Kirk EC (2019) The hominoid cranial base in relation to posture and locomotion. In: Been E, Gómez-Olivencia A, Kramer PA (eds) Spinal evolution: morphology, function, and pathology of the spine in hominoid evolution. Springer, New York, pp 15–34

Sanders WJ (1998) Comparative morphometric study of the australopithecine vertebral series Stw-H8/H41. J Hum Evol 34:249–302

Schiess R, Boeni T, Rühli F, Haeusler M (2014) Revisiting scoliosis in the KNM-WT 15000 *Homo erectus* skeleton. J Hum Evol 67:48–59.

Shapiro LJ, Russo GA (2019) Vertebral morphology in hominoids II- The lumbar spine. In: Been E, Gómez-Olivencia A, Kramer PA (eds) Spinal evolution: morphology, function, and pathology of the spine in hominoid evolution. Springer, New York, pp 51–72

Thompson NE, Almécija S (2017) The evolution of vertebral formulae in Hominoidea. J Human Evol 110:18–36

Vandermeersch B (1981) Les hommes fossiles de Qafzeh (Israël). Éditions du CNRS, Paris

Williams SA (2012a) Placement of the diaphragmatic vertebra in catarrhines: implications for the evolution of dorsostability in hominoids and bipedalism in hominins. Am J Phys Anthropol 148:111–122

Williams SA (2012b) Modern or distinct axial bauplan in early hominins? Comments on Haeusler et al. (2011). J Hum Evol 63:552–556

Williams SA, Meyer MR (2019) The spine of *Australopithecus*. In: Been E, Gómez-Olivencia A, Kramer PA (eds) Spinal evolution: morphology, function, and pathology of the spine in hominoid evolution. Springer, New York, pp 125–152

Williams SA, Russo GA (2015) Evolution of the hominoid vertebral column: the long and the short of it. Evol Anthropol 24:15–32

Williams SA, Ostrofsky KR, Frater N, Churchill SE, Schmid P, Berger LR (2013) The vertebral column of *Australopithecus sediba*. Science 340:1232996

Williams SA, Middleton ER, Villamil CI, Shattuck MR (2016) Vertebral numbers and human evolution. Am J Phys Anthropol 159:19–36

Williams SA, García-Martínez D, Bastir M, Meyer MR, Nalla S, Hawks J, Schmid P, Churchill SE, Berger LR (2017) The vertebrae and ribs of *Homo naledi*. J Hum Evol 104:136–154

Williams SA, Meyer MR, Nalla S, García-Martínez D, Nalley TK, Eyre J, Prang TC, Bastir M, Schmid P, Churchill SE, Berger LR (2018) Special Issue: *Australopithecus sediba* —The Vertebrae, Ribs, and Sternum of *Australopithecus sediba*. PaleoAnthropology 2018:156–233

Williams SA, Gómez-Olivencia A, Pilbeam D (2019) Numbers of Vertebrae in Hominoid Evolution. In: Been E, Gómez-Olivencia A, Kramer PA (eds) Spinal evolution: morphology, function, and pathology of the spine in hominoid evolution. Springer, New York, pp 97–124

Chapter 2
The Hominoid Cranial Base in Relation to Posture and Locomotion

Gabrielle A. Russo and E. Christopher Kirk

2.1 Introduction

A quick glance at the cover and title of this book promises the reader that it reviews the anatomy and evolution of the hominoid spine. The reader may therefore ask: why does this chapter focus on the *head*? In our view, there are two main reasons to introduce a book on the evolutionary anatomy of the hominoid spine with a chapter on the head. The most obvious answer is that in all vertebrates the head is directly connected to the rest of the body via the spine. The cranial base articulates with the cervical vertebral column, which initially evolved in early tetrapods to allow the head to move independently of the rest of the body (Romer 1950). In modern humans the cervical vertebral column has been modified to allow movements of the head atop an upright torso, rather than in front of the torso as in quadrupedal chimpanzees and most other primates and mammals (Lieberman 2011). Given this unusual positional relationship between the head and the rest of the body in modern humans, extensive research has been dedicated to documenting and understanding the biomechanical interactions between the cranial base and the rest of the axial skeleton among hominoids. The second answer, which is a primary driver behind biological anthropologists' motivation to conduct the aforementioned research, is that cranial anatomy plays a key role in interpreting the primate and human fossil record. Researchers have long appreciated our ability to make phylogenetically and functionally relevant inferences about aspects of postcranial anatomy using clues

G. A. Russo (✉)
Department of Anthropology, Stony Brook University, Stony Brook, NY, USA
e-mail: gabrielle.russo@stonybrook.edu

E. C. Kirk (✉)
Department of Anthropology, University of Texas at Austin, Austin, TX, USA

Jackson School Museum of Earth History, University of Texas at Austin, Austin, TX, USA
e-mail: eckirk@austin.utexas.edu

E. Been et al. (eds.), *Spinal Evolution*,
https://doi.org/10.1007/978-3-030-19349-2_2

gleaned from the cranial base, which is particularly important in the absence of direct fossil evidence of the postcranial skeleton. As we will discuss below, cranial base anatomy has historically played a key role in interpreting the postural and locomotor adaptations of some early hominin taxa (e.g., Dart 1925; White et al. 1994; Brunet et al. 2002). With these two answers in mind, in this chapter we focus on the relationship between cranial base morphology, posture, and locomotion in the Hominoidea.

2.2 What Is the Cranial Base?

The cranial base is the region of the skull that intervenes between the bones of the face (splanchnocranium/viscerocranium) and the cranial vault (calvaria). The cranial base forms the floor of the braincase (neurocranium) and supports the inferior surface of the brain. In hominoids, the cranial base is primarily formed by the ethmoid, orbital plates of the frontal, sphenoid, right and left temporals, and occipital (excluding the planum occipitale). The majority of the cranial base develops from multiple centers of ossification that appear early in fetal development within the chondrocranium. The chondrocranium itself is formed via the fusion of multiple smaller cartilages, which grow to surround many of the neurovascular structures that pass between the neck and the interior of the developing braincase. As a result, the adult bones of the cranial base that are derived at least partly from the chondrocranium (ethmoid, sphenoid, temporal, and occipital) contain numerous foramina that transmit major nerves (e.g., the cranial nerves and spinal cord) and vessels (e.g., the internal carotid artery and internal jugular vein). However, several sections of the cranial base are not derived from the chondrocranium and instead develop via intramembranous ossification. These intramembranous parts of the adult cranial base include the orbital plates of the frontal, the squamous portions of the temporals, and the pterygoid and alisphenoid portions of the sphenoid. Superiorly, the bony elements of the cranial base form fossae that accommodate key intracranial structures, including the frontal lobes and olfactory bulbs within the anterior cranial fossa, the temporal lobes within the middle cranial fossae, the pituitary gland within the hypophyseal fossa, and the cerebellum, pons, and medulla within the posterior cranial fossa (Lieberman et al. 2000; Scheuer and Black 2001).

As the bony interface between anatomical structures of the face, neck, and braincase, the cranial base provides a rich source of information about an organism's adaptations and evolutionary history. Accordingly, the morphology of the cranial base may be influenced by selection acting on many different variables, such as brain size, the anatomy of the masticatory apparatus, trunk and/or neck posture, and locomotion. Because the literature on the hominoid basicranium is quite extensive (e.g., Bolk 1909; Weidenreich 1941; Ashton and Zuckerman 1952, 1956; Biegert 1957, 1963; Demes 1985; Lieberman et al. 2000; Ross and Ravosa 1993; Russo and Kirk 2013, 2017; Neaux et al. 2017, 2018; Villamil 2017), in this chapter we primarily focus on those portions of the posterior cranial base that are most closely associated

Fig. 2.1 Inferior views of the crania of *Pan troglodytes* (left, FMNH 18406), *Homo sapiens* (middle), and *Gorilla gorilla* (right, AMNH 167236). Occipital condyles highlighted in red; FM = foramen magnum; blue asterisk = tip of mastoid process. Specimens oriented in the Frankfort horizontal and scaled to the same approximate anteroposterior length

with the cervical spine and related structures in the neck. In this context, we identify these relevant features of the cranial base as the (1) foramen magnum, which transmits the spinal cord from the braincase to the vertebral canal formed by the subjacent vertebrae; (2) occipital condyles, which form the bony articulation with the first cervical vertebra (i.e., the atlas); and (3) adjacent portions of the occipital and temporal bones that provide attachment sites for major muscles involved in head movements relative to the trunk (Fig. 2.1). For clarity, we henceforth refer to these components of the cranial base as the "cranio-cervical interface." Although our focus is on the morphology of these specific structures among hominoids, we will necessarily provide some discussion about how the cranio-cervical interface relates to other cephalic structures because the cranium as a whole is integrated (Lieberman et al. 2000; Strait 2001).

From a simplified biomechanical perspective, the cranio-cervical interface lies at the center of the first-class lever system primarily responsible for flexion and extension of the head relative to the cervical spine (Şenyürek 1938; Schultz 1942; Demes 1985). The atlanto-occipital joint is formed by the occipital condyles, located immediately lateral to the foramen magnum, and the superior articular facets (prezygapophyses) of the atlas. A point midway between the centers of the occipital condyles represents the "axis/fulcrum" of this joint, the portion of the cranium anterior to the atlanto-occipital joint represents the "resistance/load," and the nuchal musculature (and passive nuchal ligaments) positioned posterior to the joint represents the "force/effort" (Şenyürek 1938; Schultz 1942; Demes 1985). The anterior projection (i.e., resistance/load arm or out-lever) and weight (i.e., the actual resistance/load or out-force) of the facial skeleton are thus offset by the posterior projection of the neurocranium (i.e., force/effort arm or in-lever), and the force of the nuchal musculature (i.e., muscular effort or in-force) preserves neutral head posture

(i.e., maintains equilibrium) (Şenyürek 1938; Schultz 1942; Adams and Moore 1975). Because the heads of great apes have more mass located anterior to the occipital condyles than posterior to the occipital condyles (i.e., greater resistance and longer resistance arm), a large amount of effort from the neck muscles and/or bony modifications that affect the length of their force arm (e.g., spinous processes) are required to keep the head upright and level (Schultz 1942). In contrast to great apes, modern humans have a relatively smaller face (i.e., less resistance) and a more centrally located atlanto-occipital joint (i.e., shorter resistance arm), and thus less muscular effort is required to keep the head upright and level.

2.3 Foramen Magnum

The foramen magnum is the "great hole" of the occipital bone through which (1) the spinal cord exits the braincase and passes into the vertebral canal and (2) the vertebral arteries enter the braincase. The foramen magnum, along with the occipital condyles, provides a direct osteological marker of where (and to some extent how) the cervical vertebral column articulates with the head. In anatomical position, the human head is positioned superior to the torso and the head's rostro-caudal axis is essentially perpendicular to the long axis of the vertebral column. By contrast, when standing quadrupedally, the head of a chimpanzee or gorilla is positioned anterior to the torso as in most other mammals. Accordingly, a more anterior position of the foramen magnum along the midline axis of the cranial base has traditionally been linked to habitual postures in which the head is located superior to the trunk, whereas a more posterior position of the foramen magnum on the cranial base has been thought to reflect habitual postures in which the head is located more anteriorly relative to the trunk. That humans have a more anteriorly positioned foramen magnum than African apes (Figs. 2.1 and 2.2) is a distinction first observed in the mid-eighteenth century (Daubenton 1764). Most comparative research published since that time overwhelmingly favors the conclusion that the foramen magnum is more anteriorly positioned in humans than in any other living primate species (Broca 1872; Topinard 1890; Bolk 1909; Dart 1925; Dean and Wood 1981, 1982; Luboga and Wood 1990; Schaefer 1999; Ahern 2005; Russo and Kirk 2013, 2017; Russo et al. 2016; Neaux et al. 2017).

Foramen magnum position has been quantified as the anteroposterior position of basion (the anterior-most margin of the foramen magnum at midline) relative to select cranial dimensions, such as cranial length (Dart 1925). Basion position has also been assessed relative to a variety of more anteriorly placed cranial landmarks or their derivatives, including the bicarotid chord (White et al. 1994; Schaefer 1999; Ahern 2005; Suwa et al. 2009; Kimbel et al. 2014), the bitympanic and biauricular chords (Dean and Wood 1981, 1982), the biporion chord (Ahern 2005), foramen cecum, subnasale, and glabella (Luboga and Wood 1990), and the distal-most molar, posterior hard palate, anterior margin of the temporal fossa, and spheno-occipital synchondrosis (Russo and Kirk 2013, 2017; Neaux et al. 2017). Several studies

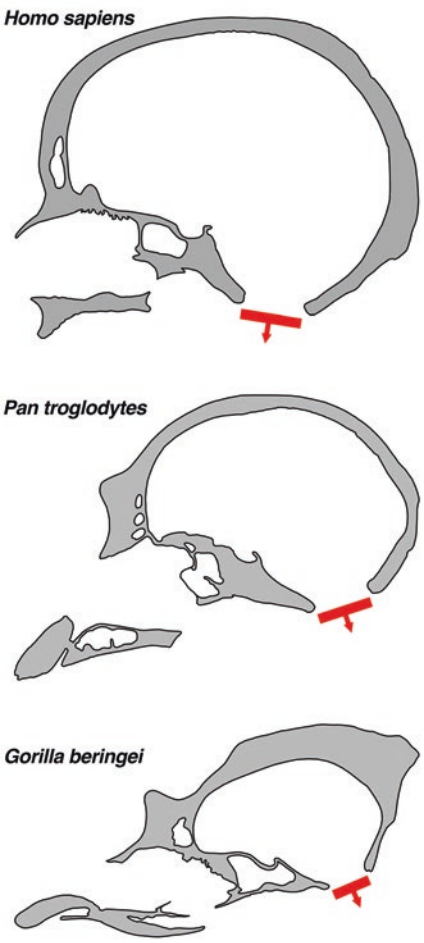

Fig. 2.2 Sagittal sections through the crania of *Homo sapiens* (top), *Pan troglodytes* (middle, USNM 395820), and *Gorilla beringei* (bottom, USNM 395636). Position and orientation of the foramen magnum indicated for each specimen by a red bar and arrow. Specimens oriented in the Frankfort horizontal and scaled to the same approximate anteroposterior length

(e.g., Weidenreich 1943; Kimbel et al. 2004; see also Russo and Kirk 2017) defined the position of the foramen magnum using opisthion (the posterior-most point on the margin of the foramen magnum at midline) rather than basion, quantifying foramen magnum position as the distance from opisthion to the posterior-most extent of the cranial vault divided by cranial length (i.e., the "Weidenreich index"; Kimbel et al. 2004). Analyses using anteriorly located landmarks as reference points for quantifying basion position have generated mixed results with varying degrees of success in distinguishing between bipedal humans and non-bipedal primates (see Russo and Kirk 2013 for a review). For example, the utility of the biporion chord for assessing relative basion position has been questioned due to its poor performance in discriminating among extant or extinct hominoids (Dean and Wood 1981; Luboga and Wood 1990; Ahern 2005). By comparison, the position of basion relative to the bicarotid chord has been used more widely and generally indicates a more forward

position of the foramen magnum in modern humans and extinct hominins compared to African apes (Schaefer 1999; Ahern 2005; Kimbel et al. 2014). The position of basion relative to the distal-most molar, the posterior edge of the bony palate at midline, the anterior-most margin of the temporal fossa, and the spheno-occipital synchondrosis also distinguishes humans from other extant hominoids (Russo and Kirk 2013, 2017; Neaux et al. 2017). However, it should be noted that the use of the spheno-occipital synchondrosis as a reference point for assessing basion position also reflects basioccipital length (the distance from basion to sphenobasion; Russo and Kirk 2017). By the same token, the use of the distal-most molars, posterior hard palate, and anterior temporal fossae to quantify relative basion position may be complicated by selection acting on the morphology of the facial skeleton and masticatory apparatus (Ruth et al. 2016; Russo and Kirk 2013, 2017; Neaux et al. 2017). Similarly, analyses that rely on the use of landmarks posterior to opisthion are evidently strongly influenced by the differences between modern humans and other extant hominoids in the posterior projection of the braincase as a result of neurocranial expansion in humans (Kimbel et al. 2004; Russo and Kirk 2017) (see below for further discussion).

While most researchers have linked the distinctive position of the foramen magnum in modern humans to habitual bipedalism, an anteriorly positioned foramen magnum has also been suggested to reflect upright (i.e., orthograde) trunk posture more generally (Kimbel and Rak 2010). In either scenario, the commonly accepted functional explanation is that a more anteroposteriorly "centered" foramen magnum along the cranial base midline in modern humans permits the head to sit atop an upright spine with minimal muscular effort (Şenyürek 1938; Schultz 1942, 1955). The relationship between an anteriorly positioned foramen magnum and bipedal locomotion receives support from comparative research demonstrating that bipedal marsupials and rodents resemble humans in possessing more anteriorly positioned foramina magna and shorter basioccipitals than their quadrupedal close relatives (Russo and Kirk 2013, 2017). In fact, the available comparative evidence indicates that anterior migration of the foramen magnum has evolved in concert with bipedalism (both striding and saltatory) in at least five mammalian clades: the Homininae, Macropodidae, Dipodidae, Heteromyidae, and Pedetidae (Russo and Kirk 2013, 2017). The hypothesis that orthograde trunk posture (rather than bipedal locomotion per se) influences foramen magnum position (Kimbel and Rak 2010) also receives some support because strepsirrhine primates known to employ orthograde positional behaviors (e.g., vertical clingers and leapers like *Propithecus* and *Lepilemur*) exhibit more anteriorly positioned foramina magna than non-orthograde strepsirrhine primates (Russo and Kirk 2013).

The apparent relationship between an anteriorly positioned foramen magnum and bipedal locomotion in extant hominoids has been used by paleoanthropologists as a basis for inferring bipedalism, and thus hominin status, in the human fossil record. The utility of the foramen magnum as an indicator of upright posture and bipedalism in fossil hominins was initially noted by Raymond Dart (1925) in his description of the "Taung child," the juvenile holotype specimen of *Australopithecus africanus*. Dart (1925) surmised that the anteriorly shifted foramen magnum of *Au.*

africanus (in comparison to a sample of baboons, chimpanzees, and modern humans) "points to the assumption by this fossil group of an attitude appreciably more erect…The improved poise of the head, and the better posture of the whole-body framework which accompanied this alteration in the angle at which its dominant member was supported, is of great significance. It means that a greater reliance was being placed by this group on the feet as organs of progression" (197). Since this report, the anterior position of the foramen magnum has been cited numerous times as morphological evidence of bipedal locomotion in putative hominins, including the Mio-Pliocene genera *Sahelanthropus* and *Ardipithecus* (e.g., Le Gros Clark 1954; Dean and Wood 1982; White et al. 1994; Brunet et al. 2002; Guy et al. 2005; Suwa et al. 2009; White et al. 2009). As a result, an anteriorly positioned foramen magnum is a commonly cited synapomorphy of hominins (e.g., White et al. 1994; Guy et al. 2005; Zollikofer et al. 2005; Kimbel et al. 2014).

In addition to differences in the anteroposterior *position* of the foramen magnum, extant hominoids also differ in the anteroinferior *inclination* of the foramen magnum (Fig. 2.2). This latter aspect of foramen magnum morphology is variously referred to as "foramen magnum orientation" (Kimbel et al. 2004; Pickford 2005; Been et al. 2014; Russo and Kirk 2017), "foramen magnum angle" (Ruth et al. 2016), "foramen magnum – orbital plane angle" (Strait and Ross 1999; Wolpoff et al. 2002; Zollikofer and Ponce de León 2005), and "inclination of occipital foramen" (Weidenreich 1943), depending on the authors and/or their choice of reference planes. The plane of the foramen magnum is defined by a chord connecting basion and opisthion. Foramen magnum orientation is typically quantified as the angle between this basion-opisthion chord and a reference plane projected into the midsagittal plane, such as the Frankfort horizontal (drawn through orbitale and porion when the cranium is viewed in *norma lateralis*) (but see Strait and Ross 1999). Previous analyses have shown that the modern human foramen magnum is distinctly anteroinferiorly oriented rather than posteroinferiorly oriented as in great apes (Daubenton 1764; Broca 1877; Bolk 1910; Luboga and Wood 1990; Pickford 2005; Zollikofer et al. 2005; Russo and Kirk 2017). In other words, although all hominoids possess foramina magna that face inferiorly to some extent, the foramina of humans are more anteriorly facing, while those of apes (and many other mammals) are more posteriorly facing (Fig. 2.2). A link between this derived foramen magnum orientation in humans and more vertical human-like neck and trunk postures is intuitively appealing and is also supported by research demonstrating a relationship between foramen magnum orientation and total cervical lordosis in intraspecific samples of modern humans (Been et al. 2014). However, the orientation of the foramen magnum relative to the orbital axis (an alternative reference plane to the Frankfort horizontal [Strait and Ross 1999]) in humans is similar to that of a wide range of other anthropoid taxa with very different neck postures (Lieberman et al. 2000). Foramen magnum orientation is also not correlated with measures of neck posture among non-human primates (Lieberman et al. 2000), suggesting that the orientation of the foramen magnum is a poor indicator of the orientation of the cervical vertebral column in interspecific samples. By extension, foramen magnum orientation is probably also a poor indicator of trunk posture. Comparisons among

great apes reveal that *Pongo* does not have a more anteriorly inclined foramen magnum (or occipital condyles) than the African apes, despite its greater reliance on orthograde trunk postures (Moore et al. 1973).

While differences in foramen magnum position and orientation between humans and other extant hominoids are readily apparent, the relationship, if any, between these two aspects of foramen magnum morphology is not clear, particularly when comparative samples are expanded to include other extant primates and mammals. Bolk (1909, 1910) speculated that foramen magnum position and orientation are linked, and some researchers have even employed foramen magnum orientation as a proxy for foramen magnum position (Ruth et al. 2016). However, a direct analysis of the relationship between these two variables in hominoids and various other mammalian clades demonstrates that foramen magnum orientation is at most only weakly correlated with foramen magnum position (Russo and Kirk 2017). Furthermore, reports that some *Australopithecus* specimens appear to exhibit human-like foramen magnum positions but more chimpanzee-like foramen magnum orientations (Kimbel and Rak 2010) indicate that foramen magnum position and orientation are not tightly coupled and may have been influenced by different selective forces during the course of hominin evolution.

Finally, as mentioned above, both foramen magnum position and orientation are likely influenced by factors other than posture and locomotion. Compared to other hominoids, humans exhibit a number of derived cephalic features (e.g., an enormously enlarged brain and neurocranium, a shortened rostrum, and a reduced size of the masticatory apparatus) that have been suggested to play a role in determining basicranial morphology. Indeed, a probable influence of brain size on foramen magnum morphology in hominoids has been recognized for nearly as long as foramen magnum morphology has been invoked to predict posture and locomotion (e.g., Bolk 1909; Le Gros Clark 1934; Weidenreich 1941; Ashton 1957; Biegert 1957, 1963). These early researchers hypothesized that increased encephalization was responsible for the pronounced basicranial flexion that distinguishes modern humans from other extant hominoids. In this evolutionary scenario, increases in brain size in hominins caused a downward rotation of the posterior cranial base relative to the facial skeleton, resulting in increased cranial base flexion (Fig. 2.2). As the cranial base became more flexed in hominins, the nuchal region deflected from a more vertical to a more horizontal orientation and the position of the foramen magnum shifted anteriorly (Biegert 1957, 1963; see also Bastir et al. 2010). Ontogenetic studies have demonstrated that the foramen magnum and occipital condyles migrate posteriorly in great apes but remain more anteriorly situated in humans during growth (Ashton and Zuckerman 1952; Schultz 1955; Ashton and Zuckerman 1956). These observations may support a link between increased basicranial flexion and increased encephalization if ontogenetic increases in brain size prevent posterior migration of the foramen magnum in humans (Ashton and Zuckerman 1952, 1956; Schultz 1955). However, other researchers have speculated that it is the acquisition of bipedal posture and locomotion that prevents posterior migration of the foramen magnum in humans (Bolk 1915). By the same token, the formation of a well-developed nuchal plane of the occipital bone as an insertion site

for the nuchal musculature during ontogeny may be tied to the more posteriorly facing foramina magna of great apes and possibly *Australopithecus* (Kimbel et al. 2004). Interspecific studies of primates and other mammals reveal that some metrics of brain size (i.e., encephalization ratio, index of relative encephalization) appear related to foramen magnum orientation (Spoor 1997; Ruth et al. 2016), while other metrics of brain size (i.e., encephalization quotient) have either a weak or nonexistent relationship with foramen magnum orientation (Russo and Kirk 2017). Although such disparate results may be attributable to a number of factors (e.g., the use or lack of phylogenetic methods), it is clear that the choice of metrics for quantifying (1) relative brain size, (2) foramen magnum orientation, and (3) foramen magnum position has a major impact on the outcome of any analysis (Russo and Kirk 2017). A similar conclusion applies to the proposed relationship between brain size and basicranial flexion, which differs according to the primate clade being considered and the metrics used to quantify basicranial flexion and relative brain size (Ross and Ravosa 1993; Ross and Henneberg 1995; Spoor 1997; Strait and Ross 1999; Lieberman et al. 2000; McCarthy 2001). Facial size either alone or considered in conjunction with brain size has also been suggested to influence basicranial anatomy in primates and other mammals (e.g., Huxley 1863; Weidenreich 1941; Biegert 1963; Ross and Ravosa 1993; Bastir et al. 2010; Ruth et al. 2016; Russo and Kirk 2017; Villamil 2017). In this scenario, smaller faces are presumably linked with more flexed basicrania and thus more anteriorly shifted cranial base structures including the foramen magnum (e.g., as in humans), whereas larger faces are linked with less flexed basicranial and thus more posteriorly shifted cranial base structures (e.g., as in great apes). However, like brain size, the results of any analysis of the relationship between foramen magnum morphology and facial size will be strongly influenced by metric choice and comparative sample composition (e.g., see results for marsupials by Russo and Kirk (2017) and Villamil (2017)).

2.4 Occipital Condyles

The occipital condyles represent the sole bony connection between the head and the rest of the axial skeleton. As noted above, the occipital condyles are paired structures located on either side of the foramen magnum that articulate with the prezygapophyses of the atlas and form the fulcrum of the atlanto-occipital joint (Schultz 1942, 1955) (Fig. 2.1). Early observations of the cranio-cervical interface recognized the utility of the occipital condyles as landmarks for determining how the head is "balanced" on the torso (e.g., Bolk 1909; Schultz 1917, 1942, 1955; Broom 1938; Şenyürek 1938; ; Le Gros Clark 1950; Moore et al. 1973). As a result, many of these papers devised methods for measuring the relative lengths and sizes of pre- and post- condylar head "segments" using indices in order to model the atlanto-occipital lever system. For example, Şenyürek (1938) divided the distance between a point in the middle of the occipital condyle articular surface and prosthion by the prosthion-opisthocranion chord in his calculation of a "cranial equilibrium index."

He concluded that the lower index observed for humans compared to other primates meant the condyles were more anteriorly situated, providing enhanced mechanical advantage in bipedal postures. Schultz (1942) (see also Schultz 1917) expanded on this work by operationalizing the head-neck lever system using an apparatus that allowed him to calculate the actual weights of the pre- and post- condylar segments[1] of the head from cadaveric specimens. Schultz (1942) concluded that modern humans exert considerably less muscular force (~16% of head weight) to "balance" the head atop the neck compared to other primates (~37% of head weight on average). These early comparative studies of extant primates generally agree that the more anteriorly positioned occipital condyles in modern humans confer an advantage compared to other primates for "balancing" the head atop an upright spine.

Researchers focused on interpreting hominin basicranial anatomy have expanded on these analyses and invoked the position of the occipital condyles as an indication of head and neck posture in extinct hominins. Le Gros Clark (1950) calculated a "condylar position index" as the distance from the center of the occipital condyle to the posterior cranial vault, divided by the distance from the center of the occipital condyle to prosthion x 100. Using this metric, he found that *Au. africanus* (represented by the adult specimen STS 5) exhibited occipital condyles more similar to modern humans and other extinct hominins than to most extant nonhuman hominoids. Le Gros Clark (1950) therefore concluded that the "bodily posture" of *Au. africanus* was similar to bipedal hominins (246). However, other studies of the STS 5 cranium using the same metric and expanded anthropoid samples found that occipital condyle position in *Au. africanus* is either more similar to African apes than to modern humans or is intermediate between the two groups (Ashton and Zuckerman 1951; Adams and Moore 1975). This later research therefore suggests that skull "balance" in *Au. africanus* was unlike modern humans despite the shared adoption of bipedal postures and locomotion. Such a finding seems consistent with the clear differences in cranial architecture between *Homo* and *Australopithecus* that would be expected to influence the biomechanics of the atlanto-occipital joint, including facial size and robusticity, rostral length, masticatory apparatus size, and brain size (Kimbel et al. 2004).

In addition to investigations of the anteroposterior position of the occipital condyles along the cranial base, the angle of condylar articular surfaces and the inferior projection of the occipital condyles have also been examined for their utility in assessing the head postures of extant hominoids and fossil hominins (Moore et al. 1973; Adams and Moore 1975; Kimbel et al. 2004). The angle of condylar articular surfaces, measured as a chord connecting the anterior- and posterior- most points on the articular surface, is generally quantified relative to the Frankfort horizontal. This metric ("condylar angle") has been presumed to reflect the orientation of the cervical vertebral column and direction of associated muscular forces relative to the cranial base (Moore et al. 1973; Demes 1985). Like the anteroposterior position of the occipital condyles, condylar angle distinguishes modern humans from other extant

[1] Schultz's (1942) study differed from that of Şenyürek (1938) by substituting the inferior-most point on the condyle for the middle of the condyle and by substituting inion for opisthocranion.

hominoids (Knese 1948 as cited in Demes 1985; Moore et al. 1973; Adams and Moore 1975). In modern humans, the articular surfaces of the occipital condyles face more ventrally than in great apes. As a result, for the presumed head/neck postures most often adopted by hominoids (i.e., more vertical in modern humans and more horizontal in great apes), reaction forces occur perpendicular to the joint surfaces (Demes 1982, 1985). These observations may also be extended to *Australopithecus*, which can be readily discriminated from African apes by its more human-like condylar angle (Moore et al. 1973; Adams and Moore 1975). This observation for condylar angle is interesting given that foramen magnum orientation, which would seemingly be linked with condylar angle, does not distinguish *Australopithecus* from African apes to the same extent (Kimbel and Rak 2010). In addition to occipital condyle angle, Kimbel et al. (2004:101) noted that, when viewed posteriorly, the occipital condyles and supramastoid crest of *Pan* form a "continuous arched outline" such that the occipital condyles project more inferiorly relative to more lateral structures in the basicranium. In *Au. afarensis*, by comparison, the mastoid region is more clearly delineated from the occipital condyles (which are invaginated into the cranial base) and the rest of the cranial base by the mastoid processes (Kimbel et al. 2004). The functional implications (if any) of this configuration are poorly understood but might be related to differing patterns of pneumatization of the temporal bone (see below).

Other than their general topographic position, little is known about the morphology of the occipital condylar articular surfaces themselves. At least one worker has noted the concordance between the areas of the occipital condyle articular surfaces and body size (Martin 1980). Much more is likely to be learned from detailed analyses of the size and shape of the occipital condyles (Coroner and Latimer 1991; Nishimura et al. 2017) and/or their inferred morphology as mirrored in the subjacent prezygapophyses of the atlas (Gommery 1996; Manfreda et al. 2006; Nalley and Grider-Potter 2017). Because the occipital condyles articulate directly with the prezygapophyses of the atlas, researchers have focused on what might be revealed from investigations of occipital condyle shape in relation to potential movements at the atlanto-occipital joint. The primary movements at this joint are sagittal plane flexion and extension (i.e., pitch) (Lopez et al. 2015). However, the articulation between the atlas and subjacent second cervical vertebra (the axis) also allows for rotational movements (i.e., yaw) such that, together, a great deal of mobility can be achieved at this bony junction of the cranio-cervical interface. Coroner and Latimer (1991) collected direct tracings of both the occipital condyles and the reciprocal facets of the atlas and determined that the atlanto-occipital joint could be modeled as two curves—an anterior curve and a posterior curve—with great apes exhibiting more acutely angled articular profiles compared to modern humans. Gommery (1996) identified distinct aspects of the prezygapophyseal articular surfaces of C1 that correspond to the occipital condyles, noting the greatest variation among a sample of strepsirrhines, platyrrhines, cercopithecoids, and hominoids in the retroglenoid tubercle,[2] which could hypothetically serve to restrict or permit movements

[2] Gommery (1996) refers to the prezygapophyses of the atlas as the "glenoid cavities," so in this sense, a retroglenoid tubercle is a bony extension of the dorsal curve of the atlas' prezygapophysis.

at the atlanto-occipital joint. With respect to the curvature of the articular surfaces, a number of workers have noted that modern humans exhibit flatter prezygapophyses of the first cervical vertebra compared to other hominoids, which exhibit more deeply dorsoventrally concave prezygapophyses (Dickman et al. 1994; Manfreda et al. 2006; Nalley and Grider-Potter 2017). A relationship between occipital condyle morphology and locomotion in an expanded primate sample has been documented by Nishimura et al. (2017), who noted subtle differences in occipital condylar morphology among suspensors and arboreal and terrestrial quadrupeds. Together, the singular and more gently curved articular profile shapes and flatter articular surfaces of the occipital condyles in modern humans are interpreted to permit movement in a greater number of directions at the atlanto-occipital joint (Coroner and Latimer 1991). In contrast, the more acutely curved articular profile shapes and dorsoventrally deeper condylar articular surfaces of hominoids and many other primates (e.g., baboons) are interpreted to provide resistance to ventral translation of the head on the neck. This configuration may be necessitated by the fact that quadrupeds typically hold their heads (which have a center of gravity that sits below the occipital condyles; Demes 1985) in front of a more horizontally oriented torso. The relationship between neck posture and occipital condyle curvature is also supported by research showing that occipital condyle curvature increases as neck inclination angle (Ross and Ravosa 1993) increases (i.e., as necks becomes increasingly horizontal) (Nalley and Grider-Potter 2017).

2.5 Additional Structures of the Cranio-cervical Interface

Immediately adjacent to the foramen magnum and occipital condyles on the posterior cranial base are the insertion sites of the muscles that move the head relative to the rest of the body. The anterior migration of the foramen magnum/occipital condyles and attendant shortening of the basioccipital noted above for modern humans has important consequences for the insertion sites of the prevertebral muscles (Dean 1984, 1985). In great apes, the mm. rectus capitis anterior, which originate from C1 and C2, insert on the basioccipital immediately anterior to the foramen magnum and are closely approximated near the midline (Dean 1985). In humans however, the mm. rectus capitis anterior have more laterally positioned insertion sites immediately anterior to the occipital condyles, with a large space intervening between their medial borders (Dean 1984; Standring 2016). Perhaps of greater functional consequence is the fact that the m. longus capitis, which originates on C3–C6 and inserts on the basioccipital anterior to the m. rectus capitis anterior, has a much smaller and anteroposteriorly shortened insertion site in humans compared to great apes (Dean 1985). This difference could conceivably be the simple consequence of basioccipital shortening in humans and an associated decrease in the area available for muscular attachment. However, because the m. longus capitis is a powerful head flexor,

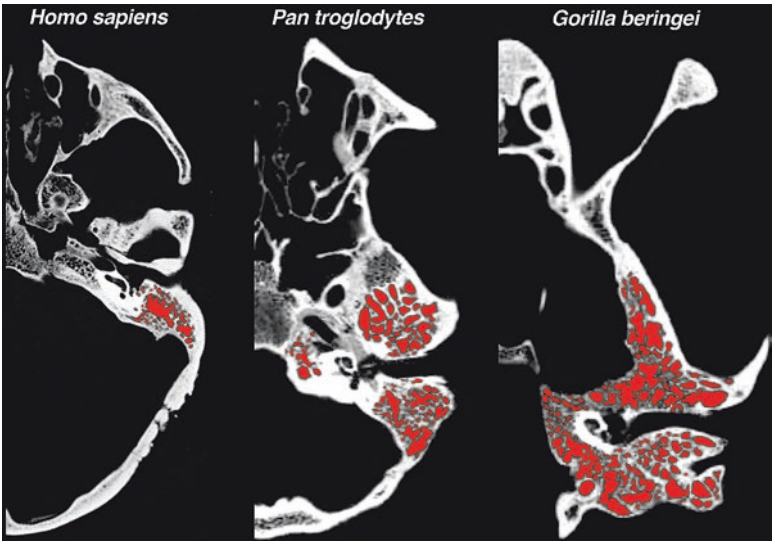

Fig. 2.3 Transverse sections through the crania of *Homo sapiens* (left), *Pan troglodytes* (middle, USNM 395820), and *Gorilla beringei* (right, USNM 395636). Pneumatic spaces of the temporal bone are shown in red. Images scaled to the same approximate anteroposterior length. The plane of each section intersects the cochlear labyrinth and external acoustic meatus, but note that the plane of sectioning for *Gorilla* is more obliquely inclined

it also seems likely that differences between great apes and humans in the size and mechanical advantage of the m. longus capitis could also be related to differences in the use of the canine teeth (sensu Dean 1984). In great apes, the canines are large and projecting and are frequently used in contests between individuals over access to mates and resources (Plavcan et al. 2012). Fighting with canines would seem to require, inter alia, the ability to powerfully flex the head in order to drive the projecting maxillary canines into the body of an opponent.[3] Modern humans, which possess incisiform canines, may be less reliant than great apes on having a large m. longus capitis because humans no longer rely on large canines for exchanging visually mediated threats or for fighting.

The bony structure of the posterior basicranium lateral to the foramen magnum and occipital condyles also differs substantially between humans and great apes. These differences partly reflect the degree of temporal bone pneumatization, which is far more extensive in African apes than in humans (Fig. 2.3; Sherwood 1999). In all great apes, the mastoid region of the temporal bone has a mastoid process that projects only a modest distance inferiorly (Lockwood et al. 2002) and lacks a groove for the origin of the posterior belly of the digastric on its medial surface (Dean 1984). Lateral to the apex of the mastoid process is a large roughened enthesis marking the

[3] Indeed, as noted by Dean (1984) saber toothed cats may require large mm. longus capitis in order to employ their maxillary canines during predation.

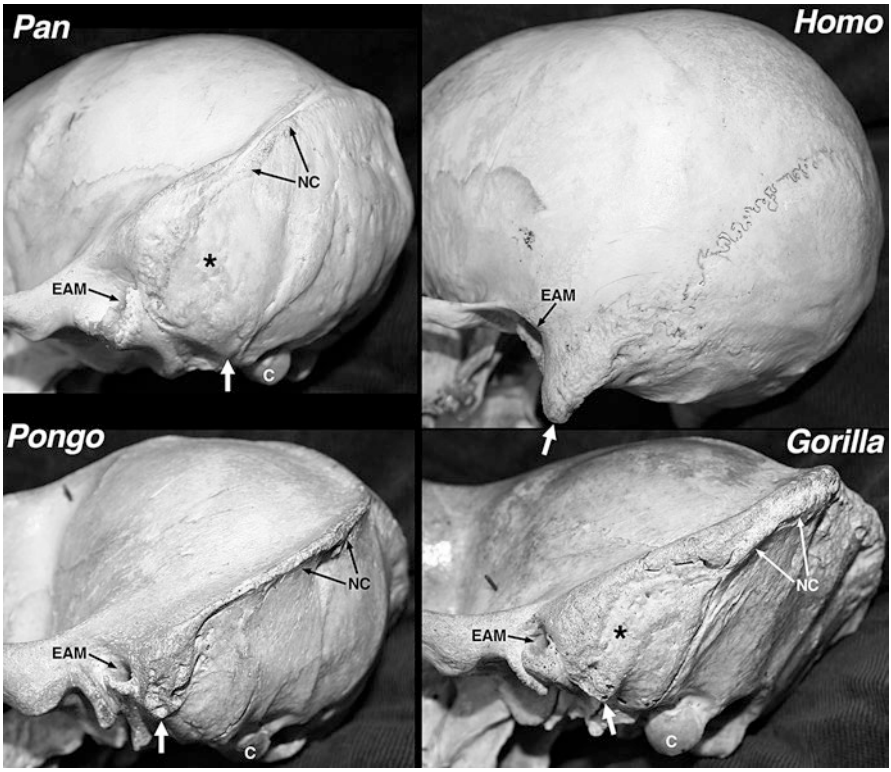

Fig. 2.4 Crania of great apes and humans in posterolateral view. Large white arrow = apex of mastoid process; asterisk = laterally projecting and extensively pneumatized mastoid region of African apes; C = occipital condyle; EAM = external acoustic meatus; NC = nuchal crest. Images not to scale. Occipital condyles of *Homo* not visible in this view due to their anteriorly shifted position. The prominent roughened entheses adjacent to the asterisks in *Pan* and *Gorilla* include the sites of origin of the m. sternocleidomastoid and m. splenius capitis (Dean 1984)

site of origin for the m. sternocleidomastoid (Fig. 2.4). This enthesis terminates superiorly at the nuchal crest,[4] immediately posterior to the external acoustic meatus. Although the mastoid process does not project far inferiorly, the entire mastoid region of great apes projects further laterally than in modern humans (Figs. 2.1, 2.4, 2.5). This extensive lateral projection of the mastoid region and anterior nuchal crest in great apes is the direct result of pneumatization of the posterolateral temporal bone (Fig. 2.5). Medial to the m. sternocleidomastoid, muscles originating from the pneumatized mastoid region of African apes include the anterior portion of the m. splenius capitis, the m. longissimus capitis, and the posterior belly of the m. digastric (Dean 1984).

[4] Note that the nuchal and supramastoid crests are confluent structures in extant great apes.

Fig. 2.5 Coronal sections through the neurocrania of *Homo sapiens* (left), *Pan paniscus* (middle, MCZ 38019), and *Gorilla gorilla* (right, MCZ 14750). The plane of each section intersects the posterior-most foramen magnum, immediately anterior to opisthion. Posterior pneumatic spaces of the temporal bone in apes are shown in pink. Specimens scaled to the same approximate supero-inferior height. Red arrows unilaterally mark the inferior margin of the nuchal crest in apes. The muscles originating from the pneumatized portions of the mastoid shown in these sections include the m. sternocleidomastoid and the m. splenius capitis (Dean 1984)

In modern humans, the mastoid process projects further inferiorly than in great apes (Lockwood et al. 2002; Fig. 2.4), and the posterior belly of the m. digastric originates from a bony groove adjacent to the medial surface of the process (Dean 1984). As in great apes, the human m. rectus capitis lateralis lies immediately lateral to the occipital condyles, suggesting that the site of origin for this muscle has migrated anteriorly with the condyles and foramen magnum. As a result, the human m. rectus capitis lateralis is positioned anteromedial to the origin of the m. digastric rather than medially adjacent to the m. digastric as in apes. The projecting mastoid process of humans is typically pneumatized (Standring 2016) but modern humans lack the extensive pneumatization of the posterolateral temporal bone seen in great apes (Figs. 2.3 and 2.5).

It is currently unclear to what extent the derived confinement of the m. digastric origin to a mediolaterally narrow digastric groove in modern humans could be related to the evolution of a more projecting mastoid process. However, the evolution of a more inferiorly projecting mastoid process in modern humans may ultimately be tied to differences in the function of the m. sternocleidomastoid, which inserts on the mastoid process. In both apes and humans, the m. sternocleidomastoid plays a key role in rotating the head from side to side (i.e., yaw rotations; Aiello and Dean 1990). However, in apes, which resemble other primate quadrupeds in having more inclined (i.e., obliquely oriented) necks than modern humans (Strait and Ross 1999), the m. sternocleidomastoid runs posteroinferiorly from origin to insertion and passes posterior to the axis of rotation of the atlanto-occipital joint (Aiello and Dean 1990). Accordingly, the ape m. sternocleidomastoid plays a role similar to the nuchal muscles in helping to keep the head elevated. This configuration differs from modern humans, in which the neck is more vertically oriented during bipedal postures (Strait and Ross 1999) and the head is positioned above the torso, so that the m. sternocleidomastoid runs inferiorly and slightly anteriorly and medially from origin to insertion. The human m. sternocleidomastoid thus plays no role in keeping

the head elevated (i.e., head extension), but modern humans presumably require little muscular effort to prevent passive flexion of the head given their smaller more gracile faces and the habitual position of the head above the torso. Inferior projection of the mastoid process may allow the m. sternocleidomastoid to play a role in returning the head to a neutral resting position (i.e., head flexion) when the head is already extended (Krantz 1963). This novel ability of the m. sternocleidomastoid to flex the head in humans may have been rendered more important by the evident decrease in the importance of the m. rectus capitis anterior as a head flexor (Dean 1985).

Posterior to the foramen magnum, the most salient osteological difference between modern humans and great apes concerns the development of the nuchal crest. The prominent nuchal crests of great apes (Fig. 2.4) probably increase the surface area available for the sites of insertion of the nuchal muscles. The nuchal muscles of great apes are massive, and this large size may be necessitated by the relatively posterior position of the occipital condyles and the need to hold up a large and projecting face (Schultz 1942; Adams and Moore 1975; Demes 1985; Aiello and Dean 1990). Both factors increase the load at the atlanto-occipital joint and increase downward torques that would passively flex the head if not compensated by muscular action (Schultz 1942; Lieberman et al. 2000; Demes 1985). Indeed, at least one electromyography study has shown that, in trained macaques, head and neck extensor musculature is more active during quadrupedal and horizontal neck postures than during seated upright and vertical neck postures, presumably in response to gravitational forces that would otherwise flex the head at the atlanto-occipital joint (Choi et al. 2003). Due to expansion of the neurocranium in modern humans, there is evidently ample room available for nuchal muscles to insert on the occipital squama (Dean 1984, 1985; Aiello and Dean 1990). Reduction in the size and anterior projection of the facial skeleton and changes in head and neck posture have also diminished the need for powerful head extensors to hold the head level. As a result, modern humans do not require the large and projecting nuchal crests that are shared by other great apes.

2.6 Summary

Comparative observations of primate basicranial anatomy indicate that evolutionary changes in head, neck, and body posture are associated with corresponding changes in the morphology of the cranio-cervical interface. Within the Hominoidea, modern humans demonstrate a profound reorganization of the cranio-cervical interface that distinguishes them from living apes. This reorganization includes a shift to a more anteriorly positioned and anteroinferiorly oriented foramen magnum, a shift to more anteriorly positioned occipital condyles with flattened articular surfaces, and a reconfiguration of the muscles that move the head relative to the neck and torso. The most significant changes in myology of the cranio-cervical interface include

reductions in the capacity of the m. longus capitis and m. sternocleidomastoid to flex and extend the head, respectively, and reductions in the size of the nuchal musculature. Shifts in the myology of the cranio-cervical interface are reflected in the bony anatomy of the region, including the evolution of a more inferiorly projecting mastoid process and diminution of the nuchal crest. Comparative and experimental studies suggest that many of these features distinguishing modern humans from living apes are the result of habitual adoption of more orthograde postures associated with bipedal locomotion. As a result, some of the derived features of the human cranial base (e.g., forward shift of the foramen magnum and shortening of the basioccipital) also characterize a variety of fossil hominin taxa.

Acknowledgments Thanks to Tim Rowe and John Kappelman at UT Austin, Larry Witmer and Ryan Ridgely at Ohio University, as well as Lauren Butaric at Des Moines University for access to CT scan data. Scans provided by Rowe, Kappelman, and Witmer were produced with funding from the National Science Foundation. Thanks also to the Field Museum of Natural History, the American Museum of Natural History, and the National Museum of Natural History for access to osteological specimens and to Abigail Nishimura for comments on a draft of this chapter.

References

Adams LM, Moore WJ (1975) Biomechanical appraisal of some skeletal features associated with head balance and posture in the Hominoidea. Acta Anatomica 92:580–594

Ahern JC (2005) Foramen magnum position variation in *Pan troglodytes*, Plio-Pleistocene hominids, and recent *Homo sapiens:* implications for recognizing the earliest hominids. Am J Phys Anthropol 127:267–276

Aiello LC, Dean C (1990) An introduction to human evolutionary anatomy. Academic Press, Cambridge

Ashton E (1957) Age changes in the basicranial axis of the Anthropoidea. Proc Zool Soc Lond. https://doi.org/10.1111/j.1096-3642.1957.tb00280.x.

Ashton E, Zuckerman S (1951) Some cranial indices of *Plesianthropus* and other primates. Am J Phys Anthropol 9:283–296

Ashton E, Zuckerman S (1952) Age changes in the position of the occipital condyles in the chimpanzee and gorilla. Am J Phys Anthropol 10:277–288

Ashton E, Zuckerman S (1956) Age changes in the position of the foramen magnum in hominoids. J Zool 126:315–326

Bastir M, Rosas A, Stringer C, Cuétara JM, Kruszynski R, Weber GW, Ross CF, Ravosa MJ (2010) Effects of brain and facial size on basicranial form in human and primate evolution. J Hum Evol 58:424–431

Been E, Shefi S, Zilka LR, Soudack M (2014) Foramen magnum orientation and its association with cervical lordosis: a model for reconstructing cervical curvature in archeological and extinct hominin specimens. Adv Anthropol 04:133–140

Biegert J (1957) Der Formwandel des Primatenschädels und seine Beziehungen zur ontogenetischen Entwicklung und den phylogenetischen Spezialisationen der Kopforgane. Gegenbaurs Morphol Jahrb 98:77–199

Biegert J (1963) The evaluation of characteristics of the skull, hands and feet for primate taxonomy. In: Washburn SL (ed) Classification and human evolution. Aldine, Chicago, pp 116–145

Bolk L (1909) On the position and displacement of the foramen magnum in the primates, vol 12. Verh Akademie van Wetenschappen, Amsterdam, pp 362–377

Bolk L (1910) On the slope of the foramen magnum in primates, vol 12. Koninklijke Akademie van Wetenschappen, Amsterdam, pp 525–534
Bolk L (1915) Über Lagerung, Verschiebung und Neigung des Foramen magnum am Schädel der Primaten. (Zehnter Beitrag zur Affenanatomie). Z Morphol Anthropol 17:611–692
Broca P (1872) Sur la direction du trou occipital. Description du niveau occipital et du goniomètre occipital. Bull Soc Anthropol Paris 7:649–668
Broca P (1877) Sur l'angle orbito-occipital. Bull Mém Soc Anthropol Paris 12:325–333
Broom R (1938) The pleistocene anthropoid apes of South Africa. Nature 3591:377–379
Brunet M, Franck G, Pilbeam D, Mackaye HT (2002) A new hominid from the Upper Miocene of Chad, Central Africa. Nature 418:145–151
Choi H, Keshner E, Peterson BW (2003) Comparison of cervical musculoskeletal kinematics in two different postures of primate during voluntary head tracking. KSME Int J 17:1140–1147
Coroner B, Latimer B (1991) Functional analysis of the atlanto-occipital joint in extant African hominoids and early hominids. Am J Phys Anthropol Suppl S12:61
Dart RA (1925) *Australopithecus africanus*: the man-ape of South Africa. Nature 115:195–199
Daubenton LJM (1764) Mémoire sur les differences de la situation du grand trou occipal dans l'homme et dans les animaux. Mem Acad Sci 66:568–575
Dean M (1984) Comparative myology of the hominoid cranial base I. The muscular relationships and bony attachments of the digastric muscle. Folia Primatol 43:234–248
Dean M (1985) Comparative myology of the hominoid cranial base II. The muscles of the prevertebral and upper pharyngeal region. Folia Primatol 44:40–51
Dean M, Wood B (1981) Metrical analysis of the basicranium of extant hominoids and *Australopithecus*. Am J Phys Anthropol 54:63–71
Dean M, Wood B (1982) Basicranial anatomy of Plio-Pleistocene hominids from East and South Africa. Am J Phys Anthropol 59:157–174
Demes B (1982) The resistance of primate skulls against mechanical stresses. J Hum Evol 11:687–691
Demes B (1985) Biomechanics of the primate skull base. Springer, New York
Dickman CA, Crawford NR, Tominaga T, Brantley AG, Coons S, Sonntag VK (1994) Morphology and kinematics of the baboon upper cervical spine: a model of the atlantoaxial complex. Spine 19:2518–2523
Gommery D (1996) New data on the morphology of the glenoid cavities of the atlas (foveae articulares superiores atlantis) in extant primates. C R Acad Sci Ser Ii Fascicule A-Sci Terre Et Des Planetes 323:1067–1072
Guy F, Lieberman DE, Pilbeam DR, Ponce de León MS, Likius A, Mackaye HT, Vignaud P, Zollikofer C, Brunet M (2005) Morphological affinities of the *Sahelanthropus tchadensis* (Late Miocene hominid from Chad) cranium. Proc Natl Acad Sci 102:18836–18841
Huxley TH (1863) On some fossil remains of man. Man's place in nature. D Appleton, New York
Kimbel WH, Rak Y (2010) The cranial base of *Australopithecus afarensis*: new insights from the female skull. Philosophical transactions of the Royal Society of London. Series B, Biological sciences 365:3365–3376
Kimbel WH, Rak Y, Johanson DC (2004) The skull of *Australopithecus afarensis*. Oxford University Press, Oxford
Kimbel WH, Suwa G, Asfaw B, Rak Y, White TD (2014) *Ardipithecus ramidus* and the evolution of the human cranial base. Proc Natl Acad Sci 111:948–953
Knese K-H (1948) Kopfgelenk, Kopfhaltung und Kopfbewegung des Menschen. Z Anat Entwicklungsgesch 114:67–107
Krantz GS (1963) The functional significance of the mastoid process in man. Am J Phys Anthropol 21:591–593
Le Gros Clark WE (1934) Early forerunners of man: a morphological study of the evolutionary origin of the primates. Baillière, Tindall and Cox, London
Le Gros Clark WE (1950) New palaeotological evidence bearing on the evolution of the Hominoidea. Q J Geol Soc 105:225–259

Le Gros Clark WE (1954) Reason and fallacy in the study of fossil man. Spottiswoode, Ballantyne & Company, London
Lieberman D (2011) The evolution of the human head. Harvard University Press, Cambridge
Lieberman DE, Ross CF, Ravosa MJ (2000) The primate cranial base: ontogeny, function, and integration. Yearb Phys Anthropol 113:117–169
Lockwood CA, Lynch JM, Kimbel WH (2002) Quantifying temporal bone morphology of great apes and humans: an approach using geometric morphometrics. J Anat 201:447–464
Lopez AJ, Scheer JK, Leibl KE, Smith ZA, Dlouhy BJ, Dahdaleh NS (2015) Anatomy and biomechanics of the craniovertebral junction. Neurosurg Focus 38:E2
Luboga S, Wood B (1990) Position and orientation of the foramen magnum in higher primates. Am J Phys Anthropol 81:67–76
Manfreda E, Mitteroecker P, Bookstein FL, Schaefer K (2006) Functional morphology of the first cervical vertebra in humans and nonhuman primates. Anat Rec B New Anat 289:184–194
Martin RD (1980) Adaptation and body size in primates. Z Morphol Anthropol 71:115–124
McCarthy RC (2001) Anthropoid cranial base architecture and scaling relationships. J Hum Evol 40:41–66
Moore W, Adams L, Lavelle C (1973) Head posture in the Hominoidea. J Zool Lond 169:409–416
Nalley TK, Grider-Potter N (2017) Functional analyses of the primate upper cervical vertebral column. J Hum Evol 107:19–35
Neaux D, Bienvenu T, Guy F, Daver G, Sansalone G, Ledogar JA, Rae TC, Wroe S, Brunet M (2017) Relationship between foramen magnum position and locomotion in extant and extinct hominoids. J Hum Evol 113:1–9
Neaux D, Sansalone G, Ledogar JA, Heins Ledogar S, Luk THY, Wroe S (2018) Basicranium and face: assessing the impact of morphological integration on primate evolution. J Hum Evol 118:43–55
Nishimura AC, Fernández PJ, Guerra JS, Russo GA (2017) Functional morphology of the occipital condyles in anthropoids. American Association of Physical Anthropologists. Am J Phys Anthropol 162(S64):300
Pickford M (2005) Orientation of the foramen magnum in Late Miocene to extant African apes and hominids. Anthropologie 43:103–110
Plavcan JM, Kay RF, Jungers WL, van Schaik CP (2012) Reconstructing social behavior from dimorphism in the fossil record. In: Plavcan JM, Kay RF, Jungers WL, van Schaik CP (eds) Reconstructing behavior in the primate fossil record. Plenum Press, New York, pp 297–338
Romer AS (1950) The vertebrate body. WB Saunders Company, London
Ross C, Henneberg M (1995) Basicranial flexion, relative brain size, and facial kyphosis in Homo sapiens and some fossil hominids. Am J Phys Anthropol 98:575–593
Ross CF, Ravosa MJ (1993) Basicranial flexion, relative brain size, and facial kyphosis in nonhuman primates. Am J Phys Anthropol 91:305–324
Russo GA, Kirk EC (2013) Foramen magnum position in bipedal mammals. J Hum Evol 65:656–670
Russo GA, Kirk EC (2017) Another look at the foramen magnum in bipedal mammals. J Hum Evol 105:24–40
Russo GA, Kirk EC, Smaers JB (2016) Elucidating the evolutionary pathways of hominoid and hominin basicranial morphology using a formal phylogenetic comparative primate approach. Am J Phys Anthropol 159:276
Ruth AA, Raghanti MA, Meindl RS, Lovejoy CO (2016) Locomotor pattern fails to predict foramen magnum angle in rodents, strepsirrhine primates, and marsupials. J Hum Evol 94:45–52
Schaefer MS (1999) Brief communication: foramen magnum–carotid foramina relationship: is it useful for species designation? Am J Phys Anthropol 110:467–471
Scheuer L, Black S (2001) Developmental juvenile osteology. Academic Press, Cambridge
Schultz AH (1917) Anthropologische Untersuchungen an der Schädelbasis. Anthropologischen. Friedr. Vieweg and Sohn: Universitat Zurich
Schultz AH (1942) Conditions for balancing the head in primates. Am J Phys Anthropol 29: 483–497

Schultz AH (1955) The position of the occipital condyles and of the face relative to the skull base in primates. Am J Phys Anthropol 13:97–120
Şenyürek MS (1938) Cranial equilibrium index. Am J Phys Anthropol 24:23–41
Sherwood RJ (1999) Pneumatic processes in the temporal bone of chimpanzee (*Pan troglodytes*) and gorilla (*Gorilla gorilla*). J Morphol 241:127–137
Spoor C (1997) Basicranial architecture and relative brain size of Sts 5 (*Australopithecus africanus*) and other Plio-Pleistocene hominids. S Afr J Sci 93:182–186
Standring S (2016) Gray's anatomy, 41st edn. Churchill Livingstone, Elsevier
Strait DS (2001) Integration, phylogeny, and the hominid cranial base. Am J Phys Anthropol 114:273–297
Strait DS, Ross CF (1999) Kinematic data on primate head and neck posture: implications for the evolution of basicranial flexion and an evaluation of registration planes used in paleoanthropology. Am J Phys Anthropol 108:205–222
Suwa G, Asfaw B, Kono RT, Kubo D, Lovejoy CO, White TD (2009) The Ardipithecus ramidus skull and its implications for hominid origins. Science 326:68–68e67
Topinard P (1890) Anthropology. Chapman and Hall, London
Villamil CI (2017) Locomotion and basicranial anatomy in primates and marsupials. J Hum Evol 111:163–178
Weidenreich F (1941) The brain and its role in the phylogenetic transformation of the human skull. Trans Am Philos Soc 31:320–442
Weidenreich F (1943) The skull of *Sinanthropus pekinensis:* a comparative study on a primitive hominid skull, Palaeontologia Sinica, vol 127. Wiley, Hoboken
White TD, Suwa G, Asfaw B (1994) *Australopithecus ramidus*, a new species of early hominid from Aramis, Ethiopia. Nature 371:306–312
White TD, Asfaw B, Beyene Y, Haile-Selassie Y, Lovejoy CO, Suwa G, WoldeGabriel G (2009) *Ardipithecus ramidus* and the paleobiology of early hominids. Science 326:64–86
Wolpoff MH, Senut B, Pickford M, Hawks J (2002) Palaeoanthropology (communication arising): *Sahelanthropus* or '*Sahelpithecus*'? Nature 419:581–582
Zollikofer CP, Ponce de León MS (2005) Virtual reconstruction: a primer in computer-assisted paleontology and biomedicine. Wiley-Interscience, Hoboken
Zollikofer CP, de León MSP, Lieberman DE, Franck G (2005) Virtual cranial reconstruction of *Sahelanthropus tchadensis*. Nature 434:755–759

Chapter 3
Vertebral Morphology in Relation to Head Posture and Locomotion I: The Cervical Spine

Thierra K. Nalley and Neysa Grider-Potter

3.1 Introduction

The cervical spine is the connection between the head and the postcranial skeleton, and as such, it has several important biological roles. These roles include providing attachment area for upper limb musculature and transmitting biomechanical loads from the head to the trunk, maintaining the visual field and natural head positions, and providing a flexible platform to permit head mobility (e.g., Schultz 1942; Swindler and Wood 1982; Kapandji 1974; Mercer and Bogduk 2001; Spoor et al. 2007). These functions are critical for many aspects of primate life, from mastication and grooming to locomotion and predator vigilance. Despite these important functions, the functional morphology of cervical vertebrae has received less attention in primates relative to other regions of the vertebral column (Toerien 1961; Mercer 1999; Manfreda et al. 2006; Nalley 2013). As a result, many questions about their form and function remain unanswered.

Many early descriptions of primate cervical morphology concluded that skeletal variation was limited and that the region was generally uninformative when investigating functional or phylogenetic questions (e.g., Toerien 1961; Ankel 1967, 1970, 1972). Exceptions include Slijper (1946) and Schultz (1961), who included the cervical spine in their analyses of the whole vertebral column. Slijper (1946) described the presacral vertebral column across large taxonomical groups and developed several body-axis models still commonly used today (e.g., Clauser 1980; Shapiro 1993; Dunbar et al. 2008; Stevens 2013). Slijper (1946) highlighted the positive scaling

T. K. Nalley (✉)
Department of Medical Anatomical Sciences, College of Osteopathic Medicine of the Pacific, Western University of Health Sciences, Pomona, CA, USA
e-mail: tnalley@westernu.edu

N. Grider-Potter
School of Human Evolution and Social Change, Institute of Human Origins, Arizona State University, Phoenix, AZ, USA

E. Been et al. (eds.), *Spinal Evolution*,
https://doi.org/10.1007/978-3-030-19349-2_3

relationship between body size and spinous process size and was one of the earliest researchers to argue that the differences in cervical spinous process length among humans, great apes, and monkeys were related to head posture and maintenance of head position. Schultz (1961) primarily focused on the thoracic and lumbar regions, but he provided general taxonomic descriptions and relative axial region lengths and weights. Like Slijper, he noted the relatively long spinous processes of apes and contrasted them with the short processes of monkeys and humans. Schultz (1961) argued that the long spinous processes observed in *Gorilla*, *Pan*, *Perodicticus*, and a few New World monkeys represented a derived condition. Schultz viewed the short processes and dorsoventrally compressed cervical vertebrae found in humans as primitive retentions, shared with most other primates. This conclusion was at odds with Slijper, who related the human condition to our reduced nuchal musculature mass relative to great apes.

More recently, researchers have aimed to further examine these relationships by expanding taxonomic sampling, incorporating 3D morphometrics and new quantification methodologies, and examining cervical variation in the context of more refined, quantified measures of head and neck posture and locomotor behaviors (Mercer 1999; Manfreda et al. 2006; Ankel-Simons 2007; Mitteroecker et al. 2007; Nalley and Grider-Potter 2015, 2017; Arlegi et al. 2017, 2018; Meyer et al. 2018; Villamil 2018). This chapter reviews what is known about the functional morphology of the cervical spine in extant primates and highlights avenues of future research and hypothesis testing.

3.2 Cervical Morphology and Head Balance

One of the primary functions of the neck is to balance and stabilize the head to maintain a stable visual field and natural head positions (Lind et al. 1989; Berthoz et al. 1992; Hayman and Donaldson 1997; Feipel et al. 1999; Panjabi et al. 2001; Dunbar 2004; Hirasaki and Kumakura 2004; Spoor et al. 2007; Takeuchi and Shono 2007; Dunbar et al. 2008; Nagamoto et al. 2011). This functional relationship has been historically modeled as a first-class lever system (Slijper 1946; Badoux 1968; Demes 1985; Jaanusson 1987; Smit 2002). According to this head-balancing model, the head is balanced on its fulcrum, the atlantooccipital joint. The downward force of gravity acts on the load arm, composed of the precondylar weight of the skull's anterior. These forces are counteracted on the effort arm by the inferiorly directed forces of the nuchal musculature (Fig. 3.1).

Since the head houses the visual and vestibular systems (e.g., Berthoz et al. 1979; Britton et al. 1993; Horak and Macpherson 1996; St George and Fitzpatrick 2011), the ability to control and maintain stable head positions during both resting and locomotor behaviors is likely to be under selection (Spoor et al. 1994, 2007; Silcox et al. 2009). Furthermore, because cranial morphology varies substantially across primates (Fleagle et al. 2010, 2016), differences in cranial shape are expected to influence

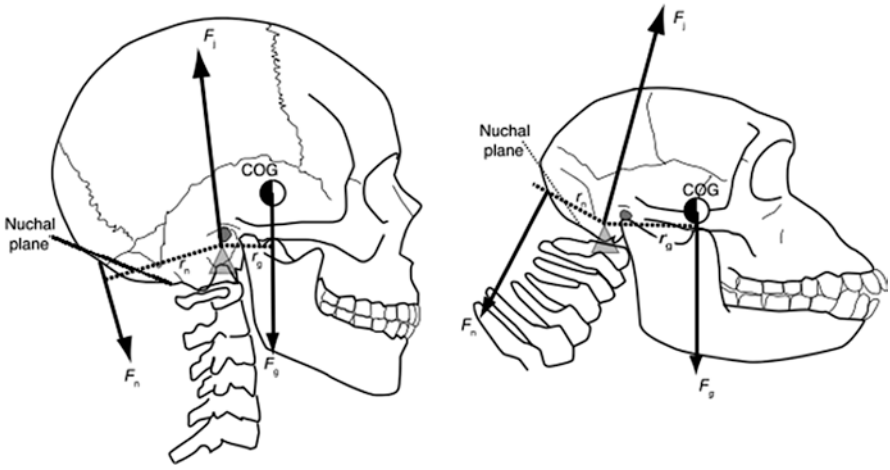

Fig. 3.1 Differences in forces at the craniocervical junction in a human (left) and chimpanzee (right). Balance of the head is dependent upon orientation of the center of gravity (COG), position and orientation of the foramen magnum, and neck posture. *Fg* gravitational force of the head; *Fj* resultant force; *Fn* force of the nuchal muscles; *rg* perpendicular distance between the gravity vertical of the head and the axis of rotation; *rn* perpendicular distance between the line of action of the nuchal muscles and the axis of rotation. Adapted from Lieberman (2011)

head-balancing mechanisms (Demes 1985; Jaanusson 1987). Many investigations support this idea (Dean 1982, 1985; Richmond et al. 2001; Nevell and Wood 2008; Russo and Kirk 2013, 2017). For example, Russo and Kirk (2013, 2017) found that, across several mammalian orders, taxa that are more orthograde exhibit more anteriorly positioned foramina magna. This morphology decreases the distance between the head's center of mass and its fulcrum, which should increase the mechanical efficiency of head-balancing muscles, allowing for a decrease in muscle cross-sectional area and a concomitant reduction in vertebral robusticity.

Relationships between overall skull size and some cervical features have been observed in extant primates. In a previous study (Nalley and Grider-Potter 2017), we found that measurements from the first two cervical vertebrae exhibit positive allometry with skull size: in the case of C1, dorsoventral width of the anterior and posterior arches, mediolateral length of the transverse process, and projection of the posterior tubercle; for C2, dorsoventral width of the pedicle and lamina. These results are consistent with the positive allometric scaling trend of overall atlas size relative to body mass observed by Manfreda et al. (2006). It is likely that positive allometry of C1 arch features reflects their proximity to the lateral masses, the primary load-bearing structures of the atlas. The ability of the lateral masses to resist compressive loading from the head is proportional to their cross-sectional area. Thus, linear dimensions of the C1 must increase disproportionately as head mass increases in order to maintain functional equivalence (e.g., Rose 1975; Jungers and Burr 1994; Polk et al. 2000; Shapiro and Simons 2002; Nakatsukasa and Hirose 2003;

Hernandez et al. 2009). Future work remains to explore the relationship between overall skull size and bony features from the subaxial cervical spine.

The head-balancing model hypothesizes a relationship between cranial shape and the cervical vertebral column. Villamil (2018) investigated the morphological integration of the hominoid cervical column and the cranial base. Her results show several patterns of integration and evolvability in the cervical features of *Homo*, *Pan*, and *Hylobates*. For example, the first cervical vertebrae (C1) has both high integration and high evolvability, indicating that C1 morphology covaries with the morphology of the other cervical vertebrae, but also responds to natural selection most rapidly (i.e., has relatively low constraint) (Villamil 2018). This indicates that C1 may be more sensitive to functional influences than other parts of the vertebral column. Villamil's (2018) results also demonstrate distinct units of integration (i.e., modules *sensu* Wagner 1996): the cranial base and C1, C2 by itself, C3–C5, and C6 and C7. These patterns support a link between cranial and cervical morphology and are similar to functional groups described in humans (e.g., Kapandji 1974; White and Panjabi 1990) and macaques (Choi et al. 2003).

A more direct examination of the head-balancing model would incorporate functionally relevant aspects of cranial morphology, such as the relative length of the cranium anterior to the foramen magnum—an estimate of the skull's load arm. Variation in relative anterior cranial length should correlate with cervical features associated with the muscles involved in counteracting the gravitational forces acting on the cranium. One expectation is that increases in anterior cranial length should elicit increases in the cross-sectional areas of the nuchal muscles, with a corresponding increase in the size of cervical features providing attachment.

To examine this prediction, we present results from a new analysis. We used phylogenetic generalized least squares to analyze data collected from female individuals representing 20 primate species, including members of Hominoidea, Cercopithecoidea, Platyrrhini, and Strepsirrhini. Relative anterior cranial length was quantified as a ratio of anterior cranial length (basion-prosthion) to total cranial length (inion-prosthion). Data for cervical traits were taken from Nalley (2013) and Nalley and Grider-Potter (2015, 2017); detailed descriptions of the measurements can be found in those sources. Cervical variables were also size-adjusted using total cranial length, and all ratios were logged for analysis.

Results show that relative anterior cranial length is significantly correlated with variation in cervical craniocaudal dimensions (Fig. 3.2). As the anterior part of the cranium lengthens, the cervical vertebrae become craniocaudally longer. These findings support expectations of the head-balancing model: increasing the craniocaudal dimensions of the neural arch structures (pedicles, laminae, and spinous process) increases their ability to resist bending and shear stresses caused by the nuchal musculature (Goel and Clausen 1998; Cripton 2000; Panzer and Cronin 2009), and larger arches also provide greater areas of attachment for larger deep nuchal muscles (e.g., transversospinales) (Kapandji 1974). Vertebral bodies also show an increase in craniocaudal length with increasing anterior cranial length. This relationship may be a by-product of changes in the neural arches, because it is unlikely that dimensions

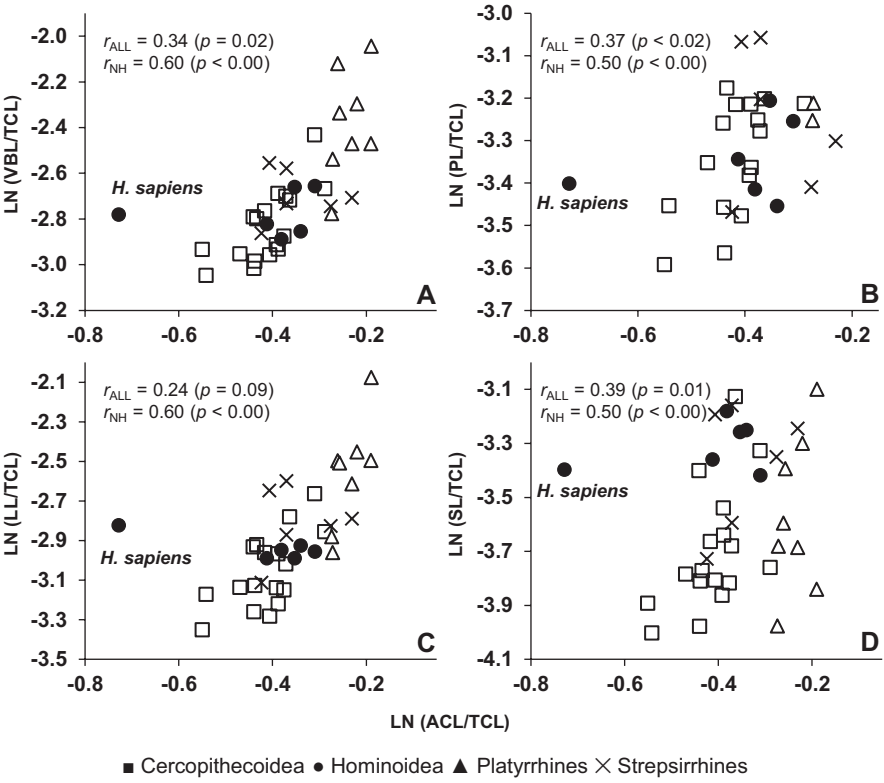

Fig. 3.2 Species means (logged) of relative anterior cranial length (anterior cranial length divided by total cranial length; ACL/TCL) plotted against species means of the (**a**) average relative vertebral body craniocaudal length (VBL/TCL) for C2–C7 levels, (**b**) average relative pedicle craniocaudal length (PL/TCL) for C1–C7 levels, (**c**) average relative laminae craniocaudal length (LL/TCL) for C1–C7 levels, and (**d**) average relative spinous process craniocaudal length (SL/TCL) for C2–C7 levels. rALL reports phylogenetic generalized least squares values for complete comparative sample. rNH reports phylogenetic generalized least squares values for sample with humans removed

of the body and arch are independent. If one component increases in craniocaudal length, the other must do so as well or a misalignment between vertebrae will occur. The global increase in cervical craniocaudal dimensions suggests a pervasive influence of head shape on cervical morphology. However, it is likely that other factors, such as head and neck posture during locomotor behaviors, play a significant role in determining cervical morphology, because humans are a notable outlier, exhibiting much larger craniocaudal dimensions than expected. How the continuous maintenance of orthograde postures might influence head-balancing structures remains to be explored.

3.3 Cervical Morphology and Maintenance of Head Stability During Locomotion

Head stability is a crucial component of locomotion because the head houses the sensory organs responsible for processing spatial orientation, acceleration, and balance. Experimental research has demonstrated that primates normally align their visual fields with their locomotor substrate (Strait and Ross 1999; Hirasaki and Kumakura 2004; Stevens and Heesy 2012) and this relationship corresponds well with how the head orients the vestibular organs relative to earth's gravity vector (Spoor et al. 1994, 2007). Previous research has also shown that axial movement varies between locomotor modes (e.g., Dunbar 2004; Dunbar et al. 2004, 2008; Hirasaki and Kumakura 2004; Xiang et al. 2008). For example, when humans and other primates walk slowly, the trunk remains stabilized (≤20° rotation), but the head frequently rotates more than 20° as subjects view their surroundings (Dunbar 2004; Hirasaki and Kumakura 2004; Xiang et al. 2008). In contrast, during faster movements (e.g., quadrupedal gallops, bipedal running), the trunk becomes less stabilized. The trunk can rotate up to 50°, while the head remains stabilized in all planes (Pozzo et al. 1990; Dunbar et al. 2004). This previous research suggests that either the head or the trunk must be rotationally stabilized to provide the brain with a reference frame for whole-body spatial orientation (Dunbar et al. 2008). Since trunk movement differs between locomotor modes and the position of the head varies with substrate orientation, the neck must likely provide compensatory movements between the two regions when transitioning between resting and various locomotor behaviors. As primates are highly variable in their postural habits and locomotor modes (e.g., Hunt et al. 1996), they make ideal subjects to examine these relationships.

Unfortunately, three-dimensional neck kinematics has yet to be investigated in nonhuman primates. Strait and Ross's (1999) data set on orbital inclinations indicate that primates range from 12° above horizontal (*Symphalangus syndactylus*) to around 28° below horizontal (*Colobus guereza*) in this variable. If the goal of the neck is to maintain visual stability, the small range of variation in orbital inclination values, in comparison to neck inclination, is to be expected because the primate should act to maintain its gaze roughly parallel to the substrate (or suprastrate). Work conducted by Stevens and Heesy (2012) seems to support this hypothesis. By measuring loris head posture during gait cycles on substrates of various inclinations, they found that head posture declines with decreasing substrate inclination. However, both studies lack the angular excursion data that are needed to answer questions about neck compensatory mechanisms and function during locomotion.

Cromwell et al. (2001) examined locomotor stability of the head, neck, and trunk in the sagittal plane during human walking. They defined the head by the apex of the skull and the atlantooccipital joint, the neck by the atlantooccipital joint and C6–C7 intervertebral joint, and the trunk by the latter joint and the lumbosacral junction (L5–S1). Their kinematic data show an average head position of 11° of flexion, the neck averages 0.03° from vertical, and the trunk 8° of flexion. In addition, the

maximum excursion of the head during one gait cycle was 12°, the neck 18°, and the trunk 7°. Despite the disparity in excursion, the head and neck tend to move together, and they are most extended during the beginning of double-limb support phase (heel strike) and most flexed during single-limb support (presumably around midswing). Based on these results, Cromwell et al. (2001) argued that the flexed position of the head is required to maintain a forward-facing and slightly substrate-directed gaze, as well as an optimally positioned vestibulocochlear apparatus. Thus, the relatively extended position of the neck acts to maintain the head's center of mass over the trunk and the neck functions to compensate for the movements of the trunk in order to facilitate head stability (Cromwell et al. 2001) (Fig. 3.3).

Similar observations have been reported in research outside of primates. For example, Dunbar et al. (2008) collected head, neck, and trunk 2D kinematics from horses. During walking, horses hold their heads in a relatively flexed position (66° below earth horizontal) and have a maximum excursion of 9°. Their necks are almost parallel to the substrate (4° below earth horizontal) and with an excursion range of ~10°. Their trunks are also parallel to earth horizontal and move ~6° in the sagittal plane. This pattern appears similar to observations made by Cromwell et al. (2001) in humans, with the trunk moving least and the neck moving to compensate for trunk

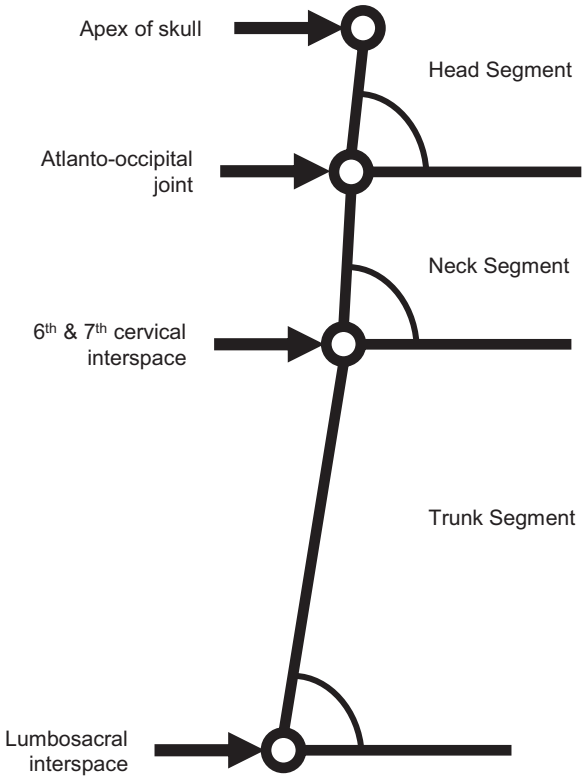

Fig. 3.3 Marker locations to define head, neck, and trunk segments from Cromwell et al. (2001). Segmental angular measurements were calculated with reference to an external horizontal plane (0″ = horizontal; 90″ = vertical). Adapted from Cromwell et al. (2001)

motion. Interestingly, these excursions increase slightly in the horse head and trunk during cantering but decrease in the neck.

The kinematics of the head during locomotion has received more attention in the literature in comparison with neck kinematics. Studies of nonhuman primates have been conducted on macaques, vervets, langurs, lorises, and gibbons (Dunbar 2004; Dunbar et al. 2004; Hirasaki and Kumakura 2004; Xiang et al. 2008). Due to differences in landmarks, however, mean head position data are not comparable, but angular excursion data can be contrasted. On average, these studies indicate that the primate head moves between 17° (*Semnopithecus entellus*) and 4° (*Macaca fuscata*) in the sagittal plane during quadrupedal walking. These data are comparable to the human and horse data. Thus, one could hypothesize that increasing locomotor head movement also increases neck movement, but this has yet to be empirically tested. Overall, further investigations into three-dimensional kinematics of the axial skeleton during locomotion and other behaviors are needed to understand how the neck moves and functions during locomotor behaviors.

This body of work is also relevant to the common critique of many analyses of primate functional morphology regarding their use of discrete postural and locomotor categories. Categorical approaches, though necessary in some cases, can oversimplify real variation that does not fit within these defined behavioral categories. As highlighted by the experimental work discussed here, commonly used primate behavioral classifications (e.g., orthograde and pronograde) are often imprecise regarding the head and neck because trunk posture and movement does not always directly reflect the posture and movements of the head. In fact, several mammalian taxa (e.g., guinea pigs, cats) with horizontal trunk postures have been observed to exhibit vertical neck postures and vice versa (e.g., indriids) (Vidal et al. 1988; Selbie et al. 1993; Keshner 1994; Graf et al. 1995a, b; Strait and Ross 1999).

When modeling the forces acting on the cervical spine, it is important to recognize that the mammalian neck is not necessarily a simple beam extending out from the torso. A potentially more informative sigmoidal model has been developed based on the experimental work of Vidal et al. (1986) and Graf et al. (1995a, b). This model describes the shape of the entire vertebral column of quadrupedal mammals and positions two major curves (in the sagittal plane) at (1) the cervicothoracic junction (concave dorsally) and (2) the thoracolumbar transition (concave ventrally). This overall axial shape often results in a vertical cervical segment relative to the torso during resting postures, regardless of locomotor category or habitual trunk position (Vidal et al. 1986). This neck orientation has been argued to accomplish several functional roles, including incorporating the cervical vertebral bodies into the mechanical support of the neck against gravity and the weight of the head. This configuration may also reduce the activity of the nuchal musculature (Demes 1985; Vidal et al. 1986; Graf et al. 1995a; Macpherson and Ye 1998; Choi et al. 2003). Electromyographic (EMG) studies of macaque nuchal muscles have observed only minor muscle activity during resting postures with a vertically oriented neck (Corneil et al. 2001; Choi et al. 2003), especially when compared to muscle recruitment when necks are more horizontally oriented (Choi et al. 2003). Choi et al. (2003) compared EMG recruitment levels and vertebral body excursion patterns in

the cervical spine of two rhesus macaques and found a significant increase in muscle EMG activation for both deep and superficial nuchal muscles during standing postures with more horizontal neck orientations (Choi et al. 2003).

When investigating the functional morphology of the primate cervical spine, especially when linking form to posture and locomotor function, it is ideal to use empirical data to construct models of how an animal is orienting its neck to stabilize the head. To date, the largest data set of primate head and neck orientation comes from the work of Strait and Ross (1999), who sampled 2D kinematic data from 29 primate species. Kinematic data were collected with mixed methods ranging from shaved, marked laboratory conditions to uncontrolled, wild, or zoo conditions. Strait and Ross (1999) report mean values of head inclination (both Frankfurt and orbital axis) and neck inclination (C2–C7) relative to the gravity vector for each species at midstance or midswing during their habitual mode of locomotion. Neck inclination angles for nonhuman primates range from relatively pronograde postures (107° relative to gravity in *Alouatta seniculus*) to semi-orthograde postures (~45° in *Saimiri* and hylobatids). Humans, unsurprisingly, are a clear outlier in their orthograde neck position, exhibiting the most vertical values (~18°).

With the availability of quantified head and neck kinematic data from several primate species, it is possible to directly test function-form hypotheses developed from head-neck biomechanical models. Taxa that habitually position the long axes of the head and neck perpendicular to the gravity vector (i.e., a more pronograde posture) should exhibit morphologies related to increasing the force output of the nuchal muscles to counter the long load arm modeled for this posture. This expectation is supported because, in comparison to humans, primate taxa with more horizontal neck postures exhibit nuchal muscles with relatively larger physiological cross-sectional areas and cranial attachment areas (Dean 1982; Richmond et al. 2001). The cervical vertebrae of these taxa should exhibit compensatory modifications for increased bending moments from the more powerful nuchal musculature and flexion-inducing force of gravity (Slijper 1946; Badoux 1968, 1974; Preuschoft 2004). Functional expectations include increases in the lengths of the transverse and spinous processes (i.e., attachment surfaces for major nuchal muscles) and larger cross-sectional areas of the neural arch components. Longer processes will increase the mechanical advantage of the attaching muscles (Slijper 1946; Shapiro 1993; Cripton 2000), and increased cross-sectional areas increase resistance to the hypothesized increased bending loads (Ruff 2000; Smit 2002; Choi et al. 2003; Cartmill and Brown 2013). Furthermore, because the intervertebral joints (uncovertebral and zygapophyseal) direct how cervical vertebral bodies move in relation to one another, they are also expected to exhibit variation related to differences in positional behavior. In general, taxa with more horizontal necks are expected to have morphologies that provide resistance to joint displacement and translation (Ankel 1972; Demes 1985; Hamrick 1996): greater curvature of C1 superior facet, a more dorsally inclined C2 odontoid process, and a more coronal orientation of the zygapophyseal joints in the subaxial spine.

In our previous work (Nalley and Grider-Potter 2015, 2017), we examined whether these cervical bony expectations were supported in primate taxa for which

data on neck position during locomotion are available (Strait and Ross 1999). Our results indicate that primates with more pronograde heads and necks exhibit (1) vertebral morphology that implies increased mechanical advantage for deep nuchal musculature (dorsally inclined dens, increased spinous process length in the subaxial vertebrae) and (2) a greater resistance to translation and ventral displacement (more curved C1 superior articular facets, coronally oriented facets at C4 and C7). Results from this study also provide support for the predictions of the Graf et al. (1995a) sigmoidal model which postulates an increase in overall cervical column range of motion and spinal segment flexibility in more pronograde taxa. This expectation is based on observations that more pronograde taxa exhibit distinct neck postures during habitual locomotor behaviors (more horizontal) versus neck postures during resting behaviors (more vertical) and likely require a greater range of movement. Our analyses report greater craniocaudal dimensions of the vertebral bodies and neural arches in quadrupedal taxa, thus supporting the sigmoidal model predictions (Nalley and Grider-Potter 2015, 2017). Overall, our results support previous research linking variation in cervical spinous process length with broader categories of posture cervical vertebrae (Slijper 1946; Schultz 1961) and more recent studies investigating new methods of cervical shape quantification (e.g., Arlegi et al. 2017, 2018; Meyer 2016; Meyer et al. 2018). These broad morphological patterns suggest that primates with more pronograde heads and necks exhibit an increased mechanical advantage for deep nuchal musculature and several mechanisms—craniocaudally long vertebral bodies and coronally oriented facets—to facilitate lordosis curve formation with a greater resistance to ventral displacement of the cervical vertebrae. Nevertheless, since both sigmoidal and head-balancing models make similar biomechanical predictions of the cervical morphology, future research is necessary to determine if both are correct or if support for one model is driven by true support for the other.

3.4 Soft Tissue

Functional analyses of the primate neck have thus far been generally limited to analyzing skeletal variation, which leaves a critical gap in understanding of soft tissue morphology. With a few notable exceptions (Swindler and Wood 1982; Dean 1982; Richmond et al. 2001; Choi et al. 2003), even the basic description and quantification of primate nuchal ligamentous and muscular anatomy remains to be conducted. These features provide crucial data for accurate biomechanical modeling and are necessary to validate functional scenarios built from bony morphology. For example, the nuchal ligament has been considered an important feature of the primate cervical vertebral region, but it remains enigmatic. Several functional roles have been hypothesized for this structure in the human medical literature, where it has been described as (1) a supportive structure for the head, (2) an attachment site for muscles, (3) a ligament to limit and control flexion, (4) a loading dampener, and

(5) a major proprioceptive structure for the head (Fielding et al. 1976; White and Panjabi 1990; Mitchell et al. 1998; Johnson et al. 2000; Mercer and Bogduk 2003; Kadri and Al-Mefty 2007).

Although the nuchal ligament has received little attention outside of medical research, its presence/absence has been incorporated into functional hypotheses regarding bipedal locomotion in fossil hominins. The absence of the nuchal ligament in the great apes (Swindler and Wood 1982) has been used to argue that it is functionally related to bipedality (Bramble and Lieberman 2004). However, the nuchal ligament is commonly found in many nonprimate mammals and has been documented in *Papio* and *Macaca* (Swindler and Wood 1982; Dean 1982), indicating that further research is required to understand its significance in hominin evolutionary history.

3.5 Conclusions

Research summarized and presented here, including new data investigating the relationship between head shape and cervical variation, provides compelling evidence for function-form relationships between cervical bony morphology and behavior. Avenues for future research include (1) expanding samples to include more orthograde and antipronograde taxa, especially strepsirrhines, (2) documenting internal bony architecture, and (3) quantifying cervical ligaments and musculature. Lowered costs and increased access to MRI and CT-scanning facilities provide nondestructive methods for visualizing and quantifying vertebral microanatomy, soft tissue structures, and in situ relationships of the primate neck.

Advances in technology have also allowed access to better methodologies for recording and quantifying primate locomotion and posture (Demes et al. 1996; Strait and Ross 1999; Isler and Thorpe 2003; Dunbar et al. 2004, 2008; Franz et al. 2005; Togasaki et al. 2005; Schoonaert et al. 2006; Larson and Stern 2007; DeSilva 2009; Carlson and Demes 2010; Patel and Wunderlich 2010; Schmitt 2011; Duarte et al. 2012), even in the wild (e.g., Isler and Grüter 2006; Thompson et al. 2018). This area of research will help provide insight into which measurements of positional behavior best explain cervical morphological variation. Moreover, technologies that observe in vivo relationships, such as XROMM (X-ray reconstruction of moving morphology), during positional behaviors will provide critical information on vertebral movement and position relative to head and neck surface structures (e.g., Brainerd et al. 2010; Menegaz et al. 2015). Focusing future efforts on the examination of the entire musculoskeletal environment, combined with capturing kinematic behavioral data during both locomotor and resting behaviors, will allow researchers to validate functional hypotheses supported by the bony morphology and more confidently apply function-form patterns in extant taxa to reconstructing positional behavior in fossil primates.

References

Ankel F (1967) Morphologie von wirbelsäule und brustkorb. Karger, Basel
Ankel F (1970) Einführung in die primatendkunde. Gustav Fischer Verlag, Stuttgart
Ankel F (1972) Vertebral morphology of fossil and extant primates. In: Tuttle R (ed) The functional and evolutionary biology of primates. Aldine, Chicago, pp 223–240
Ankel-Simons F (2007) Postcranial skeleton. In: Ankel-Simons F (ed) An introduction to primate anatomy, 3rd edn. Elsevier, Durham, NC
Arlegi M, Gómez-Olivencia A, Albessard L, Martínez I, Balzeau A, Arsuaga JL, Been E (2017) The role of allometry and posture in the evolution of the hominin subaxial cervical spine. J Hum Evol 104:80–99
Arlegi M, Gómez-Robles A, Gómez-Olivencia A (2018) Morphological integration in the gorilla, chimpanzee, and human neck. Am J Phys Anthropol 166(2):408–416
Badoux DM (1968) Some notes on the curvature of the vertebral column in vertebrates with special reference to mammals. Acta Morphol Neerl Scand 7(1):29–40
Badoux DM (1974) An introduction to biomechanical principles in primate locomotion and structure. In: Jenkins FA (ed) Primate locomotion. Academic Press, New York, pp 1–44
Berthoz A, Lacour M, Soechting JF, Vidal PP (1979) The role of vision in the control of posture during linear motion. Prog Brain Res 50:197–209
Berthoz A, Graf W, Vidal PP (eds) (1992) The head-neck sensory motor system. Oxford University Press, Oxford
Brainerd EL, Baier DB, Gatesy SM, Hedrick TL, Metzger KA, Gilbert SL, Crisco JJ (2010) X-ray reconstruction of moving morphology (XROMM): precision, accuracy and applications in comparative biomechanics research. J Exp Zool A Ecol Genet Physiol 313(5):262–279
Bramble DM, Lieberman DE (2004) Endurance running and the evolution of *Homo*. Nature 432(7015):345–352
Britton TC, Day BL, Brown P, Rothwell JC, Thompson PD, Marsden CD (1993) Postural electromyographic responses in the arm and leg following galvanic vestibular stimulation in man. Exp Brain Res 94:143–151
Carlson KJ, Demes B (2010) Gait dynamics of *Cebus apella* during quadrupedalism on different substrates. Am J Phys Anthropol 142:273–286
Cartmill M, Brown K (2013) The relative effects of locomotion and posture on vertebral scaling. Am J Phys Anthropol S150:95
Choi H, Keshner E, Peterson BW (2003) Comparison of cervical musculoskeletal kinematics in two different postures of primate during voluntary head tracking. KSME Int J 17:1140–1147
Clauser DA (1980) Functional and comparative anatomy of the primate spinal column: some locomotor and postural adaptations. Ph.D. dissertation, The University of Wisconsin-Milwaukee
Corneil BD, Olivier E, Richmond FJ, Loeb GE, Munoz DP (2001) Neck muscles in the rhesus monkey. II. Electromyographic patterns of activation underlying postures and movements. J Neurophysiol 86:1729–1749
Cripton PA (2000). Load-sharing in the human cervical spine. Ph.D. Dissertation, Queen's University
Cromwell RL, Aadland-Monahan TK, Nelson AT, Stern-Sylvestre SM, Seder B (2001) Sagittal plane analysis of head, neck, and trunk kinematics and electromyographic activity during locomotion. J Orthop Sports Phys Ther 31:255–262
Dean MC (1982) The comparative anatomy of the hominoid cranial base. Doctoral dissertation, University of London
Dean MC (1985) Comparative myology of the hominoid cranial base. Folia Primatol 44(1):40–51
Demes B (1985) Biomechanics of the primate skull base. Adv Anat Embryol Cell Biol 94:1–57
Demes B, Jungers WL, Fleagle JG, Wunderlich RE, Richmond BG, Lemelin P (1996) Body size and leaping kinematics in Malagasy vertical clingers and leapers. J Hum Evol 31:367–388, https://doi.org/10.1006/jhev.1996.0066

DeSilva JM (2009) Functional morphology of the ankle and the likelihood of climbing in early hominins. Proc Natl Acad Sci 106:6567–6572
Duarte M, Hanna J, Sanches E, Liu Q, Fragaszy D (2012) Kinematics of bipedal locomotion while carrying a load in the arms in bearded capuchin monkeys (*Sapajus libidinosus*). J Hum Evol 63:851–858
Dunbar DC (2004) Stabilization and mobility of the head and trunk in vervet monkeys (*Cercopithecus aethiops*) during treadmill walks and gallops. J Exp Biol 207:4427–4438
Dunbar DC, Badam GL, Hallgrímsson B, Vieilledent S (2004) Stabilization and mobility of the head and trunk in wild monkeys during terrestrial and flat-surface walks and gallops. J Exp Biol 207(6):1027–1042
Dunbar DC, Macpherson JM, Simmons RW, Zarcades A (2008) Stabilization and mobility of the head, neck and trunk in horses during overground locomotion: comparisons with humans and other primates. J Exp Biol 211(24):3889–3907
Feipel V, Rondelet B, Le Pallec JP, Rooze M (1999) Normal global motion of the cervical spine: an electrogoniometric study. Clin Biomech 14(7):462–470
Fielding JW, Burstein AH, Frankel VH (1976) The nuchal ligament. Spine 1:3–15
Fleagle JG, Gilbert CC, Baden AL (2010) Primate cranial diversity. Am J Phys Anthropol 142(4):565–578
Fleagle JG, Gilbert CC, Baden AL (2016) Comparing primate crania: the importance of fossils. Am J Phys Anthropol 161(2):259–275
Franz TM, Demes B, Carlson KJ (2005) Gait mechanics of lemurid primates on terrestrial and arboreal substrates. J Hum Evol 48:199–217
Goel VK, Clausen JD (1998) Prediction of load sharing among spinal components of a C5-C6 motion segment using the finite element approach. Spine 23:684–691
Graf W, de Waele C, Vidal PP (1995a) Functional anatomy of the head-neck system of quadrupedal and bipedal mammals. J Anat 186:55–74
Graf W, de Waele C, Vidal PP, Wang H, Evinger C (1995b) The orientation of the cervical vertebral column in unrestrained awake animals. II: movement strategies. Brain Behav Evol 45:209–231
Hamrick MW (1996) Articular size and curvature as determinants of carpal joint mobility and stability in strepsirhine primates. J Morphol 230:113–127
Hayman MR, Donaldson IML (1997) Changes in dorsal neck muscle activity related to imposed eye movement in the decerebrate pigeon. Neuroscience 79(3):943–956
Hernandez CJ, Loomis DA, Cotter MM, Schifle AL, Anderson LC, Elsmore L, Kunos C, Latimer B (2009) Biomechanical allometry in hominoid thoracic vertebrae. J Hum Evol 56(5):462–470
Hirasaki E, Kumakura H (2004) Head movements during locomotion in a gibbon and Japanese macaques. Neuroreport 15(4):643–647
Horak FB, Macpherson JM (1996) Postural orientation and equilibrium. In: Handbook of physiology, vol 1. Oxford University Press, Oxford, pp 255–292
Hunt KD, Cant JGH, Gebo DL, Rose MD, Walker SE, Youlatos D (1996) Standardized descriptions of primate locomotor and postural modes. Primates 37(4):363–387
Isler K, Grüter CC (2006) Arboreal locomotion in wild black-and-white snub-nosed monkeys (*Rhinopithecus bieti*). Folia Primatol 77:195–211
Isler K, Thorpe SK (2003) Gait parameters in vertical climbing of captive, rehabilitant and wild Sumatran orang-utans (*Pongo pygmaeus abelii*). J Exp Biol 206:4081–4096, https://doi.org/10.1242/jeb.00651
Jaanusson VR (1987) Balance of the head in hominid evolution. Lethaia 20(2):165–176
Johnson GM, Zhang M, Jones DG (2000) The fine connective tissue architecture of the human ligamentum nuchae. Spine 25(1):5–9
Jungers WL, Burr DB (1994) Body size, long bone geometry and locomotion in quadrupedal monkeys. Z Morphol Anthropol 80(1):89–97
Kadri PA, Al-Mefty O (2007) Anatomy of the nuchal ligament and its surgical applications. Neurosurgery 615:301–304
Kapandji I (1974) The trunk and the vertebral column. Churchill Livingstone, Edinburgh

Keshner EA (1994) Vertebral orientations and muscle activation patterns during controlled head movements in cats. Exp Brain Res 98:546–550
Larson SG, Stern JT (2007) Humeral retractor EMG during quadrupedal walking in primates. J Exp Biol 210:1204–1215
Lieberman DE (2011) Holding up and moving the head. In: Evolution of the human head. Harvard University Press, Cambridge, pp 338–373
Lind B, Sihlbom H, Nordwall A, Malchau H (1989) Normal range of motion of the cervical spine. Arch Phys Med Rehabil 70(9):692–695
Macpherson JM, Ye Y (1998) The cat vertebral column: stance configuration and range of motion. Exp Brain Res 119:324–332
Manfreda E, Mitteroecker P, Bookstein F, Schaefer K (2006) Functional morphology of the first cervical vertebra in humans and nonhuman primates. Anat Rec B New Anat 289:184–194
Menegaz RA, Baier DB, Metzger KA, Herring SW, Brainerd EL (2015) XROMM analysis of tooth occlusion and temporomandibular joint kinematics during feeding in juvenile miniature pigs. J Exp Biol 218:2573–2584
Mercer S (1999) Functional morphology of the lower cervical spine in nonhuman primates. PhD dissertation. Pittsburgh, University of Pittsburgh
Mercer S, Bogduk N (2001) Joints of the cervical vertebral column. J Orthop Sports Phys Ther 31:174–182
Mercer S, Bogduk N (2003) Clinical anatomy of ligamentum nuchae. Clin Anat 16:484–493
Meyer MR (2016) The cervical vertebrae of KSD-VP-1/1. In: Haile-Selassie Y, Su DF (eds) The postcranial anatomy of *Australopithecus afarensis*. Springer, Dordrecht, pp 63–111
Meyer MR, Woodward C, Tims A, Bastir M (2018) Neck function in early hominins and suspensory primates: insights from the uncinate process. Am J Phys Anthropol 166(3):613–637
Mitchell BS, Humphreys BK, O'Sullivan E (1998) Attachments of the ligamentum nuchae to cervical posterior spinal dura and the lateral part of the occipital bone. J Manip Physiol Ther 213:145–148
Mitteroecker P, Manfreda E, Bookstein F, Schaefer K (2007) Does the morphology of the human atlas and axis reflect bipedality? A multivariate approach to functional morphology. Am J Phys Anthropol 132:172–173
Nagamoto Y, Ishii T, Sakaura H, Iwasaki M, Moritomo H, Kashii M, Hattori T, Yoshikawa H, Sugamoto K (2011) In vivo three-dimensional kinematics of the cervical spine during head rotation in patients with cervical spondylosis. Spine 36(10):778–783
Nakatsukasa M, Hirose Y (2003) Scaling of lumbar vertebrae in anthropoids and implications for evolution of the hominoid axial skeleton. Primates 44(2):127–135
Nalley T (2013) Positional Behaviors and the Neck: A Comparative Analysis of the Cervical Vertebrae of Living Primates and Fossil Hominoids. PhD dissertation. Arizona State University
Nalley TK, Grider-Potter N (2015) Functional morphology of the primate head and neck. Am J Phys Anthropol 156(4):531–542
Nalley TK, Grider-Potter N (2017) Functional analyses of the primate upper cervical vertebral column. J Hum Evol 107:19–35
Nevell L, Wood B (2008) Cranial base evolution within the hominin clade. J Anat 212(4):455–468
Panjabi MM, Miura T, Cripton PA, Wang JL, Nain AS, DuBois C (2001) Development of a system for in vitro neck muscle force replication in whole cervical spine experiments. Spine 26(20):2214–2219
Panzer MB, Cronin DS (2009) C4–C5 segment finite element model development, validation, and load-sharing investigation. J Biomech 42:480–490
Patel BA, Wunderlich RE (2010) Dynamic pressure patterns in the hands of olive baboons (*Papio anubis*) during terrestrial locomotion: implications for cercopithecoid primate hand morphology. Anat Rec 293:710–718
Polk JD, Demes B, Jungers WL, Biknevicius AR, Heinrich RE, Runestad JA (2000) A comparison of primate, carnivoran and rodent limb bone cross-sectional properties: are primates really unique? J Hum Evol 39:297–325

Pozzo T, Berthoz A, Lefort L (1990) Head stabilization during various locomotor tasks in humans. I: normal subjects. Experimental. Brain Res 82:97–106
Preuschoft H (2004) Mechanisms for the acquisition of habitual bipedality: are there biomechanical reasons for the acquisition of upright bipedal posture? J Anat 204:363–384
Richmond FJ, Singh K, Corneil BD (2001) Neck muscles in the rhesus monkey. I. Muscle morphometry and histochemistry. J Neurophysiol 86(4):1717–1728
Rose MD (1975) Functional proportions of primate lumbar vertebral bodies. J Hum Evol 4:21–38
Ruff CB (2000) Body size, body shape, and long bone strength in modern humans. J Hum Evol 38:269–290
Russo GA, Kirk EC (2013) Foramen magnum position in bipedal mammals. J Hum Evol 65(5):656–670
Russo GA, Kirk EC (2017) Another look at the foramen magnum in bipedal mammals. J Hum Evol 105:24–40
Schmitt D (2011) Translating primate locomotor biomechanical variables from the laboratory to the field. In: D'Août K, Vereecke EE (eds) Primate locomotion: linking field and laboratory research. Springer, New York, NY, pp 7–27
Schoonaert K, D'Août K, Aerts P (2006) A dynamic force analysis system for climbing of large primates. Folia Primatol 77:246–254
Schultz A (1942) Conditions for balancing the head in primates. Am J Phys Anthropol 29: 483–497
Schultz AH (1961) Vertebral column and thorax. Primatologia 4:1–66
Selbie WS, Thomson DB, Richmond FJR (1993) Sagittal- plane mobility of the cat cervical spine. J Biomech 26:917–927
Shapiro L (1993) Functional morphology of the vertebral column in primates. In: Gebo DL, Dekalb IL (eds) Postcranial adaptation in nonhuman primates. Northern Illinois University Press, DeKalb, pp 121–149
Shapiro LJ, Simons CVM (2002) Functional aspects of strepsirrhine lumbar vertebral bodies and spinous processes. J Hum Evol 42:753–783
Silcox MT, Bloch JI, Boyer DM, Godinot M, Ryan TM, Spoor F, Walker A (2009) Semicircular canal system in early primates. J Hum Evol 56(3):315–327
Slijper E (1946) Comparative biologic-anatomical investigations on the vertebral column and spinal musculature of mammals. Verh K Ned Akad Wet 42:1–128
Smit TH (2002) The use of a quadruped as an in vivo model for the study of the spine–biomechanical considerations. Eur Spine J 11(2):137–144
Spoor F, Wood B, Zonneveld F (1994) Implications of early hominid labyrinthine morphology for evolution of human bipedal locomotion. Nature 369(6482):645–648
Spoor F, Garland T, Krovitz G, Ryan TM, Silcox MT, Walker A (2007) The primate semicircular canal system and locomotion. Proc Natl Acad Sci 104(26):10808–10812
St George RJ, Fitzpatrick RC (2011) The sense of self-motion, orientation and balance explored by vestibular stimulation. J Physiol 589(4):807–813
Stevens KA (2013) The articulation of sauropod necks: methodology and mythology. PLoS One 8(10):78572
Stevens NJ, Heesy CP (2012) Head posture and visual orientation in *Loris tardigradus* during locomotion on oblique supports. In: Masters J, Gamba M, Génin F (eds) Developments in primatology: progress and prospects: leaping ahead. Springer, New York, pp 97–104
Strait DS, Ross CF (1999) Kinematic data on primate head and neck posture: implications for the evolution of basicranial flexion and an evaluation of registration planes used in paleoanthropology. Am J Phys Anthropol 108:205–222
Swindler D, Wood C (1982) An atlas of primate gross anatomy: baboon, chimpanzee, and man. RE Krieger Publishing Company, New York
Takeuchi T, Shono Y (2007) Importance of preserving the C7 spinous process and attached nuchal ligament in French-door laminoplasty to reduce postoperative axial symptoms. Eur Spine J 16(9):1417–1422

Thompson NE, Ostrofsky KR, McFarlin SC, Robbins MM, Stoinski TS, Almécija S (2018) Unexpected terrestrial hand posture diversity in wild mountain gorillas. Am J Phys Anthropol 166:84–94

Toerien MJ (1961) The length and inclination of the primate cervical spinous processes. Trans R Soc S Afr 36:95–105

Togasaki DM, Hsu A, Samant M, Farzan B, DeLanney LE, Langston JW, Di Monte DA, Quik M (2005) The Webcam system: a simple, automated, computer-based video system for quantitative measurement of movement in nonhuman primates. J Neurosci Methods 145:159–166

Vidal PP, Graf W, Berthoz A (1986) The orientation of the cervical vertebral column in unrestrained awake animals. Exp Brain Res 61:549–559

Vidal PP, Graf W, Berthoz A (1988) Skeletal geometry underlying head movements. Ann N Y Acad Sci 545(1):228–238

Villamil CI (2018) Phenotypic integration of the cervical vertebrae in the Hominoidea (Primates). Evolution 72(3):490–517

Wagner GP (1996) Homologues, natural kinds and the evolution of modularity. Am Zool 36:36–43

White A, Panjabi M (1990) Clinical biomechanics of the spine. Lippincott, Philadelphia

Xiang Y, Yakushin SB, Kunin M, Raphan T, Cohen B (2008) Head stabilization by vestibulocollic reflexes during quadrupedal locomotion in monkey. J Neurophysiol 100:763–780

Chapter 4
Vertebral Morphology in Hominoids II: The Lumbar Spine

Liza J. Shapiro and Gabrielle A. Russo

4.1 Introduction

In hominoids, as in other mammals, the vertebral column provides both flexibility and structural support to the trunk and is a key functional component in posture and locomotion. The mammalian vertebral column is regionalized, and each region (cervical, thoracic, lumbar, sacral, caudal) is associated with distinct morphological features and functional capabilities. In the mammalian presacral vertebral column, the lumbar region is the most recently evolved and the most highly functionally differentiated among taxa (Jones et al. 2018). Lumbar vertebrae (the focus of this chapter) lie between the thoracic and sacral vertebrae. Lumbar vertebrae share the same basic skeletal components as most cervical (except the first and second), all thoracic, and some caudal vertebrae, including a vertebral body, pre- and postzygapophyses, and projecting spinous and transverse processes attached to the neural arch, which is formed by pedicles and laminae (Fig. 4.1). However, unlike thoracic vertebrae, lumbar vertebrae lack ribs and rib facets (by traditional definition; see below), and are easily distinguished from sacral vertebrae, which are fused to form the sacrum. Compared to cervical and thoracic vertebrae, lumbar vertebrae have larger vertebral bodies, more sagittally oriented zygapophyses that enhance sagittal plane flexibility while restricting rotation, and spinous and transverse processes that vary prominently across species with respect to shape and orientation. This chapter specifically addresses form and function in the lumbar region of hominoids (for cervical and thoracic regions, see Nalley and Grider-Potter, 2019). We address how the lumbar vertebrae of hominoids are morphologically and

L. J. Shapiro (✉)
Department of Anthropology, University of Texas at Austin, Austin, TX, USA
e-mail: liza.shapiro@austin.utexas.edu

G. A. Russo
Department of Anthropology, Stony Brook University, Stony Brook, NY, USA
e-mail: gabrielle.russo@stonybrook.edu

E. Been et al. (eds.), *Spinal Evolution*,
https://doi.org/10.1007/978-3-030-19349-2_4

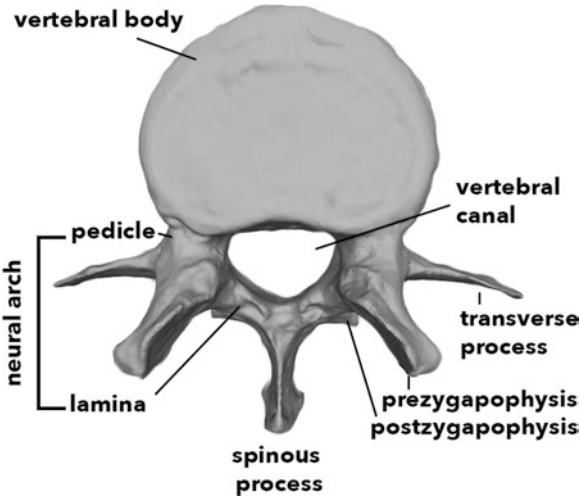

Fig. 4.1 Lumbar vertebra (*Pan troglodytes*) in cranial view with major features labeled

functionally distinct among primates with respect to the number of vertebrae and length of the lumbar region, shape of vertebral bodies and pedicles, and shape and orientation of spinous processes, transverse processes, and zygapophyses. We then discuss how traditional functional interpretations have benefited from, and been expanded by, recent comparative research on nonhominoid primates and other mammals, experimental biomechanics, and analyses of back musculature. Finally, we address recent research that has provided new perspectives on questions regarding the sequence in which features of the hominoid trunk evolved.

4.2 Distinctive Aspects of Hominoid Lumbar Vertebral Morphology

4.2.1 Vertebral Formula

Variation in vertebral formulae (the numbers of vertebrae in the different regions of the spine) among hominoids and in comparison to other primates has been of interest to researchers since at least the early 1900s (Keith 1902, 1923) and even earlier (see review in Williams et al. 2016). There are different methods one can employ when defining and counting lumbar vertebrae. The traditional definition recognizes lumbar vertebrae as those that lack ribs and lie between the rib-bearing thoracic vertebrae and the sacrum. The zygapophyseal definition recognizes lumbar vertebrae as those for which the articular surfaces of the prezygapophyses are concave and face dorsomedially, and the articular surfaces of the postzygapophyses are convex and face ventrolaterally. By this definition, thoracic vertebrae have relatively flat and more coronally oriented zygapophyses, with the articular surfaces of prezygapophyses facing dorsally and articular surfaces of the postzygapophyses,

facing ventrally (Washburn and Buettner-Janusch 1952). Depending on the position of the transitional or "diaphragmatic" vertebra ("counted" as a thoracic), in which the prezygapophyses are thoracic-like and the postzygapophyses are lumbar-like, zygapophyseal-based counts of lumbar vertebrae can be higher compared to rib-based counts. This is the case for nonhominoid primates as well as for hylobatids, in which there are usually one to three rib-bearing vertebrae caudal to the transitional vertebra. However, in great apes and humans the transitional vertebra is most often the last rib-bearing vertebra, so for these primates, lumbar counts are usually equivalent by either definition (modal counts of lumbars by both definitions are equivalent but means differ, so there is some variability within species) (Williams 2012a) (Fig. 4.2). By either definition, hominoids have fewer lumbar vertebrae than other primates (most frequently, 3–5 that lack ribs, and due to the more cranial position of the transitional vertebra in hylobatids, up to 6 by zygapophyseal definition) (Schultz 1961; Erikson 1963; Washburn 1963; Shapiro 1993a; Williams and Russo 2015; Thompson and Almécija 2017; see Williams et al., 2019). The only other primates with as few as 4–5 (traditionally defined) lumbar vertebrae are the atelids, but these numbers increase to 6–8 when defined by zygapophyses (Erikson 1963).

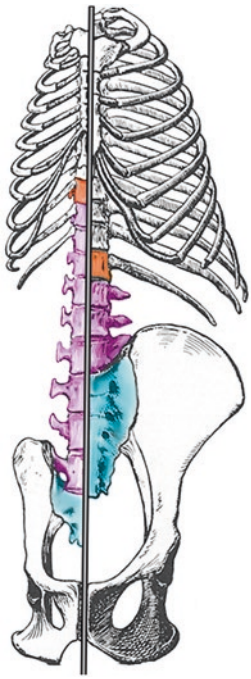

Fig. 4.2 Split (midline) ventral view of cercopithecoid (left, *Macaca*) and hominoid (right, *Pan*) bony torso morphology (modified from Schultz (1950) after Benton (1967)). Colors denote the following vertebral levels: orange = transitional ("diaphragmatic") vertebra; purple = post-transitional vertebrae; light blue = sacrum. The vertebrae situated in between the transitional vertebra and the sacrum are recognized as the lumbar vertebrae, according to the zygapophyseal definition. Note the differences in rib cage and pelvic shape, numbers of vertebrae in each region, and contrasting morphologies at corresponding vertebral levels. Images not to scale

The establishment of boundaries between the vertebral regions and differential morphological development of vertebrae is now well understood to be dependent on *Hox* genes (Kessel and Gruss 1991; Burke et al. 1995; Mallo et al. 2010). For example, Hox genes 9–11 are responsible for the distinctive morphology and regional numbers of the lower thoracic, lumbar, and sacral regions (Burke et al. 1995; Wellik and Capecchi 2003). Differences in the expression of *Hox* genes can result in changes in the location of regional morphological boundaries (i.e., homeotic changes) that are associated with variation of vertebral formulae among and within species (Pilbeam 2004; Wellik 2009; Williams 2012b; Galis et al. 2014; Williams and Russo 2015; Williams et al. 2016). For example, in the evolution of hominoids, reduction in numbers of lumbar vertebrae from the ancestral catarrhine condition was most likely the result of an anterior (i.e., cranial) homeotic shift of the lumbosacral border, in which the lower lumbar vertebrae became incorporated into the sacrum (i.e., "sacralized"; see Fig. 4.2) (Keith 1902, 1923; Pilbeam 2004; McCollum et al. 2010; Williams and Russo 2015; Williams et al. 2016). Combined with sacralization, lumbar vertebrae could also have been reduced due to incorporation into the thoracic region (bonobos) or segment loss (i.e., meristic change; chimpanzees and gorillas) (McCollum et al. 2010). At the intraspecific level, variation in vertebral formulae has been used to assess competing hypotheses about the likelihood of homoplasy in lumbar reduction among hominoids (Pilbeam 2004; McCollum et al. 2010; Williams 2012b), as well as to test for the selective effects of locomotor function. For example, reduced intraspecific variation in vertebral formulae among humans compared to other primates may reflect the biomechanical demands of bipedalism, while reduced variation in eastern gorillas and cercopithecoids may reflect functional aspects of terrestriality and cursoriality, respectively (Pilbeam 2004; Williams 2012b). More recently, analyses of intraspecific variation in aspects of vertebral morphological *shape* (rather than just numbers of regional vertebrae) have also documented a tendency toward decreased shape variation in cercopithecoids, and to some extent humans and gibbons, compared to other hominoids (Shapiro and Kemp 2019).

4.2.2 Vertebral Body Shape and Lumbar Region Length

Vertebral body craniocaudal length scales against body size with negative allometry among nonhuman catarrhines (combined, as well as within both hominoids and cercopithecoids). However, for their body size, hominoids have relatively short vertebral bodies compared to cercopithecoids (Schultz 1961; Rose 1975; Jungers 1984; Ward 1993; Sanders and Bodenbender 1994; Sanders 1998) (Figs. 4.2 and 4.3). Reduction in numbers of lumbar vertebrae combined with reduced craniocaudal length of individual vertebral bodies results in a highly reduced lumbar region length in hominoids compared to cercopithecoids (Schultz 1961; Jungers 1984). Among nonhuman catarrhines, vertebral body mediolateral width scales close to isometry (Sanders and Bodenbender 1994) but compared to cercopithecoids (and other primates in general), hominoids have mediolaterally wider vertebral bodies

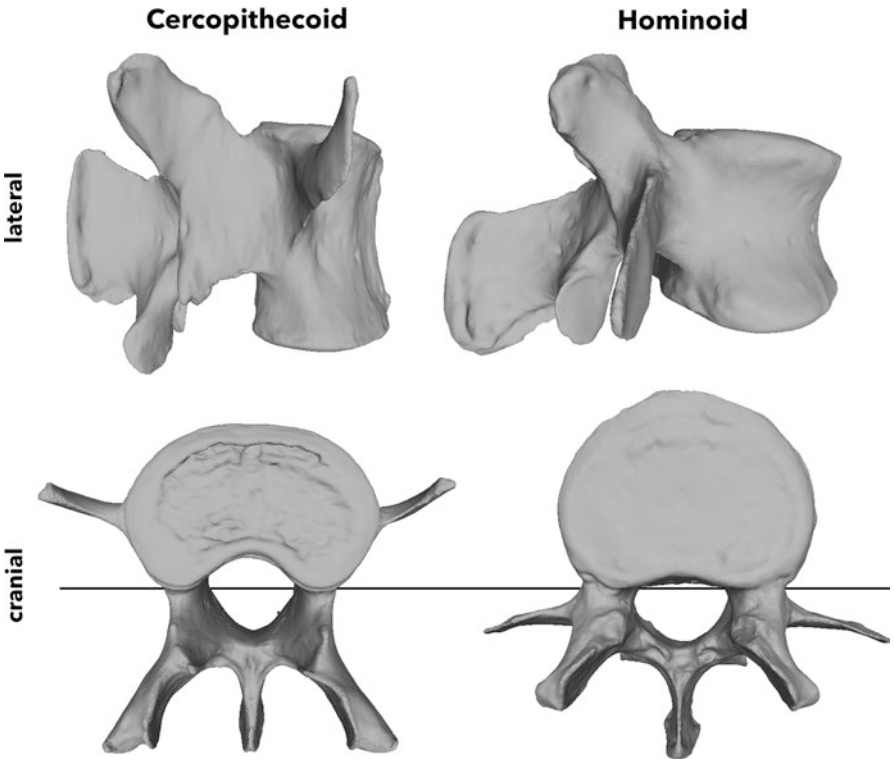

Fig. 4.3 Lateral (top panel) and cranial (bottom panel) views of cercopithecoid (*Macaca*) and hominoid (*Pan*) mid-level lumbar vertebrae. In lateral view, note the differences in craniocaudal length of vertebral bodies, craniocaudal spinous process orientation, and transverse process position and orientation. In this case, the cercopithecoid lumbar vertebra exhibits a spinous process with a craniodorsal tip that points cranially (see text for more details). In cranial view, the differences in transverse process position and orientation are apparent (reference line has been placed along the dorsalmost aspect of the cranial surfaces of the vertebral bodies for facilitating comparison). Cercopithecoid scaled to size of hominoid vertebra

relative to their overall body size (Rose 1975; Sanders and Bodenbender 1994; Sanders 1998). Vertebral body height (ventrodorsal dimension) is positively allometric among nonhuman catarrhines, providing enhanced resistance to sagittal plane spinal bending as body mass increases (Sanders and Bodenbender 1994). Vertebral body surface area scales isometrically among nonhuman catarrhines and among nonhuman hominoids (but see Nakatsukasa and Hirose 2003). Compared to those of other hominoids, the lumbar vertebral bodies of humans have relatively expanded surface areas and are relatively wider, ventrodorsally higher, and slightly craniocaudally elongated (Rose 1975; Latimer and Ward 1993; Shapiro 1993a; Sanders and Bodenbender 1994; Sanders 1998). Human lumbar vertebral bodies are also dorsally wedged in the mid-to-lower lumbar region, contributing to the unique lordotic curve of humans (Latimer and Ward 1993; Sanders 1998; Whitcome et al. 2007; Been et al. 2012; Whitcome 2012).

4.2.3 Transverse Processes, Spinous Processes, and Pedicles

In addition to reduction in relative length of the lumbar region (and the associated changes in length of individual vertebral bodies), hominoid lumbar vertebrae are distinctive with respect to the orientation and location of the transverse processes. In hylobatids, the transverse processes project laterally and originate from the body/pedicle junction. In great apes and humans, the transverse processes are oriented dorsally and originate at the pedicle/lamina junction (Figs. 4.3 and 4.4). In most other primates, the transverse processes originate on the vertebral body and are both ventrally and cranially oriented (Mivart 1865; Benton 1967, 1974; Ankel 1972; Gambaryan 1974; Shapiro 1993a, 2007; Sanders and Bodenbender 1994; Filler 2007a; Granatosky et al. 2014a, b) (Figs. 4.2 and 4.3). In addition, hominoid lumbar spinous processes have a squared-off dorsal edge and are oriented caudally, or perpendicular to the long axis of the vertebral body. In comparison, lumbar spinous processes of most pronograde primates and nonprimates are cranially oriented, either along their long axis or via a tip on the craniodorsal edge that points cranially (Slijper 1946; Gambaryan 1974; Latimer and Ward 1993; Shapiro 1993a, 2007; Granatosky et al. 2014a, b) (Fig. 4.3). All hominoids have craniocaudally shorter lumbar pedicles compared to nonhominoid primates, although gibbons have relatively longer pedicles than great apes. Great apes and humans have relatively wider and shorter (i.e., more "robust") lumbar pedicles compared to either gibbons or nonhominoids. Although hominoids as well as nonhominoid primates exhibit increased pedicular robusticity at the last lumbar vertebra, humans have especially robust (i.e., relatively wide) last lumbar pedicles suggesting a functional influence of bipedalism (Davis 1961; Shapiro 1993b; Sanders and Bodenbender 1994; Sanders 1998).

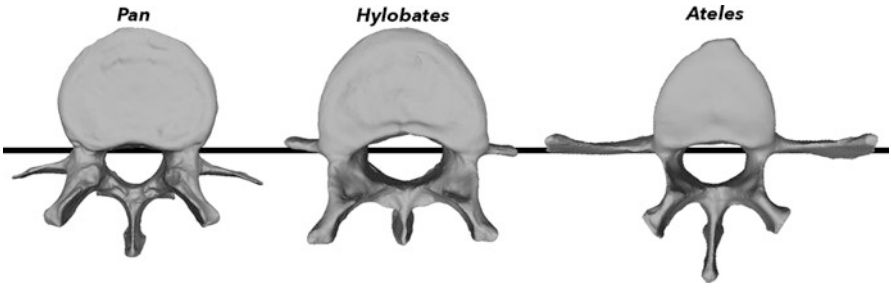

Fig. 4.4 Cranial views of (from left to right) hominid (*Pan*), hylobatid (*Hylobates*), and atelid (*Ateles*) lumbar vertebrae. Note how the transverse processes originate from the pedicle in *Pan* (as in other hominids) and more ventrally at the pedicle-body junction in *Hylobates* (reference line has been placed along the dorsalmost aspect of the cranial surfaces of the vertebral bodies for facilitating comparison). *Ateles* morphologically converges to some extent with *Hylobates* in aspects of lumbar vertebral morphology, including transverse process dorsal position and orientation. Vertebrae scaled to be similarly sized

4.2.4 Zygapophyses

As discussed above, moving from the transitional vertebra to the first (zygapophyseal-defined) lumbar vertebra, there is a shift in shape and orientation of the prezygapophyses from flat and coronally oriented in the former to curved and more sagittally oriented in the latter. The shift in prezygapophyseal morphology from the transitional vertebra to the upper lumbar vertebrae is more gradual in great apes (and to a lesser extent in *Hylobates*) compared to cercopithecoids, particularly in *Pongo* and *Gorilla* which have relatively flat and coronally oriented lumbar prezygapophyses (Russo 2010). Nonhuman hominoids also vary in upper lumbar prezygapophyseal shape and orientation, but not strictly along expected functional categories (see Russo 2010). Compared to those of other hominoids, human lumbar prezygapophyses have relatively large surface areas, and only human prezygapophyses exhibit a dramatic increase in size, angle of orientation (relative to a sagittal plane), and interfacet distance as one moves caudally along the lumbar region (Struthers 1892; Odgers 1933; Latimer and Ward 1993; Shapiro 1993a; Sanders 1998; Masharawi et al. 2004, 2007a, 2007b; Ward and Latimer 2005; Whitcome et al. 2007). In addition, human lumbar postzygapophyses accommodate the lordotic curve by exhibiting a decrease in craniocaudal length and an increase in posterior angulation moving from the upper to lower lumbar column (Latimer and Ward 1993; Masharawi et al. 2004; Been et al. 2012).

4.3 Functional Interpretations of Hominoid Lumbar Morphology

Because all living apes exhibit the aforementioned lumbar features to some extent, the specific positional behaviors to which such features might be linked is of interest to researchers, as is the issue of whether or not the ancestral crown hominoid possessed these derived vertebral features (Keith 1923; Harrison 1986; Sarmiento 1987; Benefit and McCrossin 1995; MacLatchy et al. 2000; but see Lovejoy et al. 2009; Reno 2014; Ward 2014). Researchers have spent a considerable amount of time attempting to link the lumbar vertebral features characteristic of living hominoids to specific types of postural and locomotor behaviors, including orthogrady/brachiation (Keith 1923; Erikson 1963; Gebo 1996), arm hanging (Hunt 1991), quadrumanous climbing and bridging and/or vertical climbing (Cartmill and Milton 1977; Jungers 1984; Sarmiento 1998; Lovejoy et al. 2009), orthograde clambering and arboreal bipedalism (i.e., bipedal walking along branches; Crompton et al. 2008), and orthograde trunk sitting during foraging and feeding (Jolly 1970; Andrews and Groves 1976), while a number of researchers have attributed anatomical features to a more general “combination” of these positional behaviors (Tuttle 1975; Tuttle and Basmajian 1978; Ward 1993).

Notwithstanding their relevance to any particular positional behavior, functional explanations for hominoid lumbar morphology (i.e., the "short-backed" condition; Benton 1967) emphasize its adaptive significance for providing spinal stability. This view places hominoid lumbar morphology in strong contrast to the lumbar features of "long-backed" primates (most monkeys and strepsirrhines), which function to enhance spinal flexibility (Benton 1967). For example, the relatively short lumbar region of hominoids is assumed to provide the necessary "stiffness" and resistance to bending required to enhance stability during some or all of the positional behaviors listed above, by permitting controlled trunk movements, providing resistance to bending, and/or preventing buckling (Keith 1902, 1923; Erikson 1963; Benton 1967, 1974; Cartmill and Milton 1977; Jungers 1984; Ward 1993). The unique features of human lumbar vertebral bodies (i.e., mediolateral and ventrodorsal expansion, with increased surface areas, dorsal wedging/lordosis, and craniocaudal elongation) provide increased resistance to compressive loading, bending or buckling, while also allowing the increased range of motion required for balancing the trunk over the pelvis (Sanders 1998).

The squared, dorsal edges of the hominoid spinous processes, in combination with their dorsal to caudal orientation, are assumed to limit sagittal spinal mobility due to their close proximity in extension (Erikson 1963; Latimer and Ward 1993; Shapiro 1993a). The dorsal shift of the lumbar transverse processes is thought to stabilize the upright posture of the spine by enhancing the extensor leverage of the epaxial muscles (Sanders and Bodenbender 1994; Sanders 1998; Filler 2007b). However, as a consequence of the dorsal placement and orientation of transverse processes, the area available to epaxial muscles is diminished (i.e., dorsally shallower) in hominoids, accounting for their reduced back muscle mass compared to cercopithecoids and other pronograde primates, which have a deeper dorsal "trough" due to more ventrally placed transverse processes (Keith 1940; Benton 1967, 1974). This reduction in mass (and potential force output) of the epaxial muscles was presumably offset by the enhanced leverage conferred by their more dorsal location.

The craniocaudal lengths of the pedicles and vertebral bodies are correlated in catarrhines, which likely explains the relatively short lumbar pedicles of hominoids compared to nonhominoid primates (Sanders 1998). However, differences between hominoids and nonhominoids in relative width (and thus robusticity) of lumbar pedicles is likely functionally associated with the position of the transverse processes. In great apes and humans in particular, robust pedicles may be an adaptation for resistance to increased bending forces resulting from the action of epaxial muscles inserting on the transverse processes, which originate on or near the pedicle. In contrast, pedicles might be subject to reduced loading among most nonhominoid primates, in which the transverse processes arise from the vertebral body. In this respect, hylobatids would represent an intermediate condition, with pedicles that are relatively longer and less robust than those of larger-bodied hominoids, and transverse processes located at the body-pedicle junction (Benton 1967; Ankel 1972; Shapiro 1993a; Sanders 1998). On the other hand, although transverse process position in humans is similar to that in great apes, humans have exceptionally robust (i.e., relatively wide) last lumbar pedicles. Thus, this unique human pedicular

morphology is likely related specifically to bipedalism, either for resistance to mediolateral bending forces or forces transmitted through the transverse processes via the iliolumbar ligament, which prevents the tendency of the last lumbar vertebra to slide forward on the sacrum due to lordosis (Davis 1961; Shapiro 1993b; Sanders 1998).

Compared to relatively flat, coronally oriented thoracic prezygapophyses, the more curved and sagittally oriented lumbar prezygapophyseal joints promote sagittal plane spinal flexibility and restrict rotation. Thus, the more abrupt transition in prezygapophyseal morphology at the thoracolumbar junction in "long-backed" primates (e.g., *Papio*) compared to hominoids is consistent with an adaptation in the former to sagittal spinal flexibility, while the tendency to maintain relatively more coronally oriented prezygapophyses across the junction in hominoids suggests an adaptation to more stability in this region (Russo 2010). In humans, changes in pre- and postzygapophyses along the lumbar column function to accommodate lordosis by preventing forward displacement of lower lumbar vertebrae (increase in interfacet distances and angles of orientation relative to a sagittal plane), resisting increased compressive loading (large facet areas), and preventing impingement of vertebrae (reduced length and posterior angulation of postzygapophyses) (Latimer and Ward 1993; Shapiro 1993a; Sanders 1998; Masharawi et al. 2004, 2007a, 2007b; Ward and Latimer 2005).

4.3.1 Functional Insights from Nonhominoid Primates and Other Mammals

Many workers have turned to the use of other primates or other mammals as models for understanding the functional or adaptive significance of hominoid lumbar vertebral features. Lumbar features that presumably promote lumbar spinal stability are characteristic of some nonhominoid primates that also require a "stable" spine (Mivart 1865; Schultz 1961; Erikson 1963; Benton 1967; Ankel 1972; Cartmill and Milton 1977; Shapiro 1995, 2007; Johnson and Shapiro 1998; Shapiro and Simons 2002; Shapiro et al. 2005). For example, the highly suspensory atelids, particularly *Ateles* and *Brachyteles*, exhibit the fewest lumbar vertebrae among nonhominoid primates (Erikson 1963; and see Williams et al., 2019, for a discussion of primitive primate and catarrhine conditions) and vertebral morphologies (e.g., relatively short craniocaudal vertebral body lengths, more dorsally positioned and laterally directed transverse processes) that appear convergent with hylobatids (Fig. 4.4) (Mivart 1865; Schultz 1961; Erikson 1963; Benton 1967; Ankel 1972; Shapiro 1993a; Johnson and Shapiro 1998). Additionally, while vertical clingers and leapers like *Indri* and *Propithecus* exhibit strong similarity to their pronograde quadrupedal relative *Varecia* in post-transitional vertebral numbers, they have craniocaudally shorter (though not mediolaterally wider) lumbar bodies that, at the mid-lumbar vertebral levels, tend to have more dorsally oriented transverse processes (Shapiro 1995; Shapiro and Simons

2002). Lorisids also exhibit lumbar vertebrae characterized by spinous processes that are shorter and more perpendicularly to caudally oriented relative to the vertebral body, as well as features that promote lateral bending (Shapiro 2007). Some extinct subfossil lemurs (e.g., *Palaeopropithecus*) also possess "stability"-promoting vertebral morphologies for suspensory behaviors (Shapiro et al. 2005; Granatosky et al. 2014b), and inferences about both lorisids and these extinct subfossil lemurs are supported by previous work on extant sloths (Straus and Wislocki 1932). Shared reduction in lumbar column flexibility (via short lumbar regions and more perpendicularly to caudally directed spinous processes) among hominoids, atelines, indriids, lorisids, and subfossil lemurs has therefore been interpreted to confer an advantage during suspension and/or, more generally, "antipronograde" postures (Shapiro 1995, 2007; Johnson and Shapiro 1998; Shapiro and Simons 2002; Shapiro et al. 2005; Granatosky et al. 2014b).

Nonprimate mammals that converge with hominoids on some aspects of dorsostability of the lumbar spine include perissodactyls and some artiodactyls, and their vertebral anatomy probably confers an advantage for stiff-spined running by limiting sagittal plane bending and axial rotation (Slijper 1946; Gambaryan 1974; Townsend and Leach 1984; Halpert et al. 1987; Boszczyk et al. 2001; Williams 2012a). Woolly opossums (genus *Caluromys*), known to rely on antipronograde behaviors such as cantilevering and bridging to a greater extent than other didelphids (i.e., *Monodelphis domestica*), also exhibit rigidity-promoting features such as short lumbar vertebral bodies and craniocaudally expanded spinous processes (Granatosky et al. 2014a). However, woolly opossums retain relatively long lumbar regions despite having relatively short lumbar vertebral bodies, a combination of characters unlike that observed for hominoids (Granatosky et al. 2014a). Other mammals that exhibit lumbar features associated with axial rigidity include sloths, colugos, and bats (Sargis 2001; Granatosky et al. 2014a, b). Although these taxa differ in their locomotor specializations (inverted quadrupedalism, mitten gliding, and flight, respectively), their shared lumbar adaptations for stability are likely related to the fact that they all engage in suspensory/inverted quadrupedalism (Granatosky et al. 2014b). Other gliding mammals (e.g., sugar gliders, flying squirrels) utilize above-branch pronograde quadrupedalism when not gliding and, accordingly, share lumbar features related to mobility with other pronograde quadrupeds or leapers (Granatosky et al. 2014b). Giant pandas (*Ailuropoda melanoleuca*, Carnivora) share with living hominoids a number of lumbar vertebral features that distinguish them from their close ursid (bear) relatives, including a shortened lumbar column (both in number and vertebral body craniocaudal length), more dorsally positioned and oriented transverse processes, and caudally oriented spinous processes (Russo and Williams 2015). Because giant pandas do not exhibit any of the arboreal locomotor behaviors characteristic of living apes (e.g., arm hanging, bridging, suspension) or primates generally, these morphological convergences likely reflect their shared use of orthograde trunk postures, which giant pandas employ for extensive bouts of time during bamboo foraging and feeding (Russo and Williams 2015). Moreover, the fact that lumbar reduction in giant pandas exceeds that of even large-bodied ursids (e.g., brown bears, *Ursus arctos*) suggests that the

acquisition of hominoid-like morphology is not strictly body size related among closely related taxa (Russo and Williams 2015).

In light of comparative work on nonhominoid primates and other mammals, continued comparative research may continue to inform researchers about what *general* aspects of posture (e.g., orthogrady or "antipronogrady") might select for the lumbar vertebral morphologies characteristic of apes, as opposed to pointing in the direction of *specific* aspects of locomotor behavior per se. Moreover, it appears that there are multiple configurations that can confer spinal stability and stiffness, rather than a single morphological pattern or combination of traits (i.e., more than one solution to one functional problem; Granatosky et al. 2014a). It seems increasingly likely that the evolution of hominoid-like lumbar vertebral morphologies may relate to generalized orthograde behaviors that could have later been exapted for suspensory behavior and/or other locomotor specializations (e.g., brachiation) in extant lineages (Russo and Williams 2015).

Comparative work on nonhominoid primates and other mammals has also offered insight on human lumbar morphology more specifically. For example, atelids have recently been noted to converge with humans in lacking "entrapment" of the lower lumbar vertebrae between the iliac blades, in conjunction with wide sacra, reduced iliac height, and reduced ligamentous restriction between lumbar vertebrae and ilia (Lovejoy 2005; Machnicki et al. 2016). These features are presumed to allow the lumbar mobility required for the lordotic curvature which has been visually observed (but not experimentally quantified) in atelids using bipedal postures (Machnicki et al. 2016). Further research will be needed to verify the hypothesis that the aforementioned vertebral/pelvic traits are functionally associated with lordotic capability or extended hindlimb postures in atelids (rather than suspensory behaviors or possession of a prehensile tail). Using a more phylogenetically distant model to test for convergence with humans, Cartmill and Brown (2017) examined the lumbar morphology of the gerenuk (*Litocranius walleri*), a gazelle that engages in habitual bipedal feeding postures, accompanied by a visually evident lumbar lordosis. Although increased spacing between the gerenuk's lumbar spinous processes would seem to accommodate lordosis, the gerenuk's lumbar vertebral bodies are not dorsally wedged (Cartmill and Brown 2017), a condition which in humans contributes to the lordotic curve. It would be interesting to test whether the gerenuk's zygapophyses or last lumbar pedicles are convergent with human morphology, although it seems unlikely given the overall lack of bipedal adaptations in the rest of the gerenuk's skeleton (e.g., hip joint) (Cartmill and Brown 2017).

4.3.2 Functional Insights from Experimental Biomechanics

All of the above views of the hominoid lumbar spine functionally associate the changes that occurred in the hominoid lumbar region with "stability" or "stiffness." The reduced mobility of the lumbar region is considered to be most extreme in the large-bodied apes, due to a combination of having fewer lumbar vertebrae than

hylobatids or humans, with the most caudally situated one or two lumbar vertebrae "entrapped" between the iliac blades (Lovejoy 2005; Lovejoy and McCollum 2010; Machnicki et al. 2016). Accordingly, Lovejoy (2005:99) described the great ape spine as a "stiff unibody," with no flexibility of the lower back. On the other hand, the relatively longer lumbar region in humans compared to other hominoids has been associated with a need for increased trunk mobility during bipedalism (Keith 1923; Sanders 1998; Lovejoy 2005; Whitcome 2012) and has been described as "exceedingly mobile" due to greater overall length, broadening of the ilia and sacrum, and progressive widening of the laminae and inter-zygapophyseal distance, all of which serve to liberate the lower lumbar spine from "entrapment" (Lovejoy 2005; Machnicki et al. 2016).

It should be noted that actual mobility (i.e., intervertebral range of motion) of the nonhuman hominoid spine has rarely been directly measured in vivo or even in vitro (but see Gál's (1993a, 1993b) analyses of the mammalian spine). Yet a recent in vivo biomechanical analysis that measured trunk mobility in chimpanzees walking bipedally produced the surprising results that relative to pelvic rotation, both thoracic and lumbar segment rotations were similar in magnitude between chimpanzees and humans, while lumbar relative to thoracic rotation was greater in chimpanzees (Thompson et al. 2015). The chimpanzee-human similarity was unexpected, given the relatively longer and presumably more mobile lumbar regions of humans. These observations weaken the common association between nonhuman hominoid lumbar reduction and rigidity of the spine and highlight the importance of in vivo studies of spinal kinematics for testing such hypotheses. However, Thompson et al. (2015) addressed lumbar mobility solely during bipedalism and only measured axial rotation. Therefore, this study provides a window into the rotational *capability* of the ape spine (which appears to be greater than expected), but it does not directly address whether the reduced lumbar region of hominoids provides rotational stability during arboreal behaviors such as climbing, arm swinging, or bridging, nor does it assess potential lateral or sagittal plane stability in these behaviors. More comprehensive spinal kinematic analyses in hominoids across different locomotor behaviors are needed to further enhance our understanding of the evolution of hominoid lumbar morphology.

4.3.3 Functional Insights from Back Musculature

As discussed above, hominoids have been noted for their relative reduction in lumbar epaxial muscle mass compared to most pronograde primates, and this has played a prominent role in discussions of the function and evolution of the hominoid spine. However, compared to our knowledge of form and function in lumbar osteological features, less research has been devoted to the form and function of (nonhuman) hominoid back muscles.

Early workers (e.g., Keith 1902, 1923, 1940; Elftman 1932) interested in hominoid trunk musculature noted macroscopic differences between hominoids and

nonhominoids in the size and arrangement of the lower back and pelvic musculature in relation to taillessness, one of the key defining features of the hominoid clade. Tail loss is accompanied by loss or vestigialization of the anapophyses (i.e., styloid processes), which in tail-bearing primates are situated on the pedicle ventrolateral to the postzygapophyses of lower thoracic and upper lumbar vertebrae and serve as attachment sites for longissimus and extensor caudae lateralis (Howell and Straus 1933; Sanders and Bodenbender 1994; Lemelin 1995). Muscles that flex and abduct the tail in tail-bearing primates (e.g., ischio- and ilio-caudalis) are reduced and reorganized into pelvic floor musculature in hominoids, presumably to support abdominal and pelvic viscera during orthograde posture (Keith 1902, 1923, 1940; Elftman 1932). In addition, the loss of tail extensor muscles (e.g., extensor caudae medialis, extensor caudae lateralis, which in tailed primates are extensions of multifidus and longissimus, respectively; Howell and Straus 1933; Lemelin 1995) presumably enhanced orthograde stability by providing extra attachment area for erector spinae muscles on the dorsal sacrum (Keith 1902). Although features associated with tail loss and orthograde trunk posture in extant hominoids appear functionally linked, the fossil record indicates that some of the earliest known hominoids that lacked tails were not habitually orthograde (e.g., *Nacholapithecus*, *Ekembo* [formerly *Proconsul*; McNulty et al. 2015]), complicating our evolutionary views of this scenario (Ward 1993; Nakatsukasa 2003; Nakatsukasa and Kunimatsu 2009; Russo and Shapiro 2011; Williams and Russo 2015).

Electromyographic analyses of multifidus, longissimus, and iliocostalis in chimpanzees and orangutans (compared to baboons) walking quadrupedally have revealed a basic activity pattern shared by all three species; each muscle contracts bilaterally in association with the touchdown of each foot (Shapiro and Jungers 1994). This biphasic pattern, common to other mammals as well, serves to stabilize the trunk and, significantly, appears to represent a basic mammalian function of back muscles (Schilling 2011). In addition, similarities in activity patterns of back muscles between quadrupedalism and bipedalism among hominoids (and between humans and nonhuman hominoids during bipedalism) are suggestive of a basic conservation of back muscle function in evolution (Shapiro and Jungers 1988). More research is needed to document back muscle activity patterns during other locomotor behaviors such as climbing, arm swinging, or other suspensory behaviors (see also Hurov 1982; Shapiro 1991).

In addition to insights that can be gained from comparative anatomy or electromyography, there are other aspects of muscles that can be informative functionally and from a comparative perspective, such as muscle architecture and muscle fiber type (Perry and Prufrock 2018). Analyses of muscle fiber architecture involve estimates of muscle mass, fiber length, and pennation angle, from which muscle physiological cross-sectional area (PCSA) can be estimated (Gans 1982; Lieber and Fridén 2000). Fiber length is proportional to maximum muscle excursion and contraction velocity (Bodine et al. 1982) while PCSA is proportional to the maximum force that a muscle can generate (Powell et al. 1984). Because most muscles in the body have some degree of pennation, anatomical cross-sectional area, which assumes all muscles are parallel-fibered and estimates cross-sectional area as a

volume, is thus not equivalent to PCSA: for a given volume of muscle, shorter, more pennate fibers have higher PCSAs than muscles with long, parallel fibers.

Epaxial muscle architecture has not been well studied among nonhuman primates or other mammals (but see Webster et al. 2014; Huq et al. 2015; García Liñeiro et al. 2017, 2018). However, a recent study of back muscle fiber architecture in *Galago senegalensis* and *Nycticebus coucang* (Huq et al. 2015) found that although these two species do not differ in relative PCSA, the back muscles of *G. senegalensis*, a specialized leaper, are structured to emphasize excursion and contraction velocity (longer, less pennate fibers), compared to the shorter, more pennate fibers of the slower, suspensory *N. coucang*. Some studies have addressed epaxial muscle architecture in humans (e.g., Delp et al. 2001; Ward et al. 2009; Stark et al. 2013), but not in a comparative or evolutionary context. For example, Stark et al. (2013) found that human iliocostalis and especially longissimus are structured to produce more force (larger volumes) and a wider range of motion (longer fascicles) compared to spinalis or multifidus, and Ward et al. (2009) found that human multifidus is structured for a stabilizing role, with high PCSA and low fiber length to muscle length ratio. To date, there have been no studies of nonhuman hominoid back muscle architecture despite the fact that reduced *anatomical* cross-sectional area of back muscles in hominoids (associated with derived lumbar morphology) has played a prominent role in discussions of hominoid lumbar functional morphology and evolution. However, as noted above, anatomical cross-sectional area is not likely to correspond to PCSA (Lieber and Fridén 2000), and PCSA has a more direct relationship with a muscle's maximum force-generating capacity. Therefore, our understanding of the function and evolution of the hominoid lumbar region would certainly benefit from an analysis of epaxial muscle architecture in nonhuman hominoids compared to that of other primates.

Skeletal muscle fibers are categorized into types that vary in their physiological properties, such as speed of shortening and resistance to fatigue. There are four main fiber types expressed in adult postcranial mammalian muscles. Type 1 fibers contract slowly and are fatigue resistant. In comparison, Type 2 fibers contract more quickly with several subtypes that vary in their fatigability (Lindstedt et al. 1998; Schiaffino and Reggiani 2011; Schaeffer and Lindstedt 2013). Type 1 fibers tend to predominate in more deeply located muscles or in deeper layers of individual muscles and are associated with repetitive or postural functions. Type 2 fibers are usually located more superficially and are associated with production or restriction of fast movements (Kernell 1998). This deep to superficial arrangement of Type 1 to Type 2 fibers, respectively, has been documented for the lumbar perivertebral muscles of some nonhominoid primates (lemurs; Neufuss et al. 2014; *Galago*/*Loris*; Huq et al. 2018; cercopithecoids; Yokoyama 1982; Bagnall et al. 1983; Ford et al. 1986; Kojima and Okada 1996), consistent with what appears to be the ancestral mammalian condition (Schilling et al. 2005; Schilling 2009, 2011). In contrast, in hominoids, the lumbar trunk muscles each contain about a 50–50 ratio of Type 1 to Type 2 fiber types, distributed throughout the muscle (Hesse et al. 2013; Neufuss et al. 2014), indicating that each muscle has both stabilizing and mobilizing capabilities. Hominoid back muscle fiber-type patterns are considered to be derived,

associated with the functional "versatility" presumably required for orthograde positional behaviors (Neufuss et al. 2014). It would be informative to investigate whether similar back muscle fiber-type patterns are exhibited by other orthograde primates (e.g., atelids, indriids) or nonprimate mammals (e.g., koalas, pandas). Moreover, although all hominoids fit the general pattern of homogeneity of fiber-type distribution in their perivertebral muscles, subtle interspecific differences are intriguing. For example, compared to other hominoids, gibbons and especially orangutans have relatively higher percentages of slow (Type 1) fibers overall, possibly reflecting the need for increased fatigue resistance in brachiation (gibbons) or cautious suspensory locomotion (orangutans) (Neufuss et al. 2014). *Galago senegalensis* and *Nycticebus coucang* have also been shown to differ in relative percentages of fiber types in accordance with their distinctive locomotor behaviors (Huq et al. 2018). An expanded analysis of back muscle fiber typing across a broader comparative primate sample would be a promising avenue of research for fully understanding the function of the primate lumbar region in general and the hominoid lumbar region in particular.

4.4 The Evolution of the Hominoid Body Plan

Recently, the sequence in which features of the hominoid trunk presumably evolved has been reassessed, in different ways. For example, in contrast to the traditional view, in which lumbar reduction and dorsal shifting of transverse processes were selected for as adaptations to hominoid posture and locomotion (along with changes in thorax shape and scapular position), Lovejoy, McCollum, and colleagues (Lovejoy et al. 2009; McCollum et al. 2010; Lovejoy and McCollum 2010) view the distinctive position of the lumbar transverse processes in hominoids as a *by-product* of restructuring of the thorax and shoulder in hominoid evolution. According to these researchers, it was the invagination of the thoracic vertebral column into the thorax that led to both the repositioning of the scapulae more dorsally and the dorsal placement of the lumbar transverse processes. Once the transverse processes shifted dorsally, epaxial muscles necessarily reduced in cross-sectional area and had less force available for stabilizing the lower spine. As a consequence, osteological features evolved to replace the role of muscles in stabilizing the spine—that is, the lumbar spine reduced in length and became osteologically "stiffer." Thus, lumbar region length reduction evolved *subsequent to, and as a result of,* the changes in transverse process position and concomitant reduction in size of epaxial muscles, rather than both lumbar reduction and transverse process placement being directly selected for initially as part of a broader functional complex. Lovejoy, McCollum, and colleagues (Lovejoy et al. 2009; McCollum et al. 2010; Lovejoy and McCollum 2010) view this scenario of morphological transitions as supporting evidence for the likelihood of homoplasy of lumbar shortening among hominoids, a consequence of independent adaptations for suspensory locomotion that required lumbar stability (from a longer-backed common ancestor). It should be noted though that currently

there is no consensus as to the condition of the hominoid (or *Pan-Homo*) last common ancestor with respect to lumbar region length or locomotor behavior (e.g., Haeusler et al. 2002; McCollum et al. 2010; Williams 2012b; Williams and Russo 2015; Williams et al. 2016; Thompson and Almécija 2017).

Another way in which traditional views of the hominoid body plan have been reconsidered has to do with the relationships between the thorax and pelvis, with the hominoid epaxial muscle condition playing an important role. It has long been assumed that the broadening of the thorax in hominoids and its effects on scapular position and shoulder mobility account for what appears to be the relatively broader and more coronally oriented ilia of hominoids compared to those of other anthropoids. That is, the shape and orientation of the ilia in hominoids is thought to have evolved to "mirror" the transversely broad thorax, so that musculature attaching between pelvis and thorax would lie in the same plane (e.g., Schultz 1961; Benton 1967, 1974; Ward 1993). Recent research has provided a new perspective on the relationships among the thorax, lumbar spine, and pelvis. Using 3D geometric morphometric analyses, Middleton et al. (2017) and Ward et al. (2018) provided a more nuanced understanding of the morphological differences between the ilia of apes and monkeys (platyrrhines as well as cercopithecoids), with key differences focused on the dorsal aspect of the pelvis. They found that while overall the iliac blades are more coronally oriented in apes, the iliac fossae lie in the same orientation in both apes and monkeys. Thus, the more coronal orientation of the iliac blades in apes is brought about not by an angular "rotation" but by geometric changes (i.e., narrower iliac tuberosities and sacrum in hominoids) that brought the iliac blades in hominoids closer to the midline dorsally, but not ventrally, compared to monkeys. Importantly, Middleton et al. (2017) and Ward et al. (2018) consider the hominoid pelvic condition to be the result not of thorax shape, but of the reduction in length and stiffening of the lumbar spine, which was accompanied by the dorsal shift of the transverse processes, reduction in epaxial muscle mass, and narrowing of the sacrum. In other words, it was *changes in the lower spine, not in the thorax,* that led to pelvic differences between hominoids and monkeys. In sum, Middleton et al. (2017) and Ward et al. (2018) view the lumbar spinal complex as the primary influence on hominoid pelvic morphology, whereas Lovejoy, McCollum, and colleagues (Lovejoy et al. 2009; McCollum et al. 2010; Lovejoy and McCollum 2010) view the hominoid thorax as a primary influence on the lumbar spinal complex, by way of the thorax's influence on lumbar transverse process position and orientation. These two views are not mutually exclusive—the thorax could have influenced the changes in the lumbar spine (Lovejoy et al. 2009; McCollum et al. 2010; Lovejoy and McCollum 2010), and then the changes in the lumbar spine could have in turn influenced the morphology of the ilium (Middleton et al. 2017; Ward et al. 2018). Nevertheless, both views emphasize that the placement of transverse processes and associated reduction of epaxial muscle mass had impacts on other aspects of lumbar osteology as well as on pelvic morphology, highlighting the importance of the lumbar vertebrae for understanding hominoid postural/locomotor morphology and adaptation.

4.5 Conclusions

The highly distinctive lumbar morphology of hominoids has long been functionally linked to the spinal stability necessitated by orthograde/antipronograde postures in combination with the variety of forelimb-dominated, suspensory locomotor behaviors characteristic of hominoids. The consistent documentation of lumbar morphological convergence among hominoids, nonhominoid primates, and nonprimate mammals that engage in comparable positional behaviors has strengthened the presumed functional link between lumbar skeletal features, control of trunk movements, and resistance to bending or buckling. However, there is much more research to be done before we fully understand the functional morphology of the hominoid lumbar region. For example, lumbar "rigidity" is rarely tested directly, and at least one recent biomechanical study has suggested that the ape spine may not be as rigid as often presumed. In addition, although it is clear that evolutionary changes in lumbar morphology affected the size and attachment of back musculature, only limited research is available on hominoid back muscle function as revealed by electromyography, or comparative analyses of muscle architecture and fiber typing. Future work on the biomechanics of the lumbar spine and the functional attributes of its associated musculature will greatly enhance our understanding of the evolution of this key anatomical region in hominoids.

Acknowledgments We wish to thank Ella Been, Asier Gómez-Olivencia, and Patricia Kramer for inviting us to contribute to this volume and for providing comments, along with those of the anonymous reviewer, that greatly improved the manuscript. We also thank Andrea Taylor for very helpful discussion and feedback on muscle architecture and Scott Williams for surface scans used in Figs. 4.1, 4.3, and 4.4.

References

Andrews P, Groves CP (1976) Gibbons and brachiation. In: Gibbon and Siamang, vol 4. Karger, Basel, pp 167–218

Ankel F (1972) Vertebral morphology of fossil and extant primates. In: Tuttle R (ed) The functional and evolutionary biology of primates. Aldine, Chicago, pp 223–240

Bagnall KM, Ford DM, McFadden KD, Greenhill BJ, Raso VJ (1983) A comparison of vertebral muscle fiber characteristics between human and monkey tissue. Cells Tissues Organs 117:51–57

Been E, Gómez-Olivencia A, Kramer PA (2012) Lumbar lordosis of extinct hominins. Am J Phys Anthropol 147:64–77

Benefit BR, McCrossin ML (1995) Miocene hominoids and hominid origins. Annu Rev Anthropol 24:237–256

Benton RS (1967) Morphological evidence for adaptations within the epaxial region of the primates. In: Vagtborg H (ed) The baboon in medical research, vol 2. University of Texas Press, Austin, TX, pp 201–216

Benton RS (1974) Structural patterns in the Pongidae and Cercopithecidae. Yearb Phys Anthropol 18:65–88

Bodine SC, Roy RR, Meadows DA, Zernicke RF, Sacks RD, Fournier M, Edgerton VR (1982) Architectural, histochemical, and contractile characteristics of a unique biarticular muscle: the cat semitendinosus. J Neurophysiol 48:192–201

Boszczyk BM, Boszczyk AA, Putz R (2001) Comparative and functional anatomy of the mammalian lumbar spine. Anat Rec 264:157–168

Burke AC, Nelson CE, Morgan BA, Tabin C (1995) Hox genes and the evolution of vertebrate axial morphology. Development 121:333–346

Cartmill M, Brown K (2017) Posture, locomotion and bipedality: the case of the gerenuk (*Litocranius walleri*). In: Marom A, Hovers E (eds) Human paleontology and prehistory: contributions in honor of Yoel Rak. Springer, Cham, pp 53–70

Cartmill M, Milton K (1977) The lorisiform wrist joint and the evolution of "brachiating" adaptations in the Hominoidea. Am J Phys Anthropol 47:249–272

Crompton R, Vereecke E, Thorpe S (2008) Locomotion and posture from the common hominoid ancestor to fully modern hominins, with special reference to the last common panin/hominin ancestor. J Anat 212:501–543

Davis PR (1961) Human lower lumbar vertebrae: some mechanical and osteological considerations. J Anat 95:337

Delp SL, Suryanarayanan S, Murray WM, Uhlir J, Triolo RJ (2001) Architecture of the rectus abdominis, quadratus lumborum, and erector spinae. J Biomech 34:371–375

Elftman HO (1932) The evolution of the pelvic floor of primates. Am J Anat 51:307–346

Erikson GE (1963) Brachiation in New World monkeys and in anthropoid apes. Symp Zool Soc Lond 10:135–164

Filler AG (2007a) Homeotic evolution in the mammalia: diversification of therian axial seriation and the morphogenetic basis of human origins. PLoS One 2:e1019

Filler AG (2007b) Emergence and optimization of upright posture among hominiform hominoids and the evolutionary pathophysiology of back pain. Neurosurg Focus 23:E4

Ford DM, Bagnall KM, McFadden KD, Reid DC (1986) A comparison of muscle fiber characteristics at different levels of the vertebral column in the rhesus monkey. Cells Tissues Organs 126:163–166

Gál JM (1993a) Mammalian spinal biomechanics. I. Static and dynamic mechanical properties of intact intervertebral joints. J Exp Biol 174:247–280

Gál JM (1993b) Mammalian spinal biomechanics. II. Intervertebral lesion experiments and mechanisms of bending resistance. J Exp Biol 174:281–297

Galis F, Carrier DR, van Alphen J, van der Mije SD, Van Dooren TJM, Metz JAJ, ten Broek CMA (2014) Fast running restricts evolutionary change of the vertebral column in mammals. Proc Natl Acad Sci USA 111:11401–11406

Gambaryan P (1974) How mammals run: anatomical adaptations. John Wiley and Sons, New York

Gans C (1982) Fiber architecture and muscle function. Exerc Sport Sci Rev 10:160–207

García Liñeiro JA, Graziotti GH, Rodríguez Menéndez JM, Ríos CM, Affricano NO, Victorica CL (2017) Structural and functional characteristics of the thoracolumbar multifidus muscle in horses. J Anat 230:398–406

García Liñeiro JA, Graziotti GH, Rodríguez Menéndez JM, Ríos CM, Affricano NO, Victorica CL (2018) Parameters and functional analysis of the deep epaxial muscles in the thoracic, lumbar and sacral regions of the equine spine. J Anat 233:55–63

Gebo DL (1996) Climbing, brachiation, and terrestrial quadrupedalism: historical precursors of hominid bipedalism. Am J Phys Anthropol 101:55–92

Granatosky MC, Lemelin P, Chester SGB, Pampush JD, Schmitt D (2014a) Functional and evolutionary aspects of axial stability in euarchontans and other mammals. Journal of Morphol 275:313–327

Granatosky MC, Miller CE, Boyer DM, Schmitt D (2014b) Lumbar vertebral morphology of flying, gliding, and suspensory mammals: implications for the locomotor behavior of the subfossil lemurs *Palaeopropithecus* and *Babakotia*. J Hum Evol 75:40–52

Haeusler M, Martelli SA, Boeni T (2002) Vertebrae numbers of the early hominid lumbar spine. J Hum Evol 43:621–643

Halpert AP, Jenkins FA Jr, Franks H (1987) Structure and scaling of the lumbar vertebrae in African bovids (Mammalia: Artiodactyla). J Zool 211:239–258
Harrison T (1986) A reassessment of the phylogenetic relationships of *Oreopithecus bambolii* Gervais. J Hum Evol 15:541–583
Hesse B, Fröber R, Fischer MS, Schilling N (2013) Functional differentiation of the human lumbar perivertebral musculature revisited by means of muscle fibre type composition. Ann Anat 195:570–580
Howell A, Straus W (1933) The muscular system. In: Hartman C, Straus W (eds) The anatomy of the rhesus monkey (*Macaca mulatta*). Williams and Wilkins, Baltimore, pp 89–175
Hunt K (1991) Mechanical implications of chimpanzee positional behavior. Am J Phys Anthropol 86:521–536
Huq E, Wall CE, Taylor AB (2015) Epaxial muscle fiber architecture favors enhanced excursion and power in the leaper *Galago senegalensis*. J Anat 227:524–540
Huq E, Taylor AB, Su Z, Wall CE (2018) Fiber type composition of epaxial muscles is geared toward facilitating rapid spinal extension in the leaper *Galago senegalensis*. Am J Phys Anthropol 166:95–106
Hurov J (1982) Surface EMG of superficial back mm. in human children: functions during vertical climbing and suspension and implications for the evolution of hominid bipedalism. J Hum Evol 11:117–130
Johnson SE, Shapiro LJ (1998) Positional behavior and vertebral morphology in atelines and cebines. Am J Phys Anthropol 105:333–354
Jolly CJ (1970) The seed-eaters: a new model of hominid differentiation based on a baboon analogy. Man 5:1–26
Jones KE, Angielczyk KD, Polly PD, Head JJ, Fernandez V, Lungmus JK, Tulga S, Pierce SE (2018) Fossils reveal the complex evolutionary history of the mammalian regionalized spine. Science 361:1249–1252
Jungers WL (1984) Scaling of the hominoid locomotor skeleton with special reference to lesser apes. In: Preuschoft H, Chivers D, Brockelman W, Creel N (eds) The lesser apes. Edinburgh University Press, Edinburgh, pp 146–169
Keith A (1902) The extent to which the posterior segments of the body have been transmuted and suppressed in the evolution of man and allied primates. J Anat Physiol 37:18–40
Keith A (1923) Man's posture: its evolution and disorders. Br Med J 1:587–590
Keith A (1940) Fifty years ago. Am J Phys Anthropol 26:251–267
Kernell D (1998) Muscle regionalization. Can J Appl Physiol 23:1–22
Kessel M, Gruss P (1991) Homeotic transformations of murine vertebrae and concomitant alteration of Hox codes induced by retinoic acid. Cell 67:89–104
Kojima R, Okada M (1996) Distribution of muscle fibre types in the thoracic and lumbar epaxial muscles of Japanese macaques (*Macaca fuscata*). Folia Primatol (Basel) 66:38–43
Latimer B, Ward CV (1993) The thoracic and lumbar vertebrae. In: Walker A, Leakey R (eds) The Nariokotome *Homo erectus* Skeleton. Harvard University Press, Cambridge, pp 266–293
Lemelin P (1995) Comparative and functional myology of the prehensile tail in New World monkeys. J Morphol 224:351–368
Lieber RL, Fridén J (2000) Functional and clinical significance of skeletal muscle architecture. Muscle Nerve 23:1647–1666
Lindstedt SL, McGlothlin T, Percy E, Pifer J (1998) Task-specific design of skeletal muscle: balancing muscle structural composition. Comp Biochem Physiol B Biochem Mol Biol 120:35–40
Lovejoy CO (2005) The natural history of human gait and posture: Part 1. Spine and pelvis. Gait Posture 21:95–112
Lovejoy CO, McCollum MA (2010) Spinopelvic pathways to bipedality: why no hominids ever relied on a bent-hip–bent-knee gait. Philos Trans R Soc Lond B Biol Sci 365:3289–3299
Lovejoy CO, Suwa G, Simpson SW, Matternes JH, White TD (2009) The great divides: *Ardipithecus ramidus* reveals the postcrania of our last common ancestors with African apes. Science 326:73–106

Machnicki AL, Spurlock LB, Strier KB, Reno PL, Lovejoy CO (2016) First steps of bipedality in hominids: evidence from the atelid and proconsulid pelvis. PeerJ 4:e1521

MacLatchy L, Gebo D, Kityo R, Pilbeam DR (2000) Postcranial functional morphology of *Morotopithecus bishopi*, with implications for the evolution of modern ape locomotion. J Hum Evol 39:159–183

Mallo M, Wellik DM, Deschamps J (2010) Hox genes and regional patterning of the vertebrate body plan. Dev Biol 344:7–15

Masharawi Y, Rothschild B, Dar G, Peleg S, Robinson D, Been E, Hershkovitz I (2004) Facet orientation in the thoracolumbar spine: three-dimensional anatomic and biomechanical analysis. Spine 29:1755–1763

Masharawi YM, Alperovitch-Najenson D, Steinberg N, Dar G, Peleg S, Rothschild B, Salame K, Hershkovitz I (2007a) Lumbar facet orientation in spondylolysis: a skeletal study. Spine 32:E176–E180

Masharawi Y, Dar G, Peleg S, Steinberg N, Alperovitch-Najenson D, Salame K, Hershkovitz I (2007b) Lumbar facet anatomy changes in spondylolysis: a comparative skeletal study. Eur Spine J 16:993–999

McCollum MA, Rosenman BA, Suwa G, Meindl RS, Lovejoy CO (2010) The vertebral formula of the last common ancestor of African apes and humans. J Exp Zool B Mol Dev Evol 314:123–134

McNulty KP, Begun DR, Kelley J, Manthi FK, Mbua EN (2015) A systematic revision of *Proconsul* with the description of a new genus of early Miocene hominoid. J Hum Evol 84:42–61

Middleton ER, Winkler ZJ, Hammond AS, Plavcan JM, Ward CV (2017) Determinants of iliac blade orientation in anthropoid primates. Anat Rec 300:810–827

Mivart SG (1865) Contributions towards a more complete knowledge of the axial skeleton in the primates. Proc Zool Soc London 33:545–592

Nakatsukasa M (2003) Definitive evidence for tail loss in *Nacholapithecus*, an East African Miocene hominoid. J Hum Evol 45:179–186

Nakatsukasa M, Hirose Y (2003) Scaling of lumbar vertebrae in anthropoids and implications for evolution of the hominoid axial skeleton. Primates 44:127–135

Nakatsukasa M, Kunimatsu Y (2009) *Nacholapithecus* and its importance for understanding hominoid evolution. Evol Anthropol Issues News Rev 18:103–119

Nalley TK, Grider-Potter N (2019) Vertebral morphology in relation to head posture and locomotion: the cervical spine. In: Been E, Gómez-Olivencia A, Kramer PA (eds) Spinal evolution: morphology, function, and pathology of the spine in hominoid evolution. Springer, New York, pp 35–50

Neufuss J, Hesse B, Thorpe SKS, Vereecke EE, D'Aout K, Fischer MS, Schilling N (2014) Fibre type composition in the lumbar perivertebral muscles of primates: implications for the evolution of orthogrady in hominoids. J Anat 224:113–131

Odgers PNB (1933) The lumbar and lumbo-sacral diarthrodial joints. J Anat 67:301

Perry JM, Prufrock KA (2018) Muscle functional morphology in paleobiology: the past, present, and future of "paleomyology". Anat Rec 301:538–555

Pilbeam D (2004) The anthropoid postcranial axial skeleton: comments on development, variation, and evolution. J Exp Zool B Mol Dev Evol 302:241–267

Powell PL, Roy RR, Kanim P, Bello MA, Edgerton VR (1984) Predictability of skeletal muscle tension from architectural determinations in guinea pig hindlimbs. J Appl Physiol 57:1715–1721

Reno PL (2014) Genetic and developmental basis for parallel evolution and its significance for hominoid evolution. Evol Anthropol Issues News Rev 23:188–200

Rose MD (1975) Functional proportions of primate lumbar vertebral bodies. J Hum Evol 4:21–38

Russo GA (2010) Prezygapophyseal articular facet shape in the catarrhine thoracolumbar vertebral column. Am J Phys Anthropol 142:600–612

Russo GA, Shapiro LJ (2011) Morphological correlates of tail length in the catarrhine sacrum. J Hum Evol 61:223–232

Russo GA, Williams SA (2015) Giant pandas (Carnivora: *Ailuropoda melanoleuca*) and living hominoids converge on lumbar vertebral adaptations to orthograde trunk posture. J Hum Evol 88:160–179

Sanders WJ (1998) Comparative morphometric study of the australopithecine vertebral series Stw-H8/H41. J Hum Evol 34:249–302
Sanders WJ, Bodenbender BE (1994) Morphometric analysis of lumbar vertebra UMP 67-28: implications for spinal function and phylogeny of the Miocene Moroto hominoid. J Hum Evol 26:203–237
Sargis EJ (2001) A preliminary qualitative analysis of the axial skeleton of tupaiids (Mammalia, Scandentia): functional morphology and phylogenetic implications. J Zool 253:473–483
Sarmiento EE (1987) The phylogenetic position of *Oreopithecus* and its significance in the origin of the Hominoidea. Am Mus Novit 2881:1–44
Sarmiento EE (1998) Generalized quadrupeds, committed bipeds, and the shift to open habitats: an evolutionary model of hominid divergence. Am Mus Novit 3250:1–78
Schaeffer PJ, Lindstedt SL (2013) How animals move: comparative lessons on animal locomotion. Compr Physiol 3:289–314
Schiaffino S, Reggiani C (2011) Fiber types in mammalian skeletal muscles. Physiol Rev 91:1447–1531
Schilling N (2009) Metabolic profile of the perivertebral muscles in small therian mammals: implications for the evolution of the mammalian trunk musculature. Zoology 112:279–304
Schilling N (2011) Evolution of the axial system in craniates: morphology and function of the perivertebral musculature. Front Zool 8:4
Schilling N, Arnold D, Wagner H, Fischer MS (2005) Evolutionary aspects and muscular properties of the trunk—implications for human low back pain. Pathophysiology 12:233–242
Schultz AH (1950) The physical distinctions of man. Proc Am Philos Soc 94:428–449
Schultz A (1961) Vertebral column and thorax. Primatologia 4:1–66
Shapiro LJ (1991) Functional morphology of the primate spine with special reference to orthograde posture and bipedal locomotion. PhD Thesis, State University of New York Stony Brook
Shapiro LJ (1993a) Functional morphology of the vertebral column in primates. In: Gebo D (ed) Postcranial adaptation in nonhuman primates. Northern Illinois University Press, DeKalb, pp 121–149
Shapiro LJ (1993b) Evaluation of "unique" aspects of human vertebral bodies and pedicles with a consideration of *Australopithecus africanus*. J Hum Evol 25:433–470
Shapiro LJ (1995) Functional morphology of indrid lumbar vertebrae. Am J Phys Anthropol 98:323–342
Shapiro LJ (2007) Morphological and functional differentiation in the lumbar spine of lorisids and galagids. Am J Primatol 69:86–102
Shapiro LJ, Jungers WL (1988) Back muscle function during bipedal walking in chimpanzee and gibbon: implications for the evolution of human locomotion. Am J Phys Anthropol 77:201–212
Shapiro LJ, Jungers WL (1994) Electromyography of back muscles during quadrupedal and bipedal walking in primates. Am J Phys Anthropol 93:491–504
Shapiro LJ, Kemp AD (2019) Functional and developmental influences on intraspecific variation in catarrhine vertebrae. Am J Phys Anthropol 168:131–144
Shapiro LJ, Simons C (2002) Functional aspects of strepsirrhine lumbar vertebral bodies and spinous processes. J Hum Evol 42:753–783
Shapiro LJ, Seiffert CV, Godfrey LR, Jungers WL, Simons EL, Randria GF (2005) Morphometric analysis of lumbar vertebrae in extinct Malagasy strepsirrhines. Am J Phys Anthropol 128:823–839
Slijper E (1946) Comparative biologic anatomical investigations on the vertebral column and spinal musculature of mammals, vol 17. North-Holland Publishing Company, Amsterdam, pp 1–128. Tweede Sectie
Stark H, Fröber R, Schilling N (2013) Intramuscular architecture of the autochthonous back muscles in humans. J Anat 222:214–222
Straus WL, Wislocki GB (1932) On certain similarities between sloths and slow lemurs. Bull Mus Comp Zool Harv Collect 74:45–56
Struthers J (1892) On the articular processes of the vertebrae in the gorilla compared with those in man, and on cost-vertebral variation in the gorilla. J Anat 27:131–138

Thompson NE, Almécija S (2017) The evolution of vertebral formulae in Hominoidea. J Hum Evol 110:18–36
Thompson NE, Demes B, O'Neill MC, Holowka NB, Larson SG (2015) Surprising trunk rotational capabilities in chimpanzees and implications for bipedal walking proficiency in early hominins. Nat Commun 6:8416
Townsend HGG, Leach DH (1984) Relationship between intervertebral joint morphology and mobility in the equine thoracolumbar spine. Equine Vet J 16:461–465
Tuttle RH (1975) Parallelism, brachiation, and hominid phylogeny. In: Luckett WP, Szalay FS (eds) The phylogeny of primates: a multidisciplinary approach. Plenum, New York, pp 447–480
Tuttle RH, Basmajian JV (1978) Electromyography of pongid shoulder muscles. III. Quadrupedal positional behavior. Am J Phys Anthropol 49:57–69
Ward CV (1993) Torso morphology and locomotion in *Proconsul nyanzae*. Am J Phys Anthropol 92:291–328
Ward CV (2014) Postcranial and locomotor adaptations of hominoids. In: Henke W, Tattersall I (eds) Handbook of paleoanthropology. Springer-Verlag, Berlin, pp 1011–1030
Ward CV, Latimer B (2005) Human evolution and the development of spondylolysis. Spine 30:1808–1814
Ward SR, Kim CW, Eng CM, Gottschalk LJ, Tomiya A, Garfin SR, Lieber RL (2009) Architectural analysis and intraoperative measurements demonstrate the unique design of the multifidus muscle for lumbar spine stability. J Bone Joint Surg Am 91:176–185
Ward CV, Maddux SD, Middleton ER (2018) Three-dimensional anatomy of the anthropoid bony pelvis. Am J Phys Anthropol 166:3–25
Washburn S (1963) Behavior and human evolution. In: Washburn S (ed) Classification and human evolution. Aldine, Chicago
Washburn S, Buettner-Janusch J (1952) The definition of thoracic and lumbar vertebrae. Am J Phys Anthropol 10:251–252
Webster EL, Hudson PE, Channon SB (2014) Comparative functional anatomy of the epaxial musculature of dogs (*Canis familiaris*) bred for sprinting vs. fighting. J Anat 225:317–327
Wellik DM (2009) Hox genes and vertebrate axial pattern. Curr Top Dev Biol 88:257–278
Wellik DM, Capecchi MR (2003) Hox10 and Hox11 genes are required to globally pattern the mammalian skeleton. Science 301:363–367
Whitcome KK (2012) Functional implications of variation in lumbar vertebral count among hominins. J Hum Evol 62:486–497
Whitcome KK, Shapiro LJ, Lieberman DE (2007) Fetal load and the evolution of lumbar lordosis in bipedal hominins. Nature 450:1075–1078
Williams SA (2012a) Placement of the diaphragmatic vertebra in catarrhines: implications for the evolution of dorsostability in hominoids and bipedalism in hominins. Am J Phys Anthropol 148:111–122
Williams SA (2012b) Variation in anthropoid vertebral formulae: implications for homology and homoplasy in hominoid evolution. J Exp Zool B Mol Dev Evol 318:134–147
Williams SA, Gómez-Olivencia A, Pilbeam D (2019) Numbers of Vertebrae in Hominoid Evolution. In: Been E, Gómez-Olivencia A, Kramer PA (eds) Spinal evolution: morphology,function, and pathology of the spine in hominoid evolution. Springer, New York, pp 97–124
Williams SA, Middleton ER, Villamil CI, Shattuck MR (2016) Vertebral numbers and human evolution. Am J Phys Anthropol 159:19–36
Williams SA, Russo GA (2015) Evolution of the hominoid vertebral column: the long and the short of it. Evol Anthropol Issues News Rev 24:15–32
Yokoyama Y (1982) Analyses on the fiber compositions of the lumbar back muscles in mammals. Nihon Seikeigeka Gakkai Zasshi 56:579–594

Chapter 5
Miocene Ape Spinal Morphology: The Evolution of Orthogrady

Masato Nakatsukasa

5.1 Introduction

The postcranial skeleton of living apes is characterized by a number of derived features that are attributable to forelimb-dominated orthograde positional behavior such as suspension or vertical climbing (Schultz 1930, 1961; Erikson 1963; Tuttle 1975; Andrews and Groves 1976; Larson 1998). Their axial skeleton commonly exhibits specializations such as an increase of sacral vertebrae concomitant with a decrease of lumbar vertebrae, loss of an external tail, spinal invagination into the thoracic and abdominal cavities, and craniocaudally short and dorsoventrally deep lumbar vertebral bodies (Table 5.1, Fig. 5.1; Benton 1967). Similar specializations, except tail loss, are also evolved in ateline monkeys (Schultz 1961; Erikson 1963; Johnson and Shapiro 1998; Larson 1998), reinforcing their link to forelimb-dominated orthograde positional behavior.

So far, about 20 genera of Miocene apes are known from AfroArabia and about 15 from Eurasia (Andrews 2016; Begun 2016). However, tracing the origins and evolutionary history of the living apes' orthogrady among these fossil taxa is not straightforward because of chronological and geographical bias of fossil representation and uncertainty of their phylogeny. Furthermore, fossil vertebral specimens are rare compared with limb bones. Fossil vertebral specimens are available in only eight species of apes, and their abundance and preservation vary across these species (Table 5.2). Therefore, sections of this chapter are organized to follow each anatomical character, unlike the usual review that describes morphology of each fossil taxon in the chronological order. Four major traits, which are key to the study of the spinal evolution in apes, are discussed along with several other traits (Table 5.1). Since there are diverse

M. Nakatsukasa (✉)
Laboratory of Physical Anthropology, Graduate School of Science, Kyoto University, Kyoto, Japan
e-mail: nakatsuk@anthro.zool.kyoto-u.ac.jp

E. Been et al. (eds.), *Spinal Evolution*,
https://doi.org/10.1007/978-3-030-19349-2_5

Table 5.1 Spinal characters of living apes discussed in this chapter and their function

Character	Function
Vertebral count: fewer in the lumbar spine and more in the sacrum	Dorsostability of lumbar spine (e.g., Benton 1967; Jungers 1984; Ward 1993; Lovejoy 2005; Lovejoy et al. 2009b)
Tail loss	Not clear
Spinal invagination: rib curvature, position of the lumbar transverse process	Broadening of the thorax to set the scapular glenoid laterally, which enables more versatile forelimb use (e.g., Schultz 1961; Benton 1967; Lovejoy 2005; Lovejoy et al. 2009a; Ward 2007)
Post-thoracic/lumbar vertebral body shape: craniocaudally short, dorsoventrally deep	Dorsostability of lumbar spine (e.g., Benton 1967; Erikson 1963; Sanders and Bodenbender 1994; Johnson and Shapiro 1998)
Other traits: Reduction of the accessory processes More caudal position of the transitional vertebra in the thoracic series Loss of median ventral keel of lumbar vertebral body More caudal orientation of the lumbar spinous process Enlargement of the lumbar vertebral body relative to body mass	Miscellaneous

opinions concerning which extinct non-cercopithecoid catarrhines to be included in the Hominoidea, the general term "ape" is used in this chapter, including both undoubted and potential hominoid species.

5.2 Fossils

The genus *Ekembo* is known from Kisingiri localities in Rusinga and Mfwangano Islands in Lake Victoria, western Kenya, and includes two species: *E. nyanzae* and *E. heseloni* (Walker 1997; Ward 1998; McNulty et al. 2015). The Kisingiri localities span 20–17 Ma, but most of the vertebral elements have derived from relatively young horizons (18.5–17 Ma). The hypodigm of *E. heseloni* includes a skeleton of juvenile female (KNM-RU 2036) that preserves three lumbar vertebrae (Walker and Pickford 1983). Additional vertebral specimens have been recovered from Kaswanga Primate Site (KPS) in Rusinga Island. A male partial skeleton of *E. nyanzae* (KNM-MW 13142) includes the last thoracic and four lumbar vertebrae and a fragment of sacrum (Fig. 5.2a; Ward 1993; Ward et al. 1993). Body mass (BM) of male *E. heseloni* is estimated as 20 kg or more (Harrison 2010; Nakatsukasa et al. 2016) and that of male *E. nyanzae* 35–40 kg (Rafferty et al. 1995).

Morotopithecus bishopi is an ape discovered at the site Moroto II (20.6 Ma) in eastern Uganda (Gebo et al. 1997). However, there is a claim that *M. bishopi* is a

Fig. 5.1 Lumbar vertebrae (L3) of baboon (left) and chimpanzee (right). White dotted line is drawn along the dorsal border of the vertebral centra. Black dotted lines show the axis of the spinous process. Note cranially pointed border of the spinous process of baboon. Arrow indicates the anapophysis. Not to scale

junior subjective synonym of *Afropithecus turkanensis*, which is known from northern Kenya (Patel and Grossman 2006; also see Harrison (2010) for review). Nonetheless, the Moroto primate assemblage is key to interpreting the evolution of positional behavior in fossil apes because it includes a well-preserved lumbar vertebra (UMP 67.28; Fig. 5.2b) that resembles that of modern apes in some attributes. Besides UMP 67.28, there is a smaller lumbar vertebral body (UMP 68.06; Fig. 5.2c) that may represent the same individual (Pilbeam 1969). BM of *Morotopithecus* is estimated as 34–43 kg from dimensions of UMP 67.28 (Sanders and Bodenbender 1994).

Nacholapithecus kerioi is known from Aka Aithepus Formation (16–15 Ma) at Nachola (Baragoi), northern Kenya (Ishida et al. 1999). Its postcranial anatomy is well-studied owing to a great number of fossils including a male adult skeleton KNM-BG 35250 (Nakatsukasa et al. 1998, 2007; Nakatsukasa and Kunimatsu 2009; Ishida et al. 2004; Kikuchi et al. 2015, 2016). Unfortunately, most of the *Nacholapithecus* fossils have been subjected to plastic deformation. BM of male *Nacholapithecus* is estimated ca. 20 kg (Kikuchi et al. 2018).

Table 5.2 Fossil apes whose vertebral elements are known

Taxon	Age, area	Specimens	Note	Reference
Ekembo heseloni[a]	~17–18.5 Ma, Kenya	KNM-RU 2036	CZ, CY, CD: lumbar vertebrae (none of them is the ultimate lumbar. Probably, aligned in this sequence). CY is the best-preserved one including the dorsal elements and the right transverse process	Walker and Pickford 1983
		KNM-KPS specimens	A number of vertebral specimens have been recovered from the Kaswanga Primate Site (KPS). Most of them are fragmentary and subjected to deformation. Remarkable specimens are V5/V8 (lumbar vertebral body) and V32 (last sacral vertebra)	Ward et al. 1991; Nakatsukasa et al. 2004
Ekembo nyanzae[a]	~17–18.5 Ma, Kenya	KNM-MW 13142	H (last thoracic); I (L1 or 2); J, K (juxtaposing lumbar vertebrae); L (partial lumbar vertebra with the neural arch: probably, ultimate lumbar); M (sacrum: S1–S2)	Ward 1993; Ward et al. 1993
		KNM-RU 5944	Caudal thoracic vertebral body with a detached neural arch	Nakatsukasa et al. 2004
		KNM-RU 18385	Lumbar vertebral body	
Morotopithecus bishopi	20.6 Ma[b], Uganda	Moroto II collection during 1961~1962	UMP 67.28 (well-preserved penultimate lumbar); UMP 68.06 (lumbar vertebral body); UMP 68.07, 68.08 (fragmentary dorsal elements of thoracolumbar vertebra)	Sanders and Bodenbender 1994; Nakatsukasa 2008
Nacholapithecus kerioi	~15–16 Ma, Kenya	KNM-BG 35250	BE (C1); BF (C2); BG (C4~C5); BH, BI, BJ, BW (cranial to middle thoracic vertebrae); BO (transitional vertebra); BP (post-transitional thoracic vertebra); R, P, BQ, BR, BS, BT (lumbar vertebrae)	Nakatsukasa et al. 2007
		KNM-BG 15527, 17826	Lumbar vertebral bodies. KNM-BG 15527 is the only lumbar vertebral body of *Nacholapithecus* which is not subjected to severe plastic deformation	Rose et al. 1996
		KNM-BG 17822, 42753I, 47687A	Partial sacrum	Rose et al. 1996; Kikuchi et al. 2016
		KNM-BG 40949	First coccygeal vertebra	Nakatsukasa et al. 2003a, b
		Additional specimens	13 cervical vertebrae; a caudal thoracic vertebra with a well-preserved spinous process (KNM-BG 42810B) and a lumbar vertebra	Kikuchi et al. 2012, 2015

Equatorius africanus	~15–16 Ma, Kenya	KNM-TH 28860	Y (caudal thoracic); AB (thoracic or lumbar vertebral body)	Sherwood et al. 2002
Otavipithecus namibiensis	~12–13 Ma	#BA 91-104	Atlas	Conroy et al. 1996
Pierolapithecus catalaunicus	~12 Ma, Spain	IPS-21350	IPS-21350-64 (middle lumbar vertebra); −65 (ultimate lumbar vertebral body)	Moyà-Solà et al. 2004
Hispanopithecus laietanus	9.6 Ma, Spain	IPS-18800	IPS-18800.8 (upper thoracic vertebra); IPS-18800.9 (1st or 2nd lumbar vertebra); IPS-18800.6 (penultimate or last lumbar vertebra); IPS-18800.5, 7, 10, 11, 12 (fragmentary lumbar body or neural arch)	Moyà-Solà and Köhler 1996; Susanna et al. 2014
Oreopithecus bambolii	~6.7–9 Ma, Italy	IGF 11778, #50	IGF 11778 (male young adult skeleton with the whole lumbar series); Bac 72 (last three lumbar vertebrae and S1–S2); Bac 50 (sacrum)	Schultz 1960; Straus 1963; Harrison 1991; Köhler and Moyà-Solà 1997; Russo and Shapiro 2013

[a]Previously classified as *Proconsul*

[b]This age as well as the taxonomic validity of *Morotopithecus* is contentious (e.g., Pickford 2002; Patel and Grossman 2006; Harrison 2010)

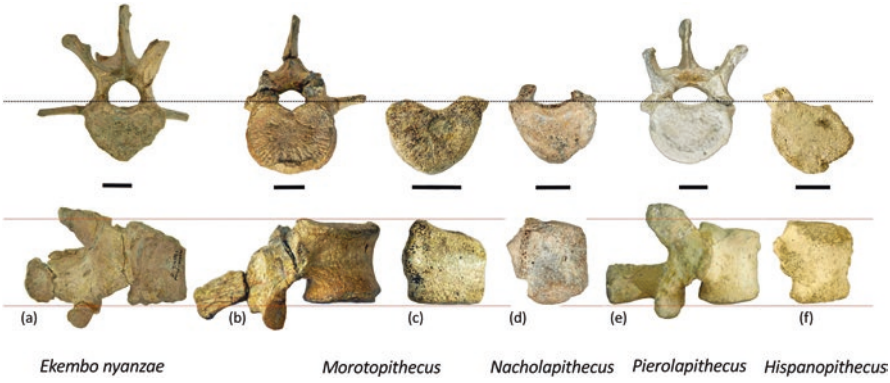

Fig. 5.2 Lumbar vertebra of fossil apes. Left to right, *Ekembo nyanzae* KNM-MW 13142J (**a**), *Morotopithecus* UMP 67.28 (**b**), UMP 68.06 (**c**), *Nacholapithecus* KNM-BG 15527 (**d**), *Pierolapithecus* IPS-21350-64 (**e**), *Hispanopithecus* IPS-18800-9 (**f**). Images of IPS-21350-64 and IPS-18800-9 are reversed for comparative purpose. Images are scaled to a comparable vertebral body length (craniocaudal length on the dorsal side). Cranial surface of the centrum of KNM-MW 13142J is ventrally eroded (Ward et al. 1993). Scale bar = 1 cm

Equatorius africanus (16–15 Ma) is known from sites on Maboko Island in Lake Victoria and the Tugen Hills in Kenya (Benefit and McCrossin 1995; Ward et al. 1999). Two vertebral specimens are included in a male skeleton discovered from the Tugen Hills (KNM-TH 28860; Sherwood et al. 2002). Unfortunately, these vertebrae are badly damaged by postmortem compression. BM of this male is estimated as ca. 27 kg (Ward et al. 1999).

Otavipithecus namibiensis (13–12 Ma) is known from Berg Aukas in the Otavi Mountain region of northern Namibia (Conroy et al. 1992, 1996). An almost complete atlas (#BA 91-104) has been attributed to this species. It approximates an atlas of female *Papio ursinus* (weighing ca. 15 kg) in size (Conroy et al. 1996). BM of *Otavipithecus* is also estimated as 14–20 kg from molar size of the type mandible (probably male) (Conroy et al. 1992).

Pierolapithecus catalaunicus (12 Ma) was discovered at Els Hostalets de Pierola, Catalonia, Spain (Moyà-Solà et al. 2004; Casanovas-Vilar et al. 2011). The holotype IPS-21350 (male skeleton) includes a nearly complete middle lumbar vertebra (IPS-21350-64; Fig. 5.2e) and a partial body of the ultimate lumbar vertebra (IPS-21350-65). In addition to these vertebrae, three ribs are also associated with the holotype, which add insight regarding torso morphology (Moyà-Solà et al. 2004). BM of IPS-21350 is estimated as 30–35 kg from lumbar vertebral body and molar dimensions (Moyà-Solà et al. 2004).

Hispanopithecus laietanus (9.6 Ma) is known from Can Llobateres, Catalonia, Spain (Moyà-Solà and Köhler 1996; Moyà-Solà et al. 2009). A male skeleton of *Hispanopithecus* (IPS-18800) from the locality CLL2 includes several thoracic/lumbar vertebral specimens (Fig. 5.2f; Susanna et al. 2014). BM of IPS-18800 is estimated as ca. 39 kg from femoral head dimensions (Moyà-Solà et al. 2009).

Oreopithecus bambolii (8–7 Ma) is known from Tuscany and Sardinia, Italy (Begun 2002). Information on the spinal morphology is available from a male young

adult skeleton (IGF 11778), an adhered lumbosacral specimen (last three lumbar vertebrae and S1–2: Bac. 72), and an isolated sacrum (Bac. 50) (Schultz 1960; Straus 1963; Harrison 1991; Köhler and Moyà-Solà 1997; Russo and Shapiro 2013). IGF 11778 was discovered in articulated position in lignite, and the caudal half of the spine is well preserved except L4 (which is very fragmentary) and sacrum. BM of IGF 11778 is estimated as 32 kg (Jungers 1987).

5.3 Vertebral Formula

Pilbeam (2004) hypothesized the modal formula of precaudal vertebra in the stem catarrhine as either 7:13:6:3 (cervical:thoracic:lumbar:sacral) or 7:13:7:3 based on living catarrhines' variation. Narita and Kuratani (2005) proposed that a total thoracic and lumbar vertebral number of 19 was the ancestral condition for the primates since this number is common in many mammalian orders (see Williams et al. 2019). This hypothesized condition (six or seven lumbar and three sacral vertebrae) is concordant with the condition in the fossil catarrhine *Epipliopithecus* (15–14 Ma) (Zapfe 1958). In living cercopithecids, dominant formulae are either 7:13:6:3 or 7:12:7:3, with the total precaudal vertebral number of 29 (Schultz and Straus Jr. 1945; Schultz 1961; Williams and Russo 2015). Thus, cercopithecids are conservative. In contrast, living apes have fewer lumbar vertebrae and more sacral vertebrae compared to cercopithecids (Table 5.3). Additionally, the transitional vertebra is

Table 5.3 Precaudal vertebral formula in fossil and living apes[a]

Taxon	Vertebral formula: C-T-L-S	Total number	Note or frequency in living species
Ekembo nyanzae	(7)-(13)-6/7-3	Prob. 29 or 30	Lumbar vertebral count is likely 6. Sacral vertebral count of 3 is tentative.
Nacholapithecus kerioi	(7)-(13)-6/7-3	Prob. 29 or 30	Sacral vertebral count of 3 is tentative.
Oreopithecus bambolii	(7)-(12/13)-5-6	30 or 31	Lumbar and sacral vertebral counts are from different individuals.
Hylobates lar	7-13-5-5 7-13-5-4	30 29	44.8% 21.0%
Symphalangus syndactylus	7-13-5-4 7-13-5-5	29 30	21.5% 18.5%
Pongo pygmaeus	7-12-4-5 7-12-4-6	28 29	37.2% 18.3%
Gorilla gorilla	7-13-4-5 7-13-4-6	29 30	27.9% 23.3%
Pan troglodytes	7-13-4-6 7-13-4-5	30 29	24.6% 24.0%
Pan paniscus	7-13-4-6 7-13-4-7	30 29	22.6% 19.4%
Homo sapiens	7-12-5-5 7-12-5-6	29 30	57.5% 22.1%

[a]Data for living hominoids are from McCollum et al. (2010). Two most frequent formulae are shown. See also Williams et al. 2019

also more caudally located in the thoracic series (Williams 2012; Williams et al. 2016). The reduction of the lumbar vertebral number and the more caudal position of the transitional vertebra are considered to be related to the dorsostability (see below). Here, the lumbar vertebrae are defined as presacral vertebra which do not have a rib.

There are only three species of fossil apes whose precaudal vertebral formula can be estimated: *E. nyanzae*, *Nacholapithecus*, and *Oreopithecus*. A partial skeleton of *E. nyanzae* (KNM-MW 13142) includes several vertebral elements (Ward et al. 1993). KNM-MW 13142H is the last thoracic vertebra, and -I is the first lumbar vertebra (L1). KNM-MW 13142 J and K are juxtaposed lumbar vertebrae and probably an antepenultimate and a penultimate vertebra, respectively. KNM-MW 13142L is a partial lumbar vertebra and, probably, the ultimate lumbar. Ward (1993) inferred that two lumbar vertebrae are missing between KNM-MW 13142I and -J based on the sequential change of lumbar vertebral size and morphology. The lumbar vertebral count of 6 is widely accepted (though 7 is not completely precluded). Although a partial sacrum (S1– S2 segment) is also preserved, it is too fragmentary to estimate the original number of sacral vertebrae.

As for *Nacholapithecus*, the holotype skeleton (KNM-BG 35250) preserves six lumbar vertebrae (Nakatsukasa et al. 2007). Because of preservation issues, it is difficult to decide whether an additional lumbar vertebra was present or not. Thus, Nakatsukasa et al. (2007) proposed that it had either six or seven lumbar vertebrae assuming *Nacholapithecus* retained the primitive catarrhine condition. No complete sacrum is available. However, partial sacral specimens (S1) show relatively strong caudal tapering of the body, like cercopithecids (Fig. 5.3a; Rose et al. 1996; Kikuchi et al. 2016), suggesting a smaller number of sacral vertebrae. However, since *Nacholapithecus* lacked an external tail (see below), its last sacral vertebra could

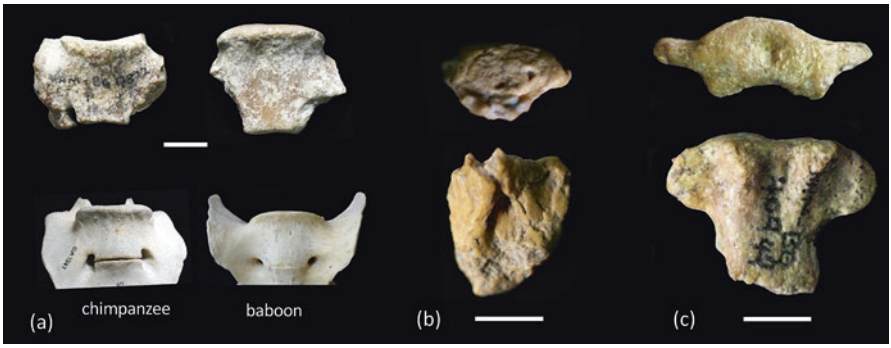

Fig. 5.3 Sacral and coccygeal specimens. (**a**) Sacral fragment (S1) of *Nacholapithecus*. KNM-BG 17822 (left) and KNM-BG 42753I (right) compared to sacrum of chimpanzee and baboon. KNM-BG 17822 is subjected to craniocaudal compression. Scale bar = 1 cm. Chimpanzee and baboon specimens are not to scale. (**b**) Last sacral vertebra of a juvenile *E. heseloni* (KPS V42) in cranial and dorsal view. Scale = 5 mm. (**c**) First coccygeal vertebra of *Nacholapithecus* KNM-BG 40949 in cranial and dorsal view. Scale bar = 5 mm

have been smaller than that of similar-sized cercopithecids. Thus, a sacral vertebral number greater than three is also possible.

The case for *Oreopithecus* is clear. The IGF 11778 skeleton possesses five lumbar vertebrae. An isolated sacrum (#50) is composed of six sacral vertebrae (Straus 1963). This vertebral formula of *Oreopithecus* is derived and, comparatively, (living) ape-like (Table 5.3). However, a combination of five lumbar and six sacral vertebrae is rare in living apes (Pilbeam 2004; McCollum et al. 2010) although a caveat should be noted that the *Oreopithecus* formula is derived from lumbar and sacral vertebral counts obtained from different individuals.

Whether a fossil primate had either a long back or short back can be inferred even if only a fraction of the whole lumbar series is preserved. The magnitude of ventral wedging of the lumbar vertebral body (especially more cranially) is stronger in cercopithecid monkeys and lower in great apes, with hylobatids being intermediate, although the ranges of monkeys and great apes overlap (Ward et al. 1993). Wedged lumbar vertebrae in cercopithecids contribute to the formation of a long and arched (dorsoflexible) lumbar spine. *E. nyanzae* and *Nacholapithecus* lumbar vertebrae exhibit strong wedging (Fig. 5.2a, c; Ward et al. 1993; Nakatsukasa 2008; Susanna et al. 2014). The middle lumbar vertebra of *Pierolapithecus* also shows strong wedging while those of *Hispanopithecus* (both cranial and caudal ones) show only slight wedging (Fig. 5.2e, f; Susanna et al. 2014). This may suggest a smaller number of lumbar vertebrae in *Hispanopithecus*, like living great apes. *Morotopithecus* lumbar vertebra (UMP 67.28) has little wedging (Ward et al. 1993; Sanders and Bodenbender 1994; Susanna et al. 2014). However, another lumbar vertebra (UMP 68.06), from a more cranial level, shows strong wedging, complicating its interpretation (Fig. 5.2c; Nakatsukasa 2008). These two vertebrae exhibit a large size difference suggesting that *Morotopithecus* could have had a long back if these two vertebrae represent the same individual.

5.4 Tail Loss

Tail loss is a diagnostic feature of living hominoids. The living apes (and humans) not only lack an external tail but also have modified vestigial tail bones into the ventrally directed coccygeal vertebrae, which anchor the ligaments, fasciae, and muscles that support the pelvic floor (Elftman 1932). No fossil of early catarrhine (or ape progenitor) documenting the process of tail loss has been discovered. However, many researchers agree that very powerful pollical/hallucal assisted grip that is observed in Early and Middle Miocene apes (Walker and Pickford 1983; Begun et al. 1994; Nakatsukasa et al. 2003a) had taken over the dynamic balancing function that the tail originally had born (Kelley 1997; Ward 1998). Ancestral apes were above-branch quadrupeds and probably decreased reliance on arboreal running/leaping and increased frequencies of deliberate above-branch locomotion and cautious climbing as body size increased, dissipated the functional efficiency of a long tail as a balancing organ (Cartmill and Milton 1977; Begun et al. 1994; Ward

2007; Williams and Russo 2015). Some macaques have extremely reduced or absent tails (Napier and Napier 1967). However, their tail reduction is generally related to enhanced terrestriality or thermoregulation (e.g., Wilson 1972) and may not be a good analogy for the case in the apes.

The earliest evidence of tail loss in apes is documented in *E. heseloni*. A last sacral vertebra of a juvenile *E. heseloni* (KPS V42; Fig. 5.3b) was discovered from the KPS in Rusinga Island. Ward et al. (1991) focused on the strong tapering of this vertebra and concluded that this vertebra could not bear a substantial number of caudal vertebrae distally. Although the tapering angle of this vertebra cannot be measured accurately due to postmortem distortion, follow-up studies (Nakatsukasa et al. 2004; Russo 2016) reported additional characters of this specimen which justified the original interpretation (e.g., absence of the postzygapophyses, formation of sacral hiatus, dorsoventral flatness, small caudal articular surface area, weak development of the transverse process). The sacrum of *Oreopithecus* (#50) also displays a tapered distal end, testifying to the absence of a tail (Straus 1963).

So far, only a single coccygeal vertebra of fossil ape has been discovered. KNM-BG 40949 is a first coccygeal vertebra of *Nacholapithecus* (Fig. 5.3c; Nakatsukasa et al. 2003b). The mid-distal part of the body is much narrower than the proximal end. Thus, it is T-shaped rather than trapezoidal, unlike the first coccyx of living apes. However, this bone shares several derived features (shallow dorsal groove instead of neural arch, absence of the prezygapophyses, dorsoventral flatness, reduced transverse processes, tapered distal end) with the first coccygeal vertebra of living apes. The combination of these features is not found in any other tailless or short-tailed primates (see Nakatsukasa et al. 2003b; Russo 2015). The suite of derived features of KPS V42 is also unique to living hominoids (Nakatsukasa et al. 2004). Therefore, tail loss in fossil and living apes is almost certainly a shared derived feature, which predated the acquisition of orthograde adaptations in later apes.

5.5 Spinal Invagination

The thoracolumbar spine of living apes is more ventrally positioned than that of Old World monkeys (Schultz 1956, 1961; Benton 1967; Lovejoy 2005). The spinal invagination into the thoracic cavity is linked with the dorsal arrangement of the scapula on a mediolateral broadened thoracic cage, which allows greater mobility of the arm dorsolaterally (Ward 2007). In living apes (especially in great apes), broadening of the thoracic cage, coupled with dorsal orientation of the gluteal plane of the ilium, lower iliac elongation, and lumbar shortening, forms a rigid thoraco-pelvic link (Lovejoy 2005: Lovejoy et al. 2009a).

Spinal invagination has been evaluated from several osteological features such as the orientation of the transverse process of the thoracic vertebra, dorsoventral position of the costal fovea, rib curvature, and dorsoventral position of the lumbar transverse process. Due to the relatively fragile nature, thoracic bone specimens are not abundant. However, the position of the transverse process on the lumbar vertebra

has been extensively discussed (e.g., Shapiro 1993; Sanders and Bodenbender 1994; Ward 1993; Moyà-Solà et al. 2004; Nakatsukasa 2008; Susanna et al. 2014). Dorsal migration of the transverse processes may be associated with a reduction of the cross-sectional area of the erector spinae muscle, which is linked with restricted dorsomobility of the lumbar spine (Benton 1967; Lovejoy 2005). Reduced cross-sectional area of the erector spinae is also reflected in more dorsal orientation of the transverse process in a coronal plane (Benton 1967). A relatively dorsal position of the transverse process may increase the moment arm for the erector spinae to extend the spine, increasing mechanical efficiency (Shapiro 1993; Ward 1993; Johnson and Shapiro 1998).

The lumbar vertebrae of *E. heseloni*, *E. nyanzae*, and *Nacholapithecus* have transverse processes which arise from a relatively ventral position (Fig. 5.2a, d). In cranial view, the transverse process arises from the widest and most dorsal part of the body. This contrasts with the condition in living great apes and *Hispanopithecus* where the base of the transverse process is situated on the pedicle (Figs. 5.1 and 5.2f; Susanna et al. 2014). Damage of the *Hispanopithecus* vertebral centrum (IPS-18800.6) makes the exact positioning difficult. The base of the transverse process might be more dorsally positioned than that in Fig. 5.2f. In *Pierolapithecus*, the transverse process is positioned on both the body and pedicle, like non-*Symphalangus* gibbons or *Ateles* (Fig. 5.2e; Moyà-Solà et al. 2004). Researchers agree that the condition of *Morotopithecus* (UMP 67.28; Fig. 5.2b) differs from that of other African Miocene apes such as *Ekembo* or *Nacholapithecus* and more similar to that of living apes (MacLatchy 2004; Harrison 2010; Begun 2013; Fleagle 2013 and references therein) although its character state is described a little differently by different authors: body-pedicle juncture (Moyà-Solà et al. 2004; Nakatsukasa 2008) and pedicle near the centro-pedicular junction (Sanders and Bodenbender 1994). Metrically, its position is similar to *Symphalangus* (in cranial view; Susanna et al. 2014) or *Pongo* (in caudal view; Sanders and Bodenbender 1994). However, another more cranial lumbar vertebra (UMP 68.06; Fig. 5.2c) has a large part of the base of the transverse process positioned on the vertebral body. This suggest that this character varies by segmental level (Nakatsukasa 2008) and that invagination of the thoracic spine might not be developed in *Morotopithecus* despite a relatively dorsostable lumbar spine.

Rib curvature is another good measure to evaluate spinal invagination (Schultz 1960; Kagaya et al. 2008). Schultz (1960) compared the neck-body angle of a second rib in *Oreopithecus* and living catarrhines. The neck of the rib in *Oreopithecus*, like that of living hominoids, displays a strong bend suggesting marked spinal invagination. Moyà-Solà et al. (2004) reported a similar observation on a third (or fourth) rib of *Pierolapithecus*. The neck angle is less useful as a proxy of spinal invagination at more caudal (ca. sixth~) levels (Kagaya et al. 2008). However, the body of a caudal (seventh to ninth) rib of *Pierolapithecus* exhibits a great ape-like pronounced curvature in concert with greater spinal invagination as inferred from the lumbar transverse process position (Moyà-Solà et al. 2004). Moyà-Solà and Köhler (1996) noted that the costal fovea of the *Hispanopithecus* thoracic vertebra is situated relatively dorsally and suggested a relatively ventral position of the spinal column, i.e., a strong invagination, in this ape.

5.6 Vertebral Body Shape

A dorsostable lumbar spine is a hallmark of living apes, especially great apes (Slijper 1946; Ankel 1967; Benton 1967, 1974; Erikson 1963; Rose 1975; Jungers 1984; Ward 1993). Decreased number of lumbar vertebrae in living apes is related to enhanced dorsostability against lumbar spinal buckling. Other than their number, the shape of each vertebral body also affects dorsostability (e.g., Benton 1967; Erikson 1963; Johnson and Shapiro 1998).

Relative vertebral body length is a standard metric trait to infer the lumbar dorsostability from single lumbar vertebra (hereafter, the vertebral *length* refers to craniocaudal dimension of the vertebral body and the *height* to the dorsoventral dimension of the body). Vertebral body length is often standardized by centrum articular surface diameter(s) or the geometric mean of vertebral measurements. Relative vertebral body (dorsal side) length distinguishes living apes from most monkeys with *Ateles* being intermediate (Susanna et al. 2014). On the one hand, in most monkeys, relative vertebral length increases toward the caudal levels and then decreases in the penultimate and ultimate lumbar vertebrae (Ward 1993; Sanders and Bodenbender 1994; Nakatsukasa 2008; Susanna et al. 2014). On the other hand, in apes and *Ateles*, the magnitude of their length change is less marked, being constant or with a weak, continuous decrease. However, it should be noted that vertebral body length has a negative allometric relationship to BM among cercopithecids and apes (Ward 1993; Sanders and Bodenbender 1994), an important caveat when comparing relative vertebral body length among taxa covering a wide size range. Fortunately, estimated BMs of most fossil apes fall within a relatively narrow range of 20–40 kg, and it is still useful to calculate relative vertebral body length for comparison among fossil apes and similar-sized living primates. Relative vertebral body (dorsal side) length is high in *E. nyanzae* and *Nacholapithecus*, as in cercopithecids (Ward 1993; Nakatsukasa et al. 2007; Susanna et al. 2014; Figs. 5.1 and 5.2). In contrast, the lumbar vertebral body of *Pierolapithecus* and *Hispanopithecus* is proportionally shorter, being close to hylobatids, while *Morotopithecus* (UMP 67.28) is well within the range of chimpanzee (Susanna et al. 2014). Although relative length UMP 67.28 has been reported to be as long as male baboon vertebra (Sanders and Bodenbender 1994), their measurement was *ventral* length and standardized by the cranial surface breadth (remember that vertebral body of UMP 67.28 lacks ventral wedging). When the ventral length is standardized by GM, UMP 67.28 takes a position between living apes and *Papio* (Susanna et al. 2014).

Shape of the centrum articular surface can also affect the stability of the lumbar spine. As the vertebral body height increases against a given mediolateral breadth (and thus the articular shape becomes more circular), articular surface area increases so that the lumbar spine can bear a greater magnitude of stress (Fig. 5.1; Ward 1991; Susanna et al. 2014). Regarding the relative height of the centrum articular surface, fossil apes are separated into two groups, either the short (*Ekembo*, *Nacholapithecus*) or tall (*Hispanopithecus*, *Pierolapithecus*, *Morotopithecus*) group, the latter group being morphologically close to *Gorilla* or *Symphalangus* (Susanna et al. 2014).

5.7 Other Characters

There are several other characters in which early fossil apes differ from living apes. They include reduction of the anapophyses, caudal shift of the transitional vertebra, loss of median ventral keel of lumbar vertebral body, orientation of the lumbar spinous process, and enlargement of the thoracolumbar vertebral body relative to BM.

5.7.1 Anapophysis

Anapophysis is a bony process (or eminence) arising from the caudal part of the pedicle ventral to the postzygapophysis in caudal thoracic and lumbar vertebrae of mammals (Ankel 1967). Although this process is often called an "accessory process," this term refers to both anapophysis and metapophysis. Anapophyses tend to be reduced in dorsostable mammal species (Sanders 1995). Cercopithecids exhibits well-developed anapophyses in post-transitional thoracic and cranial-middle lumbar vertebrae (Fig. 5.1). In these primates, the anapophysis reduces its length to the caudal levels and is absent (or greatly diminished) in the last two lumbar vertebrae (Ward 1991). These processes serve as insertion sites of spinal extensors, most importantly the longissimus muscle (Ward 1993 and references therein). In great apes, anapophyses are not present since the transverse process arises from the pedicle and occupies the position where they would originate, taking over the role as the longissimus insertion (Ward 1993; Williams and Russo 2015). In these primates, a rudimentary tubercle is present on the inferior margin of the transverse process for this role (Benton 1967). Hylobatids have anapophyses. However, they are relatively reduced in size compared to cercopithecids (Ward 1991).

Anapophyses are observed in lumbar vertebrae of fossil apes which maintain a relatively ventral position of the transverse process though not prominent as those of cercopithecids: *E. nyanzae* (Ward et al. 1993), *E. heseloni* (Walker and Pickford 1983), and *Nacholapithecus* (Nakatsukasa et al. 2007). For other fossil apes, the presence/absence of the anapophysis in the caudal thoracic and lumbar series (other than penultimate and ultimate lumbar vertebrae) is unknown.

5.7.2 Position of the Transitional Vertebra

Orientation of the prezygapophyseal articular surface differs between "typical" thoracic vertebrae and lumbar vertebrae. Compared to dorsally oriented surfaces of thoracic vertebra, sagittally oriented (and curved) surfaces of lumbar vertebra restrict rotation while permitting flexion-extension (Rockwell et al. 1938; Kapandji 1987).

The transitional vertebra is the caudal thoracic vertebra which has thoracic-type prezygapophyseal surfaces and lumbar-type postzygapophyseal surfaces. In many

cercopithecids, the transitional vertebra is located at T10, positioned 2–3 levels cranial to the last thoracic vertebra, a condition considered to be plesiomorphic for catarrhines (Williams 2012). Although mobility of each post-transitional thoracic vertebra is probably not identical to that of lumbar vertebrae due to thoracic wall structures, a greater number of those thoracic vertebrae would contribute to enhance dorsomobility of the spine during locomotion (Erikson 1963; Williams and Russo 2015). In living apes, the position of the transitional vertebra tends to shift caudally and appears at the last thoracic level in the majority of species (Williams 2012; Williams and Russo 2015).

It would be interesting to know the evolutionary sequence of this shift and the changes of the modal lumbar and sacral vertebral count (and other characters presumably related to the enhanced dorsostability in living apes), but only limited information is available from fossils apes. One post-transitional thoracic vertebra is included in the KNM-MW 13142 *E. nyanzae* skeleton (Ward 1993) and two in the KNM-BG 35250 *Nacholapithecus* skeleton (Ishida et al. 2004; Nakatsukasa et al. 2007). Given the generally less derived nature of the trunk skeleton of *E. nyanzae* (Ward 1993), it is very likely that both of them retained the primitive catarrhine condition in terms of the position of the transitional vertebra. For other fossil apes, no information is available.

5.7.3 Median Ventral Keel of Lumbar Vertebral Body

Lumbar (and caudal thoracic) vertebral bodies of monkeys and prosimians (and many non-primate mammals as well) exhibit a prominent ventral midsagittal keel (Straus 1963; Fig. 5.4). In cercopithecids, this keel is well-developed as the

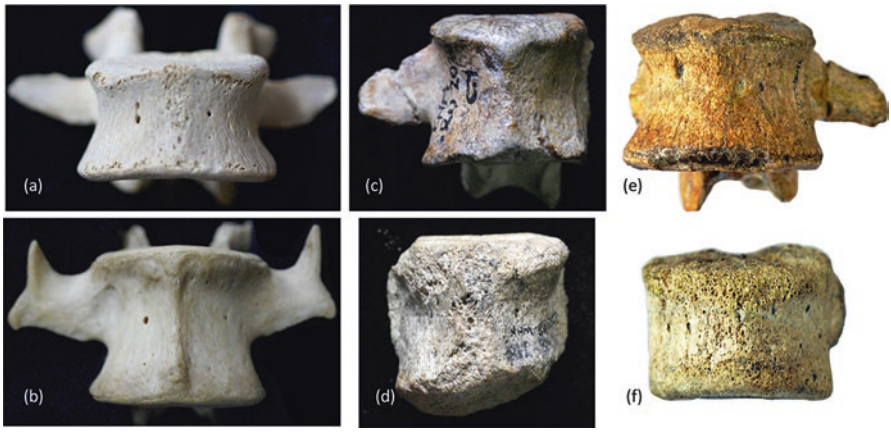

Fig. 5.4 Lumbar vertebral centra of extant and fossil primates. (**a**) Chimpanzee, (**b**) baboon, (**c**) *Ekembo heseloni* KNM-RU 2036CY, (**d**) *Nacholapithecus* KNM-BG 15527, (**e**) and (**f**) *Morotopithecus* UMP 67.28 and UMP 68.06, respectively. Not to scale

attachment site of the ventral longitudinal ligament and its ventrolateral sides are often hollowed. In living apes, such a keel is not developed, and the ventral surface of the vertebral body is transversally rounded (Ward 1993; Sanders and Bodenbender 1994). The significance of the development of this ligamentous attachment is not fully understood. However, it is feasible that disappearance of this bony feature in living apes is related to a series of specializations for dorsostability in the lumbar spine.

Caudal thoracic and lumbar vertebral bodies of *Ekembo*, *Nacholapithecus*, and *Equatorius* exhibit a ventral median keel although its development (e.g., sharpness, presence/absence of ventrolateral hollowing) is variable (Fig. 5.4; Walker and Pickford 1983; Ward 1993; Sherwood et al. 2002; Ishida et al. 2004; Nakatsukasa et al. 2007; Kikuchi et al. 2015). In *Morotopithecus*, lumbar vertebrae lack a ventral median keel (Walker and Rose 1968; Ward 1993; Sanders and Bodenbender 1994). However, the more cranial lumbar vertebra (UMP 68.06) shows a prominent median bulge (Nakatsukasa 2008; Figs. 5.2c and 5.4f) unlike the penultimate lumbar vertebra (UMP 67.28) or the lumbar vertebrae of living apes. In *Pierolapithecus* and *Hispanopithecus*, the lumbar vertebrae lack a distinct keel (Moyà-Solà et al. 2004; Susanna et al. 2014), coinciding with their dorsostable lumbar anatomy. However, the thoracolumbar vertebrae of *Oreopithecus* (the last thoracic and all-preserved lumbar vertebrae in IGF 11778) exhibit prominent ventral median keels (Straus 1963), implying that interpretation of this trait is not always straightforward.

5.7.4 Orientation of the Lumbar Spinous Process

Craniocaudal orientation of the spinous process of lumbar vertebrae (and post-transitional thoracic vertebrae as well) relates to the degree of dorsostability. Caudally oriented lumbar spinous processes suggest emphasized activities of the multifidus muscle to extend the lumbar spine (Slijper 1946; Shapiro 1993) and may restrict the range of dorsal extension by engaging with a caudally adjacent spinous process (Erikson 1963; Nakatsukasa et al. 2007). The orientation of the spinous processes is classified as either "cranial" or "caudal" based on the overall shape. In most monkeys, the cranial edge of the process (or its dorsal portion at least) shows ventrocaudal-to-dorsocranial inclination accentuating the dorsal orientation of the process (Fig. 5.1; Shapiro 1993). The axis of the spinous process is dorsal or dorsocranially oriented in monkeys while it is more caudal in living apes (Ward 1991).

The lumbar spinous process of *E. nyanzae* shows a caudal orientation as in living apes (Ward et al. 1993; Fig. 5.2a) irrespective of the otherwise primitive (or cercopithecid-like) condition of the lumbar spine. This suggests some similarity of intrinsic back muscle anatomy/function between *E. nyanzae* and living apes. The spinous process of the *Morotopithecus* lumbar vertebra UMP 67.28 is broken along the dorsal border but perhaps had a similar orientation to that in *E. nyanzae* (Fig. 5.2b). The spinous process of a *Nacholapithecus* post-transitional thoracic vertebra (KNM-BG 42810B) exhibits a more emphasized caudal orientation

Fig. 5.5 Lumbar vertebra of *E. nyanzae* KNM-MW 13142J and *Nacholapithecus* KNM-BG 35250BT and KNM-BG 42753C (left to right) in dorsal view. Note that the spinous process is projecting caudally dividing the notch between the right and left postzygapophyses in *Nacholapithecus* (arrows). Scale bar = 1 cm

resembling the condition in *Gorilla* and *Pongo* (Kikuchi et al. 2015). Likewise, an emphasized caudal orientation on the spinous process in the lumbar series can be inferred from the morphology of the process base despite the fact that there is no lumbar vertebral specimen that preserves a large part of the spinous process. In *Nacholapithecus*, the basal part of the spinous process projects caudally into the notch that separates the right and left postzygapophyses, unlike in *Ekembo* and *Morotopithecus*, which lack a comparable caudal protrusion (Fig. 5.5; Nakatsukasa et al. 2007; Kikuchi et al. 2015). Among European fossil apes, *Pierolapithecus* resembles *E. nyanzae*/*Morotopithecus* while *Hispanopithecus* is more similar to *Nacholapithecus* in the orientation of the spinous process (Moyà-Solà and Köhler 1996; Susanna et al. 2014; Williams and Russo 2015).

5.7.5 Lumbar Vertebral Body Size

Lumbar vertebrae of some fossil apes have a comparatively small centrum articular surface compared to those of living catarrhines. For example, centrum articular surface area of lumbar vertebrae of a male *E. nyanzae* is close to that of male proboscis monkey, which weighs less than two-thirds of the predicted BM of male *E. nyanzae* (Sanders and Bodenbender 1994). Similarly, uniquely small lumbar vertebral bodies are known for *E. heseloni* and *Nacholapithecus* (Harrison and Sanders 1999; Nakatsukasa and Hirose 2003; Nakatsukasa et al. 2007; Kikuchi et al. 2015). In the case of *Nacholapithecus*, small centrum articular size is recognized through the thoracolumbar spine (Nakatsukasa et al. 2007; Kikuchi et al. 2015, 2016). Reason for this unique tendency is not well understood. It might be related to postural or locomotor mode (see Harrison and Sanders 1999; Nakatsukasa et al. 2007) or proportion of load bearing between the ventral (vertebral bodies) and dorsal pillars

(zygapophyses and lamina) (Pal and Routal 1987; Russo 2010). The only currently known fossil ape whose lumbar vertebral centrum size scales with limb joint size as in modern catarrhines is *Hispanopithecus* (IPS-18800; Susanna et al. 2014).

5.8 Discussion

Fossil evidence indicates that fossil apes (~19–15 Ma) in East Africa from the beginning and mid-part of the Miocene were essentially arboreal pronograde quadrupeds as illustrated by *Ekembo* and *Nacholapithecus*, though *Nacholapithecus* shows a hint of early departure for more orthograde positional behavior (Ward 1998, 2007; Nakatsukasa and Kunimatsu 2009; Begun 2010). Their vertebral spinal anatomy was largely conservative retaining the presumed ancestral catarrhine condition except the loss of external tail. Thus, tail loss in hominoids predated specialization for forelimb-dominated arboreal orthogrady which is commonly observed in extant terminal lineages of apes (Ward et al. 1993; Nakatsukasa et al. 2003a, b). The origins and dispersal history of the hylobatid into Eurasia are vague. A small-sized ape *Pliobates* (from 11.6 Ma-old Catalonia) exhibits similarity with hylobatids in its cranial morphology (Alba et al. 2015) and may provide a clue to infer the morphotype of the last common ancestor (LCA) of the crown hominoids despite the chronological gap between its geologic age and the estimated hylobatid split time from the great ape clade (17 Ma, Carbone et al. 2014; or ~ 20 Ma, Matsudaira and Ishida 2010). However, it is important to note that *Pliobates* lacks various postcranial apomorphies shared by extant apes (Alba et al. 2015). Unfortunately, no spinal element of this species is available.

It is generally accepted that Eurasian great apes originated from postcranially unspecialized stem great apes which spread into Eurasia between 17 and 16 Ma (Casanovas-Vilar et al. 2011; Alba 2012; Begun et al. 2012). This dispersal is documented by *Griphopithecus*, which is known from a wide area encompassing from Turkey to Germany. Postcranially, *Griphopithecus* is less well-known compared to the contemporary African fossil apes (Begun 1992a; Ersoy et al. 2008). However, known bony elements show no derived features for orthogrady, and its spine most probably also lacked these derived features. Diversification of Eurasian apes perhaps resulted in parallel evolution of orthograde taxa in Europe and Asia (Casanovas-Vilar et al. 2011; Alba 2012; Begun et al. 2012). In Europe, an orthograde ape (*Pierolapithecus*) first appeared around 12 Ma. *Pierolapithecus* was orthograde but probably less dorsostable compared to extant great apes and *Hispanopithecus*. It was not specialized for suspension (Moyà-Solà et al. 2004; but see Deane and Begun 2008, 2010). However, the 2 Ma younger *Hispanopithecus* had acquired a full suite of orthograde characters like living great apes although it was not exactly like any living apes (Almécija et al. 2007). *Oreopithecus* is another ape with a fully orthograde spine. However, its lumbar vertebrae have some features distinct from *Hispanopithecus* (ventral median keel: also see Nakatsukasa et al. 2016 for hand bones) and might be a lineage that became specialized for full orthogrady independently of *Hispanopithecus*.

Morotopithecus is somewhat inconsistent with the chronological and geographic pattern described above. Its lumbar anatomy is more similar to European fossil apes and living apes. Curiously, its craniodental elements show close affinity with *Afropithecus* (17 Ma, Kenya), which is, like *Ekembo*, considered to be an arboreal pronograde quadruped based on limb bone morphology (Ward 1998). On the other hand, the morphology of the nasoalveolar clivus in *Nacholapithecus* is derived toward extant great apes compared to Early Miocene apes/hylobatids despite its primitive spinal anatomy (Nakatsukasa and Kunimatsu 2009). This inconsistency has been a problem in interpreting the early evolutionary history of apes (e.g., MacLatchy 2004; Nakatsukasa and Kunimatsu 2009).

In recent years, however, the opinion with regard to the derived lumbar anatomy of *Morotopithecus* as an independent adaptation for some sort of orthograde positional behavior is becoming dominant (Ward 2007; Begun 2010, 2013; Harrison 2010; Alba 2012; Machnicki et al. 2016). Lumbar vertebral morphology of *Morotopithecus* is unique, especially when information from a previously less studied specimen (UMP 68.06) is included (Nakatsukasa 2008). Its lumbar spine was relatively dorsostable, but thoracic spinal invagination might be weak. This unique morphology itself is not a proof of homoplasy because it could be a nascent stage from which specialized lumbar anatomy of later apes originated. However, when the dentognathic information and the European fossil record after 16 Ma are taken into account, the author agrees with the view that its derived lumbar anatomy is a homoplasy with living apes (also see Kunimatsu et al. 2019). It is noteworthy that recent advances of evolutionary developmental biology are unveiling genetic and developmental mechanisms which may explain repeated evolution of similar anatomical structures in closely related living organisms (see Reno 2014 for review).

In contrast to the comparatively rich fossil record of European apes which illustrates a progressive evolution toward orthogrady, postcranial fossils in African apes are totally absent after ~12 Ma (Berg Aukas) until the appearance of the earliest putative hominins (e.g., *Sahelanthropus*), and this fossil dearth spurs an argument over the evolutionary scenario of the living African apes and humans (AAH). Some authors propose that a European orthograde ape lineage dispersed into Africa during the Late Miocene and gave rise to the AAH clade (Stewart and Disotell 1998; Begun 2010, 2013; Begun et al. 2012). However, there is criticism of this interpretation from the site representation and paleoecology (Cote 2004), and some researchers (Moyà-Solà et al. 2009; Alba 2012; Pérez de los Ríos et al. 2012) question usefulness of craniodental traits that were used to validate the Homininae status of some European Miocene apes (see Begun 2007). If such a dispersal had not occurred, orthogrady would have evolved in European and African ape lineages independently. Although this is merely a speculation, the author does not see this as impossible when recalling that a similar parallel evolution is suggested in western and eastern Eurasia (*Hispanopithecus*, *Oreopithecus* in the west vs. hylobatids, *Pongo* in the east, e.g., Casanovas-Vilar et al. 2011).

Besides this issue, an argument persists whether the dorsostable spine (or, more broadly speaking, adaptations for forelimb-dominated orthograde behavior) in the extant African apes is homologous (Begun 1992b, 1994; Pilbeam 1996; Wrangham

and Pilbeam 2001; Young 2003) or homoplastic (Larson 1998; Ward 2007; Almécija et al. 2015). The vertebral formula of the AAH's LCA is also controversial (Haeusler et al. 2002; Pilbeam 2004; McCollum et al. 2010; Williams 2011; Williams and Russo 2015; Williams et al. 2016; Thompson and Almécija 2017). Some authors (e.g., Lovejoy et al. 2009b; White et al. 2015) propose that the LCA of the AAH had an intermediate body plan between pronogrady and orthogrady (i.e., "multigrady"), having spinal invagination but not enhanced dorsostability as that in extant great apes inferring from the postcranial anatomy of *Ardipithecus ramidus* (spinal invagination is predicted from the reduction of the retroauricular region of the os coxa: see Lovejoy et al. 2009a, b). However, the debate continues (e.g., Wood and Harrison 2011; Begun 2016). For further clarification of evolution of hominoid spine, new discoveries of postcranial skeletal elements of Late Miocene African apes such as *Nakalipithecus* (10 Ma, Kenya) or *Chororapithecus* (8 Ma, Ethiopia) as well as more complete fossils from Eurasia are eagerly awaited.

Acknowledgments I thank the editors for inviting me to contribute to this volume and the National Museums of Kenya for permission to study original specimens under their care. I am grateful to Salvador Moyà-Solà, David Alba, Ivette Susanna, Sergio Almécija, and Yasuhiro Kikuchi for providing me photographs of original fossil specimens and David Begun, Sergio Almécija, and the editors for their careful reading and constructive comments on drafts of this article. This work is supported by JSPS KAKENHI (16H02757) and Primate Institute Cooperative Research, Kyoto University.

References

Alba DM (2012) Fossil Apes from the Valles-Penedés Basin. Evol Anthropol 21:254–269

Alba DM, Almécija S, DeMiguel D, Fortuny J, Pérez de los Ríos M, Pina M, Robles JM, Moyà-Solà S (2015) Miocene small-bodied ape from Eurasia sheds light on hominoid evolution. Science 350:aab2625

Almécija S, Alba DM, Moyá-Solá S, Köhler M (2007) Orang-like manual adaptations in the fossil hominoid *Hispanopithecus laietanus*: first steps towards great ape suspensory behaviours. Proc R Soc B Biol Sci 274:2375–2384

Almécija S, Smaers JB, Jungers WL (2015) The evolution of human and ape hand proportions. Nat Commun 6:7177

Andrews P (2016) An ape's view of human evolution. Cambridge University Press, Cambridge

Andrews P, Groves CP (1976) Gibbons and brachiation. In: Rumbaugh DM (ed) Gibbons and Siamang: suspensory behavior, locomotion, and other behaviors of captive gibbons: cognition. Karger, Basel, pp 167–218

Ankel F (1967) Morphologie von Wirbelsaule und Brustkorb. Primatologia 4:1–120

Begun DR (1992a) Phyletic diversity and locomotion in primitive European hominids. Am J Phys Anthropol 87:311–340

Begun DR (1992b) Miocene fossil hominids and the chimp-human clade. Science 257:1929–1933

Begun DR (1994) Relations among the great apes and humans: new interpretations based on the fossil great ape *Dryopithecus*. Yearb Phys Anthropol 37:11–63

Begun DR (2002) European hominoids. In: Hartwig W (ed) The primate fossil record. Cambridge University Press, Cambridge, pp 231–253

Begun DR (2007) Fossil record of Miocene hominoids. In: Henke W, Tattersall I (eds) Handbook of paleoanthropology. Springer, Berlin, pp 921–977

Begun DR (2010) Miocene hominids and the origins of the African apes and humans. Annu Rev Anthropol 39:67–84
Begun DR (2013) The Miocene hominoid radiation. In: Begun DR (ed) A companion to paleoanthropology. Wiley-Blackwell, Chichester, pp 398–416
Begun DR (2016) The real planet of the apes: a new story of human origins. Princeton University Press, Princeton, NJ
Begun DR, Teaford MF, Walker A (1994) Comparative and functional anatomy of *Proconsul* phalanges from the Kaswanga Primate Site, Rusinga Island, Kenya. J Hum Evol 26:89–165
Begun DR, Nargolwalla MC, Kordos L (2012) European Miocene hominids and the origin of the African ape and human clade. Evol Anthropol 21:10–23
Benefit BR, McCrossin ML (1995) Miocene hominoids and hominid origins. Annu Rev Anthropol 24:237–256
Benton RS (1967) Morphological evidence for adaptations within the epaxial region of the primates. In: Vagtborg H (ed) The baboon in medical research. University of Texas Press, Austin, pp 201–216
Benton RS (1974) Structural patterns in the Pongidae and Cercopithecidae. Am J Phys Anthropol S18:65–88
Carbone L, Harris RA, Gnerre S, Veeramah KR, Lorente-Galdos B, Huddleston J, Meyer TJ, Herrero J, Roos C, Aken B, Anaclerio F, Archidiacono N, Baker C, Barrell D, Batzer MA, Beal K, Blancher A, Bohrson CL, Brameier M, Campbell MS, Capozzi O, Casola C, Chiatante G, Cree A, Damert A, de Jong PJ, Dumas L, Fernandez-Callejo M, Flicek P, Fuchs NV, Gut I, Gut M, Hahn MW, Hernandez-Rodriguez J, Hillier LW, Hubley R, Ianc B, Izsvák Z, Jablonski NG, Johnstone LM, Karimpour-Fard A, Konkel MK, Kostka D, Lazar NH, Lee SL, Lewis LR, Liu Y, Locke DP, Mallick S, Mendez FL, Muffato M, Nazareth LV, Nevonen KA, O'Bleness M, Ochis C, Odom DT, Pollard KS, Quilez J, Reich D, Rocchi M, Schumann GG, Searle S, Sikela JM, Skollar G, Smit A, Sonmez K, ten Hallers B, Terhune E, Thomas GW, Ullmer B, Ventura M, Walker JA, Wall JD, Walter L, Ward MC, Wheelan SJ, Whelan CW, White S, Wilhelm LJ, Woerner AE, Yandell M, Zhu B, Hammer MF, Marques-Bonet T, Eichler EE, Fulton L, Fronick C, Muzny DM, Warren WC, Worley KC, Rogers J, Wilson RK, Gibbs RA (2014) Gibbon genome and the fast karyotype evolution of small apes. Nature 513:195–201
Cartmill M, Milton K (1977) The lorisiform wrist joint and the evolution of "brachiating" adaptations in the hominoidea. Am J Phys Anthropol 47:249–272
Casanovas-Vilar I, Alba DM, Garcés M, Robles JM, Moyà-Solà S (2011) Updated chronology for the Miocene hominoid radiation in Western Eurasia. Proc Natl Acad Sci U S A 108:5554–5559
Conroy GC, Pickford M, Senut B, Van Couvering J, Mein P (1992) *Otavipithecus namibiensis*, first Miocene hominoid from southern Africa. Nature 356:144–148
Conroy GC, Senut B, Gommery D, Pickford M, Mein P (1996) New primate remains from the Miocene of Namibia, Southern Africa. Am J Phys Anthropol 99:487–492
Cote SM (2004) Origins of the African hominoids: an assessment of the paleobiogeographical evidence. C R Palevol 3:323–340
Deane AS, Begun DR (2008) Broken fingers: retesting locomotor hypotheses for fossil hominoids using fragmentary proximal phalanges and high-resolution polynomial curve fitting (HR-PCF). J Hum Evol 55:691–701
Deane AS, Begun DR (2010) *Pierolapithecus* locomotor adaptations: a reply to Alba et al.'s comment on Deane and Begun (2008). J Hum Evol 59:150–154
Elftman HO (1932) The evolution of the pelvic floor of primates. Am J Anat 51:307–339
Erikson GE (1963) Brachiation in new world monkeys and in anthropoid apes. In: Napier J, Barnicot NA (eds) Symposia of the zoological society of London. Zoological Society of London, London, pp 135–164
Ersoy A, Kelley J, Andrews P, Alpagut B (2008) Hominoid phalanges from the middle Miocene site of Paşalar, Turkey. J Hum Evol 54:518–529
Fleagle JG (2013) Primate adaptation and evolution, 3rd edn. Academic Press, San Diego
Gebo DL, MacLatchy L, Kityo R, Dino A, Kingston J, Pilbeam D (1997) A hominoid genus from the early Miocene of Uganda. Science 276:401–404

Haeusler M, Martelli SA, Boeni T (2002) Vertebrae numbers of the early hominid lumbar spine. J Hum Evol 43:621–643

Harrison T (1991) The implications of *Oreopithecus bambolii* for the origins of bipedalism. In: Coppens Y, Senut B (eds) Origine(s) de la bipédie chez les hominidés. CNRS, Paris, pp 235–244

Harrison T (2010) Dendropithecoidea, Proconsuloidea and Hominoidea (Catarrhini, Primates). In: Werdelin L, Sanders WJ (eds) Cenozoic mammals of Africa. University of California Press, Berkeley, pp 429–469

Harrison T, Sanders WJ (1999) Scaling of lumbar vertebrae in anthropoid primates: its implications for the positional behavior and phylogenetic affinities of *Proconsul*. Am J Phys Anthropol S28:146

Ishida H, Kunimatsu Y, Nakatsukasa M, Nakano Y (1999) New hominoid genus from the middle Miocene of Nachola, Kenya. Anthropol Sci 107:189–191

Ishida H, Kunimatsu Y, Takano T, Nakano Y, Nakatsukasa M (2004) *Nacholapithecus* skeleton from the Middle Miocene of Kenya. J Hum Evol 46:67–101

Johnson SE, Shapiro LJ (1998) Positional behavior and vertebral morphology in atelines and cebines. Am J Phys Anthropol 105:333–354

Jungers WL (1984) Scaling of the hominoid locomotor skeleton with special reference to lesser apes. In: Preuschoft H, Chivers DJ, Brockelman WY, Creel N (eds) The lesser apes: evolutionary and behavioural biology. Edinburgh University Press, Edinburgh, pp 146–169

Jungers WL (1987) Body size and morphometric affinities of the appendicular skeleton in *Oreopithecus bambolii* (IGF11778). J Hum Evol 16:445–456

Kagaya M, Ogihara N, Nakatsukasa M (2008) Morphological study of the anthropoid thoracic cage: scaling of thoracic width and an analysis of rib curvature. Primates 49:89–99

Kapandji IA (1987) The physiology of the joints: annotated diagrams of the mechanics of the human joints. Churchill Livingstone, New York, NY

Kelley J (1997) Paleobiological and phylogenetic significance of life history in Miocene hominoids. In: Begun DR, Ward CV, Rose MD (eds) Function, phylogeny, and fossils. Miocene hominoid evolution and adaptations. Plenum Press, New York, pp 173–208

Kikuchi Y, Nakano Y, Nakatsukasa M, Kunimatsu Y, Shimizu D, Ogihara N, Tsujikawa H, Takano T, Ishida H (2012) Functional morphology and anatomy of cervical vertebrae in *Nacholapithecus kerioi*, a middle Miocene hominoid from Kenya. J Hum Evol 62:677–695

Kikuchi Y, Nakatsukasa M, Nakano Y, Kunimatsu Y, Shimizu D, Ogihara N, Tsujikawa H, Takano T, Ishida H (2015) Morphology of the thoracolumbar spine of the middle Miocene hominoid *Nacholapithecus kerioi* from northern Kenya. J Hum Evol 88:25–42

Kikuchi Y, Nakatsukasa M, Nakano Y, Kunimatsu Y, Shimizu D, Ogihara N, Tsujikawa H, Takano T, Ishida H (2016) Sacral vertebral remains of the Middle Miocene hominoid *Nacholapithecus kerioi* from northern Kenya. J Hum Evol 94:117–125

Köhler M, Moyà-Solà S (1997) Ape-like or hominid-like? The positional behavior of *Oreopithecus bambolii* reconsidered. Proc Natl Acad Sci U S A 94:11747–11750

Kunimatsu Y, Nakatsukasa M, Shimizu D, Nakano Y, Ishida H (2019) Loss of the subarcuate fossa and the phylogeny of Nacholapithecus. J Hum Evol 131:22–27

Larson SG (1998) Parallel evolution in the hominoid trunk and forelimb. Evol Anthropol 6:87–99

Lovejoy CO (2005) The natural history of human gait and posture. Part 1. Spine and pelvis. Gait Posture 21:95–112

Lovejoy CO, Suwa G, Spurlock L, Asfaw B, White TD (2009a) The pelvis and femur of *Ardipithecus ramidus*: the emergence of upright walking. Science 326:e71–e76

Lovejoy CO, Suwa G, Simpson SW, Matternes JH, White TD (2009b) The great divides: *Ardipithecus ramidus* reveals the postcrania of our last common ancestors with African apes. Science 326:100–106

Machnicki AL, Spurlock LB, Strier KB, Reno PL, Lovejoy CO (2016) First steps of bipedality in hominids: evidence from the atelid and proconsulid pelvis. PeerJ 4:e1521

MacLatchy L (2004) The oldest ape. Evol Anthropol 13:90–103

Matsudaira K, Ishida T (2010) Phylogenetic relationships and divergence dates of the whole mitochondrial genome sequences among three gibbon genera. Mol Phylogenet Evol 55:454–459
McCollum MA, Rosenman BA, Suwa G, Meindl RS, Lovejoy CO (2010) The vertebral formula of the last common ancestor of African apes and humans. J Exp Zool B Mol Dev Evol 314B:123–134
McNulty KP, Begun DR, Kelley J, Manthi FK, Mbua EN (2015) A systematic revision of *Proconsul* with the description of a new genus of early Miocene hominoid. J Hum Evol 84:42–61
Moyà-Solà S, Köhler M (1996) A *Dryopithecus* skeleton and the origins of great-ape locomotion. Nature 379:156–159
Moyà-Solà S, Köhler M, Alba DM, Casanovas-Vilar I, Galindo J (2004) *Pierolapithecus catalaunicus*, a new middle Miocene great ape from Spain. Nature 306:1339–1344
Moyà-Solà S, Köhler M, Alba DM, Casanovas-Vilar I, Galindo J, Robles JM, Cabrera L, Garcés M, Almécija S, Beamud E (2009) First partial face and upper dentition of the Middle Miocene hominoid *Dryopithecus fontani* from Abocador de Can Mata (Vallès-Penedès Basin, Catalonia, NE Spain): taxonomic and phylogenetic implications. Am J Phys Anthropol 139:126–145
Nakatsukasa M (2008) Comparative study of Moroto vertebral specimens. J Hum Evol 55:581–588
Nakatsukasa M, Hirose Y (2003) Scaling of lumbar vertebrae in anthropoids and implications for evolution of the hominoid axial skeleton. Primates 44:127–135
Nakatsukasa M, Kunimatsu Y (2009) *Nacholapithecus* and its importance for understanding hominoid evolution. Evol Anthropol 18:103–119
Nakatsukasa M, Yamanaka A, Kunimatsu Y, Shimizu D, Ishida H (1998) A newly discovered *Kenyapithecus* skeleton and its implications for the evolution of positional behavior in Miocene East African hominoids. J Hum Evol 34:657–664
Nakatsukasa M, Kunimatsu Y, Nakano Y, Takano T, Ishida H (2003a) Comparative and functional anatomy of phalanges in *Nacholapithecus kerioi*, a Middle Miocene hominoid from northern Kenya. Primates 44:371–412
Nakatsukasa M, Tsujikawa H, Shimizu D, Takano T, Kunimatsu Y, Nakano Y, Ishida H (2003b) Definitive evidence for tail loss in *Nacholapithecus*, an East African Miocene hominoid. J Hum Evol 45:179–186
Nakatsukasa M, Ward CV, Walker A, Teaford MF, Kunimatsu Y, Ogihara N (2004) Tail loss in *Proconsul heseloni*. J Hum Evol 46:777–784
Nakatsukasa M, Kunimatsu Y, Nakano Y, Ishida H (2007) Vertebral morphology of *Nacholapithecus kerioi* based on KNM-BG 35250. J Hum Evol 52:347–369
Nakatsukasa M, Almécija S, Begun DR (2016) The hands of Miocene hominoids. In: Kivell TL, Lemelin P, Richmond BG, Schmitt D (eds) The evolution of the primate hand. Springer, New York, pp 485–514
Napier JR, Napier PH (1967) A handbook of living primates. Academic Press, London
Narita Y, Kuratani S (2005) Evolution of the vertebral formulae in mammals: a perspective on developmental constraints. J Exp Zool B Mol Dev Evol 304:91–106
Pal TGP, Routal RV (1987) Transmission of weight through the lower thoracic and lumbar regions of the vertebral column in man. J Anat 152:93–105
Patel BA, Grossman A (2006) Dental metric comparison of *Morotopithecus* and *Afropithecus*: implications for the validity of the genus *Morotopithecus*. J Hum Evol 51:506–512
Pérez de los Ríos M, Moyà-Solà S, Alba DM (2012) The nasal and paranasal architecture of the Middle Miocene ape *Pierolapithecus catalaunicus* (primates: Hominidae): Phylogenetic implications. J Hum Evol 63:497–506
Pickford M (2002) New reconstruction of the Moroto hominoid snout and a reassessment of its affinities to *Afropithecus turkanensis*. Hum Evol 17:1–19
Pilbeam DR (1969) Tertiary Pongidae of East Africa: evolutionary relationships and taxonomy. Bulletin (Peabody Mus Nat Hist) 31:1–185
Pilbeam D (1996) Genetic and morphological records of the Hominoidea and hominid origins: a synthesis. Mol Phylogenet Evol 5:155–168
Pilbeam D (2004) The anthropoid postcranial axial skeleton: comments on development, variation, and evolution. J Exp Zool B Mol Dev Evol 302B:241–267

Rafferty KL, Walker A, Ruff CB, Rose MD, Andrews PJ (1995) Postcranial estimates of body weight in *Proconsul*, with a note on a distal tibia of *P. major* from Napak, Uganda. Am J Phys Anthropol 97:391–402

Reno PL (2014) Genetic and developmental basis for parallel evolution and its significance for hominoid evolution. Evol Anthropol 23:188–200

Rockwell H, Evans FG, Pheasant HC (1938) The comparative morphology of the vertebrate spinal column. Its form as related to function. J Morphol 63:87–117

Rose MD (1975) Functional proportions of primate lumbar vertebral bodies. J Hum Evol 4:21–38

Rose MD, Nakano Y, Ishida H (1996) *Kenyapithecus* postcranial specimens from Nachola, Kenya. Afr Study Monogr S24:3–56

Russo GA (2010) Prezygapophyseal articular facet shape in the catarrhine thoracolumbar vertebral column. Am J Phys Anthropol 142:600–612

Russo GA (2015) Postsacral vertebral morphology in relation to tail length among primates and other mammals. Anat Rec 298:354–375

Russo GA (2016) Comparative sacral morphology and the reconstructed tail lengths of five extinct primates: *Proconsul heseloni*, *Epipliopithecus vindobonensis*, *Archaeolemur edwardsi*, *Megaladapis grandidieri*, and *Palaeopropithecus kelyus*. J Hum Evol 90:135–162

Russo GA, Shapiro LJ (2013) Reevaluation of the lumbosacral region of *Oreopithecus bambolii*. J Hum Evol 65:253–265

Sanders WJ (1995) Function, allometry, and evolution of the australopithecine lower precaudal spine. Ph.D. Dissertation. New York University

Sanders WK, Bodenbender BE (1994) Morphometric analysis of lumbar vertebra UMP 67-28: implications for spinal function and phylogeny of the Miocene Moroto hominoid. J Hum Evol 26:203–237

Schultz AH (1930) The skeleton of the trunk and limbs of the higher primates. Hum Biol 2:303–408

Schultz AH (1956) Postembryonic age change. Primatologia 1:887–964

Schultz AH (1960) Einige Beobachtungen und Mass am Skelett von *Oreopithecus* im Vergleich mit anderen catarrhinen Primaten. Z Morphol Anthropol 50:136–149

Schultz AH (1961) Vertebral column and thorax. Primatologia 4:1–66

Schultz AH, Straus WL Jr (1945) The numbers of vertebrae in primates. Proc Am Philos Soc 89:601–626

Shapiro L (1993) Functional morphology of the vertebral column in primates. In: Gebo DL (ed) Postcranial adaptation in nonhuman primates. Northern Illinois University Press, Dekalb, pp 121–149

Sherwood RJ, Ward S, Hill A, Duren DL, Brown B, Downs W (2002) Preliminary description of the *Equatorius africanus* partial skeleton (KNM-TH 28860) from Kipsaramon, Tugen Hills, Baringo District, Kenya. J Hum Evol 42:63–73

Slijper E (1946) Comparative biologic-anatomical investigations on the vertebral column and spinal musculature of mammals. Verh K Ned Akad Wet 42:1–128

Stewart CB, Disotell TR (1998) Primate evolution- in and out of Africa. Curr Biol 8:582–588

Straus WL (1963) The classification of *Oreopithecus*. In: Washburn SL (ed) Classification and human evolution. Aldine Publishing Co, Chicago, pp 146–177

Susanna I, Alba DM, Almécija S, Moyà-Solà S (2014) The vertebral remains of the late Miocene great ape *Hispanopithecus laietanus* from Can Llobateres 2 (Vallès-Penedès Basin, NE Iberian Peninsula). J Hum Evol 73:15–34

Thompson NE, Almécija S (2017) The evolution of vertebral formulae in Hominoidea. J Hum Evol 110:18–36

Tuttle RH (1975) Parallelism, brachiation, and hominoid phylogeny. In: Luckett WP, Szalay FS (eds) Phylogeny of the primates. Plenum Press, New York, pp 447–480

Walker A (1997) *Proconsul*: function and phylogeny. In: Begun DR, Ward CV, Rose MD (eds) Function, phylogeny, and fossils: miocene hominoid evolution and adaptations. Plenum Press, New York, pp 209–224

Walker AC, Pickford M (1983) New postcranial fossils of *Proconsul africanus* and *Proconsul nyanzae*. In: Ciochon RL, Corruccini RS (eds) New interpretations of ape and human ancestry. Plenum Press, New York, pp 325–351

Walker AC, Rose MD (1968) Fossil hominoid vertebra from the Miocene of Uganda. Nature 217:980–981

Ward CV (1991) Functional anatomy of the lower back and pelvis of the Miocene hominoid *Proconsul nyanzae* from Mfangano Island, Kenya. Ph.D. Dissertation. The Johns Hopkins University

Ward CV (1993) Torso morphology and locomotion in *Proconsul nyanzae*. Am J Phys Anthropol 92:291–328

Ward CV (1998) Afropithecus, Proconsul, and the primitive hominoid skeleton. In: Strasser E, Fleagle J, Rosenberger A, McHenry H (eds) Primate locomotion: recent advances. Plenum Press, New York, pp 337–352

Ward CV (2007) Postcranial and locomotor adaptations of hominoids. In: Henke W, Tattersall I (eds) Handbook of paleoanthropology. Springer, Berlin, pp 1011–1030

Ward CV, Walker A, Teaford MF (1991) *Proconsul* did not have a tail. J Hum Evol 21:215–220

Ward CV, Walker A, Teaford MF, Odhiambo I (1993) Partial skeleton of *Proconsul nyanzae* from Mfangano Island. Am J Phys Anthropol 90:77–111

Ward S, Brown B, Hill A, Kelley J, Downs W (1999) *Equatorius*: A new hominoid genus from the middle Miocene of Kenya. Science 285:1382–1386

White TD, Lovejoy CO, Asfaw B, Carlson JP, Suwa G (2015) Neither chimpanzee nor human, *Ardipithecus* reveals the surprising ancestry of both. Proc Natl Acad Sci U S A 112:4877–4884

Williams SA (2011) Variation in anthropoid vertebral formulae: implications for homology and homoplasy in hominoid evolution. J Exp Zool B Mol Dev Evol 318:134–147

Williams SA (2012) Placement of the diaphragmatic vertebra in catarrhines: implications for the evolution of dorsostability in hominoids and bipedalism in hominins. Am J Phys Anthropol 148:111–122

Williams SA, Russo GA (2015) Evolution of the hominoid vertebral column: the long and the short of it. Evol Anthropol 24:15–32

Williams SA, Middleton ER, Villamil CI, Shattuck MR (2016) Vertebral numbers and human evolution. Am J Phys Anthropol 159(S61):19–36

Williams SA, Gómez-Olivencia A, Pilbeam D (2019) Numbers of Vertebrae in Hominoid Evolution. In: Been E, Gómez-Olivencia A, Kramer PA (eds) Spinal evolution: morphology, function, and pathology of the spine in hominoid evolution. Springer, New York, pp 97–124

Wilson DR (1972) Tail reduction in *Macaca*. In: Tuttle R (ed) The functional and evolutionary biology of primates. Aldine, New York, pp 241–261

Wood B, Harrison T (2011) The evolutionary context of the first hominins. Nature 470:347–352

Wrangham R, Pilbeam D (2001) African apes as time machines. In: Galdikas BMF, Briggs NE, Sheeran LK, Shapiro GL, Goodall J (eds) All apes great and small: volume 1: African apes. Kluwer Academic, New York, pp 5–17

Young NM (2003) A reassessment of living hominoid postcranial variability: implications for ape evolution. J Hum Evol 45:441–464

Zapfe H (1958) The skeleton of *Pliopithecus* (*Epipliopithecus*) *vindobonensis* Zapfe and Hürzeler. Am J Phys Anhropol 16:441–458

Chapter 6
Numbers of Vertebrae in Hominoid Evolution

Scott A. Williams, Asier Gómez-Olivencia, and David R. Pilbeam

6.1 Introduction

One of the most obvious and well-studied aspects of the vertebral column is the regional numbers of vertebrae composing the spine. Modern humans normally have 7 cervical (7 C), 12 thoracic (12 T), and 5 lumbar (5 L) vertebrae, along with 5 elements of the sacrum (5 S) and 4 variably fused coccygeal elements. This is uncontroversial and reported in human anatomy and osteology textbooks. Variation in human vertebral numbers is less well-known, as are numbers of vertebrae in our closest living relatives, the nonhuman apes, especially the lesser apes, or gibbons (family Hylobatidae). In a larger framework, extant hominoids (humans and other apes, superfamily Hominoidea) are characterized by the absence of an external tail (instead possessing a coccyx), a reduced number of trunk (thoracolumbar) vertebrae, a spine that is invaginated ventrally into the thorax, and morphological differences in individual vertebrae primarily associated with biomechanical changes

S. A. Williams (✉)
Center for the Study of Human Origins, Department of Anthropology, New York University, New York, NY, USA

New York Consortium in Evolutionary Primatology, New York, NY, USA
e-mail: sawilliams@nyu.edu

A. Gómez-Olivencia
Departamento de Estratigrafía y Paleontología, Facultad de Ciencia y Tecnología, Universidad del País Vasco/Euskal Herriko Unibertsitatea (UPV/EHU), Leioa, Spain

IKERBASQUE. Basque Foundation for Science, Bilbao, Spain

Centro Mixto UCM-ISCIII de Evolución y Comportamiento Humanos, Madrid, Spain

D. R. Pilbeam
Department of Human Evolutionary Biology, Harvard University, Cambridge, MA, USA

E. Been et al. (eds.), *Spinal Evolution*,
https://doi.org/10.1007/978-3-030-19349-2_6

related to orthograde posture and forelimb-dominated locomotion compared to their closest relatives, the Old World monkeys (cercopithecoids) and known stem anthropoids, catarrhines, and hominoids (reviewed in Williams and Russo 2015). Additionally, extant hominoids differ from most primates, and from cercopithecoids in particular, in demonstrating high levels of variation in regional numbers of vertebrae (Williams et al. 2016, 2019). The paucity of the fossil record makes controversial our interpretation of the sequence of evolutionary changes that led to the current configurations of vertebrae in modern humans and other living apes (Haeusler et al. 2002; Pilbeam 2004; McCollum et al. 2010; Williams 2012c; Gómez-Olivencia and Gómez-Robles 2016; Williams et al. 2016; Pilbeam and Lieberman 2017; Thompson and Almécija 2017).

Ancestral primates, anthropoids, and catarrhines are thought to have retained a primitive mammalian vertebral formula (Ji et al. 2002; Bi et al. 2014) consisting of 7 cervical vertebrae (7 C), 19 thoracolumbar (19 TL) vertebrae (either 13 T and 6 L or 12 T and 7 L), and a sacrum composed of 3 fused vertebral elements (3 S) (Todd 1922; Schultz and Straus 1945; Zapfe 1958; Pilbeam 2004; Williams 2011; Thompson and Almécija 2017). Although none preserve a complete vertebral column, stem catarrhines (e.g., *Epipliopithecus vindobonensis*) and stem hominoids (e.g., *Ekembo nyanzae*, *Nacholapithecus kerioi*) seem to conform to this pattern (Zapfe 1960; Ward 1993; Ishida et al. 2004; Nakatsukasa and Kunimatsu 2009). Extant hominoids demonstrate a reduced number of thoracolumbar vertebrae from the primitive mammalian number of 19 retained by most mammals, including many primates (Todd 1922; Schultz and Straus 1945; Pilbeam 2004; Narita and Kuratani 2005; Williams 2011). Among hominids (i.e., great apes and humans; family Hominidae), the putative stem hominid *Oreopithecus bambolii* is the only Miocene hominoid that preserves a complete sacrum. Together with a reduced lumbar column consisting of five lumbar vertebrae (Schultz 1960), a preserved sacrum has either six (Harrison 1986) or five (Haeusler et al. 2002) vertebral elements. Other Miocene hominids may also have reduced lumbar regions (Susanna et al. 2014). Known early hominins seem to have the same number of vertebrae as modern humans (Robinson 1972; Haeusler et al. 2011; Williams et al. 2013; Meyer et al. 2015; Ward et al. 2017).

Researchers are divided on the regional numbers of vertebrae that characterized the last common ancestor of humans and chimpanzees/bonobos (LCA; see Pilbeam and Lieberman 2017). The largest disagreements concern the numbers of vertebrae in the lumbar region and in the thoracolumbar and precaudal (CTLS) combined regions, together with debate over the absolute position of the transitional (or diaphragmatic) vertebra, the level at which the zygapophyses change in shape and orientation from transverse to roughly parasagittal. The position of the transitional vertebra (with transversely oriented superior articular facets and parasagittally oriented lower articular facets) has been identified as the limit between regions with different biomechanical roles due to the constraints on mobility related to facet orientation (Rockwell et al. 1938; Erikson 1963; Washburn 1963; Clauser 1980; Shapiro 1993; Williams 2012b). Because the cervical region is nearly invariable at seven (7 C) in most mammals, including hominoids, its inclusion in precaudal or exclusion in presacral (C+TL) counts does not affect results.

Lovejoy and colleagues (Lovejoy et al. 2009; Lovejoy and McCollum 2010; McCollum et al. 2010; Machnicki et al. 2016) propose a "long-backed" ancestor with numerically long lumbar (6–7 L), thoracolumbar (18–19 TL), and precaudal (30–31 CTLS) regions. Their proposal is based on two principal sources of information, the first of which is the interpretation that early hominins had 18 or more thoracolumbar vertebrae (12 T and 6 L) (Robinson 1972; Latimer and Ward 1993; Sanders 1998; Pilbeam 2004; Lovejoy et al. 2009). However, this hypothesis has largely been rejected in favor of a shorter trunk (17 TL) in known early hominins (Benade 1990; Haeusler et al. 2002, 2011; Toussaint et al. 2003; Williams 2012b; Williams et al. 2013, 2016, 2018; Ward et al. 2017; Gómez-Olivencia and Gómez-Robles 2016). What differs between early hominins and modern humans is that the transitional vertebra occurs at the penultimate thoracic (rib-bearing) level (i.e., T11) in *Australopithecus afarensis*, *Au. africanus*, *Au. sediba*, and *Homo erectus* (Haeusler et al. 2002, 2011; Williams et al. 2013, 2018; Meyer et al. 2015; Ward et al. 2017), whereas it modally occurs at the level of the last thoracic vertebra (i.e., T12) in modern humans (Williams 2012a, b; Williams et al. 2016; contra Haeusler et al. 2011, 2012). Lovejoy et al. (2009) predict 6 lumbar (6 L) and 12 thoracic vertebrae (12 T; 18 TL) in the ARA-VP-6/500 *Ardipithecus ramidus* partial skeleton, but this is hypothetical rather than inferred from preserved vertebral elements. The second factor influencing Lovejoy and colleagues' long-backed hypothesis is the hypothesis that the number of precaudal vertebrae present in bonobos (*Pan paniscus*), which is larger than in modern humans or common chimpanzees (*Pan troglodytes*), is primitive (McCollum et al. 2010).

Pilbeam, Williams, and others (Pilbeam 2004; Williams 2011, 2012c; Fulwood and O'Meara 2014; Williams and Russo 2015; Williams et al. 2016; Pilbeam and Lieberman 2017; Thompson and Almécija 2017) argue for a "short-backed" LCA with fewer numbers of vertebrae (4 L, 17 TL, 29–30 CTLS) with a transitional vertebra located at the same position as the last thoracic (rib-bearing) vertebra (i.e., V20, where V1 is the first cervical vertebra). Still others have argued for an "intermediate" lumbar column (5 L) within a short torso (17 TL, 29 CTLS) (Haeusler et al. 2002) based on the interpretation that the modern human configuration represents the ancestral condition. Gómez-Olivencia and Gómez-Robles (2016) proposed a functionally "intermediate" lower back with five post-transitional vertebrae (i.e., the transitional vertebra at V19) despite the presence of a short lumbar spine (4 L, with 17 TL and 29 CTLS). These opposing scenarios have implications for reconstructing the positional behaviors that characterized the LCA and preceded bipedalism and for the evolutionary history of hominoid evolution and amount of homoplasy that occurred during it. The long-back models invoke extensive homoplasy in the repeated reduction of vertebral numbers in extant apes and humans, whereas the short-back model relies on the homology of reduced vertebral numbers in ancestral hominoids. The strict short-back model implies that the absolute position of the transitional vertebra changed from V20 in the LCA to V18 in early hominins, then to V19 in modern humans (Williams et al. 2016). Fossil hominins have been interpreted as supporting all three models: long (Lovejoy et al. 2009; Machnicki

et al. 2016), intermediate (Haeusler et al. 2002; Gómez-Olivencia and Gómez-Robles 2016), and short (Pilbeam 2004; Williams 2012c; Williams et al. 2016; Pilbeam and Lieberman 2017; Thompson and Almécija 2017).

In order to move this debate forward, the first step is to establish vertebral formulae in as many extant taxa as possible. Here, we provide an exhaustive dataset of cervical, thoracic, lumbar, and sacral numbers of vertebrae in extant hominoids; coccygeal numbers are not reported here due to difficulty in ascertaining full counts in skeletal remains. We report descriptive statistics on the largest samples of living apes yet compiled, along with a large sample of modern humans (data on fossil hominins are reported in Gómez-Olivencia and Been 2019; Meyer and Williams 2019; Williams and Meyer 2019). We provide data on two species of *Pongo*, the Borneo (*Pongo pygmaeus*) and Sumatran (*P. abelii*) orangutans. We also present data on subspecies of *Pan*—eastern (*Pan troglodytes schweinfurthii*), central (*P. t. troglodytes*), and western (*P. t. verus*) chimpanzees—in addition to the largest sample of bonobos (*P. paniscus*) yet published. For gorillas, we include both western (*Gorilla gorilla*) and eastern (*G. beringei*) species, as well as subspecies of the latter, mountain (*G. b. beringei*) and eastern lowland (*G. b. graueri*) gorillas. Finally, we explore diversity within Hylobatidae by including 10 of the 14 or more hylobatid species (Kim et al. 2011; Zichello 2018).

6.2 Materials and Methods

Our dataset is rooted in the Schultz/Pilbeam dataset (see Williams et al. 2016), combined with data collected by AGO (see Gómez-Olivencia and Gómez-Robles 2016) at a number of European collections. Overlapping specimens allowed for an assessment of repeatability, which was high, and care was taken to not include the same specimen more than once in the combined dataset. Species and subspecies affiliation was determined using museum accession and locality information. We sample 2599 complete hominoid vertebral columns including 2075 hominids (763 humans and 1312 great apes) representing all species and subspecies except *Pongo tapanuliensis* (Nater et al. 2017) and *Pan troglodytes ellioti* (Hey 2010; Prado-Martinez et al. 2013) and 524 hylobatids from 10 species representing all 4 genera (Carbone et al. 2014; Zichello 2018) (Appendix). Two cercopithecoid species, one colobine, *Trachypithecus cristatus* ($n = 88$), and one cercopithecine, *Papio cynocephalus* ($n = 50$), are included for comparison and bring the total sample size of the dataset to 2737.

We use the Schultz criteria for defining vertebral regions (Schultz 1961; Williams and Russo 2015; Williams et al. 2016), allowing for intermediate vertebrae at regional boundaries (i.e., half-and-half count vertebrae with diagnostic morphological features presented asymmetrically). We also record the absolute level at which the transitional vertebra occurs in the series (e.g., V19, the 19th vertebra, which would be T12 in a spine with seven cervical vertebrae), which is defined as the thoracolumbar vertebra in a series that bears flat, coronally oriented prezygapophyses and curved, sagittally oriented postzygapophyses (Washburn 1963; Shapiro 1993; Williams 2012b; Williams and Russo 2015; Gómez-Olivencia and

Gómez-Robles 2016; Williams et al. 2016). Completely asymmetrical transitions, where the zygapophyses on one side are flat and coronally oriented and curved and sagittally oriented on the other, are recorded across two levels (e.g., V19–20, or V19.5). Sample sizes (total $N = 2180$) for position of the transitional vertebra are lower, in part because Schultz did not record it. Hominids are represented by 1690 specimens from the same species and subspecies as above (732 humans and 958 great apes), while 352 hylobatid specimens from 7 species and 3 genera are included. The cercopithecoids species and sample sizes are the same as listed above.

We use measures of intraspecific/subspecific heterogeneity (morphological heterogeneity index) and interspecific/subspecific similarity (normalized morphological similarity index) (Pilbeam 2004; Williams 2012c; Williams et al. 2016) to quantify patterns of variation in hominoid vertebral formulae. The heterogeneity index is measured in each taxon as:

$$1-\sum_{i=1} f_i^2\left[\frac{n}{n-1}\right],$$

where f is the frequency of a single vertebral formula and n is the taxon sample size. The heterogeneity index can range from 0 (no variation) to 1 (number of different formulae = n). The similarity index is used to compare vertebral formulae between pairs of taxa and is calculated as:

$$\sum x_i y_i \,/\left(\sum x_i^2 y_i^2\right)^{1/2},$$

where $x_i\, y_i$ is the probability of sampling formula i from both taxon x and taxon y. The similarity index can range from 0 (no shared formulae) to 1 (identical frequencies of formulae).

6.3 Results

Summary statistics of vertebral regions, combined regions, and position of the transitional vertebra are provided in the Appendix, along with the vertebral profile (modal formula and other formulae present in a population at ≥10% frequency). A second vertebral profile including the position of the transitional vertebra (C, T, L, S + position of the transitional vertebra) is also listed for each taxon. Extant hominoids broadly vary in having 6 to 8 cervical vertebrae, 11 to 15 thoracic vertebrae, 2 to 6 lumbar vertebrae, and 3 to 8 sacral vertebrae. The transitional vertebra varies in placement from V17 to V23, situated most commonly at the level of the last thoracic vertebra. Each extant hominid genus is characterized by a different modal vertebral formula (7 C: 12 T: 5 L: 5 S in *Homo*, 7:13:4:6 in *Pan*, 7:12:4:5 in *Pongo*, and within *Gorilla*, 7:13:4:5 in *G. gorilla* and 7:13:3:6 in *G. beringei*). Most hylobatid species are characterized by one of two modal vertebral formulae (7:13:5:4, 7:13:5:5), with the exception of *Hylobates pileatus*, which possesses one fewer

thoracic vertebra modally (7:12:5:4), and *Nomascus gabriellae*, with one additional thoracic vertebra in its modal formula (7:14:5:5). It should be noted, however, that the latter two hylobatid species are represented by low sample sizes in this study (n = 8 and 14, respectively). The two cercopithecoids present different vertebral formula modes: 7:12:7:3 in *T. cristatus* and 7:13:6:3 in *P. cynocephalus*, the former being the most common pattern in cercopithecoids (Schultz and Straus 1945; Clauser 1980; Pilbeam 2004; Williams 2011, 2012c).

In contrast to full vertebral formulae, combined regional counts are more similar within and across hominoid taxa, although combined thoracolumbar region is more phylogenetically structured than total precaudal count (Tables 6.1 and 6.2). Modal precaudal number (CTLS) is 29 in hominines (African apes and humans) except *P. paniscus* and *P. t. schweinfurthii*, where it is 30, although high, nearly bimodal frequencies of 29 and 30 are found across *Pan* species and subspecies. *Homo* and *Gorilla* are characterized by high frequencies of 29 precaudal vertebrae. Hylobatids are somewhat more variable, ranging from modes of 28 (*H. pileatus* and *N. concolor*) to 31 (*N. gabriellae*) precaudal vertebrae, with all other genera and species

Table 6.1 Frequencies of precaudal numbers of vertebrae in hominoid taxa

N	Taxon	26	27	28	29	30	31	32
88	*Trachypithecus cristatus*			8.5%	**90.3%**	1.1%		
50	*Papio cynocephalus*		2.0%	18.0%	**76.0%**	4.0%		
260	*Hylobates lar*			11.9%	**73.7%**	13.3%	1.2%	
32	*Hylobates agilis*			10.9%	**59.4%**	29.7%		
35	*Hylobates muelleri*		5.7%	10.0%	**44.3%**	35.7%	4.3%	
12	*Hylobates klossii*			8.3%	20.8%	**70.8%**		
8	*Hylobates pileatus*			**57.1%**	42.9%			
30	*Hylobates moloch*			3.3%	40.0%	**56.7%**		
24	*Nomascus concolor*		4.2%	**54.2%**	33.3%	4.2%	4.2%	
14	*Nomascus gabriellae*					28.6%	**64.3%**	7.1%
25	*Hoolock hoolock*			16.0%	**66.0%**	18.0%		
84	*Symphalangus syndactylus*		1.2%	9.5%	**47.6%**	36.9%	4.8%	
163	*Pongo pygmaeus*	1.4%	14.7%	**55.2%**	24.1%	4.5%		
46	*Pongo abelii*		17.4%	**57.6%**	22.8%	2.2%		
264	*Pongo*	0.8%	18.6%	**56.8%**	21.0%	2.8%		
71	*Gorilla beringei beringei*			9.6%	**84.6%**	5.9%		
28	*Gorilla beringei graueri*		3.6%	0.0%	**85.7%**	10.7%		
119	*Gorilla beringei*		0.8%	6.7%	**86.6%**	5.9%		
375	*Gorilla gorilla*		0.8%	12.3%	**58.3%**	27.6%	0.9%	0.1%
52	*Pan troglodytes schweinfurthii*			3.1%	22.9%	**65.6%**	8.3%	
241	*Pan troglodytes troglodytes*			4.7%	**48.9%**	43.8%	2.6%	
24	*Pan troglodytes verus*			4.2%	**58.3%**	33.3%	4.2%	
499	*Pan troglodytes*			4.6%	**47.5%**	45.1%	2.8%	
55	*Pan paniscus*			1.8%	9.1%	**44.5%**	37.3%	7.3%
763	*Homo sapiens*		0.1%	4.3%	**72.5%**	22.7%	0.3%	

Table 6.2 Frequencies of thoracolumbar numbers of vertebrae in hominoid taxa

N	Taxon	14	15	16	17	18	19	20
88	*T.cri.*						**97.7%**	2.3%
50	*P.cyn.*				2.0%	6.0%	**90.0%**	2.0%
260	*H.lar*				4.2%	**72.9%**	22.9%	
32	*H.agi.*				18.8%	**73.4%**	7.8%	
35	*H.mue.*			8.6%	11.4%	**72.9%**	7.1%	
12	*H.klo.*				8.3%	**75.0%**	16.7%	
8	*H.pil.*				**57.1%**	42.9%		
30	*H.mol.*				20.0%	**75.0%**	5.0%	
24	*N.con.*				16.7%	**75.0%**	8.3%	
14	*N.gab.*					25.0%	**67.9%**	7.1%
25	*H.hoo.*				22.0%	**74.0%**	4.0%	
84	*S.syn.*			2.4%	34.5%	**58.9%**	4.2%	
163	*P.pyg.*	0.3%	17.1%	**71.7%**	10.8%			
46	*P.abe.*		2.2%	**87.0%**	10.9%			
264	*Pongo*	0.2%	15.0%	**76.1%**	8.7%			
71	*G.b.ber.*		1.5%	**91.2%**	7.4%			
28	*G.b.gra.*		3.6%	**96.4%**				
119	*G.ber.*		2.1%	**92.9%**	**5.0%**			
375	*G.gor.*		0.8%	42.5%	**55.5%**	1.2%		
52	*P.t.sch.*			12.5%	**79.2%**	8.3%		
241	*P.t.tro.*		0.4%	24.4%	**71.4%**	3.8%		
24	*P.t.ver.*			41.7%	**50.0%**	8.3%		
499	*P.tro.*		0.4%	25.5%	**70.4%**	3.7%		
55	*P.pan.*			11.8%	**73.6%**	14.5%		
763	*H.sap.*		0.1%	7.5%	**87.5%**	4.9%		

possessing 29 or 30. The cercopithecoids both have modes of 29 precaudal vertebrae. Thoracolumbar counts are more stable within Hominidae and Hylobatidae, with *Homo*, all *Pan* species and subspecies, and *G. gorilla* characterized by 17 thoracolumbar vertebrae. *G. beringei* and its subspecies and both studied species of *Pongo* have modes of 16 TL. In hylobatids, nearly all species are modal at 18 TL; *H. pileatus* and *N. gabriellae* are the exceptions, with modes of 17 and 19 TL vertebrae, respectively. *Trachypithecus cristatus* and *P. cynocephalus* retain the primitive number of 19 TL vertebrae. Cercopithecoid sacral segment modes are both strongly three (3 S), whereas hylobatids' are either four or five (4–5 S) and hominids' are five or six (5–6 S) (Table 6.3).

Interspecific similarity and intraspecific/subspecific heterogeneity indices are reported in Figs. 6.1, 6.2, and 6.3. Generally, hylobatid species are more similar to each other in vertebral formulae than hominids are to each other (Fig. 6.1). The hylobatids' average similarity index is 0.568 for vertebral formulae comparisons, whereas the hominid average is 0.303. The average similarity index for thoracolumbar count of hylobatids (0.828) is also higher than that of hominids (0.654);

Table 6.3 Frequencies of sacral vertebra numbers in hominoid taxa

N	Taxon	2	3	4	5	6	7	8
88	*T.cri.*	9.7%	**90.3%**					
50	*P.cyn.*	12.0%	**86.0%**	2.0%				
260	*H.lar*		23.8%	**67.2%**	9.0%			
32	*H.agi.*		1.6%	**67.2%**	31.3%			
35	*H.mue.*		1.4%	**58.6%**	37.1%	2.9%		
12	*H.klo.*			45.8%	**54.2%**			
8	*H.pil.*			**100.0%**				
30	*H.mol.*		1.7%	36.7%	**56.7%**	5.0%		
24	*N.con.*			45.8%	**50.0%**	4.2%		
14	*N.gab.*			7.1%	**89.3%**	3.6%		
25	*H.hoo.*		4.0%	**72.0%**	24.0%			
84	*S.syn.*			38.1%	**54.2%**	7.7%		
163	*P.pyg.*			11.9%	**53.5%**	32.9%	1.7%	
46	*P.abe.*			18.5%	**60.9%**	20.7%		
264	*Pongo*			15.0%	**56.3%**	27.5%	1.3%	
71	*G.b.ber.*				13.2%	**81.6%**	5.1%	
28	*G.b.gra.*				3.6%	**85.7%**	10.7%	
119	*G.ber.*				10.1%	**84.5%**	5.5%	
375	*G.gor.*			1.5%	41.7%	**52.7%**	3.9%	0.3%
52	*P.t.sch.*			1.0%	20.8%	**72.9%**	5.2%	
241	*P.t.tro.*			1.3%	34.2%	**62.2%**	2.4%	
24	*P.t.ver.*				35.4%	**56.3%**	8.3%	
499	*P.tro.*			0.9%	34.0%	**60.5%**	4.6%	
55	*P.pan.*				14.5%	**43.6%**	34.5%	7.3%
763	*H.sap.*			1.0%	**76.3%**	22.5%	0.1%	

however, the average precaudal similarity index in both groups is nearly identical (hylobatids: 0.634, hominids: 0.629). *Trachypithecus cristatus* and *P. cynocephalus* are fairly dissimilar to each other in vertebral formulae (SI = 0.605) but much more similar in thoracolumbar (SI = 0.998) and precaudal (SI = 0.988) counts. Average heterogeneity indices are similar in both hominoid families, although hylobatids are higher in each comparison: vertebral formulae (hylobatids: 0.790, hominids: 0.736) and thoracolumbar (hylobatids: 0.481, hominids: 0.389) and precaudal (hylobatids: 0.600, hominids: 0.548) counts. *Papio cynocephalus* is similar to hominoids in vertebral formula heterogeneity (0.720), but lower in precaudal (0.396) and particularly thoracolumbar (0.189) heterogeneity indices. Heterogeneity is much lower in *T. cristatus* than in any hominoid taxon or in *P. cynocephalus* (vertebral formulae HI = 0.230; precaudal HI = 0.190; thoracolumbar HI = 0.045).

The transitional vertebra is positioned at vertebra 20 (V20) in the African great apes and at V19 in humans and orangutans (Table 6.4 and Appendix). Only 4 of 11 hylobatids are sampled adequately to quantify intraspecific variation, and each has the transitional vertebra at V20, although *H. lar* is nearly bimodal at V19 and V20.

C:T:L:S	*H.sap.*	*P.pan.*	*P.t.sch.*	*P.t.tro.*	*P.t.ver.*	*G.gor.*	*G.b.ber.*	*G.b.gra.*	*P.pyg.*	*P.abe.*
H.sap.	**0.576**									
P.pan.	0.008	**0.944**								
P.t.sch.	0.013	0.712	**0.779**							
P.t.tro.	0.018	0.668	**0.882**	**0.851**						
P.t.ver.	0.007	0.486	0.599	0.784	**0.873**					
G.gor.	0.017	0.487	0.623	**0.877**	**0.907**	**0.859**				
G.b.ber.	0.006	0.088	0.103	0.128	0.752	0.634	**0.568**			
G.b.gra.	0.001	0.084	0.090	0.312	0.741	0.598	**0.982**	**0.323**		
P.pyg.	0.069	0.024	0.065	0.063	0.035	0.105	0.103	0.018	**0.850**	
P.abe.	0.035	0.044	0.095	0.126	0.055	0.128	0.079	0.012	**0.961**	**0.735**

C:T:L:S	*S.syn.*	*H.hoo.*	*H.lar.*	*H.agi.*	*H.klo.*	*H.mol.*	*H.mue.*	*H.pil.*	*N.con.*	*N.gab.*
S.syn.	**0.890**									
H.hoo.	0.682	**0.727**								
H.lar.	0.555	**0.942**	**0.757**							
H.agi.	0.753	**0.935**	**0.873**	**0.835**						
H.klo.	0.714	0.504	0.368	0.689	**0.758**					
H.mol.	**0.859**	0.701	0.576	**0.828**	**0.905**	**0.782**				
H.mue.	0.777	0.817	0.770	**0.907**	0.736	**0.834**	**0.903**			
H.pil.	0.319	0.601	0.510	0.516	0.156	0.279	0.399	**0.810**		
N.con.	**0.831**	**0.891**	0.802	**0.938**	0.756	**0.906**	**0.880**	0.411	**0.757**	
N.gab.	0.170	0.026	0.003	0.076	0.107	0.111	0.086	0.000	0.066	**0.681**

Fig. 6.1 Matrix of similarity (off-diagonal) and heterogeneity indices (diagonal) calculated for hominid (top) and hylobatid (bottom) vertebral formulae. Darker shading within the lower triangle represents stronger similarity indices, determined by pooling all hominoid comparisons and separating into quintiles

CTLS	*H.sap.*	*P.pan.*	*P.t.sch.*	*P.t.tro.*	*P.t.ver.*	*G.gor.*	*G.b.ber.*	*G.b.gra.*	*P.pyg.*	*P.abe.*
H.sap.	**0.467**									
P.pan.	0.374	**0.777**								
P.t.sch.	0.594	0.830	**0.515**							
P.t.tro.	0.910	0.640	0.873	**0.672**						
P.t.ver.	**0.975**	0.545	0.756	**0.978**	**0.569**					
G.gor.	**0.982**	0.467	0.694	**0.953**	**0.988**	**0.621**				
G.b.ber.	**0.971**	0.207	0.394	0.790	0.898	0.930	**0.350**			
G.b.gra.	**0.982**	0.245	0.440	0.819	0.919	0.933	**0.991**	**0.262**		
P.pyg.	0.442	0.142	0.235	0.400	0.426	0.544	0.454	0.403	**0.630**	
P.abe.	0.399	0.513	0.187	0.349	0.379	0.499	0.489	0.367	**0.998**	**0.615**

CTLS	*S.syn.*	*H.hoo.*	*H.lar.*	*H.agi.*	*H.klo.*	*H.mol.*	*H.mue.*	*H.pil.*	*N.con.*	*N.gab.*
S.syn.	**0.653**									
H.hoo.	0.921	**0.560**								
H.lar.	0.888	**0.994**	**0.514**							
H.agi.	**0.978**	**0.979**	**0.960**	**0.613**						
H.klo.	**0.948**	0.761	0.710	0.876	**0.595**					
H.mol.	0.811	0.533	0.457	0.686	0.945	**0.561**				
H.mue.	**0.997**	0.911	0.875	**0.970**	**0.947**	0.818	**0.776**			
H.pil.	0.591	0.746	0.709	0.660	0.384	0.258	0.594	**0.571**		
N.con.	0.583	0.699	0.652	0.626	0.394	0.303	0.593	**0.989**	**0.616**	
N.gab.	0.314	0.104	0.085	0.178	0.330	0.385	0.315	0.000	0.085	**0.538**

Fig. 6.2 Matrix of similarity (off-diagonal) and heterogeneity indices (diagonal) calculated for hominid (top) and hylobatid (bottom) precaudal number. Darker shading within the lower triangle represents stronger similarity indices, determined by pooling all hominoid comparisons and separating into quintiles

TL	*H.sap.*	*P.pan.*	*P.t.sch.*	*P.t.tro.*	*P.t.ver.*	*G.gor.*	*G.b.ber.*	*G.b.gra.*	*P.pyg.*	*P.abe.*
H.sap.	**0.227**									
P.pan.	**0.988**	**0.430**								
P.t.sch.	**0.996**	**0.996**	**0.358**							
P.t.tro.	0.971	0.976	0.984	**0.432**						
P.t.ver.	0.819	0.862	0.860	0.932	**0.594**					
G.gor.	0.842	0.867	0.876	0.947	**0.993**	**0.573**				
G.b.ber.	0.165	0.233	0.234	0.398	0.694	0.670	**0.262**			
G.b.gra.	0.085	0.155	0.155	0.323	0.635	0.608	**0.997**	**0.262**		
P.pyg.	0.227	0.291	0.292	0.449	0.722	0.703	0.974	0.970	**0.478**	
P.abe.	0.208	0.240	0.276	0.437	0.724	0.702	**0.999**	**0.992**	0.978	**0.277**

TL	*S.syn.*	*H.hoo.*	*H.lar.*	*H.agi.*	*H.klo.*	*H.mol.*	*H.mue.*	*H.pil.*	*N.con.*	*N.gab.*
S.syn.	**0.567**									
H.hoo.	0.971	**0.457**								
H.lar.	0.866	0.943	**0.514**							
H.agi.	0.960	**0.998**	0.962	**0.458**						
H.klo.	0.963	**1.000**	0.952	**0.999**	**0.434**					
H.mol.	0.903	0.971	**0.995**	0.984	0.977	**0.439**				
H.mue.	0.928	0.984	0.968	**0.989**	**0.987**	0.985	**0.479**			
H.pil.	0.920	0.802	0.616	0.775	0.784	0.669	0.709	**0.571**		
N.con.	0.951	**0.996**	0.969	**1.000**	**0.998**	**0.988**	**0.991**	0.755	**0.420**	
N.gab.	0.353	0.378	0.607	0.427	0.392	0.535	0.425	0.206	0.725	**0.473**

Fig. 6.3 Matrix of similarity (off-diagonal) and heterogeneity indices (diagonal) calculated for hominid (top) and hylobatid (bottom) thoracolumbar count. Darker shading within the lower triangle represents stronger similarity indices, determined by pooling all hominoid comparisons and separating into quintiles

Table 6.4 Frequencies of the serial level of the transitional vertebra (TV)

N	Taxon	16	17	18	19	20	21	22	23	24
88	*T.cri.*		**97.7%**	2.3%						
50	*P.cyn.*	10.0%	**82.0%**	8.0%						
239	*H.lar*			0.8%	47.7%	**50.8%**	0.6%			
20	*H.agi.*				10.0%	**70.0%**	20.0%			
31	*H.mue.*				33.9%	**62.9%**	3.2%			
5	*H.klo.*					**80.0%**	20.0%			
6	*H.mol.*				**50.0%**	**50.0%**				
6	*N.con.*				**50.0%**	16.7%	33.3%			
45	*S.syn.*			2.2%	20.0%	**73.3%**	4.4%			
83	*P.pyg.*			12.7%	**66.9%**	20.5%				
32	*P.abe.*			6.3%	**57.8%**	32.8%	3.1%			
163	*Pongo*			12.6%	**62.3%**	24.5%	0.6%			
41	*G.b.ber.*			7.3%	24.4%	**48.8%**	9.8%	2.4%	7.3%	
27	*G.b.gra.*			7.4%	18.5%	**55.6%**	3.7%	11.1%	3.7%	
83	*G.ber.*		1.2%	7.8%	26.5%	**48.8%**	6.0%	4.8%	4.8%	
319	*G.gor.*			1.6%	18.0%	**63.6%**	13.2%	1.4%	1.9%	0.3%
44	*P.t.sch.*				26.1%	**68.2%**	5.7%			
203	*P.t.tro.*			1.0%	31.3%	**62.8%**	4.7%	0.2%		
17	*P.t.ver.*			2.9%	23.5%	**73.5%**				
342	*P.tro.*		0.1%	1.9%	28.7%	**69.3%**				
51	*P.pan.*				7.8%	**61.8%**	30.4%			
732	*H.sap.*		0.5%	33.9%	**60.9%**	4.7%				

Three additional species are inadequately sampled but are included in Table 6.4 for comparative purposes: one species shows the transitional vertebra at V20, one at V19, and one is bimodal (Table 6.4). The cercopithecoids both have the transitional vertebra at V18 at high frequency. Results are summarized and presented visually in Fig. 6.4.

6.4 Discussion

The ancestral number of precaudal vertebrae has been relatively unchanged throughout primate and hominoid evolution. Twenty-nine precaudal vertebrae are found in cercopithecoids and many platyrrhines and are thought to represent the ancestral condition in primates, anthropoids, and hominoids (7:13:6:3 or 7:12:7:3 = 29 CTLS; see above). Both cercopithecoid species included here and the majority of hylobatid and hominid taxa retain 29 precaudal vertebrae, although reductions to 28 and increases to 30 or 31 occur in some species (see Table 6.1). Non-hominoid primates commonly possess 29 precaudal vertebrae, varying infrequently from 19 thoracolumbar vertebrae and 3 sacral segments (Schultz and Straus 1945; Clauser 1980; Pilbeam 2004; Williams 2011, 2012c; Williams et al. 2016). *Trachypithecus cristatus* and *P. cynocephalus* conform to that pattern (Tables 6.1, 6.2, and 6.3 and Appendix). Hominoid thoracolumbar count is derived in its reduction, at 18 in many hylobatids (although 1 species, *Nomascus gabriellae*, has 19) and 17 (humans, chimpanzees, bonobos, and western gorillas) or 16 (eastern gorillas and orangutans) in hominids (Table 6.2). Concomitant increases in the numerical composition of the sacrum are found in hominoids, with hylobatids possessing four or five sacral vertebrae modally and hominids with five or six (Table 6.3 and Appendix). This reduction is correlated with a rostral shift in expression boundaries of the *Hox11*-mediated complex (see Martelli 2019) leading to a cranially directed homeotic shift at the lumbosacral border and, given no reduction in original somite number, a numerically longer sacrum along with fewer thoracolumbar vertebrae (Keith 1902; Benton 1967; Jungers 1984; Abitbol 1987; Pilbeam 2004; Williams and Russo 2015; Williams et al. 2016).

The inclusion of a large sample of hominoid species and subspecies allows us to expand on similar work (Schultz and Straus 1945; Pilbeam 2004) that is underappreciated in the recent literature on vertebral number evolution (McCollum et al. 2010; Williams 2012c; Fulwood and O'Meara 2014; Williams et al. 2016; Thompson and Almécija 2017). Hylobatid species are particularly variable in vertebral numbers, with modes ranging across more thoracolumbar and precaudal levels (17–19 TL, 28–31 CTLS) than hominids (16–17 TL, 28–30 CTLS) (Tables 6.1 and 6.2), consistent with their greater genetic diversity (Chen et al. 2013). The hylobatid species most commonly included in analyses, *Hylobates lar*, is probably not representative of hylobatids generally: *H. lar* has a relatively high frequencies of 3 sacral and 19 thoracolumbar vertebrae, whereas most hylobatid species have lower frequencies of those variants. Additionally, *H. lar* has a relatively low similarity index

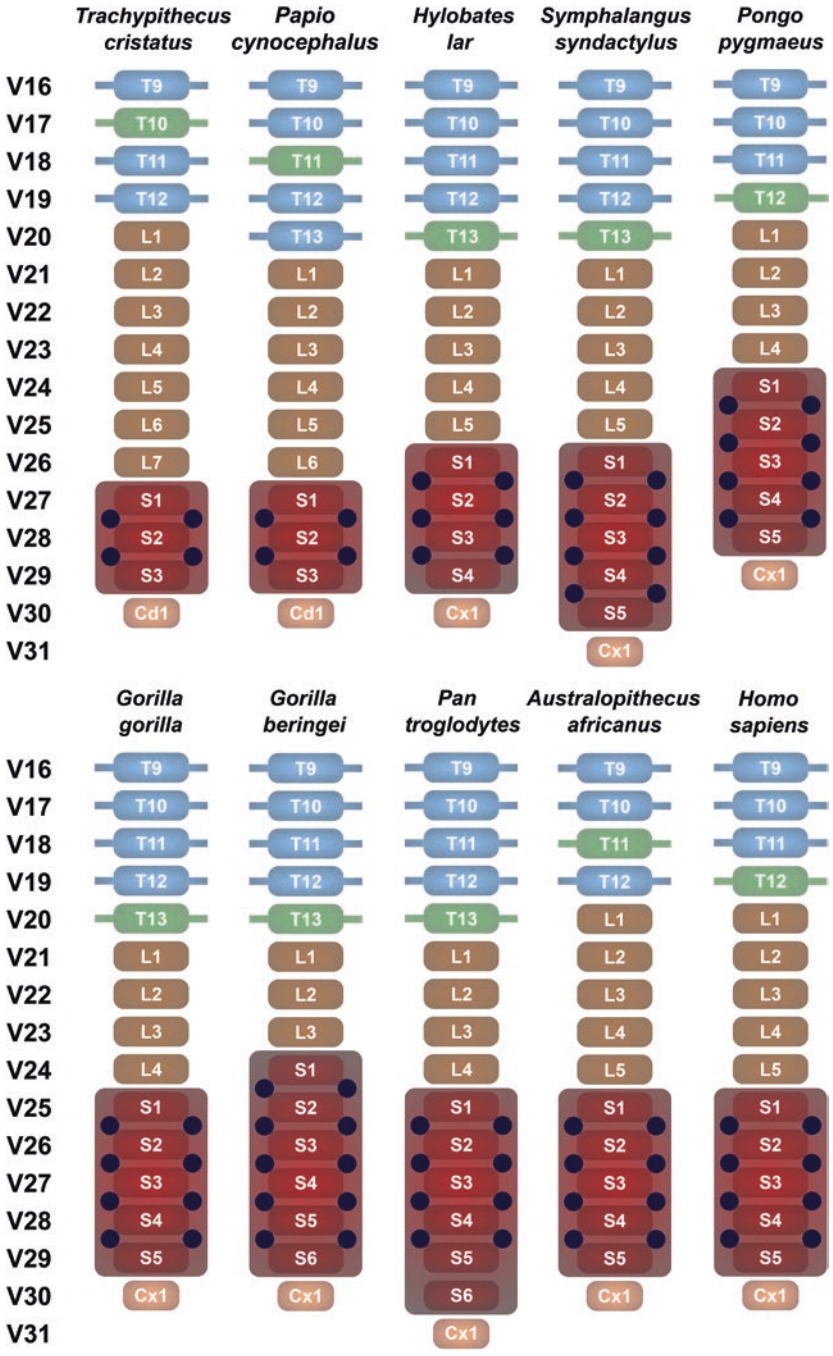

Fig. 6.4 Schematic representation of the lower back of hominoid and representative cercopithecoid species showing the number of thoracic (T), lumbar (L), and sacral (S) vertebrae and also the absolute position of the transitional vertebra (represented in blue). Vertebral segment numbers (V), where the count starts at the first cervical vertebra (V1), are shown on the left side. The first 15 segments are not shown, so each series starts at T9 (V16). Note that only the first caudal (Cd1) or coccygeal (Cx1) vertebra has been represented. *Australopithecus africanus* vertebral configurations are from Robinson (1972) and Haeusler et al. (2002)

(SI = 0.600) with other hylobatids, whereas other species can be considered more representative of hylobatids (*Hylobates agilis*: 0.724, *Nomascus concolor*: 0.720, *Hylobates muelleri*: 0.690, *Hoolock hoolock*: 0.678, *Hylobates moloch*: 0.667, *Symphalangus syndactylus*: 0.629). *Hylobates klossii* (SI = 0.548), *H. pileatus* (SI = 0.355), and particularly *Nomascus gabriellae* (0.072) differ from other hylobatids (Fig. 6.1).

Within hominids, two species of *Pongo* overlap extensively in vertebral formulae (SI = 0.961), more so than the two species of *Pan* (SI = 0.674) and *Gorilla* (SI = 0.618). The two *Gorilla beringei* subspecies are also very similar in vertebral formulae (SI = 0.982). In contrast, three subspecies of chimpanzees are more dissimilar to one another than expected but conform to phylogenetic and geographic relationships (Hey 2010; Prado-Martinez et al. 2013): central (*Pan troglodytes troglodytes*) and eastern (*P. t. schweinfurthii*) chimpanzees are most similar (SI = 0.882), followed by central and western (*P. t. verus*) (SI = 0.784) chimpanzees, and eastern and western chimpanzees are least similar (SI = 0.599) (Fig. 6.1). This is consistent with neutral evolutionary processes (e.g., genetic drift) affecting vertebral number variation, similar to what others have found in analyses of cranial morphology of chimpanzee subspecies (Weaver 2014; Weaver and Stringer 2014; Schroeder and von Cramon-Taubadel 2017; Zichello et al. 2018).

Humans overlap very little with other hominids in vertebral formulae, not surpassing 10% similarity in any comparison (Fig. 6.1). In this regard, *Homo sapiens* are least similar to other hominoids. Given their clearly derived body plan and positional behavior (i.e., vertical trunk and bipedal locomotion), this result is not unexpected. Hominins are distinct from other extant hominids in showing a relatively long lumbar column, which could have facilitated lumbar lordosis (Lovejoy 2005; Williams 2012a; Williams et al. 2013) and contributes to the presence of a substantial gap between the ribcage and iliac blades. This waist functions to allow counter-rotation of the trunk relative to the hips, maintaining balance during strides (Bramble and Lieberman 2004). Humans are not as dissimilar, however, in combined regions of vertebrae: humans are among the least dissimilar hominids in precaudal counts, and humans have very high similarity indices with *P. paniscus* (0.988), *P. troglodytes* (SI = 0.967), and *G. gorilla* (SI = 0.842) in thoracolumbar counts (Figs. 6.2 and 6.3). This suggests that the derived configuration of human vertebral formulae is largely achieved via homeotic rather than meristic change; that is, shifts in *Hox* gene expression boundaries modify vertebral formulae without change to combined regional numbers of vertebrae. Modally, humans have 12 thoracic vertebrae and 5 lumbar vertebrae (12 T, 5 L), whereas chimpanzees, bonobos, and western gorillas have 13 thoracic vertebrae and 4 lumbar vertebrae (13 T, 4 L), both configurations within a 17-element thoracolumbar spine. A rostral shift in *Hox10* complex expression can account for the homeotic change necessary to derive a human from an African ape-like ancestor (Pilbeam 2004; Williams 2012c; Williams and Russo 2015; Williams et al. 2016).

As with modern humans compared to African great apes, the two cercopithecoid species included here are very similar to one another in precaudal (SI = 0.988) and thoracolumbar (SI = 0.998) counts but are less similar when vertebral formulae are

compared (SI = 0.605). This is due, in part, to different modes of thoracic and lumbar vertebrae in *T. cristatus* (7:12:7:3) and *P. cynocephalus* (7:13:6:3) within the same modal thoracolumbar (19 TL) and precaudal (29 CTLS) framework. *Papio cynocephalus* is nearly bimodal in thoracic and lumbar numbers of vertebrae and vertebral formulae, with 7:12:7:3 as its second most common formula (Appendix). In this regard, *T. cristatus* is a better representative of most cercopithecoids than *P. cynocephalus* (see Clauser 1980; Schultz and Straus 1945; Pilbeam 2004; Williams 2011, 2012c). Although we only include two species of cercopithecoids in this study, we sampled one relatively invariant species with regard to vertebral formulae (*T. cristatus*) and one highly polymorphic species (*P. cynocephalus*), each from a different subfamily.

Heterogeneity indices are similar across hominoids, with notable exceptions (Fig. 6.1). For vertebral formulae, all taxa produce fairly high heterogeneity indices, particularly *S. syndactylus* (HI = 0.890), *H. muelleri* (HI = 0.859), and especially *P. paniscus* (HI = 0.944). In contrast, humans (HI: 0.526) and eastern gorillas (*G. b. beringei*: 0.568, *G. b. graueri*: 0.323) are exceptions: their heterogeneity indices are much lower than the average of other hominids (0.842). An index of 1.0 means that every individual sampled has a different vertebral formula: for example, of 55 bonobos, 24 different vertebral formulae are sampled, while in contrast, our sample of 71 mountain gorillas (*G. b. beringei*) has just 12 formulae. Results are similar for heterogeneity indices of thoracolumbar and precaudal counts, although the differences between modern humans/eastern gorillas and other hominoids are not as stark (Figs. 6.2 and 6.3). *Papio cynocephalus* heterogeneity in vertebral formulae (0.720) is similar to hominoids (average HI = 0.763), whereas precaudal number heterogeneity is similar to modern humans and eastern gorillas (HI = 0.396), and thoracolumbar count heterogeneity is lower than any hominoid (HI = 0.189). Heterogeneity indices are lower in *T. cristatus* than other species, particularly in thoracolumbar count (HI = 0.045), where numbers of vertebrae are nearly invariable. Low heterogeneity in vertebral formulae (HI = 0.230) and precaudal numbers (HI = 0.190) in *T. cristatus* are approached only by *G. beringei graueri* (HI = 0.323 and 0.262, respectively).

Cercopithecoids are similar to many mammal species in being relatively stable in their vertebral formulae and combined regional counts. Stabilizing selection on presacral numbers of vertebrae to avoid partial homeotic transformations of lumbosacral vertebrae, which may impede running and leaping ability (Galis et al. 2014), might explain low heterogeneity in *P. cynocephalus* and especially *T. cristatus*. Hominoids are more heterogeneous, both within and between species, potentially due to relaxed selection on vertebral formulae associated with adaptation to suspensory locomotion and departure from the typical mammalian body plan (Williams et al. 2019). Regarding humans and eastern gorillas, there are at least two hypotheses to explain the results. First, humans and eastern gorillas have experienced relatively strong stabilizing selection on their numbers of vertebrae, perhaps through adaptation to near-exclusive terrestriality (Williams 2012c). Other studies have identified ecological correlates of postcranial morphological differences between gorilla taxa attributable to locomotion (Schultz 1934; Sarmiento 1994;

Inouye 2003; Tocheri et al. 2011; Dunn et al. 2014). We additionally note that the lower heterogeneity index of eastern lowland gorillas (*G. b. graueri*) relative to mountain gorillas (*G. b. beringei*) might be attributable to more terrestrial travel by the former than the latter (Yamagiwa and Mwanza 1994). The second hypothesis is one of demography and population history that small population sizes and genetic drift limited the range of variation in vertebral formulae available in either or both humans and eastern gorillas (Williams 2012c). Bottlenecks have occurred recently in both species (Manica et al. 2007; Scally et al. 2012; see also Prado-Martinez et al. 2013), which could account for reduced heterogeneity.

The position of the transitional (or diaphragmatic) vertebra is studied in two ways here: its serial position in the vertebral column (equivalent to original somite number) as described in the methods (Gómez-Olivencia and Gómez-Robles 2016) and its position relative to the last thoracic vertebra (Williams 2012b, c; Williams et al. 2016). The transitional vertebra is also used to define the thoracolumbar border under an alternative, "functional" definition of thoracic and lumbar vertebrae, where the transitional vertebra and trunk vertebrae that precede it—those bearing flat, coronally oriented prezygapophyses that are hypothesized to allow lateral bending but limit sagittal flexibility—are considered thoracic vertebrae, and those that follow it and bear curved, sagittally oriented prezygapophyses that allow sagittal flexion and extension but restrict rotation (Rockwell et al. 1938; Erikson 1963; Washburn 1963; Clauser 1980; Shapiro 1993). Rather than tallying up the alternate numbers of thoracic and lumbar vertebrae as some studies have done (e.g., Washburn 1963; Shapiro 1993; Williams et al. 2016), we compare its position across hominoids. In stem hominoids, it is probable that the transitional vertebra was positioned at V17, two to three levels cranial to the last thoracic vertebra (Williams 2012b; Thompson and Almécija 2017), as it is found in stem hominoids (e.g., *Ekembo nyanzae, Nacholapithecus kerioi*; Ward 1993; Ishida et al. 2004; Nakatsukasa and Kunimatsu 2009).

Cercopithecoids have the transitional vertebra at V17, generally two (sometimes three) levels above the last thoracic vertebra (Tables 6.3 and 6.4), which is probably a primitive retention (Williams 2011, 2012b). In extant hominoids, modal positions of the transitional vertebra are at V20 (8 out of 11 of the adequately sampled species) or V19 (the remaining 3 species), coincident with either the last thoracic vertebra (10 out of 11 species) or the penultimate thoracic level (1 species) (Table 6.5). In humans and orangutans, the species that have 12 thoracic vertebrae (*H. pileatus* has 12 thoracic vertebrae as well, but is not represented adequately in our dataset), the transitional vertebra occurs at V19 (concurrent with the last thoracic vertebra). In 7 species, all of which have 13 thoracic vertebrae, the transitional vertebra occurs at V20 (the level of the last thoracic vertebra). One species, *H. lar*, is essentially bimodal in transitional vertebra position at V20 (50.8%) and V19 (47.7%), either at the level of the penultimate (54.0%) or last (44.4%) thoracic vertebra (Table 6.4).

As with regional boundaries, *Hox* gene expression patterns also affect the shape and orientation of the zygapophyses and therefore the position of the transitional vertebra (Pollock et al. 1995; Carapuço et al. 2005). Given that, modally, extant hominoids are characterized by the transitional vertebra at the last rib-bearing

Table 6.5 Frequencies of the position of the transitional vertebra (TV) relative to the last thoracic vertebra (0 = together at the same level; + = # levels cranial; − = # levels caudal)

N	Taxon	4	3	2	1	0	−1	−2	−3	−4
88	*T.cri.*		0.6%	**98.9%**	0.6%					
50	*P.cyn.*	2.0%	46.0%	**52.0%**						
239	*H.lar*			0.8%	**54.0%**	44.4%	0.8%			
20	*H.agi.*				15.0%	**80.0%**	5.0%			
31	*H.mue.*			1.6%	43.5%	**51.6%**	3.2%			
5	*H.klo.*					**90.0%**	10.0%			
6	*H.mol.*				**50.0%**	**50.0%**				
6	*N.con.*				**50.0%**	**50.0%**				
45	*S.syn.*			2.2%	30.0%	**67.8%**				
83	*P.pyg.*				1.8%	**81.3%**	16.9%			
32	*P.abe.*				12.5%	**51.6%**	35.9%			
163	*Pongo*				5.2%	**72.7%**	22.1%			
41	*G.b.ber.*			2.4%	24.4%	**51.2%**	9.8%	2.4%	9.8%	
27	*G.b.gra.*			3.7%	22.2%	**55.6%**	3.7%	11.1%	3.7%	
83	*G.ber.*		1.2%	7.8%	24.1%	**50.0%**	6.0%	4.8%	6.0%	
319	*G.gor.*			0.9%	17.4%	**69.6%**	9.1%	0.9%	1.9%	0.2%
44	*P.t.sch.*			2.3%	31.8%	**64.8%**	1.1%			
203	*P.t.tro.*			0.2%	36.5%	**61.1%**	2.2%			
17	*P.t.ver.*			8.8%	29.4%	**61.8%**				
342	*P.tro.*			0.9%	32.9%	**65.6%**	0.6%			
51	*P.pan.*				32.4%	**63.7%**	3.9%			
732	*H.sap.*			0.3%	32.5%	**62.8%**	4.3%	0.1%		

(i.e., thoracic) level and that many hominoid species seem to share a pattern in which a high frequency of individuals present the transitional vertebra at the penultimate level (~33% in humans, bonobos, and chimpanzees; ~20% in gorillas; and between 15 and 54% of available hylobatid species), it has been proposed that in extant hominoids, the transitional and last thoracic vertebrae are somewhat associated (Williams 2012b) but that variation in their position relative to one another can and does occur both within and between species and subspecies (Table 6.5). Orangutans are the only hominoid species with relatively high frequencies of the transitional vertebra occurring at the level of the first lumbar vertebra, and interestingly, *P. abelii* (35.9%) demonstrates this pattern more commonly than *P. pygmaeus* (16.9%). It should also be noted that orangutans have 28 precaudal (CTLS) vertebrae, a derived pattern from the ancestral condition of 29 precaudal vertebrae. Humans are the only species with a moderate frequency (33.9%) of transitional vertebra position at V18.

In all known early hominins, which seem to conform to the modal *H. sapiens* vertebral formula, the position of the transitional vertebra is at the level of the penultimate thoracic vertebra, probably V18 (Robinson 1972; Haeusler et al. 2011; Williams et al. 2013; Meyer et al. 2015; Ward et al. 2017). Although theoretically an

additional vertebra allowing sagittal flexibility might be advantageous in bipedal locomotion (e.g., in facilitating lordosis) (Lovejoy 2005; Williams 2012a, b), the function of the transitional vertebra and pre- versus post-transitional vertebrae is not well understood (Haeusler et al. 2012, 2014). Experimental work with humans and nonhuman primates (e.g., Preuschoft et al. 1988; Nakatsukasa et al. 1995; Shapiro et al. 2001; Thompson et al. 2015; Castillo et al. 2017) may elucidate the role of the transitional vertebra and other aspects of vertebral formula evolution. Although we do not test competing models of hominoid vertebral number evolution in a hypothetico-deductive framework here, we do think it is reasonable to draw a few conclusions regarding the evolutionary history of hominoid vertebral formulae. It seems plausible to us to infer that the number of precaudal vertebrae in hominoid has remained relatively unchanged from the primitive number of 29 in catarrhines, anthropoids, primates, and many mammal groups (Schultz and Straus 1945; Clauser 1980; Abitbol 1987; Pilbeam 2004; Williams 2011; Williams et al. 2016). In contrast, the number of thoracolumbar vertebrae and segments of the sacrum have been negatively correlated during hominoid evolution, with decreases in the former associated with increases in the latter, suggesting that in hominoids, there has been selection to decrease the number of thoracolumbar vertebrae, a relatively rare occurrence in mammals (Welcker 1881; Todd 1922; Pilbeam 2004; Narita and Kuratani 2005; Williams 2011; Russo and Williams 2015; Williams et al. 2019). When and how many times this occurred is a matter of debate (Haeusler et al. 2002; Pilbeam 2004; Lovejoy et al. 2009; McCollum et al. 2010; Thompson and Almécija 2017; Gómez-Olivencia and Gómez-Robles 2016), the resolution of which will depend in part on future fossil discoveries of already known (and unknown) fossil taxa, particularly certain Miocene hominoids (e.g., *Ekembo*, *Morotopithecus*, "dryopithecines," and potential stem pongines), together with less ambiguity in phylogenetic interpretations of those fossil taxa.

Acknowledgments We thank Ella Been for her leadership in organizing this volume and for inviting us to contribute to it. Peer review improved the manuscript. We thank N. Duncan, G. Garcia, E. Hoeger, S. Ketelsen, A. Marcato, B. O'Toole, M. Surovy, and E. Westwig (American Museum of Natural History); M. Milella, M. Ponce de León, and C. Zollikofer (Anthropological Institute and Museum, University of Zurich); H. Taboada (Center for the Study of Human Origins, New York University); Y. Haile-Selassie and L. Jellema (Cleveland Museum of Natural History); D. Katz and T. Weaver (Department of Anthropology, U.C. Davis); B. Patterson, A. Goldman, M. Schulenberg, L. Smith, and W. Stanley (Field Museum of Natural History); C. McCaffery and D. Reed (Florida Museum of Natural History, University of Florida); S. McFarlin (the George Washington University); J. Ashby (Grant Museum of Zoology; University College London); J. Chupasko, J. Harrison, and M. Omura (Harvard Museum of Comparative Zoology); E. Gilissen and W. Wendelen (Musée Royal de l'Afrique Centrale); S. Jancke, N. Lange, and F. Mayer, (Musée für Naturkunde, Berlin); C. Lefèvre (Muséum national d'Histoire naturelle); C. Conroy (Museum of Vertebrate Zoology, U.C. Berkeley); N. Edmison, L. Gordon, K. Helgen, E. Langan, D. Lunde, J. Ososky, and R. Thorington (National Museum of Natural History, Smithsonian Institution); P. Jenkins, L. Tomsett, and R. Portela (Natural History Museum, London); J. Soderberg and M. Tappen (Neil C. Tappen Collection, University of Minnesota); M. Nowak-Kemp (Oxford University Museum of Natural History); S. Bruaux and G. Lenglet (Royal Belgian Institute of Natural Sciences); A. Zihlman, C. Underwood, and J. Hudson (University of California, Santa Cruz); R. Asher (University Museum of Zoology, University of Cambridge); B. Zipfel, S. Jirah,

L. Berger, B. Billings, and J. Hemmingway (University of the Witwatersrand); and M. Hiermeier (Zoologische Staatssammlung München) for facilitating access to specimens in their care. SAW has been funded by the National Science Foundation (BCS-0925734), the Leakey Foundation, and the New York University Research Challenge Fund. Part of the data collection done by AGO was possible thanks to the support from the SYNTHESYS Project http://www.synthesys.info/ which is financed by the European Community Research Infrastructure Action under the FP7 "Capacities" Program (projects BE-TAF-4132 and GB-TAF-3674). AGO has received support from the Spanish Ministerio de Ciencia y Tecnología (project: CGL-2015-65387-C3-2-P, MINECO/FEDER), the Spanish Ministerio de Ciencia, Innovación y Universidades (project PGC2018-093925-B-C33), Research Group IT1418-19 from the Eusko Jaurlaritza-Gobierno Vasco. We gratefully acknowledge the Rwandan government for permission to study skeletal remains curated by the Mountain Gorilla Skeletal Project (MGSP). The authors also thank the continuous efforts of researchers, staff, and students from the Rwanda Development Board's Department of Tourism and Conservation, Gorilla Doctors, DFGFI, the George Washington University, New York University College of Dentistry, Institute of National Museums of Rwanda, and other universities in Rwanda and the USA.

Appendix

Taxon	Cervical	Thoracic	Lumbar	Sacral	TV level[a]	TL[b]	CTLS[c]	Total N/TV N (top) and # form. (bottom), freq.[d]
H. sapiens								
Mean	7.00	11.99	4.98	5.22	18.70	16.97	29.19	784/732
CTLS mode[e]	7	12	5	5	–	17	29	63.2%
CTLS 2nd[f]	7	12	5	6	–	17	30	14.9%
CTLS+TV mode[g]	7	12	5	5	19	17	29	36.6%
CTLS+TV 2nd[h]	7	12	5	5	18	17	29	20.4%
CTLS+TV 3rd	7	12	5	6	19	17	30	10.9%
Range	(6–7.5)	(11–13)	(4–6)	(4–7)	(18–20)	(15–18)	(27–31)	39/75
P. paniscus								
Mean	7.01	13.51	3.55	6.35	20.17	17.06	30.42	72/51
CTLS mode	7	13	4	6	–	17	30	18.2%
CTLS 2nd	7	14	3	7	–	17	31	10.9%
CTLS+TV mode	7	13	4	6	20	17	30	11.8%
Range	(6.5–8)	(12.5–14)	(2–4)	(5–8)	(19–21)	(16–18)	(28–32)	24/35
P. troglodytes								
Mean	7.00	13.11	3.67	5.69	19.78	16.77	29.46	526/342
CTLS mode	7	13	4	6	–	17	30	28.5%

Taxon	Cervical	Thoracic	Lumbar	Sacral	TV level[a]	TL[b]	CTLS[c]	Total N/TV N (top) and # form. (bottom), freq.[d]
CTLS 2nd	7	13	4	5	–	17	29	21.0%
CTLS 3rd	7	13	3	6	–	16	29	13.6%
CTLS+TV mode	7	13	4	6	20	17	30	24.3%
CTLS+TV 2nd	7	13	4	5	20	17	29	16.4%
Range	(6–7.5)	(12–14)	(2–5)	(4–7)	(18–20)	(15–18)	(28–31)	45/60
P. t. schweinfurthii								
Mean	7.01	13.15	3.83	5.84	19.81	16.99	29.84	52/44
CTLS mode	7	13	4	6	–	17	30	45.8%
CTLS 2nd	7	13	4	5	–	17	29	10.4%
CTLS+TV mode	7	13	4	6	20	17	30	36.4%
CTLS+TV 2nd	7	13	4	6	19	17	30	11.4%
Range	(7–7.5)	(12–14)	(2–5)	(4.5–7)	(19–21)	(16–18)	(28–31)	19/22
P. t. troglodytes								
Mean	7.00	13.06	3.72	5.65	19.74	16.78	29.44	241/203
CTLS mode	7	13	4	6	–	17	30	29.5%
CTLS 2nd	7	13	4	5	–	17	29	20.5%
CTLS 3rd	7	13	3	6	–	16	29	12.0%
CTLS+TV mode	7	13	4	6	20	17	30	20.2%
CTLS+TV 2nd	7	13	4	5	20	17	29	14.8%
Range	(6.5–7.5)	(12–14)	(2–5)	(4–7)	(18–21.5)	(15–18)	(28–31)	35/50
P. t. verus								
Mean	6.98	13.23	3.44	5.73	19.71	16.67	29.38	24/17
CTLS mode	7	13	3	6	–	16	29	8.5%
CTLS 2nd	7	13	4	5	–	17	29	16.7%
CTLS 3rd	7	13	4	6	–	17	30	16.7%
CTLS+TV mode	7	13	4	6	20	17	30	23.5%
CTLS+TV 2nd	7	13	4	5	20	17	29	17.6%
CTLS+TV 3rd	7	13	3	6	20	16	29	11.8%
CTLS+TV 4th	7	14	3	6	20	17	30	11.8%

Taxon	Cervical	Thoracic	Lumbar	Sacral	TV level[a]	TL[b]	CTLS[c]	Total N/TV N (top) and # form. (bottom), freq.[d]
Range	(6.5–7)	(13–14)	(3–4)	(5–7)	(18.5–20)	(16–18)	(28–31)	10/10
G. gorilla								
Mean	6.99	13.03	3.53	5.59	20.01	16.57	29.16	375/319
CTLS mode	7	13	4	5	–	17	29	24.0%
CTLS 2nd	7	13	3	6	–	16	29	21.9%
CTLS 3rd	7	13	4	6	–	17	30	16.3%
CTLS+TV mode	7	13	4	5	20	17	29	17.9%
CTLS+TV 2nd	7	13	3	6	20	16	29	15.7%
Range	(6–7)	(12–15)	(2–5)	(4–8)	(18–23)	(16–18)	(27–31.5)	42/81
G. beringei								
Mean	6.99	12.90	3.16	5.96	19.81	16.06	29.01	126/83
CTLS mode	7	13	3	6	–	16	29	71.4%
CTLS+TV mode	7	13	3	6	20	16	29	39.8%
CTLS+TV 2nd	7	13	3	6	19	16	29	19.3%
Range	(6–7)	(12–13)	(2–4)	(5–7)	(17–23)	(15–17)	(27–30)	14/24
G. b. beringei								
Mean	6.99	12.86	3.19	5.92	19.95	16.06	28.96	71/41
CTLS mode	7	13	3	6	–	16	29	64.7%
CTLS 2nd	7	12	4	6	–	16	29	11.8%
CTLS+TV mode	7	13	3	6	20	16	29	39.0%
CTLS+TV 2nd	7	13	3	6	19	16	29	12.2%
Range	(6–7)	(12–13)	(3–4)	(5–7)	(18–23)	(15–17)	(28–30)	12/19
G. b. graueri								
Mean	7.00	12.96	3.00	6.07	20.04	15.96	29.04	28/27
CTLS mode	7	13	3	6	–	16	29	82.1%
CTLS 2nd	7	13	3	7	–	16	30	10.7%
CTLS 3rd	7	13	3	6	20	16	29	44.4%
CTLS+TV mode	7	13	3	6	19	16	29	18.5%
CTLS+TV 2nd	7	13	3	6	22	16	29	11.1%

Taxon	Cervical	Thoracic	Lumbar	Sacral	TV level[a]	TL[b]	CTLS[c]	Total N/TV N (top) and # form. (bottom), freq.[d]
Range	–	(12–13)	(2–4)	(5–7)	(18–23)	(15–16)	(27–30)	4/9
Pongo								
Mean	6.98	11.95	4.01	5.12	19.13	15.96	28.07	330/163
CTLS mode	7	12	4	5	–	16	28	39.0%
CTLS 2nd	7	12	4	6	–	16	29	14.0%
CTLS+TV mode	7	12	4	5	19	16	28	30.1%
Range	(6–7)	(11–13)	(3–5)	(4–7)	(18–21)	(14.5–17)	(26–30)	39/53
P. pygmaeus								
Mean	6.98	11.90	4.02	5.24	19.07	15.92	28.15	148/83
CTLS mode	7	12	4	5	–	16	28	33.6%
CTLS 2nd	7	12	4	6	–	16	29	16.8%
CTLS+TV mode	7	12	4	5	19	16	28	27.7%
CTLS+TV 2nd	7.0	12.0	4.0	6.0	19	16	29	13.3%
Range	(6–7)	(11–13)	(3–5)	(4–7)	(18–20)	(14.5–17)	(27–30)	31/36
P. abelii								
Mean	7.0	12.1	4.0	5.0	19.3	16.10	28.11	50/32
CTLS mode	7	12	4	5	–	16	28	47.8%
CTLS+TV mode	7	12	4	5	19	16	28	28.1%
CTLS+TV 2nd	7	12	4	4	19	16	27	12.5%
Range	(6.5–7)	(11–13)	(3–5)	(4–6)	(18–21)	(15–17)	(27–30)	12/17
S. syndactylus								
Mean	7.00	13.11	4.53	4.70	19.83	17.64	29.34	87/45
CTLS mode	7	13	5	5	–	18	30	20.2%
CTLS 2nd	7	13	5	4	–	18	29	17.9%
CTLS 3rd	7	13	4	5	–	17	29	17.9%
CTLS+TV mode	7	13	5	5	20	18	30	20.0%
CTLS+TV 2nd	7	13	5	4	20	18	29	13.3%
CTLS+TV 3rd	7	13	4	5	20	17	29	11.1%

Taxon	Cervical	Thoracic	Lumbar	Sacral	TV level[a]	TL[b]	CTLS[c]	Total N/TV N (top) and # form. (bottom), freq.[d]
Range	–	(12–14)	(4–5)	(4–6)	(18–21)	(16–19)	(27–31)	21/22
H. hoolock								
Mean	7	12.9	4.92	4.2	19.5	17.82	29.02	25/4
CTLS mode	7	13	5	4	–	18	29	52.0%
CTLS 2nd	7	13	5	5	–	18	30	12.0%
Range	–	(12–13.5)	(4–6)	(3–5)	(19–20)	(17–19)	(28–30)	10/4
H. lar								
Mean	7.00	13.05	5.13	3.86	19.57	18.19	29.04	262/239
CTLS mode	7	13	5	4	–	18	29	47.7%
CTLS+TV mode	7	13	5	4	20	18	29	23.4%
CTLS+TV 2nd	7	13	5	4	19	18	29	23.4%
Range	(6–8)	(12–14)	(4–6)	(3–5)	(18.5–21)	(17–19)	(28–31)	37/50
H. agilis								
Mean	7.00	13.00	4.87	4.30	20.00	17.87	29.16	34/20
CTLS mode	7	13	5	4	–	18	29	37.5%
CTLS 2nd	7	13	5	5	–	18	30	18.8%
CTLS+TV mode	7	13	5	4	20	18	29	30.0%
CTLS+TV 2nd	7	13	5	5	20	18	30	15.0%
CTLS+TV 3rd	7	13	5	4	19	18	29	10.0%
Range	–	(12–14)	(4–6)	(3.5–5)	(19–21)	(17–19)	(28–30)	15/12
H. moloch								
Mean	7.00	13.06	4.77	4.66	19.50	17.83	29.49	33/6
CTLS mode	7	13	5	5	–	18	30	40.0%
CTLS 2nd	7	13	5	4	–	18	29	26.7%
Range	(7–8)	(12–14)	(4–5.5)	(3.5–6)	(19–20)	(17–19)	(28–30)	11/5
H. klossii								
Mean	7.00	13.04	5.04	4.54	20.17	18.08	29.62	13/5
CTLS mode	7	13	5	5	–	18	30	50.0%
CTLS 2nd	7	13	5	4	–	18	29	16.7%
CTLS+TV mode	7	13	5	4	20	18	29	40.0%
CTLS+TV 2nd	7	13	5	5	20	18	30	40.0%

Taxon	Cervical	Thoracic	Lumbar	Sacral	TV level[a]	TL[b]	CTLS[c]	Total N/TV N (top) and # form. (bottom), freq.[d]
Range	–	(13–13.5)	(4–6)	(4–5)	(20–21)	(17–19)	(28–30)	6/3
H. muelleri								
Mean	7.03	13.09	4.70	4.41	19.69	17.79	29.23	35/31
CTLS mode	7	13	5	4	–	18	29	25.7%
CTLS 2nd	7	13	5	5	–	18	30	17.1%
CTLS 3rd	7	13	5	4.5	–	18	30	11.4%
CTLS+TV mode	7	13	5	4	20	18	29	12.9%
CTLS+TV 2nd	7	13	5	5	20	18	30	12.9%
Range	(7–8)	(12–14)	(3.5–6)	(4–5)	(19–21)	(16–19)	(27–31)	18/20
H. pileatus								
Mean	7.00	12.44	5.07	4.00	19.67	17.51	28.51	8/2
CTLS mode	7	12	5	4	–	17	28	42.9%
CTLS 2nd	7	13	5	4	–	18	29	28.6%
Range	–	(12–13)	(4.5–6)	(4–4)	19–20	(17–18)	(28–29)	4/2
N. concolor								
Mean	7.00	13.12	4.92	4.58	20.21	18.04	29.62	25/6
CTLS mode	7	13	5	4	–	18	29	41.7%
CTLS 2nd	7	13	5	5	–	18	30	29.2%
CTLS+TV mode	7	13	5	5	19.5	18	30	33.3%
Range	–	(12–14.5)	(4–6)	(4–6)	(19–21)	(17–19)	(28–32)	8/5
N. gabrielle								
Mean	7.00	13.93	4.89	4.96	21.00	18.82	30.79	21/2
CTLS mode	7	14	5	5	–	19	31	57.1%
CTLS 2nd	7	14	4	5	–	18	30	14.3%
Range	–	(13–14)	(4–6)	(4–5.5)	(21–21)	(18–20)	(30–32)	6/2
T. cristatus								
Mean	7.00	12.02	7.00	2.90	17.02	19.02	28.93	50/50
CTLS mode	7	12	7	3	–	19	29	87.5%
CTLS+TV mode	7	12	7	3	17	19	29	87.5%
Range	–	(12–13)	(6.5–7.5)	(2–3)	(17–18)	(19–20)	(28–30)	6/6
P. cynocephalus								
Mean	7.00	12.48	6.44	2.90	16.98	18.92	28.82	88/88
CTLS mode	7	13	6	3	–	19	29	42.0%
CTLS 2nd	7	12	7	3	–	19	29	32.0%
CTLS 3rd	7	12	7	2	–	19	28	10.0%

Taxon	Cervical	Thoracic	Lumbar	Sacral	TV level[a]	TL[b]	CTLS[c]	Total N/TV N (top) and # form. (bottom), freq.[d]
CTLS+TV mode	7	13	6	3	17	19	29	20.5%
CTLS+TV 2nd	7	12	7	3	17	19	29	18.2%
Range	–	(11.5–13)	(5.5–7)	(2–4)	(16–18)	(17–20)	(27–30)	9/12

[a]TV level: the absolute vertebral level at which the transitional vertebra occurs
[b]TL: Number of thoracic and lumbar (thoracolumbar) vertebrae
[c]CTLS: Number of cervical, thoracic, lumbar, and sacral (precaudal) vertebrae
[d]The first row of each taxon contains the total N and N of transitional vertebra data (shown as N/N); the last row contains the number of vertebral formulae sampled for the total N and N of transitional vertebra data (shown as N/N); the rows in between the first and last show the frequency of vertebral formulae sampled at ≥10%
[e]CTLS mode: The modal vertebral formula sampled in each taxon (not including the position of the transitional vertebra)
[f]CTLS 2nd, etc.: The second (and third, etc.) most common vertebral formula sampled (sans the TV)
[g]CTLS+TV mode: The modal vertebral formula (with position of the transitional vertebra) sampled in each taxon
[h]CTLS+TV 2nd, etc.: The second (and third, etc.) most common vertebral formula (with position of the transitional vertebra) sampled in each taxon

References

Abitbol MM (1987) Evolution of the sacrum in hominoids. Am J Phys Anthropol 74:65–81

Benade MM (1990) Thoracic and lumbar vertebrae of African hominids ancient and recent: morphological and functional aspects with special reference to upright posture. Master's Thesis, University of the Witwatersrand

Benton RS (1967) Morphological evidence for adaptations within the epaxial region of the primates. In: van der Hoeven F (ed) The baboon in medical research, vol II. University of Texas Press, Austin, TX, pp 201–216

Bi S, Wang Y, Guan J, Sheng X, Meng J (2014) Three new Jurassic euharamiyidan species reinforce early divergence of mammals. Nature 514:579–584

Bramble DM, Lieberman DE (2004) Endurance running and the evolution of *Homo*. Nature 432:345–352

Carapuço M, Nóvoa A, Bobola N, Mallo M (2005) *Hox* genes specify vertebral types in the presomitic mesoderm. Genes Dev 19:2116–2121

Carbone L, Alan Harris R, Gnerre S, Veeramah KR, Lorente-Galdos B, Huddleston J, Meyer TJ, Herrero J, Roos C, Aken B, Anaclerio F, Archidiacono N, Baker C, Barrell D, Batzer MA, Beal K, Blancher A, Bohrson CL, Brameier M, Campbell MS, Capozzi O, Casola C, Chiatante G, Cree A, Damert A, de Jong PJ, Dumas L, Fernandez-Callejo M, Flicek P, Fuchs NV, Gut I, Gut M, Hahn MW, Hernandez-Rodriguez J, Hillier LW, Hubley R, Ianc B, Izsvák Z, Jablonski NG, Johnstone LM, Karimpour-Fard A, Konkel MK, Kostka D, Lazar NH, Lee SL, Lewis LR, Liu Y, Locke DP, Mallick S, Mendez FL, Muffato M, Nazareth LV, Nevonen KA, O'Bleness M, Ochis C, Odom DT, Pollard KS, Quilez J, Reich D, Rocchi M, Schumann GG, Searle S, Sikela JM, Skollar G, Smit A, Sonmez K, Hallers B, Terhune E, Thomas GWC, Ullmer B, Ventura

M, Walker JA, Wall JD, Walter L, Ward MC, Wheelan SJ, Whelan CW, White S, Wilhelm LJ, Woerner AE, Yandell M, Zhu B, Hammer MF, Marques-Bonet T, Eichler EE, Fulton L, Fronick C, Muzny DM, Warren WC, Worley KC, Rogers J, Wilson RK, Gibbs RA (2014) Gibbon genome and the fast karyotype evolution of small apes. Nature 513:195–201

Castillo ER, Hsu C, Mair RW, Lieberman DE (2017) Testing biomechanical models of human lumbar lordosis variability. Am J Phys Anthropol 163:110–121

Chen Y-C, Roos C, Inoue-Murayama M, Inou E, Shih C-C, Pei KJ-C, Vigilant L (2013) Inferring the evolutionary histories of divergences in *Hylobates* and *Nomascus* gibbons through multilocus sequence data. BMC Evol Biol 13:82

Clauser D (1980) Functional and comparative anatomy of the primate spinal column: some locomotor and postural adaptations. PhD Dissertation, University of Wisconsin-Milwaukee

Dunn RH, Tocheri MW, Orr CM, Jungers WL (2014) Ecological divergence and talar morphology in gorillas. Am J Phys Anthropol 153:526–541

Erikson G (1963) Brachiation in New World monkeys and in anthropoid apes. Symp Zool Soc Lond 10:135–163

Fulwood EL, O'Meara BC (2014) A phylogenetic approach to the evolution of anthropoid lumbar number. Am J Phys Anthropol 153(S58):123

Galis F, Carrier DR, van Alphen J, van der Mije SD, Van Dooren TJM, Metz JAJ, ten Broek CMA (2014) Fast running restricts evolutionary change of the vertebral column in mammals. Proc Natl Acad Sci U S A 111:11401–11406

Gómez-Olivencia A, Been E (2019) The spine of late Homo. In: Been E, Gómez-Olivencia A, Kramer PA (eds) Spinal evolution: morphology, function, and pathology of the spine in hominoid evolution. Springer, New York, pp 185–212

Gómez-Olivencia A, Gómez-Robles A (2016) Evolution of the vertebral formula in hominoids: insights from ancestral state reconstruction approaches. Proc Eur Soc Study Human Evol 5:109

Haeusler M, Martelli SA, Boeni T (2002) Vertebrae numbers of the early hominid lumbar spine. J Hum Evol 43:621–643

Haeusler M, Schiess R, Boeni T (2011) New vertebral material point to modern bauplan of the Nariokotome *Homo erectus* skeleton. J Hum Evol 61:575–582

Haeusler M, Regula S, Boeni T (2012) Modern or distinct axial bauplan in early hominins? A reply to Williams (2012). J Hum Evol 63:557–559

Haeusler M, Frater N, Bonneau N (2014) The transition from thoracic to lumbar facet joint orientation at T11: functional implications of a more cranially positioned transitional vertebra in early hominids. Am J Phys Anthropol 153(S58):133

Harrison T (1986) A reassessment of the phylogenetic relationships of *Oreopithecus bambolii* Gervais. J Hum Evol 15:541–583

Hey J (2010) The divergence of chimpanzee subspecies and subspecies as revealed in multipopulation isolation-with-migration analyses. Mol Biol Evol 27:921–933

Inouye SE (2003) Intraspecific and ontogenetic variation in the forelimb morphology of *Gorilla*. In: Taylor AB, Goldsmith ML (eds) Gorilla biology: a multidisciplinary perspective. Cambridge University Press, Cambridge, pp 194–235

Ishida H, Kunimatsu Y, Takano T, Nakano Y, Nakatsukasa M (2004) *Nacholapithecus* skeleton from the Middle Miocene of Kenya. J Hum Evol 46:69–103

Ji Q, Luo Z-X, Yuan C-X, Wible JR, Zhang JP, Georgi JA (2002) The earliest known eutherian mammal. Nature 416:816–822

Jungers WL (1984) Scaling of the hominoid locomotor skeleton with special reference to lesser apes. In: Preuschoft H, Chivers DJ, Brockelman WY, Creel N (eds) The lesser apes: evolutionary and behavioral biology. Edinburgh University Press, Edinburgh, pp 146–169

Keith A (1902) The extent to which the posterior segments of the body have been transmuted and suppressed in the evolution of man and allied primates. J Anat Physiol 37:18–40

Kim SK, Carbone L, Becquet C, Mootnick AR, Li DJ, de Jong PJ, Wall JD (2011) Patterns of genetic variation within and between gibbon species. Mol Biol Evol 28:2211–2218

Latimer B, Ward CV (1993) The thoracic and lumbar vertebrae. In: Walker A, Leakey R (eds) The Nariokotome Homo erectus skeleton. Harvard University Press, Cambridge, pp 266–293

Lovejoy CO (2005) The natural history of human gait and posture Part 1. Spine and pelvis. Gait Posture 21:95–112

Lovejoy CO, McCollum MA (2010) Spinopelvic pathways to bipedality: why no hominids ever relied on a bent-hip-bent-knee gait. Philos Trans R Soc B 365:3289–3299

Lovejoy CO, Suwa G, Simpson SW, Matternes JH, White TD (2009) The great divides: *Ardipithecus ramidus* reveals the postcrania of our last common ancestors with African apes. Science 326:100–106

Machnicki AL, Lovejoy CO, Reno PL (2016) Developmental identity versus typology: Lucy has only four sacral segments. Am J Phys Anthropol 160:729–739

Manica A, Amos W, Balloux F, Hanihara T (2007) The effect of ancient population bottlenecks on human phenotypic variation. Nature 448:346–348

Martelli S (2019) The modern and fossil hominoid spinal ontogeny. In: Been E, Gómez-Olivencia A, Kramer PA (eds) Spinal evolution: morphology, function, and pathology of the spine in hominoid evolution. Springer, New York, pp 246–282

McCollum MA, Rosenman BA, Suwa G, Meindl RS, Lovejoy CO (2010) The vertebral formula of the last common ancestor of African apes and humans. J Exp Zool 314B:123–134

Meyer MR, Williams SA (2019) The spine of early Pleistocene Homo. In: Been E, Gómez-Olivencia A, Kramer PA (eds) Spinal evolution: morphology, function, and pathology of the spine in hominoid evolution. Springer, New York, pp 153–184

Meyer MR, Williams SA, Smith MP, Sawyer GJ (2015) Lucy's back: reassessment of fossils associated with the A.L. 288-1 vertebral column. J Hum Evol 85:174–180

Nakatsukasa M, Kunimatsu Y (2009) *Nacholapithecus* and its importance for understanding hominoid evolution. Evol Anthropol 18:103–119

Nakatsukasa M, Hayama S, Preuschoft H (1995) Postcranial skeleton of a macaque trained for bipedal standing and walking and implications for functional adaptation. Folia Primatol 64:1–29

Narita Y, Kuratani S (2005) Evolution of the vertebral formulae in mammals: a perspective on developmental constraints. J Exp Zool 304B:91–106

Nater A, Mattle-Greminger MP, Nurcahyo A, Nowak MG, de Manuel M, Desai T, Groves C, Pybus M, Sonay TB, Roos C, Lameira AR, Wich SA, Askew J, Davila-Ross M, Fredriksson G, de Valles G, Casals F, Prado-Martinez J, Goossens B, Verschoor EJ, Warren KS, Singleton I, Marques DA, Pamungkas J, Perwitasari-Farajallah D, Rianti P, Tuuga A, Gut IG, Gut M, Orozco-terWengel P, van Schaik CP, Bertranpetit J, Anisimova M, Scally A, Marques-Bonet T, Meijaard E, Krützen M (2017) Morphometric, behavioral, and genomic evidence for a new orangutan species. Curr Biol 27:3487–3498

Pilbeam D (2004) The anthropoid postcranial axial skeleton: comments on development, variation, and evolution. J Exp Zool 302:241–267

Pilbeam DR, Lieberman DE (2017) Reconstructing the last common ancestor of chimpanzees and humans. In: Muller MN, Wrangham RW, Pilbeam DR (eds) Chimpanzees and human evolution. The Belknap Press of Harvard University Press, Cambridge, pp 22–141

Pollock RA, Sreenath T, Ngo L, Bieberich CJ (1995) Gain of function mutations for paralogous *Hox* genes: implications for the evolution of *Hox* gene function. Proc Natl Acad Sci U S A 92:4492–4496

Prado-Martinez J, Sudmant PH, Kidd JM, Li H, Kelley JL, Lorente-Galdos B, Veeramah KR, Woerner AE, O'Connor TD, Santpere G, Cagan A, Theunert C, Casals F, Laayouni H, Munch K, Hobolth A, Halager AE, Malig M, Hernandez-Rodriguez J, Hernando-Herraez I, Prüfer K, Pybus M, Johnstone L, Lachmann M, Alkan C, Twigg D, Petit N, Baker C, Hormozdiari F, Fernandez-Callejo M, Dabad M, Wilson ML, Stevison L, Camprubí C, Carvalho T, Ruiz-Herrera A, Vives L, Mele M, Abello T, Kondova I, Bontrop RE, Pusey A, Lankester F, Kiyang JA, Bergl RA, Lonsdorf E, Myers S, Ventura M, Gagneux P, Comas D, Siegismund H, Blanc J, Agueda-Calpena L, Gut M, Fulton L, Tishkoff SA, Mullikin JC, Wilson RK, Gut IG, Gonder MK, Ryder OA, Hahn BH, Navarro A, Akey JM, Bertranpetit J, Reich D, Mailund T, Schierup MH, Hvilsom C, Andrés AM, Wall JD, Bustamante CD, Hammer MF, Eichler EE, Marques-Bonet T (2013) Great ape genetic diversity and population history. Nature 499:471–475

Preuschoft H, Hayama S, Günther MM (1988) Curvature of the lumbar spine as a consequence of mechanical necessities in Japanese macaques trained for bipedalism. Folia Primatol 50:42–58
Robinson J (1972) Early hominid posture and locomotion. University of Chicago Press, Chicago
Rockwell H, Evans FG, Pheasant HC (1938) The comparative morphology of the vertebrate spinal column. Its form as related to function. J Morphol 63:87–117
Russo GA, Williams SA (2015) Giant pandas (Carnivora: *Ailuropoda melanoleuca*) and living hominoids converge on lumbar vertebral adaptations to orthograde trunk posture. J Hum Evol 88:160–179
Sanders WJ (1998) Comparative morphometric study of the australopithecine vertebral series Stw-H8/H41. J Hum Evol 34:249–302
Sarmiento EE (1994) Terrestrial traits in the hands and feet of gorillas. Am Mus Novit 309:1–56
Scally A, Dutheil JY, Hillier LW, Jordan GE, Goodhead I, Herrero J, Hobolth A, Lappalainen T, Mailund T, Marques-Bonet T, McCarthy S, Montgomery SH, Schwalie PC, Tang YA, Ward MC, Xue Y, Yngvadottir B, Alkan C, Andersen LN, Ayub Q, Ball EV, Beal K, Bradley BJ, Chen Y, Clee CM, Fitzgerald S, Graves TA, Gu Y, Heath P, Heger A, Karakoc E, Kolb-Kokocinski A, Laird GK, Lunter G, Meader S, Mort M, Mullikin JC, Munch K, O'Connor TD, Phillips AD, Prado-Martinez J, Rogers AS, Sajjadian S, Schmidt D, Shaw K, Simpson JT, Stenson PD, Turner DJ, Vigilant L, Vilella AJ, Whitener W, Zhu B, Cooper DN, de Jong P, Dermitzakis ET, Eichler EE, Flicek P, Goldman N, Mundy NI, Ning Z, Odom DT, Ponting CP, Quail MA, Ryder OA, Searle SM, Warren WC, Wilson RK, Schierup MH, Rogers J, Tyler-Smith C, Durbin R (2012) Insights into hominid evolution from the gorilla genome sequence. Nature 483:169–175
Schroeder L, von Cramon-Taubadel N (2017) The evolution of hominoid cranial diversity: a quantitative genetic approach. Evolution 71-11:2634–2649
Schultz AH (1934) Some distinguishing characters of the mountain gorilla. J Mammal 15:51–61
Schultz AH (1960) Einige Beobachtungen und Maße am Skelett von *Oreopithecus* im Vergleich mit anderen catarrhinen Primaten. Z Morphol Anthropol 50:136–149
Schultz AH (1961) Vertebral column and thorax. Primatologia 4:1–66
Schultz AH, Straus WL (1945) The numbers of vertebrae in primates. Proc Am Philos Soc 89:601–626
Shapiro L (1993) Functional morphology of the vertebral column in primates. In: Gebo DL (ed) Postcranial adaptation in nonhuman primates. Northern Illinois University Press, Dekalb, pp 121–149
Shapiro LJ, Demes B, Cooper J (2001) Lateral bending of the lumbar spine during quadrupedalism in strepsirhines. J Hum Evol 40:231–259
Susanna I, Alba DM, Almécija S, Moyà-Solà S (2014) The vertebral remains of the late Miocene great ape *Hispanopithecus laietanus* from Can Llobateres 2 (Vallès-Penedès Basin, NE Iberian Peninsula). J Hum Evol 73:15–34
Thompson NE, Almécija S (2017) The evolution of vertebral formulae in Hominoidea. J Hum Evol 110:18–36
Thompson NE, Demes B, O'Neill MC, Holowka NB, Larson SG (2015) Surprising trunk rotational capabilities in chimpanzees and implications for bipedal walking proficiency in early hominins. Nat Commun 6:8416
Tocheri MW, Solhan CR, Orr CM, Femiani J, Frohlich B, Groves CP, Harcourt-Smith WE, Richmond BG, Shoelson B, Jungers WL (2011) Ecological divergence and medial cuneiform morphology in gorillas. J Hum Evol 60:171–184
Todd TW (1922) Numerical significance in the thoracicolumbar vertebrae of the Mammalia. Anat Rec 24:261–286
Toussaint M, Macho GA, Tobias PV, Patridge TC, Hughes AR (2003) The third partial skeleton of a late Pliocene hominin (Stw 431) from Sterkfontein, South Africa. S Afr J Sci 99:215–223
Ward CV (1993) Torso morphology and locomotion in *Proconsul nyanzae*. Am J Phys Anthropol 92:291–328
Ward CV, Nalley TK, Spoor F, Tafforeau P, Alemseged Z (2017) Thoracic vertebral count and thoracolumbar transition in *Australopithecus afarensis*. Proc Natl Acad Sci U S A 114:6000–6004

Washburn SL (1963) Behavior and human evolution. In: Washburn SL (ed) Classification and human evolution. Aldine, Chicago

Weaver TD (2014) Quantitative- and molecular-genetic differentiation in humans and chimpanzees: implications for the evolutionary processes underlying cranial diversification. Am J Phys Anthropol 154:615–620

Weaver TD, Stringer CB (2014) Unconstrained cranial evolution in Neandertals and modern humans compared to common chimpanzees. Proc R Soc B 282:20151519

Welcker H (1881) Die neue anatomische Anstalt zu Halle durch einen Vortrag über Wirbelsäule und Becken eingeweiht von dem derzeitigen Director. Archiv für Anatomie und Physiologie (Anatomische Abtheilung). Jahrgang 1881:161–192

Williams SA (2011) Evolution of the hominoid vertebral column. PhD Dissertation, University of Illinois, Urbana-Champaign

Williams SA (2012a) Modern of distinct axial bauplan in early hominins? Comments on Haeusler et al. (2011). J Hum Evol 63:552–556

Williams SA (2012b) Placement of the diaphragmatic vertebra in catarrhines: implications for the evolution of dorsostability in hominoids and bipedalism in hominins. Am J Phys Anthropol 148:111–122

Williams SA (2012c) Variation in anthropoid vertebral formulae: implications for homology and homoplasy in hominoid evolution. J Exp Zool 318B:134–147

Williams SA, Meyer MR (2019) The spine of Australopithecus. In: Been E, Gómez-Olivencia A, Kramer PA (eds) Spinal evolution: morphology, function, and pathology of the spine in hominoid evolution. Springer, New York, pp 125–152

Williams SA, Russo GA (2015) Evolution of the hominoid vertebral column: the long and the short of it. Evol Anthropol 24:15–32

Williams SA, Ostrofsky KR, Frater N, Churchill SE, Schmid P, Berger LR (2013) The vertebral column of *Australopithecus sediba*. Science 340:1232996

Williams SA, Middleton ER, Villamil CI, Shattuck MR (2016) Vertebral numbers and human evolution. Am J Phys Anthropol 159(S61):S19–S36

Williams SA, Meyer MR, Nalla S, García-Martínez D, Nalley TK, Eyre J, Prang TC, Bastir M, Schmid P, Churchill SE, Berger LE (2018) The vertebrae, ribs, and sternum of *Australopithecus sediba*. PaleoAnthropology 2018:156–233

Williams SA, Spear JK, Petrullo L, Goldstein D, Lee AB, Peterson AL, Miano DA, Kaczmarek EB, Shattuck MR (2019) Increased variation in numbers of presacral vertebrae in suspensory mammals. Nat Ecol Evol 3:949–956

Yamagiwa J, Mwanza N (1994) Day-journey length and daily diet of solitary male gorillas in lowland and highland habitats. Int J Primatol 15:207–244

Zapfe H (1958) The skeleton of *Pliopithecus* (*Epipliopithecus*) *vindobonensis* Zapfe and Hürzeler. Am J Phys Anthropol 16:441–458

Zapfe H (1960) A new fossil anthropoid from the Miocene of Austria. Curr Anthropol 1:428–429

Zichello JM (2018) Look in the trees: hylobatids as evolutionary models for extinct hominins. Evol Anthropol 27:142–146

Zichello JM, Baab KL, McNulty KP, Raxworthy CJ, Steiper ME (2018) Hominoid intraspecific cranial variation mirrors neutral genetic diversity. Proc Natl Acad Sci U S A 115:11501–11506

Chapter 7
The Spine of *Australopithecus*

Scott A. Williams and Marc R. Meyer

7.1 Introduction

Early hominins evolved in the late Miocene (roughly 5–7 million years ago) and proliferated into many varieties, one lineage of which gave rise to the australopiths. This ancestor was ape-like in many ways yet was probably a facultative biped that spent its time both on the ground and in the trees, as demonstrated by analyses of *Ardipithecus ramidus* (Lovejoy et al. 2009a, b; White et al. 2009, 2015; Prang 2019). A subsequent group of species colloquially referred to as australopiths (after the genus *Australopithecus*) initially evolved in the early Pliocene and demonstrate unequivocal evidence for bipedal locomotion on the ground (Lovejoy 2005a, b, 2007; Prang 2015). Restricted to parts of East, Central, and Southern Africa, the ten or so species of australopiths differed in size, diet, and behavior, in addition to the environments in which they lived (see Reed et al. 2013).

Bipedal locomotion is one of the defining characteristics of hominins and is thought to be one of the earliest autapomorphies that appeared in the hominin lineage. Fossils of the ca. 4.4 Ma *Ardipithecus ramidus* demonstrate that a non-grasping, adducted hallux, long considered a primary adaptation to bipedalism, did not accompany the initial evolution of bipedalism (Lovejoy et al. 2009a). Therefore, a grasping, abducted hallux persisted for the first few million years of hominin evolution and eventually evolved into a foot with distinct weight transfer and propulsion mechanisms known in later fossil hominins and modern humans

S. A. Williams (✉)
Center for the Study of Human Origins, Department of Anthropology, New York University, New York, NY, USA

New York Consortium in Evolutionary Primatology, New York, NY, USA
e-mail: sawilliams@nyu.edu

M. R. Meyer
Department of Anthropology, Chaffey College, Rancho Cucamonga, CA, USA

E. Been et al. (eds.), *Spinal Evolution*,
https://doi.org/10.1007/978-3-030-19349-2_7

(Haile-Selassie et al. 2012; Prang 2015, 2019). Morphologies related to hip (Lovejoy et al. 1973; Lovejoy 1988, 2007), knee (Johanson and Taieb 1976; Leakey et al. 1995; Lovejoy 2005b), and spine posture (Lovejoy 2005a; Whitcome et al. 2007), then, may have been some of the first skeletal structures modified for bipedal locomotion. Indeed, *Ar. ramidus* demonstrates a mosaic pelvic morphology, with a derived, *Australopithecus*-like upper pelvis and a more primitive, ape-like ischium (Lovejoy et al. 2009c); nevertheless, Kozma et al. (2018) showed that *Ar. ramidus* would have been capable of human-like hip extension.

Spinal posture is contributed to by both soft and hard tissues (Shapiro and Frankel 1989; Been et al. 2010a, 2014; Been and Kalichman 2014; Nalley and Grider-Potter 2015, 2017), including the vertebral bodies, intervertebral discs, zygapophyseal morphology, and epaxial and hypaxial musculature. The vertical orientation and sigmoid curvature of the vertebral column balance the upper body over the pelvis, and the strap-like erector spinae muscles provide support and allow extension of the spine. Morphologies related to spinal orientation and curvature on the cranial base and vertebral column may have been some of the earliest adaptations to bipedalism, along with changes in *Hox* gene expression patterns to generate a homeotic shift at the thoracolumbar border and a longer lumbar column (Pilbeam 2004; Williams et al. 2016).

7.2 Numbers of Vertebrae

The last common ancestor (LCA) of hominins and panins (chimpanzees and bonobos) most likely possessed 17 thoracolumbar vertebrae with a panin-like vertebral formula consisting of 13 thoracic vertebrae and 4 lumbar vertebrae (Pilbeam 2004; Williams 2011; Williams and Russo 2015; Williams et al. 2016, 2019a, b; Thompson and Almécija 2017; but see Haeusler et al. 2002; McCollum et al. 2010). At some point in early hominin evolution, a rostral shift in *Hox* gene expression at the thoracolumbar border was selected for, resulting in the regionalization of 12 thoracic and 5 lumbar vertebrae, with no meristic change in total thoracolumbar number (Pilbeam 2004; Williams 2012a; Williams et al. 2016). Such homeotic shifts involve not only costal components (i.e., rib presence or absence, and hence what determines thoracic and lumbar identification traditionally) (Wellik and Capecchi 2003; Mallo et al. 2010) but also the shape and orientation of the articular facets (and thus the location of the transitional or diaphragmatic vertebra, that vertebra with flat, coronally oriented "thoracic-like" superior articular facets and curved, sagittally oriented "lumbar-like" inferior articular facets, which serve as an alternate demarcation of thoracic and lumbar regions; see Washburn 1963; Shapiro 1993; Whitcome 2012) (Pollock et al. 1995; Carapuço et al. 2005). All known early fossil hominins with adequate preservation of the vertebral column possess five lumbar vertebrae (Haeusler et al. 2002, 2011; Williams et al. 2013); however, the transitional vertebra is not the last thoracic vertebra as is the case with modern humans and other extant

hominoids (Williams 2012a, b), but rather the penultimate thoracic vertebra (Haeusler et al. 2002, 2011; Williams et al. 2013; Meyer et al. 2015). Ward et al.'s (2017) analysis of the "Dikika child" (DIK-1-1) confirmed this configuration, and although lacking a lumbar column, this infant *Au. afarensis* preserves 12 thoracic vertebrae, with the 11th thoracic (T11) the transitional vertebra. Together, the fossil evidence suggests that, by the Pliocene, early hominins evolved an elongated lumbar column and an even longer post-transitional vertebral column (5 and 6 elements, respectively), in both cases at the expense of the numerical composition of the thoracic and pre-transitional columns (12 and 11 elements, respectively). This configuration probably facilitated the evolution of bipedalism by allowing for sufficient lordosis and thus overall spinal posture (Lovejoy 2005a; Williams et al. 2013).

7.3 Fossil Record

The oldest known vertebral material in the hominin fossil record belongs to 4.4 Ma *Ardipithecus ramidus* from the Middle Awash site of Aramis (White et al. 2009). The best preserved element is a somewhat crushed subaxial cervical vertebra (ARA-VP-6/500-057); a crushed partial thoracic vertebra (ARA-VP-6/500-084) and an inferior segment of the sacrum (ARA-VP-6/500-038) are both associated with the inferred female partial skeleton known as "Ardi" (ARA-VP-6/500). Several other partial vertebrae from the site are associated with *Ar. ramidus*, but do not belong to the partial skeleton (White et al. 2009). Detailed studies of these vertebrae have not been published but when carried out will provide glimpses into the posture and locomotor repertoire of one of the earliest putative bipeds.

The oldest vertebral material belonging to a member of the genus *Australopithecus* hails from the site of Asa Issie in the Middle Awash of Ethiopia attributed to *Australopithecus anamensis* (White et al. 2006; Meyer and Williams 2019). Several partial vertebrae, including an atlas (ASI-VP-2-220), an axis (ASI-VP-2-214), and lower cervical and thoracic vertebrae, are known but not associated with a single individual. White et al. (2006) point out that the axis and thoracic neural arch are larger than those from A.L. 333 and A.L. 288 (belonging to *Au. afarensis*). The vertebral fragments are described in Meyer and Williams (2019).

Australopithecus afarensis is the earliest hominin with fully described, reasonably complete vertebrae, and all of the vertebrae known for this species derive from the Afar region of Ethiopia. The earliest *Au. afarensis* vertebrae yet discovered belong to KSD-VP-1/1 dated to ~3.6 Ma from Woranso-Mille in Ethiopia (Haile-Selassie et al. 2010). The vertebrae of Kadanuumuu, the "Big Man," include parts of six cervical vertebrae (C2–C6), none of which are well-preserved, although several of the vertebral bodies are nearly complete (Meyer 2016). The Dikika child is the partial skeleton of a young juvenile *Au. afarensis* dated to ~3.3 Ma (Alemseged et al. 2006). It includes the most complete cervical and thoracic vertebral columns in the early hominin fossil record (Ward et al. 2017). These vertebrae are essentially

complete, but the centra are not yet fused to the neural arches due to the young age of this individual (Ward et al. 2017).

The partial skeleton of an adult female from ~3.2 Ma Hadar, A.L. 288-1 ("Lucy"), preserves eight vertebral elements (one of the original nine, a neural arch fragment, was shown not to belong to Lucy; Meyer et al. 2015). Fossil hominin vertebrae are shown in a comparative context in Figs. 7.1, 7.2, 7.3, 7.4, 7.5, 7.6, 7.7, 7.8, 7.9, 7.10, 7.11, 7.12, 7.13, 7.14, 7.15, 7.16, and 7.17. Johanson et al. (1982) and Cook et al. (1983) describe nonconsecutive thoracic vertebrae, but Meyer et al. (2015) make a case that the thoracic elements are consecutive (T6–T11) (see Fig. 7.10). In addition, there is a nearly complete lumbar vertebra (sans lumbar transverse processes) (Fig. 7.13) and an isolated lumbar spinous process. Vertebrae from other sites at Hadar (A.L. 333 and A.L. 444) represent all three presacral regions, some of which are nearly complete (Lovejoy et al. 1982; Ward et al. 2012). These vertebrae are isolated and have not been associated with one another, although A.L. 444-7, a large lumbar vertebral body (Fig. 7.14), has been suggested to belong to the same individual as the A.L. 444-2 male skull (Kimbel et al. 2004; Ward et al. 2012).

Potentially the oldest hominin material from South Africa comes from the lower members of Sterkfontein Caves (Granger et al. 2015; but see Pickering et al. 2019a). StW 573 is a yet fully described partial skeleton from Member 2 in Silberberg Grotto (Clarke 2019). Clarke (2019) reports 16 preserved vertebrae in this individual: an atlas, 4 other cervical vertebrae, 6 thoracic vertebrae, and 5 lumbar vertebrae

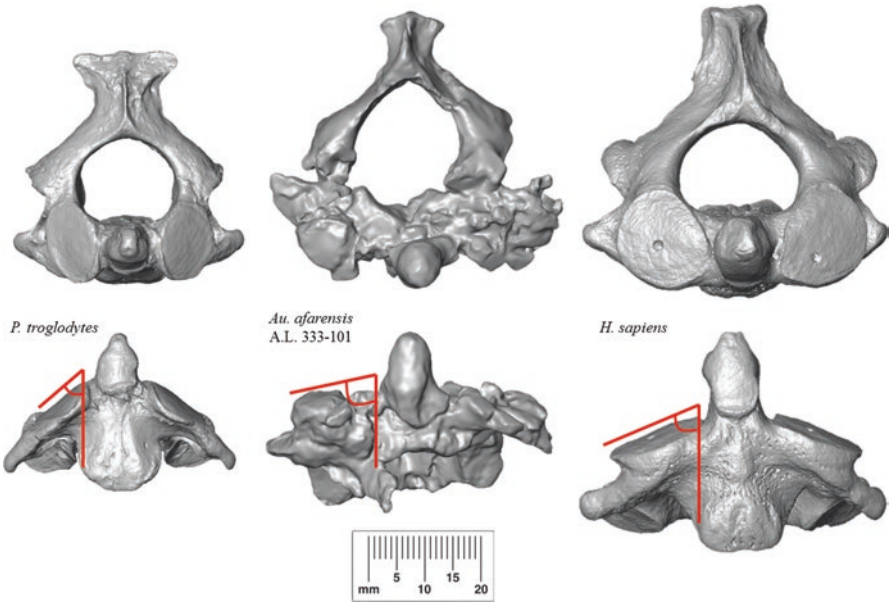

Fig. 7.1 Axis vertebrae in superior and anterior views. Angles indicate the angle of the superior articular facets, which are more steeply sloped in *Au. afarensis* and modern humans than in chimpanzees

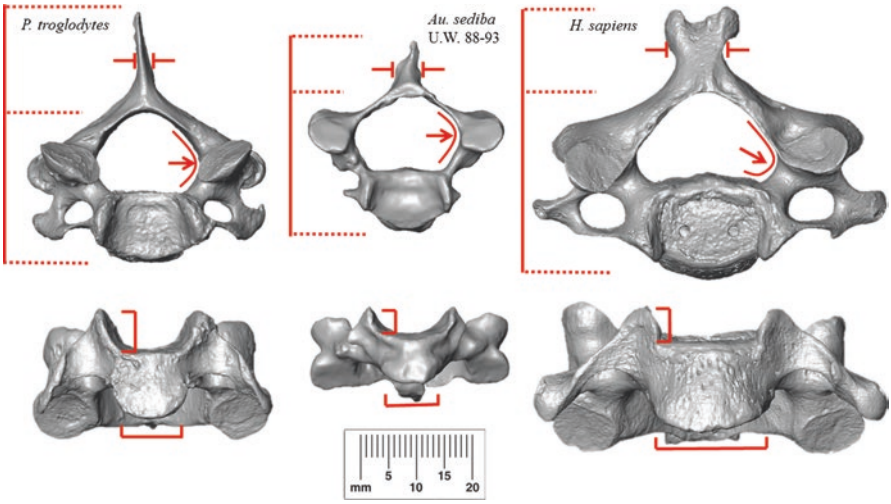

Fig. 7.2 Third cervical vertebrae in superior and anterior views. Spinous processes are shorter and wider in *Au. sediba* and modern humans than in chimpanzees. Arrows indicate the widest part of the spinal canal, which is more posteriorly located in *Au. sediba* and chimpanzees than in modern humans. Brackets show the height of the uncinated processes, which are shorter in *Au. sediba* and modern humans than in chimpanzees, and the width of the vertebral body, which is narrower in *Au. sediba* and chimpanzees than in modern humans

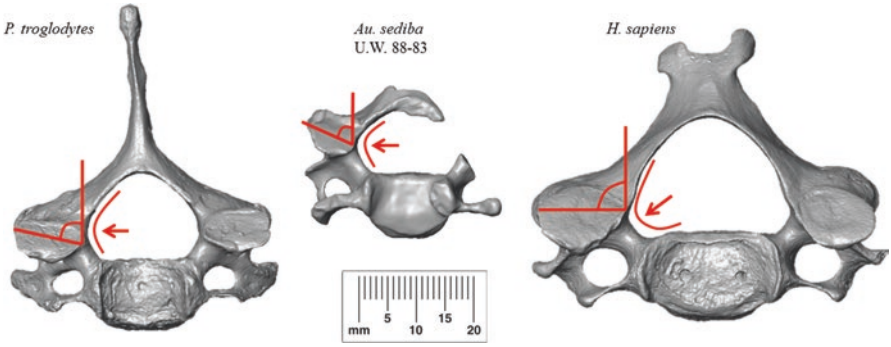

Fig. 7.3 Fourth cervical vertebrae in superior view. Orientations of the superior articular facets are more acute in *Au. sediba* and chimpanzees than in modern humans, which are obtuse. As with the third cervical vertebra, the widest portion of the spinal canal is more posterior in *Au. sediba* and chimpanzees than in modern humans

(in addition to a badly crushed sacrum). It is currently unknown whether StW 573 belongs to *A. africanus* or a second species in the lower members at Sterkfontein, the latter of which has been suggested by Clarke (2008). Two additional, mostly complete lumbar vertebrae are known from Member 2 of Jacovec Cavern in Sterkfontein: middle lumbar vertebrae (StW 656) and last lumbar vertebrae

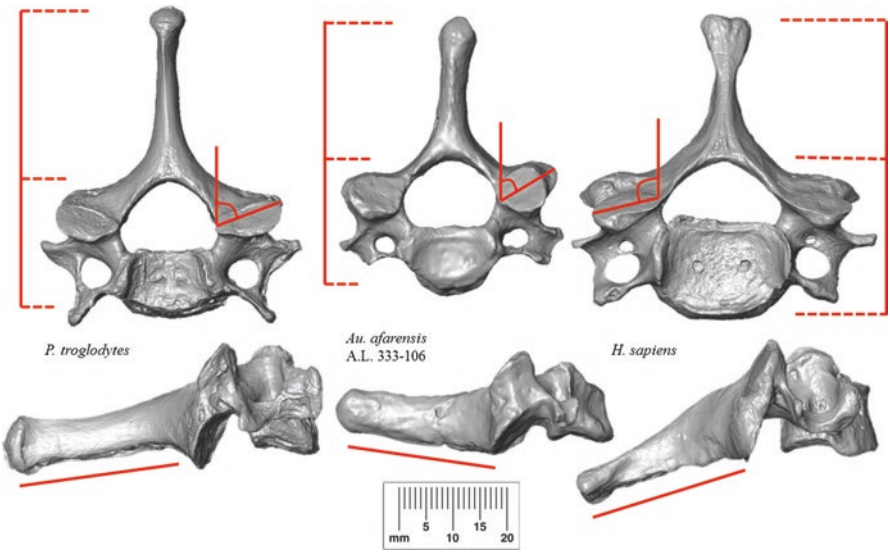

Fig. 7.4 Sixth cervical vertebrae in superior and lateral view. The relative length of the spinous process is shorter in *Au. afarensis* and humans than in chimpanzees. The superior articular facets are acutely angled in *Au. afarensis* and chimpanzees and obtusely angled in modern humans. The spinous process is cranially oriented in *Au. afarensis*, slightly caudally oriented in chimpanzees, and more strongly caudally oriented in modern humans

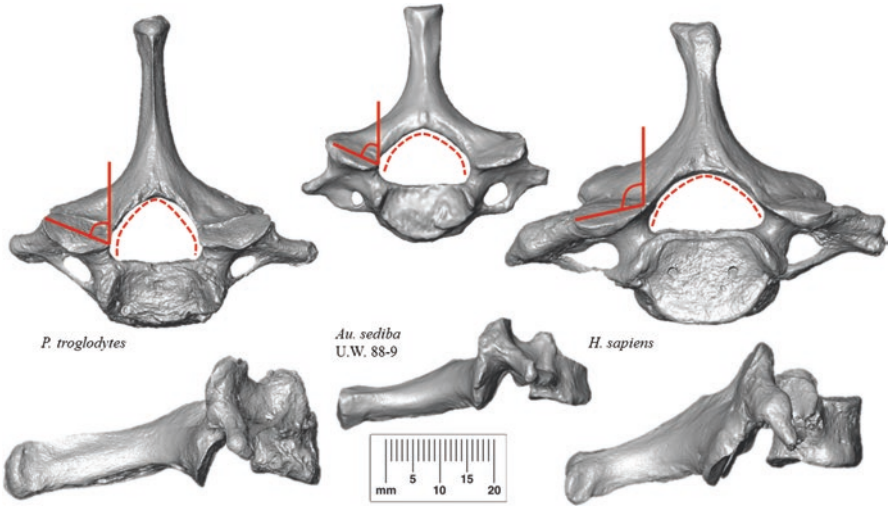

Fig. 7.5 Last cervical vertebrae in superior and lateral view. Superior articular facets are acutely angled in *Au. sediba* and chimpanzees and obtusely angled in modern humans. Spinal canal shape is wider in *Au. sediba* and modern humans than in chimpanzees

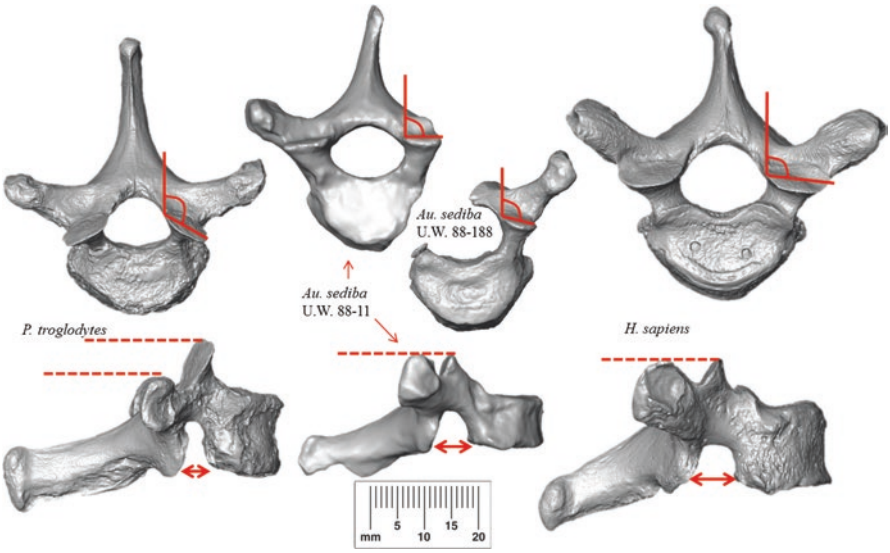

Fig. 7.6 Second thoracic vertebrae in superior and lateral view. Superior articular facets are less obtusely angled in Au. sediba and modern humans than in chimpanzees. The transverse processes are more superiorly positioned relative to the superior articular facets in *Au. sediba* and modern humans than in chimpanzees. The vertebral notch is wider in *Au. sediba* and modern humans than in chimpanzees

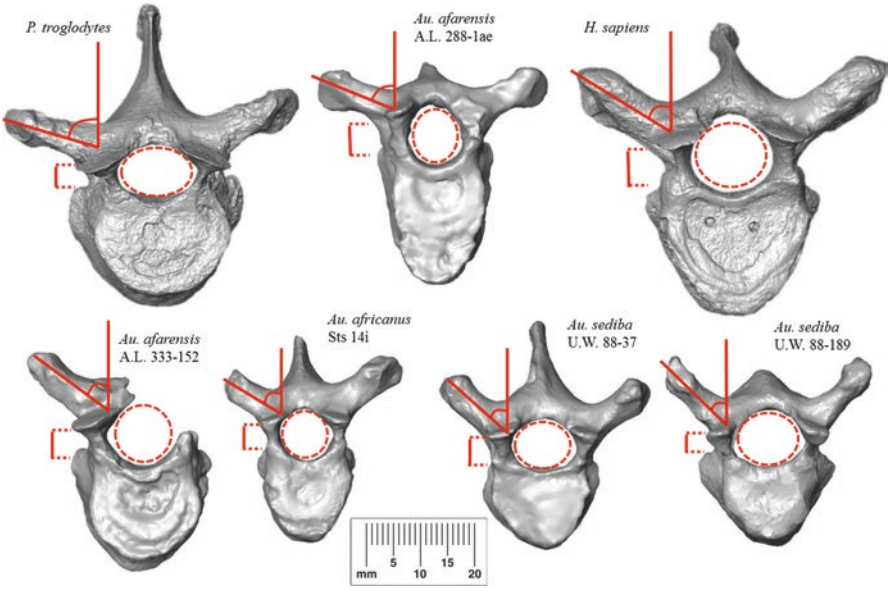

Fig. 7.7 Middle thoracic vertebrae in superior view. Transverse processes are generally more dorsally oriented in hominins than in chimpanzees (A.L. 288-1ae, but not A.L. 333-152, is an exception). Pedicles are anteroposteriorly longer in hominins than in chimpanzees (U.W. 88-189, but not U.W. 88-37, is an exception). Spinal canal shape is more round in hominins than in chimpanzees

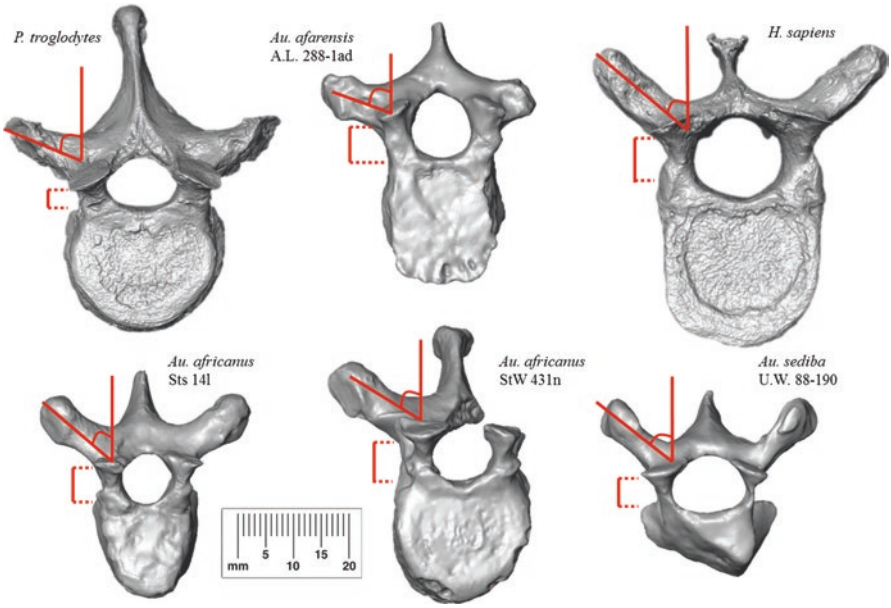

Fig. 7.8 Ninth thoracic vertebrae (tenth thoracic in a chimpanzee) in superior view. Transverse process orientation is more acute in *Au. africanus*, *Au. sediba*, and modern humans than in *Au. afarensis* and chimpanzees. Pedicles are anteroposteriorly longer in hominins than in chimpanzees

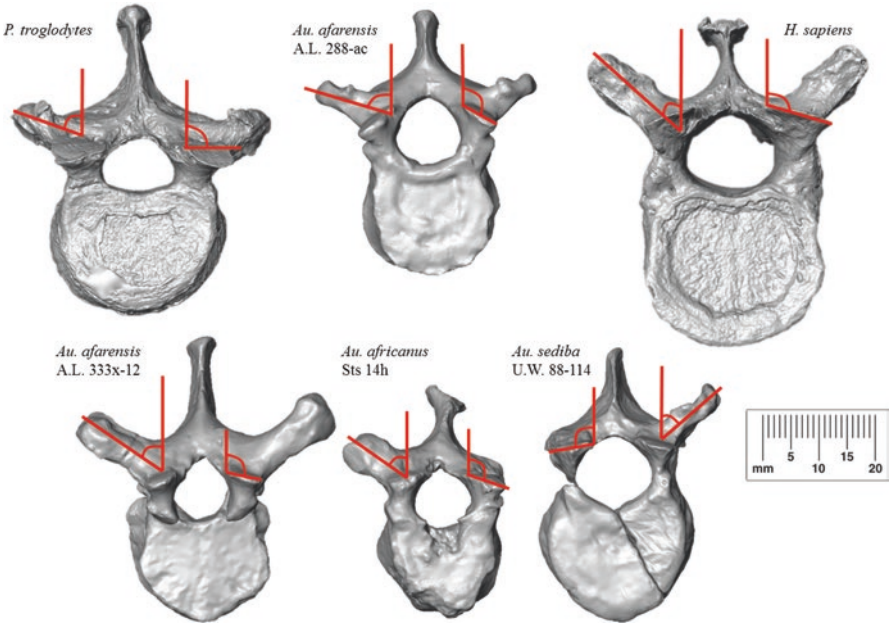

Fig. 7.9 Antepenultimate thoracic vertebrae in superior view. Transverse processes are generally more dorsally oriented in hominins than in chimpanzees (A.L. 288–1 ac, but not A.L. 333x-12, is an exception). Superior articular facets are more obtusely oriented in hominins than in chimpanzees

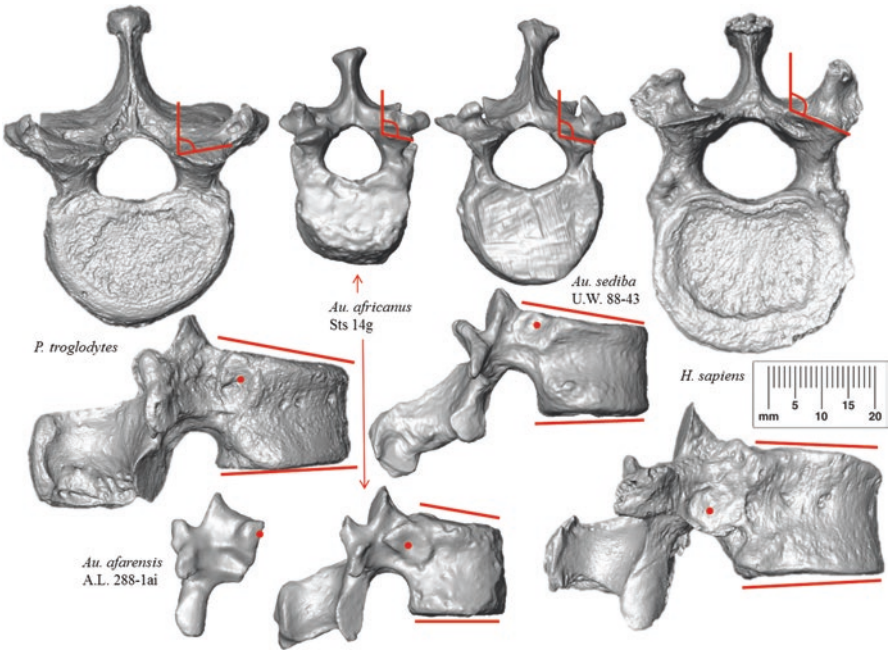

Fig. 7.10 Penultimate thoracic vertebrae in superior and lateral view. Superior articular facets are obtusely oriented in hominins and acutely oriented in chimpanzees. Vertebral bodies are more strongly ventrally wedged in *Australopithecus* and chimpanzees than in modern humans. Red dots indicate the center of the costal facets, which are located more cranially and anteriorly in fossil hominins and chimpanzees than in modern humans. Notice that extant taxa with the transitional vertebra located at the penultimate thoracic level were chosen, whereas the transitional vertebra occurs modally at the last thoracic vertebra in modern humans and chimpanzees

(StW 600) (Partridge et al. 2003; Pickering et al. 2019b). Both vertebrae are similar to those of *Au. africanus* discussed below (Pickering et al. 2019b).

Arguably, *Au. africanus* vertebrae are the best known in the early hominin fossil record, although, as we previously mentioned, no cervical vertebrae are known for this species. All specimens discussed here derive from Member 4 of Sterkfontein. The first early hominin partial skeleton recovered (d. 1947), Sts 14, was announced in Broom et al. (1950) and fully described in Robinson (1972). This individual's vertebral and sacral annular epiphyses are in various stages of fusion, and the iliac crest is not fully fused, suggesting that Sts 14 is a subadult (Bonmatí et al. 2008). The original identification and seriation of the vertebrae was challenged by Haeusler et al. (2002), who argued for a consecutive series of 15 thoracolumbar vertebrae (T3–L5). The fossils were found in cement-like breccia alongside a partial pelvis and were treated with acid for removal, which unfortunately dissolved some morphological aspects of the vertebrae. Additionally, a number of the vertebrae were "reconstructed" with plaster permanently applied directly to the fossils, in some cases fairly extensively (e.g., Sts 14a, the last lumbar vertebra; see Fig. 7.15).

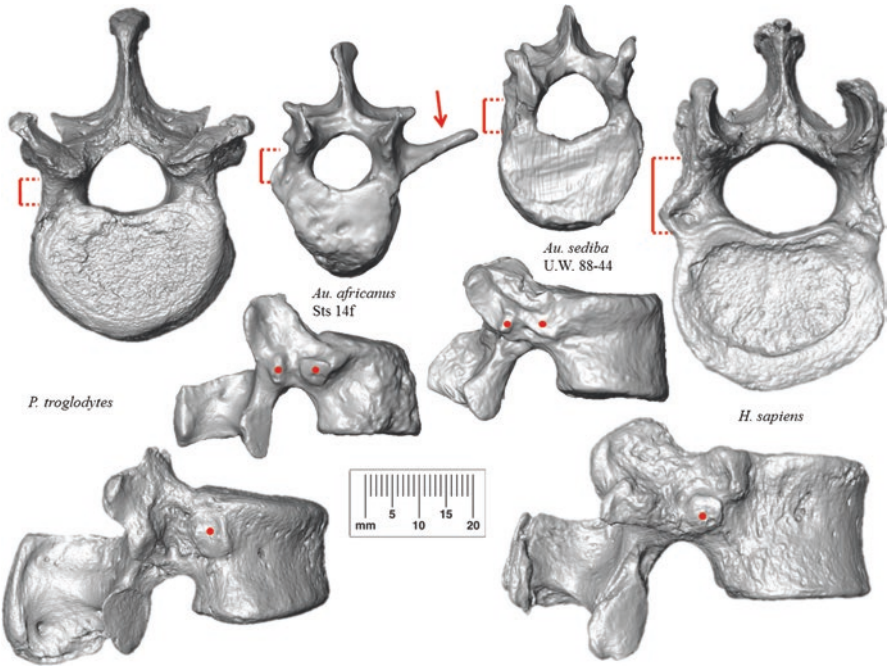

Fig. 7.11 Ultimate thoracic vertebrae in superior and lateral views. Anteroposterior pedicle length is short in chimpanzees, long in modern humans, and somewhat intermediate in fossil hominins. Costal facets are indicated with red dots: notice that those of *Au. africanus* and *Au. sediba* are bifurcate. The red arrow indicates a lumbar transverse process or ankylosed last rib of Sts 14f. Both Sts 14f and U.W. 88-44 are fairly lumbar-like in their overall morphology. Extant taxa with post-transitional thoracic vertebrae are shown for comparison with the fossil hominins

Another *Au. africanus* partial skeleton, StW 431, was discovered in 1987 and published by Toussaint et al. (2003), although the vertebrae were fully described previously by Benade (1990). Haeusler et al. (2002) reassessed the vertebrae and seriated them as ten consecutive elements (T8–L5). StW 431 is an adult and, given its large size compared to Sts 14, is probably a male. Similar-sized adult vertebrae recovered in 1969 and 1975, StW 8, a series of four articulated lumbar vertebrae, and StW 41, two articulated lower thoracic vertebrae, were proposed to be from the same individual by Tobias (1978). Seriation attempts were made by Benade (1990) and Sanders (1998), with the consensus that a continuous series of lower thoracic and lumbar vertebrae (T11–L4) are represented. Two other vertebrae from Member 4 at Sterkfontein, attributed by Robinson (1972) to *Au. africanus*, are the large lower thoracic vertebral body Sts 73 (Robinson 1972) and the partial lumbar vertebra Sts 65 associated with the homonymous female ilium and pubis (Claxton et al. 2016).

The site of Malapa bears *Au. sediba* fossils dated to just under 2 Ma and yields vertebrae from two individuals: an adult female (MH2) and a juvenile male (MH1) (Berger et al. 2010). Additional vertebrae are described in Williams et al. (2013, 2018), with analyses of cervical vertebrae published in Meyer et al. (2017). Eight

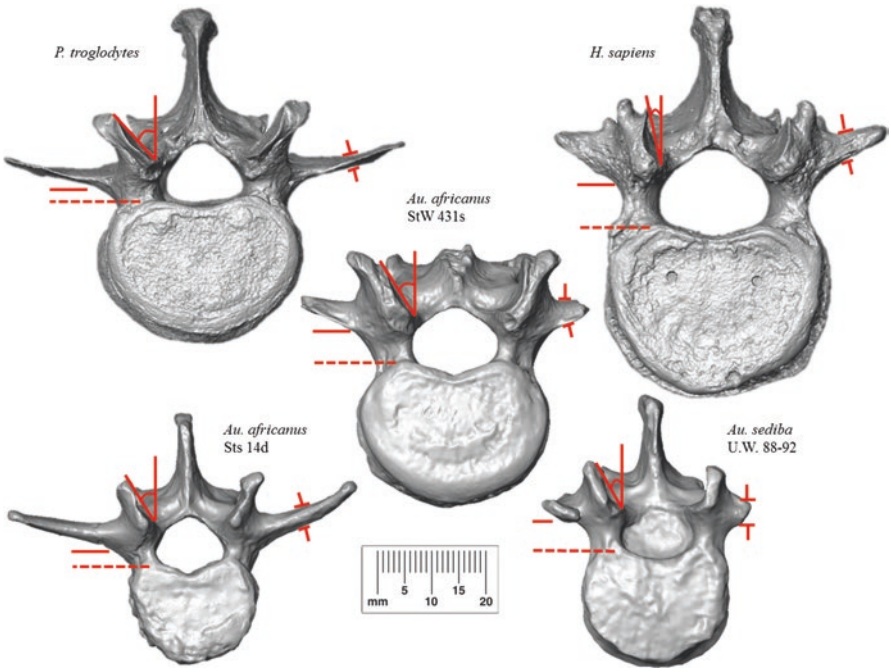

Fig. 7.12 First lumbar vertebrae in superior view. Superior articular facets are more acutely oriented in hominins than in chimpanzees. This is the opposite pattern than what is found at the last lumbar level. Pedicles are longer and lumbar transverse processes are anteroposteriorly more robust in hominins than in chimpanzees

nonconsecutive cervical, thoracic, and lumbar vertebrae are associated with MH1, while 14 vertebrae of MH2 have been recovered, with at least 3 consecutive thoracic vertebrae and 2 lower lumbar vertebrae preserved in articulation with a sacrum (Kibii et al. 2011; Williams et al. 2013, 2018). Overlapping elements belonging to MH1 and MH2 allow for unprecedented comparisons of contemporaneous adult and juvenile, female and male australopiths, which will provide insights into ontogeny and sexual dimorphism of this species.

7.4 Head Carriage and Neck Mobility

Basicranial morphology and cervical vertebral morphology correlate with positional behavior and head and neck posture in primates (Strait and Ross 1999; Manfreda et al. 2006; Russo and Kirk 2013, 2017; Nalley and Grider-Potter 2015; but see caveats in Ruth et al. 2016; Nalley and Grider-Potter 2017; Villamil 2017). Upright posture and bipedal locomotion in early hominins were first inferred from the cranial base in the Taung child, a juvenile member of *Australopithecus africanus*

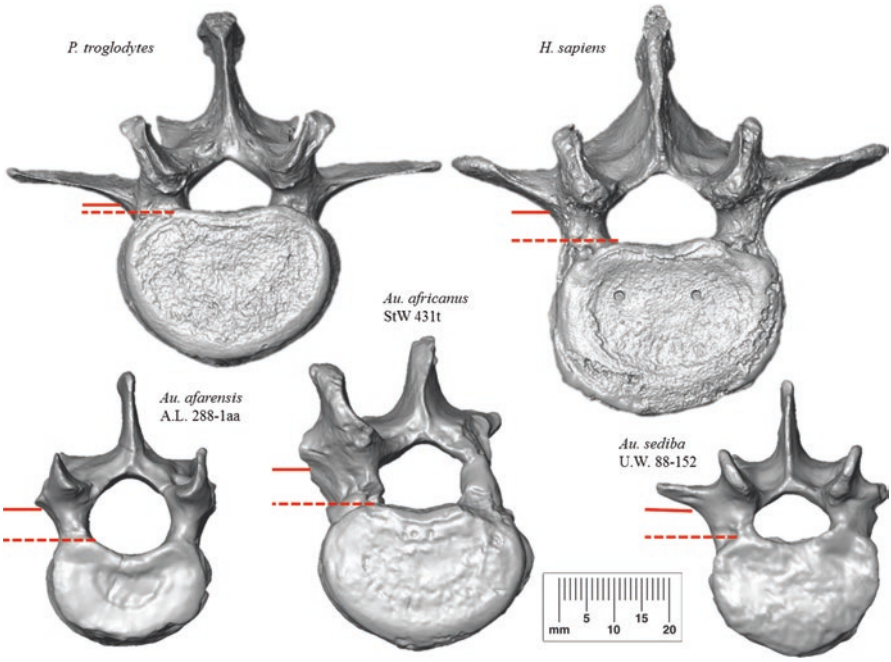

Fig. 7.13 Middle lumbar vertebrae in superior view. Pedicles are anteroposteriorly longer in hominins than in chimpanzees. Notice that superior articular facet orientation is similar across taxa at this level

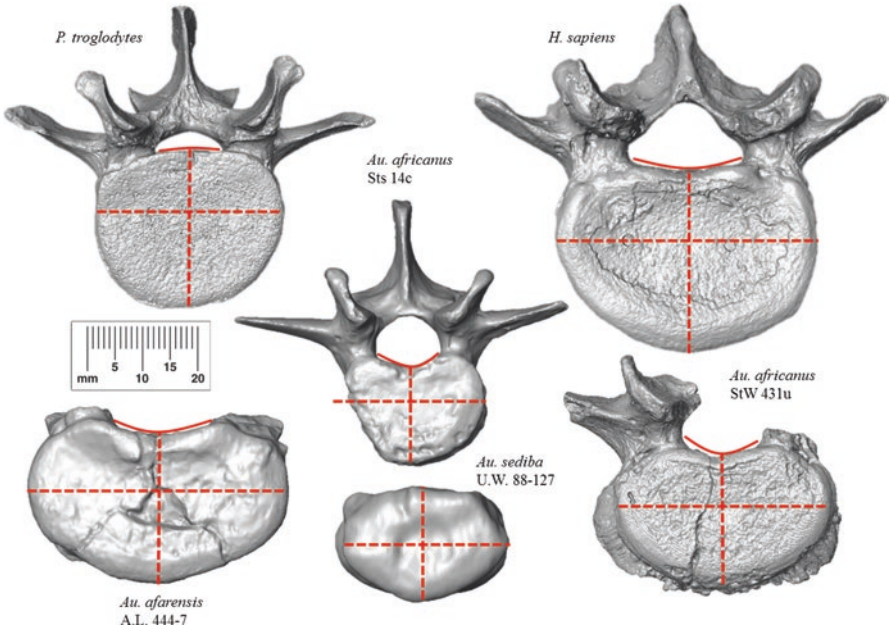

Fig. 7.14 Penultimate lumbar vertebrae (middle lumbar vertebra of *Au. africanus*) in superior view. The hominin vertebral body is kidney-shaped (reniform), with a dorsal concavity that the chimpanzee lacks. Notice that the mediolateral width of the hominin vertebral body is greater than its dorsoventral dimension

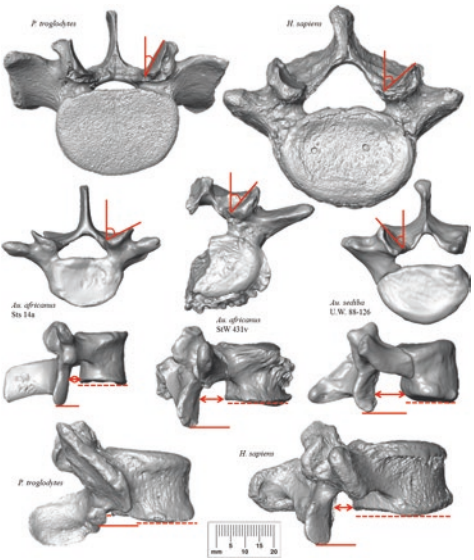

Fig. 7.15 Ultimate lumbar vertebrae in superior and lateral views. Hominin superior articular facets are less acutely angled than chimpanzees. This reflects the oblique (more coronal) orientation of hominin inferior articular facets, which meet the articular facets of the sacrum. The inferior articular facets project more caudally in hominins than in chimpanzees. Hominins also have wider vertebral notches than chimpanzees, although Sts 14a demonstrates a fairly narrow notch compared to other hominins

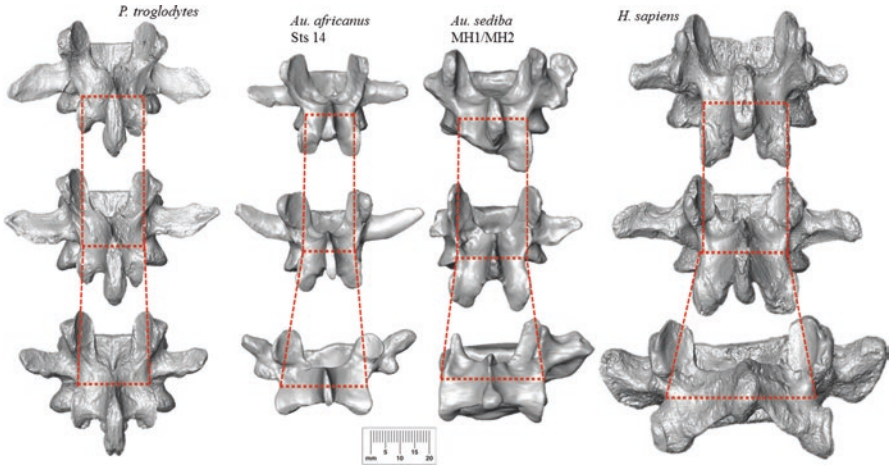

Fig. 7.16 Upper, middle, and lower lumbar vertebrae in posterior view in fossil hominins and extant taxa. Notice that lamina breadth increases caudally in hominins and remains consistently narrow in chimpanzees

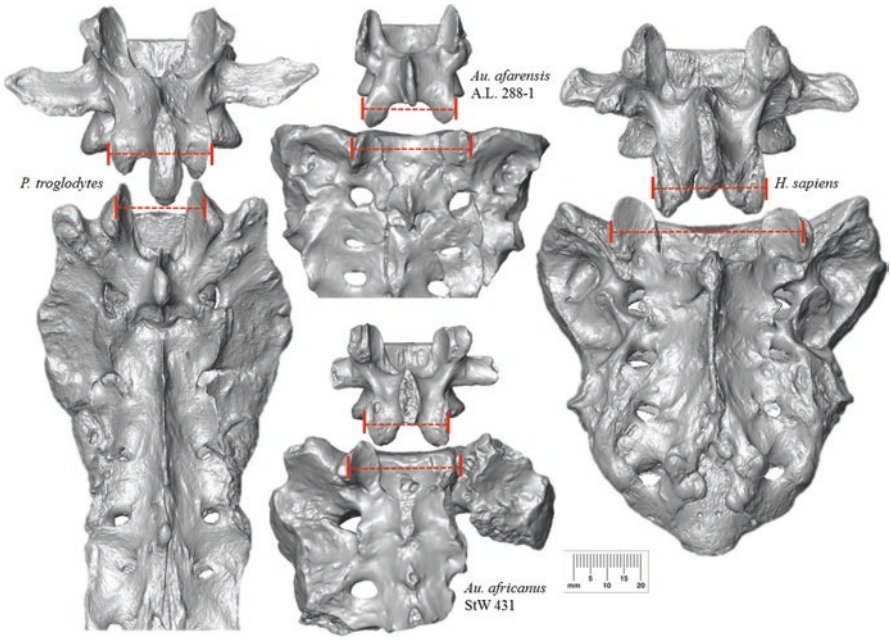

Fig. 7.17 Second lumbar vertebrae and sacra in posterior view in fossil hominins and extant taxa. Comparing the lower articular facet breadth of L2 to superior articular facet breadth of the sacrum reveals an increase in hominins (more drastic in modern humans than in *Australopithecus*) and a decrease or consistency in breadth in chimpanzees. Notice that the sacral alae are much broader in hominins than in chimpanzees

(Dart 1925). The cranial base has also been used to infer bipedalism, and, by implication, hominin status, of the late Miocene *Sahelanthropus tchadensis* cranium, a candidate for the earliest known member of the human lineage (Brunet et al. 2002; Zollikofer et al. 2005; but see Wolpoff et al. 2002). An anteriorly positioned and anteriorly oriented foramen magnum characterizes modern humans to the exclusion of chimpanzees and other apes (Strait and Ross 1999; Russo and Kirk 2013; Been et al. 2014). This places the human skull atop a vertical vertebral column, with minimal neck musculature needed to support the head compared to great apes (Le Gros Clark 1947; Adams and Moore 1975; Aiello and Dean 1990; Lieberman 2011). Neck posture, quantified as cervical lordosis, is correlated with foramen magnum orientation in modern humans, suggesting that cranial base morphology can be informative for reconstructing neck posture in extinct hominins (Been et al. 2014, 2017; see reference to Zollikofer et al. 2005 and Kimbel and Rak 2010 below).

Cervical vertebrae are rare in early hominins. Associated cervical vertebrae are even rarer and are currently known only for *Au. afarensis* (KSD-VP-1/1) and *Au. sediba* (MH1 and MH2). Recent work has shown that australopith cervical vertebrae are intermediate in morphology (and potentially in terms of function) between chimpanzees and modern humans (Gommery 2006; Kimbel and Rak 2010; Nalley 2013; Meyer 2016; Arlegi et al. 2017; Meyer et al. 2017; see also Lovejoy et al.

Table 7.1 List of specimens and species to which they belong

Level	Specimen	Comments	References
Ardipithecus ramidus, Aramis			
?	ARA-VP-6/500-070	Possible vertebra	White et al. (2009)
?	ARA-VP-6/500-086	Possible vertebra	White et al. (2009)
C	ARA-VP-6/500-057	Mostly complete	White et al. (2009)
T	ARA-VP-6/500-084	Thoracic arch	White et al. (2009)
T	ARA-VP-6/1001	Thoracic arch	White et al. (2009)
T	ARA-VP-6/1012	Thoracic spine	White et al. (2009)
Australopithecus anamensis, Asa Issie			
C1	ASI-VP-2/219	Neural arch fragment	Meyer and Williams (2019)
C1	ASI-VP-2/220	Neural arch fragment	White et al. (2006), Meyer and Williams (2019)
C2	ASI-VP-2/214	Body/partial arch	Meyer and Williams (2019)
C6	ASI-VP-2/218	Partial neural arch	Meyer and Williams (2019)
T1	ASI-VP-2/224	Neural arch fragment	White et al. (2006), Meyer and Williams (2019)
T1	ASI-VP-2/470	Body	Meyer and Williams (2019)
T9	ASI-VP-2/223	Partial neural arch	White et al. (2006), Meyer and Williams (2019)
Australopithecus afarensis, Woranso Mille			
C2	KSD-VP-1/1h	Body/partial arch	Haile-Selassie et al. (2010), Meyer (2016)
C3	KSD-VP-1/1i,x	Body/partial arch	Haile-Selassie et al. (2010), Meyer (2016)
C4	KSD-VP-1/1j,ac,z	Body/partial arch	Haile-Selassie et al. (2010), Meyer (2016)
C5	KSD-VP-1/1k,aa,y	Body/partial arch	Haile-Selassie et al. (2010), Meyer (2016)
C6	KSD-VP-1/1l	Body	Haile-Selassie et al. (2010), Meyer (2016)
C7	KSD-VP-1/1ad,ae,af,ag,ab	Partial neural arch	Haile-Selassie et al. (2010), Meyer (2016)
?	KSD-VP-1/1m	Body	Haile-Selassie et al. (2010)
Australopithecus afarensis, Dikika			
C1	DIK-1-1 C1	Mostly complete	Alemseged et al. (2006)
C2	DIK-1-1 C2	Mostly complete	Alemseged et al. (2006)
C3	DIK-1-1 C3	Mostly complete	Alemseged et al. (2006)
C4	DIK-1-1 C4	Mostly complete	Alemseged et al. (2006)
C5	DIK-1-1 C5	Mostly complete	Alemseged et al. (2006)
C6	DIK-1-1 C6	Mostly complete	Alemseged et al. (2006)
C7	DIK-1-1 C7	Mostly complete	Alemseged et al. (2006)
T1	DIK-1-1 T1	Mostly complete	Alemseged et al. (2006), Ward et al. (2017)
T2	DIK-1-1 T2	Mostly complete	Alemseged et al. (2006), Ward et al. (2017)
T3	DIK-1-1 T3	Mostly complete	Alemseged et al. (2006), Ward et al. (2017)
T4	DIK-1-1 T4	Mostly complete	Alemseged et al. (2006), Ward et al. (2017)
T5	DIK-1-1 T5	Mostly complete	Alemseged et al. (2006), Ward et al. (2017)
T6	DIK-1-1 T6	Mostly complete	Alemseged et al. (2006), Ward et al. (2017)
T7	DIK-1-1 T7	Mostly complete	Alemseged et al. (2006), Ward et al. (2017)

(continued)

Table 7.1 (continued)

Level	Specimen	Comments	References
T8	DIK-1-1 T8	Mostly complete	Alemseged et al. (2006), Ward et al. (2017)
T9	DIK-1-1 T9	Mostly complete	Alemseged et al. (2006), Ward et al. (2017)
T10	DIK-1-1 T10	Mostly complete	Alemseged et al. (2006), Ward et al. (2017)
T11	DIK-1-1 T11	Mostly complete	Alemseged et al. (2006), Ward et al. (2017)
T12	DIK-1-1 T12	Mostly complete	Alemseged et al. (2006), Ward et al. (2017)
Australopithecus afarensis, Hadar			
T6	A.L. 288-1ae/ah	Mostly complete	Johanson et al. (1982), Cook et al. (1983)
T7	A.L. 288-1af	Body	Johanson et al. (1982), Cook et al. (1983)
T8	A.L. 288-1ag/aj	Mostly complete	Johanson et al. (1982), Cook et al. (1983)
T9	A.L. 288-1ad	Mostly complete	Johanson et al. (1982), Meyer et al. (2015)
T10	A.L. 288-1ac	Mostly complete	Johanson et al. (1982), Meyer et al. (2015)
T11	A.L. 288-1ai	Partial dorsal pillar	Johanson et al. (1982), Meyer et al. (2015)
L2	A.L. 288-1ab	Spinous process	Johanson et al. (1982), Meyer et al. (2015)
L3	A.L. 288-1aa/ak/al	Mostly complete	Johanson et al. (1982), Meyer et al. (2015)
C1	A.L. 333-83	Partial neural arch	Lovejoy et al. (1982)
C2	A.L. 333-101	Mostly complete	Lovejoy et al. (1982)
C5/6	A.L. 333-106	Mostly complete	Lovejoy et al. (1982), Cook et al. (1983)
T2	A.L. 333-81	Mostly complete	Lovejoy et al. (1982), Cook et al. (1983)
T6	A.L. 333-152	Body/partial arch	Ward et al. (2012)
T7/8/9	A.L. 333-51	Body	Lovejoy et al. (1982), Cook et al. (1983)
L3	A.L. 333-73	Body	Lovejoy et al. (1982), Cook et al. (1983)
C/T	A.L. 333w-14	Lower C/Upper T spinous process	Lovejoy et al. (1982), Cook et al. (1983)
T10	A.L. 333x-12	Mostly complete	Lovejoy et al. (1982), Cook et al. (1983)
C	A.L. 444-9	Partial neural arch	Ward et al. (2012)
T	A.L. 444-8	Spinous process	Ward et al. (2012)
T	A.L. 444-10	Partial neural arch	Ward et al. (2012)
T	A.L. 444-11	Partial neural arch	Ward et al. (2012)
L	A.L. 444-7	Body	Ward et al. (2012)
?	A.L. 444-12	Partial neural arch	Ward et al. (2012)
Australopithecus sp., Sterkfontein			
L3	StW 656	Mostly complete	Pickering et al. (2019a)
L5	StW 600	Mostly complete	Partridge et al. (2003), Pickering et al. (2019a)
L	StW 573	Partial column	Clarke (2002, 2019)
Australopithecus africanus, Sterkfontein			
T3	Sts 14p	Partial arch, body	Robinson (1972), Haeusler et al. (2002)
T4	Sts 14n	Mostly complete	Robinson (1972), Haeusler et al. (2002)
T5	Sts 14m	Mostly complete	Robinson (1972), Haeusler et al. (2002)
T6	Sts 14i	Mostly complete	Robinson (1972), Haeusler et al. (2002)
T7	Sts 14k	Mostly complete	Robinson (1972), Haeusler et al. (2002)
T8	Sts 14l	Mostly complete	Robinson (1972), Haeusler et al. (2002)
T9	Sts 14o	Body	Robinson (1972), Haeusler et al. (2002)

(continued)

Table 7.1 (continued)

Level	Specimen	Comments	References
T10	Sts 14h	Mostly complete	Robinson (1972), Haeusler et al. (2002)
T11	Sts 14g	Mostly complete	Zihlmann (1971), Robinson (1972), Haeusler et al. (2002)
T12	Sts 14f	Mostly complete	Robinson (1972), Haeusler et al. (2002)
L1	Sts 14e	Mostly complete	Robinson (1972), Haeusler et al. (2002)
L2	Sts 14d	Mostly complete	Robinson (1972), Haeusler et al. (2002)
L3	Sts 14c	Mostly complete	Robinson (1972), Haeusler et al. (2002)
L4	Sts 14b	Partial arch, body	Robinson (1972), Haeusler et al. (2002)
L5	Sts 14a	Partial arch, body	Zihlmann (1971), Robinson (1972). Haeusler et al. (2002)
T8	StW 431o	Body	Toussaint et al. (2003), Haeusler et al. (2002)
T9	StW 431n	Mostly complete	Toussaint et al. (2003), Haeusler et al. (2002)
T10	StW 431ma/mb	Partial arch, body	Toussaint et al. (2003), Haeusler et al. (2002)
T11	StW 431l	Partial arch	Toussaint et al. (2003), Haeusler et al. (2002)
T12	StW 431qa/qb	Partial arch, body	Toussaint et al. (2003), Haeusler et al. (2002)
L1	StW 431r	Body	Toussaint et al. (2003), Haeusler et al. (2002)
L2	StW 431s	Mostly complete	Toussaint et al. (2003), Haeusler et al. (2002)
L3	StW 431t	Body, partial arch	Toussaint et al. (2003), Haeusler et al. (2002)
L4	StW 431u	Body, partial arch	Toussaint et al. (2003), Haeusler et al. (2002)
L5	StW 431v	Partial arch, body	Toussaint et al. (2003), Haeusler et al. (2002)
T11	StW H41a	Body	Tobias (1992), Sanders (1998)
T12	StW H41b	Body	Tobias (1992), Sanders (1998)
L1	StW H8a	Partial arch, body	Tobias (1992), Sanders (1998)
L2	StW H8b	Body, partial arch	Tobias (1992), Sanders (1998)
L3	StW H8c	Body, arch fragment	Tobias (1992), Sanders (1998)
L4	StW H8d	Partial body	Tobias (1992), Sanders (1998)
T12	Sts 73	Body	Zihlmann (1971), Robinson (1972), Sanders (1998)
Australopithecus sediba, Malapa			
C3	U.W. 88-72 (MH1)	Partial arch, body	Berger et al. (2010), Williams et al. (2013, 2018), Meyer et al. (2017)
C7	U.W. 88-09 (MH1)	Mostly complete	Berger et al. (2010), Williams et al. (2013, 2018), Meyer et al. (2017)

(continued)

Table 7.1 (continued)

Level	Specimen	Comments	References
Upr T	U.W. 88-11 (MH1)	Mostly complete	Berger et al. (2010), Williams et al. (2013, 2018), Meyer et al. (2017)
Mid T	U.W. 88-37 (MH1)	Mostly complete	Berger et al. (2010), Williams et al. (2013, 2018)
Lwr T	U.W. 88-70 (MH1)	Partial arch, body	Berger et al. (2010), Williams et al. (2013, 2018)
Lwr T	U.W. 88-90 (MH1)	Partial arch, body	Berger et al. (2010), Williams et al. (2013, 2018)
Mid L	U.W. 88-92 (MH1)	Mostly complete	Berger et al. (2010), Williams et al. (2013, 2018)
Mid L	U.W. 88-152 (MH1)	Mostly complete	Williams et al. (2013, 2018)
C3	U.W. 88-93 (MH2)	Mostly complete	Berger et al. (2010), Williams et al. (2013, 2018), Meyer et al. (2017)
C6	U.W. 88-83 (MH2)	Body, partial arch	Berger et al. (2010), Williams et al. (2013, 2018), Meyer et al. (2017)
Upr T	U.W. 88-188 (MH2)	Body, partial arch	Williams et al. (2013, 2018)
Mid T	U.W. 88-189 (MH2)	Mostly complete	Williams et al. (2013, 2018)
T	U.W. 88-190 (MH2)	Partial arch, body	Williams et al. (2013, 2018)
T	U.W. 88-191 (MH2)	Partial arch, body	Williams et al. (2013, 2018)
T	U.W. 88-96 (MH2)	Mid-Lower T neural arch fragment	Berger et al. (2010), Williams et al. (2013, 2018)
Lwr T	U.W. 88-114 (MH2)	Mostly complete	Williams et al. (2013, 2018)
Lwr L	U.W.88-43 (MH2)	Mostly complete	Berger et al. (2010), Williams et al. (2013, 2018)
Ult T	U.W. 88-44 (MH2)	Mostly complete	Berger et al. (2010), Williams et al. Williams (2012a, b), (2018)
Lwr L	U.W. 88-127/153/234	Body, partial arch	Williams et al. (2013, 2018)
Ult L	U.W. 88-126/138	Body, partial arch	Williams et al. (2013, 2018)

1982) (Figs. 7.1, 7.2, 7.3, 7.4, and 7.5). However, the presumed retention of primitive features (present in extant great apes) in *Au. sediba* cervical vertebrae such as relatively gracile vertebral bodies and robust dorsal pillar morphologies; acute (versus obtuse) superior articular facet angles; long, dorsally oriented lower cervical spinous processes; and inferred lack of the nuchal ligament (Meyer et al. 2017; see Figs. 7.2, 7.3, 7.5) suggests limited neck mobility in australopiths relative to modern humans (Nalley 2013; Meyer 2016; Arlegi et al. 2017). While only the latter two features are shared by the KSD-VP-1/1 *Au. afarensis* (Meyer 2016), this morphofunctional condition appears corroborated by evidence for posteriorly oriented foramina magna on australopith basicrania (Zollikofer et al. 2005; Kimbel and Rak 2010). However, relatively short spinous processes on upper subaxial cervical vertebrae and vertebral body wedging angles similar to modern humans suggest cervical lordosis and a human-like neck posture (Meyer 2016; Meyer et al. 2017; Arlegi et al. 2017) (Figs. 7.2, 7.4).

7.5 Number and Configuration of Thoracic and Lumbar Vertebrae

Regional vertebral numbers are relatively stable in mammals, with nearly all possessing seven cervical vertebrae, and many clades fixed at either 19 or 20 thoracolumbar vertebrae, with little variation (Galis 1999; Narita and Kuratani 2005; Asher et al. 2011; Williams et al. 2019). The same is true for the majority of primate clades (Schultz and Straus 1945; Pilbeam 2004). In particular, reduction in the number of thoracolumbar vertebrae in primates and other mammals is rare, with bats, giant pandas, and hominoids as notable exceptions (Schultz and Straus 1945; Pilbeam 2004; Williams 2011; Russo and Williams 2015; Williams and Russo 2015; Williams et al. 2017, 2019). No single fossil hominin skeleton preserves a complete thoracolumbar column. As Table 7.1 indicates, Sts 14 and StW 431 (*Au. africanus*) preserve five lumbar vertebrae each, but neither preserves a complete thoracic column. DIK-1-1 (*Au. afarensis*), on the other hand, does preserve a putatively complete thoracic (and cervical) column but lacks any lumbar vertebrae (Ward et al. 2017). A.L. 288-1 (*Au. afarensis*) preserves a series of thoracic vertebrae and parts of two lumbar vertebrae, StW 8/41 (*Au. africanus*) probably represents the last two thoracic vertebrae and the first four lumbar vertebrae, and MH1 and MH2 (*A. sediba*) preserve a number of thoracic vertebrae and two lumbar vertebrae each (Table 7.1).

Thoracolumbar vertebrae have also been identified functionally (as opposed to developmentally, based on the presence or absence of ribs) on the basis of articular facet (zygapophysis) orientation and location of the transitional vertebra (e.g., Shapiro 1993; Whitcome 2012). This so-called zygapophyseal definition of thoracic versus lumbar vertebrae identifies the transitional vertebra as the last thoracic vertebra (but see Haeusler et al. 2002; Williams 2012a; Williams et al. 2013). Whereas the distinction does not affect regional counts in most hominoids because the transitional vertebra is modally the last rib-bearing vertebra, it is located one to several elements cranial to the last thoracic vertebra in non-hominoid primates (e.g., at the T10 level in a primate with 12 or 13 thoracic vertebrae), which retain the primitive mammalian configuration (Shapiro 1993; Williams 2012a). Importantly, fossil hominins seem to be distinct from modern humans and other hominoids in this regard (Williams 2012b; Williams et al. 2016). The transitional vertebra is located at the penultimate thoracic level in all early hominins preserving this region (Haeusler et al. 2002; Williams 2012a; Williams et al. 2013, 2016; Meyer et al. 2015; Ward et al. 2017). This displacement of transitional and last thoracic vertebra morphologies has led to confusion and debate over the total number of thoracolumbar vertebrae in hominin evolution (Robinson 1972; Sanders 1995; Pilbeam 2004; Lovejoy et al. 2009d; McCollum et al. 2010; Williams and Russo 2015; Williams et al. 2013, 2017; Thompson and Almécija 2017).

7.6 Lumbar Morphology

Due to both lack of ribs and sagittal mobility allowed by post-transitional vertebrae, the lumbar column is thought to be particularly relevant to function and locomotion. Compared to the short, stable lower backs of great apes, hominins have longer, more mobile lower backs. In addition to a numerically longer lumbar column than great apes (five lumbar vertebrae as opposed to four or even just three), hominins have fewer rib pairs (and fewer thoracic vertebrae resulting from a cranially directed homeotic shift at the thoracolumbar border; see Pilbeam 2004; Williams et al. 2017) and fewer lower lumbar vertebrae "entrapped" between the iliac blades (Lovejoy 2005b; Lovejoy and McCollum 2010; McCollum et al. 2010; Machnicki et al. 2016). The presence of an additional post-transitional vertebra in early hominins would conceivably allow more sagittal mobility, which may be related to the achievement of adequate lumbar lordosis for bipedal posture and locomotion (Lovejoy 2005a; Williams et al. 2013).

Hominins are characterized by lumbar lordosis (ventral convexity of the lower back), a combination of bony and soft tissue wedging of lumbar vertebrae, and angulation of the sacrum that counters the primary kyphotic curve (ventrally concavity of the upper back) of the vertebral column, which is found in nonhuman primates and many other mammals. In addition to wedging of the vertebral body and intervertebral discs, the lamina and articular facets increase in width starting in the middle of the lumbar column (Lovejoy 2005a; Ward and Latimer 2005), the postzygapophyses (inferior articular processes) are more dorsally angled (Been et al. 2010b, 2012), and laminar fossae (also known as "imbrication pockets") form via bone remodeling on nonarticular areas of the pars interarticularis from hyperextension of the articular facet joints (Latimer and Ward 1993; Ward and Latimer 2005; Williams et al. 2013; see Fig. 7.16). In combination with thoracic kyphosis, lumbar lordosis contributes to the sinusoidal curvature of the human spine and is considered a primary adaptation to bipedalism and of our lineage. This configuration evolved to balance and stabilize the upright trunk over two legs and dissipate loads through the vertebral column, pelvis, and lower limbs during bipedal posture and locomotion (Sanders 1995; Lovejoy 2005b). Australopiths are widely considered to have possessed modern human-like lordosis, evidenced by dorsal wedging of lower lumbar vertebrae and a pattern of caudad widening of the lamina and articular facets in *Au. africanus* (Sts 14, StW 431) and *Au. sediba* (MH2) (Robinson 1972; Sanders 1995; Whitcome et al. 2007; Been et al. 2012; Williams et al. 2013) and caudally progressive widening of the articular facets in *Au. afarensis* (A.L. 288-1) (Lovejoy 2005a) (Figs. 7.16 and 7.17). Additionally, sexual dimorphism in lumbar lordosis is present in both modern humans (Masharawi et al. 2010; Ostrofsky and Churchill 2015) and *Au. africanus* (Whitcome et al. 2007) and presumably in other australopiths.

7.7 Paleopathology

The evolution of bipedalism seems to have taken a toll on the lower back, a region prone to injury and chronic pain in modern human populations (Balagué et al. 2012; Castillo and Lieberman 2015). Although prolonged use of furniture and the poor postures promoted by its use are a probable culprit for many of these maladies (Black et al. 1996; Castillo and Lieberman 2015), vertebral pathologies are prevalent in the hominin fossil record (see Haeusler 2019). The A.L. 288-1 vertebral column shows evidence of the modern human disease known as Scheuermann's kyphosis, where the thoracic vertebral bodies are characterized by "hyperostotic" anterior bone growth that affects the wedging of vertebrae and increases thoracic kyphosis (Johanson et al. 1982; Cook et al. 1983) (Figs. 7.7 and 7.8). Cook et al. (1983) proposed that habitual ventral flexion of the trunk during flexed trunk climbing or object carrying might be responsible for Lucy's vertebral pathologies. The degree of anterior bone growth in her spine appears to be greater than that normally seen in modern humans with Scheuermann's disease (DiGiovanni et al. 1989). The isolated thoracic vertebra A.L. 333-51 and middle thoracic vertebrae of Sts 14 (Fig. 7.8) show evidence of slight to moderate anterior bone growth, suggesting Scheuermann's kyphosis or something like it occurred frequently in the australopiths.

Juvenile male *Au. sediba* MH1 bears the earliest evidence in the hominin fossil record for a neoplasm. A middle thoracic vertebra (U.W. 88-37) from this individual (Fig. 7.7) carries a lytic lesion on its right lamina and base of the spinous process that was diagnosed as an osteoid osteoma, a benign tumor that probably resulted in chronic pain and affected the individual's use of his right arm (Randolph-Quinney et al. 2016). Finally, the male *Au. africanus* partial skeleton StW 431 includes lower lumbar vertebrae with lesions and lipping (Figs. 7.14 and 7.15) that were originally interpreted as pathological (osteophytic lipping; Toussaint et al. 2003). D'Anastasio et al. (2009) later interpreted the lesions as a possible case of early brucellosis, an infectious disease often caused by ingestion of *Brucella*-infected animal proteins such as milk and meat. Recently, however, Odes et al. (2017) proposed taphonomic and pathological origins of the lesions, a combination of degenerative joint disease and insect burrowing in the bone prior to fossilization.

Acknowledgments We thank Ella Been and Asier Gómez for their leadership in organizing this volume and for inviting us to contribute to it. Recommendations from peer reviewers improved the paper. We acknowledge the curatorial staff at the following institutions for allowing us access to fossil specimens in their care: University of the Witwatersrand, Ditsong National Museum of Natural History, National Museum of Ethiopia, and Authority for Research and Conservation of Cultural Heritage.

References

Adams LM, Moore WJ (1975) Biomechanical appraisal of some skeletal features associated with head balance and posture in the Hominoidea. Acta Anat 92:580–584

Aiello L, Dean C (1990) An introduction to human evolutionary anatomy. Academic Press, London

Alemseged Z, Spoor F, Kimbel WH, Bobe R, Geraads D, Reed D, Wynn JG (2006) A juvenile early hominin skeleton from Dikika, Ethiopia. Nature 443:296–301

Arlegi M, Gómez-Olivencia A, Albessard L, Martínez I, Balzeau A, Arsuaga JL, Been E (2017) The role of allometry and posture in the evolution of the hominin subaxial cervical spine. J Hum Evol 104:80–99

Asher RJ, Lin KH, Kardjilov N, Hautier L (2011) Variability and constraint in the mammalian vertebral column. J Evol Biol 24:1080–1090

Balagué F, Mannion AF, Pellisé F, Cedraschi C (2012) Non-specific low back pain. Lancet 379:482–491

Been E, Kalichman L (2014) Lumbar lordosis. Spine J 14:87–97

Been E, Barash A, Marom A, Kramer PA (2010a) Vertebral bodies or discs: which contributes more to human-like lumbar lordosis? Clin Orthop Relat Res 468:1822–1829

Been E, Barash A, Marom A, Aizenberg I, Kramer PA (2010b) A new model for calculating the lumbar lordosis angle in early hominids and the spine of the Neanderthal from Kebara. Anat Rec 293:1140–1145

Been E, Gómez-Olivencia A, Kramer PA (2012) Lumbar lordosis of extinct hominins. Am J Phys Anthropol 147:64–77

Been E, Shefi S, Zilka LR, Soudack M (2014) Foramen magnum orientation and its association with cervical lordosis: a model for reconstructing cervical curvature in archaeological and extinct hominin specimens. Adv Anthropol 4:133–140

Been E, Gómez-Olivencia A, Shefi S, Soudack M, Bastir M, Barash A (2017) Evolution of spino-pelvic alignment in hominins. Anat Rec 300:900–911

Benade MM (1990) Thoracic and lumbar vertebrae of African hominids ancient and recent: morphological and functional aspects with special reference to upright posture. MA thesis, University of the Witwatersrand

Berger LR, de Ruiter DJ, Churchill SE, Schmid P, Carlson KJ, Dirks PHGM, Kibii JM (2010) *Australopithecus sediba*: a new species of *Homo*-like australopith from South Africa. Science 328:195–204

Black KM, McClure P, Polansky M (1996) The influence of different sitting positions on cervical and lumbar posture. Spine 21:65–70

Bonmatí A, Arsuaga J-L, Lorenzo C (2008) Revisiting the developmental stage and age-at-death of the ''Mrs. Ples'' (Sts 5) and Sts 14 specimens from Sterkfontein (South Africa): do they belong to the same individual? Anat Rec 291:1707–1722

Broom R, Robinson JT, Schepers GWH (1950) Sterkfontein Ape-Man *Plesianthropus*. Transvaal Museum Memoir No. 4. Voortrekkerpers, Beperk, Johannesburg

Brunet M, Guy F, Pilbeam D, Mackaye HT, Likius A, Ahounta D, Beauvilain A, Blondel C, Bocherens H, Bolsserie J-R, de Bonis L, Coppens Y, Dejax J, Denys C, Duringer P, Eisenmann V, Fanone G, Fronty P, Geraads D, Lehmann T, Lihoreau F, Louchart A, Mahamat A, Merceron G, Mouchelin G, Otero O, Campomanes PP, Ponce de Leon M, Rage J-C, Sapanet M, Schuster M, Sudre J, Tassy P, Valentin X, Vignaud P, Viriot L, Zazzo A (2002) A new hominid from the Upper Miocene of Chad, Central Africa. Nature 418:145–151

Carapuço M, Nóvoa A, Bobola N, Mallo M (2005) *Hox* genes specify vertebral types in the presomitic mesoderm. Genes Dev 19:2116–2121

Castillo ER, Lieberman DE (2015) Lower back pain. Evol Med Public Health 2015:2–3

Clarke RJ (2002) Newly revealed information on the Sterkfontein Member 2 *Australopithecus* skeleton. S Afr J Sci 98:523–526

Clarke RJ (2008) Latest information on Sterkfontein's *Australopithecus* skeleton and a new look at *Australopithecus*. S Afr J Sci 104:443–449
Clarke RJ (2019) Excavation, reconstruction and taphonomy of the StW 573 *Australopithecus prometheus* skeleton from Sterkfontein Caves, South Africa. J Hum Evol 127:41–53
Claxton AG, Hammond AS, Romano J, Oleinik E, DeSilva JM (2016) Virtual reconstruction of the *Australopithecus africanus* pelvis Sts 65 with implications for obstetrics and locomotion. J Hum Evol 99:10–24
Cook DC, Buikstra JE, Buikstra JE, DeRousseau CJ, Johanson DC (1983) Vertebral pathology in the Afar australopithecines. Am J Phys Anthropol 60:83–101
D'Anastasio R, Zipfel B, Moggi-Cecchi J, Stanyon R, Capasso L (2009) Possible brucellosis in an early hominin skeleton from Sterkfontein, South Africa. PLoS One 4:e6439
Dart RA (1925) *Australopithecus africanus*: the man-ape of South Africa. Nature 115:195–199
DiGiovanni BF, Scoles PV, Latimer BM (1989) Anterior extension of the thoracic vertebral bodies in Scheuermann's kyphosis: An anatomic study. Spine 14:712–716
Galis F (1999) Why do almost all mammals have seven cervical vertebrae? Developmental constraints, *Hox* genes, and cancer. J Exp Zool 285:19–26
Gommery D (2006) Evolution of the vertebral column in Miocene hominoids and Plio-Pleistocene hominids. In: Ishida H, Tuttle R, Pickford M, Ogihara N, Nakatsukasa M (eds) Human origins and environmental backgrounds. Springer, New York, pp 31–43
Granger DE, Gibbon RJ, Kuman K, Clarke RJ, Bruxelles L, Caffee MW (2015) New cosmogenic burial ages for Sterkfontein Member 2 *Australopithecus* and Member 5 Oldowan. Nature 522:85–88
Haeusler M (2019) Spinal pathologies in fossil hominins. In: Been E, Gómez-Olivencia A, Kramer PA (eds) Spinal evolution: morphology, function, and pathology of the spine in hominoid evolution. Springer, New York, pp 213–246
Haeusler M, Martelli SA, Boeni T (2002) Vertebrae numbers of the early hominid lumbar spine. J Hum Evol 43:621–643
Haeusler M, Schiess R, Boeni T (2011) New vertebral and rib material point to modern bauplan of the Nariokotome *Homo erectus* skeleton. J Hum Evol 61:575–582
Haile-Selassie Y, Latimer BM, Alene M, Deino AL, Gibert L, Melillo SM, Saylor BZ, Scott GR, Lovejoy CO (2010) An early *Australopithecus afarensis* postcranium from Woranso-Mille, Ethiopia. Proc Natl Acad Sci U S A 107:12121–12126
Haile-Selassie Y, Saylor BZ, Deino A, Levin NE, Alene M, Latimer BM (2012) A new hominin foot from Ethiopia shows multiple Pliocene bipedal adaptations. Nature 483:565–569
Johanson DC, Taieb M (1976) Plio-Pleistocene hominid discoveries in Hadar, Ethiopia. Nature 260:293–297
Johanson DC, Lovejoy CO, Kimbel WH, White TD, Ward SC, Bush ME, Latimer BM, Coppens Y (1982) Morphology of the Pliocene partial hominid skeleton (A.L. 288-1) from the Hadar Formation, Ethiopia. Am J Phys Anthropol 57:403–451
Kibii JM, Churchill SE, Schmid P, Carlson KJ, Reed ND, de Ruiter DJ, Berger LR (2011) A partial pelvis of *Australopithecus sediba*. Science 333:1407–1411
Kimbel WH, Rak Y (2010) The cranial base of *Australopithecus afarensis*: new insights from the female skull. Philos Trans R Soc Lond B Biol Sci 365:3365–3376
Kimbel WH, Rak Y, Johanson DC (2004) The skull of *Australopithecus afarensis*. Oxford University Press, New York
Kozma EE, Webb NM, Harcourt-Smith WEH, Raichlen DA, D'Août K, Brown MH, Finestone EM, Ross SR, Aerts P, Pontzer H (2018) Hip extensor mechanics and the evolution of walking and climbing capabilities in humans, apes, and fossil hominins. Proc Natl Acad Sci U S A 115:4134–4139
Latimer B, Ward CV (1993) The thoracic and lumbar vertebrae. In: Walker A, Leakey R (eds) The Nariokotome *Homo erectus* Skeleton. Harvard University Press, Cambridge MA, pp 266–293

Le Gros Clark WE (1947) Observations on the anatomy of the fossil Australopithecinae. J Anat 81:300–333
Leakey MG, Feibel CS, McDougall I, Walker A (1995) New four-million-year-old hominid species from Kanapoi and Allia Bay, Kenya. Nature 376:565–571
Lieberman D (2011) The evolution of the human head. Belknap Press of Harvard University Press, Cambridge MA
Lovejoy CO (1988) Evolution of human walking. Sci Am 259:118–125
Lovejoy CO (2005a) The natural history of human gait and posture, Part 1. Spine and pelvis. Gait Posture 21:95–112
Lovejoy CO (2005b) The natural history of human gait and posture, Part 2. Hip and thigh. Gait Posture 21:113–124
Lovejoy CO (2007) The natural history of human gait and posture, Part 3. The knee. Gait Posture 25:325–341
Lovejoy CO, McCollum MA (2010) Spinopelvic pathways to bipedality: why no hominids ever relied on a bent-hip-bent-knee gait. Philos Trans R Soc B 365:3289–3299
Lovejoy CO, Heiple KG, Burnstein AH (1973) The gait of *Australopithecus*. Am J Phys Anthropol 38:757–780
Lovejoy CO, Johanson DC, Coppens Y (1982) Elements of the axial skeleton recovered from the Hadar formation: 1974–1977 Collections. Am J Phys Anthropol 57:631–635
Lovejoy CO, Latimer B, Suwa G, Asfaw B, White TD (2009a) Combining prehension and propulsion: the foot of *Ardipithecus ramidus*. Science 326:72e1–72e8
Lovejoy CO, Simpson SW, White TD, Asfaw B, Suwa G (2009b) Careful climbing in the Miocene: the forelimbs of *Ardipithecus ramidus* and humans are primitive. Science 326:70e1–70e8
Lovejoy CO, Suwa G, Spurlock L, Asfaw B, White TD (2009c) The pelvis and femur of *Ardipithecus ramidus*: the emergence of upright walking. Science 326:71e1–71e6
Lovejoy CO, Suwa G, Simpson SW, Matternes JH, White TD (2009d) The great divides: *Ardipithecus ramidus* reveals the postcrania of our last common ancestor with African apes. Science 326:100–106
Machnicki AL, Spurlock LB, Strier KB, Reno PL, Lovejoy CO (2016) First steps of bipedality in hominids: evidence from the atelid and proconsulid pelvis. PeerJ 4:e1521
Mallo M, Wellik DM, Deschamps J (2010) *Hox* genes and regional patterning of the vertebrate body plan. Dev Biol 344:7–15
Manfreda E, Mitteroecker P, Bookstein FL, Schaefer K (2006) Functional morphology of the first cervical vertebra in humans and nonhuman primates. Anat Rec 289B:184–194
Masharawi Y, Dar G, Peleg S, Steinberg N, Medlej B, May H, Abbas J, Hershkovitz I (2010) A morphological adaptation of the thoracic and lumbar vertebrae to lumbar hyperlordosis in young and adult females. Eur Spine J 19:768–773
McCollum MA, Rosenman BA, Suwa G, Meindl RS, Lovejoy CO (2010) The vertebral formula of the last common ancestor of African apes and humans. J Exp Zool 314B:123–134
Meyer MR (2016) The cervical vertebrae of KSD-VP-1/1. In: Haile-Selassie Y, Su DF (eds) The postcranial anatomy of *Australopithecus afarensis*: new insights from KSD-VP-1/1. Springer, Dordrecht, pp 63–111
Meyer MR, Williams SA (2019) Earliest axial fossils from the genus *Australopithecus*. J Human Evol 132:189–214
Meyer MR, Williams SA, Smith MP, Sawyer GJ (2015) Lucy's back: reassessment of fossils associated with the A.L. 288-1 vertebral column. J Hum Evol 85:174–180
Meyer MR, Williams SA, Schmid P, Churchill SE, Berger LR (2017) The cervical spine of *Australopithecus sediba*. J Hum Evol 104:32–49
Nalley TK (2013) Positional behaviors and the neck: a comparative analysis of the cervical vertebrae of living primates and fossil hominoids. PhD dissertation, Arizona State University
Nalley TK, Grider-Potter N (2015) Functional morphology of the primate head and neck. Am J Phys Anthropol 156:531–542

Nalley TK, Grider-Potter N (2017) Functional analyses of the primate upper cervical vertebral column. J Hum Evol 107:19–35
Narita Y, Kuratani S (2005) Evolution of the vertebral formulae in mammals: a perspective on developmental constraints. J Exp Zool 304B:91–106
Odes EJ, Parkinson AH, Randolph-Quinney PS, Zipfel B, Jakata K, Bonney H, Berger LR (2017) Osteopathology and insect traces in the *Australopithecus africanus* skeleton StW 431. S Afr J Sci 113:1–7
Ostrofsky KR, Churchill SE (2015) Sex determination by discriminant function analysis of lumbar vertebrae. J Forensic Sci 60:21–28
Partridge TC, Granger DE, Caffee MW, Clarke RJ (2003) Lower Pliocene hominid remains from Sterkfontein. Science 300:607–612
Pickering R, Herries AIR, Woodhead JD, Hellstrom JC, Green HE, Paul B, Ritzman T, Strait DS, Schoville BJ, Hancox PJ (2019a) U-Pb-dated flowstones restrict South African early hominin record to dry climate phases. Nature 565(7738):226–229. https://doi.org/10.1038/s41586-018-0711-0
Pickering TR, Heaton JL, Clarke RJ, Stratford D (2019b) Hominin vertebrae and upper limb bone fossils from Sterkfontein Caves, South Africa (1998-2003 excavations). Am J Phys Anthropol 168(3):459–480. https://doi.org/10.1002/ajpa.23758
Pilbeam D (2004) The anthropoid postcranial axial skeleton: comments on development, variation, and evolution. J Exp Zool 302B:241–267
Pollock RA, Sreenath T, Ngo L, Bieberich CJ (1995) Gain of function mutations for paralogous *Hox* genes: implications for the evolution of *Hox* gene function. Proc Natl Acad Sci U S A 92:4492–4496
Prang TC (2015) Calcaneal robusticity in Plio-Pleistocene hominins: implications for locomotor diversity and phylogeny. J Hum Evol 80:135–146
Prang TC (2019) The African ape-like foot of *Ardipithecus ramidus* and its implications for the origin of bipedalism. eLife 8:e44433
Randolph-Quinney PS, Williams SA, Steyn M, Meyer MR, Smilg JS, Churchill SE, Odes EJ, Augustine T, Tafforeau P, Berger LR (2016) Osteogenic tumour in *Australopithecus sediba*: earliest hominin evidence for neoplastic disease. S Afr J Sci 112:1–7
Reed K, Fleagle JG, Leakey RE (2013) The Paleobiology of *Australopithecus*. Springer, Dordrecht
Robinson JT (1972) Early hominid posture and locomotion. University of Chicago Press, Chicago
Russo GA, Kirk EC (2013) Foramen magnum position in bipedal mammals. J Hum Evol 65:656–670
Russo GA, Kirk EC (2017) Another look at the foramen magnum in bipedal mammals. J Hum Evol 105:24–40
Russo GA, Williams SA (2015) Giant pandas (Carnivora: *Ailuropoda melanoleuca*) and living hominoids converge on lumbar vertebral adaptations to orthograde trunk posture. J Hum Evol 88:160–179
Ruth AA, Raghanti MA, Meindl RS, Lovejoy CO (2016) Locomotor pattern fails to predict foramen magnum angle in rodents, strepsirrhine primates, and marsupials. J Hum Evol 94:45–52
Sanders WJ (1995) Function, allometry, and evolution of the australopithecine lower precaudal spine. PhD Dissertation, New York University
Sanders WJ (1998) Comparative morphometric study of the australopithecine vertebral series Stw-H8/H41. J Hum Evol 34:249–302
Schultz AH, Straus WL (1945) The numbers of vertebrae in primates. Proc Am Philos Soc 89:601–626
Shapiro L (1993) Functional morphology of the vertebral column in primates. In: Gebo DL (ed) Postcranial Adaptation in Nonhuman Primates. Northern Illinois University Press, DeKalb, pp 121–149

Shapiro I, Frankel VH (1989) Biomechanics of the cervical spine. In: Nordin M, Frankel VH (eds) Basic Biomechanics of the musculoskeletal system. Lea and Febiger, Philadelphia, pp 209–224
Strait DS, Ross CF (1999) Kinematic data on primate head and neck posture: implications for the evolution of basicranial flexion and an evaluation of registration planes used in paleoanthropology. Am J Phys Anthropol 108:205–222
Thompson NE, Almécija S (2017) The evolution of vertebral formulae in Hominoidea. J Hum Evol 110:18–36
Tobias PV (1978) The place of *Australopithecus africanus* in hominid evolution. In: Chivers DJ, Joysey KA (eds) Recent advances in primatology, Evolution, vol III. Academic Press, London, pp 373–394
Tobias PV (1992) New researches at Sterkfontein and Taung with a note on Piltdown and its relevance to the history of palaeo-anthropology. Trans R Soc S Afr 48:1–14
Toussaint M, Macho GA, Tobias PV, Partridge TC, Hughes AR (2003) The third partial skeleton of a late Pliocene hominin (Stw 431) from Sterkfontein, South Africa. S Afr J Sci 99:215–223
Villamil CI (2017) Locomotion and basicranial anatomy in primates and marsupials. J Hum Evol 111:163–178
Ward CV, Latimer B (2005) Human evolution and the development of spondylolysis. Spine 30(16):1808–1814
Ward CV, Kimbel WH, Harmon EH, Johanson DC (2012) New postcranial fossils of *Australopithecus afarensis* from Hadar, Ethiopia (1990-2007). J Hum Evol 63:1–51
Ward CV, Nalley TK, Spoor F, Tafforeau P, Alemseged Z (2017) Thoracic vertebral count and thoracolumbar transition in *Australopithecus afarensis*. Proc Natl Acad Sci U S A 114:6000–6004
Washburn SL (1963) Behavior and human evolution. In: Washburn SL (ed) Classification and human evolution. Aldine, Chicago, pp 190–203
Wellik DM, Capecchi MR (2003) *Hox10* and *Hox11* genes are required to globally pattern the mammalian skeleton. Science 301:363–367
Whitcome KK (2012) Functional implications of variation in lumbar vertebral count among hominins. J Hum Evol 62:486–497
Whitcome KK, Shapiro LJ, Lieberman DE (2007) Fetal load and the evolution of lumbar lordosis in bipedal hominins. Nature 450:1075–1078
White TD, WoldeGabriel G, Asfaw B, Ambrose S, Beyene Y, Bernor RL, Boisserie J-R, Currie B, Gilbert H, Haile-Selassie Y, Hart WK, Hlusko LJ, Howell FC, Kono RT, Lehmann T, Louchart A, Lovejoy CO, Renne PR, Saegusa H, Vrba ES, Wesselman H, Suwa G (2006) Asa Issie, Aramis and the origin of *Australopithecus*. Nature 440:883–889
White TD, Asfaw B, Beyene Y, Haile-Selassie Y, Lovejoy CO, Suwa G, WoldeGabriel G (2009) *Ardipithecus ramidus* and the paleobiology of early hominids. Science 326:75–86
White TD, Lovejoy CO, Asfaw B, Carlson JP, Suwa G (2015) Neither chimpanzee nor human, *Ardipithecus* reveals the surprising ancestry of both. Proc Natl Acad Sci U S A 11:4877–4884
Williams SA (2011) Variation in anthropoid vertebral formulae: implications for homology and homoplasy in hominoid evolution. J Exp Zool 318:134–147
Williams SA (2012a) Placement of the diaphragmatic vertebra in catarrhines: implications for the evolution of dorsostability in hominoids and bipedalism in hominins. Am J Phys Anthropol 148:111–122
Williams SA (2012b) Modern or distinct axial bauplan in early hominins? Comments on Haeusler et al. (2011). J Hum Evol 63:552–556
Williams SA, Russo GA (2015) Evolution of the hominoid vertebral column: the long and the short of it. Evol Anthropol 24:15–32
Williams SA, Ostrofsky KR, Frater N, Churchill SE, Schmid P, Berger LR (2013) The vertebral column of *Australopithecus sediba*. Science 340:1232996
Williams SA, Middleton ER, Villamil CI, Shattuck MR (2016) Vertebral numbers and human evolution. Yearb Phys Anthropol 159:S19–S36
Williams SA, García-Martínez D, Bastir M, Meyer MR, Nalla S, Hawks J, Schmid P, Churchill SE, Berger LR (2017) The vertebrae and ribs of *Homo naledi*. J Hum Evol 104:136–154

Williams SA, Meyer MR, Nalla S, García-Martínez D, Nalley TK, Eyre J, Prang TC, Bastir M, Schmid P, Churchill SE, Berger LR (2018) The vertebrae, ribs, and sternum of *Australopithecus sediba*. PaleoAnthropology 2018:156–233

Williams SA, Gómez-Olivencia A, Pilbeam D (2019a) Numbers of vertebrae in hominoid evolution. In: Been E, Gómez-Olivencia A, Kramer PA (eds) Spinal evolution: morphology, function, and pathology of the spine in hominoid evolution. Springer, New York, pp 97–124

Williams SA, Spear JK, Petrullo L, Goldstein DM, Lee AB, Peterson AL, Miano DA, Kaczmarek EB, Shattuck MR (2019b) Increased variation in numbers of presacral vertebrae in suspensory mammals. Nat Ecol Evol 3:949–956

Wolpoff MH, Senut B, Pickford M, Hawks J (2002) *Sahelanthropus* or '*Sahelpithecus*'? Nature 419:581–582

Zihlmann AL (1971) The question of locomotor differences in *Australopithecus*. In: Biegert J, Leutenegger W (eds) Proceedings of the third international congress of primatology, Zurich 1970, Taxonomy, anatomy, and reproduction, vol 1. S. Karger, Basel, pp 54–66

Zollikofer CPE, Ponce de León MS, Lieberman DE, Guy F, Pilbeam D, Likius A, Mackaye HT, Vignaud P, Brunet M (2005) Virtual cranial reconstruction of *Sahelanthropus tchadensis*. Nature 434:755–759

Chapter 8
The Spine of Early Pleistocene *Homo*

Marc R. Meyer and Scott A. Williams

8.1 Introduction

There is a general consensus that there was a shift in postcranial morphology with the evolutionary transition from *Australopithecus* to the genus *Homo* (Aiello and Dean 1990; Aiello and Wells 2002; Ward et al. 2015). Some postcranial changes in *Homo* have been hypothesized to associate with changes in body size and ranging ecology (Martin 1981; Walker and Leakey 1993a; McHenry 1994a), improved terrestrial locomotor efficiency and increased distance running ability (Jungers 1982; Bramble and Lieberman 2004; Steudel-Numbers 2006; Pontzer 2007), greater load bearing ability (Meyer 2005, 2008), and increased neurological endowment of the brain (Aiello and Wheeler 1995) and spinal cord (MacLarnon 1993). However, recent work suggests traits assumed to be derived in *Homo* (1) are present in *Australopithecus*, such as larger limb joints and longer hind limbs (Haile-Selassie et al. 2010, 2016; Holliday 2012), and (2) are thought to be the product of positive allometry (Holliday and Franciscus 2009; Pontzer 2012, 2017). If australopiths are ancestral to early *Homo*, body size may have actually decreased slightly (Jungers et al. 2016). Both australopiths and *Homo* appear to share extended limb posture and spring-like plantar arch (Lovejoy 2007; DeSilva 2009; Barak et al. 2013; Prang 2015), challenging the hypothesis that the postcranium of early *Homo* was radically specialized for terrestrial locomotion relative to its putative forbears and that the

M. R. Meyer (✉)
Department of Anthropology, Chaffey College, Rancho Cucamonga, CA, USA
e-mail: marc.meyer@chaffey.edu

S. A. Williams
Department of Anthropology, Centre for the Study of Human Origins, New York University, New York, NY, USA

New York Consortium in Evolutionary Primatology, New York, NY, USA

E. Been et al. (eds.), *Spinal Evolution*,
https://doi.org/10.1007/978-3-030-19349-2_8

two groups belonged to distinct adaptive grades (Holliday 2012; Antón et al. 2014; Villmoare 2018).

The axial skeleton is not unlike other biological regions revealing aspects of an anatomical continuum from australopiths to *Homo* (Robinson 1965; Haile-Selassie et al. 2010, 2016; Grabowski et al. 2015; Kimbel and Villmoare 2016; Meyer and Haile-Selassie 2016; Garvin et al. 2017). In this chapter, we explore the vertebral column of early *Homo* (Table 8.1), with an emphasis on spinal form and function in *H. erectus*. We also examine fossil vertebrae from *H. naledi* dated to the late Middle Pleistocene (Dirks et al. 2017), and although the taxon may not represent the origin of the genus, it is a morphologically primitive hominin in many respects (Berger et al. 2015; Hawks et al. 2017). We also discuss isolated vertebrae from Swartkrans and Koobi Fora and suggest reasons for a reappraisal of their taxonomic designations.

8.2 *Homo erectus* from Dmanisi

Five vertebrae discovered in 2001 at the site of Dmanisi in Georgia (Fig. 8.1) presently represent the oldest presently known vertebral series for the genus *Homo* (Meyer 2005). Dated to 1.77 Ma, two cervical and two thoracic vertebrae and one lumbar vertebra are associated with the adolescent D2700 *H. erectus* partial skeleton. Dental and long bone development suggest an age between 14 and 17 years based on modern human standards, and the morphology and lack of fusion of the ring apophyses agree with this estimation (Meyer 2005). Corresponding developmental schedules in the Dmanisi skeleton and modern humans accord with recent evidence demonstrating that the rate of growth and development in *H. erectus* was within the range of modern humans (Dean and Liversidge 2015; Smith et al. 2015; Dean 2016), in contrast to earlier work positing accelerated skeletal age in *H. erectus* (Dean et al. 2001; Robson and Wood 2008). Other than its smaller size, Meyer (2005) found very few differences between the Dmanisi spine and modern humans in terms of form or function.

8.3 *Homo erectus* from Nariokotome

A larger, similarly aged adolescent partial skeleton for *H. erectus* is KNM-WT 15000 from Nariokotome, West Lake Turkana, Kenya (Brown et al. 1985; Walker and Leakey 1993a). This skeleton preserves a total of 16 vertebrae (Latimer and Ward 1993; Walker and Leakey 1993b), consisting of one cervical, ten thoracic, and five lumbar vertebrae (Haeusler et al. 2011) (Fig. 8.2). Fused primary ossification centers but unfused ring apophyses and billowing on the vertebral bodies indicate its adolescent status. Many of the vertebrae are remarkably preserved, with only a

Table 8.1 Current inventory of preserved vertebrae in the fossil record for early Pleistocene and other hominins discussed in this chapter

Level	Specimen	Comments	References
***Homo erectus*, Dmanisi**			
C2	D2673	Mostly complete	Meyer (2005)
C3	D2674	Mostly complete	Meyer (2005)
T3	D2721	Mostly complete	Meyer (2005)
T11	D2715	Mostly complete	Meyer (2005)
L2	D2672	Mostly complete	Meyer (2005)
***Homo erectus*, Nariokotome**			
C7	KNM-WT 15000 r	Mostly complete	Walker and Leakey (1993a, 1993b)
T1	KNM-WT 15000 s	Mostly complete	Walker and Leakey (1993a, 1993b)
T2	KNM-WT 15000 t	Mostly complete	Walker and Leakey (1993a, 1993b)
T3	KNM-WT 15000 u	Mostly complete	Walker and Leakey (1993a, 1993b)
T4	KNM-WT 15000 ca	Mostly complete	Walker and Leakey (1993a, 1993b); modified by Haeusler et al. (2011)
T6	KNM-WT 15000 w	Mostly complete	Walker and Leakey (1993a, 1993b); modified by Haeusler et al. (2011)
T7	KNM-WT 15000 v	Mostly complete	Walker and Leakey (1993a, 1993b); modified by Haeusler et al. (2011)
T9	KNM-WT 15000 bi	Partial dorsal pillar	Walker and Leakey (1993a, 1993b)
T10	KNM-WT 15000 x	Partial dorsal pillar	Walker and Leakey (1993a, 1993b)
T11	KNM-WT 15000 y	Mostly complete	Walker and Leakey (1993a, 1993b)
T12	KNM-WT 15000 ar/ba	Mostly complete	Walker and Leakey (1993a, 1993b); modified by Haeusler et al. (2011)
L1	KNM-WT 15000 av/aa	Body and dorsal pillar	Walker and Leakey (1993a, 1993b); modified by Haeusler et al. (2011)
L2	KNM-WT 15000 z/bw	Body and dorsal pillar	Walker and Leakey (1993a, 1993b); modified by Haeusler et al. (2011)
L3	KNM-WT 15000 ab	Mostly complete	Walker and Leakey (1993a, 1993b); modified by Haeusler et al. (2011)
L4	KNM-WT 15000 bm	Mostly complete	Walker and Leakey (1993a, 1993b); modified by Haeusler et al. (2011)
L5	KNM-WT 15000 ac	Mostly complete	Walker and Leakey (1993a, 1993b); modified by Haeusler et al. (2011)
***Homo erectus*, Koobi Fora**			
C1	KNM-ER 1808 z	Partial, articular facets	Walker et al. (1982); Leakey and Walker (1985)
***Homo erectus*, Swartkrans**			
T12	SK 3981a	(*P*) Mostly complete	Robinson (1970); Robinson (1972); reconsidered here
L1	SK 853	Mostly complete	Broom and Robinson (1949)
L5	SK 3981b	(*P*) Partially complete	Robinson (1970); Robinson (1972); reconsidered here

(continued)

Table 8.1 (continued)

Level	Specimen	Comments	References
***Homo naledi*, Dinaledi Chamber**[a]			
C1	U.W. 101-651	Neural arch fragment	Williams et al. (2017)
C1	U.W. 101-331	Neural arch fragment	Williams et al. (2017)
C2	U.W. 101-1279/489	Body	Williams et al. (2017)
C2	U.W. 101-1692	Body fragment	Williams et al. (2017)
C2	U.W. 101-732	Neural arch fragment	Williams et al. 2017)
T10	U.W. 101-855	Mostly complete	Williams et al. (2017)
T11	U.W. 101-1733	Mostly complete	Williams et al. (2017)
***Homo naledi*, Lesedi Chamber**			
T10	U.W. 102a-036	Mostly complete	Hawks et al. (2017)
T11	U.W. 102a-151	Mostly complete	Hawks et al. (2017)
T12	U.W. 102a-154a	Articulated with 154b	Hawks et al. (2017)
L1	U.W. 102a-154b	Articulated with 154a	Hawks et al. (2017)
L2	U.W. 102a-322	Body	Hawks et al. (2017)
L4	U.W. 102a-306	Body	Hawks et al. (2017)
L5	U.W. 102a-139	Body	Hawks et al. (2017)
***Homo* sp. or *Paranthropus*, Cooper's Cave**			
T10-T12	CD 5773	Body, left pedicle	de Ruiter et al. (2009)
***Homo* sp. or *Paranthropus*, Swartkrans**			
Mid Thor	SKX 3342	Body fragment	Susman (1988)
T10	SKX 41692	(*P*) Mostly complete	Susman (1989)
Homo sp.* or *Paranthropus, Ileret			
C1	KNM-ER 1825	Partial, articular facets	Leakey and Walker (1985)
***Homo floresiensis*, Liang Bua**			
C1	LB5/1	Two fragments	Morwood et al. (2005); Groves (2007)
***Homo sapiens*, Koobi Fora (intrusive human burial)**			
C7, T1	KNM-ER 164 c	(*E*) 2 articulated elements	Day and Leakey (1974); modified by Meyer (2005)

(E) Previously attributed to *H. erectus*
(P) Previously attributed to *Paranthropus*
[a]See Williams et al. (2017), Table S1, for a complete inventory of Dinaledi hominin postcranial axial material

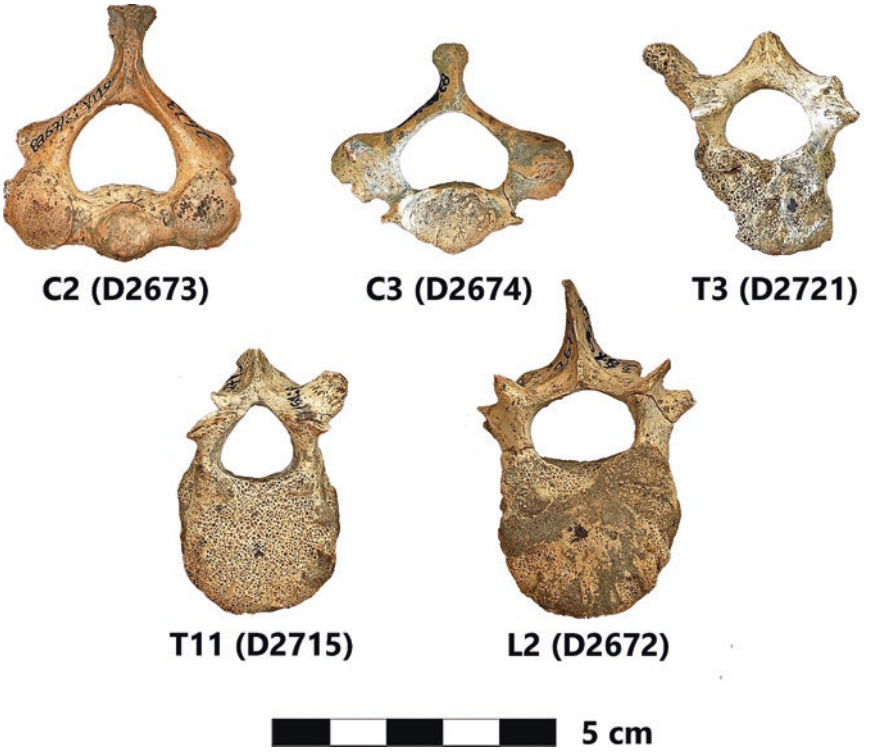

Fig. 8.1 Superior view of fossil vertebrae attributed to the D2700 *Homo erectus* from Dmanisi. Published vertebral level attributions (Meyer 2005) are accompanied by specimen catalog numbers in parentheses

few exceptions, such as the L2 where the vertebral body is separated from the pedicles and dorsal structures.

Walker and Leakey (1993b) originally assessed that three thoracic vertebrae were missing (T4, T6, and T12) and that six lumbar vertebrae were preserved; however, while working at the National Museums of Kenya, Nairobi, Haeusler and colleagues identified three previously undescribed vertebral fragments stored in several plastic bags within the skull box of the fossil, prompting a reassessment of the vertebral attributions (Haeusler et al. 2011). It is now apparent that only two thoracic vertebrae are absent (T5 and T8) and that the sixth presacral level was rib-bearing, resulting in its attribution to the ultimate thoracic level (T12) rather than to the first lumbar (L1) as previously suggested.

The postcranial anatomy of KNM-WT 15000 may be more intermediate between *Australopithecus* and modern humans (Holliday 2012) than first reported (Brown et al. 1985). Nonetheless, despite a relatively constricted lower cervical and upper thoracic spinal canal (Meyer and Haeusler 2015), few differences exist in overall vertebral functional morphology between KNM-WT 15000 and modern humans.

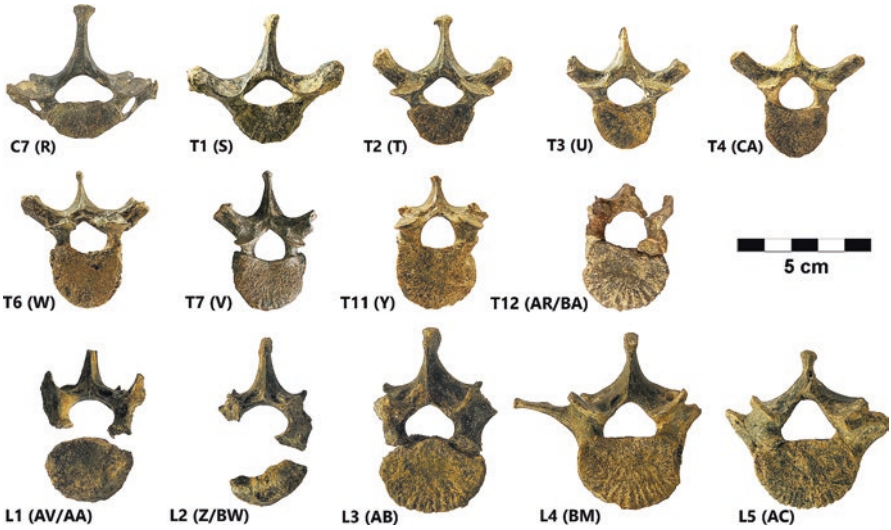

Fig. 8.2 Superior view of most well-preserved fossil vertebrae from the *Homo erectus* from Nariokotome, West Turkana. Published vertebral level attributions are accompanied by specimen catalog numbers in parentheses (Walker and Leakey 1993a). Specimen number prefixes are KNM-WT 15000. Revised attributions in accordance with Haeusler et al. (2011)

Meyer and Haeusler (2015) argued that spinal canal constriction only would have become symptomatic (and thus pathological) after spinal trauma or spinal degenerations with osteophytes that further narrow the spinal canal. The most notable difference between the spines of KNM-WT 15000 and modern humans would be proportionally longer and more horizontal spinous processes in the former (Latimer and Ward 1993; Carretero et al. 1999; Haeusler et al. 2011; Arlegi et al. 2017).

8.4 *Homo erectus* from Koobi Fora

Securely attributed to one of the more complete skeletons for *H. erectus*, KNM-ER 1808-Z is a partial C1 atlas from Koobi Fora, East Lake Turkana, Kenya dated to 1.7 Ma (Walker et al. 1982; Leakey and Walker 1985; Brown 1995). This fossil preserves the left lateral mass, left articular facets, and a thin anterior arch extending nearly to the midline. The superior articular facet is deeply concave and large, measuring approximately 20 mm in dorsoventral length and 10 mm in transverse width. The inferior articular facet is planar and inclined inferolaterally away from the midline. While the foramen transversarium is not preserved, both roots are preserved and are equal in size, as is the derived condition in humans.

8.5 *Homo* sp. from Ileret

KNM-ER 1825 is a first cervical vertebral fragment from Ileret, East Lake Turkana, Kenya attributed to early *Homo* sp. (Leakey and Walker 1985) and dated to 1.7 Ma (Brown 1995). This fossil preserves the left lateral mass, left transverse process and attendant foramen transversarium, and the left superior and inferior articular facets. The superior articular facet is deeply concave, while the inferior articular facet is large, planar, and generally square in its outline. Like all known hominins, both roots of the foramen transversarium of this vertebra are equal in size, unlike the nonhuman condition where the dorsal root is much thicker dorsoventrally than the anterior root (Meyer and Williams Forthcoming). This vertebra has alternatively been classified as *Paranthropus boisei* (Grausz et al. 1988) based on its recovery from Area 6A below the Ileret Tuff Complex from which several individuals of *Paranthropus* (KNM-ER 801,802, and others) were collected. Nonetheless, in the absence of associated craniodental evidence, we are agnostic with respect to its taxonomic affiliation.

8.6 *Homo naledi* from Rising Star Cave

Vertebrae from this cave system for *H. naledi* include those from the LES1 partial skeleton ("Neo") from the Lesedi Chamber (area 102a) of the Rising Star cave system in South Africa (Hawks et al. 2017) (Fig. 8.3), and an abundance of isolated vertebral fragments from the nearby Dinaledi chamber (Williams et al. 2017) (Fig. 8.4). *H. naledi* has been described as primitive in many respects (Berger et al. 2015; Hawks et al. 2017) including its cranium, body mass, limbs, shoulder and upper limb, hand, and thorax (Kivell et al. 2015; Feuerriegel et al. 2017; Garvin et al. 2017; Laird et al. 2017; Williams et al. 2017). However, Berger et al. (2015) argued that humanlike features of the cranium, hand and wrist, and foot and hind limb (see also Harcourt-Smith et al. 2015; Kivell et al. 2015) justified placing *H. naledi* within the genus *Homo.* Dated to between 236 and 335 ka (Dirks et al. 2017), it is unclear if the taxon represents a late-surviving lineage that diverged from early *Homo* or a diminutive relict population of Middle Pleistocene *Homo*.

Two nearly complete lower thoracic vertebrae (T10 and T11) from the Dinaledi Chamber were recovered in association with a small-bodied adult individual and are among the smallest known in the hominin fossil record (Williams et al. 2017). The T10 presents a single demifacet superiorly at the body–pedicle border and articulates with the T11, which presents a full costal facet at the body–pedicle border and articulates with a preserved 11th rib. Like most modern humans and other Middle Pleistocene hominins, the zygapophyses of the T11 are oriented coronally (thoracic-like), signaling that the penultimate thoracic vertebra is not the transitional vertebra as in all early hominins.

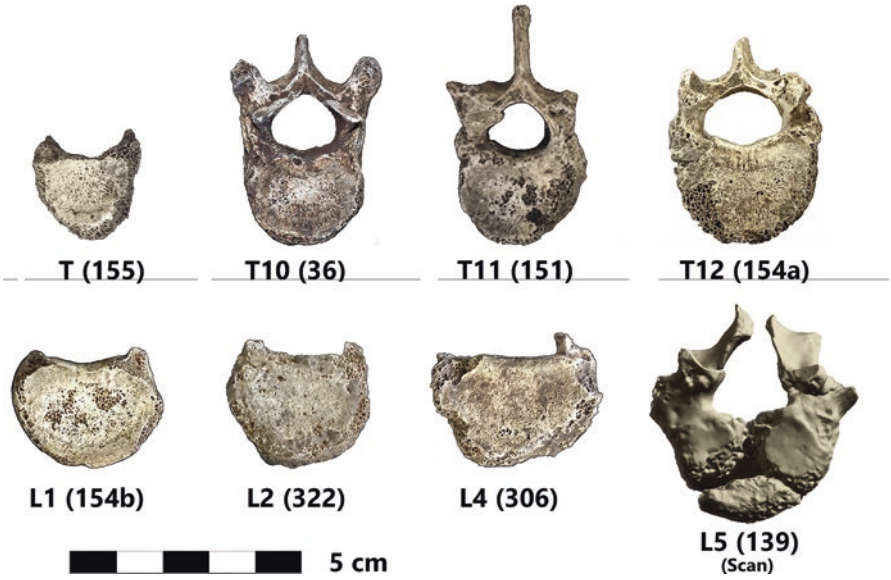

Fig. 8.3 Superior view of most well-preserved fossil vertebrae from the Lesedi Chamber of the Rising Star cave system in South Africa attributed to the LES1 ("Neo") *Homo naledi*. Published vertebral level attributions are accompanied by specimen catalog numbers in parentheses (Hawks et al. 2017). Specimen number prefixes are U.W. 102

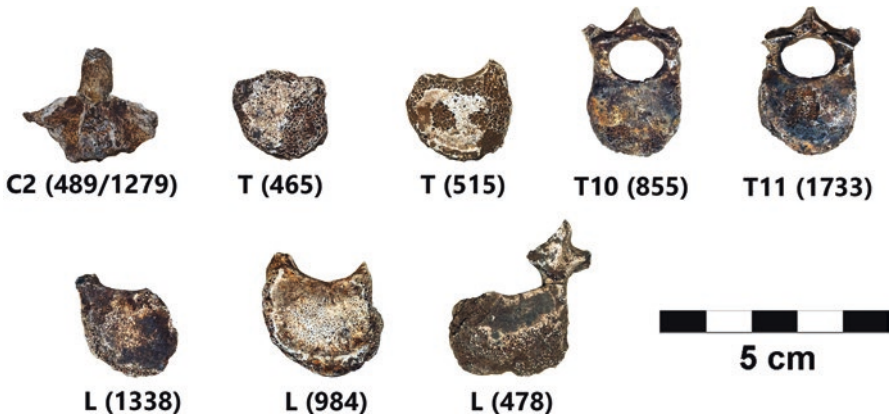

Fig. 8.4 Superior view of most well-preserved fossil vertebrae from the Dinaledi Chamber of the Rising Star cave system in South Africa attributed to *Homo naledi*. Published vertebral level attributions are accompanied by specimen catalog numbers in parentheses (Williams et al. 2017). Specimen number prefixes are U.W. 101

Approximately 30 additional vertebral fragments and 21 probable vertebral fragments were also found from each vertebral region for at least two separate individuals (see Tables S1-S2 in Williams et al. 2017), ranging from the first cervical to a sacrococcygeal vertebrae, which to date have not received detailed analyses.

Williams et al. (2017) note that the lower thoracic vertebrae from the Dinaledi Chamber are some of the most diminutive in the fossil record. A model based on the two adult thoracic vertebrae and long bones from the Dinaledi assemblage produces a stature of 122 cm (previously unpublished) when combined with postcranial dimensions below the 50% mean from the fossil sample (e.g., means method for a putative female, as the *H. naledi* vertebrae are some of the smallest in the fossil record). Our estimate was produced by comparative data from a modern human sample of South Africans ($N = 11$) and African Americans ($N = 63$). We estimated stature via the means method model, standard least squares regression ($R^2 = 0.94$, $p < 0.0001$) on human T11 vertebral body (ventral and dorsal superoinferior heights, superior and inferior transverse and dorsoventral lengths), and appendicular dimensions (superoinferior femur head, transverse and dorsoventral femur midshaft widths, superoinferior humerus head, and transverse talus condyle width). Without vertebral dimensions in their calculations, Garvin et al. (2017) published a larger stature populational estimate for *Homo naledi* at 143.6 cm, similar to that predicted for *H. erectus* from Dmanisi. Estimated mean body weight estimates for *H. naledi* are also near to the Dmanisi hominins, ranging between 37.4 and 44.0 kg (Grabowski et al. 2015; Jungers et al. 2016; Garvin et al. 2017) despite *H. naledi* vertebrae being considerably smaller than those from Dmanisi at every vertebral level (Williams et al. 2017).

There are seven thoracic and lumbar vertebrae of various completeness from the Lesedi Chamber (area 102a) attributed to the LES1 skeleton "Neo" (Hawks et al. 2017). The sequence is nearly uninterrupted from the T10 to the L5 level, with only the L3 missing, although the three most caudal elements (L2, L4, and L5) only preserve vertebral bodies. The transitional vertebra in LES1 is asymmetrical, with the T11 possessing one curved inferior articular facet (lumbar-like with an angle with the midsagittal plane less than 90°) and one flat, coronally oriented facet (thoracic-like). Additional vertebral remains include a mid-thoracic vertebral body, as well as cervical fragments from the C1 and C2 levels.

In both the Dinaledi and Lesedi lower thoracic vertebrae, the pedicles and transverse processes of the T10 and T11 vertebrae are mediolaterally thick, the latter of which are almost directly oriented posteriorly on the parasagittal plane (Hawks et al. 2017; Williams et al. 2017). This unusual configuration forms a nearly continuous line from the pedicles through the transverse processes, which is also a condition approximated in Neandertals (Bastir et al. 2017; Been et al. 2017a).

This morphology appears to reflect a reduction in the size of the epaxial muscles by constricting the space for the muscles that occupy the space between the transverse processes (*Mm. intertransversarii thoracis* and the *Mm. intertransversarii laterales lumborum*) in exchange for an increase in hypaxial musculature (i.e., quadratus lumborum, psoas). This configuration suggests a pattern of trunk stabilization in *H. naledi* dissimilar from other *Homo* taxa and similar in many respects to

Australopithecus. Cumulative evidence from the postcranium appears consistent with this interpretation, such as ilia positioned posteriorly relative to the acetabulum, flared iliac blades, and a broad lower ribcage consistent with orthogrady and an obligate bipedal locomotor regime at variance with that of modern humans (Harcourt-Smith et al. 2015; Throckmorton et al. 2016; Williams et al. 2017; VanSickle et al. 2018).

Despite an endocranial volume for LES1 estimated at 610 mL and an even smaller 460 mL for DH3, each of the vertebrae exhibits a large, transversely ovoid spinal canal in both absolute and relative terms (Hawks et al. 2017; Williams et al. 2017), and as with their larger-brained congenerics, signaling an increased neurovascular capacity relative to the australopith thoracic and lumbar spine (Meyer and Haeusler 2015).

The unusual similarities in the axial skeleton of *H. naledi* and Neandertals are surprising, considering these shared vertebral and thorax features appear in some of the respectively smallest and largest hominins in the fossil record. These similarities may simply reflect homoplasy if the *H. naledi* population represents ancient relict hominin lineage or, more speculatively, represents a case of apomorphy, with the *H. naledi* group representing a population descended from a group of Late to Middle Paleolithic hominins of considerably larger body size.

8.7 *Homo erectus* from Swartkrans

SK 853 is a small subadult lumbar vertebra from the Swartkrans site in South Africa alternatively attributed to *Homo* (Broom and Robinson 1949; Benade 1990; Susman 1993) or *Paranthropus* (McHenry 1994b; Sanders 1998) (Fig. 8.5). This vertebra is nearly complete, with only the right transverse process broken laterally, and a part of the right superior articular process absent. The lack of fused epiphyses and its billowed vertebral body signal its immature status. Because of its differences with the Sts 14 *A. africanus* and its similarity to modern humans in terms of its short, stocky vertebral body and thick spinous process, both Robinson (1972) and Benade (1990) attributed the fossil to *H. erectus.* The vertebral body has a larger cross-sectional surface area than observed in australopiths in absolute and relative terms when compared to overall vertebral body size (geometric mean of six vertebral body dimensions). Robinson placed this specimen at the L1 level, and our observations support Robinson's level and taxonomic designations.

8.8 *Homo floresiensis* from Liang Bua Cave, Flores Island

Brown et al.'s (2004) initial description of the diminutive *H. floresiensis* fossils from Liang Bua Cave on Flores Island, Indonesia, was met with considerable (and oftentimes acrimonious) debate on its taxonomic affinity. The dispute surrounding

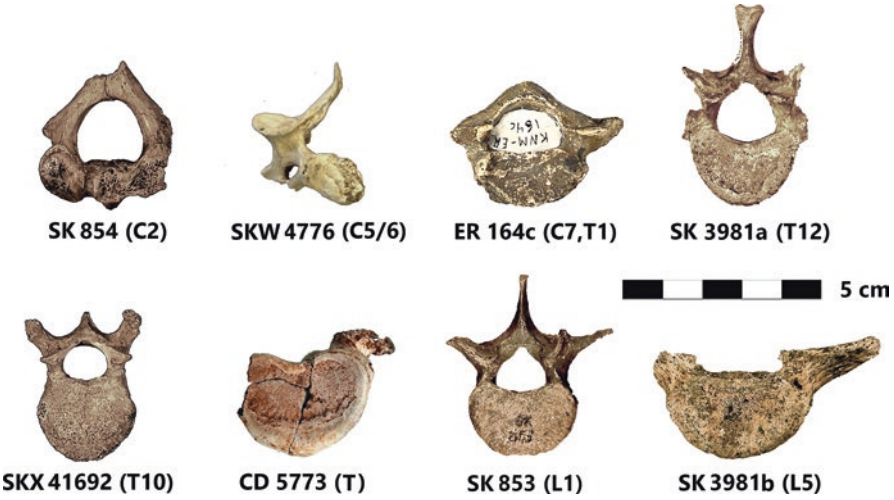

Fig. 8.5 Superior view of early Pleistocene hominin fossil vertebrae with uncertain taxonomic attribution. KNM-ER 164c consists of two articulated vertebrae (C7, T1) and was previously attributed to *Homo erectus* (Day and Leakey 1974) but may represent *Homo sapiens* from an intrusive burial (Alan Walker, personal communication). CD 5775 is modified from de Ruiter et al. (2009) with permission. Specimen catalog numbers are accompanied by vertebral levels

whether the fossils represent a primitive hominin (i.e., Brown et al. 2004; Morwood et al. 2004, 2005; Falk et al. 2005; Groves 2007; Baab and McNulty 2009; Baab et al. 2016); or a pygmoid or pathological modern human (Jacob et al. 2006; Martin 2006; Martin et al. 2006; Hershkovitz et al. 2007; Eckhardt and Henneberg 2010) appears to have settled in recent years. A battery of cladistic tests on cranial, dental, and postcranial characters place *H. floresiensis* as a sister taxon either to *H. habilis* or to a clade consisting of at least *H. habilis* and early Pleistocene *Homo*, including *H. erectus* (Morwood et al. 2005; Argue et al. 2006, 2009, 2017; Baab 2016).

Only one vertebra, LB5/1, an incomplete adult C1 represented by two fragments, has been reported for the taxon (Morwood et al. 2005). The individual LB5 is only further represented by this vertebra and a metacarpal. Other than its announcement, no analysis and no images of this vertebra has been published at present; however, Groves (2007:125) describes fossils discovered subsequent to LB1, including LB5, as "smaller than their counterparts in LB1."

Because some postcranial elements in *H. floresiensis* exhibit unique morphologies not shared with any other known hominin species (e.g., humeral torsion, ulna morphology) which might reflect adaptation to insular island-specific conditions (Groves 2007; Baab 2016), future research on LB5/1 might be directed to examining whether similar vertebral autapomorphies are present in *H. floresiensis*.

8.9 Vertebrae of Uncertain Taxonomic Affinity

The discovery of both *Paranthropus robustus* and *H. erectus* at Swartkrans makes the taxonomic designation of postcranial fossils both difficult and tenuous (Broom and Robinson 1949; Kimbel and Rak 1993; Susman et al. 2001), especially in the case of vertebrae which offer very low phyletic valence. Early workers assigned postcranial fossils to *Homo* if they observed some aspects of "derived" morphology (as in SK 853 above), while fossils exhibiting some "primitive" morphology were assigned to *Paranthropus* (Robinson 1972). Other workers combined morphology with size differences to sort out taxonomic affinities at Swartkrans, with larger and smaller fossils tending to be assigned to *Homo* and *Paranthropus*, respectively (Susman et al. 2001). Confounding the taxonomic attributions based on size is the large degree of sexual dimorphism among Swartkrans hominins, and the overlap between body size between females of both *Paranthropus* and *Homo*, with both estimated at 30 kg (McHenry 1991; Susman et al. 2001). In light of the discovery of similarly sized early *Homo* exhibiting a mosaic of primitive and derived features (i.e., Dmanisi *H. erectus*, *H. naledi*), we suggest a reassessment of some attributions of the vertebral remains (see Fig. 8.5).

Two vertebral specimens that might be reassessed are SK 3981a, an ultimate thoracic vertebra (T12), and SK 3981b, an ultimate lumbar (L5) attributed to *P. robustus* found in two blocks of breccia just outside the cave site having been excavated and discarded by miners in the 1930s (Robinson 1970, 1972). Unfortunately, Robinson's comparative hominin sample in 1970 was limited to the Sts 14 *A. africanus* partial skeleton and had no *H. erectus* specimens to compare with the SK 3981a T12. Moreover, Robinson was unaware of the more cranial position in the transitional vertebra in early hominins when compared to later *Homo* (Haeusler 2002; Williams 2011; Meyer et al. 2015; Ward et al. 2017), and as such, its taxonomic and level ascriptions warrant reappraisal.

The tenuous taxonomic attribution of the SK 3981a and SK 3981b Swartkrans specimens were alluded to by Ward and colleagues but not specifically addressed (Ward et al. 2012). Our unpublished data support Robinson's contention that SK 3981a has a proportionately longer spinous process than most modern humans (but not outside their range) but, as in the genus *Homo*, presents a short transverse process and transversely wider and more robust vertebral body than australopiths. Notwithstanding his attribution to *Paranthropus*, Robinson (1970: 1218) described the vertebral body as more similar to "modern man" than Sts 14, an observation expanded on by Sanders (1998) who saw the vertebral body as more compressed dorsoventrally and consequently has a higher cranial surface shape index than comparable vertebrae in australopiths. Similarly, Meyer and Haeusler (2015) found the cross-sectional area of the SK 3981a spinal canal similar to both modern humans and the KNM-WT 15000 *H. erectus* in absolute and relative size, and well above the range seen in australopiths. Based on these observations, we suggest that this vertebra be provisionally reassigned to *Homo* sp., although future research is needed.

The ultimate lumbar vertebra from Swartkrans SK 3981b should be considered Hominini indet. Sanders (1998) noted that this specimen shares with humans a marked increase in pedicle width and cross-sectional area, unlike the last two lumbar levels in nonhuman apes and australopiths where pedicle widths do not increase caudally. This feature is thought to facilitate loads associated with long distance travel, frequent or sustained running, and lifting and carrying objects associated with *H. erectus* (see discussion below). The neural arch, while incomplete, nonetheless exhibits a broad transverse width as in *Homo* in contrast to nonhuman apes with constricted neural arch widths. Both Robinson (1970) and Sanders (1998) described the transverse process as very long. However, we find its transverse width (measured from the neural arch) of 28.2 mm very close to the human mean of 27.3 mm, and far from the 21.5 mm of the Sts 14 *A. africanus*. Yet Robinson (1970) noted the surface area of the inferior vertebral body as small, indicating a smaller lumbosacral joint area than expected for *Homo*. Wedging angles in the L5 appear to segregate some South African hominins from others (Williams et al. 2013); however, wedging angles based on Digiovanni and colleagues' methodology (Digiovanni et al. 1989) do not help resolve its affinity. With an angle of −3.5°, SK 3981b is close to wedging values in the ultimate lumbar of both Sts 14 and *H. naledi* (U.W. 102–139) with wedging values of −4° and −4.7°, respectively (authors' unpublished data). Our cursory assessment of the morphology of the SK 3981b vertebra places it in an ambiguous taxonomic position. With craniodental remains from Swartkrans indicating the presence of *P. robustus* and early *Homo* at Swartkrans, and new discoveries such as penecontemporaneous *A. sediba* and the later *H. naledi* in close proximity to Swartkrans Cave, a comprehensive taxonomic assessment is justified.

Several other fossil vertebrae that are contemporaneous with the genus *Homo* from South Africa have been attributed to *Paranthropus*, including SK 854, a C2 from the hanging remnant of Member 1 at Swartkrans dated to roughly 1.8 Ma (Fig. 8.5) (Broom and Robinson 1949; Napier 1959). Attributed to *Paranthropus* by Robinson (1972), this specimen exhibits a morphology different from that of the genus *Homo*, *Australopithecus*, and most extant great apes, with a strong ventral crest and projecting anterior tubercle similar to that of bonobos, and appears to signal greater sagittal flexion, perhaps related to climbing (Gommery 2000, 2006). Because this distinct morphology is absent in the genus *Homo*, along with other attributes of the neural canal (Meyer 2005), we do not contest its attribution to *Paranthropus*.

Similarly, SKW 4776 is a fragmentary cervical vertebra from the Lower Bank of Member 1 at Swartkrans (Fig. 8.5), which has been attributed to *Paranthropus* (Susman 1989, 1993). Originally seriated to the C3 level, we reposition it caudally, perhaps to the C5 level, although further investigation is warranted. However, we find no reason at present to dispute its taxonomic designation, as the vertebral body is ventrally eccentric as in *Pan* and some australopiths, and unlike the dorsally eccentric cervical vertebral body of *Homo* (Meyer 2016a). Moreover, most craniodental fossils (96%) in this deposit are paranthropine, and those that have been attributed to *Homo* from Swartkrans consist largely of fragments and isolated teeth,

which has led to considerable controversy regarding their taxonomic affinities (Grine 1988; Brain 1993; Grine 2005; Pickering et al. 2011).

SKX 3342 is the right half of an adult middle thoracic vertebral body (T6–T9) recovered from Member 2 of Swartkrans (Susman 1988). The vertebral body features a well-preserved costal demifacet superiorly and a faint costal demifacet inferiorly. Both the superior and inferior epiphyseal plates are fused. This fossil also preserves a small remnant of the right pedicle. This vertebra is described as being similar in size to its mid-thoracic counterpart in the Sts 14 *A. africanus* vertebral column, and considerably smaller than that of modern humans. While Susman (1988) denotes its taxonomic attribution as uncertain, the deposit from which this vertebral fragment was recovered contains mostly craniodental remains from *Homo*. Member 2 also preserves manual and pedal fragments with "humanlike" characteristics except for their extreme degree of curvature (Susman 1988). In light of new discoveries where small vertebrae are associated with a high degree of metacarpal curvature in the genus *Homo* (Berger et al. 2015; Kivell et al. 2015), we suggest a reappraisal of this fossil in the future.

SKX 41692 is a presumed *P. robustus* T10 vertebra from Swartkrans (Susman 1989) and is largely complete except for bone attrition on the vertebral body surface. The planiform articular facets superiorly and inferiorly indicate that this fossil is not the transitional vertebra. This vertebra possesses marked posterior orientation of the transverse processes that is unique among australopiths, but also observed in *H. naledi* (Hawks et al. 2017; Williams et al. 2017). Another difference between SKX 41692 and *H. naledi* and other members of the genus *Homo* is its relatively small neural foramen in relation to its vertebral body, suggesting it is not best assigned to the genus *Homo*; however, more research is needed.

Lastly, CD 5773 is a lower thoracic vertebra (T10-T12) attributed to *Paranthropus robustus* from Cooper's Cave, South Africa (Fig. 8.5). This specimen consists of an essentially complete vertebral body and the preserved left pedicle (de Ruiter et al. 2009). We find no particular reason to justify de Ruiter and colleagues' attribution of this specimen to Hominidae gen. et sp. indet. and suggest that it likely represents the same taxon as the dental remains of *P. robustus* found in close proximity to Cooper's Cave.

8.10 *Homo erectus* from Koobi Fora?

The KNM-ER 164c fossil originally attributed to *Homo* sp. indet. was discovered in 1969 in Area 104 at Koobi Fora, consisting of two consecutive adult vertebrae from the C7 and T1 levels (Day and Leakey 1974; Leakey and Leakey 1978) (Fig. 8.5). The vertebrae were described as Plio-Pleistocene in age; although because they were found at least 15 meters above the post-KBS erosional surface, KNM-ER 164C must be younger than 1.8 Ma (Findlater 1978). Heavily damaged and fused

together by matrix, these two vertebrae preserve aspects of both vertebral bodies, laminae and spinal canal. The fusion of these two elements is not pathological; rather it is clear that they were too fragile to separate them manually, so not all matrix was removed. The vertebrae were later attributed to *H. erectus*, but are only briefly mentioned in literature, because as Latimer and Ward (1993) point out, the fossil is too poorly preserved for use in comparative analyses. The fossils' preserved spinal canal falls within modern human values for absolute and relative size (Meyer 2003, 2005). This specimen likely comes from an intrusive modern human burial (Alan Walker, personal communication to MRM). Although the Koobi Fora team has not published the details for this correction, the likely intrusive nature of KNM-ER 164c has previously been reported in the literature (Meyer 2005; Meyer and Haeusler, 2014; Meyer and Haeusler 2015). In short, KNM-ER 164c appears to be an intrusive specimen and should no longer be attributed to *H. erectus*. Further research into the morphology and taxonomic affinity of this specimen is warranted.

8.11 Vertebral Numbers

Robinson's (1972) interpretation of the Sts 14 (*A. africanus*) thoracolumbar vertebral column began a long line of researchers inferring that early hominins possessed six lumbar vertebrae (Robinson 1972; Shapiro and Simons 2002; Lovejoy 2005a; Whitcome et al. 2007). The spine of early *Homo* was no exception. Based on the nearly parasagittal orientation of the superior articular facets (prezygapophysis) of the ultimate thoracic element, most researchers classified it as a lumbar vertebra. Subsequently, researchers have found evidence that early hominins, including the KNM-WT 15000 *H. erectus*, did not differ from modern humans in having 12 thoracic and five lumbar vertebrae, finding that previous reconstructions had missed the presence of costal facets on fossil specimens, and erroneously relied on the nearly parasagittal prezygapophysis orientation as the defining feature of lumbars (Haeusler 2002, 2011; Williams 2012; Tardieu et al. 2013).

However, this strict zygapophyseal criterion is problematic, since in large percentages of humans the last rib-bearing vertebra is not transitional in facet orientation, but rather the transition from the coronally oriented thoracic facets to the parasagittally oriented lumbar facets is shifted cranially to the T11, and in roughly half of humans, the transition is gradual, spanning several elements (Singer et al. 1988; Williams 2011, 2012; Williams et al. 2017). The former condition appears to be the norm in nearly all early hominins, and the T12 vertebrae in these taxa are rib-bearing despite having lumbar-like zygapophyses (Haeusler 2002, 2011; Meyer et al. 2015; Ward et al. 2017; Williams et al. 2017). Thus, early *Homo* did not differ from modern humans in the modal configuration of the vertebral column with twelve thoracic and five lumbar vertebrae.

8.12 Spinal Cord

The brain and spinal cord are both larger in humans than those of the African great apes. Since body and brain size exhibit strong covariance, increases in body size in *Homo* may have been a by-product of selection for larger brains (Grabowski 2016). Yet recent discoveries suggest that an independent increase in the size of the hominin spinal cord appears to antedate the advent of both body and brain size, and may have been independently selected for (Meyer 2016b). Evidence for this comes from the large-bodied KSD-VP-1/1 *A. afarensis* partial skeleton from Woranso-Mille, Ethiopia, which features a humanlike cervical spinal canal that is enlarged (especially transversely) relative to nonhuman apes, suggesting that hominin cervical spinal cord enlargement was completed by at least 3.6 million years ago (Meyer 2016a).

This increase in spinal cord size is apparently retained in members of the genus *Homo* in the early Pleistocene, despite initial reports of the KNM-WT 15000 *Homo erectus* skeleton from Nariokotome having a small, *Pan*-sized spinal canal (Brown et al. 1985; MacLarnon 1993; Walker and Leakey 1993a). The discovery of additional vertebrae for *H. erectus* at Dmanisi (Meyer 2005) and a careful reanalysis of the Nariokotome vertebrae revealed that the absolute and relative size of the vertebral foramina in all of the Dmanisi fossils and most of the KNM-WT 15000 vertebrae were within the human range of variation (Meyer and Haeusler 2014, 2015). Only the vertebral foramina of C7, T2, and T3 in the KNM-WT 15000 column appear constricted, but rather than retaining the primitive *Pan*-like condition, these vertebrae appear to exhibit spinal stenosis (Latimer and Ohman 2001), a pathology often associated with childhood malnutrition, or physical trauma (Clark et al. 1985; Papp et al. 1997; Cantu 1998; Meyer 2005). Meyer and Haeusler (2015) argued that this constriction would only have become symptomatic (and thus pathological) after spinal trauma or spinal degenerations with osteophytes that further narrow the spinal canal, but the "constriction" in KNM-WT 15000 is not associated with physical trauma and probably also not with childhood malnutrition (for which there is absolutely no evidence).

Thus, evidence from the Dmanisi spinal canal dated to 1.77 Ma and the unaffected levels of KNM-WT 15000 dated to 1.5 Ma suggest that like subsequent larger-brained taxa such as *H. antecessor*, European Middle Pleistocene hominins from Sima de los Huesos, and Neandertals (Gómez-Olivencia 2005; Gómez-Olivencia et al. 2007), *H. erectus* possessed a postcranial neurological endowment at minimum that was at least intermediate to *Pan* and *H. sapiens*, but clearly within the lower range of modern humans. Relatively large spinal canals are also observed in *H. naledi* (Hawks et al. 2017; Williams et al. 2017), but not australopiths such as the MH1 *A. sediba* (Meyer et al. 2017). The increase in cervical spinal cord dimensions in the genus *Homo* from the early Pleistocene would augment the neurological capacity for fine-motor coordination of the arm and hand, affording the anatomical potential for accurate throwing and precision toolmaking (Meyer 2016a; Meyer and Haile-Selassie 2016). Increases in lower thoracic, lumbar, and sacral spinal canals

also allow for the proportionately large spinal nerve roots of humans thought to associate with high demands for control of the lower limbs during bipedalism (Sanders and Bodenbender 1994). Likewise, the expanded lumbar spinal canal in *Homo* allows for the enlarged internal venous plexus of humans, facilitating the high vascular demands of extended bouts of orthogrady and bipedal locomotion (MacLarnon 1993; Plaisant et al. 1996). Transversely, wider spinal canals in *Homo* also have the effect of widening lumbar interfacet distances, increasing the base of support and passively conferring greater stability in orthograde posture (Meyer 2005). In addition, caudad expansion of the lumbar spinal canals engender a pyramidal pattern of articular facet spacing, allowing for the imbrication of the posterior elements of adjacent vertebrae necessary for lumbar lordosis (Latimer and Ward 1993). In short, the increased spinal canal dimensions would confer early Pleistocene *Homo* neurological, structural, and vascular advantages over *Pan* and *Australopithecus*, providing the anatomical underpinnings for toolmaking, accurate throwing, and distance running.

8.13 Spinal Curvature

The accentuated series of spinal curvatures in humans is the product of vertebral body and intervertebral disc wedging, which provides balance and stability in erect posture while permitting torque equilibrium between spinal segments (Gracovetsky et al. 1987; Wagner et al. 2012; Castillo et al. 2017). Because intervertebral discs do not preserve, paleoanthropologists must exclusively rely on osseous remains in the reconstruction of hominin spinal curvature. Based on wedging angles of the caudalmost lumbar vertebra, vertebral bodies, and broad sacral ala (which free the most caudal lumbars from the "trapping" effect of narrow sacra that confer lower trunk rigidity during suspension), it has long been posited that both australopithecines and early *Homo* possessed the well-developed lumbar lordosis of humans (Robinson 1972; Latimer and Ward 1993; Sanders 1998; Lovejoy 2005a, 2005b, 2007; Meyer 2005; Whitcome et al. 2007; Williams et al. 2013).

The KNM-WT 15000 *H. erectus* features a well-developed lumbar lordosis and thoracic kyphosis described as humanlike in terms of morphology and function at 1.5 Ma (Latimer and Ward 1993; Walker and Leakey 1993a). A similar condition in the 1.77 Ma Dmanisi *H. erectus* is suggested by the D2672 L2 vertebra from Dmanisi, including features such as strong posterior lamina fossae (Meyer 2005), also known as imbrication pockets (Lovejoy 2005a), that are the direct result of mechanical deformation on the laminae from the suprajacent inferior articular facets in habitual lordosis. Posterior lamina fossae may be thought of as analogs of "squatting facets" on the tibia and talus, indicating a specific habitual postural behavior, or in the case of lumbar vertebrae, indicating the presence of lordosis. Additional evidence for lordosis comes from the inferior articular facets of the D2672 vertebra, which are inclined posteriorly relative to the transverse plane of the

superior vertebral body epiphyseal surface as in humans, in contrast to their craniocaudal orientation in chimpanzees and gorillas.

Been et al. (2012) reconstructed spinal curvature based on the correlation between two morphological parameters of the lumbar vertebrae and lumbar lordosis: vertebral wedging and the orientation of the post-zygapophyses with respect to the superior surface of the vertebral body, as well as by way of the relationship between the orientation of the foramen magnum and cervical lordosis. This method accords with clinical data showing that any surgical alteration in one region of spinal curvature incurs reciprocal compensation in another to preserve stable sagittal balance of the trunk above the hip joints (Lafage et al. 2012; Oh et al. 2015). Using this method, Been et al. (2017b) estimate the degree of spinal curvature in *H. erectus* and *H. sapiens* to be very similar, with both groups featuring accentuated sinusoidal spinal curvatures while australopiths, Neandertals, and the Sima de los Huesos hominins did not, implying that the latter group employed a somewhat different mode in maintaining the line of gravity above the acetabulum (Been et al. 2010, 2017a; Bonmatí et al. 2010; Arsuaga et al. 2015; Gómez-Olivencia et al. 2017). Been et al. (2017a) hypothesized that australopiths featured less cervical lordosis, but a similar degree to modern humans in terms of lumbar lordosis, while based on evidence from pelvic incidence and the angle of the inferior articular process, Neandertals and the Sima de los Huesos hominins possessed reduced spinal curvatures overall. Given past debates on the modal number of lumbar vertebrae in australopiths and early *Homo* (i.e., five or six), it is important to note that variation in the number of lumbar vertebrae has no effect on the lordosis angle in modern humans (Whitcome 2012).

Another method for reconstructing spinal curvature in extinct hominins is based on a chain of known correlations between lumbar vertebrae morphology, lumbar lordosis, and pelvic incidence (the orientation of the basis ossis sacralis in relation to the acetabulum) in modern humans (Duval-Beaupere et al. 1992; Tardieu et al. 2006, 2017; Been et al. 2014, 2017b; Yilgor et al. 2017). Data from *H. erectus* produced a lumbar lordosis angle ranging between 45° and 47°, with similar lordosis angles in australopiths (A.L. 288-1, Sts 14, StW 431, Sts 14, MH2) ranging between 36° and 45° (Been et al. 2014). While the MH2 fossil presents the lowest value in the latter group, a new reconstruction of the MH2 pelvis suggests that its incidence angle has been much more humanlike than previously appreciated (Fornai and Haeusler 2016; Haeusler et al. 2016), which would translate into a more human lordosis angle (see also Williams et al. 2013, 2018). This brings both the australopithecine and early *Homo* predicted lordosis values well within fossil and modern human values (mean 51°, with ranges of 49°–51° and 32°–78°, respectively). Similar mean values were found by Tardieu et al. (2013) in the angle of sacral incidence of the Gona pelvis and in the australopiths A.L. 288-1 and Sts 14, which would predict humanlike degrees of lordosis in these individuals. Similar values obtained for the male KNM-WT 15000 and female Gona fossil offer a preliminary indication that the angle of incidence in *H. erectus* is not sexually dimorphic, as is also the case in humans (Tardieu et al. 2013). Thus, all available evidence currently suggests that a humanlike lordosis and overall degree of spinal curvature was present in early *H. erectus*.

8.14 Vertebrae and Locomotion

The apparent stasis in australopith postcranial form has prompted hypotheses suggesting stabilizing selection for the retention of some primitive, arboreal features (Ward 2002), while other lines of evidence from the lower limb and foot have led to proposals that *H. erectus* was more specialized for distance locomotion than its antecedents (Bramble and Lieberman 2004; Lieberman et al. 2006; Rolian et al. 2009; Ward 2013). Carrier (1984) hypothesized that distance running emerged in *H. erectus* with the advent of a new behavioral niche, persistence hunting (or scavenging, see Pickering and Bunn 2007), where subsistence depended on the biological capacity for distance running. This was later proposed to explain in several skeletal modification in *Homo* that are unique among primates (summarized in Bramble 2000; Bramble and Lieberman 2004). These features include marked postcranial robusticity (Trinkaus 1983), which can be a response to fatigue stress (Lanyon 1982) promoted by activities such as endurance running (Trinkaus 1987).

Changes to the lumbar and cervical spinal column also support hypotheses surrounding the advent of distance running in *Homo erectus*. Lumbar vertebral body size is largely independent of body mass in terrestrial mammals after taking phylogeny into account, suggesting that these elements offer utility in morpho-functional analyses (Álvarez et al. 2013) and allow for locomotor inferences in fossil taxa with minimal bias for body size. Relatively enlarged lumbar vertebral body epiphyses (compared to the geometric mean of multiple linear vertebral dimensions) are commonplace among cursorial mammals, offering resistance to ground reaction forces incumbent to running (Cartmill and Brown 2013, 2014, 2017). Unlike their *Australopithecus* predecessors, *H. erectus* at Dmanisi and Nariokotome feature these enlarged lumbar epiphysis surfaces (Latimer and Ward 1993; Meyer 2005, 2008) and, accompanied with other increased postcranial joint surfaces are thought to enhance cursorial behaviors (Jungers 1988; Bramble and Lieberman 2004; Meyer 2005, 2008; Cartmill and Brown 2017). Although Schiess and Haeusler (2013) suggest that epiphyses in the Nariokotome vertebrae are somewhat smaller than in modern humans, in contrast to *H. erectus*, the surprisingly small lumbar vertebrae of australopiths are not well-suited for the dynamic vertical loads incurred during extended bouts of running (Meyer 2008; Cartmill and Brown 2013). However, the australopith vertebral column appears to have been underprepared for the transmission of heavy vertical loads incumbent to bipedality, and as a result, they appear to have suffered unusually high frequencies of vertebral body pathology (Cook et al. 1983; Meyer 2016a). Bipedal locomotion engenders a unique set of loading demands on the spine (Schultz 1961; Williams and Russo 2015), which apparently frequently manifests in the form of spinal pathologies that are virtually unknown in knuckle-walking apes (Lovell 1990; Gunji et al. 2003; Latimer 2005; Lovejoy 2005a; Hernandez et al. 2009).

In addition to enhanced mitigation of loads, larger vertebral epiphyseal areas also augment energy return from ground reaction forces during running through larger intervertebral discs. Efficient human running exchanges kinetic and potential energy

through a mass-spring mechanism in the legs, as elastic strain energy stored in collagen-rich tendons and ligaments releases energy through recoil during propulsion (Cavagna et al. 1976; Ker et al. 1987). Similarly, the spine provides additional energy return through the intervertebral discs which are composed of alternate layers of collagen fibers exhibiting viscoelastic properties that respond to an applied load (Gracovetsky and Iacono 1987). Intervertebral discs offer energy return from spinal rotations (axial torque) mandated by the contralateral movement of the pelvis and shoulders in bipedality (Gracovetsky and Iacono 1987), and may help return energy from the marked vertical displacements of the center of mass due to the bouncing gait incumbent to bipedal running (Cavagna et al. 1976).

The cervical vertebrae of early Pleistocene *Homo* present corroborating anatomical evidence for the advent of distance running. Like humans, short cervical spinous processes in the Dmanisi *H. erectus* would have resulted in a physiological "void" unoccupied by the large trapezius, splenius capitis, and rhomboid muscles of the African great apes (Meyer 2005). Reduction of these muscles in humans results in a thin dorsal raphe and a fascial septum of dense connective tissue running from the midline ventrally to the interspinous ligaments between the spinous processes (Mercer and Bogduk 2003). This elastic ligamentous band, the nuchal ligament, is an important character in cursorial mammals functioning to passively maintain head stability during distance running (Bianchi 1989; Bramble 2000). The nuchal ligament connects the C7 vertebra to the inferior aspect of the cranium, resulting in an everted median nuchal line on the occipital. Since both *Pan* and *Australopithecus* possess relatively long cervical spinous processes and lack an everted median nuchal line on the basicranium, it appears that the nuchal ligament was absent in the hominin lineage until these features appear in concert in *H. erectus* (Bramble 2000; Meyer 2005, 2008, 2016a; Lieberman et al. 2006, 2007; Lieberman 2011). Weakening the running hypothesis is evidence from Vallois (1926) who showed that the nuchal ligament also evolved in carnivores and large ungulates not known to be long-distance runners (i.e., the giraffe) and work by Bianchi (1989) demonstrating that nuchal ligament strength relates to body size in ruminants with no apparent relationship to cursorial behavior. However, compared with large ungulates, the relatively small body and head masses in early Pleistocene *Homo* argue for the near exclusivity of a nuchal ligament among primates for functional reasons other than static head support.

Short spinous processes may also promote wider degrees of motion through avoidance of mechanical interference otherwise unavoidable with longer spinous processes (Gambaryan 1974; Salesa et al. 2008). Several studies have hypothesized that with short cervical spinous processes and shallow subaxial uncinate processes, cervical anatomy in the genus *Homo* gained flexibility and relinquished a set of musculoskeletal constraints coupling the head and neck with the torso (Ward 2002; Bramble and Lieberman 2004; Meyer 2005, 2008; Meyer et al. 2018). In this model, *Homo naledi* appears to share the derived axial bauplan and lower limb morphology of early *Homo* for distance running, but its elevated shoulder and broad lower thorax suggest that this taxon was not adapted to efficient long-distance locomotion (Williams et al. 2017). By contrast, the vertebral column of early *Homo* by 1.8 Ma

apparently presents a derived combination of features, along with other postcranial regions, promoting efficient bipedal running not observed in earlier hominin species or in *H. naledi* from the Middle Pleistocene.

8.15 Out of Africa

It is generally accepted that a form of early *Homo* represented the initial hominin movement from Africa, and the consensus view is that a more modern body shape and an efficient striding gait were compulsory for traveling long distances (Gabunia et al. 1988; Antón 2003; Gabunia and Vekua 1995; Zhu et al. 2008; Pontzer et al. 2010; Antón et al. 2014; van den Bergh et al. 2016; Argue et al. 2017). Because the postcranium of *H. erectus* appears to be the first hominin to fully accord with this expectation, it has been the likely candidate for expansion from the ancestral continent, although the presence of the primitive hominin *H. floresiensis* in Indonesia has suggested that a more primitive taxon cannot be ruled out (Morwood and Jungers 2009; Argue et al. 2009, 2017; Dembo et al. 2015). Supporting this latter hypothesis is relative leg length in *H. habilis* (i.e., OH 35, OH 62) which appears humanlike, despite the ape-like upper-to-lower arm proportions (Haeusler and McHenry 2004, 2007). On the other hand, the discovery of *H. floresiensis* with its surprisingly short legs and primitive body shape (Brown et al. 2004; Holliday and Franciscus 2009) opens the possibility that a modern body shape and long legs were not necessary for dispersal out of Africa.

Notwithstanding, if leg length and body shape provide the biological underpinnings for efficient bipedal locomotion, equally important for the hominin expansion out of Africa would be the capacity for the axial skeleton to bear high magnitudes of compressive loading incumbent to endurant bipedal locomotion, especially among gravid females and in the transportation of infants (Meyer 2005, 2008). While no vertebrae are known for *H. habilis*, the vertebral column in both the D2700 and KNM-WT 15000 *H. erectus* partial skeletons reveals an aggregate morphology better suited to resist vertical compression (Latimer and Ward 1993), load bearing, and distance travel than australopithecines (Bramble and Lieberman 2004; Meyer 2005, 2008). This is consistent with other postcranial evidence suggesting that load bearing increased in *Homo erectus* relative to the australopithecines (Wang et al. 2002; Wang and Crompton 2004; cf. Preuschoft 2004).

Like the knuckle-walking apes, australopithecines had relatively tall but small vertebral bodies (especially with respect to dorsoventral length) compared to structures of the neural arch (articular facets, laminae, pedicles) and were predisposed to channel proportionately greater forces through these dorsal structures than through the vertebral body (Sanders 1990, 1995; Shapiro 1991, 1993). Unlike humans, where the majority of loads are accommodated by the vertebral body (Pal and Routal 1986), this configuration left australopiths unprepared for the higher magnitudes of vertebral body loading incumbent to bipedality, resulting in an unusually high rate of thoracolumbar vertebral body pathologies (Cook et al. 1983; Latimer 2005; Meyer 2005, 2016b; de Ruiter et al. 2009). By contrast, the vertebral column

of early Pleistocene *Homo* reveals a relative reduction in the craniocaudal height of the vertebral bodies relative to the African great apes, which decreases bending moments but increases stability, explaining its predominance among primates with a more terrestrial adaptation than their more arboreal counterparts (Ward 1993; Mazelis 2014; Williams and Russo 2015).

Axial stability in terrestrial locomotion is of foremost importance with increasing body size, and the vertebral column of large mammals typically tends to be more rigid in order to support their body mass (Galis et al. 2014; Jones 2015). However, spinal rigidity tends to limit their locomotor repertoire and is typically not seen in fast-running taxa (Slijper 1946; Gambaryan 1974; Hildebrand 1974; Schilling and Hackert 2006; Galis et al. 2014). Despite the fact that humans are not particularly fast runners, as a relatively large-bodied primate, *Homo* is exceptional in that the spine offers increased flexibility relative to their putative *Australopithecus* ancestors and the African great apes (Meyer 2012; Meyer et al. 2018). The spine of australopiths, however, appears to have lacked the flexibility and load-carrying capacity of early Pleistocene *Homo*, and their more primitive configuration was apparently overburdened by the higher magnitudes of longitudinal loads incurred with obligate terrestrial bipedality. But the axiom that "behavior precedes biology" applies here, as ventral pillar (i.e., vertebral body) pathology in *Australopithecus* is common, and especially severe in small-bodied females such as A.L. 288 and Sts 14, begging the question of whether this liability most keenly affected females burdened with carrying their infants both in utero and postnatally and reduced their ranging behaviors (Meyer 2005). After all, such is the case in *Pan* females (Pontzer and Wrangham 2004).

To offset extra loading patterns inherent to gravidity (Griffin and Price 2000; Sabino and Grauer 2008; Vermani et al. 2010), parturient human females possess specialized vertebral features, including more horizontally and ventrally oriented transverse processes and greater lumbar lordosis (Whitcome et al. 2007; Bastir et al. 2014). While future fossil discoveries will be needed to test this hypothesis, it may be that without this suite of features, combined with the enhanced load-bearing capacity derived in the vertebral column of *Homo*, our *Australopithecus* ancestors may have been bound to the ancestral continent (Meyer 2005).

Acknowledgements The authors would like to thank Ella Been and Asier Gómez for taking the lead in organizing this volume and for their dedicated editorial assistance. We would also like to express our gratitude to two anonymous reviewers for their superb insights in improving an earlier draft of this chapter.

References

Aiello LC, Dean C (1990) An introduction to human evolutionary anatomy. Academic Press, London

Aiello LC, Wells JCK (2002) Energetics and the evolution of the genus *Homo*. Annu Rev Anthropol 31:323–338

Aiello LC, Wheeler P (1995) The expensive–tissue hypothesis: the brain and the digestive system. Curr Anthropol 36:199–221

Álvarez A, Ercoli MD, Prevosti FJ (2013) Locomotion in some small to medium–sized mammals: a geometric morphometric analysis of the penultimate lumbar vertebra, pelvis and hindlimbs. Zoology 116:356–371

Antón SC (2003) Natural history of *Homo erectus*. Am J Phys Anthropol 122(S37):126–170

Antón SC, Potts R, Aiello LC (2014) Evolution of early *Homo*: an integrated biological perspective. Science 345:6192

Argue D, Donlon D, Groves C, Wright R (2006) *Homo floresiensis*: microcephalic, pygmoid, *Australopithecus*, or *Homo*? J Hum Evol 51(4):360–374

Argue D, Morwood MJ, Sutikna T, Jatmiko, Saptomo EW (2009) *Homo floresiensis*: a cladistic analysis. J Hum Evol 57(5):623–639

Argue D, Groves CP, Lee MSY, Jungers WL (2017) The affinities of *Homo floresiensis* based on phylogenetic analyses of cranial, dental, and postcranial characters. J Hum Evol 107:107–133

Arlegi M, Gómez-Olivencia A, Albessard L, Martínez I, Balzeau A, Arsuaga JL, Been E (2017) The role of allometry and posture in the evolution of the hominin subaxial cervical spine. J Hum Evol 104:80–99

Arsuaga JL, Carretero JM, Lorenzo C, Gómez-Olivencia A, Pablos A, Rodriguez L, Garcia-González R, Bonmatí A, Quam RM, Pantoja-Pérez A, Martínez I, Aranburu A, Gracia-Téllez A, Poza-Rey E, Sala N, García N, Alcazar de Velasco A, Cuenca-Bescós G, Bermúdez de Castro JM, Carbonell E (2015) Postcranial morphology of the middle Pleistocene humans from Sima de los Huesos, Spain. Proc Natl Acad Sci USA 112(37):11524–11529

Baab KL (2016) The place of *Homo floresiensis* in human evolution. J Anthropol Sci 94:5–18

Baab KL, McNulty KP (2009) Size, shape, and asymmetry in fossil hominins: the status of the LB1 cranium based on 3D morphometric analyses. J Hum Evol 57(5):608–622

Baab KL, Brown P, Falk D, Richtsmeier JT, Hildebolt CF, Smith K, Jungers W (2016) A critical evaluation of the down syndrome diagnosis for LB1, type specimen of *Homo floresiensis*. PLoS One 11(6):e0155731

Barak MM, Lieberman DE, Raichlen D, Pontzer H, Warrener AG, Hublin JJ (2013) Trabecular evidence for a human–like gait in *Australopithecus africanus*. PLoS One 8:e77687

Bastir M, Higuero A, Ríos L, García Martínez D (2014) Three-dimensional analysis of sexual dimorphism in human thoracic vertebrae: implications for the respiratory system and spine morphology. Am J Phys Anthropol 155:513–521

Bastir M, García Martínez D, Rios L, Higuero A, Barash A, Martelli S, García Tabernero A, Estalrrich A, Huguet R, De La Rasilla M, Rosas A (2017) Three-dimensional morphometrics of thoracic vertebrae in Neandertals and the fossil evidence from El Sidrón (Asturias, northern Spain). J Hum Evol 108:47–61

Been E, Peleg S, Marom A, Barash A (2010) Morphology and function of the lumbar spine of the Kebara 2 Neandertal. Am J Phys Anthropol 142:549–557

Been E, Gómez-Olivencia A, Kramer PA (2012) Lumbar lordosis of extinct hominins. Am J Phys Anthropol 147:64–77

Been E, Gómez-Olivencia A, Kramer PA (2014) Lumbar lordosis in extinct hominins: implications of the pelvic incidence. Am J Phys Anthropol 154:307–314

Been E, Gómez-Olivencia A, Kramer PA, Barash A (2017a) 3D reconstruction of spinal posture of the Kebara 2 Neanderthal. In: Marom A, Hovers E (eds) Human paleontology and prehistory contributions in honor of Yoel Rak. Springer, New York, pp 239–251

Been E, Gómez-Olivencia A, Shefi S, Soudack M, Bastir M, Barash A (2017b) Evolution of spino-pelvic alignment in hominins. Anat Rec 300:900–911

Benade MM (1990) Thoracic and lumbar vertebrae of African hominids ancient and recent: morphological and functional aspects with special reference to upright posture. University of the Witwatersrand, Johannesburg

Berger LR, Hawks J, de Ruiter DJ, Churchill SE, Schmid P, Delezene LK, Kivell TL, Garvin HM, Williams SA, DeSilva JM, Skinner MM, Musiba CM, Cameron N, Holliday TW, Harcourt-

Smith W, Ackermann RR, Bastir M, Bogin B, Bolter D, Brophy J, Cofran ZD, Congdon KA, Deane AS, Dembo M, Drapeau M, Elliott MC, Feuerriegel EM, García-Martínez D, Green DJ, Gurtov A, Irish JD, Kruger A, Laird MF, Marchi D, Meyer MR, Nalla S, Negash EW, Orr CM, Radovcic D, Schroeder L, Scott JE, Throckmorton Z, Tocheri MW, van Sickle C, Walker CS, Wei P, Zipfel B (2015) *Homo naledi*, a new species of the genus *Homo* from the Dinaledi chamber, South Africa. elife 4:e09560. https://doi.org/10.7554/eLife.09560

Bianchi MS (1989) The thickness, shape and arrangement of the elastic fibres within the nuchal ligament from various animal species. Anat Anz 169:53–66

Bonmatí A, Gómez-Olivencia A, Arsuaga JL, Carretero JM, Gracia A, Martínez I, Lorenzo C, Bermúdez de Castro JM, Carbonell E (2010) Middle Pleistocene lower back and pelvis from an aged human individual from the Sima de los Huesos site, Spain. Proc Natl Acad Sci U S A 107(43):18386–18391

Brain CK (1993) Swartkrans: a cave's chronicle of early man. Transvaal Museum, Pretoria

Bramble DM (2000) Head stabilization in human running: implications for hominid evolution. Am J Phys Anthropol 30(S41):111

Bramble DM, Lieberman DE (2004) Endurance running and the evolution of *Homo*. Nature 432:345–352

Broom R, Robinson JT (1949) A new type of fossil man. Nature 164:322–323

Brown F (1995) Development of Pliocene and Pleistocene chronology in the Turkana Basin, East Africa and its relation to other sites. In: Corruchini RS, Ciochon RL (eds) Integrative paths to the past: paleoanthropological advances in honor of F. Clark Howell. Prentice Hall, Englewood Cliffs, pp 285–312

Brown F, Harris J, Leakey R, Walker A (1985) Early *Homo erectus* skeleton from West Lake Turkana, Kenya. Nature 316:788–792

Brown P, Sutikna T, Morwood MJ, Soejono RP, Jatmiko WS, Due R (2004) A new small-bodied hominin from the late Pleistocene of Flores, Indonesia. Nature 431:1055–1061

Cantu RC (1998) The cervical spinal stenosis controversy. Clin Sports Med 17:121–126

Carretero JM, Lorenzo C, Arsuaga JL (1999) Axial and appendicular skeleton of *Homo antecessor*. J Hum Evol 37:459–499

Carrier DR (1984) The energetic paradox of human running and hominid evolution. Curr Anthropol 25:483–495

Cartmill M, Brown K (2013) The relative effects of locomotion and posture on vertebral scaling. Am J Phys Anthropol 150(S54):95

Cartmill M, Brown K (2014) Vertebral body area profiles in primates and other mammals. Am J Phys Anthropol 153(S55):91

Cartmill M, Brown K (2017) Posture, locomotion and bipedality: the case of the gerenuk (*Litocranius walleri*). In: Marom A, Hovers E (eds) Human paleontology and prehistory: contributions in honor of Yoel Rak. Springer, New York, pp 53–70

Castillo ER, Hsu C, Mair RW, Lieberman DE (2017) Testing biomechanical models of human lumbar lordosis variability. Am J Phys Anthropol 163:110–121

Cavagna GA, Thys H, Zamboni A (1976) The sources of external work in level walking and running. J Physiol 262:639–657

Clark GA, Panjabi MM, Wetzel FT (1985) Can infant malnutrition cause adult vertebral stenosis? Spine 10:165–170

Cook DC, Buikstra JE, DeRousseau CJ, Johanson DC (1983) Vertebral pathology in the Afar australopithecines. Am J Phys Anthropol 60:83–101

Day MH, Leakey RE (1974) New evidence of the genus *Homo* from east Rudolf, Kenya (III). Am J Phys Anthropol 41:367–380

Dean MC (2016) Measures of maturation in early fossil hominins: events at the first transition from australopiths to early *Homo*. Philos Trans R Soc Lond B 371:1698

Dean MC, Liversidge HM (2015) Age estimation in fossil hominins: comparing dental development in early *Homo* with modern humans. Ann Hum Biol 42:415–429

Dean C, Leakey MG, Reid D, Schrenk F, Schwartz GT, Stringer C, Walker A (2001) Growth processes in teeth distinguish modern humans from *Homo erectus* and earlier hominins. Nature 414:628–631

Dembo M, Matzke NJ, Mooers AØ, Collard M (2015) Bayesian analysis of a morphological supermatrix sheds light on controversial fossil hominin relationships. Proc R Soc Lond B Biol Sci 282:1812

de Ruiter DJ, Pickering R, Steininger CM, Kramers JD, Hancox PJ, Churchill SE, Berger LR, Backwell L (2009) New *Australopithecus robustus* fossils and associated U-Pb dates from Cooper's cave (Gauteng, South Africa). J Hum Evol 56:497–513

DeSilva JM (2009) Functional morphology of the ankle and the likelihood of climbing in early hominins. Proc Natl Acad Sci U S A 106:6567–6572

Digiovanni BF, Scoles PV, Latimer BM (1989) Anterior expansion of the thoracic vertebral bodies in Scheuermann's kyphosis: an anatomic study. Spine 14:712–716

Dirks P, Roberts EM, Hilbert-Wolf H, Kramers JD, Hawks J, Dosseto A, Duval M, Elliott M, Evans M, Grün R, Hellstrom J, Herries AIR, Joannes-Boyau R, Makhubela TV, Placzek CJ, Robbins J, Spandler C, Wiersma J, Woodhead J, Berger LR (2017) The age of *Homo naledi* and associated sediments in the rising star cave, South Africa. elife 6:e24231

Duval-Beaupere G, Schmidt C, Cosson P (1992) A Barycentremetric study of the sagittal shape of spine and pelvis: the conditions required for an economic standing position. Ann Biomed Eng 20:451–462

Eckhardt RB, Henneberg M (2010) LB1 from Liang Bua, Flores: craniofacial asymmetry confirmed, plagiocephaly diagnosis dubious. Am J Phys Anthropol 143(3):331–334

Falk D, Hildebolt C, Smith K, Morwood MJ, Sutikna T, Brown P, Jatmiko, Brunsden B, Prior F (2005) The Brain of LB1, *Homo floresiensis*. Science 308(5719):242–245

Feuerriegel EM, Green DJ, Walker CS, Schmid P, Hawks J, Berger LR, Churchill SE (2017) The upper limb of *Homo naledi*. J Hum Evol 104:155–173

Findlater IC (1978) Stratigraphy. In: Leakey M, Leakey R (eds) Koobi fora research project: the fossil hominids and an introduction to their context, 1968–1974. Clarendon Press, Oxford, pp 14–31

Fornai C, Haeusler M (2016) Virtual reconstruction of the *Australopithecus sediba* pelvis and reconsideration of its morphological affinities. Proc Eur Soc Human Evol 5:96

Gabunia L, Vekua A (1995) A plio-pleistocene hominid from Dmanisi, East Georgia, Caucasus. Nature 373:509–512

Gabunia L, Vekua A, Bugianishvili T (1988) The Dmanisi site. Newsletter of the Georgian Academy of Science, Biology 14:344

Galis F, Carrier DR, van Alphen J, van der Mije SD, Van Dooren TJ, Metz JA, ten Broek CM (2014) Fast running restricts evolutionary change of the vertebral column in mammals. Proc Natl Acad Sci U S A 111:11401–11406

Gambaryan PP (1974) How mammals run. Wiley, New York

Garvin HM, Elliott MC, Delezene LK, Hawks J, Churchill SE, Berger LR, Holliday TW (2017) Body size, brain size, and sexual dimorphism in *Homo naledi* from the Dinaledi chamber. J Hum Evol 111:119–138

Gómez-Olivencia A (2005) Estudio de la columna cervical de los humanosde la Sima de los Huesos (Sierra de Atapuerca, Burgos). Masters Thesis, Universidad Complutense de Madrid

Gómez-Olivencia A, Carretero JM, Arsuaga JL, Rodríguez-García L, García-González R, Martínez I (2007) Metric and morphological study of the upper cervical spine from the Sima de los Huesos site (sierra de Atapuerca, Burgos, Spain). J Hum Evol 53:6–25

Gómez-Olivencia A, Arlegi M, Barash A, Stock JT, Been E (2017) The Neandertal vertebral column 2: the lumbar spine. J Hum Evol 106:84–101

Gommery D (2000) Superior cervical vertebrae of a Miocene hominoid and a Plio–Pleistocene hominid from southern Africa. Palaeontologica Africana 36:139–145

Gommery D (2006) Evolution of the vertebral column in Miocene hominoids and Plio–Pleistocene hominids. In: Ishida H, Tuttle R, Pickford M, Ogihara N, Nakatsukasa M (eds) Human origins and environmental backgrounds. Springer, Boston, pp 31–43

Grabowski M (2016) Bigger brains led to bigger bodies? The correlated evolution of human brain and body size. Curr Anthropol 57:174–196

Grabowski M, Hatala KG, Jungers WL, Richmond BG (2015) Body mass estimates of hominin fossils and the evolution of human body size. J Hum Evol 85:75–93
Gracovetsky SA, Iacono S (1987) Energy transfers in the spinal engine. J Biomed Eng 9:99–114
Gracovetsky SA, Zeman V, Carbone AR (1987) Relationship between lordosis and the position of the Centre of reaction of the spinal disc. J Biomed Eng 9:237–248
Grausz HM, Leakey RE, Walker A, Ward CV (1988) Associated cranial and post–cranial bones of *Australopithecus boisei*. In: Grine F (ed) Evolutionary history of the robust australopithecines. Aldine de Gruyter, Chicago, pp 127–132
Griffin SD, Price VJ (2000) Living with lifting: Mothers' perceptions of lifting and back strain in childcare. Occup Ther Int 7:1–20
Grine FE (1988) New craniodental fossils of *Paranthropus* from the Swartkrans formation and their significance in 'robust' australopithecine evolution. In: Grine FE (ed) Evolutionary history of the robust australopithecines. Aldine de Gruyter, New York, pp 223–243
Grine FE (2005) Early *Homo* at Swartkrans, South Africa: a review of the evidence and an evaluation of recently proposed morphs. S Afr J Sci 101:43–52
Groves C (2007) The *Homo floresiensis* controversy. J Biosci 14:123–126
Gunji H, Hosaka K, Huffman MA, Kawanaka K, Matsumoto-Oda A, Hamada Y, Nishida T (2003) Extraordinarily low bone mineral density in an old female chimpanzee *(Pan troglodytes schweinfurthii*) from the Mahale Mountains National Park. Primates 44:145–149
Haeusler M (2002) New insights into the locomotion of *Australopithecus africanus* based on the pelvis. Evol Anthropol 11:53–57
Haeusler M, McHenry HM (2004) Body proportions of *Homo habilis* reviewed. J Hum Evol 46:433–465
Haeusler M, McHenry HM (2007) Evolutionary reversals of limb proportions in early hominids? Evidence from KNM-ER 3735 (*Homo habilis*). J Hum Evol 53:383–405
Haeusler M, Martelli SA, Boeni T (2002) Vertebrae numbers of the early hominid lumbar spine. J Hum Evol 43:621–643
Haeusler M, Schiess R, Boeni T (2011) New vertebral and rib material point to modern bauplan of the Nariokotome *Homo erectus* skeleton. J Hum Evol 61:575–582
Haeusler M, Fremondiere P, Fornai C, Frater N, Mathews S, Thollon L, Marchal F (2016) Virtual reconstruction of the MH2 pelvis (*Australopithecus sediba*) and obstetrical implications. Am J Phys Anthropol 57(S62):165
Haile-Selassie Y, Latimer B, Alene M, Deino A, Gibert L, Melillo SM, Saylor BZ, Scott GR, Lovejoy CO (2010) An early *Australopithecus afarensis* postcranium from Woranso-mille, Ethiopia. Proc Natl Acad Sci U S A 107:12121–12126
Haile-Selassie Y, Lovejoy C, Latimer B, Melillo SM, Meyer MR (2016) Implications of KSD-VP-1/1 for early hominin paleobiology and insights into the last common ancestor (LCA). In: Haile-Selassie Y, Su D The postcranial anatomy of *Australopithecus afarensis*: new insights from KSD-VP-1/1. Springer, Netherlands, 179–187
Harcourt-Smith WEH, Throckmorton Z, Congdon KA, Zipfel B, Deane AS, Drapeau MSM, Churchill SE, Berger LR, DeSilva JM (2015) The foot of *Homo naledi*. Nat Commun 6:8432
Hawks J, Elliott M, Schmid P, Churchill SE, Ruiter DJ, Roberts EM, Hilbert-Wolf H, Garvin HM, Williams SA, Delezene LK, Feuerriegel EM, Randolph-Quinney P, Kivell TL, Laird MF, Tawane G, JM DS, Bailey SE, Brophy JK, Meyer MR, Skinner MM, Tocheri MW, Van Sickle C, Walker CS, Campbell TL, Kuhn B, Kruger A, Tucker S, Gurtov A, Hlophe N, Hunter R, Morris H, Peixotto B, Ramalepa M, Dv R, Tsikoane M, Boshoff P, Dirks P, Berger LR (2017) New fossil remains of *Homo naledi* from the Lesedi chamber, South Africa. elife 6:e24232
Hernandez CJ, Loomis DA, Cotter MM, Schifle AL, Anderson LC, Elsmore L, Kunos C, Latimer B (2009) Biomechanical allometry in hominoid thoracic vertebrae. J Hum Evol 56:462–470
Hershkovitz I, Kornreich L, Laron Z (2007) Comparative skeletal features between *Homo floresiensis* and patients with primary growth hormone insensitivity (Laron syndrome). Am J Phys Anthropol 134(2):198–208
Hildebrand M (1974) Analysis of vertebrate structure. Wiley, New York

Holliday TW (2012) Body size, body shape, and the circumscription of the genus *Homo*. Curr Anthropol 53:330–345
Holliday TW, Franciscus RG (2009) Body size and its consequences: Allometry and the lower limb length of Liang Bua 1 (*Homo floresiensis*). J Hum Evol 57:223–228
Jacob T, Indriati E, Soejono RP, Hsü K, Frayer DW, Eckhardt RB, Kuperavage AJ, Thorne A, Henneberg M (2006) Pygmoid Australomelanesian *Homo sapiens* skeletal remains from Liang Bua, Flores: population affinities and pathological abnormalities. Proc Natl Acad Sci 103(36):13421–13426
Jones KE (2015) Evolutionary allometry of lumbar shape in Felidae and Bovidae. Biol J Linn Soc 116(3):721–740
Jungers WL (1982) Lucy's limbs: skeletal allometry and locomotion in *Australopithecus afarensis*. Nature 297:676–678
Jungers WL (1988) Relative joint size and hominid locomotor adaptations with implications for the evolution of hominid bipedalism. J Hum Evol 17:247–265
Jungers WL, Grabowski M, Hatala KG, Richmond BG (2016) The evolution of body size and shape in the human career. Philos Trans R Soc Lond B 371:1698
Ker RF, Bennett MB, Bibby SR, Kester RC, Alexander RM (1987) The spring in the arch of the human foot. Nature 325:147–149
Kimbel W, Rak Y (1993) The importance of species taxa in paleoanthropology and an argument for the phylogenetic concept of the species category. In: Kimbel W, Martin L (eds) Species, species concepts and primate evolution. Plenum Press, New York, pp 461–484
Kimbel W, Villmoare B (2016) From *Australopithecus* to *Homo*: the transition that wasn't. Philos Trans R Soc Lond B 371:1698
Kivell TL, Deane AS, Tocheri MW, Orr CM, Schmid P, Hawks J, Berger LR, Churchill SE (2015) The hand of *Homo naledi*. Nat Commun 6:8431
Lafage V, Ames C, Schwab F, Klineberg E, Akbarnia B, Smith J, Boachie-Adjei O, Burton D, Hart R, Hostin R, Shaffrey C, Wood K, Bess S (2012) Changes in thoracic kyphosis negatively impact sagittal alignment after lumbar pedicle subtraction osteotomy: a comprehensive radiographic analysis. Spine 37:E180–E187
Laird MF, Schroeder L, Garvin HM, Scott JE, Dembo M, Radovčić D, Musiba CM, Ackermann RR, Schmid P, Hawks J, Berger LR, de Ruiter D (2017) The skull of *Homo naledi*. J Hum Evol 104:100–123
Lanyon LE (1982) Mechanical function and bone remodeling. In: Sumner-Smith G (ed) Bone in clinical orthopaedics. WB Saunders, Philadelphia
Latimer B (2005) The perils of being bipedal. Ann Biomed Eng 33:3–6
Latimer B, Ohman JC (2001) Axial displasia in *Homo erectus*. J Hum Evol 40:12
Latimer B, Ward CV (1993) The thoracic and lumbar vertebrae. In: Walker A, Leakey R (eds) The nariokotome *Homo erectus* skeleton. Harvard University Press, Cambridge, pp 266–293
Leakey MG, Leakey RE (1978) Koobi Fora research project, volume 1: the fossil hominids and an introduction to their context, 1968–1974. Clarendon Press, Oxford
Leakey RE, Walker A (1985) Further hominids from the Plio–Pleistocene of Koobi Fora, Kenya. Am J Phys Anthropol 67:135–163
Lieberman D (2011) The evolution of the human head. Belknap Press of Harvard University Press, Cambridge
Lieberman D, Bramble D, Raichlen D, Shea J (2006) Brains, brawn, and the evolution of human endurance running capabilities. In: Grine F, Fleagle J, Leakey RE (eds) Contributions from the third stony brook human evolution symposium and workshop. Springer, Dordrecht, pp 77–92
Lieberman D, Bramble D, Raichlen D, Shea J (2007) The evolution of endurance running and the tyranny of ethnography: a reply to Pickering and Bunn (2007). J Hum Evol 53:439–442
Lovejoy CO (2005a) The natural history of human gait and posture: part 1. Spine and pelvis. Gait Posture 21:95–112
Lovejoy CO (2005b) The natural history of human gait and posture: part 2. Hip and thigh. Gait Posture 21:113–124

Lovejoy CO (2007) The natural history of human gait and posture: part 3. The knee. Gait Posture 25:325–341
Lovell NC (1990) Patterns of injury and illness in great apes: a skeletal analysis. Smithsonian Institution Press, Washington
MacLarnon A (1993) The vertebral canal. In: Walker A, Leakey RE (eds) The nariokotome *Homo erectus* skeleton. Springer–Verlag, Berlin, pp 359–390
Martin RA (1981) On extinct hominid population densities. J Hum Evol 10:427–428
Martin RD (2006) Comment on "the brain of LB1, *Homo floresiensis*". Science 312(5776):999
Martin RD, MacLarnon AM, Phillips JL, Dobyns WB (2006) Flores hominid: new species or microcephalic dwarf? Anat Rec A: Discov Mol Cell Evol Biol 288A(11):1123–1145
Mazelis EJ (2014) Covariation of locomotor behavior and vertebral shape in Cercopithecidae. Am J Phys Anthr 153:179–180
McHenry HM (1991) Petite bodies of the “robust” australopithecines. Am J Phys Anthropol 86:445–454
McHenry HM (1994a) Behavioral ecological implications of early hominid body size. J Hum Evol 27:77–87
McHenry HM (1994b) Early hominid postcrania: phylogeny and function. In: Corruccini RS, Ciochon RL (eds) Integrative paths to the past: paleoanthropological advances in honor of F. Clark Howell. Prentice Hall, Englewood Cliffs, pp 251–268
Mercer SR, Bogduk N (2003) Clinical anatomy of ligamentum nuchae. Clin Anat 16:484–493
Meyer MR (2003) Vertebrae and language ability in early hominids. PaleoAnthropology 1:20–21
Meyer MR (2005) Functional biology of the *Homo erectus* axial skeleton from Dmanisi, Georgia. Ph.D. Dissertation, University of Pennsylvania
Meyer MR (2008) Skeletal indications for distance locomotion in early *Homo erectus*. Am J Phys Anthropol 135(S46):155
Meyer MR (2012) Functional anatomy of the thoracic vertebrae in early *Homo*. Am J Phys Anthropol 147(S54):214
Meyer MR (2016a) The cervical vertebrae of KSD-VP-1/1. In: Haile–Selassie Y, Su D (eds) the postcranial anatomy of *Australopithecus afarensis*: new insights from KSD-VP-1/1. Springer, Netherlands, pp 63–112
Meyer MR (2016b) The spinal cord in hominin evolution. In: Encyclopedia of life sciences. John Wiley & Sons, Chichester. https://doi.org/10.1002/9780470015902.a0027058
Meyer MR, Haeusler M (2014) Spinal stenosis in *Homo erectus*. Eur Soc Study Human Evol 3:117
Meyer MR, Haeusler M (2015) Spinal cord evolution in early *Homo*. J Hum Evol 88:43–53
Meyer MR, Haile-Selassie Y (2016) The KSD-VP-1/1 postcranial skeleton from Woranso Mille, Ethiopia: brachial plexus enlargement and the capacity for fine motor skills in *Australopithecus afarensis*. Am J Phys Anthropol 159(S62):228
Meyer MR, Williams SA (Forthcoming) Earliest axial fossils from the genus *Australopithecus*
Meyer MR, Williams SA, Smith MP, Sawyer GJ (2015) Lucy's back: reassessment of fossils associated with the A.L. 288-1 vertebral column. J Hum Evol 85:174–180
Meyer MR, Williams SA, Schmid P, Churchill SE, Berger LR (2017) The cervical spine of *Australopithecus sediba*. J Hum Evol 104:32–49
Meyer MR, Woodward C, Tims A, Bastir M (2018) Neck function in early hominins and suspensory primates: insights from the uncinate process. Am J Phys Anthropol 166:613–637
Morwood MJ, Jungers WL (2009) Conclusions: implications of the Liang Bua excavations for hominin evolution and biogeography. J Hum Evol 57:640–648
Morwood MJ, Soejono RP, Roberts RG, Sutikna T, Turney CS, Westaway KE, Rink WJ, Zhao JX, van den Bergh GD, Due RA, Hobbs DR, Moore MW, Bird MI, Fifield LK (2004) Archaeology and age of a new hominin from Flores in eastern Indonesia. Nature 431(7012):1087–1091
Morwood MJ, Brown P, Jatmiko ST, Saptomo EW, Westaway KE, Due RA, Roberts RG, Maeda T, Wasisto S, Djubiantono T (2005) Further evidence for small-bodied hominins from the late Pleistocene of Flores, Indonesia. Nature 437(7061):1012–1017
Napier JR (1959) Fossil metacarpals from Swartkrans. Fossil Mamm Africa 17:1–18

Oh T, Scheer JK, Eastlack R, Smith JS, Lafage V, Protopsaltis TS, Klineberg E, Passias PG, Deviren V, Hostin R, Gupta M, Bess S, Schwab F, Shaffrey CI, Ames CP (2015) Cervical compensatory alignment changes following correction of adult thoracic deformity: a multicenter experience in 57 patients with a 2-year follow-up. J Neurosurg Spine 22:658–665

Pal GP, Routal RV (1986) A study of weight transmission through the cervical and upper thoracic regions of the vertebral column in man. J Anat 148:245–261

Papp T, Porter RW, Craig CE, Aspden RM, Campbell DM (1997) Significant antenatal factors in the development of lumbar spinal stenosis. Spine 22:1805–1810

Pickering TR, Bunn HT (2007) The endurance running hypothesis and hunting and scavenging in savanna-woodlands. J Hum Evol 53:434–438

Pickering R, Kramers JD, Hancox PJ, de Ruiter D, Woodhead J (2011) Contemporary flowstone development links early hominin bearing cave deposits in South Africa. Earth Planet Sci Lett 306(1e2):23e32

Plaisant O, Sarrazin JL, Cosnard G, Schill H, Gillot C (1996) The lumbar anterior epidural cavity: the posterior longitudinal ligament, the anterior ligaments of the dura mater and the anterior internal vertebral venous plexus. Acta Anat (Basel) 155:274–281

Pontzer H (2007) Effective limb length and the scaling of locomotor cost in terrestrial animals. J Exp Biol 210:1752–1761

Pontzer H (2012) Ecological energetics in early *Homo*. Curr Anthropol 53:S346–S358

Pontzer H (2017) Economy and endurance in human evolution. Curr Biol 27:R613–R621

Pontzer H, Wrangham RW (2004) Climbing and the daily energy cost of locomotion in wild chimpanzees: implications for hominoid locomotor evolution. J Hum Evol 46:315–333

Pontzer H, Rolian C, Rightmire GP, Jashashvili T, Ponce de Leon MS, Lordkipanidze D, Zollikofer CP (2010) Locomotor anatomy and biomechanics of the Dmanisi hominins. J Hum Evol 58:492–504

Prang TC (2015) Rearfoot posture of *Australopithecus sediba* and the evolution of the hominin longitudinal arch. Sci Rep 5:17677

Preuschoft H (2004) Mechanisms for the acquisition of habitual bipedality: are there biomechanical reasons for the acquisition of upright bipedal posture? J Anat 204:363–384

Robinson JT (1965) Homo 'habilis' and the australopithecines. Nature 205:121

Robinson JT (1970) Two new early hominid vertebrae from Swartkrans. Nature 225:1217–1219

Robinson JT (1972) Early hominid posture and locomotion. University of Chicago Press, Chicago

Robson SL, Wood B (2008) Hominin life history: reconstruction and evolution. J Anat 212:394–425

Rolian C, Lieberman DE, Hamill J, Scott JW, Werbel W (2009) Walking, running and the evolution of short toes in humans. J Exp Biol 212:713–721

Sabino J, Grauer JN (2008) Pregnancy and low back pain. Curr Rev Musculoskelet Med 1:137–141

Salesa MJ, Antón M, Peigne S, Morales J (2008) Functional anatomy and biomechanics of the postcranial skeleton of *Simocyon batalleri* (Viret, 1929) (Carnivora, Ailuridae) from the late Miocene of Spain. Zool J Linnean Soc 152:593–621

Sanders WJ (1990) Weight transmission through the lumbar vertebrae and sacrum in australopithecines. Am J Phys Anthropol 81:289

Sanders WJ (1995) Function, allometry, and evolution of the australopithecine lower precaudal spine. New York University, PhD Dissertation

Sanders WJ (1998) Comparative morphometric study of the australopithecine vertebral series Stw-H8/H41. J Hum Evol 34:249–302

Sanders WJ, Bodenbender BE (1994) Morphometric analysis of lumbar vertebra UMP 67-28: implications for spinal function and phylogeny of the Miocene Moroto hominoid. J Hum Evol 26:203–237

Schiess R, Haeusler M (2013) No skeletal dysplasia in the Nariokotome boy KNM-WT 15000 (*Homo erectus*): a reassessment of congenital pathologies of the vertebral column. Am J Phys Anthropol 150:365–374

Schilling N, Hackert R (2006) Sagittal spine movements of small therian mammals during asymmetrical gaits. J Exp Biol 209:3925–3939

Schultz AH (1961) Vertebral column and thorax. Primatologica 4:1–66
Shapiro L (1991) Functional morphology of the primate spine with special reference to orthograde posture and bipedal locomotion. Ph.D., State University of New York at Stony Brook
Shapiro L (1993) Evaluation of unique aspects of human vertebral bodies and pedicles with a consideration of *Australopithecus africanus*. J Hum Evol 25:433–470
Shapiro LJ, Simons CV (2002) Functional aspects of strepsirrhine lumbar vertebral bodies and spinous processes. J Hum Evol 42:753–783
Singer KP, Breidahl PD, Day RE (1988) Variations in zygapophyseal joint orientation and level of transition at the thoracolumbar junction. Surg Radiol Anat 10:291–295
Slijper EJ (1946) Comparative biologic–anatomical investigations on the vertebral column and spinal musculature of mammals. Koninklijke Nederlandse Akademie van Wetenschappen 42:1–128
Smith TM, Tafforeau P, Le Cabec A, Bonnin A, Houssaye A, Pouech J, Moggi-Cecchi J, Manthi F, Ward C, Makaremi M, Menter CG (2015) Dental ontogeny in Pliocene and early Pleistocene hominins. PLoS One 10(2):e0118118
Steudel-Numbers KL (2006) Energetics in *Homo erectus* and other early hominins: the consequences of increased lower-limb length. J Hum Evol 51(5):445–453
Susman RL (1988) New postcranial remains from Swartkrans and their bearing on the functional morphology and behavior of *Paranthropus robustus*. In: Grine FE (ed) Evolutionary history of the "robust" australopithecines. Aldine de Gruyter, New York, pp 149–172
Susman RL (1989) New hominid fossils from the Swartkrans formation (1979–1986 excavations): postcranial specimens. Am J Phys Anthropol 79(4):451–474
Susman RL (1993) Hominid postcranial remains from Swartkrans. In: Brain CK (ed) Swartkrans: a Cave's chronicle of early man Capetown. CTP Book Printers, Capetown, pp 117–136
Susman RL, de Ruiter D, Brain CK (2001) Recently identified postcranial remains of *Paranthropus* and early *Homo* from Swartkrans cave, South Africa. J Hum Evol 41(6):607–629
Tardieu C, Hecquet J, Barrau A, Loridon P, Boulay C, Legaye J, Carlier R, Marty C, Duval-Beaupere G (2006) Le basin, interfacearticulaire entre rachis et membres inferieurs: analyse par le logiciel DE–VISU. Comptes Rendus Palévol 5:583–595
Tardieu C, Bonneau N, Hecquet J, Boulay C, Marty C, Legaye J, Duval-Beaupère G (2013) How is sagittal balance acquired during bipedal gait acquisition? Comparison of neonatal and adult pelves in three dimensions: evolutionary implications. J Hum Evol 65(2):209–222
Tardieu C, Hasegawa K, Haeusler M (2017) How did the pelvis and vertebral column become a functional unit during the transition from occasional to permanent bipedalism? Anat Rec 300(5):912–931
Throckmorton Z, Weh HS, Congcon K, Zipfel B, DeSilva JM, VanSickle C, Williams SA, Meyer MR, Prang TC, Walker CS, Marchi D, Garcia-Martínez D, Churchill S, Hawks J, Berger LR (2016) *Homo naledi* strides again: preliminary reconstructions of an extinct hominin's gait. Am J Phys Anthropol 159(S62):314
Trinkaus E (1983) Neandertal postcrania and the adaptive shift to modern humans. In: Trinkaus E (ed) The Mousterian legacy British archaeological reports, 165–200
Trinkaus E (1987) Bodies, brawn, brains and noses: human ancestors and human predation. In: Nitecki MH, Nitecki DV (eds) The evolution of human hunting. Plenum Press, New York, pp 107–145
van den Bergh GD, Kaifu Y, Kurniawan I, Kono R, Brumm A, Setiyabudi E, Aziz F, Morwood MJ (2016) *Homo floresiensis*-like fossils from the early middle Pleistocene of Flores. Nature 534:245–248
Vallois HV (1926) La sustentation de la tête et le ligament cervical postérieur chez l'homme et les anthropoïdes. Anthropologie 36:191–207
VanSickle C, Cofran Z, García-Martínez D, Williams SA, Churchill SE, Berger LR, Hawks J (2018) *Homo naledi* pelvic remains from the Dinaledi chamber, South Africa. J Hum Evol 125:122–136
Vermani E, Mittal R, Weeks A (2010) Pelvic girdle pain and low back pain in pregnancy: a review. Pain Pract 10(1):60–71

Villmoare B (2018) Early *Homo* and the role of the genus in paleoanthropology. Am J Phys Anthropol 165:72–89
Wagner H, Liebetrau A, Schinowski D, Wulf T, de Lussanet M (2012) Spinal lordosis optimizes the requirements for a stable erect posture. Theoret Biol Med Model 9(1):13
Walker A, Leakey RE (1993a) Perspectives on the Nariokotome discovery. In: Walker A, Leakey RE (eds) The Nariokotome *Homo erectus* skeleton. Harvard University Press, Cambridge, pp 411–430
Walker A, Leakey RE (1993b) The postcranial bones. In: Walker A, Leakey RE (eds) The Nariokotome *Homo erectus* skeleton. Harvard University Press, Cambridge, pp 95–160
Walker A, Zimmerman MR, Leakey RE (1982) A possible case of hypervitaminosis a in *Homo erectus*. Nature 296:248–250
Wang W, Crompton R (2004) The role of load-carrying in the evolution of modern body proportions. J Anat 204:417–430
Wang W, Crompton R, Li Y, Günther M (2002) Optimum ratio of upper to lower limb lengths under the assumptions of frequency coordination and hand-carrying of a load. J Biomech 36:249–252
Ward CV (1993) Torso morphology and locomotion in: *Proconsul nyanzae*. Am J Phys Anthropol 92(3):291–328
Ward CV (2002) Interpreting the posture and locomotion of *Australopithecus afarensis*: where do we stand? Am J Phys Anthropol S35:185–215
Ward CV (2013) Postural and locomotor adaptations of *Australopithecus* species. In: Reed KE, Fleagle KG, Leakey RE (eds) The paleobiology of *Australopithecus* Springer, Dordrecht, 235–245
Ward CV, Kimbel WH, Harmon EH, Johanson DC (2012) New postcranial fossils of *Australopithecus afarensis* from Hadar, Ethiopia (1990–2007). J Hum Evol 63(1):1–51
Ward CV, Feibel CS, Hammond AS, Leakey LN, Moffett EA, Plavcan JM, Skinner MM, Spoor F, Leakey MG (2015) Associated ilium and femur from Koobi Fora, Kenya, and postcranial diversity in early *Homo*. J Hum Evol 81:48–67
Ward CV, Nalley TK, Spoor F, Tafforeau P, Alemseged Z (2017) Thoracic vertebral count and thoracolumbar transition in *Australopithecus afarensis*. Proc Natl Acad Sci U S A 114(23):6000–6004
Whitcome KK (2012) Functional implications of variation in lumbar vertebral count among hominins. J Hum Evol 62(4):486–497
Whitcome KK, Shapiro LJ, Lieberman DE (2007) Fetal load and the evolution of lumbar lordosis in bipedal hominins. Nature 450(7172):1075–1078
Williams SA (2011) Evolution of the hominoid vertebral column. University of Illinois at Urbana-Champaign, Doctoral Dissertation
Williams SA (2012) Modern or distinct axial bauplan in early hominins? Comments on Haeusler et al. (2011). J Hum Evol 63:552–559
Williams SA, Russo GA (2015) Evolution of the hominoid vertebral column: the long and the short of it. Evolution Anthropol 24(1):15–32
Williams SA, Ostrofsky KR, Frater N, Churchill SE, Schmid P, Berger LR (2013) The vertebral column of *Australopithecus sediba*. Science 340:6129
Williams SA, Garcia-Martinez D, Bastir M, Meyer MR, Nalla S, Hawks J, Schmid P, Churchill SE, Berger LR (2017) The vertebrae and ribs of Homo Naledi. J Hum Evol 104:136–154
Williams SA, Meyer MR, Nalla S, García-Martínez D, Nalley TK, Eyre J, Prang TC, Bastir M, Schmid P, Churchill SE, Berger LR (2018) The vertebrae, ribs, and sternum of *Australopithecus sediba*. 2018:156–233
Yilgor C, Sogunmez N, Yavuz Y, Abul K, Boissiere L, Haddad S, Obeid I, Kleinstuck F, Sánchez Pérez-Grueso FJ, Acaroglu E, African M, Pellise F, Alanay A (2017) Relative lumbar lordosis and lordosis distribution index: individualized pelvic incidence-based proportional parameters that quantify lumbar lordosis more precisely than the concept of pelvic incidence minus lumbar lordosis. Neurosurg Focus 43(6):E5
Zhu RX, Potts R, Pan YX, Yao HT, Lu Q, Zhao X, Gao X, Chen LW, Gao F, Deng CL (2008) Early evidence of the genus *Homo* in East Asia. J Hum Evol 55(6):1075–1085

Chapter 9
The Spine of Late *Homo*

Asier Gómez-Olivencia and Ella Been

9.1 Introduction

Similar to what happens in the study of the costal skeleton, the study of the evolution of the vertebral column is hampered by the fragility (and thus, scarceness) of these anatomical elements in the fossil record, the difficulty in establishing the exact anatomical position due to the similarity among these serial elements, and the difficulty in amassing large comparative samples (Franciscus and Churchill 2002). Thus, for a long time (mainly the second half of the twentieth century), the study of the vertebral column of "late" *Homo* (understood here as the hominin groups which existed approximately one million years ago or later, and which do not show early *Homo* or australopithecine affinities, i.e., excluding *H. floresiensis, H. luzonensis* and *H. naledi*) has been relegated to chapters of minor importance within monographs in which the general conclusion was that there were only few differences related to robusticity between these hominins and recent *H. sapiens* (e.g., the Neandertal case in Trinkaus 1983; Arensburg 1991).

Recent studies during the last 15–20 years have dramatically changed this perception. First, new efforts have been put in providing more accurate inventories,

A. Gómez-Olivencia (✉)
Departamento de Estratigrafía y Paleontología, Facultad de Ciencia y Tecnología, Universidad del País Vasco/Euskal Herriko Unibertsitatea (UPV/EHU), Leioa, Spain

IKERBASQUE, Basque Foundation for Science, Bilbao, Spain

Centro Mixto UCM-ISCIII de Evolución y Comportamiento Humanos, Madrid, Spain
e-mail: asier.gomezo@ehu.eus

E. Been
Department of Sports Therapy, Faculty of Health Professions, Ono Academic College, Kiryat Ono, Israel

Department of Anatomy and Anthropology, Sackler Faculty of Medicine, Tel Aviv University, Tel Aviv, Israel

E. Been et al. (eds.), *Spinal Evolution*,
https://doi.org/10.1007/978-3-030-19349-2_9

which is a prerequisite before performing a proper metric analysis (Gómez-Olivencia 2013a, b). Second, appropriate statistical analyses have been used to test for morphological differences between different "late" *Homo* species and modern humans (e.g., Carretero et al. 1999; Gómez-Olivencia et al. 2007, 2013a, b, 2017b; Been et al. 2010, 2012, 2014a, 2017a). Third, the discovery of new fossil remains (e.g., Gran Dolina, Sima de los Huesos, El Sidrón), the presence of casts of the most complete Neandertal spine (Kebara 2) in many research institutions, and the application of geometric morphometrics to the study of the postcranial axial skeleton (e.g., Bastir et al. 2017; see Bastir et al. 2019) have been of paramount importance in the shift of perception regarding the morphology and function in different extinct *Homo* species.

Here, we review the vertebral column fossil record for "late" *Homo* during the last million years and emphasize the morphological differences found between Neandertals and their Middle Pleistocene ancestral populations, and *H. sapiens*. We also explore the functional and postural implications of these differences (Table 9.1).

9.2 Late Lower and Middle Pleistocene *Homo*

9.2.1 Homo antecessor *from Gran Dolina-TD6*

The TD6 level of Gran Dolina (Sierra de Atapuerca, Burgos, Spain) yielded its first human remains in the field season of 1994. At that time, with an age between 780 and 949 ka (*kilo anne* = 10^3 years), these hominin fossils were the oldest known from Europe (Carbonell et al. 1995; Pares and Perez-Gonzalez 1995, 1999; Duval et al. 2018). Additional fossils were found and a new human species, *Homo antecessor*, was defined. This new species was first proposed to be ancestral to Neandertals and modern humans (Bermúdez de Castro et al. 1997; but see Gómez-Robles et al. 2013). The taphonomic analysis of the TD6 human remains indicates that they were cannibalized to be consumed (Fernández-Jalvo et al. 1996, 1999). However, the age distribution of the cannibalized individuals does not correspond with other cases of exocannibalism by hominins. This age profile, on the other hand, is consistent with that present in intergroup aggression in chimpanzees, which has led to Saladié et al. (2012) to propose that the TD6 hominins mounted low-risk attacks on members of neighboring groups (or new groups in the same area) in order to protect the catchment territory of the group and to try to expand their territory.

The field seasons of the mid-1990s yielded seven vertebral remains (four cervical, two thoracic, and one lumbar vertebrae), including a nearly complete atlas, which was suggested to belong to a female individual based on its small size (Carretero et al. 1999). This atlas shows a caudally projecting anterior tubercle of the anterior arch and protruding (large) tubercles for the attachment of the transverse ligament (Gómez-Olivencia et al. 2007). New excavations and the restudy of the faunal remains recovered from the excavations in the mid-1990s have increased

Table 9.1 Selected morphological traits in "late *Homo*" compared to modern humans as a baseline

Vertebra	Trait	*H. antecessor*	Sima de los Huesos	*H. neanderthalensis*	Recent *H. sapiens*	References
C1	Vertebral canal dorsoventral diameter		Longer	Longer	Shorter	Carretero et al. (1999); Gómez-Olivencia et al. (2007, 2013b); Arsuaga et al. (2015)
	Anterior tubercle of the anterior arch	Caudally projected (ATD6-90)	Caudally projected	Caudally projected	Caudally projected	
	Size of the tubercles for the insertion of the transverse ligament	Large (ATD6-90)	Variable: Large (33.3%); Small (66.7%)	Small (83.3 %)	Large (74.4–83.3%)	
	Size of the posterior arch	Robust (ATD6-90)	Robust	Slender	Robust	
C2	Overall morphology		Relatively low and wide	Relatively low and wide	Relatively high and narrow	
C3–C7	Vertebral body			Craniocaudally smaller	Craniocaudally longer	
C3–C7	General shape			Dorsoventrally longer (C4–C7) and mediolaterally wider (C3–C7)	Dorsoventrally shorter and mediolaterally narrower	
C5	Length of the spinous process		Longer	Longer	Shorter	
C6–C7	Length of the spinous process			Longer	Shorter	
C6–C7	Orientation of the spinous process	More horizontal	More horizontal	Very horizontal	More caudally oriented	

(continued)

Table 9.1 (continued)

Vertebra	Trait	*H. antecessor*	Sima de los Huesos	*H. neanderthalensis*	Recent *H. sapiens*	References
Thoracic vertebrae	Orientation of the transverse processes in mid-thoracic vertebrae			More dorsally oriented	Less dorsally oriented	Bastir et al. (2017); Gómez-Olivencia et al. (2018)
T2	Width of the vertebral foramen			Wider	Narrower	Gómez-Olivencia et al. (2013a)
Lumbar spine	Vertebral body wedging		More ventrally wedged in at least L2 and L4	More ventrally wedged (L1–L3, L4?)	Default	Been et al. (2010, 2012, 2014a); Bonmatí et al. (2010); Arsuaga et al. (2015); Gómez-Olivencia et al. (2017a, b)
	Lower articular facet angle			More closed angle (L3?, L4–L5)	More open angle	
	Lumbar lordosis		Small	Small	Default	
	Transverse process: length		Very long	Long	Shorter	
	Transverse process: orientation in cranial view		Dorsolateral	Laterally oriented (L2–L4)	Dorsolateral	
	Transverse process: orientation in dorsal view		More laterally oriented	More cranially oriented (L1–L3)	More laterally oriented	
L4–L5	Vertebral canal shape		Same as modern humans	Dorsoventrally enlarged	Default	
Sacrum	General orientation within the pelvis		More vertical	More vertical	Less vertical	Been et al. (2010); Rmoutilová et al. (in preparation)
	Canal shape			Dorsoventrally enlarged	Default	

the number of identified human vertebral specimens. The current hypodigm from Gran Dolina-TD6 includes 16 fossil vertebrae from all the presacral anatomical regions: six cervical, six thoracic, one thoracic or lumbar, and three lumbar remains. These fossils represent a minimum of five individuals of different ages-at-death (Gómez-Olivencia et al. 2017a) from the eight individuals represented in the TD6 hypodigm (Bermúdez-De-Castro et al. 2017). It should be noted that, while most of these remains are fragmentary as they were cannibalized, a virtually complete adult sixth cervical vertebra, which shows a very horizontal spinous process, is known. This feature, which has been proposed as primitive within genus *Homo*, is also present in the KNM-WT 15000 *Homo erectus* C7 (Gómez-Olivencia et al. 2017a).

9.2.2 Zhoukoudian Locality 1

The Zhoukoudian Locality 1 (Dragon Hill, Northern China) has provided a large sample of hominin fossils modified by hyaenids, representing allochthonous members of the fossil assemblage (Boaz et al. 2004). Locality 1 has a long Middle Pleistocene stratigraphic sequence and fossils have been found in multiple layers (Grün et al. 1997; Goldberg et al. 2001; Shen et al. 2001; Boaz et al. 2004 and references therein). The fossil assemblage includes cranial and postcranial remains, but the spinal elements are restricted to a fragmentary atlas, which shows damage produced by hyaenids at the right transverse process (Boaz et al. 2004). This atlas was found in Locus I, level 22 in 1936 and it has been associated with Skull VI on spatial, stratigraphical, and morphological bases, thus being considered part of the I1 ("eye-one") individual (Boaz et al. 2004), older than 600 ka BP (Shen et al. 2001).

9.2.3 Caune de l'Arago

The Caune de l'Arago (Tautavel, Roussillon, Occitanie, France) is a classic site with a long Middle Pleistocene stratigraphic sequence which has yielded a total of 148 human remains belonging to 18 adults and 12 immature individuals (de Lumley 2015). These fossils have been proposed to belong to a population different from that represented from the mandible of Mauer, and the taxon *H. erectus tautavelensis* has been proposed for this assemblage, representing one of the richest Middle Pleistocene fossil assemblages from Europe. To explain the accumulation of certain of these remains, a ritual cannibalism has been proposed (de Lumley 2015). Among the 148 fossils, those belonging to the spine are restricted to an atlas (C1) and an axis (C2) from sublevel Gm (level G; Middle stratigraphic assemblage; c. 450 ka; Moigne et al. 2006) which may have belonged to the same individual and which were found close to the cranium Arago 21–47 (de Lumley 2015). These remains have not been described in detail yet.

9.2.4 Sima de los Huesos

The Sima de los Huesos (SH) site is located in the lower level of the Cueva Mayor–Cueva del Silo karstic system in the Sierra de Atapuerca (Burgos, Spain; Ortega et al. 2013). More than 7000 human fossils belonging to a minimum of 28 individuals (Bermúdez de Castro et al. 2004) have been found in the lithostratigraphic unit 6, dated to around 430 ka BP (Arsuaga et al. 2014). This site has also yielded thousands of carnivore remains, especially *Ursus deningeri*, micromammals, and a single stone tool (Cuenca-Bescós et al. 1997; García et al. 1997; Carbonell et al. 2003; García and Arsuaga 2011; Arsuaga et al. 2014). Regarding the cranium, this paleodeme shows derived Neandertal features in the anterior vault and in the face, mostly related to the masticatory apparatus (Arsuaga et al. 1993, 1997b, 2014). The postcranial skeleton shows anatomical features that are similar to those of Neandertals, but others are plesiomorphic or of uncertain phylogenetic polarity. While there are a few Neandertal apomorphies, the SH hominins do not show the full suite of Neandertal-derived craniodental and postcranial features (Carretero et al. 1997; Pablos et al. 2013, 2014, 2017; Arsuaga et al. 2014, 2015). Several taphonomical studies have dealt with the origin of the accumulation of SH (Arsuaga et al. 1990, 1997a; Sala et al. 2014, 2015a, b), which propose that SH was a natural trap for the carnivores and that the human remains accumulated at SH because complete corpses were thrown purposefully by other humans. The most recent taphonomic and geological analyses (Sala et al. 2014, 2015a, b; Aranburu et al. 2017) reject previous claims of the human accumulation due to a geological catastrophic event and/or carnivore activity (e.g., Andrews and Fernández-Jalvo 1997). For practical reasons, this paleodeme was included within a particular definition of *H. heidelbergensis*, which would include all the known European Middle Pleistocene fossils, except Ceprano and those which are very Neandertal-like (e.g., Biache-Saint-Vaast, La Chaise-Abri Suard) (Arsuaga et al. 1997b). In that analysis, the presence of Neandertal-derived features in the Mauer mandible (the holotype of *H. heidelbergensis*) was considered likely (Arsuaga et al. 1997b). More recent analyses of Middle Pleistocene mandibles show, however, the very distinct morphology of Mauer (Rak et al. 2011) and the more Neandertal-like morphology of SH (Rosas 2001; Arsuaga et al. 2014). Thus, the Atapuerca researchers currently avoid the *H. heidelbergensis* designation to refer to the SH paleodeme.

There is a minimum of 212 vertebrae preserved in SH, belonging to a minimum of 12 individuals (Gómez-Olivencia et al. 2017a). While most of the vertebrae are isolated, associating vertebrae among them and to other anatomical elements like crania or pelves has begun (e.g., Bonmatí et al. 2010; Gómez-Olivencia et al. 2011; Arsuaga et al. 2014). The morphology of the upper cervical spine (C1 and C2) and on the pathological lesions of the lumbar and pelvic region of the Pelvis 1 individual have been published in detail (Gómez-Olivencia et al. 2007). Preliminary information regarding the morphology of the cervical and lumbar regions has been published as parts of other studies (Carretero et al. 1999; Gómez-Olivencia et al. 2011, 2017a; Gómez-Olivencia and Arsuaga 2015; Martínez et al. 2013; Arsuaga et al. 2015), but the thoracic spine remains undescribed. Below, we review the current studies on the cervical and lumbar spines and sacrum.

Cervical Spine

The atlas displays a large maximum dorsoventral canal diameter, related to the size of the foramen magnum of the SH crania. Similar to Neandertals, the atlases from SH show a caudal projection of the anterior tubercle of the atlas. The SH paleodeme shows a higher percentage of large tubercles for the attachment of the transverse ligament when compared to Neandertals, but still lower than that present in modern humans (Fig. 9.1). The posterior tubercle is more robust than in Neandertals (Gómez-Olivencia et al. 2007, 2013b). The axis is craniocaudally low, and the atlantoaxial joint is mediolaterally (ML) expanded, with a general shape similar to that of Neandertals (Gómez-Olivencia et al. 2007) (Fig. 9.1). The SH hominins show C6 and C7 spinous processes that are more horizontally oriented than in modern humans and shorter and more robust than in Neandertals (Gómez-Olivencia et al. 2011; Arsuaga et al. 2015) (Fig. 9.2). Finally, it has been possible to associate a complete cervical spine to Cranium 5 (see Arsuaga et al. 2014), and it has been possible to measure the total (skeletal) neck length from C2 to C7. The length is below the modern human male mean, but within 1 standard deviation of it (Martínez et al. 2013).

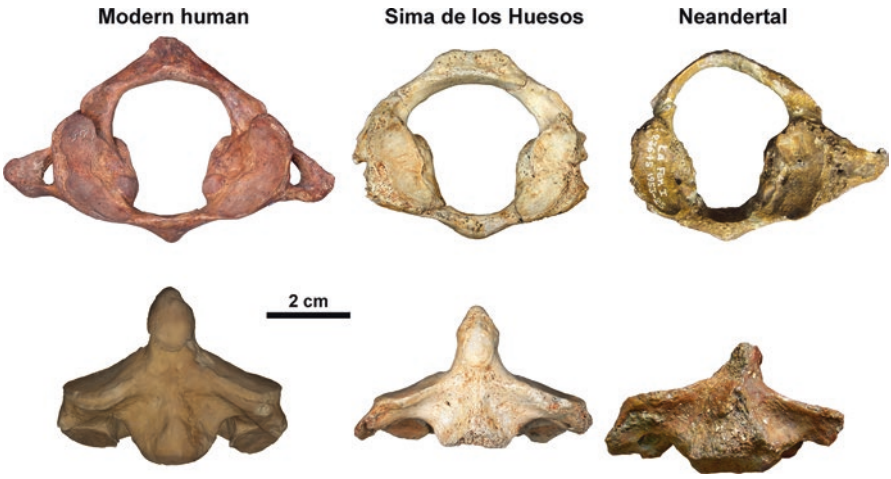

Fig. 9.1 Upper cervical spine (first cervical vertebra or atlas in cranial view on the top row and second cervical vertebra or axis in ventral view on the lower row): comparison of the morphology between recent modern humans, Sima de los Huesos (SH), and Neandertals. Note the more robust posterior arch in both modern humans compared to Neandertals and the relatively low and wide axes of the Neandertal lineage compared to that of modern humans. SH: the atlas is VC7, and the axis is VC4 and they do not belong to the same individual (Gómez-Olivencia et al. 2007). Neandertals: the atlas belongs to La Ferrassie 1 (Heim 1976; Gómez-Olivencia 2013a) and the axis to La Chapelle-aux-Saints 1 (LC1) (Boule 1913; Gómez-Olivencia 2013b). Note that the LC1 axis is eroded and it is also oriented in a different fashion compared to the axis from SH

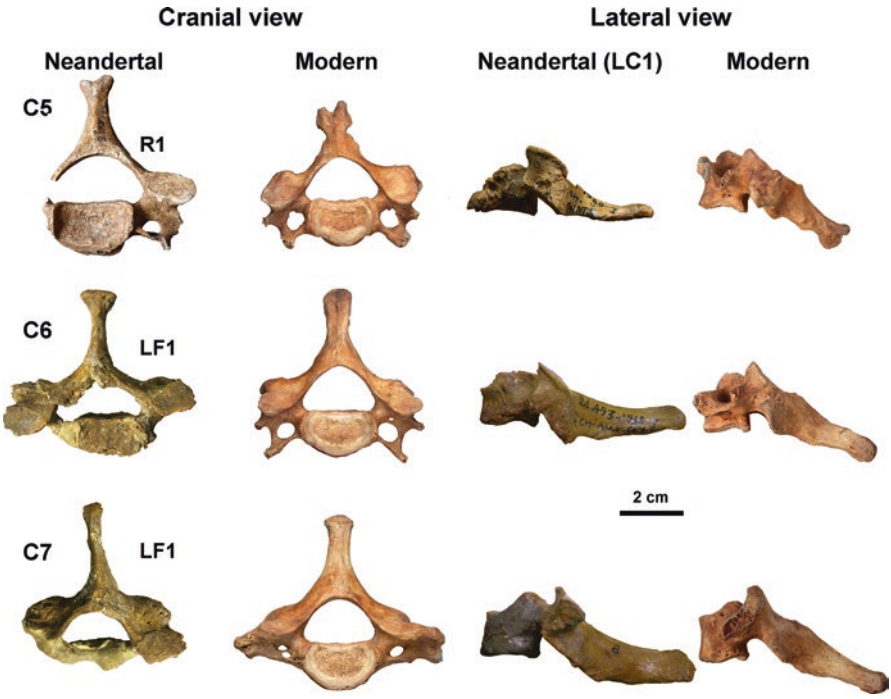

Fig. 9.2 The fifth, sixth, and seventh cervical vertebrae (C5–C7) of Neandertals compared to modern humans. Note the longer and more horizontally oriented spinous processes in Neandertals. Also note that LF1 shows some reconstruction problems (Gómez-Olivencia 2013a) and that LC1 has some pathologies (Trinkaus 1985). LC1 = La Chapelle-aux-Saints 1 (Boule 1913; Gómez-Olivencia 2013b); LF1 = La Ferrassie 1 (Heim 1976; Gómez-Olivencia 2013a); R1 = Regourdou 1 (Piveteau 1966; Gómez-Olivencia et al. 2013a)

Lumbar Spine

The maximum dorsoventral dimensions of the most complete lumbar vertebrae associated to Pelvis 1 individual are either similar to the mean of a modern human male sample (L4) or significantly longer than this modern human sample, and also longer than Neandertals (Bonmatí et al. 2010). The lumbar (costo)transverse processes are rarely preserved complete in the hominin fossil record, and SH is no exception. At least the L3 and L5 lumbar vertebrae display very long (longer even than Neandertals) and dorsolaterally oriented transverse processes (Bonmatí et al. 2010; Arsuaga et al. 2015). This dorsolateral orientation has been proposed as primitive for genus *Homo* and the lateral orientation that is present in Neandertals as derived (Been et al. 2010; Arsuaga et al. 2015; Gómez-Olivencia et al. 2017b). Regarding the lumbar lordosis of the SH hominins, the evidence from the vertebral wedging and the pelvic incidence suggests a low degree of curvature, similar to that present in Neandertals (Bonmatí et al. 2010).

In summary, the spinal morphology of this population is significantly different from that of modern humans, and while it shows some Neandertal derived features (e.g., a reduced lumbar lordosis), it also retains some primitive features like the orientation of the mid-lumbar transverse processes (dorsolateral). In other words, this population does not display the full suite of derived Neandertal features. This is consistent with the pattern of mosaic evolution also present in the cranium and other elements of the postcranium (Arsuaga et al. 2014, 2015).

9.2.5 Jebel Irhoud

The recent discovery of additional human fossils from the Middle Stone Age site of Jebel Irhoud (Morocco), with new dates of the associated stone tools and direct dates of human fossils, provides new information regarding the emergence of *H. sapiens* (Hublin et al. 2017; Richter et al. 2017). The study of the fossils from Jebel Irhoud reveals a mosaic morphology with features in the face skeleton, mandible, and dentition aligning these hominins with early or recent anatomically modern humans, but with neurocranial and endocranial morphology placing them with more primitive hominins (Hublin et al. 2017). This pattern is similar to that seen in the first representatives of the Neandertal lineage from Sima de los Huesos, where characteristics related to the masticatory apparatus evolved first, with maintenance of a more primitive neurocranium (Arsuaga et al. 2014). Dating of fire-heated flint lithic tools found during the new excavations of Jebel Irhoud has provided a weighted average age of 315 ± 34 ka, compatible with the age obtained from a tooth of the juvenile hominin Irhoud 3 mandible found in 1968 (286 ± 32 ka) obtained from the recalculated uranium series with electron spin resonance (Richter et al. 2017). The most recent excavations between 2004 and 2011 have reported the presence of a lumbar vertebra (Irhoud 18; ID = 2838) found in the initial cleaning in 2007 and a cervical vertebra (Irhoud 20; ID = 3751) found in the initial cleaning in 2009 (Hublin et al. 2017). These vertebrae have not been described in detail yet.

9.2.6 Jinniushan

The Middle Pleistocene (c. 260 ka BP) partial skeleton from Jinniushan (northeastern China) preserves six vertebrae: one cervical and five thoracic (Lü 1990; Tiemei et al. 1994; Rosenberg et al. 2006). This skeleton belonged to a female individual of c. 168 cm and 77.6 kg (Rosenberg et al. 2006). This individual has been assigned to cf. *H. heidelbergensis* (Lu et al. 2011), although this taxon is problematic (Rak et al. 2011). The study of this specimen is restricted to body size, body proportions, encephalization, and the pedal remains (Rosenberg et al. 2006; Lu et al. 2011), and thus, no detailed analysis of the vertebrae has yet been performed.

9.2.7 *Broken Hill*

A series of cranial and postcranial remains were recovered from a lead quarry between 1921 and 1925 at Broken Hill (then Northern Rhodesia; now Kabwe, Zambia), including the Broken Hill 1 cranium (Pycraft et al. 1928; Balzeau et al. 2017). While the faunal remains found with the human fossil remains suggested a date between 700 and 300 ka (Klein 1973), new ESR and U-series datings suggest a date of approximately 250–300 ka (Buck and Stringer 2015). Among the human fossil remains is a nearly complete sacrum (E.688) that was described in the original publication by Pycraft et al. (1928). This sacrum was compared to four modern human individuals. The description was limited with only the relatively small size of the sacrum compared to a Bantu individual, and its similarity to a female Australian individual was noted. In terms of shape, the Broken Hill's sacrum is dolichoheiric, i.e., relatively mediolaterally narrow relative to its craniocaudal length, as were two of the four individuals with which it was compared (Pycraft et al. 1928). To our knowledge, a methodologically modern statistical analysis has yet to be performed on this specimen.

9.3 Neandertals (*Homo neanderthalensis*)

Despite probably being the most abundant hominin fossil species, most of what is known regarding the Neandertal presacral spine is thanks to a handful of specimens classified either as males or that have a size compatible with being males: Kebara 2, La Chapelle-aux-Saints 1, La Ferrassie 1, Regourdou 1, and individuals 1 to 5 from Shanidar (Boule 1913; Piveteau 1966; Heim 1976, 1982a; Trinkaus 1983; Arensburg 1991; Been et al. 2010; Gómez-Olivencia et al. 2007, 2013a, b, 2017b; Gómez-Olivencia 2013a, b; Pomeroy et al. 2017). The Krapina remains (Gorjanović-Kramberger 1906) have been used as comparative samples in different studies (e.g., Gómez-Olivencia et al. 2007, 2013b) but have only recently been metrically described in detail (Trinkaus 2016). More recently, the thoracic spine remains from El Sidrón were described (Bastir et al. 2017). The Sima de las Palomas postcranial axial remains are fragmentary in nature (Walker et al. 2011a, b; Trinkaus et al. 2017) and some potentially important specimens, such as the La Quina H5 vertebral remains (Martin 1923), are currently lost.

Vertebral remains from several immature Neandertal individuals (e.g., Dederiyeh 1 and 2, Kebara 1, La Ferrassie 4, 5, 6, 8, Le Moustier 2, Mezmaiskaya, Roc-de-Marsal, Amud 7 (Smith and Arensburg 1977; Heim 1982b; Madre-Dupouy 1992; Kondo and Dodo 2003; Kondo and Ishida 2003; Golovanova et al. 1999; Maureille 2002; Been and Rak 2012; Gómez-Olivencia et al. 2015; Ponce de León et al. 2008) as well as from isolated remains (e.g., Harvati et al. 2013) are known. In most cases, the description of these remains is merely inventories due to the intrinsic difficulty of studying fragmentary juvenile remains. The recent description of the ontogeny of

the J1 individual from El Sidrón has, however, shown that, despite the estimated age at death of 7.7 years, based on dental histology, the atlas and mid-thoracic vertebrae remained at the 5- to 6-year stage of development and the endocranial features suggest an extended brain growth (Rosas et al. 2017).

9.3.1 Cervical Spine Morphology

Several studies have pointed to the presence of differences in basically each cervical vertebra (e.g., Gorjanović-Kramberger 1906; Boule 1913; Martin 1923; Stewart 1962; Piveteau 1966; Heim 1976; Arensburg 1991). Despite these differences, the view that Neandertals display "little indication of a form fundamentally different from that of modern human" (Stewart 1962: 152; see also Trinkaus 1983; Arensburg 1991) remained. The most in-depth study of the Neandertal cervical spine morphology was recently published by Gómez-Olivencia et al. (2013b). These researchers found significant differences between Neandertals and modern humans in each cervical vertebra. In the atlas, the vertebral foramen is dorsoventrally elongated paralleling the elongated foramen magnum present in Neandertals (Rak et al. 1994), the tubercles for the attachment of the transverse ligament are small, and the posterior tubercle is small. The atlantoaxial joint is mediolaterally larger (Fig. 9.1). The axis also shows a wider vertebral foramen and a small craniocaudal dimension (Fig. 9.1). The vertebrae are dorsoventrally longer in C4–C7, which could be related to the long (C5–C7) and very horizontally oriented spinous processes (C6–C7, but also likely in C5, although no comparison was done), although the differences in the spinous process length decrease in the caudal direction (Fig. 9.2). The vertebral bodies are craniocaudally smaller in the subaxial cervical spine, and together with the craniocaudal dimension of the axis, this results in a shorter neck than modern humans, although only in a marginally significant way ($0.1 > p > 0.05$). Also, the vertebral bodies of C3, C4, and potentially C5 are anteroposteriorly larger. All the subaxial cervical vertebrae (C3–C7) show wider vertebral foramina, potentially due to a more lateral position of the upper articular facets. The laminae are craniocaudally shorter in C3 but thicker in C5, C6, and possibly in C7. In the C3–C5 segment, the bituberculosity of the tip of the spinous process is variably present (25–40%), only one of five (20%) C6 vertebrae exhibit a partial bituberculosity, and no bituberculosity appears in C7. In modern humans, there are higher proportions of bituberculosity in all the subaxial cervical vertebrae.

Boule (1913) suggested the presence of a reduced cervical lordosis in Neandertals based on the orientation of both the articular facets and the spinous process of La Chapelle-aux-Saints 1 specimen. In modern humans, there is a significant relationship between the orientation of the foramen magnum and cervical lordosis (Been et al. 2014b). Based on the orientation of the foramen magnum in Neandertals, a cervical lordosis of around 26° has been proposed for this species, which would be significantly below that of modern humans (c. 35–37°; Been et al. 2017b).

The morphological differences found between Neandertals and modern humans are likely related to one another due to the strong integration present in the cervical subaxial spine (Arlegi et al. 2018). For example, the thickness in the Neandertal laminae has been proposed to be related to the loads applied to them (Pal and Routal 1996) and as the consequence of the weight transmission of the long and horizontal spinous process (Gómez-Olivencia et al. 2013b). From a biomechanical point of view, longer and more horizontal spinous processes increase the lever arm for the muscles and ligaments attached to them (i.e., the head and neck rotators and extensors; Shapiro 2007). These longer dorsoventral dimensions of the vertebrae, together with wider dimension of the cervical vertebrae (more laterally located articular pillars), and the slightly shorter neck indicate a more stable cervical spine in both sagittal and coronal planes. These differences with modern humans and within the Neandertal lineage (e.g., compared to SH) have been proposed to be related to neck biomechanics and to the head stabilization and equilibrium due to differences in skull shape (Gómez-Olivencia et al. 2011, 2013b).

9.3.2 Thoracic Spine

Unlike the cervical and lumbar spines, our knowledge of the Neandertal thoracic spine is restricted to the information provided by only a handful of studies. Bastir et al. (2017) presented 15 thoracic vertebral remains from El Sidrón (Asturias, Spain) and used geometric morphometrics (GMM) to understand the two best preserved remains, comparing them to other Neandertal specimens and to a modern human comparative sample. Based on centroid size comparison, despite the similarity in size between the El Sidrón sample and their modern human comparative sample, Bastir et al. (2017) suggested that Neandertals may have had larger T1 and probably T2s. The El Sidrón sample was found to be morphologically similar to other Neandertals, and the latter as a group differs from modern humans in several features, particularly in the central lower regions (T6–T10): more dorsally and cranially oriented transverse processes, less caudally (i.e., less vertically) oriented spinous processes, and anteroposteriorly and craniocaudally short vertebral bodies (Bastir et al. 2017). The more dorsal orientation of the transverse processes has also been demonstrated using traditional morphometrics (Gómez-Olivencia et al. 2018). In fact, due to the similar length of the transverse processes, their more dorsal orientation results in a smaller maximum transverse diameter (a measurement taken between the most lateral points of the transverse processes) in the T4–T8 of Kebara 2 (significantly smaller in T4, T7, and T8; Gómez-Olivencia et al. 2018). A greater dorsal orientation of the transverse processes has been interpreted to indicate a greater overall invagination of the spine within the ribcage (Bastir et al. 2017), which has been recently demonstrated in the 3D virtual reconstruction of the thorax of Kebara 2 (Gómez-Olivencia et al. 2018) (Fig. 9.3).

The thoracic kyphosis has been only estimated in one Neandertal individual: Kebara 2. Been et al. (2017a) used Goh et al.'s (1999) method, based on the ratio

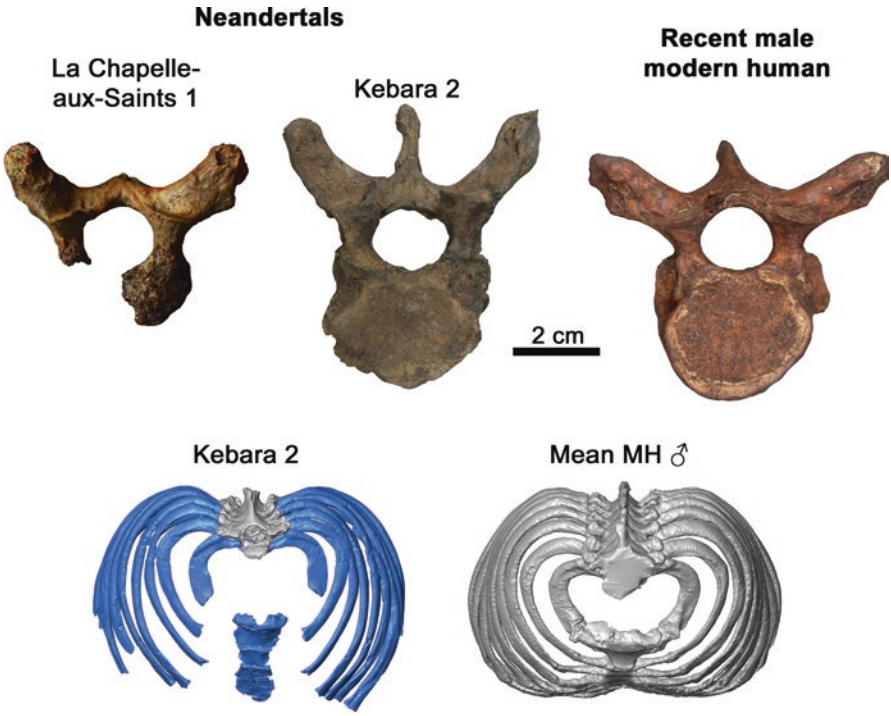

Fig. 9.3 Top: cranial view of eighth thoracic (T8) vertebrae of two Neandertal males and a modern human male. Note the more dorsally oriented transverse processes in Neandertals. This orientation is related to a more invaginated position of the vertebral column within the Neandertal thorax. Bottom: comparison of the reconstruction of the Kebara 2 thorax to the mean of modern male sample (Gómez-Olivencia et al. 2018) in which it is possible to see the more invaginated spine within the Neandertal thorax

between the anterior and the posterior craniocaudal heights of the vertebrae. This resulted in a value of kyphosis for this Neandertal individual of 44° which is below but near the mean for modern humans (Been et al. 2017a).

9.3.3 Lumbar Spine

The Neandertal lumbar spine shows significant differences with modern humans at all the vertebral levels (Been et al. 2010; Gómez-Olivencia et al. 2017b). The vertebral bodies are dorsoventrally large in L1–L5, but in L1–L3 they show smaller ventral craniocaudal dimensions (heights) (Fig. 9.4), resulting in more ventrally wedged shapes. This ventral wedging is related to a lower degree of lumbar lordosis (see below). The vertebral foramina in L4–L5 are larger dorsoventrally and, to a lesser extent, mediolaterally. Additionally, the union of the laminae is distinct in the

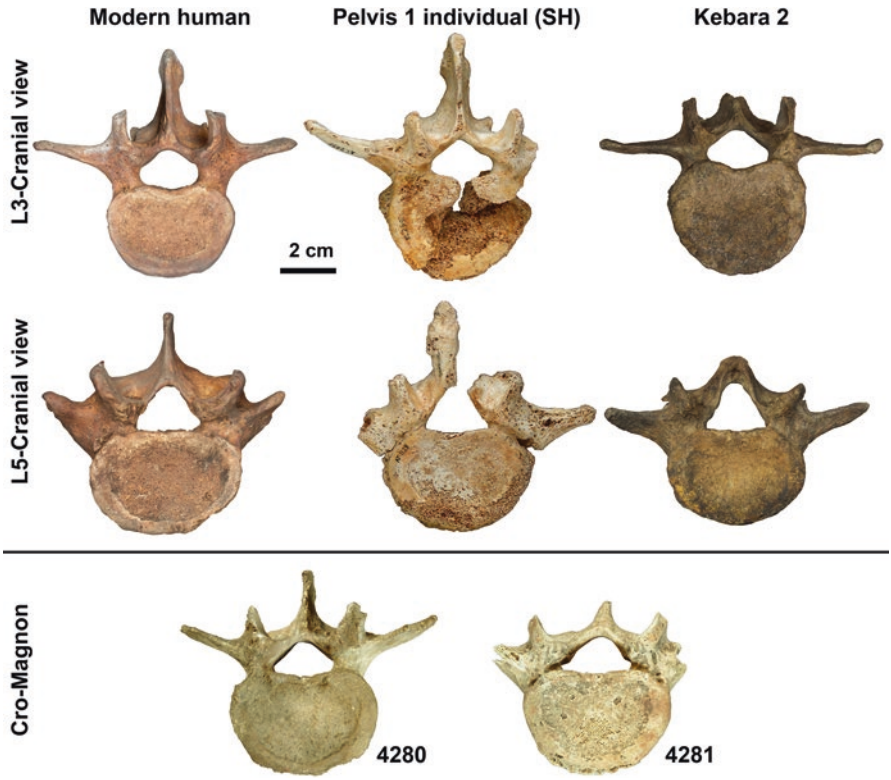

Fig. 9.4 Top: cranial view of the third (L3) and fifth (L5) lumbar vertebrae of a modern human compared to the Pelvis 1 individual from Sima de los Huesos (SH) and the Kebara 2 Neandertal. The transverse processes of the L3 of the SH Pelvis 1 individual are longer than those of Kebara 2, which are themselves longer than the modern human mean (Been et al. 2010; Bonmatí et al. 2010; Gómez-Olivencia et al. 2017b). In L2–L4, both modern humans and SH share the primitive pattern of a dorsolateral orientation of the transverse processes compared to the lateral orientation of Neandertals. In L5, Neandertals show an expanded dorsoventral vertebral foramen. Note that the SH Pelvis 1 individual shows several pathological lesions (Gómez-Olivencia 2009; Bonmatí et al. 2010; see Haeusler 2019). Bottom: 4280 (L4?) and 4281 (L5) lumbar vertebrae from Cro-Magnon. Note that the morphology of these vertebrae is similar to that of recent modern humans and morphologically different from Neandertals

Neandertal L5 (Fig. 9.4). The transverse processes (TPs) are longer in L4 and L5, and in the only individual in which all the TPs are present (Kebara 2), the maximum length occurs at L4 rather than at L3 as in modern humans. The TPs are more laterally oriented in L2–L4 and, in Kebara 2, are also more cranially oriented in L1–L3. The upper articular facets are more sagittally oriented in L2–L3, which increases the minimum distance between the facets. The neural arches are wider in all the lumbar vertebrae (L1–L5) and craniocaudally longer in L1–L3, and spinous processes are craniocaudally smaller in L1 but longer in L2–L3.

Regarding lumbar curvature, Weber and Pusch (2008) suggested, based on the lumbar spines of Kebara 2 and Shanidar 3 Neandertal individuals, the presence of a kyphotic lumbar spine as the natural anatomy of these two Neandertals. This assertion was based on the comparison of the ventral and dorsal craniocaudal dimensions (heights) of these two specimens to modern humans (Weber and Pusch 2008); however, no quantitative method was used to calculate the lumbar lordosis (LL). More recently, several methods have been used in the reconstruction of the LL of Neandertals. First, Been et al. (2012) used the correlation between LL and the angle of the lower articular processes to estimate the LL of three Neandertal individuals: La Chapelle-aux-Saints 1, Kebara 2, and Shanidar 3 (average: 29° ± 4), significantly lower LL than modern humans (51° ± 11) (Been et al. 2012). A second study (Been et al. 2014a) used pelvic incidence (PI) to estimate LL based in the chain of correlation between these two parameters (Boulay et al. 2006). The PI (measured as explained by Peleg et al. 2007) and lumbar lordosis of 47 modern humans and 8 nonhuman hominoids were measured, from which regression formulae were derived, and this regression was later applied to the fossil hominins. From this method, a lordosis angle between 29° and 36° (depending on the formula used) was calculated for Kebara 2 (Been et al. 2014a), a result consistent with previous estimations (Been et al. 2012) (Fig. 9.5).

9.3.4 Sacrum

Despite the argument that there is no difference between the Neandertal and modern human sacrum (e.g., Pap et al. 1996), some studies have pointed out significant differences in the Neandertal sacral morphology when compared to that of modern and early *H. sapiens*. First, Neandertals show an anteroposteriorly, and in some individuals also mediolaterally, large canal (Rmoutilová et al. in review), likely related to the dorsoventrally large canal present in L5 (see above). Second, it has been proposed that Neandertals show a relatively narrow sacrum in relation to their pelvic inlet circumferences (Fraipont and Lohest 1887; Boule 1913; Tague 1992). Third, Neandertals show a more vertically oriented sacrum due to a reduced pelvic incidence, which is related to lower lumbar lordosis (Been et al. 2014a). Fourth, in some sacra, a large sacral hiatus has been noted (e.g., Shanidar 1 and Shanidar 4; Trinkaus 1983). Finally, a more ventral relative position of the first sacral vertebra within the pelvic inlet has been proposed (Rak 1991; Gómez-Olivencia et al. 2018). The study of additional sacra should provide new information in the near future (Toussaint et al. in press; Rmoutilová et al. submitted). It is important to note that future study of the sacrum should explore this bone not only in isolation but also as part of the pelvic ring and as the base for the rest of the spine.

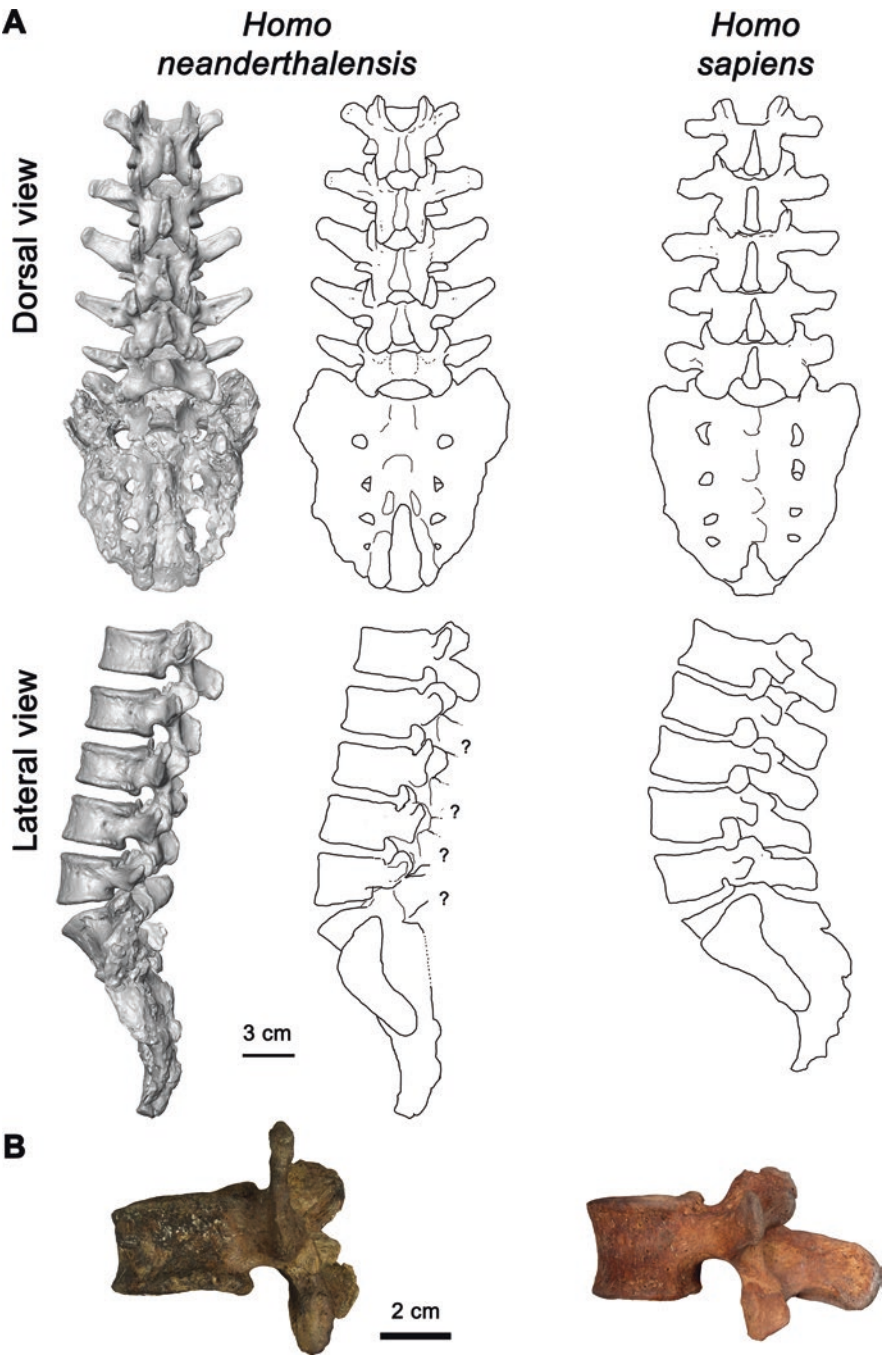

Fig. 9.5 Morphological comparison between Neandertals and modern humans. (**a**) Dorsal and lateral views of the 3D virtual reconstruction of the lumbar spine and sacrum of Kebara 2 compared to a modern human (Been et al. 2017a; Gómez-Olivencia et al. 2017b). Note the more vertically oriented sacrum, the lower lumbar lordosis of Kebara 2, and the cranially oriented transverse processes. (**b**) Third lumbar vertebra (L3) of Kebara 2 compared to a modern human L3. Note the more ventrally wedged vertebral body of Kebara 2 compared to modern humans

9.3.5 Coccygeal Vertebrae

The fossil record of Neandertal coccyx is limited to the first coccygeal vertebrae (Cx1) from a handful of Neandertal individuals: La Ferrassie 1, Shanidar 4, and Kebara 2 (Heim 1976; Trinkaus 1983; Arensburg 1991; Gómez-Olivencia 2013a). The analysis of the Cx1 of Shanidar 4 suggests that this vertebra is similar to that of modern humans in size and morphology (Trinkaus 1983). The morphology and evolution of the coccyx has been overlooked by scholars for many years and perhaps it is time to evaluate the morphology of this bone.

9.4 Pre-MIS 3 Fossil *Homo sapiens*

The fossil record of the late Middle Pleistocene and Upper Pleistocene *H. sapiens* is relatively abundant (e.g., Dolní Věstonice, Pavlov, Cro-Magnon, Gough's cave, El Mirón, Sunghir), and it is generally described as falling within the variation of recent *H. sapiens* (Vallois and Billy 1965; Sládek et al. 2000; Holliday 2006; Churchill and Holliday 2002; Been et al. 2010; Trinkaus et al. 2014; Carretero et al. 2015). However, older remains from our species are restricted to a handful of sites. Here, we will briefly enumerate the evidence from the Omo and Klasies River Mouth sites and discuss the vertebral remains from Skhul and Qafzeh.

The Omo valley (Ethiopia) has yielded one of the oldest *Homo sapiens* skeleton, the Omo I skeleton, dated around 195 ka (Pearson et al. 2008 and references therein). Seventeen vertebral fragments, including six cervical fragments, nine thoracic fragments, and two lumbar fragments, have been associated and, to our notice, just preliminarily described by Pearson et al. (2008).

The Klasies River main site is located between Plettenberg Bay and Cape St. Francis, on the southern coast of South Africa (Rightmire and Deacon 2001). The oldest (LBS) levels that have yielded two fragmentary human maxillae are dated to approximately 110 ka (MIS 5d), while most of the human remains have been recovered in the overlying (SAS) member with dates in excess of 90 ka (MIS 5c) (Grün et al. 1990). Rightmire and Deacon (1991) preliminarily described a lumbar vertebra (KRM 20927A/SAM-AP 6113A) from Cave 1 SAS member. Grine et al. (1998) provided evidence of an atlas (C1) fragment that had been identified among the faunal remains.

The Israeli site of Skhul is located in Nahal Mearot, adjacent to Tabun cave, on the western slopes of Mount Carmel, facing the Mediterranean Sea. The Skhul skeletons belong to *H. sapiens* dated around 100–135 ka (Stringer et al. 1989; Grün et al. 2005). Studies of their skeletal morphologies demonstrate close similarities to the hominins from Qafzeh cave in the Lower Galilee, Israel. At least four individuals from Skhul retain parts of their vertebral spine—Skhul 1, 4, 5, and 7. Skhul 5 is the most complete with an intact cervical spine (C1–C7) (Fig. 9.6), dorsal parts of the thoracic vertebrae T1–T12, and the lamina and transverse processes of the five

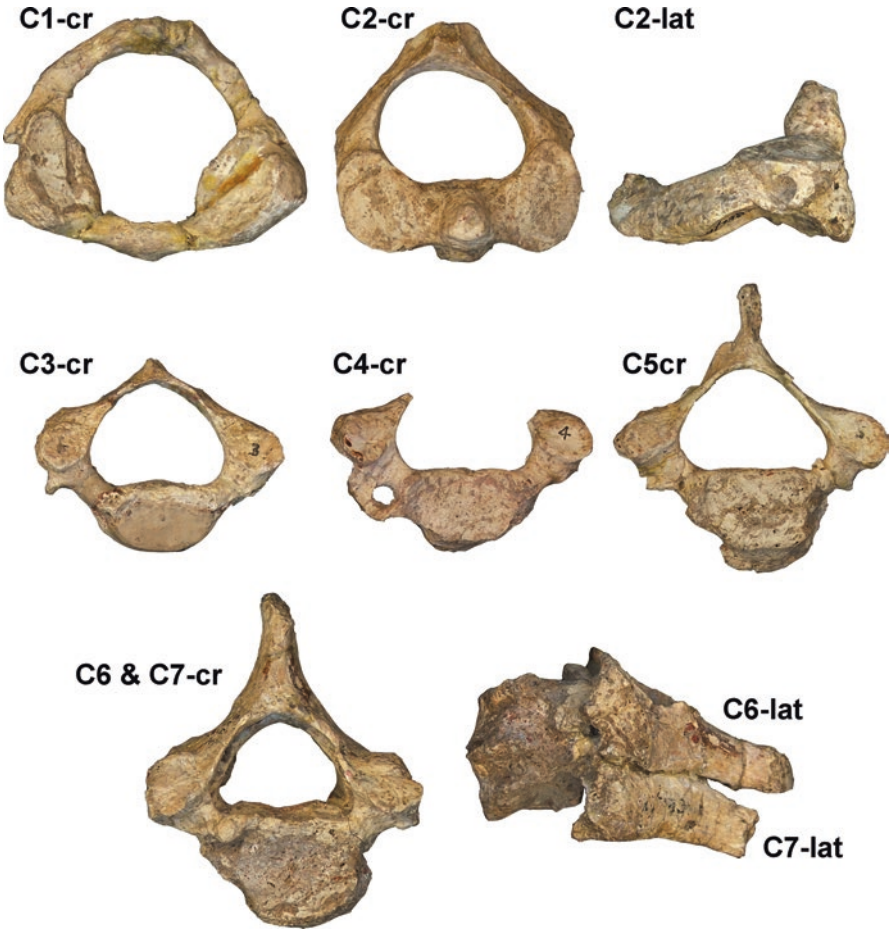

Fig. 9.6 The cervical vertebrae of the fossil *Homo sapiens* Skhul 5. The asymmetry in the vertebral foramen of the C2 vertebra is artificial due to excessive erosion produced when the fossils were liberated from the matrix (Gómez-Olivencia, personal assessment). Note that the sixth (C6) and seventh (C7) cervical vertebrae are still connected via matrix, which makes it difficult to measure the orientation of the spinous process. cr = cranial; lat = lateral view

lumbar vertebrae L1–L5 (McCown and Keith 1939). The main feature highlighted by McCown and Keith (1939) concerning the vertebral column of the Skhul individuals is related to the craniocaudal shortness of all the vertebral vertebrae, especially when the length of the long limbs is taken into account.

The site of Qafzeh is near the city of Nazareth in the Lower Galilee, Israel, and it has yielded the remains of several Mousterian *H. sapiens* individuals with a chronology in the range of 90–130 ka BP (Schwarcz et al. 1988; Valladas et al. 1988). The human remains of seven adults (Q 3, 5, 6, 7, 8, 9, 25) and several juveniles (Q 4, 10, 11, 12, 13, 14, 15, 21, 22), as well as a few isolated bones and teeth, were

found during the two series of excavations at the site (Vandermeersch 1981; Tillier 1999). Vandermeersch (1981) studied the adult individuals and Tillier (1999) studied the infants from Qafzeh. Few vertebrae are preserved within the Qafzeh adults (Vandermeersch 1981): Qafzeh 3 (Q3) is the most complete despite the fact that not all the vertebrae are represented and none of those represented is complete. In Q9, the vertebral column is complete but crushed, and only a few cervical elements can be measured. Finally, Q8 preserves only vertebral fragments (Vandermeersch 1981).

9.4.1 Cervical Spine

McCown and Keith (1939) described minor anatomical differences between the cervical spines of the Skhul hominins and those of recent modern humans. First, they argue that the more horizontal articular process in the Skhul hominins (compared to modern humans) created strong lateral columns, with more weight bearing on the articular processes and less mobility. They also describe the cervical spine as craniocaudally short with the presence of long and horizontal spinous process, and a small cervical lordosis compared to modern humans.

More recent research on the spine of Skhul/Qafzeh hominins variably supported or contradicted the findings of McCown and Keith (1939). Arensburg et al. (1990) demonstrated a craniocaudally shorter cervical spine in Skhul 5 compared to modern humans. Trinkaus (1995), on the other hand, found similarity between the shapes of the cervical vertebrae of the Skhul/Qafzeh hominins and those of modern humans. The length of the spinous process of the fifth cervical vertebrae of Qafzeh 3 (19 mm) and of Skhul 5 (17.5 mm) is similar to those of recent modern humans and smaller than those of Neandertals (Vandermeersch 1981). Whether a short spinous process in C5 is primitive or derived within genus *Homo* is currently unknown. Been et al. (2017b) calculated the cervical lordosis based on the orientation of the foramen magnum. The calculated cervical lordosis for Skhul 5 between the foramen magnum and the seventh cervical vertebra is 39.5°, close to the mean lordosis found in modern humans (38.6° ± 10.6). Another interesting finding involves the spine of a child from Qafzeh. Tillier et al. (2001) described a relatively narrow cervical spinal canal in Qafzeh 12, a 3-year-old toddler that probably suffered from hydrocephalus.

9.4.2 Lumbar Spine

Generally, the lumbar spine of early *H. sapiens* resembles that of recent modern humans. McCown and Keith (1939) describe an overall short lumbar spine with lumbar lordosis similar to that of recent modern humans. They describe long and horizontal spinous processes in the five lumbar vertebrae compared to modern humans. They also describe the presence of kyphotic wedging of L4 of Skhul 4 and

7. Been et al. (2010) found that the vertebral wedging of late Pleistocene *H. sapiens* (Cro-Magnon 1, 2, and 3, and Skhul 4) resembles that of modern humans, with the exception of kyphotic wedging in L4 of Skhul 4. The length and orientation of the transverse processes and that of the laminae in Cro-Magnon 1 and 3 (Fig. 9.4), as well as in Skhul 4 and 5, appear to resemble that of modern humans. The amount of lumbar lordosis calculated for Skhul 4, based on pelvic incidence, is 58°, and that of Cro-Magnon 1 and 3 are 44° and 64°, respectively, based on the angle of the lower articular processes (Been et al. 2012, 2017). The average lordosis for fossil *H. sapiens* is 53.3° ± 8.4°, which is within the normal range for modern humans (51.2° ± 11.1), although slightly higher than the mean value.

Nonetheless, the vertebral spine of early *H. sapiens* remains understudied. A thorough examination of the vertebral spines of the Omo, Klasies River Mouth, and Skhul/Qafzeh hominins, with traditional and new methodologies, is needed in order to enhance our understanding of spinal morphology in *H. sapiens*.

9.5 Final Considerations

In the last two decades, substantial changes in the way the vertebral column is studied have occurred, due to a combination of new fossil evidence and new methodological approaches to this anatomical region. This has resulted in a plethora of new information that suggests the presence of at least two different morphologies within genus *Homo* during the Middle and Late Pleistocene: that of the Neandertal lineage, with evolutionary changes between the Middle and Late Pleistocene demes/chronospecies, and that of the *H. sapiens*. The evolution of *H. sapiens* is not well understood due to the near absence of a Middle Pleistocene fossil record for populations ancestral to our species and to the lack of application of new research methods to the current hypodigm of spinal remains of early *H. sapiens*. A large gap in the spinal record between *H. erectus* and the Middle Pleistocene populations also exists, but this gap may be partially filled in once the TD6 level of Gran Dolina is excavated over a larger surface. The distinct morphology of Neandertals in their cervical and lumbar spine and, to a lesser extent, in the thoracic spine and sacrum has been documented and characterized. Most of what is currently known about the Neandertal spine is, however, based on specimens which have been either classified as males or have sizes compatible with them being males. Studies in modern humans have demonstrated the presence of sexual dimorphism expressed in both size and shape. For example, male thoracic vertebrae tend to show more dorsally oriented transverse processes and have relatively larger vertebral bodies in the upper and lower thoracic vertebrae than females (Bastir et al. 2014). Additionally, modern human females seem to have more lumbar lordosis which would compensate for the shift of the center of mass during pregnancy. In fact, this larger degree of lumbar lordosis present in females appears to have been already present in *Australopithecus africanus* (Whitcome et al. 2007). Given this pattern in modern humans (and probably in *A. africanus*), it would be interesting to know whether Neandertals (as well as in their

Middle Pleistocene ancestors), who show (derived) lower lumbar lordosis compared to *H. erectus*, also exhibit the same pattern of sexual dimorphism as recent humans in this feature. In summary, despite being the fossil human species with the most fossil evidence, large gaps in understanding Neandertal spinal anatomy exist. Even less well understood is the morphology of the spine of early *H. sapiens*. The description of new fossil material and the application of new technologies promise a near future full of important results.

Acknowledgments This work has received support from the Spanish Ministerio de Ciencia y Tecnología (Project: CGL-2015-65387-C3-2-P, MINECO/FEDER), from the Spanish Ministerio de Ciencia, Innovación y Universidades (Project: PGC2018-093925-B-C33) and from the European Community Research Infrastructure Action (SYNTHESYS Project; http://www.synthesys.info/; FP6 "Structuring the European Research Area" Programme; project FR-TAF-109). The first author is part of the Research Group IT1418-19 from the Eusko Jaurlaritza-Gobierno Vasco. We would like to thank the rest of the authors of this book for fruitful discussions and also to M. Arlegi, A. García, O. Pearson, J.M. Carretero, J.L. Arsuaga, and the Atapuerca Research Team. Thanks to M. Meyer and P. Kramer for their comments on a previous version of this paper.

References

Andrews P, Fernández-Jalvo Y (1997) Surface modifications of the Sima de los Huesos fossil humans. J Hum Evol 33:191–217

Aranburu A, Arsuaga JL, Sala N (2017) The stratigraphy of the Sima de los Huesos (Atapuerca, Spain) and implications for the origin of the fossil hominin accumulation. Quat Int 433(Part A): 5–21

Arensburg B (1991) The vertebral column, thoracic cage and hyoid bone. In: Bar-Yosef O, Vandermeersch B (eds) Le squelette moustérien de Kébara 2. Éditions du CNRS, Paris, pp 113–147

Arensburg B, Schepartz LA, Tillier A-M, Vandermeersch B, Rak Y (1990) A reappraisal of the anatomical basis for speech in Middle Palaeolithic hominids. Am J Phys Anthropol 83:137–146

Arlegi M, Gómez-Robles A, Gómez-Olivencia A (2018) Morphological integration in the gorilla, chimpanzee, and human neck. Am J Phys Anthropol 166:408–416

Arsuaga JL, Carretero JM, Gracia A, Martínez I (1990) Taphonomical analysis of the human sample from the Sima de los Huesos Middle Pleistocene site (Atapuerca/Ibeas, Spain). Hum Evol 5:505–513

Arsuaga JL, Martínez I, Gracia A, Carretero JM, Carbonell E (1993) Three new human skulls from the Sima de los Huesos Middle Pleistocene site in Sierra de Atapuerca, Spain. Nature 362:534–537

Arsuaga JL, Martínez I, Gracia A, Carretero JM, Lorenzo C, Garcia N, Ortega AI (1997a) Sima de los Huesos (Sierra de Atapuerca, Spain). The site. J Hum Evol 33:109–127

Arsuaga JL, Martínez I, Gracia A, Lorenzo C (1997b) The Sima de los Huesos crania (Sierra de Atapuerca, Spain). A comparative study. J Hum Evol 33:219–281

Arsuaga JL, Martínez I, Arnold LJ, Aranburu A, Gracia-Téllez A, Sharp WD, Quam RM, Falguères C, Pantoja-Pérez A, Bischoff J, Poza-Rey E, Parés JM, Carretero JM, Demuro M, Lorenzo C, Sala N, Martinón-Torres M, García N, Alcázar De Velasco A, Cuenca-Bescós G, Gómez-Olivencia A, Moreno D, Pablos A, Shen C-C, Rodríguez L, Ortega AI, García R, Bonmatí A, Bermúdez De Castro JM, Carbonell E (2014) Neandertal roots: cranial and chronological evidence from Sima de los Huesos. Science 344:1358–1363

Arsuaga JL, Carretero J-M, Lorenzo C, Gómez-Olivencia A, Pablos A, Rodríguez L, García-González R, Bonmatí A, Quam RM, Pantoja-Pérez A, Martínez I, Aranburu A, Gracia-Téllez A, Poza-Rey E, Sala N, García N, Alcázar De Velasco A, Cuenca-Bescós G, Bermúdez De Castro JM, Carbonell E (2015) Postcranial morphology of the middle Pleistocene humans from Sima de los Huesos, Spain. Proc Natl Acad Sci U S A 112:11524–11529

Balzeau A, Buck LT, Albessard L, Becam G, Grimaud-Hervé D, Rae TC, Stringer CB (2017) The Internal Cranial Anatomy of the Middle Pleistocene Broken Hill 1 Cranium. PaleoAnthropology 2017:107–138

Bastir M, Higuero A, Ríos L, García Martínez D (2014) Three-dimensional analysis of sexual dimorphism in human thoracic vertebrae: implications for the respiratory system and spine morphology. Am J Phys Anthropol 155:513–521

Bastir M, García Martínez D, Rios L, Higuero A, Barash A, Martelli S, García Tabernero A, Estalrrich A, Huguet R, De La Rasilla M, Rosas A (2017) Three-dimensional morphometrics of thoracic vertebrae in Neandertals and the fossil evidence from El Sidrón (Asturias, Northern Spain). J Hum Evol 108:47–61

Bastir M, Torres-Tamayo N, Palancar CA, Zlolniski SL, García-Martínez D, Riesco-López A, Vidal D, Blanco-Pérez E, Barash A, Nalla S, Martelli S, Sanchis-Gimeno JL, Schlager S (2019) Geometric morphometric studies in the human spine. In: Been E, Gómez-Olivencia A, Kramer PA (eds) Spinal evolution: morphology, function, and pathology of the spine in hominoid evolution. Springer, New York, pp 360–386

Been E, Rak Y (2012) Amud 7, a Neandertal infant from Amud Cave, Israel. Am J Phys Anthropol 147(S54):94

Been E, Peleg S, Marom A, Barash A (2010) Morphology and function of the lumbar spine of the Kebara 2 Neandertal. Am J Phys Anthropol 142:549–557

Been E, Gómez-Olivencia A, Kramer PA (2012) Lumbar lordosis of extinct hominins. Am J Phys Anthropol 147:64–77

Been E, Gómez-Olivencia A, Kramer PA (2014a) Brief Communication: Lumbar lordosis in extinct hominins: implications of the pelvic incidence. Am J Phys Anthropol 154:307–314

Been E, Shefi S, Zilka LR, Soudack M (2014b) Foramen magnum orientation and its association with cervical lordosis: a model for reconstructing cervical curvature in Archeological and extinct hominin specimens. Advances Anthropol 4:133–140

Been E, Gómez-Olivencia A, Kramer PA, Barash A (2017a) 3D reconstruction of spinal posture of the Kebara 2 Neandertal. In: Marom A, Hovers E (eds) Human paleontology and prehistory: contributions in honor of Yoel Rak. Springer, Heidelberg, pp 239–251

Been E, Gómez-Olivencia A, Shefi S, Soudack M, Bastir M, Barash A (2017b) Evolution of spinopelvic alignment in hominins. Anat Rec 300:900–911

Bermúdez De Castro JM, Arsuaga JL, Carbonell E, Rosas A, Martínez I, Mosquera M (1997) A hominid from the Lower Pleistocene of Atapuerca, Spain: possible ancestor to neandertals and modern humans. Science 276:1392–1395

Bermúdez De Castro JM, Martinón-Torres M, Lozano M, Sarmiento S, Muela A (2004) Paleodemography of the Atapuerca-Sima de los Huesos hominin sample: a revision and new approaches to the paleodemography of the european Middle Pleistocene population. J Anthropol Res 60:5–26

Bermúdez-De-Castro J-M, Martinón-Torres M, Martín-Francés L, Modesto-Mata M, Martínez-De-Pinillos M, García C, Carbonell E (2017) *Homo antecessor*: the state of the art eighteen years later. Quat Int 433(Part A):22–31

Boaz NT, Ciochon RL, Xu Q, Liu J (2004) Mapping and taphonomic analysis of the *Homo erectus* loci at Locality 1 Zhoukoudian, China. J Hum Evol 46:519–549

Bonmatí A, Gómez-Olivencia A, Arsuaga JL, Carretero JM, Gracia A, Martínez I, Lorenzo C, Bermúdez De Castro JM, Carbonell E (2010) Middle Pleistocene lower back and pelvis from an aged human individual from the Sima de los Huesos site, Spain. Proc Natl Acad Sci U S A 107:18386–18391

Boulay C, Tardieu C, Hecquet J, Benaim C, Mouilleseaux B, Marty C, Prat-Pradal D, Legaye J, Duval-Beaupère G, Pélissier J (2006) Sagittal alignment of spine and pelvis regulated by pelvic incidence: standard values and prediction of lordosis. Eur Spine J 15:415–422

Boule M (1913) L'homme fossile de la Chapelle aux Saints. Annales de Paléontologie 6:111–172. 7:21–56, 85–192; 8: 1–70

Buck LT, Stringer CB (2015) A rich locality in South Kensington: the fossil hominin collection of the Natural History Museum, London. Geol J 50:321–337

Carbonell E, Bermúdez De Castro JM, Arsuaga JL, Díez JC, Rosas A, Cuenca-Bescós G, Sala R, Mosquera M, Rodríguez XP (1995) Lower pleistocene hominids and artefacts from Atapuerca-TD6 (Spain). Science 269:826–830

Carbonell E, Mosquera M, Ollé A, Rodríguez XP, Sala R, Vergès JM, Arsuaga JL, Bermúdez De Castro JM (2003) Les premiers comportements funéraires auraient-ils pris place à Atapuerca, il y a 350 000 ans? Anthropologie 107:1–14

Carretero JM, Arsuaga JL, Lorenzo C (1997) Clavicles, scapulae and humeri from the Sima de los Huesos site (Sierra de Atapuerca, Spain). J Hum Evol 33:357–408

Carretero JM, Lorenzo C, Arsuaga JL (1999) Axial and appendicular skeleton of *Homo antecessor*. J Hum Evol 37:459–499

Carretero JM, Quam RM, Gómez-Olivencia A, Castilla M, Rodríguez L, García-González R (2015) The Magdalenian human remains from El Mirón Cave, Cantabria (Spain). J Archaeol Sci 60:10–27

Churchill SE, Holliday TW (2002) Gough's Cave 1 (Somerset, England): a study of the axial skeleton. Bulletin of The Natural History Museum Geology Series 58:1–11

Cuenca-Bescós G, Laplana Conesa C, Canudo JI, Arsuaga JL (1997) Small mammals from Sima de los Huesos. J Hum Evol 33:175–190

De Lumley M-A (2015) L'homme de Tautavel. Un *Homo erectus* européen évolué. *Homo erectus tautavelensis*. Anthropologie 119:303–348

Duval M, Grün R, Parés JM, Martín-Francés L, Campaña I, Rosell J, Shao Q, Arsuaga JL, Carbonell E, Bermúdez De Castro JM (2018) The first direct ESR dating of a hominin tooth from Atapuerca Gran Dolina TD-6 (Spain) supports the antiquity of Homo antecessor. Quat Geochronol 47:120–137

Fernández-Jalvo Y, Díez JC, Bermúdez De Castro JM, Carbonell E, Arsuaga JL (1996) Evidence of early cannibalism. Science 271:277–278

Fernández-Jalvo Y, Carlos Díez J, Cáceres I, Rosell J (1999) Human cannibalism in the Early Pleistocene of Europe (Gran Dolina, Sierra de Atapuerca, Burgos, Spain). J Hum Evol 37:591–622

Fraipont J, Lohest M (1887) La race humaine de Néanderthal ou de Canstadt en Belgique. Arch Biol 7:587–757

Franciscus RG, Churchill SE (2002) The costal skeleton of Shanidar 3 and a reappraisal of Neandertal thoracic morphology. J Hum Evol 42:303–356

García N, Arsuaga JL (2011) The Sima de los Huesos (Burgos, northern Spain): palaeoenvironment and habitats of *Homo heidelbergensis* during the Middle Pleistocene. Quat Sci Rev 30:1413–1419

García N, Arsuaga JL, Torres T (1997) The carnivore remains from the Sima de los Huesos Middle Pleistocene site (Sierra de Atapuerca, Spain). J Hum Evol 33:155–174

Goh S, Price RI, Leedman PJ, Singer KP (1999) The relative influence of vertebral body and intervertebral disc shape on thoracic kyphosis. Clin Biomech 14:439–448

Goldberg P, Weiner S, Bar-Yosef O, Xu Q, Liu J (2001) Site formation processes at Zhoukoudian, China. J Hum Evol 41:483–530

Golovanova LV, Hoffecker JF, Kharitonov VM, Romanova GP (1999) Mezmaiskaya cave: a neanderthal occupation in the Northern caucasus. Curr Anthropol 40:77–86

Gómez-Olivencia A (2009) Estudios paleobiológicos sobre la columna vertebral y la caja torácica de los humanos fósiles del Pleistoceno, con especial referencia a los fósiles de la Sierra de Atapuerca. (PhD thesis), Universidad de Burgos, Burgos

Gómez-Olivencia A (2013a) The presacral spine of the La Ferrassie 1 Neandertal: a revised inventory. Bulletins et Mémoires de la Societé d'Anthropologie de Paris 25:19–38
Gómez-Olivencia A (2013b) Back to the old man's back: reassessment of the anatomical determination of the vertebrae of the Neandertal individual of La Chapelle-aux-Saints. Annales de Paléontologie 99:43–65
Gómez-Olivencia A, Arsuaga JL (2015) The vertebral column and thorax in the Middle Pleistocene: the case of the Sima de los Huesos. Am J Phys Anthropol 156(S60):155
Gómez-Olivencia A, Carretero JM, Arsuaga JL, Rodríguez-García L, García-González R, Martínez I (2007) Metric and morphological study of the upper cervical spine from the Sima de los Huesos site (Sierra de Atapuerca, Burgos, Spain). J Hum Evol 53:6–25
Gómez-Olivencia A, Arsuaga JL, Carretero JM, Gracia A, Martínez I (2011) A complete neck from Sima de los Huesos and the evolution of the cervical spine in Neandertal lineage. Proceedings of the First annual meeting, European Society for the study of Human Evolution:41
Gómez-Olivencia A, Couture-Veschambre C, Madelaine S, Maureille B (2013a) The vertebral column of the Regourdou 1 Neandertal. J Hum Evol 64:582–607
Gómez-Olivencia A, Been E, Arsuaga JL, Stock JT (2013b) The Neandertal vertebral column 1: the cervical spine. J Hum Evol 64:608–630
Gómez-Olivencia A, Crevecoeur I, Balzeau A (2015) La Ferrassie 8 Neandertal child reloaded: New remains and re-assessment of the original collection. J Hum Evol 82:107–126
Gómez-Olivencia A, Arsuaga JL, Bermúdez De Castro JM, Carbonell E (2017a) The vertebral column of the Gran Dolina-TD6 and Sima de los Huesos hominins: new remains and new results. Am J Phys Anthropol 162(S64):197
Gómez-Olivencia A, Arlegi M, Barash A, Stock JT, Been E (2017b) The Neandertal vertebral column 2: the lumbar spine. J Hum Evol 106:84–101
Gómez-Olivencia A, Barash A, García-Martínez D, Arlegi M, Kramer P, Bastir M, Been E (2018) 3D virtual reconstruction of the Kebara 2 Neandertal thorax. Nat Commun 9:4387
Gómez-Robles A, Bermúdez De Castro JM, Arsuaga J-L, Carbonell E, Polly PD (2013) No known hominin species matches the expected dental morphology of the last common ancestor of Neanderthals and modern humans. Proc Natl Acad Sci U S A 110:18196–18201
Gorjanović-Kramberger K (1906) Der diluviale Mensch von Krapina. C.W. Kreidel's verlag, Wiesbaden
Grine FE, Pearson OM, Klein RG, Rightmire GP (1998) Additional human fossils from Klasies River Mouth, South Africa. J Hum Evol 35:95–107
Grün R, Shackleton NJ, Deacon HJ (1990) Electron-spin-resonance dating of tooth enamel from Klasies River Mouth. Curr Anthropol 31:427–432
Grün R, Huang P-H, Wu X, Stringer CB, Thorne AG, Mcculloch M (1997) ESR analysis of teeth from the palaeoanthropological site of Zhoukoudian, China. J Hum Evol 32:83–91
Grün R, Stringer C, Mcdermott F, Nathan R, Porat N, Robertson S, Taylor L, Mortimer G, Eggins S, Mcculloch M (2005) U-series and ESR analyses of bones and teeth relating to the human burials from Skhul. J Hum Evol 49:316–334
Haeusler M (2019) Spinal pathologies in fossil hominins. In: Been E, Gómez-Olivencia A, Kramer PA (eds) Spinal evolution: morphology, function, and pathology of the spine in hominoid evolution. Springer, New York, pp 213–246
Harvati K, Darlas A, Bailey SE, Rein TR, El Zaatari S, Fiorenza L, Kullmer O, Psathi E (2013) New Neanderthal remains from Mani peninsula, Southern Greece: The Kalamakia Middle Paleolithic cave site. J Hum Evol 64:486–499
Heim J-L (1976) Les Hommes fossiles de la Ferrassie. I. Le gisement. Les squelettes adultes (crâne et squelette du tronc). Masson, Paris
Heim J-L (1982a) Les hommes fossiles de La Ferrassie. II. In: Les squelettes d'adultes: squelettes des membres, Paris, Masson
Heim J-L (1982b) Les enfants néandertaliens de la Ferrassie. Étude anthropologique et analyse ontogénique des hommes de Néandertal. Masson, Paris

Holliday TW (2006) The vertebral columns. In: Trinkaus E, Svoboda J (eds) Early Modern Human Evolution in Central Europe. The People of Dolní Věstonice and Pavlov. Oxford University Press, Oxford, pp 242–294

Hublin J-J, Ben-Ncer A, Bailey SE, Freidline SE, Neubauer S, Skinner MM, Bergmann I, Le Cabec A, Benazzi S, Harvati K, Gunz P (2017) New fossils from Jebel Irhoud, Morocco and the pan-African origin of *Homo sapiens*. Nature 546:289–292

Klein RG (1973) Geological antiquity of Rhodesian Man. Nature 244:311–312

Kondo O, Dodo Y (2003) The postcranial bones of the Neanderthal child of burial n°1. In: Akazawa T, Muhesen T (eds) Neanderthal Burials. Excavations of the Dederiyeh Cave, Afrin, Syria. KW Publications Ltd., Auckland, pp 93–137

Kondo O, Ishida H (2003) The postcranial bones of the Neanderthal child of burial n°2. In: Akazawa T, Muhesen T (eds) Neanderthal Burials. Excavations of the Dederiyeh Cave, Afrin, Syria. KW Publications Ltd., Auckland, pp 299–321

Lü Z (1990) La découverte de l'homme fossile de Jing-Niu-Shan. Première étude L'Anthropologie (Paris) 94:899–902

Lu Z, Meldrum DJ, Huang Y, He J, Sarmiento EE (2011) The Jinniushan hominin pedal skeleton from the late Middle Pleistocene of China. Homo 62:389–401

Madre-Dupouy M (1992) L'enfant du Roc de Marsal. Éditions du CNRS, Paris

Martin H (1923) L'Homme fossile de la Quina. Librairie Octave Doin, Paris

Martínez I, Rosa M, Quam R, Jarabo P, Lorenzo C, Bonmatí A, Gómez-Olivencia A, Gracia A, Arsuaga JL (2013) Communicative capacities in Middle Pleistocene humans from the Sierra de Atapuerca in Spain. Quat Int 295:94–101

Maureille B (2002) A lost Neanderthal neonate found. Nature 419:33–34

McCown TD, Keith A (1939) The stone age of Mount Carmel. The fossil human remains from the levalloiso-mousterian. Clarendon press, Oxford

Moigne A-M, Palombo MR, Belda V, Heriech-Briki D, Kacimi S, Lacombat F, De Lumley M-A, Moutoussamy J, Rivals F, Quilès J, Testu A (2006) Les faunes de grands mammifères de la Caune de l'Arago (Tautavel) dans le cadre biochronologique des faunes du Pléistocène moyen italien. Anthropologie 110:788–831

Ortega AI, Benito-Calvo A, Pérez-González A, Martín-Merino MA, Pérez-Martínez R, Parés JM, Aramburu A, Arsuaga JL, Bermúdez De Castro JM, Carbonell E (2013) Evolution of multi-level caves in the Sierra de Atapuerca (Burgos, Spain) and its relation to human occupation. Geomorphology 196:122–137

Pablos A, Martínez I, Lorenzo C, Gracia A, Sala N, Arsuaga JL (2013) Human talus bones from the Middle Pleistocene site of Sima de los Huesos (Sierra de Atapuerca, Burgos, Spain). J Hum Evol 65:79–92

Pablos A, Martínez I, Lorenzo C, Sala N, Gracia-Téllez A, Arsuaga JL (2014) Human calcanei from the Middle Pleistocene site of Sima de los Huesos (Sierra de Atapuerca, Burgos, Spain). J Hum Evol 76:63–76

Pablos A, Pantoja-Pérez A, Martínez I, Lorenzo C, Arsuaga JL (2017) Metric and morphological analysis of the foot in the Middle Pleistocene sample of Sima de los Huesos (Sierra de Atapuerca, Burgos, Spain). Quat Int 433:103–113

Pal GP, Routal RV (1996) The role of the vertebral laminae in the stability of the cervical spine. J Anat 188:485–489

Pap I, Tillier A-M, Arensburg B, Chech M (1996) The Subalyuk Neanderthal remains (Hungary): a re-examination. Annales Historico-Naturales Musei Nationalis Hungarici 88:233–270

Pares JM, Perez-Gonzalez A (1995) Paleomagnetic age for hominid fossils at Atapuerca archaeological site, Spain. Science 269:830–832

Parés JM, Pérez-González A (1999) Magnetochronology and stratigraphy at Gran Dolina section, Atapuerca (Burgos, Spain). J Hum Evol 37:325–342

Pearson OM, Fleagle JG, Grine FE, Royer DF (2008) Further new hominin fossils from the Kibish Formation, southwestern Ethiopia. J Hum Evol 55:444–447

Peleg S, Dar G, Medlej B, Steinberg N, Masharawi Y, Latimer B, Jellema L, Peled N, Arensburg B, Hershkovitz I (2007) Orientation of the human sacrum: Anthropological perspectives and methodological approaches. Am J Phys Anthropol 133:967–977

Piveteau J (1966) La grotte de Regourdou (Dordogne). Paléontologie humaine. Annales de Paléontologie (Vertébrés) 52:163–194

Pomeroy E, Mirazón Lahr M, Crivellaro F, Farr L, Reynolds T, Hunt CO, Barker G (2017) Newly discovered Neanderthal remains from Shanidar Cave, Iraqi Kurdistan, and their attribution to Shanidar 5. J Hum Evol 111:102–118

Ponce De León MS, Golovanova L, Doronichev V, Romanova G, Akazawa T, Kondo O, Ishida H, Zollikofer CPE (2008) Neanderthal brain size at birth provides insights into the evolution of human life history. Proc Natl Acad Sci U S A 105:13764–13768

Pycraft WP, Smith GE, Yearsley M, Carter JT, Smith RA, Hopwood AT, Bate DMA, Swinton WE (1928) Rhodesian man and associated remains. British Museum (Natural History, London

Rak Y (1991) The pelvis. In: Bar-Yosef O, Vandermeersch B (eds) Le squelette moustérien de Kébara 2. Éditions du CNRS, Paris

Rak Y, Kimbel WH, Hovers E (1994) A Neandertal infant from Amud Cave, Israel. J Hum Evol 26:313–324

Rak Y, Hylander W, Quam R, Martínez I, Gracia A, Arsuaga JL (2011) The problematic hypodigm of *Homo heidelbergensis*. Am J Phys Anthropol 144(S52):247

Richter D, Grün R, Joannes-Boyau R, Steele TE, Amani F, Rué M, Fernandes P, Raynal J-P, Geraads D, Ben-Ncer A, Hublin J-J, Mcpherron SP (2017) The age of the hominin fossils from Jebel Irhoud, Morocco, and the origins of the Middle Stone Age. Nature 546:293–296

Rightmire GP, Deacon HJ (1991) Comparative studies of Late Pleistocene human remains from Klasies River Mouth, South Africa. J Hum Evol 20:131–156

Rightmire GP, Deacon HJ (2001) New human teeth from Middle Stone Age deposits at Klasies River, South Africa. J Hum Evol 41:535–544

Rmoutilová R, Gómez-Olivencia A, Brůžek J, Holliday T, Ledevin R, Couture-Veschambre C, Madelaine S, Džupa V, Velemínská J, Maureille B (submitted) A case of marked bilateral asymmetry in the sacral alae of the Neandertal specimen Regourdou 1 (Périgord, France). Am J Phys Anthropol

Rosas A (2001) Occurrence of Neanderthal features in mandibles from the Atapuerca-SH site. Am J Phys Anthropol 114:74–91

Rosas A, Ríos L, Estalrrich A, Liversidge H, García-Tabernero A, Huguet R, Cardoso H, Bastir M, Lalueza-Fox C, De La Rasilla M, Dean C (2017) The growth pattern of Neandertals, reconstructed from a juvenile skeleton from El Sidrón (Spain). Science 357:1282–1287

Rosenberg KR, Züne L, Ruff CB (2006) Body size, body proportions, and encephalization in a Middle Pleistocene archaic human from northern China. Proc Natl Acad Sci U S A 103:3552–3556

Sala N, Arsuaga JL, Martínez I, Gracia-Téllez A (2014) Carnivore activity in the Sima de los Huesos (Atapuerca, Spain) hominin sample. Quat Sci Rev 97:71–83

Sala N, Arsuaga JL, Martínez I, Gracia-Téllez A (2015a) Breakage patterns in Sima de los Huesos (Atapuerca, Spain) hominin sample. J Archaeol Sci 55:113–121

Sala N, Arsuaga JL, Pantoja-Pérez A, Pablos A, Martínez I, Quam RM, Gómez-Olivencia A, Bermúdez De Castro JM, Carbonell E (2015b) Lethal Interpersonal Violence in the Middle Pleistocene. PLoS One 10:e0126589

Saladié P, Huguet R, Rodríguez-Hidalgo A, Cáceres I, Esteban-Nadal M, Arsuaga JL, Bermúdez De Castro JM, Carbonell E (2012) Intergroup cannibalism in the European Early Pleistocene: The range expansion and imbalance of power hypotheses. J Hum Evol 63:682–695

Schwarcz HP, Grün R, Vandermeersch B, Bar-Yosef O, Valladas H, Tchernov E (1988) ESR dates for the hominid burial site of Qafzeh in Israel. J Hum Evol 17:733–737

Shapiro LJ (2007) Morphological and functional differentiation in the lumbar spine of lorisids and galagids. Am J Primatol 69:86–102

Shen G, Ku T-L, Cheng H, Edwards RL, Yuan Z, Wang Q (2001) High-precision U-series dating of Locality 1 at Zhoukoudian, China. J Hum Evol 41:679–688
Sládek V, Trinkaus E, Hillson SW, Holliday TW (2000) The people of the Pavlovian. Skeletal catalogue of the Gravettian fossil hominids from Dolní Vestonice and Pavlov. Academy of Sciences of the Czech Republic, Institute of Archaeology in Brno, Brno
Smith P, Arensburg B (1977) A mousterian skeleton from Kebara cave. Eretz-Israel 13:164–176
Stewart TD (1962) Neanderthal cervical vertebrae with special attention to the Shanidar Neanderthals from Iraq. Bibl primat 1:130–154
Stringer CB, Grün R, Schwarcz HP, Goldberg P (1989) ESR dates for the hominid burial site of Es Skhul in Israel. Nature 338:756–758
Tague RG (1992) Sexual dimorphism in the human bony pelvis, with a consideration of the Neandertal pelvis from Kebara cave, Israel. Am J Phys Anthropol 88:1–21
Tiemei C, Quan Y, En W (1994) Antiquity of *Homo sapiens* in China. Nature 368:55
Tillier A-M (1999) Les enfants moustériens de Qafzeh. Interprétation phylogénétique et paléoauxologique. CNRS Editions, Paris
Tillier A-M, Arensburg B, Duday H, Vandermeersch B (2001) Brief communication: an early case of hydrocephalus: The Middle Paleolithic Qafzeh 12 child (Israel). Am J Phys Anthropol 114:166–170
Toussaint M, Gómez-Olivencia A, Been E (in press) The Spy Neandertal spinal bones (the sacrum and one lumbar vertebra). In: Rougier H, Semal P (eds) Spy Cave, State of 125 Years of Pluridisciplinary Research on the Betche-aux-Rotches from Spy (Jemeppe-sur-Sambre, Province of Namur, Belgium), vol 2. Royal Belgian Institute of Natural Sciences & NESPOS Society, Brussels
Trinkaus E (1983) The Shanidar Neandertals. Academic Press, New York
Trinkaus E (1985) Pathology and the posture of the La Chapelle-aux-Saints Neandertal. Am J Phys Anthropol 67:19–41
Trinkaus E (1995) Near Eastern late archaic humans. Paléorient 21(2):9–24
Trinkaus E (2016) The Krapina human postcranial remains: morphology, morphometrics and paleopathology. FF-Press, Zagreb
Trinkaus E, Buzhilova AP, Mednikova MB, Dobrovolskaya MV (2014) The People of Sunghir. Burials, Bodies, and Behavior in the Earlier Upper Paleolithic. Oxford University Press, Oxford
Trinkaus E, Robson Brown KA, Ortega J, Karaková K (2017) The palomas postcrania. In: Trinkaus E, Walker M J The people of Palomas. Neandertals from the Sima de las Palomas del Cabezo Gordo, Southeastern Spain. Texas A&M University Press, College Station, Texas, 183–228
Valladas H, Reyss JL, Joron JL, Valladas G, Bar-Yosef O, Vandermeersch B (1988) Thermoluminescence dating of Mousterian Proto-Cro-Magnon remains from Israel and the origin of modern man. Nature 331:614–616
Vallois HV, Billy G (1965) Nouvelles recherches sur les hommes fossiles de l'Abri de Cro-Magnon. L'Anthropologie (Paris) 69:249–272
Vandermeersch B (1981) Les hommes fossiles de Qafzeh (Israël). Éditions du CNRS, Paris
Walker MJ, Ortega J, López MV, Parmová K, Trinkaus E (2011a) Neandertal postcranial remains from the Sima de las Palomas del Cabezo Gordo, Murcia, southeastern Spain. Am J Phys Anthropol 144:505–515
Walker MJ, Ortega J, Parmová K, López MV, Trinkaus E (2011b) Morphology, body proportions, and postcranial hypertrophy of a female Neandertal from the Sima de las Palomas, southeastern Spain. Proc Natl Acad Sci U S A 108:10087–10091
Weber J, Pusch CM (2008) The lumbar spine in Neanderthals shows natural kyphosis. Eur Spine J 17:S327–S330
Whitcome KK, Shapiro LJ, Lieberman DE (2007) Fetal load and the evolution of lumbar lordosis in bipedal hominins. Nature 450:1075–1078

Chapter 10
Spinal Pathologies in Fossil Hominins

Martin Haeusler

10.1 Introduction

Back problems are the foremost musculoskeletal disorder of modern humans with 60–80% of all people being affected by low back pain at some point in their life (Andersson 1999). The Global Burden of Disease 2010 study demonstrated that low back and neck pains are in all countries among those disorders that cause the highest socioeconomic costs and more disability than any other condition (Hoy et al. 2014; Dieleman et al. 2016). In Western societies, chronic disability from back disorders has exponentially risen since the last decades. Yet, there is no indication that back disorders are significantly more common or more severe than they have always been. Waddell (1996) therefore suggested that it is mainly our attitude towards them that has changed. Although hard physical labour seems to have a protective effect, the prevalence of back disorders is globally surprisingly similar independent of the occupation, behaviour, environment or culture of the patient, so that back disability cannot be viewed as a disorder of civilisation (Leino et al. 1994; Volinn 1997).

Krogman (1951) was one of the first who conjectured that our back disorders might be a trade-off to the evolution of upright bipedalism. Already Gregory (1928) compared quadrupeds with a living suspension bridge whose two towers are formed by the shoulder and pelvic girdles, between which the backbone is spread out, supported by an elaborate trestlework of the ribs and the pectoral and abdominal muscles. According to Krogman (1951), most mechanical advantages of this sophisticated construction were lost during the acquisition of upright bipedalism. This would have had an adverse effect on the mechanical balance of the vertebral column. The primitive single-curved arch of the spine that is still present at birth in modern humans is

M. Haeusler (✉)
Institute of Evolutionary Medicine, University of Zürich, Zürich, Switzerland
e-mail: Martin.Haeusler@iem.uzh.ch

E. Been et al. (eds.), *Spinal Evolution*,
https://doi.org/10.1007/978-3-030-19349-2_10

broken up into a double S-curve when children begin to stand up (Tardieu et al. 2017; Tardieu and Haeusler 2019). This brings the centre of body mass close to the hip joints and thus guarantees an ergonomic bipedal locomotion (Kummer 1975). In addition, the spinal curves are essential for dampening the thrusts that particularly occur during bipedal running (Castillo and Lieberman 2018).

The curvatures of the vertebral column make us, however, also vulnerable to mechanical failure. Thus, degenerative changes of the intervertebral discs, disc herniation, isthmic spondylolysis and spondylolisthesis, facet joint osteoarthritis and also spinal stenosis predominantly occur at the caudalmost segments of the lumbar curve, i.e. L4–L5 and L5–S1 (Hensinger 1989; Pietilä et al. 2001; Tischer et al. 2006; Kalichman and Hunter 2007; Takatalo et al. 2009; Tsirikos and Garrido 2010). On the other hand, the peaks of the spinal curves are particularly susceptible during the adolescent growth spurt to disc lesions and mechanical overloading. These seem to play a role in the aetiology of Scheuermann's disease. This disease is characterised by a thoracic hyperkyphosis or lumbar kyphosis and is the most common spinal pathology in adolescents, having a prevalence of 0.4–8.3% in modern humans (Scheuermann 1921; Sørensen 1964; Schlenzka and Arlet 2008; Tsirikos and Jain 2011; Palazzo et al. 2014). A similarly high prevalence with 1.0–3.3% has adolescent idiopathic scoliosis (defined by a Cobb angle >10°; Suh et al. 2011; Rogala et al. 1978; Lonstein et al. 1982; Daruwalla et al. 1985). Although the aetiology of this deformity is still unknown (Schlösser et al. 2015), its development is apparently related to the thoracic and lumbar curves of the spinal column. Moreover, like in Scheuermann's disease, upright bipedalism seems to play an important role as adolescent idiopathic scoliosis is also restricted to humans (in contrast to other types of scoliosis; Kouwenhoven and Castelein 2008; Schiess et al. 2014).

Spinal pathologies are remarkably uncommon in quadrupedal animals including chimpanzees and gorillas (Jurmain 2000), though the axial loading of the spine is often much higher in quadrupedalism than in bipedal locomotion (Smit 2002; Bergknut et al. 2012). Yet, if disc degeneration occurs, e.g. in captive macaques and baboons at an advanced age, no regional differences are found between the spinal levels from T10–T11 to L6–L7 (Lauerman et al. 1992; Nuckley et al. 2008). This strongly contrasts with the modern human pattern, where disc degeneration generally begins in the lowermost lumbar region (Takatalo et al. 2009). The important role of prolonged upright posture has also been demonstrated in animal experiments with bipedal rats, where degenerative changes in the intervertebral discs were induced (Goff and Landmesser 1957; Gloobe and Nathan 1973; Shi et al. 2007; Liang et al. 2008; but see Bailey et al. 2001).

Although it is often speculated that low back disorders are trade-offs to the evolution of bipedalism (Krogman 1951; Anderson 1999; Olshansky et al. 2003; Latimer 2005), no study so far has substantiated this association. On the contrary, Putz and Müller-Gerbl (1996) suggested that our spine is an optimised compromise between stability and mobility and that occasional failures of this system should primarily be attributed to our increased lifespan and a changed lifestyle compared to that of our ancestors.

The aim of this study is the analysis of all known spinal pathologies in the fossil record of early hominins up to the Neanderthals to provide an evolutionary approach to our back problems.

10.2 Vertebral Pathologies in the Fossil Hominin Record

10.2.1 Australopithecus afarensis

KSD-VP-1/1

Apart from a handful of small, crushed vertebral fragments and a segment of the inferior sacrum of *Ardipithecus ramidus* (White et al. 2009), the 3.58-Ma-old KSD-VP-1/1 specimen (*Australopithecus afarensis*) is the earliest hominin fossil that preserves a partial vertebral column (Haile-Selassie et al. 2010; Haile-Selassie and Su 2016). It belongs to a large, fully adult and probably male individual. Small to moderate osteophytes (i.e. second- to third-degree ventral osteophytes according to the staging of Nathan 1962) are present on the vertebral bodies of C4, C5 and C6 (Meyer 2016). They are most marked in the inferior cervical spine. This pattern with the greatest development of osteophytes in the vicinity of the peak of the cervical lordosis is typical of modern humans (Nathan 1962) but is not observed in great apes (Jurmain 2000). The presence of this pathology has thus been interpreted to indicate a human-like posture of the neck in *Australopithecus* (Meyer 2016).

The development of osteophytes is related to the degeneration of intervertebral discs with resultant increased strain on the anterior longitudinal ligament (Schmorl and Junghans 1968). Twin studies demonstrated that intervertebral disc degeneration is largely a function of genetic predisposition and ageing, while inter-individual variation in physical loading plays a subordinate role (Battié et al. 1995, 2009; Sambrook et al. 1999). Accordingly, skeletal studies did not find a correlation between vertebral osteophytosis and intense physical activity (Bridges 1991). Because cervical osteophytes usually develop later in life than those in the thoracic and lumbar region and rarely appear before the third decade of life in modern humans (Nathan 1962; Schmorl and Junghans 1968), they also suggest that KSD-VP-1/1 was of relatively advanced age.

A.L. 288-1

A second *Australopithecus afarensis* partial skeleton is the 3.2-Ma-old A.L. 288-1 ("Lucy") from Hadar, Ethiopia, an individual that died in its mid-20s. It preserves vertebral bodies T6–T10 and L3 (Johanson et al. 1982; Meyer et al. 2015). Their sagittal diameter is elongated, most markedly at T6, due to an anterior appositional bone growth (Fig. 10.1). Moreover, T10 and L3 are abnormally anteriorly wedged with an angle of 6° between the superior and inferior vertebral surfaces.

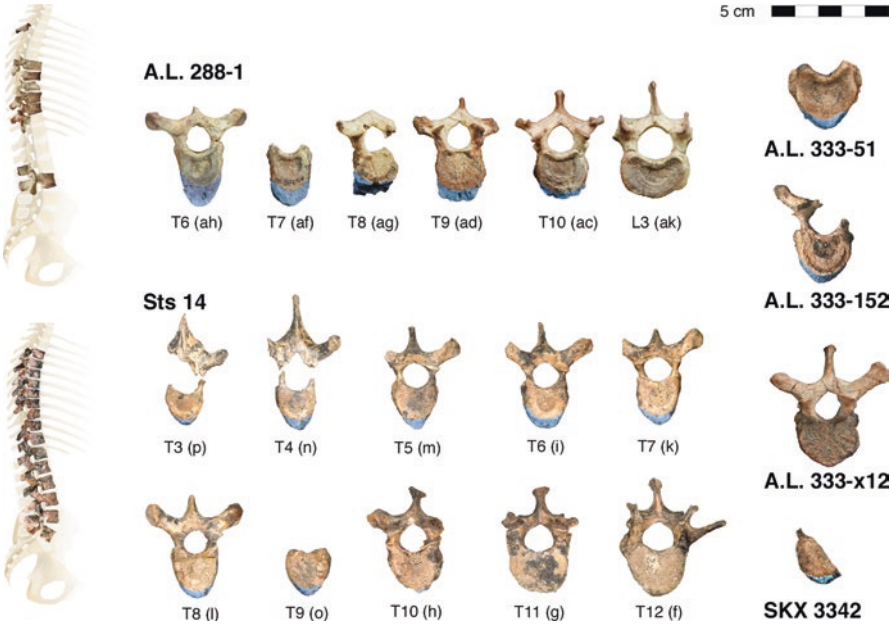

Fig. 10.1 Ventral appositional bone growth (coloured in light blue) suggestive of Scheuermann's disease in the mid- and lower thoracic vertebrae of A.L. 288-1 (*Australopithecus afarensis*), the isolated vertebrae A.L. 333-51, A.L. 333-152 and A.L. 333-x12 from Hadar, Sts 14 (*A. africanus*) and SKX 3342 (*Paranthropus robustus*)

Cook et al. (1983), therefore, suggested that A.L. 288-1 suffered from juvenile kyphosis or Scheuermann's disease although the radiological criteria for the thoracic form of Scheuermann's kyphosis require abnormal wedging of at least 5° at three or more adjacent vertebrae (Sørensen 1964; Lowe 2007; Schlenzka and Arlet 2008; Palazzo et al. 2014). Noteworthy is, however, the absence of additional signs of Scheuermann's disease in A.L. 288-1 such as endplate irregularities with Schmorl's nodes. On the other hand, the typical ventral extension has not been observed in normal modern human spines or in other disorders than Scheuermann's disease (Scoles et al. 1991).

Isolated *A. afarensis* Vertebrae

The characteristic anterior appositional bone growth of Scheuermann's disease leading to an elongation of the sagittal diameter has also been observed in a few isolated *A. afarensis* thoracic vertebrae from Hadar, including the adult A.L. 333-51 and A.L. 333-152 and the juvenile A.L. 333x-12 (Fig. 10.1; Cook et al. 1983; Ward et al. 2012).

10.2.2 Australopithecus africanus

Sts 14

Sts 14 is an approximately 2.5-Ma-old adolescent *A. africanus* partial skeleton from Sterkfontein Member 4, South Africa, that preserves 15 thoracolumbar vertebrae and the first 2 sacral segments (Robinson 1972). The anomalous sixth last presacral vertebra caused some confusion about the number of lumbar vertebrae in Sts 14 and in early hominins in general. This vertebra possesses on the left side an unusual costal process with a costotransverse foramen caused by an ontogenetically incomplete fusion of the rib anlage with the vertebra. The right side, on the other hand, displays a protuberant, convex rib facet articulating to a movable last rib (Haeusler et al. 2002). Rather than interpreting this partial border shift of the thoracolumbar junction as an incomplete lumbarisation, Robinson (1972) and others suggested that Sts 14 and by implication early hominins on average possessed six instead of five lumbar vertebrae as modally present in modern humans. Latimer and Ward (1993) conjectured that this presumed lengthening of the lumbar spine facilitated the critical adoption of lumbar lordosis in human evolution. An analysis of further early hominin vertebral columns, including StW 431 (*A. africanus*) and MH2 (*A. sediba*), and the recovery of additional vertebral fragments of KNM-WT 15000 (*H. erectus*) demonstrated, however, that all of them have a modern human segmentation pattern with five lumbar vertebrae (Haeusler et al. 2002, 2011; Williams et al. 2013). Nevertheless, Sts 14 and all other early hominin skeletons seem to differ from the majority of modern humans in a more cranially located transition between anterolaterally oriented, thoracic-like facet joints and dorsomedially oriented, lumbar-like facet joints. This transition is located in all known specimens at the penultimate rather than at the last thoracic vertebra (Haeusler et al. 2012; Williams et al. 2013; Ward et al. 2017).

In a cast of a lower thoracic vertebra of Sts 14, Cook et al. (1983) noted a ventral expansion of the vertebral body similar to that of A.L. 288-1, which they attributed to normal variation. An analysis of the entire thoracolumbar vertebral column of this partial skeleton shows, however, that the pathognomonic new bone formation at the ventral border of the vertebrae affects the whole series from T3 to T9 (T10–T12 being ventrally eroded), with a maximum at T8 (Fig. 10.1). In addition, Sørensen's (1964) diagnostic criteria of Scheuermann's disease are fully met, i.e. a kyphotic wedging angle greater than 5° in more than three adjacent vertebrae. Hence, also Sts 14 suffered from this form of juvenile kyphosis.

StW 431

The second partial *A. africanus* skeleton from Sterkfontein Member 4, Stw 431, preserves the ten last presacral vertebrae from T8 to L5 and the first three sacral vertebrae (Benade 1990; Haeusler et al. 2002; Toussaint et al. 2003; Haeusler and

Ruff 2019). Marked submarginal osteophyte formation is present at the vertebral body L5 cranially and to a lesser degree at the vertebral body L4 caudally while the vertebral margin is partly destructed by lytic lesions. D'Anastasio et al. (2009) interpreted this as signs of brucellosis, a bacterial infection associated with the consumption of contaminated meat or milk.

Mays (2007) argued, however, that vertebral marginal lesions should not be used to diagnose brucellosis in the absence of additional evidence. He suggested that a limbus vertebra (i.e. a traumatic anterior disc herniation; Schmorl and Junghans 1968) is a much more likely cause of vertebral marginal lesions. Thus, Mays (2007) observed a prevalence of 4% of limbus vertebrae in a sample of 135 skeletons from rural medieval England with complete lumbar spines. In the majority of them, lumbar vertebrae L4 and L3 were affected. This corresponds well with StW 431, where vertebrae L4/L5 are affected. Moreover, the morphology of the submarginal osteophytes and the porotic surface of the partly destructed vertebral margin in a limbus vertebra (Fig. 2 in Mays 2007) are nearly identical to that of Stw 431. It has been hypothesised that limbus vertebrae result in the subadult spine from traumatic anterior disc herniation due to excessive tensile strain (Schmorl and Junghans 1968). This leads to the avulsion of a small bone fragment mostly at the superior vertebral margin close to the attachment of the ring apophysis. Limbus vertebrae are thus pathogenetically related to Scheuermann's disease and Schmorl's nodes. As Scheuermann's disease, they predominantly occur in young, physically active individuals and do not cause pain (Hellström et al. 1990).

StW 8/41

StW 8/41 is a fragmentary six-element-long *A. africanus* vertebral series from Sterkfontein Member 4, probably representing T11 to L4 (Tobias 1973; Sanders 1998). A small, blunt osteophyte has been described at the right ventral aspect of the vertebral body L2 (Sanders 1998). Because of its unusual morphology, a location not in direct association with the vertebral margin, and the extensive damage to the specimen, it is, however, unclear whether this bump indeed represents an osteophyte.

10.2.3 Australopithecus sediba

Two partial skeletons with well-preserved vertebral columns are known of *A. sediba* (Berger et al. 2010; Williams et al. 2013, 2018). Thoracic vertebra T6 of the juvenile male skeleton MH1 shows in the right lamina a 12 × 5 × 15-mm-large lytic lesion with smooth, sclerotic margins. The morphology is characteristic of an osteoid osteoma (Randolph-Quinney et al. 2016), a benign primary bone tumour that mostly occurs in younger individuals. It is mostly associated with pain that is worse at night and typically resolves untreated after about 3 years (Kneisl and Simon 1992).

10.2.4 Paranthropus robustus

Only a few, mostly fragmentary remains of the vertebral column of *Paranthropus* are known. SKX 3342 is a partial midthoracic vertebral body from Swartkrans Member 2 that is dated to 1.7–1.1 Ma (Susman 1989; Herries et al. 2009). It shows ventral appositional bone growth characteristic of Scheuermann's disease (Fig. 10.1).

An isolated fragmentary lower thoracic vertebral body, CD 5773, is described from Cooper's D, South Africa, a dolomitic cave site in the vicinity of Swartkrans and Sterkfontein dating to 1.5–1.4 Ma (de Ruiter et al. 2009). As only *P. robustus* remains have been discovered at that site, the vertebra can probably be also attributed to that taxon. The vertebral body is markedly anteriorly wedge-shaped and shows submarginal osteophytic lipping. The costal facet shows degenerative changes.

10.2.5 Homo erectus

The 1.47-million-year-old KNM-WT 15000 *Homo erectus* skeleton is the best-preserved early hominin fossil discovered to date (Walker and Leakey 1993; McDougall et al. 2012). Additional vertebral and rib fragments were described by Haeusler et al. (2011) so that now all 5 lumbar vertebrae and 10 of 12 thoracic and the last cervical vertebrae are known. Epiphyseal closure pattern and skeletal development are comparable to 13.5- to 15-year-old modern humans, while tooth microanatomy indicates an age at death of approximately 8 years (Smith 1993; Tardieu 1998; Dean et al. 2001; Zihlman et al. 2004). The long bones imply a stature at death of 157 cm (Ruff and Walker 1993; Ruff 2007). Yet, when Ohman et al. (2002) summed up the heights of all vertebral bodies, they obtained an apparently short trunk length, which suggested to them a stature at death of only 141–147 cm. They concluded that KNM-WT 15000 suffered from disproportionate dwarfism due to platyspondylic and diminutive vertebrae (Ohman et al. 2002). A reanalysis of the vertebrae demonstrated, however, that the unfused ring apophyses are missing in KNM-WT 15000 due to its juvenile age. In fact, vertebral body height is exactly what is expected for a modern human of the same age (Schiess and Haeusler 2013).

Latimer and Ohman (2001) further asserted that KNM-WT 15000 suffered from spina bifida, condylus tertius, spinal stenosis and scoliosis, which led them to claim a novel form of congenital skeletal dysplasia in this individual. Yet, the reassessment by Schiess and Haeusler (2013) revealed no evidence for any form of spina bifida in the thoracic, lumbar and sacral vertebrae. A literature review also showed no indication for an association between a condylus tertius and skeletal dysplasia. In addition, a comparison with the subadult *H. erectus* specimen from Dmanisi rejected the hypothesis of spinal stenosis in KNM-WT 15000. While the spinal foramen dimensions of the Dmanisi specimen are in the lower range of the modern

human distribution, they are slightly below the modern human range of variation in KNM-WT 15000. It, therefore, seems that *H. erectus* as a species had a slightly narrower spinal canal than modern humans. This is a primitive characteristic but has nothing to do with pathology (Meyer and Haeusler 2015). Finally, a morphometric analysis of the vertebrae failed to support the hypothesis of scoliosis (Schiess et al. 2014), and the observed unsystematic asymmetries of the thorax disappeared with a rearrangement of the ribs (Haeusler et al. 2011). Moreover, the pattern of asymmetry present in the uppermost thoracic vertebrae T1–T2 and the facet joints of the lower lumbar vertebrae L3–L5 is incompatible with adolescent idiopathic scoliosis or other types of scoliosis, including congenital, neuromuscular or syndromic scoliosis. Rather, they might reflect developmental or possibly trauma-related anomalies (Schiess et al. 2014).

The asymmetries at the lower lumbar spine of KNM-WT 15000 are restricted to the shape and size of the articular processes of L3–L5 (Haeusler et al. 2013). The left superior facet of L5 is osteophytically remodelled and articulates to a knoblike nearthrosis at the inferior side of the left pedicle of L4. This is characteristic of advanced disc space narrowing leading to telescoping subluxation (Jinkins 2004). The most likely cause for disc space narrowing in KNM-WT 15000 is disc herniation that often leads to unilateral subluxation as in KNM-WT 15000 (Fig. 10.2; Haeusler et al. 2013). In contrast to disc herniation in adults, the majority of juvenile disc herniations are traumatic in origin or related to sports injury, rather than degenerative (Slotkin et al. 2007). The levels L4–L5 of the affected intervertebral disc in KNM-WT 15000 also perfectly fit the frequency distribution of disc herniations in modern human adolescents with 97% occurring at L4–L5 and L5–S1 (Pietilä et al. 2001).

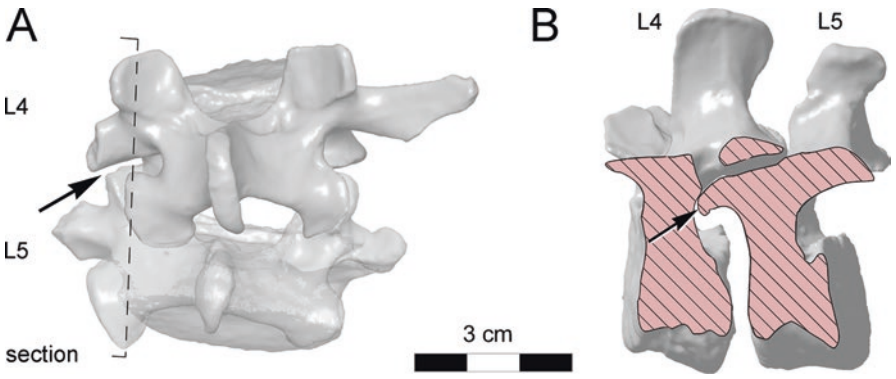

Fig. 10.2 (**a**) Articulated vertebrae L4 and L5 of KNM-WT 15000 (3D surface scan generated models, dorsal view). The nearthrosis (arrow) and the asymmetric articular processes imply an oblique position of the vertebrae relative to each other. (**b**) Section through the nearthrosis and the remodelled superior articular facet of L5 (arrow), left lateral view. Cropped parts of the vertebrae are hatched. Adapted from Haeusler et al. (2013)

The extensive bony remodelling of these facet joints indicates that KNM-WT 15000 survived a considerable period of time with a potentially disabling condition. Patients with a similar degree of bony remodelling usually have a history of between at least 6 months and several years of recurrent low back pain and sciatica (Hadley 1936, 1951, 1961). Since paediatric patients with lumbar disc hernias are often more disabled than adults (Rugtveit 1966; Slotkin et al. 2007), it can be hypothesised that KNM-WT 15000 was temporarily restricted in walking, bending and other daily activities. Despite the difficulties in deducing inferences for social care from the fossil record (Degusta 2002), this contributes to the growing evidence that *Homo erectus* was already capable to support and care for disabled group members (Walker and Shipman 1996; Lordkipanidze et al. 2005; Bonmatí et al. 2010; Tilley 2015).

10.2.6 Sima de los Huesos and Neanderthals

Sima de los Huesos Pelvis 1 Individual

The Pelvis 1 individual from the Sima de los Huesos (SH) in the Sierra de Atapuerca, Spain, dated to ca. 430,000 years ago, is associated with five lumbar vertebrae in addition to the sacrum and both hipbones (Bonmatí et al. 2010; Arsuaga et al. 2014). Based on the degree of bony remodelling of the pubic symphysis, the sacroiliac joint surface and the acetabulum, an individual age of over 45 years was estimated. The lumbar vertebrae L2–L4 show marked kyphotic wedging and remodelling of the ventral surface. Bonmatí et al. (2010) interpreted this as degenerative lumbar kyphosis, which would imply osteoporotic compression fractures. However, in accordance with the generally more robust skeletons and thicker trabeculae of non-sedentary populations compared to recent humans (Chirchir et al. 2015; Ryan and Shaw 2015), the published radiograph of L5 (Bonmatí et al. 2010) shows a high trabecular bone density, which would make it unlikely that vertebrae L2–L4 were affected by osteoporotic compression fractures. An alternative interpretation is lumbar Scheuermann's disease, which is typically associated with a kyphotic deformity of the lumbar spine (Sørensen 1964). This diagnosis is supported by the presence of a large Schmorl's node in lumbar vertebra L5 (Bonmatí et al. 2010).

Pérez (2003) and Bonmatí et al. (2010) further described a spondylolisthesis of the last lumbar vertebra of the SH Pelvis 1 individual. This is accompanied by intense unilateral remodelling of the left facet joint L5–S1, which is located more dorsally than its counterpart on the right side. In combination with a sacral slanting of 5° to the left with respect to the hip joint axis, this suggested a clockwise rotational component of the slippage of L5 over S1. The spondylolisthesis led to a characteristic trapezoidal deformation of L5 and a dome-shaped remodelling of the superior sacral surface as well as an osteophytic distortion of the ventral rim of the sacrum (see also Antoniades et al. 2000). This indicates disc degeneration and narrowing of the intervertebral spaces L5–S1, which is also implied by a nearthrosis on

the underside of the left pedicle for an extra articulation with the sacrum. There is no evidence for a traumatic origin of the spondylolisthesis as assumed by Pérez (2003), nor for a spondylolysis with an isthmic defect of L5. Rather, the more dorsally positioned left inferior articular process of L5 compared to the right side is indicative of an elongation of the posterior element secondary to repeated microfractures and subsequent healing (see Hammerberg 2005). A non-union of the left lamina of L5, which is a developmental defect and by definition represents a variant of spina bifida occulta (e.g. Kumar and Tubbs 2011), suggests that the spondylolisthesis is of developmental low dysplastic origin according to the aetiology-based classification system of Marchetti and Bartolozzi (1997). Low dysplastic spondylolisthesis results from defects of the lumbosacral junction such as asymmetric and deformed facet joints and is often associated with spina bifida (Hammerberg 2005). Patients with the low dysplastic form of spondylolisthesis usually become symptomatic as young adults rather than adolescents (Hammerberg 2005), which explains the relatively moderate bony remodelling in the SH Pelvis 1 individual. The lamina and median sacral crest are also missing on the first sacral vertebra, but due to postmortem damage it is unknown whether the spina bifida occulta extended to S1.

Spondylolisthesis is a uniquely human condition that has not been observed in patients that never walked (Rosenberg et al. 1981). In modern humans, it is correlated with an increased pelvic incidence and lumbar lordosis (e.g. Merbs 1996; Labelle et al. 2004). This seems to be at odds with the kyphotic lumbar deformity of the SH Pelvis 1 individual and the reported low pelvic incidence of 27.6° (Bonmatí et al. 2010). The pelvic incidence is the angle between the ray from the midpoint of the hip joint axis to the midpoint of the superior sacral surface and the normal to the superior sacral surface (Duval-Beaupère et al. 1992; Tardieu et al. 2017). It is characteristic of each individual and well correlated with lumbar lordosis. In the SH Pelvis 1 individual, the pelvic incidence is, however, misleading because of the spondylolisthesis-induced dome-shaped distortion of the superior sacral surface and the presence of a second promontorium that implies partial lumbarisation of the first sacral vertebra. Both morphologies significantly affect the pelvic incidence. While the impact of the dome-shaped distortion of the superior sacral surface is difficult to quantify, the lumbar lordosis estimate of 32° (Been et al. 2014) based on the published pelvic incidence of the SH Pelvis 1 individual might be up to 20° too low due to the presence of a partial lumbarisation of the first sacral vertebra (Price et al. 2016).

A second individual from Sima de los Huesos has been reported to have a similarly low pelvic incidence as the SH Pelvis 1 individual (Bonmatí et al. 2010). However, in the absence of a published description of this specimen, it is unknown whether this value is affected by taphonomic deformation or a lumbosacral transitional anomaly similar to that of the SH Pelvis 1 individual.

On the other hand, the spinous processes L4–L5 of the SH Pelvis 1 individual display the characteristic osteophytic remodelling of Baastrup's disease (Bonmatí et al. 2010). This implies that the spinous processes of the lower lumbar vertebrae were in long-term close contact. Baastrup's disease most often results from disc space narrowing or an increased lordosis, or a combination of both

(Bachmann 1956; Alonso et al. 2017). The increased lordosis of the lower lumbar spine might, therefore, have at least partially compensated the kyphotic deformity of the upper lumbar spine of the SH Pelvis 1 individual, which is a typical mechanism to restore sagittal spinopelvic balance in younger individuals (Roussouly and Pinheiro-Franco 2011).

La Chapelle-aux-Saints 1

An adult male Neanderthal skeleton with severe osteoarthritic changes affecting all large joints and the entire vertebral column was discovered in 1908 in the Bouffia Bonneval cave at La Chapelle-aux-Saints in southwestern France (Raynal 1990; about 50,000 years BP; Boule 1911–1913; Fig. 10.3). His age at death has recently been revised to 63 ± 12 years based on acetabulur morphology, which suggests that he was one of the oldest Neaderthal individuals (Haeusler et al. 2019).

Because it is the first nearly complete Neanderthal skeleton that was discovered, it played a crucial role in the discussion of the posture of these late archaic humans. La Chapelle-aux-Saints 1 was originally portrayed by Boule (1911–1913) as having a primitive, forward inclined head position coupled with a straight neck and weak spinal curvatures, including a faint thoracic kyphosis and lumbar lordosis, as well as flexed hips and flexed knees. This gave rise to the once popular view of Neanderthals as primitive beasts with a semierect posture. In 1955, Arambourg challenged this interpretation by showing that Boule misaligned the cranial base. Moreover, he suggested that a primitive, ape-like cervical curvature cannot be inferred from a horizontal orientation of the cervical spinous processes in La Chapelle-aux-Saints 1 due to the high variability of this characteristic among modern humans. Straus and Cave (1957) seconded by attributing the distinct spinal curvature of La Chapelle-aux-Saints 1 mainly to its severe spinal osteoarthritis and disc degeneration; the posture of a healthy Neanderthal, however, would have been indistinguishable from modern humans. Trinkaus (1985), in contrast, argued that Boule's interpretation of the spinal curvature cannot be attributed to pathology as the degenerative changes did not affect the shape of the vertebral bodies. Rather, Boule's reconstruction of La Chapelle-aux-Saints' posture might have been biased by his evolutionary preconceptions. A geometric analysis of the vertebrae provided further support for a well-developed vertebral curvature in this fossil close to the average of modern humans (Cleuvenot 1999). Recently, however, Been and co-workers (2012, 2017) challenged this view. Their studies of the orientation of the inferior articular processes of the lumbar vertebra and foramen magnum orientation again suggested a hypolordotic lower back and a weak cervical lordosis in La Chapelle-aux-Saints 1 in line with their reconstruction of other Neanderthal specimens.

La Chapelle-aux-Saints 1 preserves 19 vertebrae and the first 2 sacral segments (Boule 1911–1913; Gómez-Olivencia 2013a). The thoracic region is most severely damaged and the majority of the vertebral bodies are missing. Nevertheless, Schmorl's nodes can be recognised in vertebral bodies T8–T10 on both the superior and inferior surfaces. Osteophytes only survive in the lower cervical spine as

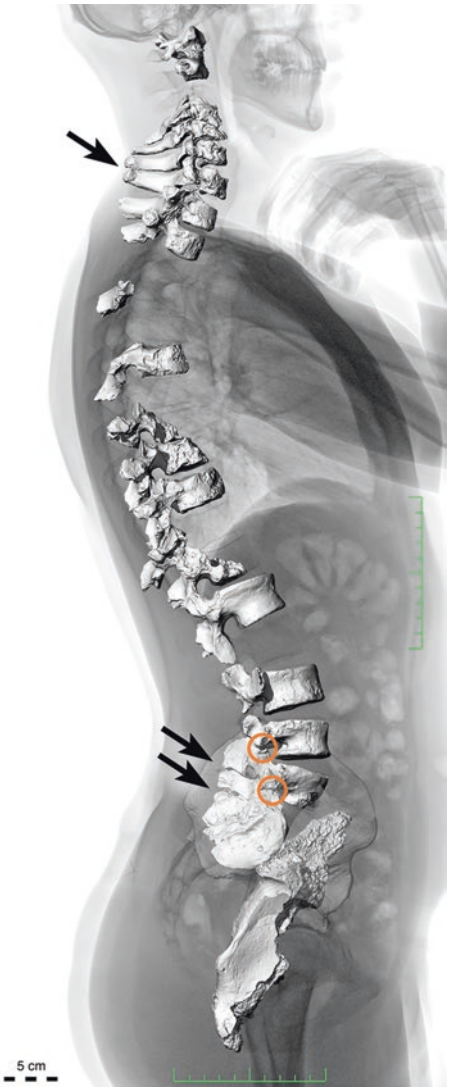

Fig. 10.3 The La Chapelle-aux-Saints 1 vertebrae (3D surface scans) superimposed on a standing EOS radiograph of a modern human. Note Baastrup's disease that affects spinous processes C6–C7, L4–L5 and L5–S1 (arrows) and the notch-shaped nearthroses between L4 and L5 as well as between L5 and the sacrum (circles). The right hipbone of La Chapelle-aux-Saints 1 is semitransparent for better visualisation of the sacrum and lower lumbar vertebrae. The exact identification of the two isolated midthoracic vertebral fragments is unclear, and their position on the figure is only symbolic. The patient's pelvic incidence is 52° and the lumbar lordosis 67°, which both seems to be slightly lower than in La Chapelle-aux-Saints 1

the ventral margins of the vertebral bodies are damaged throughout the entire thoracolumbar spine (Trinkaus 1985; Haeusler et al. 2017, 2019). Facet joint osteoarthritis, however, can be recognised in all vertebrae. This pattern of generalised spinal osteoarthritis suggests ageing as the most important aetiological factor in its development rather than localised trauma as proposed by Dawson and Trinkaus (1997). The degenerative changes are most severe in the lower cervical, upper and lower thoracic spine, where also telescoping facet joint subluxation can be observed. Baastrup's disease with osteophytic remodelling of the tips of the spinous processes of C6 and C7 suggests that they were in close contact (Haeusler et al. 2019).

Another region with Baastrup's disease is at vertebral levels L4–L5 (see also Ogilvie et al. 1998) and L5–S1. Baastrup's disease ("kissing spines") is caused by close approximation and contact of the spinous processes of adjacent vertebrae during upright posture and repeated strains of the interspinous ligament (Mayer 1826; Brailsford 1929; Baastrup 1933; Bachmann 1956; Lerch and Wurm 1964; Bywaters and Evans 1982; Kwong et al. 2011). Initially, this leads to the development of interspinous bursae and, with prolonged stress, to osteophytically enlarged tips of the spinous processes. Risk factors for Baastrup's disease include large spinous processes, increased lordosis during advanced age and reduced intervertebral space (Bachmann 1956; Lerch and Wurm 1964; Kwong et al. 2011; Filippiadis et al. 2015; Alonso et al. 2017). Although repetitive flexion and extension of the spine in gymnasts may also lead to the development of interspinous bursitis (Keene et al. 1989), morphological changes of the spinous process have not been observed by that study.

The spinous processes of L4–S1 show marked osteophytic remodelling in La Chapelle-aux-Saints 1, which indicates a long-term, habitually close contact between them. In addition, facet joint subluxations led to the formation of extra joints on the inferior sides of the bases of the right costal processes of L4 and L5 that articulate with notch-like nearthroses at the right superior articular processes of L5 and S1, respectively. Articulation of the vertebrae after restoration of the median sacral crest shows that these subluxations with nearthroses on the right side of the neural arches together with the nearthroses between the spinous processes L4–L5 and L5–S1 led to a virtually immobile lower lumbar spine of La Chapelle-aux-Saints 1. Such a fixed lordosis that prevents further flexion and extension of the lumbar region is typical for patients with advanced Baastrup's disease (Bachmann 1956). The immobility of this spinal region might also explain Dawson and Trinkaus' (1997) observation of its lower degree of facet joint osteoarthritis with the absence of eburnations compared to the rest of the vertebral column.

Articulation of the lower lumbar vertebrae taking into account the close contact of the spinous processes and the unilateral nearthroses further indicates markedly reduced intervertebral spaces L4–L5 and L5–S1 with a right-convex scoliotic misalignment, which is to a lesser degree also present in the cervical spine. Because of the fixed articulation of the lower lumbar vertebrae, it is possible to estimate lumbar lordosis in La Chapelle-aux-Saints 1. A least squares regression of the lordosis angle S1–L1 against the segmental lordosis S1–L4 for a sample of 63 lateral lumbar radiographs thus predicts a high lumbar lordosis angle of 74°–79° in La Chapelle-aux-Saints 1 that exceeds the range of the modern human reference sample (Haeusler et al. 2019). On the other hand, a new virtual reconstruction of the La Chapelle-aux-Saints 1 pelvis based on 3D surface scans of the fragmentary left hipbone and sacrum as well as a high-resolution cast of the better preserved, but currently missing, right hipbone provided a pelvic incidence of 56° (Haeusler et al. 2019). This is slightly above of the mean of modern humans, indicating that the lumbar lordosis was close to the average of modern humans when La Chapelle-aux-Saints 1 was young and healthy and only intensified later in life, when the individual suffered from extensive degenerative changes of the vertebral column.

The analysis of the degenerative changes of the La Chapelle-aux-Saints 1 vertebral column thus corroborates the presence of a well-developed cervical and lumbar lordosis in this individual as suggested previously (Arambourg 1955; Straus and Cave 1957; Trinkaus 1985; Cleuvenot 1999), although it challenges the most recent reconstructions of a faint spinal curvature in this individual (estimated lumbar lordosis 34°, SEE 8.6°; estimated cervical lordosis 21.5°, RSME 6.9°; Been et al. 2012, 2017). Further research will be needed to resolve this apparent contradiction.

La Ferrassie 1

The nearly complete Neanderthal skeleton of an older male from La Ferrassie, Dordogne, France, was discovered in 1909 and is most likely dated to ~43–45 ka (Peyrony 1934; Guérin et al. 2015). Except for one sacral and two thoracic elements, all vertebrae are preserved, although most of them are very fragmentary (Heim 1976; Gómez-Olivencia 2013b). All vertebrae that can be assessed show facet joint osteoarthritis. The osteoarthritic changes are mostly of an advanced stage in the cervical spine with marked osteophytic enlargement of the joint facets and subchondral porosity, although the degree of the osteoarthritic changes does not yet parallel that of La Chapelle-aux-Saints 1. Ventral osteophytes of the vertebral bodies can only be observed in C5 and T2, a newly identified midthoracic vertebral fragment (Gómez-Olivencia et al. 2018) and a midlumbar vertebra due to damage to the vertebral body in the other elements. Osteophytic remodelling of the facet joints and the formation of nearthroses also indicate degenerative telescoping subluxation of L4–L5 and L5–S1 (Gómez-Olivencia 2013b). These degenerative changes are surprisingly advanced for the estimated age at death of about 40–55 years (Trinkaus and Smith 1995).

Moreover, the facet joints and the orientation of the spinous processes show slight asymmetries. This was interpreted as evidence for scoliosis by Gómez-Olivencia et al. (2018). However, the diagnostic criteria of scoliosis are not meet, and the asymmetries do not show a systematic pattern that would be compatible with a usual curve pattern of scoliotic curves (see Schiess et al. 2014). Alternatively, some of the asymmetries might be due to developmental anomaly. Similar to La Chapelle-aux-Saints 1, other asymmetries might also be explained by degenerative scoliotic misalignment related to the unilateral subluxation of the lower lumbar vertebrae. Moreover, Gómez-Olivencia et al. (2018) speculated about a possible relationship of the vertebral remodelling with a fracture of the right greater trochanter through a compensatory crooked posture.

Regourdou 1

The collapsed cave of Regourdou (Dordogne, France) has provided a partial skeleton of a young adult, probably male Neanderthal with fragments of at least seven cervical, nine thoracic and four lumbar vertebrae as well as a partial sacrum

(Piveteau 1959; Gómez-Olivencia et al. 2013; Maureille et al. 2015). The cervical vertebrae C2–C7 have been described to show mild facet joint and uncovertebral osteoarthritis, and the vertebral body T11 shows mild osteophytes at the dorsal edge of its inferior surface (Gómez-Olivencia et al. 2013).

The sacrum of Regourdou 1 is remarkable for facet joint tropism and its asymmetric alae (Rmoutilová et al. 2018). Together with the observation of some asymmetrical facet joints and two rotated and twisted spinous processes, Gómez-Olivencia et al. (2013) proposed that this asymmetry might reflect some kind of postural asymmetry or mild scoliosis. However, before the presence of scoliosis can be established, the corresponding diagnostic criteria need to be assessed (see Schiess et al. 2014). Moreover, the pelvis usually shows no significant asymmetries in patients with scoliosis (Rigo 1997; Qiu et al. 2012).

El Sidrón

Two out of three atlases among the vertebral remains from El Sidrón, northwestern Spain, present defects of ossification (Ríos et al. 2015; Trinkaus 2018). In SD-1643, the right posterior lamina is broken off, but the left posterior lamina terminates in a tapered tip close to the midline, suggesting non-fusion of the posterior arch. This form of spina bifida occulta occurs at the atlas in about 0.7–3.8% of the individuals within modern populations (Ríos et al. 2015). On the other hand, the fragmentary SD-1094 atlas shows a congenital cleft of the anterior arch. Like spina bifida occulta, it is not associated with clinical symptoms. With a prevalence of about 0.1% in contemporary humans, it is, however, less common. Together with the presence of dental anomalies in two individuals from El Sidrón, this accumulation of rare developmental defects at this but also at other sites was taken as evidence for a high level of consanguinity in Pleistocene populations (Ríos et al. 2015; Trinkaus 2018).

Krapina

The rock shelter at the foot of the Hušnjak hill overlooking the Krapinica river at Krapina, Croatia, yielded a large number of fragmentary and mostly isolated Neanderthal vertebral remains that are dated to a mean age of 130 ± 10 ka (Gorjanović-Kramberger 1906; Rink et al. 1995).

The lower cervical vertebral series Krapina 106/108–110 (C4–C7) shows moderate to severe facet joint osteoarthritis despite the probably young adult age of that individual (Trinkaus 2016). The changes are most marked at the left C4/C5 facet joint with osteophytes, surface pitting and eburnation. Osteophytes at the left C5/C6 facet joint might have compromised the spinal nerve root (Trinkaus 2016).

Gardner and Smith (2006) suggested that the relatively minor osteophytic lipping at the posterior vertebral body of Krapina 106 (C4) also led to spinal stenosis. The vertebral foramen of this vertebra still has, however, an anteroposterior diameter of 15.8 mm (Trinkaus 2016), which is well above the radiological threshold of

13 mm for spinal stenosis in modern humans (Cantu 1998). There is therefore no evidence for spinal stenosis in Krapina 106/108–110.

In analogy with the extensive cervical osteoarthritis of La Chapelle-aux-Saints 1, for which Dawson and Trinkaus (1997) proposed a traumatic origin, Gardner and Smith (2006) inferred a similar aetiology for the pathology in Krapina 106/108–110. The reanalysis of La Chapelle-aux-Saints 1 by Haeusler et al. (2019) revealed, however, a more generalised pattern of spinal osteoarthritis in this individual than previously suggested, which is incompatible with localised trauma. Consequently, the degenerative changes in Krapina 106/108–110 might also be best explained by advanced age.

Minor osteophytes have also been reported at the ventral margin of the body and at the facets of Krapina 112.1 and 112.6 (probably C6 and C7) as well as at the facets of the thoracolumbar vertebrae Krapina 113.1 and 116.4 (Trinkaus 2016).

Shanidar 1

Shanidar 1 is an older adult (35- to 50-year-old) male Neanderthal from Shanidar Cave, Iraqi Kurdistan, that is dated to ca. 75–50 ka BP (Solecki 1971; Trinkaus 1983). The skeleton is best known for its stunted right shoulder and arm, probably resulting from a traumatic amputation above the elbow during childhood (Trinkaus 1983). The vertebral column preserves a fragmentary C1, most of C5–T1, fragments of T2(?) and T12 as well as of several further thoracic vertebrae, the crushed bodies of L1 and L2, large portions of the bodies of L3–L5 and a crushed sacrum. The poor preservation prevents an adequate assessment of the vertebral pathologies. Trinkaus (1983) and Crubézy and Trinkaus (1992) described an osteophyte at the anteroinferior margin of the C5 body, a large beak-shaped osteophyte at the left inferior body of L3 that projects 13.4 mm inferiorly and probably bridged to L4, a broad broken-off osteophyte on the upper left anterolateral margin of L5 and osteophytic remodelling of the left inferior facet joint of L5. Trinkaus (1983) interpreted these alterations as degenerative, while Crubézy and Trinkaus (1992) suggested that Shanidar 1 suffered from a moderate form of diffuse idiopathic skeletal hyperostosis (DISH) based on the additional extraspinal involvement such as enthesophytes at the left olecranon, the superior pole of both patellae and both calcaneal tuberosities.

DISH is a systemic disease of unknown aetiology characterised by progressive ossification of entheses and ligaments (Forestier and Rotés-Querol 1950; Mader et al. 2013). Patients affected by DISH are mostly asymptomatic, but the condition is frequently associated with obesity; metabolic risk factors such as diabetes mellitus, dyslipidaemia, hyperuricaemia and hypertension; and advanced age (Mader et al. 2013). These metabolic derangements are unexpected in a Neanderthal.

DISH has to be differentiated from degenerative spondylosis (see, e.g. Mader et al. 2013). Characteristic of DISH is the ossification of the anterior longitudinal ligament particularly of the thoracic spine, while in spondylosis the thoracic spine is only involved in later stages. Second, the intervertebral disc space is usually preserved, whereas it is reduced in spondylosis. Third, the osteophytes in DISH are broad, vertical and bridging, flowing like a band over the anterolateral aspects of

multiple vertebrae. On the other hand, osteophytes in degenerative spondylosis are produced by the periosteum. They are therefore located submarginally, i.e. they originate a few millimetres caudally or cranially from the edge of the vertebral body. They first grow in a transverse direction and then bend cranially or caudally, which leads to the characteristic beak-shaped osteophytes. In contrast to DISH, they thus become bridging only at advanced stages.

As noted by Crubézy and Trinkaus (1992), the diagnosis of DISH cannot be definitively established in Shanidar 1. Most importantly, there is no indication of the pathognomonic ossification of the anterior longitudinal ligament in the preserved lumbar vertebrae L3–L5 (see Fig. 1 in Crubézy and Trinkaus 1992), and due to damage to the thoracic region, it is not possible to assess whether four contiguous thoracic vertebrae were connected by bony bridges as required by the most commonly used diagnostic criteria of DISH (Resnick and Niwayama 1976). Moreover, bridging osteophytes are also absent in the remainder of the vertebral column of Shanidar 1. The tip of the large beak-shaped osteophyte on the left side of L3 is not broken off, and there is therefore no reason to assume that it once was bridging. Its shape best corresponds to a third-degree submarginal osteophyte (Nathan 1962) characteristic of degenerative spondylosis. Rather than with the anterior longitudinal ligament, it has been associated with the left interior intervertebral ligament (Trinkaus 1983), whose fibres radiate into the intervertebral disc. In addition, osteoarthritis of the facet joint L5–S1 indicates intervertebral disc space narrowing, while disc space typically is preserved in DISH. More study is therefore needed to establish the diagnosis of DISH in Shanidar 1.

Shanidar 2

Shanidar 2 is a 20- to 30-year-old male Neanderthal from Shanidar Cave, northern Iraq (Solecki 1971; Trinkaus 1983). It preserves significant parts of all seven cervical vertebrae, fragments of eight thoracic and four lumbar vertebrae (Trinkaus 1983). Only minor facet joint osteoarthritis is described for the right occipital condyle and the superior articular facets and the left inferior articular facet of the L4 (Trinkaus 1983).

The tips of the spinous processes L2–L4 are robust, and their inferior margins are bifurcated. Ogilvie et al. (1998) inferred from this that Shanidar 2 suffered from Baastrup's disease despite its young age. However, in accordance with the minor degenerative changes of the lumbar facet joints, the spinous processes show no osteophytic remodelling suggestive of a close contact between them. In addition, impingement of the spinous processes is expected to lead to a shallow groove rather than to the sharp, V-shaped notch that separates the two knobs at the inferior side of the spinous processes in Shanidar 2 (see also Le Double 1912).

Similar bifurcations of the inferior margin of the spinous processes have been described in additional Neanderthals, including Shanidar 3, the fragmentary L4 spinous process of Shanidar 4 and the L2 spinous process of Shanidar 6 (Trinkaus 1983). The latter specimen is like Shanidar 2 a young adult, and its skeleton also shows little evidence for degenerative processes, which would be uncharacteristic

for Baastrup's disease. As bifurcated lumbar spines are often also found in male gorillas, they might simply reflect the general robusticity of these Neanderthal skeletons without being caused by Baastrup's disease. Rather, they might aetiologically be related to the bifurcation of the cervical spinous processes (see also Woodruff 2014; von Eggeling 1922).

Shanidar 3

Shanidar 3 is a ca. 40- to 45-year-old male Neanderthal from Shanidar Cave, northern Iraq (Solecki 1971; Trinkaus 1983; Trinkaus and Thompson 1987). The vertebral column preserves major parts of the thoracic, lumbar and sacral region. Instead of costal processes, the fifth last presacral element shows well-developed bilateral rib facets on the pedicles. Trinkaus (1983) and Ogilvie et al. (1998) interpreted this vertebra as an L1 that had bilateral lumbar ribs. Alternatively, the rib facets could have articulated with true thoracic ribs since the well-developed rib facets suggest correspondingly well-developed ribs. This would imply that the lumbar spine counted only four elements. Both interpretations are equally likely. In fact, a number of 4 lumbar vertebrae and either 12 or 13 thoracic elements occur in about 5% of modern humans (Schultz and Straus 1945; Pilbeam 2004). Lumbar ribs also have a reported prevalence of 5%, although bilateral lumbar ribs are rarer (Hueck 1930). Crucial for the difference between a lumbar vertebra with bilateral lumbar ribs and a last thoracic vertebra would be the morphology of this pair of ribs. A lumbar rib would be blunt, thick and laterally or cranially directed and therefore appears morphologically like a detached flat, expanded costal process (Haeusler et al. 2002). Shanidar 3 preserves fragments of 12 rib pairs (Trinkaus 1983; Franciscus and Churchill 2002), but it is unknown whether one of them articulated with the fifth last presacral vertebra. In the absence of these ribs, it cannot be decided whether Shanidar 3 possessed four or five lumbar vertebrae. In any case, no functional difference has been associated with these anomalies.

The preserved vertebrae of Shanidar 3 show several different pathologies. A cavitation of 8.5 mm mediolaterally by 4.5 mm superoinferiorly is visible on the dorsal aspect of the left costal process of the penultimate vertebra. This lesion might represent a developmental defect (Ogilvie et al. 1998). Another cavitation is visible in the same vertebra on the right inferior aspect of the spinous process.

The preserved lower thoracic and lumbar vertebrae of Shanidar 3 show moderate degenerative changes with slight to moderate facet joint osteoarthritis. Submarginal osteophytes are most marked at the right lateral side of the vertebral bodies of the fourth, fifth and sixth last presacral elements. Ogilvie et al. (1998) erroneously interpreted them as syndesmophytes. Syndesmophytes would be pathognomonic of ankylosing spondylitis, a progressive inflammatory autoimmune disorder primarily affecting the axial skeleton that typically begins in young adults. Syndesmophytes represent ossifications of the outer lamella of the annulus fibrosus of the intervertebral disc and the immediately adjacent connective tissue and therefore grow right from the margin of the vertebral endplate in a longitudinal direction. In contrast, degenerative osteophytes of the vertebral bodies (also called spondylophytes) are of

periostal origin and therefore originate at some distance away from the vertebral margin. They initially grow in lateral and ventral directions before they bend cranially or caudally and are, therefore, beak-shaped as in Shanidar 3 (Freyschmidt 2008; see also Shanidar 1).

Like in Shanidar 2, Shanidar 4 and Shanidar 6, the tips of the lumbar spinous processes of Shanidar 3 are bifurcated at their inferior aspect, which is most marked in the penultimate and antepenultimate lumbar vertebrae; the spinous processes are not preserved in the last lumbar vertebra and in the first two sacral elements where they have been reconstructed with plaster of Paris (see, e.g. Fig. S1 in Gómez-Olivencia et al. 2017). Ogilvie et al. (1998) inferred from this bifurcation that Shanidar 3 was affected by Baastrup's disease. As in the other Shanidar specimens, the deep, V-shaped notch is still visible that separates the two knobs at the inferior side of the bifurcated spinous processes in the penultimate and antepenultimate lumbar vertebrae of Shanidar 3. However, the knobs themselves show osteophytic remodelling, suggesting long-term impingement of the lower lumbar spinous processes. The presence of Baastrup's disease in Shanidar 3 in combination with facet joint osteoarthritis and submarginal osteophytes at the lumbar vertebral bodies indicates a reduced intervertebral space and possibly an increased lumbar lordosis during his last years of life.

Remarkable is also the strong kyphotic wedging of about 9° of both the sixth and the fifth last presacral vertebrae (corresponding either to the last two thoracic vertebrae or the last thoracic and first lumbar vertebrae). This is accompanied by an abnormal 6° kyphotic wedging of the fourth last presacral vertebra, while the third last presacral vertebra is with 4° within the normal range of variation of modern humans. Kyphotic wedging of ≥5° in three or more vertebrae in combination with vertebral endplate irregularities that are also present in these vertebrae of Shanidar 3 is diagnostic of Scheuermann's disease (Sørensen 1964; Schlenzka and Arlet 2008; Palazzo et al. 2014).

Shanidar 4

Shanidar 4 is a male Neanderthal from Shanidar Cave, northern Iraq, of advanced age, whose teeth are similarly worn down as those of Shanidar 1 (Trinkaus 1983). His vertebral column is badly preserved. Moderately pronounced submarginal osteophytes have been described ventrally at the C4 vertebral body and at one of the thoracic or upper lumbar body fragments. In addition, all three of the lumbar left superior articular facets and one of the two lumbar left inferior articular facets show facet joint osteoarthritis (Trinkaus 1983).

Kebara 2

The adult male Neanderthal skeleton from Kebara preserves a nearly complete, though partially crushed, vertebral column (Arensburg 1991). Several developmental anomalies have been described. The first lumbar vertebra possesses typical

lumbar ribs. They are flat, about 2 cm long with a concave superior border, and thus look like detached costal processes (Duday and Arensburg 1991). The apophysis of the spinous process of L1 seems to be unfused, while L2–L5 have an almost complete agenesis of the spinous processes. This developmental defect is a variant of occult spinal dysraphism, a group of disorders that includes spina bifida occulta, and is typically not associated with an underlying neural pathology (Kumar and Tubbs 2011). The sacrum, on the other hand, shows a transitional first sacral element that is partially lumbarised, leading to a double promontorium (Duday and Arensburg 1991).

Duday and Arensburg (1991) described a considerable ventral expansion of the ring apophyses of the midthoracic vertebrae T2–T8. They hesitated, however, to attribute this to Scheuermann's disease. Thus, only vertebra T5 shows an abnormal kyphotic wedging of 6° based on the measurements of Arensburg (1991), and a single small Schmorl's node of 3.0 × 3.4 mm has been observed in the superior surface of vertebral body L2 (Duday and Arensburg 1991). Sørensen's (1964) classic radiological criteria for Scheuermann's disease of kyphotic wedging in at least three adjacent vertebrae of 5° or greater are therefore not met. Yet, some authors consider one abnormally wedged vertebra as sufficient to diagnose Scheuermann's disease if associated with increased kyphosis and endplate irregularities such as Schmorl's nodes (Bradford 1981; Palazzo et al. 2014).

The lower thoracic and upper lumbar vertebral bodies (T10, L1–L4) show minor submarginal osteophytes. Facet joint osteoarthritis is present in vertebrae C2/C3, T11 and T12 and L5–S1 (Duday and Arensburg 1991).

10.3 Discussion

Although the fragile elements of the vertebral column are less often preserved in the hominin fossil record than harder bone tissues such as those from the long bones and the skull, the relatively small sample size shows a remarkably high prevalence of pathologies. So far, the only specimens, for which no pathologies have been described, are the Dikika child (*A. afarensis*), the adult female MH2 (*A. sediba*) and the subadult skeleton from Dmanisi (*Homo erectus*), if we focus on fossil hominin skeletons that preserve significant parts of the vertebral column.

The described pathologies fall into various major aetiological groups, including congenital, neoplastic, degenerative and traumatic conditions. Thus, there is one case of a congenital agenesis of the lumbar spinous processes in the Kebara 2 Neanderthal (Duday and Arensburg 1991), two cases of spina bifida-like developmental defects in the El Sidrón Neanderthal sample (Ríos et al. 2015; Trinkaus 2018) and one case of a neoplasia—the benign bone tumour in MH2 (*A. sediba*) (Randolph-Quinney et al. 2016). Other pathologies are summarised in the following sections.

10.3.1 Degenerative Processes of the Vertebral Column

More common are degenerative processes of the vertebral column. Facet joint osteoarthritis has already been observed in the earliest hominin fossil that preserves a substantial portion of the cervical spine, the 3.58-Ma-old KSD-VP-1/1 (*A. afarensis*). Degenerative osteoarthritic changes become, however, only widespread in Neanderthals and their direct ancestors, where the vertebral columns of the SH Pelvis 1 individual, La Chapelle-aux-Saints 1, La Ferrassie 1, Shanidar 1, Shanidar 3 and Shanidar 4, Kebara 2 and, to a lesser degree, Regourdou 1 are affected. Ogilvie et al. (1998) attributed this to the strenuous physical activities associated with the foraging lifestyle of Neanderthals. Yet, although a comparison of the prevalence and pattern of osteoarthritis between Neanderthals and early modern humans is missing so far, an analysis of traumatic injuries demonstrated no difference in the prevalence to modern humans (Beier et al. 2018). It is thus not possible to infer a more strenuous lifestyle in Neanderthals than in Upper Palaeolithic modern humans. Moreover, osteoarthritis is not a suitable indicator of habitual activity and strain in prehistoric human populations in general (e.g. Bridges 1991; Weiss and Jurmain 2007). Although there are no specific data for spinal osteoarthritis available, a recent review confirmed that, in the absence of previous joint injury, increased levels of sport and physical activity are not associated with an increased level of osteoarthritis (Richmond et al. 2013). Rather, intense physical activity might be protective of hip, knee or ankle osteoarthritis. Likewise, elite athletes participating in high-level long-distance running do not have an elevated risk of hip joint osteoarthritis, in contrast to those participating in high-impact sports (Vigdorchik et al. 2017).

The main factor influencing the onset and severity of osteoarthritis is, however, age (Weiss and Jurmain 2007). The high prevalence of advanced spinal osteoarthritis, including Baastrup's disease, in Neanderthals might therefore reflect the dramatic increase in longevity in the Late Pleistocene inferred from tooth wear (Mann 1975; Trinkaus 2011; Mori et al. 2013).

Nevertheless, biomechanical factors related to bipedalism may play a role in the aetiology of spinal osteoarthritis. This is insinuated by the remarkably low prevalence of such alterations in non-human primates (Jurmain 2000) and the absence of regional differences between the spinal levels, if spinal osteoarthritis develops at an advanced age (Lauerman et al. 1992; Nuckley et al. 2008). The human-like pattern of the distribution of osteoarthritic lesions in the cervical spine of KSD-VP-1/1 might thus simply reflect bipedal locomotion in *A. afarensis* and is compatible with a well-developed cervical lordosis.

The analysis of osteoarthritic changes has a great potential of inferring spinal posture in other fossil hominins as well. Thus, advanced spinal osteoarthritis with Baastrup's disease and telescoping subluxations with the formation of nearthroses at the cervical and lumbar spine of the La Chapelle-aux-Saints 1 Neanderthal imply that this individual had a well-developed cervical lordosis coupled with a lumbar lordosis exceeding that of our modern human reference sample (Haeusler et al. 2019).

Further evidence for a well-developed lumbar lordosis in Neanderthals comes from Shanidar 3, whose lower lumbar vertebrae were probably also affected by Baastrup's disease. These findings challenge previous studies based on vertebral wedging, the orientation of the inferior articular processes of the lumbar vertebrae and on foramen magnum orientation suggesting a flat lower back and a weak cervical lordosis in La Chapelle-aux-Saints 1 and other Neanderthals (Weber and Pusch 2008; Been et al. 2010, 2012, 2017). More studies are therefore needed to resolve this apparent conflict.

10.3.2 Spinal Pathologies Related to Biomechanical Failure

The great majority of spinal pathologies in fossil hominins are related to biomechanical failure and trauma sensu lato. They mostly affect juvenile and young adult individuals. This includes spondylolisthesis, a uniquely hominin condition related to upright bipedal posture (Merbs 1996) that can be observed in the last lumbar vertebra of the Middle Pleistocene SH Pelvis 1 individual (Bonmatí et al. 2010). A major risk factor is an increased lumbar lordosis and pelvic incidence (Labelle et al. 2004; the presence of a second promontorium and the deformed superior sacral surface need to be taken into account to predict lumbar lordosis in this individual).

A further pathology related to biomechanical failure is the traumatic juvenile disc herniation that has been inferred for KNM-WT 15000 but is extremely rare in modern humans (Haeusler et al. 2013). Otherwise, this individual seems to be a healthy *Homo erectus* youth with no evidence for congenital skeletal dysplasia or other claimed pathologies (Schiess and Haeusler 2013; Schiess et al. 2014; Meyer and Haeusler 2015). Traumatic juvenile disc herniation is pathogenetically related to anterior disc herniation (also known as limbus vertebra) that probably can be observed in L4–L5 of StW 431 (*A. africanus*). The differential diagnosis of brucellosis proposed by D'Anastasio et al. (2009) for these alterations is less likely according to the argumentation of Mays (2007).

The most common spinal disorder in the hominin fossil record is, however, Scheuermann's disease. Evidence for Scheuermann's disease is found in A.L. 288-1 (*A. afarensis*) and in three other isolated thoracic vertebrae from Hadar (A.L. 333-51, A.L. 333-152 and A.L. 333x-12; Cook et al. 1983; Ward et al. 2012), Sts 14 (*A. africanus*), SKX 3342 (*P. robustus*), in the SH Pelvis 1 individual, and perhaps Kebara 2 and Shanidar 3. This suggests that at least seven out of two dozen early hominin vertebral columns suffered from this condition. Also today, Scheuermann's disease is the most common spinal deformity, affecting about 0.4–8.3% of modern humans (Sørensen 1964; Schlenzka and Arlet 2008; Palazzo et al. 2014). Yet, the prevalence in early hominins seems to significantly surpass that in contemporary populations.

Juvenile disc herniation, traumatic anterior disc herniation and Scheuermann's disease have been argued to be different manifestations of the same phenomenon (Schmorl and Junghans 1968; Cleveland and Delong 1981; Heithoff et al. 1994; Parisini et al. 2001). These entities all occur during the increased vulnerability

phase of the pubertal growth spurt, result from displacement of disc material and have a higher incidence following trauma. In this context, the disc herniation of the Nariokotome boy loses some of its singularity despite being rare among adolescents today.

Surprisingly, no evidence of scoliosis has been found so far in fossil hominins, although this deformity today has a similarly high prevalence as Scheuermann's disease (1.0–3.3%; Rogala et al. 1978; Lonstein et al. 1982; Daruwalla et al. 1985; Suh et al. 2011). Assertions for scoliosis in KNM-WT 15000 (Latimer and Ohman 2001) have been rejected by Schiess et al. (2014), while the claimed presence of scoliosis in La Ferrassie 1 (Gómez-Olivencia et al. 2018) and Regourdou 1 (Gómez-Olivencia et al. 2013) is hampered by the fragmentarity of these specimens that prevents assessment of the diagnostic criteria of scoliosis (see Schiess et al. 2014). Like Scheuermann's disease, adolescent idiopathic scoliosis is also related to upright bipedalism (Kouwenhoven and Castelein 2008), and its absence in the fossil record thus emphasises the remarkably high prevalence of Scheuermann's disease and related conditions in our ancestors.

10.4 Summary and Conclusions

This survey found a remarkably high prevalence of degenerative disorders of the spinal column. They can already be observed in the earliest australopithecine fossils, although they become more common and more severe in the Late Pleistocene only. This might reflect the dramatically increased lifespan of these populations rather than a physically more demanding lifestyle.

The hominin fossil record shows, however, also an extraordinarily high prevalence of disorders testifying to mechanical strains to the axial skeleton in our ancestors that particularly affected the adolescent spine such as Scheuermann's disease and related conditions. A possible explanation for this might be that the early hominin spine is characterised by relatively smaller vertebral cross-sectional areas compared to modern humans (McHenry 1992; Schiess and Haeusler 2013). Because stress is directly proportional to the force over the loaded area, a small cross section makes vertebrae and discs more susceptible to injury (Haeusler et al. 2013). We, therefore, hypothesise that the early hominin intervertebral discs were more vulnerable to injury due to their relatively smaller vertebral cross-sectional area compared with that of modern humans. Conversely, we might speculate that our spinal column has been shaped by a long process of natural selection to become less vulnerable than that of our ancestors. Increased vertebral cross-sectional area might indeed be considered as one of the most important vertebral adaptations to habitual bipedal locomotion (Haeusler et al. 2013). It is likely that this makes our vertebral column better adapted to vertical loading than that of early hominins. Consequently, we seem to have less problems with our spine than our ancestors.

These adaptations considerably predate industrialisation and the spread of agriculture. Our data, therefore, do not support the hypothesis that the changed lifestyle

of contemporary humans and a mismatch of our body to modern-day environments (Stearns et al. 2010) are related to our widespread back problems. In addition, we have no evidence that the high prevalence of low back problems of contemporary populations might primarily be attributed to our increased lifespan, as advocated by Putz and Müller-Gerbl (1996).

A corollary of our data is that they emphasise the importance of biomechanical factors in the aetiology of back problems. This seems to contradict the findings of twin studies that variation in physical loading exposure related to occupation and sports only explains between 2 and 7% of the variation in disc degeneration at L4–S1 and T12–L4, respectively, while genetic influences explained between 34 and 51% (Battié et al. 1995; Battié et al. 2009). However, the physical loading accompanying everyday upright posture and locomotion is not considered in these epidemiologic studies (Battié et al. 2004). Moreover, moderate physical loading has been shown to be beneficiary to the disc (Videman et al. 2007; Adams et al. 2015). This is in line with the well-known tenet of evolutionary medicine that we weren't born to sit, and if we must, we should keep our back muscles active by constantly moving and changing the mechanics (Crawford et al. 2016). The predominance of back disorders today may, therefore, relate to external influences like our society's perception of back pain (Waddell 1996). The majority of back pain may actually be "normal". Perhaps the knowledge about the evolutionary background of our vertebral column may improve the patient's ability to cope with low back pain.

The high prevalence of spinal pathologies in the fossil hominin record on the other hand also reminds us that a peculiar morphology in a fossil specimen might be due to pathology rather than representing a derived trait. A careful comparison with normal and pathological reference samples is therefore always needed.

Acknowledgements I thank Asier Gómez-Olivencia and Leonid Kalichman for comments to the manuscript that greatly helped to improve it. Access to the fossils was granted by Yohannes Haile-Selassie, Yared Assefa, Metasebia Endalamaw and Mamitu Yilma (National Museum of Ethiopia, Addis Ababa); Fredrick Manthi, Emma Mbua and Meave Leakey (National Museums of Kenya, Nairobi); Stephany Potze and Francis Thackeray (Ditsong National Museum of Natural History, Pretoria); Lee Berger, Bernhard Zipfel and the late Philippe Tobias (University of the Witwatersrand, South Africa); Dominique Grimaud-Hervé, Liliana Huet, Véronique Laborde and Antoine Balzeau (Musée de l'Homme, Paris); Antonio Rosas and Markus Bastir (Museo Nacional de Ciencias Naturales, Madrid); and Richard Potts (Smithsonian National Museum of Natural History, Washington). Financial support was provided by the Swiss National Science Foundation Grants No. 31003A_156299 and 31003A_176319 as well as the Mäxi Foundation, Switzerland.

References

Adams MA, Lama P, Zehra U, Dolan P (2015) Why do some intervertebral discs degenerate, when others (in the same spine) do not? Clin Anat 28:195–204

Alonso F, Bryant E, Iwanaga J, Chapman JR, Oskouian RJ, Tubbs RS (2017) Baastrup's disease: a comprehensive review of the extant literature. World Neurosurg 101:331–334

Anderson R (1999) Human evolution, low back pain, and dual-level control. In: Trevathan WR, Smith EO, McKenna JJ (eds) Evolutionary medicine. Oxford University Press, Oxford, pp 333–349

Andersson GBJ (1999) Epidemiological features of chronic low-back pain. Lancet 354:581–585
Antoniades SB, Hammerberg KW, DeWald RL (2000) Sagittal plane configuration of the sacrum in spondylolisthesis. Spine 25:1085–1091
Arambourg C (1955) Sur l'attitude, en station verticale, des Néanderthaliens. Comptes Rendus Hebdomadaires des Séances de l'Académie des Sciences 240:804–806
Arensburg B (1991) The vertebral column, thoracic cage and hyoid bone. In: Bar Yosef O, Vandermeersch B (eds) Le squelette Moustérien de Kébara 2. Éditions du CNRS, Paris, pp 113–146
Arsuaga JL, Martínez I, Arnold LJ, Aranburu A, Gracia-Téllez A, Sharp WD, Quam RM, Falguères C, Pantoja-Pérez A, Bischoff J, Poza-Rey E, Parés JM, Carretero JM, Demuro M, Lorenzo C, Sala N, Martinón-Torres M, García N, Alcázar de Velasco A, Cuenca-Bescós G, Gómez-Olivencia A, Moreno D, Pablos A, Shen C-C, Rodríguez L, Ortega AI, García R, Bonmatí A, Bermúdez de Castro JM, Carbonell E (2014) Neandertal roots: cranial and chronological evidence from Sima de los Huesos. Science 344:1358–1363
Baastrup I (1933) On the spinous processes of the lumbar vertebrae and the soft tissues between them, and on pathological changes in that region. Acta Radiologica 14:52–55
Bachmann R (1956) Über die osteoarthrotischen Formveränderungen an den Dornfortsätzen der Lendenwirbelsäule. Arch Orthop Unfall-Chir 48:171–179
Bailey AS, Adler F, Min Lai S, Asher MA (2001) A comparison between bipedal and quadrupedal rats: do bipedal rats actually assume an upright posture? Spine 26:E308–E313
Battié MC, Videman T, Gibbons LE, Fisher LD, Manninen H, Gill K (1995) 1995 Volvo Award in clinical sciences. Determinants of lumbar disc degeneration. A study relating lifetime exposures and magnetic resonance imaging findings in identical twins. Spine 20:2601–2612
Battié MC, Videman T, Kaprio J, Gibbons LE, Gill K, Manninen H, Saarela J, Peltonen L (2009) The Twin Spine Study: contributions to a changing view of disc degeneration. Spine J 9:47–59
Battié MC, Videman T, Parent E (2004) Lumbar disc degeneration: epidemiology and genetic influences. Spine 29:2679–2690
Been E, Barash A, Marom A, Aizenberg I, Kramer PA (2010) A new model for calculating the lumbar lordosis angle in early hominids and in the spine of the Neanderthal from Kebara. Anat Rec 293:1140–1145
Been E, Gómez-Olivencia A, Kramer PA (2012) Lumbar lordosis of extinct hominins. Am J Phys Anthropol 147:64–77
Been E, Gómez-Olivencia A, Kramer PA (2014) Lumbar lordosis in extinct hominins: implications of the pelvic incidence. Am J Phys Anthropol 154:307–314
Been E, Gómez-Olivencia A, Shefi S, Soudack M, Bastir M, Barash A (2017) Evolution of spinopelvic alignment in hominins. Anat Rec 300:900–911
Beier J, Anthes N, Wahl J, Harvati K (2018) Similar cranial trauma prevalence among Neanderthals and Upper Palaeolithic modern humans. Nature 563:686–690
Benade MM (1990) Thoracic and lumbar vertebrae of African hominids ancient and recent: morphological and functional aspects with special reference to upright posture. Master's Thesis, Master's Thesis, University of the Witwatersrand, Johannesburg
Berger LR, de Ruiter DJ, Churchill SE, Schmid P, Carlson KJ, Dirks PH, Kibii JM (2010) *Australopithecus sediba*: a new species of *Homo*-like australopith from South Africa. Science 328:195–204
Bergknut N, Rutges JP, Kranenburg HJ, Smolders LA, Hagman R, Smidt HJ, Lagerstedt AS, Penning LC, Voorhout G, Hazewinkel HA, Grinwis GC, Creemers LB, Meij BP, Dhert WJ (2012) The dog as an animal model for intervertebral disc degeneration? Spine 37:351–358
Bonmatí A, Gómez-Olivencia A, Arsuaga JL, Carretero JM, Gracia A, Martínez I, Lorenzo C, Bermúdez de Castro JM, Carbonell E (2010) Middle Pleistocene lower back and pelvis from an aged human individual from the Sima de los Huesos site, Spain. Proc Natl Acad Sci U S A 107:18386–18391
Boule M (1911–1913) L'homme fossile de La Chapelle-aux-Saints. Annales de Paléontologie 6–8:1–271
Bradford DS (1981) Vertebral osteochondrosis (Scheuermann's kyphosis). Clin Orthop Relat Res 158:83–90

Brailsford JF (1929) Deformities of the lumbosacral region of the spine. Br J Surg 16:562–627
Bridges PS (1991) Degenerative joint disease in hunter–gatherers and agriculturalists from the Southeastern United States. Am J Phys Anthropol 85:379–392
Bywaters EGL, Evans S (1982) The lumbar interspinous bursae and Baastrup's syndrome – an autopsy study. Rheumatol Int 2:87–96
Cantu RC (1998) The cervical spinal stenosis controversy. Clin Sports Med 17:121–126
Castillo ER, Lieberman DE (2018) Shock attenuation in the human lumbar spine during walking and running. J Exp Biol 221:jeb177949
Chirchir H, Kivell TL, Ruff CB, Hublin J-J, Carlson KJ, Zipfel B, Richmond BG (2015) Recent origin of low trabecular bone density in modern humans. Proc Natl Acad Sci U S A 112:366–371
Cleuvenot E (1999) Courbures sagittales de la colonne vertébrale déterminées par la morphologie des vertèbres. Développement d'une nouvelle méthodologie et application chez *Homo sapiens.* PhD dissertation, Université Bordeaux I
Cleveland RH, Delong GR (1981) The relationship of juvenile lumbar disc disease and Scheuermann's disease. Pediatr Radiol 10:161–164
Cook DC, Buikstra JE, DeRousseau CJ, Johanson DC (1983) Vertebral pathology in the Afar australopithecines. Am J Phys Anthropol 60:83–101
Crawford R, Melloh M, Rühli F, Haeusler M (2016) Low back pain as a trade-off to efficient walking: a new perspective on connecting evolutionary medicine with public health. ISEMPH 2016: International Society for Evolution, Medicine and Public Health 2016 Meeting. Durham, June 22–25
Crubézy E, Trinkaus E (1992) Shanidar 1: a case of hyperostotic disease (DISH) in the Middle Paleolithic. Am J Phys Anthropol 89:411–420
D'Anastasio R, Zipfel B, Moggi-Cecchi J, Stanyon R, Capasso L (2009) Possible brucellosis in an early hominin skeleton from Sterkfontein, South Africa. PLoS One 4:e6439
Daruwalla JS, Balasubramaniam P, Chay SO, Rajan U, Lee HP (1985) Idiopathic scoliosis. Prevalence and ethnic distribution in Singapore schoolchildren. J Bone Joint Surg Br 67:182–184
Dawson JE, Trinkaus E (1997) Vertebral osteoarthritis of the La Chapelle-aux-Saints 1 Neanderthal. J Archaeol Sci 24:1015–1021
de Ruiter DJ, Pickering R, Steininger CM, Kramers JD, Hancox PJ, Churchill SE, Berger LR, Backwell L (2009) New *Australopithecus robustus* fossils and associated U-Pb dates from Cooper's Cave (Gauteng, South Africa). J Hum Evol 56:497–513
Dean MC, Leakey MG, Reid DJ, Schrenk F, Schwartz GT, Stringer C, Walker A (2001) Growth processes in teeth distinguish modern humans from *Homo erectus* and earlier hominins. Nature 414:628–631
Degusta D (2002) Comparative skeletal pathology and the case for conspecific care in Middle Pleistocene hominids. J Archaeol Sci 29:1435–1438
Dieleman JL, Baral R, Birger M, Bui AL, Bulchis A, Chapin A, Hamavid H, Horst C, Johnson EK, Joseph J, Lavado R, Lomsadze L, Reynolds A, Squires E, Campbell M, DeCenso B, Dicker D, Flaxman AD, Gabert R, Highfill T, Naghavi M, Nightingale N, Templin T, Tobias MI, Vos T, Murray CJ (2016) US spending on personal health care and public health, 1996–2013. JAMA 316:2627–2646
Duday H, Arensburg B (1991) La pathologie. In: Bar-Yosef O, Vandermeersch B (eds) Le Squelette Moustérien de Kébara 2. Éditions du CNRS, Paris, pp 179–193
Duval-Beaupère G, Schmidt C, Cosson P (1992) A barycentremetric study of the sagittal shape of spine and pelvis: the conditions required for an economic standing position. Ann Biomed Eng 20:451–462
Filippiadis DK, Mazioti A, Argentos S, Anselmetti G, Papakonstantinou O, Kelekis N, Kelekis A (2015) Baastrup's disease (kissing spines syndrome): a pictorial review. Insights Imaging 6:123–128
Forestier J, Rotés-Querol J (1950) Senile ankylosing hyperostosis of the spine. Ann Rheum Dis 9:321–330

Franciscus RG, Churchill SE (2002) The costal skeleton of Shanidar 3 and a reappraisal of Neandertal thoracic morphology. J Hum Evol 42:303–356
Freyschmidt J (2008) Skeletterkrankungen klinisch-radiologische Diagnose und Differenzialdiagnose. Springer, Berlin
Gardner JC, Smith FH (2006) The paleopathology of the Krapina Neandertals. Period Biol 108:471–484
Gloobe H, Nathan H (1973) Osteophyte formation in experimental bipedal rats. J Comp Pathol 83:133–141
Goff CW, Landmesser W (1957) Bipedal rats and mice; laboratory animals for orthopaedic research. J Bone Joint Surg 39-A:616–622
Gómez-Olivencia A (2013a) Back to the old man's back: reassessment of the anatomical determination of the vertebrae of the Neandertal individual of La Chapelle-aux-Saints. Annales de Paléontologie 99:43–65
Gómez-Olivencia A (2013b) The presacral spine of the La Ferrassie 1 Neandertal: a revised inventory. Bulletin et Mémoires de la Société d'Anthropologie de Paris 25:19–38
Gómez-Olivencia A, Arlegi M, Barash A, Stock JT, Been E (2017) The Neandertal vertebral column 2: the lumbar spine. J Hum Evol 106:84–101
Gómez-Olivencia A, Couture-Veschambre C, Madelaine S, Maureille B (2013) The vertebral column of the Regourdou 1 Neandertal. J Hum Evol 64:582–607
Gómez-Olivencia A, Quam R, Sala N, Bardey M, Ohman JC, Balzeau A (2018) La Ferrassie 1: New perspectives on a "classic" Neandertal. J Hum Evol 117:13–32
Gorjanović-Kramberger D (1906) Der diluviale Mensch von Krapina in Kroatien. Ein Beitrag zur Paläoanthropologie. Kreidel, Wiesbaden
Gregory WK (1928) The upright posture of man: a review of its origin and evolution. Proc Am Philos Soc 67:339–374
Guérin G, Frouin M, Talamo S, Aldeias V, Bruxelles L, Chiotti L, Dibble HL, Goldberg P, Hublin J-J, Jain M, Lahaye C, Madelaine S, Maureille B, McPherron SJP, Mercier N, Murray AS, Sandgathe D, Steele TE, Thomsen KJ, Turq A (2015) A multi-method luminescence dating of the Palaeolithic sequence of La Ferrassie based on new excavations adjacent to the La Ferrassie 1 and 2 skeletons. J Archaeol Sci 58:147–166
Hadley LA (1936) Apophyseal subluxation. J Bone Joint Surg 53:428–433
Hadley LA (1951) Intervertebral joint subluxation, bony impingement and foramen encroachment with nerve root changes. Am J Roentgenol Radium Ther 65:377–402
Hadley LA (1961) Anatomico-roentgenographic studies of the posterior spinal articulations. Am J Roentgenol Radium Ther 86:270–276
Haeusler M, Fornai C, Frater N, Bonneau N (2017) The vertebral column of La Chapelle-aux Saints: the evidence of spinal osteoarthritis for Neanderthal spinal curvature. Am J Phys Anthropol 162(Suppl 64):206
Haeusler M, Martelli S, Boeni T (2002) Vertebrae numbers of the early hominid lumbar spine. J Hum Evol 43:621–643
Haeusler M, Ruff CB (2019) Pelvis. In: Richmond BG, Ward CV, Zipfel B (eds) Hominid postcranial remains from Sterkfontein, South Africa. Oxford University Press, Oxford
Haeusler M, Schiess R, Boeni T (2011) New vertebral and rib material point to modern bauplan of the Nariokotome *Homo erectus* skeleton. J Hum Evol 61:575–582
Haeusler M, Schiess R, Boeni T (2012) Modern or distinct axial bauplan in early hominins? A reply to Williams (2012). J Hum Evol 63:557–559
Haeusler M, Schiess R, Boeni T (2013) Evidence for juvenile disc herniation in a *Homo erectus* boy skeleton. Spine 38:123–128
Haeusler M, Trinkaus E, Fornai C, Müller J, Bonneau N, Boeni T, Frater NT (2019) Morphology, pathology and the vertebral posture of the La Chapelle-aux-Saints Neandertal. Proc Natl Acad Sci U S A 116:4923–4927
Haile-Selassie Y, Latimer BM, Alene M, Deino AL, Gibert L, Melillo SM, Saylor BZ, Scott GR, Lovejoy CO (2010) An early *Australopithecus afarensis* postcranium from Woranso-Mille, Ethiopia. Proc Natl Acad Sci U S A 107:12121–12126

Haile-Selassie Y, Su FD (eds) (2016) The postcranial anatomy of *Australopithecus afarensis*: new insights from KSD-VP-1/1. Springer, Dordrecht
Hammerberg KW (2005) New concepts on the pathogenesis and classification of spondylolisthesis. Spine 30:S4–S11
Heim J-L (1976) Les hommes fossiles de La Ferrassie. Tome I – Le gisement. Les squelettes adultes (crâne et squelette du tronc). Masson, Paris
Heithoff KB, Gundry CR, Burton CV, Winter RB (1994) Juvenile discogenic disease. Spine 19:335–340
Hellström M, Jacobsson B, Sward L, Peterson L (1990) Radiologic abnormalities of the thoracolumbar spine in athletes. Acta Radiologica 31:127–132
Hensinger RN (1989) Spondylolysis and spondylolisthesis in children and adolescents. J Bone Joint Surg Br 71:1098–1107
Herries AIR, Curnoe D, Adams JW (2009) A multi-disciplinary seriation of early *Homo* and *Paranthropus* bearing palaeocaves in southern Africa. Quatern Int 202:14–28
Hoy D, March L, Brooks P, Blyth F, Woolf A, Bain C, Williams G, Smith E, Vos T, Barendregt J, Murray C, Burstein R, Buchbinder R (2014) The global burden of low back pain: estimates from the Global Burden of Disease 2010 study. Ann Rheum Dis 73:968–974
Hueck H (1930) Ueber Anomalien der Lendenwirbelsäule, insbesondere die verschiedenen Formen der Lendenrippe. Archiv für klinische Chirurgie 162:58–60
Jinkins JR (2004) Acquired degenerative changes of the intervertebral segments at and suprajacent to the lumbosacral junction. A radioanatomic analysis of the nondiscal structures of the spinal column and perispinal soft tissues. Eur J Radiol 50:134–158
Johanson DC, Lovejoy OC, Kimbel WH, White TD, Ward SC, Bush ME, Latimer BM, Coppens Y (1982) Morphology of the Pliocene partial skeleton (A.L. 288-1) from the Hadar Formation, Ethiopia. Am J Phys Anthropol 57:403–451
Jurmain RD (2000) Degenerative joint disease in African great apes: an evolutionary perspective. J Hum Evol 39:185–203
Kalichman L, Hunter DJ (2007) Lumbar facet joint osteoarthritis: a review. Semin Arthritis Rheum 37:69–80
Keene JS, Albert MJ, Springer SL, Drummond DS, Clancy WG Jr (1989) Back injuries in college athletes. Clin Spine Surg 2:190–195
Kneisl JS, Simon MA (1992) Medical management compared with operative treatment for osteoid-osteoma. J Bone Joint Surg Am 74:179–185
Kouwenhoven JW, Castelein RM (2008) The pathogenesis of adolescent idiopathic scoliosis: review of the literature. Spine 33:2898–2908
Krogman WM (1951) The scars of human evolution. Sci Am 185:54–57
Kumar A, Tubbs RS (2011) Spina bifida: a diagnostic dilemma in paleopathology. Clin Anat 24:19–33
Kummer BKF (1975) Functional adaptation to posture in the pelvis of man and other primates. In: Tuttle RH (ed) Primate functional morphology and evolution. Mouton, The Hague, pp 281–290
Kwong Y, Rao N, Latief K (2011) MDCT findings in Baastrup disease: disease or normal feature of the aging spine? AJR Am J Roentgenol 196:1156–1159
Labelle H, Roussouly P, Berthonnaud E, Transfeldt E, O'Brien M, Chopin D, Hresko T, Dimnet J (2004) Spondylolisthesis, pelvic incidence, and spinopelvic balance: a correlation study. Spine 29:2049–2054
Latimer B (2005) The perils of being bipedal. Ann Biomed Eng 33:3–6
Latimer B, Ohman JC (2001) Axial dysplasia in *Homo erectus*. J Hum Evol 40:A12
Latimer B, Ward CV (1993) The thoracic and lumbar vertebrae. In: Walker A, Leakey R (eds) The Nariokotome *Homo erectus* skeleton. Springer, Berlin, pp 266–293
Lauerman WC, Platenberg RC, Cain JE, Deeney VFX (1992) Age-related disk degeneration: preliminary report of a naturally-occurring baboon model. J Spinal Disord 5:170–174
Le Double A-F (1912) Traité des variations de la colonne vertebrale de l'homme et de leur signification au point de vue de l'anthropologie zoologique. Vigot Frères, Paris

Leino PI, Berg MA, Puska P (1994) Is back pain increasing? Results from national surveys in Finland during 1978/9–1992. Scand J Rheumatol 23:269–276
Lerch H, Wurm H (1964) Schmerzzustände an den Dornfortsätzen der Wirbelsäule und anderen Knochenprominenzen des Rückens. Arch Orthop Unfall-Chir 56:108–122
Liang QQ, Zhou Q, Zhang M, Hou W, Cui XJ, Li CG, Li TF, Shi Q, Wang YJ (2008) Prolonged upright posture induces degenerative changes in intervertebral discs in rat lumbar spine. Spine 33:2052–2058
Lonstein JE, Bjorklund S, Wanninger MH, Nelson RP (1982) Voluntary school screening for scoliosis in Minnesota. J Bone Joint Surg 64:481–488
Lordkipanidze D, Vekua A, Ferring R, Rightmire GP, Agustí J, Kiladze G, Mouskhelishvili A, Nioradze M, Ponce de León M, Tappen M, Zollikofer CPE (2005) The earliest toothless hominin skull. Nature 434:717–718
Lowe TG (2007) Scheuermann's kyphosis. Neurosurg Clin N Am 18:305–315
Mader R, Verlaan J-J, Buskila D (2013) Diffuse idiopathic skeletal hyperostosis: clinical features and pathogenic mechanisms. Nat Rev Rheumatol 9:741–750
Mann AE (1975) Some Paleodemographic aspects of the south African australopithecines. University of Pennsylvania Publications in Anthropology, Philadelphia
Marchetti PG, Bartolozzi P (1997) Classification of spondylolisthesis as a guideline for treatment. In: Bridwell KH, DeWald RL (eds) The textbook for spinal surgery, 2nd edn. Lippincott-Raven, Philadelphia, pp 1211–1254
Maureille B, Gómez-Olivencia A, Couture-Veschambre C, Madelaine S, Holliday T (2015) Nouveaux restes humains provenant du gisement de Regourdou (Montignac-sur-Vézère, Dordogne, France). Paleo 26:117–138
Mayer O (1826) Über zwei neu entdeckte Gelenke an der Wirbelsäule des menschlichen Körpers. Z Phys 2:29–35
Mays SA (2007) Lysis at the anterior vertebral body margin: evidence for brucellar spondylitis? Int J Osteoarchaeol 17:107–118
McDougall I, Brown FH, Vasconcelos PM, Cohen BE, Thiede DS, Buchanan MJ (2012) New single crystal 40Ar/39Ar ages improve time scale for deposition of the Omo group, Omo-Turkana Basin, East Africa. J Geol Soc 169:213–226
McHenry HM (1992) Body size and proportions in early hominids. Am J Phys Anthropol 87:407–431
Merbs CF (1996) Spondylolysis and spondylolisthesis: a cost of being an erect biped or a clever adaptation? Yearb Phys Anthropol 39:201–228
Meyer MR (2016) The cervical vertebrae of KSD-VP-1/1. In: Haile-Selassie Y, Su D (eds) The postcranial anatomy of *Australopithecus afarensis*: new insights from KSD-VP-1/1. Springer, New York, pp 63–111
Meyer MR, Haeusler M (2015) Spinal cord evolution in early *Homo.* J Hum Evol 88:43–53
Meyer MR, Williams SA, Smith MP, Sawyer GJ (2015) Lucy's back: reassessment of fossils associated with the A.L. 288-1 vertebral column. J Hum Evol 85:174–180
Mori T, Moggi-Cecchi J, Pickering TR, Menter CG (2013) Distribution of ages-at-death of fossil hominins from the early Pleistocene site of Drimolen, South Africa: preliminary results and behavioral implications. Proc Eur Soc Stud Hum Evol 2:156
Nathan H (1962) Osteophytes of the vertebral column – an anatomical study of their development according to age, race, and sex with considerations as to their etiology and significance. J Bone Joint Surg 44:243–268
Nuckley DJ, Kramer PA, Del Rosario A, Fabro N, Baran S, Ching RP (2008) Intervertebral disc degeneration in a naturally occurring primate model: radiographic and biomechanical evidence. J Orthop Res 26:1283–1288
Ogilvie MD, Hilton CE, Ogilvie CD (1998) Lumbar anomalies in the Shanidar 3 Neandertal. J Hum Evol 35:597–610
Ohman JC, Wood C, Wood B, Crompton RH, Günther MM, Yu L, Savage R, Wang W (2002) Stature-at-death of KNM-WT 15000. Hum Evol 17:79–94

Olshansky SJ, Carnes BA, Butler RN (2003) If humans were built to last. Sci Am (Special Edition) 13(2):94–100
Palazzo C, Sailhan F, Revel M (2014) Scheuermann's disease: an update. Joint Bone Spine 81:209–214
Parisini P, Di Silvestre M, Greggi T, Miglietta A, Paderni S (2001) Lumbar disc excision in children and adolescents. Spine 26:1997–2000
Pérez PJ (2003) Recopilación de diagnósticos paleopatológicos en fósiles humanos, con casos relativos a homínidos de Atapuerca. In: Isidro A, Malgosa A (eds) Paleopatología. La enfermedad no escrita. Masson, Barcelona, pp 295–306
Peyrony D (1934) La Ferrassie. Moustérien, Périgordien, Aurignacien. Préhistoire 3:1–92
Pietilä TA, Stendel R, Kombos T, Ramsbacher J, Schulte T, Brock M (2001) Lumbar disc herniation in patients up to 25 years of age. Neurol Med Chir 41:340–344
Pilbeam D (2004) The anthropoid postcranial axial skeleton: comments on development, variation, and evolution. J Exp Zool 302B:241–267
Piveteau J (1959) Les restes humains de la grotte de Regourdou (Dordogne). Comptes Rendus Hebdomadaires des Séances de l' Académie des Sciences 248:40–44
Price R, Okamoto M, Le Huec JC, Hasegawa K (2016) Normative spino-pelvic parameters in patients with the lumbarization of S1 compared to a normal asymptomatic population. Eur Spine J 25:3694–3698
Putz RLV, Müller-Gerbl M (1996) The vertebral column – a phylogenetic failure? A theory explaining the function and vulnerability of the human spine. Clin Anat 9:205–212
Qiu XS, Zhang JJ, Yang SW, Lv F, Wang ZW, Chiew J, Ma WW, Qiu Y (2012) Anatomical study of the pelvis in patients with adolescent idiopathic scoliosis. J Anat 220:173–178
Randolph-Quinney PS, Williams SA, Steyn M, Meyer MR, Smilg JS, Churchill SE, Odes E, Augustine T, Tafforeau P, Berger LR (2016) Primary osteogenic tumor of the spine in *Australopithecus sediba*: earliest evidence for neoplastic disease in the human lineage. S Afr J Sci 112:2015–0470
Raynal J (1990) Essai de datation directe. La Chapelle-aux-Saints et la préhistoire en Corrèze. La Nef, Bordeaux, pp 43–46
Resnick D, Niwayama G (1976) Radiographic and pathologic features of spinal involvement in diffuse idiopathic skeletal hyperostosis (DISH). Radiology 119:559–568
Richmond SA, Fukuchi RK, Ezzat A, Schneider K, Schneider G, Emery CA (2013) Are joint injury, sport activity, physical activity, obesity, or occupational activities predictors for osteoarthritis? A systematic review. J Orthop Sports Phys Ther 43:515–B519
Rigo M (1997) Pelvis asymmetry in idiopathic scoliosis. Evidence of whole torsional body deformity? In: Sevastik JA, Diab KM (eds) Research into spinal deformities. IOS Press, Amsterdam
Rink WJ, Schwarcz HP, Smith FH, Radovčić J (1995) ESR ages for Krapina hominids. Nature 378:24
Ríos L, Rosas A, Estalrrich A, García-Tabernero A, Bastir M, Huguet R, Pastor F, Sanchís-Gimeno JA, de la Rasilla M (2015) Possible further evidence of low genetic diversity in the El Sidrón (Asturias, Spain) Neandertal group: congenital clefts of the atlas. PLoS One 10:e0136550
Rmoutilová R, Gómez-Olivencia A, Brůžek J, Ledevin R, Couture-Veschambre C, Holliday T, Madelaine S, Velemínská J, Maureille B (2018) Extreme asymmetry of sacral alae in the Neandertal Regourdou 1 (Montignac-Sur-Vézère, Dordogne, France). Proc Eur Soc Stud Hum Evol 7:164
Robinson JT (1972) Early hominid posture and locomotion. University of Chicago Press, Chicago
Rogala EJ, Drummond DS, Gurr J (1978) Scoliosis: incidence and natural history. A prospective epidemiological study. J Bone Joint Surg Am 60:173–176
Rosenberg NJ, Bargar WL, Friedman B (1981) The incidence of spondylolysis and spondylolisthesis in nonambulatory patients. Spine 6:35–38
Roussouly P, Pinheiro-Franco JL (2011) Biomechanical analysis of the spino-pelvic organization and adaptation in pathology. Eur Spine J 20:609
Ruff C (2007) Body size prediction from juvenile skeletal remains. Am J Phys Anthropol 133:698–716

Ruff CB, Walker A (1993) Body size and body shape. In: Walker A, Leakey R (eds) The Nariokotome *Homo erectus* skeleton. Springer, Berlin, pp 234–265
Rugtveit A (1966) Juvenile lumbar disc herniations. Acta Orthop Scand 37:348–356
Ryan TM, Shaw CN (2015) Gracility of the modern *Homo sapiens* skeleton is the result of decreased biomechanical loading. Proc Natl Acad Sci U S A 112:372–377
Sambrook PN, MacGregor AJ, Spector TD (1999) Genetic influences on cervical and lumbar disc degeneration: a magnetic resonance imaging study in twins. Arthritis Rheum 42:366–372
Sanders WJ (1998) Comparative morphometric study of the australopithecine vertebral series Stw-H8/H41. J Hum Evol 34:249–302
Scheuermann HW (1921) Kyphosis dorsalis juvenilis. Zeitschrift für Orthopädische Chirurgie 41:305–317
Schiess R, Boeni T, Rühli F, Haeusler M (2014) Revisiting scoliosis in the KNM-WT 15000 *Homo erectus* skeleton. J Hum Evol 67:48–59
Schiess R, Haeusler M (2013) No skeletal dysplasia in the Nariokotome boy KNM-WT 15000 (*Homo erectus*): a reassessment of congenital pathologies of the vertebral column. Am J Phys Anthropol 150:365–374
Schlenzka D, Arlet V (2008) Juvenile kyphosis (Scheuermann's disease). In: Boos N, Aebi M (eds) Spinal disorders. Springer, Berlin, pp 765–796
Schlösser TPC, Colo D, Castelein RM (2015) Etiology and pathogenesis of adolescent idiopathic scoliosis. Semin Spine Surg 27:2–8
Schmorl G, Junghans H (1968) Die gesunde und die kranke Wirbelsäule in Röntgenbild und Klinik. Thieme (English translation: Schmorl G, Junghans H. 1971. The human spine in health and disease, New York, Grune & Stratton), Stuttgart
Schultz AH, Straus WL (1945) The numbers of vertebrae in primates. Proc Am Philos Soc 89:601–626
Scoles PV, Latimer BM, DiGiovanni BF, Vargo E, Bauza S, Jellema LM (1991) Vertebral alterations in Scheuermann's kyphosis. Spine 16:509–515
Shi CD, Matsumura A, Takahashi H, Yamashita M, Kimura T (2007) Effects of erect bipedal standing on the morphology of rat vertebral bodies. Anthropol Sci 115:9–15
Slotkin JR, Mislow JM, Day AL, Proctor MR (2007) Pediatric disk disease. Neurosurg Clin N Am 18:659–667
Smit TH (2002) The use of a quadruped as an in vivo model for the study of the spine–biomechanical considerations. Eur Spine J 11:137–144
Smith BH (1993) The physiological age of KNM-WT 15000. In: Walker A, Leakey R (eds) The Nariokotome *Homo erectus* skeleton. Springer, Berlin, pp 195–220
Solecki R (1971) Shanidar: the first flower people. Alfred A. Knopf, New York
Sørensen KH (1964) Scheuermann's juvenile kyphosis. Clinical appearances, radiography, aetiology, and prognosis. Munksgaard, Copenhagen
Stearns SC, Nesse RM, Govindaraju DR, Ellison PT (2010) Evolution in health and medicine Sackler colloquium: evolutionary perspectives on health and medicine. Proc Natl Acad Sci U S A 107(Suppl 1):1691–1695
Straus WL, Cave AJE (1957) Pathology and the posture of Neanderthal man. Q Rev Biol 32:348–363
Suh S-W, Modi HN, Yang J-H, Hong J-Y (2011) Idiopathic scoliosis in Korean schoolchildren: a prospective screening study of over 1 million children. Eur Spine J 20:1087–1094
Susman RL (1989) New hominid fossils from the Swartkrans formation (1979–1986 excavations): postcranial specimens [published erratum appears in the American Journal of Physical Anthropology1990 Jun;82:243]. Am J Phys Anthropol 79:451–474
Takatalo J, Karppinen J, Niinimaki J, Taimela S, Nayha S, Jarvelin MR, Kyllonen E, Tervonen O (2009) Prevalence of degenerative imaging findings in lumbar magnetic resonance imaging among young adults. Spine 34:1716–1721
Tardieu C (1998) Short adolescence in early hominids: infantile and adolescent growth of the human femur. Am J Phys Anthropol 107:163–178

Tardieu C, Haeusler M (2019) The acquisition of human verticality with an emphasis on sagittal balance. In: Roussouly P, Pinheiro-Franco JL, Labelle H, Gehrchen M (eds) Sagittal balance of the spine. Thieme, New York

Tardieu C, Hasegawa K, Haeusler M (2017) How the pelvis and vertebral column became a functional unit in human evolution during the transition from occasional to permanent bipedalism? Anat Rec 300:912–931

Tilley L (2015) Theory and practice in the bioarchaeology of care. Springer, Cham

Tischer T, Aktas T, Milz S, Putz RV (2006) Detailed pathological changes of human lumbar facet joints L1–L5 in elderly individuals. Eur Spine J 15:308–315

Tobias PV (1973) A new chapter in the history of the Sterkfontein early hominid site. J S Afr Biol Soc 14:30–44

Toussaint M, Macho GA, Tobias PV, Partridge TC, Hughes AR (2003) The third partial skeleton of a late Pliocene hominin (Stw 431) from Sterkfontein, South Africa. S Afr J Sci 99:215–223

Trinkaus E (1983) The Shanidar Neandertals. Academic Press, New York

Trinkaus E (1985) Pathology and the posture of the La Chapelle-aux-saints Neandertal. Am J Phys Anthropol 67:19–41

Trinkaus E (2011) Late Pleistocene adult mortality patterns and modern human establishment. Proc Natl Acad Sci U S A 108:1267–1271

Trinkaus E (2016) The Krapina human postcranial remains – morphology, Morphometrics and paleopathology. FF-Press, Zagreb

Trinkaus E (2018) An abundance of developmental anomalies and abnormalities in Pleistocene people. Proc Natl Acad Sci U S A 115:11941–11946

Trinkaus E, Smith FH (1995) Neanderthal mortality patterns. J Archaeol Sci 22:121–142

Trinkaus E, Thompson DD (1987) Femoral diaphyseal histomorphometric age determinations for the Shanidar 3, 4, 5, and 6 Neandertals and Neandertal longevity. Am J Phys Anthropol 72:123–129

Tsirikos AI, Garrido EG (2010) Spondylolysis and spondylolisthesis in children and adolescents. J Bone Joint Surg Br 92:751–759

Tsirikos AI, Jain AK (2011) Scheuermann's kyphosis; current controversies. J Bone Joint Surg Br 93:857–864

Videman T, Levalahti E, Battie MC (2007) The effects of anthropometrics, lifting strength, and physical activities in disc degeneration. Spine 32:1406–1413

Vigdorchik JM, Nepple JJ, Eftekhary N, Leunig M, Clohisy JC (2017) What is the association of elite sporting activities with the development of hip osteoarthritis? Am J Sports Med 45:961–964

von Eggeling H (1922) Die Gabelung der Halswirbeldornen und ihre Ursachen. Anat Anz 55(33–94):201–211

Volinn E (1997) The epidemiology of low back pain in the rest of the world. A review of surveys in low- and middle-income countries. Spine 22:1747–1754

Waddell G (1996) Low back pain: a twentieth century health care enigma. Spine 21:2820–2825

Walker A, Leakey R (eds) (1993) The Nariokotome *Homo erectus* skeleton. Springer, Berlin

Walker A, Shipman P (1996) The wisdom of the bones: in search of human origins. Knopf, New York

Ward CV, Kimbel WH, Harmon EH, Johanson DC (2012) New postcranial fossils of *Australopithecus afarensis* from Hadar, Ethiopia (1990–2007). J Hum Evol 63:1–51

Ward CV, Nalley TK, Spoor F, Tafforeau P, Alemseged Z (2017) Thoracic vertebral count and thoracolumbar transition in *Australopithecus afarensis*. Proc Natl Acad Sci U S A 114:6000–6004

Weber J, Pusch CM (2008) The lumbar spine in Neanderthals shows natural kyphosis. Eur Spine J 17(S2):327–330

Weiss E, Jurmain R (2007) Osteoarthritis revisited: a contemporary review of aetiology. Int J Osteoarchaeol 17:437–450

White TD, Asfaw B, Beyene Y, Haile-Selassie Y, Lovejoy CO, Suwa G, WoldeGabriel G (2009) *Ardipithecus ramidus* and the paleobiology of early hominids. Science 326:75–86

Williams SA, Meyer MR, Nalla S, García-Martínez D, Nalley TK, Eyre J, Prang TC, Bastir M, Schmid P, Churchill SE, Berger LR (2018) The vertebrae, ribs, and sternum of *Australopithecus sediba*. PaleoAnthropology 2018:156–233

Williams SA, Ostrofsky KR, Frater N, Churchill SE, Schmid P, Berger LR (2013) The vertebral column of *Australopithecus sediba*. Science 340:1232996

Woodruff DC (2014) The anatomy of the bifurcated neural spine and its occurrence within Tetrapoda. J Morphol 275:1053–1065

Zihlman A, Bolter D, Boesch C (2004) Wild chimpanzee dentition and its implications for assessing life history in immature hominin fossils. Proc Natl Acad Sci U S A 101:10541–10543

Chapter 11
The Modern and Fossil Hominoid Spinal Ontogeny

Sandra A. Martelli

11.1 Introduction

This chapter presents an overview over the pre- and postnatal ontogeny of the modern human and modern great and lesser ape vertebral column. During pre- and postnatal ontogeny, the human vertebral column undergoes significant changes both in shape and size. There are differences in growth patterns which lead to the distinct and species-specific adult vertebral column morphology of modern humans and great and lesser modern apes that is important to interpret fossil hominoid vertebral material in its phylogenetic and functional context.

Understanding these processes can provide some explanation as to how different adult forms marked by differences such as sexual dimorphism (intraspecific variation) or between related taxa (interspecific variation) both modern and fossil establish.

The first part of the chapter introduces key events of the prenatal development of the human vertebral column. The second part sums up the postnatal development of the size and shape of the vertebrae, the intervertebral discs, the spinal segments (cervical, thoracic, lumbar and sacral) and the vertebral column as a whole including its associated characteristic sagittal curves.

The final part gives a summary of what is known about the pre- and postnatal ontogeny of the modern ape vertebral column. This is followed by an overview on how the postnatal growth of various fossil specimens (*Australopithecus*, *Homo*) compare to both the modern ape and human patterns.

S. A. Martelli (✉)
Department of Cell and Developmental Biology, University College London, London, UK
e-mail: s.martelli@ucl.ac.uk

E. Been et al. (eds.), *Spinal Evolution*,
https://doi.org/10.1007/978-3-030-19349-2_11

11.2 Embryogenesis of the General Mammalian Vertebrae with Special Reference to the Modern Human Embryonal Development

11.2.1 Somite, Sclerotome and Dermomyotome Formation

Primate vertebrae follow the general mammalian vertebrate pattern of spinal and vertebral embryogenesis. Vertebrae arise from somites and embryonal structures which form through segmentation from (paraxial) mesoderm on both sides of the forming notochord and neural tube during week 5 of the embryogenesis (Kaplan et al. 2005). The formation of somites follows in an anteroposterior direction along the future body axis. Somites are temporary embryonal structures which completely disappear as they differentiate into two further structures called sclerotomes and dermomyotomes (Christ et al. 2000; Gilbert 2003; Kaplan et al. 2005). The sclerotomes will eventually give rise to the vertebrae and intervertebral discs and ribs in the thoracic region of the spine. The dermomyotomes are the origin of the accompanying paravertebral musculature, also known as the autochthonous back muscles and the overlying dermis.

The different parts of the developing intervertebral discs have a more mixed origin compared with the vertebrae. The *annulus fibrosus* is formed by sclerotomes (see re-segmentation section below). The other part of the intervertebral disc, the *nucleus pulposus*, develops from the notochord, a structure formed by axial mesoderm. The notochord is the common structure which defines all chordate embryos of the phylum *Chordata* (Wehner and Gehring 2007). In humans, the notochord forms as a midline structure of the mesoderm in week 3 of the embryonal development and at the time of somite formation is found ventrally to the developing neural plate and neural tube. The notochord plays an essential role in several embryonic processes. It might provide directional information for the migration of the sclerotomes, particularly where they surround the notochord (Ward et al. 2018).

11.2.2 Re-segmentation of the Sclerotomes

The sclerotomes do not directly transform into vertebrae. Rather, in the wake of spinal nerve development (peripheral portion), the sclerotomes undergo a re-segmentation, a process in which the sclerotomes split into a cranial and a caudal segment (Huang et al. 1996; Aoyama and Asamoto 2000; Christ et al. 2000; Afonso and Catala 2003) (Fig. 11.1).

The cranial portion of the sclerotome consists of loosely arranged tissue which contains the glycoprotein tenascin-C in its extracellular matrix. The protein encourages the growth of axonal neurons, which assists in the split of the cranial and caudal portion of each sclerotome (Bernhardt et al. 1998). Conversely, the caudal portion of the sclerotome consists of very dense mesenchymal tissue which does not

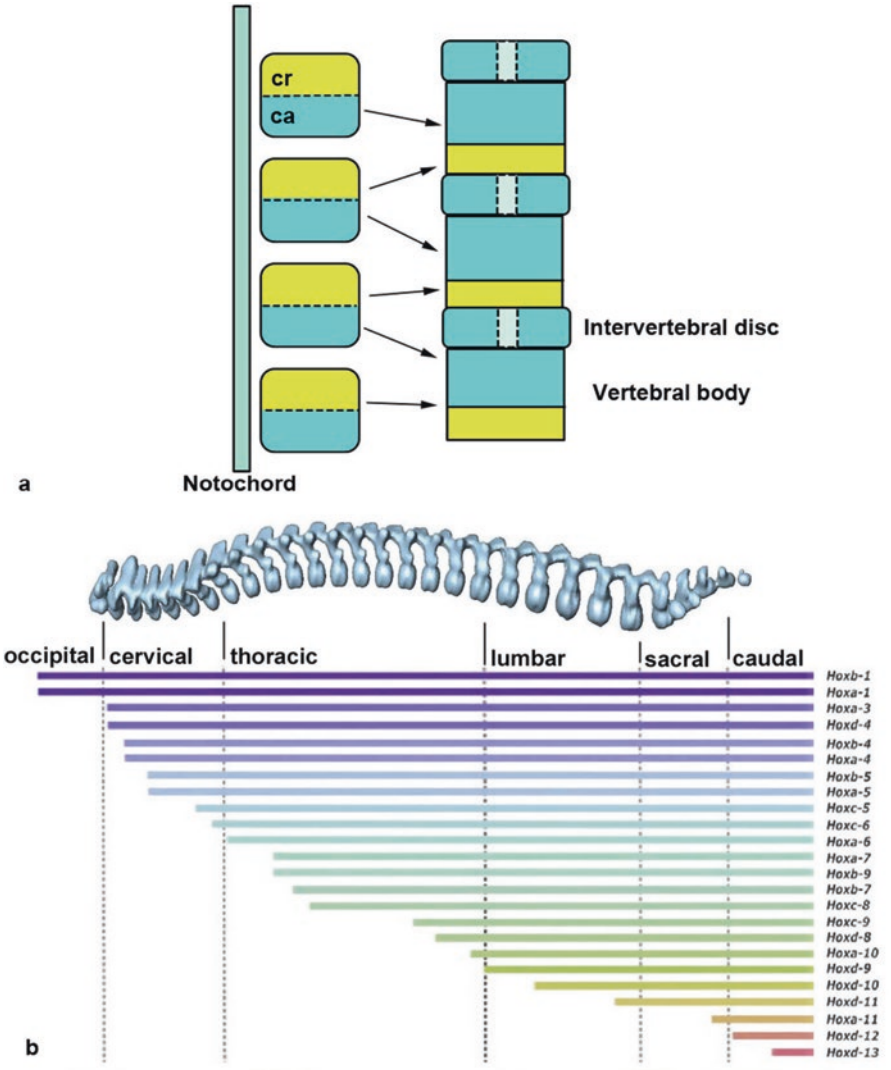

Fig. 11.1 Prenatal vertebral development, key events: (**a**) re-segmentation process of the sclerotomes; *cr* cranial portion of sclerotome, *ca* caudal portion of sclerotome; (**b**) differentiation of vertebral morphology under the control of specific Hox gene expression

encourage the growth of nerves. Subsequently, the cranial portion of a sclerotome will form the caudal part of the vertebral body, and the caudal part of the sclerotome will eventually differentiate into cells forming the *annulus fibrosus* of the intervertebral discs, vertebral arch, transverse processes and ribs. Therefore, two adjacent sclerotomes are involved in the formation of each vertebra.

The first and second vertebrae, the atlas and axis, need further attention as their formation from re-segmentation of sclerotomes is more complex than that of other vertebrae. In many vertebrates, the caudal part of the fourth occipital somite and the cranial part of the first vertebral somite contribute to the formation of a protoatlas. However, this is not the case in humans, where these somite portions are assimilated into the occipital condyles and also form the superior-most tip (apex) of the odontoid process (dens) of the second cervical vertebra (axis). The base of the dens of the axis forms from the caudal part of the first cervical somite and the cranial portion of the second vertebral somite. The body of the axis and the neural arch of the axis form from the caudal part of the second vertebral somite and the cranial part of the third vertebral somite (Cunningham et al. 2016).

11.2.3 The Role of Hox Genes in the Differentiation of the Number of Vertebrae, Vertebral Size and Vertebral Morphology

Somitogenesis, the differentiation into vertebrae with distinctive morphology (cervical, thoracic, lumbar and sacral) from them and the final number of vertebrae, is under the control of the expression of Hox genes, a group of genes instrumental in the development of body plan and anatomical structures. The expression of these Hox genes varies along the anteroposterior body axis (Kessel and Gruss 1990; Burke et al. 1995; Richardson et al. 1998).

In the first instance, Hox genes control the amount as well as the size of somites being formed. This in turn influences the total number of vertebrae that can be formed. Vertebrates with very long presacral spines such as snakes (*Reptilia*) can produce up to 300 somites before vertebral differentiation whereas vertebrates with very short presacral spines such as frogs (*Amphibia*) only produce 6 to 8 somites, resulting in 4–6 vertebrae.

Humans initially produce 42 to 44 pairs of somites. However, that number is reduced to around 37 somites prior to re-segmentation (Richardson et al. 1998). Although somites look identical, the resulting vertebrae are morphologically different according to different spinal regions such as the cervical, thoracic, lumbar and sacral region of the spine. The regional differences in vertebral morphology are established prenatally and are determined by both differences in Hox gene expression and their expression boundaries along the anteroposterior body axis (Kessel and Gruss 1991; Burke et al. 1995; Gilbert 2003). Of particular importance for morphology differentiation are the Hox gene families 5 and 6 (at cervico-thoracic boundary), Hox 9 and 10 (at thoracolumbar boundary), Hox 10 (at lumbosacral boundary) and Hox 10 and 11 (at sacro-caudal boundary) (Burke et al. 1995) (see Fig. 11.1b).

For example, the expression boundary of the Hoxa-9, Hoxb-9 and Hoxc-9 genes seem closely linked with the morphological transition from thoracic to lumbar

vertebrae in mice and chicks (Fromental-Ramain et al. 1996; de la Cruz et al. 1999). Homozygotic mutant mice which lack the Hoxa-9 gene have an anteriorised lumbar region. This means that these mice produced a supernumerary pair of ribs on the vertebra in the position of the usual first lumbar vertebra. Furthermore, the orientation of the vertebra's superior articular processes and joint facets changed from the lumbar to the thoracic type. These mutants sometimes also displayed an anteriorisation of the first sacral vertebra to a lumbar one. Therefore, the relative shifts in Hox gene expression boundaries reflect the relative expansion and contraction of morphological regions, i.e. the lengthening and shortening of thoracic and lumbar regions between related taxa during evolution (Burke et al. 1995; Fromental-Ramain et al. 1996). In the case of fossil and modern hominoids, this can be of importance as the length of the thoracic and lumbar segments of the vertebral column can carry both phylogenetic and functional weight (Schultz 1953, 1961; Haeusler et al. 2002; Pilbeam 2004; Williams et al. 2016; Ward et al. 2017; Williams et al. 2019).

11.2.4 Prenatal Formation of Primary Ossification Centres

Following on the formation process, vertebrae first undergo a chondrification (cartilage formation) process, followed by an ossification (bone formation) process. During the sixth week of embryonal development, the mesenchymal vertebrae start to develop chondrification centres in the centrum (embryonal vertebral body), the two neural arch elements and the transverse and spinous processes (Moore and Persaud 2008). The cartilaginous vertebrae mineralise via endochondral ossification processes, both pre- and postnatally. In humans, the ossification of vertebrae begins during the embryonic period and ends around the 25th postnatal year of age.

In the seventh and eighth embryonal weeks, the first ossification centres appear in the centra, encompassing the original chondrification centres positioned posterior to the notochord and shortly fusing into one centrum ossification centre (Moore and Persaud 2008). The two neural or vertebral arch elements each develop their own ossification centre shortly after the ossification centres of the centra have started forming. These three ossification centres (one centrum, two arch elements) are the primary ossification centres of the vertebrae.

Differing from this pattern are the atypical cervical vertebrae axis and atlas and the sacral vertebrae which develop more than three primary ossification centres. The atlas develops a total of six primary ossification centres, three located on each of the lateral masses. The axis has five primary centres – one for each half of the neural arch, one for the actual body of the axis and two for the upper and lower half of the odontoid process (*dens axis*). Sacral primary ossification centres appear at each of the centra, the arch elements and the costal elements (*alae*).

The pattern of ossification centre appearance differs slightly for centra and arch elements, and the different types of vertebrae are summarised in Table 11.1. For the centra, ossification centres first appear in the lower thoracic and upper lumbar elements (T10–L1) (Cunningham et al. 2016). The appearance of vertebral body

Table 11.1 Prenatal formation of human primary ossification centres

	Prenatal appearance of primary ossification centres	
Vertebrae	Centrum	Vertebral arch elements
Atlas	1–2 years postnatal	7–8 w
Axis	16–24 w	8–9 w
C3–C7	12–16 w ↑[a]	8–12 w↑
T1–T9	9–10 w ↑	8–10 w↓
T11–T12	8–9 w ↑	12–16 w↕[c]
L1–L5	9–10 w ↓[b]	12–16 w↓
S1–S5	12–20 w ↓	16–32 w ↓

[a]Formation continues in cranial direction
[b]Formation continues in caudal direction
[c]Formation continues in both cranial and caudal directions

ossification centres then progresses bidirectionally, towards the fifth lumbar and second cervical vertebrae. These endpoints of progression are reached by the end of the third and fourth foetal months, respectively (Cunningham et al. 2016). It should be noted that the atlas and axis arch element centres appear before the body centres (Table 11.1).

For the neural arch elements, primary ossification centres first appear in the atlas, lower cervical and upper thoracic region. The pattern of progression is somewhat debated but can be summarised as having various points of origin and a bidirectional progression in cranio-caudal direction of appearance of further centres. By the end of the fourth foetal month, all vertebrae have developed their primary ossification centres (Cunningham et al. 2016) (Table 11.1).

Ossification centres for the sacral centra of S1 and S2 appear in the third foetal month. By the fourth month, ossification centres both centra of S1–S4 and arch elements for S1–S3 are visible. The costal element ossification centres appear around foetal months 6–8. At birth, the primary centres of ossification are present but in the lowest sacral elements. It is possible that the primary centres of the lowest sacral elements might be present. However, they might be very small, and the distinctive character of each sacral element is not well established until the end of the first postnatal year.

11.2.5 Secondary Ossification Centres

Vertebrae develop secondary ossification centres during the postnatal development period. These ossification centres appear as growth zones at the tips of each spinous process, the transverse/costal processes, and as two annular epiphyseal plates on the superior and inferior surfaces of the vertebral bodies (Bogduk 2005; Cunningham et al. 2016). Reports vary as to when these secondary epiphyses appear, but in humans they are visible at or around onset of puberty and can indeed be used to estimate the onset of puberty (Moore and Persaud 2008; Ríos and Cardoso 2009;

Cunningham et al. 2016). The secondary ossification centres of the atlas are restricted to epiphyses on the tips of the transverse processes only (Cunningham et al. 2016). The axis has five to six secondary ossification centres if the *ossiculum terminale* of the odontoid process is included. The sacral vertebrae sport a multitude of irregular, rather small secondary, ossification centres along the lateral margins and the sacral spinous processes. The fusion of the secondary ossification centres will be described in the postnatal growth section.

11.3 Postnatal Ontogeny of the Human Vertebral Column: From Birth to Adulthood

11.3.1 Modern Human Growth Patterns

The onset and distribution of peak growth velocity for vertebral column length generally follow a musculoskeletal growth pattern (Tanner et al. 1966). This is characterised by an early growth spurt during the first 2 years of postnatal life, followed by a period of relatively stable and small growth increments and a secondary growth spurt during the late juvenile period (adolescence). It is of note that in females the adolescent growth spurt initiates around the age of 11–12 years, whereas in males, the onset is delayed to around the age of 13–14 years (Tanner et al. 1966; Schlösser et al. 2015). Consequently, the trailing off from peak growth rates occurs earlier in females, around the age of 14–16 years and around the age of 16–18 years in males (Schlösser et al. 2015). This in turn influences the size and shape of the vertebral column as a whole and the relationship between sagittal curves of the vertebral column.

11.3.2 The Neonatal Spine

At birth (Fig. 11.2a), the human vertebral column's overall appearance is best described as C-shaped. Of the characteristic sagittal spinal curves observed in the adult vertebral column, the thoracic kyphosis is present to some degree, and an angle is observed between the last lumbar and the first sacral vertebrae (promontorium angle). The postnatal development of these curves will be addressed later in this chapter.

All presacral vertebrae consist of at least three separate elements at birth: a vertebral body and two vertebral arch elements. The atypical cervical and the sacral vertebrae vary again. The atlas consists of two bone elements with large concave articular facets connecting to the occipital bone. The axis consists of five separate elements as the odontoid process is separate from the body of the axis and consists of two elements. The unfused sacral vertebrae have additional separate costal (alar)

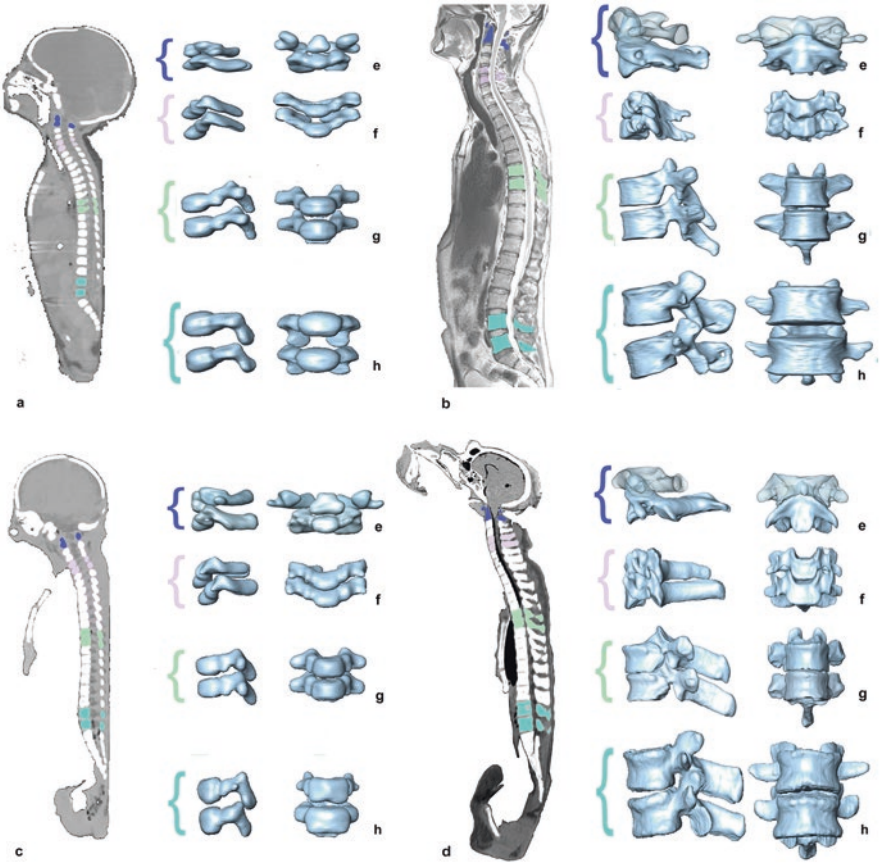

Fig. 11.2 The neonate (**a**) and adult (**b**) human and neonate (**c**) and adult (**d**) chimpanzee vertebral column in midsagittal section with atlas and axis (dark blue) (**e**) and selected cervical (purple) (**f**), thoracic (green) (**g**) and lumbar (turquoise) (**h**) segments highlighted. Note spinal curvature development and differences in vertebral and intervertebral disc height and shape between neonates and adults and between taxa. Cervical segment C5–C6, thoracic segment T7–T8, lumbar segment L4–L5 (human) and L3–L4 (chimpanzee). Adult atlas representations shown semitransparent for better visibility of axis morphology. Sagittal sections and vertebral representations not to scale

elements. These alar masses provide the articulation with the iliac element of the pelvis and form the sacroiliac joint.

Neonate vertebrae already differ in size along the vertebral column (small to large cranio-caudally), but these size differences are considerably less than in the adult. Equally, differences in vertebral morphology are also already established at birth (see previous section), but the vertebrae, with the exception of the atlas and axis, appear more uniform at this point in time.

Vertebral bodies and intervertebral discs appear uniformly square in the midsagittal plane along the length of the vertebral column. However, it should be noted that the intervertebral discs in the lumbar region already appear large compared to other

intervertebral discs and, particularly, the disc at the level of L5/S1 is distinct both in size and orientation. This might be linked to the observation of an increased height gain prenatally in the lumbar discs compared to other spinal regions. This is to the point that the increase in disc height is sometimes bigger than the increase in prenatal centrum height (Cunningham et al. 2016).

11.3.3 The Postnatal Ontogeny of Vertebral Column Length

Throughout childhood and by the end of the adolescent growth spurt, the neonate trunk height (i.e. thoracolumbar spine length) of approximately 34 cm will have increased on average by 88 cm in females and 92 cm in males (Dimeglio and Canavese 2012). The largest increase in trunk height is achieved in the first 2 years of postnatal life. Growth increments of approximately 12 cm in year 1 and about 5 cm in year 2 have been reported by Dimeglio and Canavese (2012). In other words, vertebral bodies and intervertebral discs achieve approximately 50% of their adult length around the age of 2 years.

Until the onset of the adolescent growth spurt, trunk length increases in decreasing (age 2–5 years) and later stable (age 6 years to puberty onset) increments (Taylor and Twomey 1984). Since the onset of puberty is generally earlier in females, they have larger increments of trunk height growth between the ages of about 11 and 13 years than males of the same age. In males, the largest increase in trunk height after the early infant growth spurt is usually observed from 13 to 15 years of age (Taylor and Twomey 1984). Around the age of 18 years, adult trunk height is usually achieved.

A closer inspection of the growth patterns indicates that adult vertebral body length is already established at the age of 10 years and thus prior to the onset of puberty (Dickson and Deacon 1987). Nevertheless, the vertebral body growth zone remains active up to 25 years of age. Whereas not much longitudinal vertebral body growth is achieved during this time period, it allows for adaptation of the shape of the vertebral body (Dickson and Deacon 1987) in the anteroposterior and lateral dimensions. This might represent a crucial adjustment of vertebral morphology to vertically applied spinal loads. The increase in disc height during this time might also further increase trunk height.

11.3.4 Postnatal Ontogeny of Cervical, Thoracic and Lumbar Spinal Segment Length

The different presacral vertebral column segments (cervical, thoracic and lumbar) reach their adult length at different stages of the postnatal ontogeny. At birth, the cervical segment (C1–C7) is the shortest and measures approximately 5–6 cm in

length (Schultz 1961). It will at least double its length at birth and on average increase by about 11 cm in females and 13 cm in males (Johnson et al. 2016).

The overall growth period for the cervical segment is reported to be sexually dimorph with females reaching their final cervical segment length around the age of 14 years and males extending that growth period up to 18 years (Johnson et al. 2016). Therefore, in males, up to 50% of growth is achieved after the 9th year of age whereas in females only 33% of the total growth was achieved after that age. In both males and females, about 25% of total cervical spine length can be attributed to an increase in the length of the cranio-vertebral junction, i.e. atlas and predominantly axis. The majority of longitudinal growth of the cervical spine is achieved by the increase in vertebral body and intervertebral disc height of C3 to C7.

The thoracic segment (T1–T12) usually measures around 20 cm at birth and reaches about 45 cm around the age of 18 years or older (Dimeglio and Canavese 2012). At skeletal maturity, the thoracic segment accounts for approximately 30% of total spine length. Adult thoracic segment length of less than 18–22 cm is tightly associated with severe respiratory insufficiencies (Dimeglio and Canavese 2012).

At approximately 7.5 cm, the lumbar spinal segment (L1–L5) is considerably shorter at birth than the thoracic spinal segment. At skeletal maturity, its length reaches about 16 cm. Although the lumbar spinal segment reaches approximately 90% of its adult length by the age of 10 years, it does not achieve more than 60% of its total volume (i.e. vertebral body width and height) at that age. This indicates that vertebral body width and height increase considerably in the juvenile and adolescent period (Taylor 1975; Dimeglio and Canavese 2012). The different parameters of the vertebral bodies (height, width and length) achieve adult proportions at different times during the postnatal ontogeny.

11.3.5 Postnatal Ontogeny of the Spinal Sagittal Curvature of the Modern Human Vertebral Column

The adult presacral vertebral column characteristically shows three anteroposterior curves when viewed in the sagittal plane: the cervical lordosis, thoracic kyphosis and lumbar lordosis (Fig. 11.2a). Clinically asymptomatic ranges of these spinal curvatures are difficult to establish as they seem to vary widely, e.g. see Willner and Johnson (1983). Partially, curve angles are influenced by sex and ethnic background and potentially other factors such as geographic affinity. For example, the range of adult asymptomatic lordosis angles ranged from 15° to 75° in a Nigerian population (Okpala 2014) but from 11° to 95° in an asymptomatic Greek population (Korovessis et al. 1998). More important than the range of the degree of lordosis and/or kyphosis is (a) how and when the lordosis and kyphosis develop during postnatal ontogeny in order to form a functional unit and (b) the relationship between the spinal curves and sacro-pelvic parameters which can influence their development. The relationships between the spinal curves and sacro-pelvic parameters will be discussed elsewhere, e.g. Been and Bailey (2019).

The establishment and increase in curve angles during postnatal ontogeny follow again an overall musculoskeletal growth pattern (Schlösser et al. 2015). However, the onset for curve establishment varies for the different vertebral column segments.

Cervical Lordosis

The first curve to develop significantly postnatally is the cervical lordosis. The cervical spine starts to develop an anterior convex curvature around the age of 3–6 months. This coincides with children's gradual increase in neck muscle control which allows them to carry their head upright and unassisted (Kapandji 1992; Byrd and Comiskey 2007). From about 4 months until about 9 to 12 months, the degree of the cervical lordosis increases rapidly (Byrd and Comiskey 2007). During this period of time, the occipital condyles of the skull also undergo substantial, species-specific remodelling which is likely linked to both face development and developing head carriage and locomotion (Ashton and Zuckerman 1952; Schultz 1955; Dean and Wood 1982; Kimbel and Rak 2010; Neaux et al. 2017). In any case, the repositioning of the occipital condyles will interact tightly with the development of the cervical lordosis.

After that period, the lordotic curve appears to flatten out until about the age of 9 years after which the lordosis angle increases again for the reminder of the postnatal growth period. The cervical lordosis reaches adult configuration around 17 years of age. The secondary lordosis curve increase seems to be linked to the peak thoracic kyphosis curve increase, particularly after the age of 9 years (Lee et al. 2012; Been et al. 2017), and helps maintain a functionally balanced upright spine and head carriage.

Thoracic Kyphosis

The thoracic kyphosis is already present at birth and thereafter linked tightly to lung function as well as sexual dimorphism in both thorax and lung morphology (Dimeglio and Canavese 2012; Bastir et al. 2014; Torres-Tamayo et al. 2018). It has also been shown that insufficient increase in normal thoracic kyphosis (e.g. due to severe scoliosis) during postnatal growth severely restricts the formation of alveoli in the lungs, leading to diminished lung function (Karol et al. 2008).

For most of the postnatal growth period, specifically between 5–9 years and 15–20 years of age, there is little difference observed in the growth increments of the kyphosis angle of males and females (Taylor 1975; Taylor and Twomey 1984; Voutsinas and MacEwen 1986; Schlösser et al. 2015). There is little or no statistically significant male/female difference in the adult kyphosis angle of young adults (Giglio and Volpon 2007). Many studies, however, find statistically significant sexual dimorphism in the kyphosis angle during the period of 8–14 years of age (e.g.

Willner and Johnson 1983; Schlösser et al. 2015). In all studies, males usually show a larger degree of kyphosis than females. In both sexes, the peak in curve increase occurs around 14 years of age albeit it that females and males show differences in the onset of the adolescent growth spurt (Willner and Johnson 1983). In other words, the increase in the degree of thoracic curvature peaks later than the maximum growth velocity of the spinal segmental length increase (Poussa et al. 2005).

This has consequences in that female vertebral columns have not developed the same degree of kyphosis angle when they undergo their most rapid thoracic segment length increase. At this time, the female vertebral column is also still more posteriorly inclined (see section below). Males, on the other hand, have developed substantially larger degrees of their kyphosis angle when their spine reaches the peak growth velocity of length increase (Schlösser et al. 2015). In both sexes, the upper age limit for the establishment of the adult kyphosis seems to be approximately 22 years (Stagnara et al. 1982; Poussa et al. 2005).

Lumbar Lordosis

Generally, the increase in lordosis angle is less when compared to the kyphosis angle (Schlösser et al. 2015). The lumbar lordosis is acquired once upright walking becomes habitual and the vertebral column is exposed to vertical axial loads (Kimura et al. 2001). The last and second to last lumbar segments (usually L5 and L4) contribute substantially to the formation of the lumbar lordosis. This configuration is maintained during adulthood (Korovessis et al. 1998). However, the relatively smaller lordosis in children can also be attributed to a less curved L1–L3 segment whereas the L4–L5 segment is not much different from that of adult spines (Cil et al. 2005). The inclination of the L2–L4 segments contributes 50% and the L5 segment alone the other 50% (Shefi et al. 2013).

Unsurprisingly, the establishment of the lumbar lordosis angle is tightly linked to the establishment of the kyphosis angle (Voutsinas and MacEwen 1986). Like the kyphosis angle, the development of the lordosis angle follows a linear growth trajectory for both males and females. There is no sexual dimorphism detected in these patterns (Giglio and Volpon 2007). There is, however, sexual dimorphism in the degree of lordotic curvature. From the age of 6 to 9 years onwards (Willner and Johnson 1983) and particularly from 11 to 22 years, females have a larger degree of lordotic curve than males (Poussa et al. 2005). Shefi et al. (2013) show that the lordosis angle increases continuously from 2 to approximately 13 years of age but then increases at higher increments from 14 to 16 years after which the increments drop again until skeletal maturity is reached. As with the kyphosis, the lumbar lordosis shows increased, steady growth rates from 5 to 20 in boys and between 5 and 15 in girls. This indicates an earlier establishment of the lordotic curvature in females when compared to males (Voutsinas and MacEwen 1986).

The earlier increase in lumbar lordosis in females indicates that the lordosis establishment is tightly linked with the increase in lumbar vertebral body length

during the adolescent growth spurt. In this, the lordosis angle development differs from that of the kyphosis angle (Poussa et al. 2005).

11.3.6 Development of Spinal Inclination

The infant spine is not a scaled version of the adult spine. It is characterised by a relatively larger thoracic kyphosis but smaller lumbar lordosis when compared to the adult spine (Voutsinas and MacEwen 1986; Cil et al. 2005). Non-adult vertebral columns tend to have a more posterior tilt of the thoracic and lumbar segments than adults (Mac-Thiong et al. 2007; Schlösser et al. 2015). A more posterior tilt means that more vertebrae of the thoracolumbar segment are posteriorly angled in comparison to the vertical plane through the body of C7 and the femoral heads. Besides the infant/adult difference, there is sexual dimorphism observed in the spinal tilt. When measured between T1 and L5, it is larger in females, and the individual vertebral angles are also bigger (Mac-Thiong et al. 2007; Janssen et al. 2009; Schlösser et al. 2014, 2015). This is especially the case for the more cranial segments of both the thoracic and the lumbar spinal segment.

The relationship between the lumbar lordosis and the thoracic kyphosis is tight and highly significant (Hellsing et al. 1987). The degree of thoracic kyphosis and lumbar lordosis changes throughout the postnatal ontogeny, and at the same time, the relationship between the two curves changes as well. This is influenced by the differences in the onset of the adolescent growth spurt between males and females (Hellsing et al. 1987; Widhe 2001). Therefore, the degree of the kyphosis decreases relatively when compared to the lordosis in females. In males, on the other hand, the kyphosis-lordosis relationship remains stable during the adolescent growth phase (later than 14 years of age) (Widhe 2001; Poussa et al. 2005). The relationship between the thoracic kyphosis and lumbar lordosis segments can be further differentiated. The degree of thoracic kyphosis correlates well with the proximal half of the lumbar lordosis but poorly or hardly with the distal half of the lordosis (L3–5) (Yong et al. 2012; Clément et al. 2013).

11.3.7 Postnatal Ontogeny of Individual Vertebrae: Fusion Patterns of Vertebral Elements

The postnatal development of vertebral column length and the spinal curves is achieved through postnatal growth of the individual vertebral elements and intervertebral discs. In the first instance, these growth processes consist of the fusion of the individual vertebral elements observed at birth (Fig. 11.3). The secondary ossification centres orchestrate the growth of vertebral processes and lateral and anteroposterior vertebral body dimensions. These patterns of vertebral ossification are both species- (see Sect. 11.4) and spinal segment-specific.

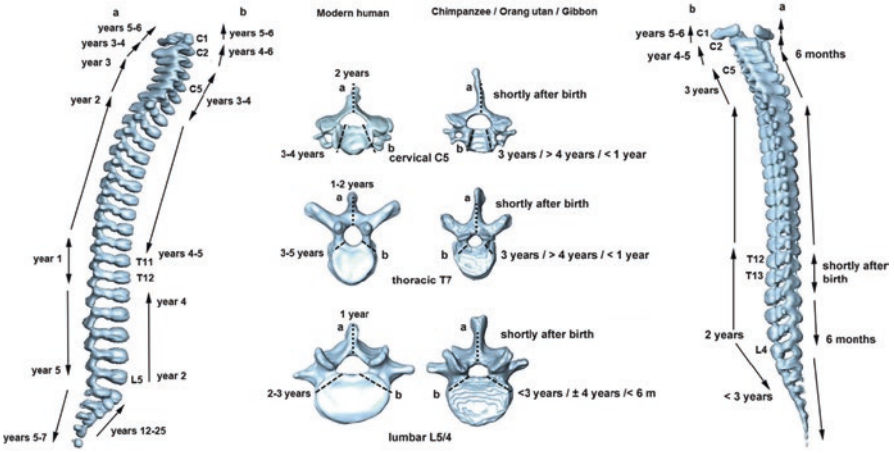

Fig. 11.3 Comparison of human and modern ape patterns of postnatal ossification processes: (*a*) arch element fusion pattern, (*b*) vertebral body and arch fusion. Note similar age at particular fusion events does not correspond with the same postnatal growth period (infant, juvenile) between taxa. For information on varying growth periods, see Table 11.2

The patterns of arch element union and arch elements uniting with vertebral bodies differ from each other (Fig. 11.3). The arch elements of the lower thoracic vertebrae (T11/T12) unite by the end of the first year of postnatal life. The union of further arch elements then continues in both directions cranio-caudally. By 2 years of age, the thoracic and typical cervical vertebrae all have united arch elements.

The fusion of the vertebral arch and body commences around the age of 3–4 years in the region of the lower cervical vertebrae (C4–C6). The uncinate processes of the cervical vertebrae are not present at birth but develop after the vertebral bodies and arch elements have fused and are fully formed by age of 6 years.

From there, fusions between arch and body elements continue cranio-caudally and bidirectionally along the vertebral column. The union of vertebral arches and bodies continues along the thoracic segment and reaches the lower thoracic vertebrae around 4–5/6 years of age. In the lumbar segment, the first vertebral arch and bodies to unite is L5. The arch-body fusion for the other lumbar vertebrae follows in a cranial direction, and in L1 the elements are usually united around the age of 4 years.

The atypical cervical vertebrae axis and atlas differ from other vertebrae for both arch element fusion and arch and body fusion.

The arch element fusion somewhat lags behind that of other vertebrae. The axis arch elements unite between 3 and 4 years of age, and the posterior atlas arch elements unite between 3 and 5 years of age (see Fig. 11.4). The arch of the atlas can however persist unfused into adulthood as a *spina bifida atlantis*.

Towards the end of the first postnatal year, the atlas also starts to develop an anterior bar element instead of a vertebral body. Considerable variation is observed in the amount of ossification centres for the formation of the anterior bar: there can

Table 11.2 Comparison of dental development/years of age equivalents of modern humans, great and lesser apes

	Prenatal period (days/weeks)	Postnatal period (years)	Definition of postnatal developmental periods based on dental eruption patterns[a]	Key dental eruptions
Chimpanzee Orangutan	238/34 275/39	11–12 11–12	**Infant period: 1–3 years** Early infant: year 1 Late infant: >1 to <3 years	Completion of deciduous dentition (around 2.5–3 years)
			Juvenile period: 3–8 years Early juvenile: >3 to <6 years Late juvenile: >6 to <8 years	M1 and M2 eruptions
				M1 eruption (~3–3.5 years)
				M2 eruption (~6–7 years)
			Subadult/adult period: from 8 years Subadult: >8 to <11 years Adult: >11 years	M3 eruption (~8–10 years), M3 fully matured after 11 years
Gibbon	210/30	7–8	**Infant period: year 1** Early infant: ~ first 4 months Late infant: >4 to <12 months	Completion of deciduous dentition (around 6–12 months)
			Juvenile period: 1–4 years Early juvenile: >1 to <2 years Late juvenile: >2 to <4 years	M1 and M2 eruptions
				M1 eruption (~1–1.5 year)
				M2 eruption (~2–3 years)
			Subadult/adult period: from 4 years Subadult: >4 to <8 years Adult: >8 years	M3 eruption (~4–6 years), M3 fully matured after 8 years
Modern human	280/38–40	18–20	**Infant period: 1–6 years** Early infant: <3 years Late infant: >3 to <6 years	Completion of deciduous dentition (around 3 years)
			Juvenile period: 6–16 years Early juvenile: >6 to <12 years Late juvenile: >12 to <16 years	M1 and M2 eruptions
				M1 eruption (~5–6 years)
				M2 eruption (~11–12 years)
			Subadult/adult period: >16 to <21 years Subadult: >16 to <21 years Adult: >21 years	M3 eruption, usually not before 18 years, full maturation of M3 can occur until late in adulthood

[a]Based on data provided by Dean and Wood (2003), Dirks et al. (2013) and Rowe (1996)

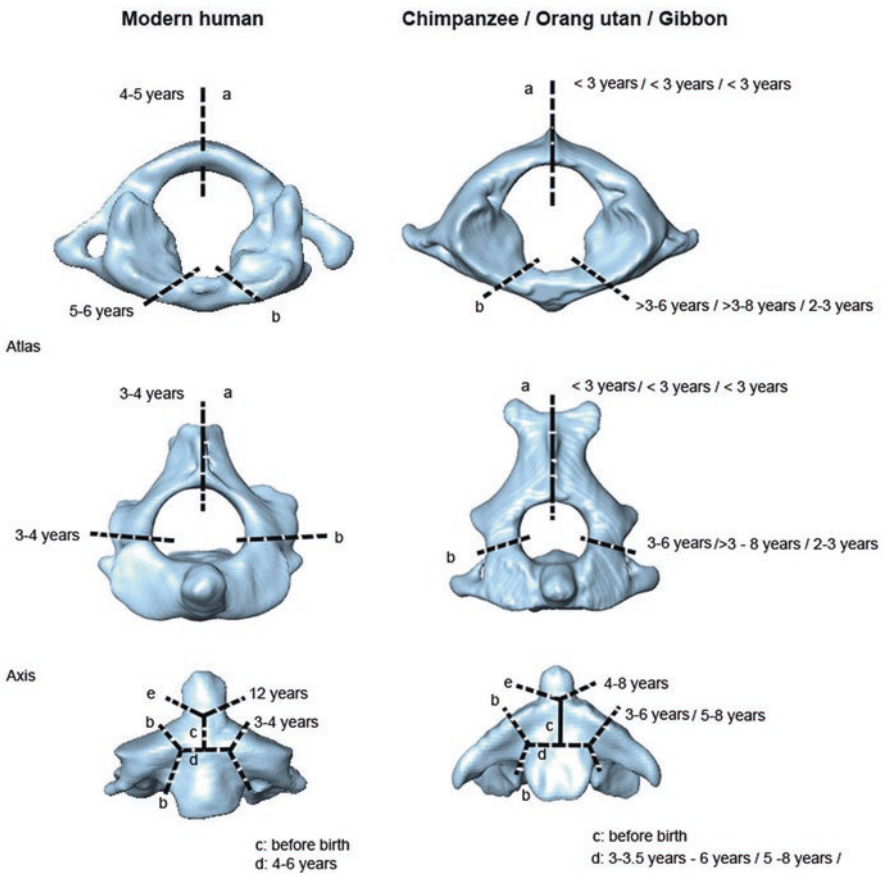

Fig. 11.4 Comparison of human and modern ape patterns of postnatal ossification processes of the atlas and axis: (*a*) arch element fusion pattern, (*b*) vertebral body and arch fusion pattern. Atlas- and axis-specific fusion patterns, (*c*) fusion of left and right odontoid process base halves, (*d*) fusion of odontoid process base with axis vertebral body, (*e*) fusion of odontoid process base and dens axis. Note similar age at particular fusion events does not correspond with the same postnatal growth period (infant, juvenile) between taxa. For information on varying growth periods, see Table 11.2

be none, one or two centres, but the element is usually fully formed by 3–4 years of age (Cunningham et al. 2016).

In the axis, the pattern is even more elaborate (Fig. 11.4), with the base of the odontoid process fusing with the axis arch around the age of 3–4 years. This is followed by the base of the odontoid process fusing with the vertebral body of the axis and the body of the axis simultaneously fusing with the arch element between the ages of 4 and 6 years.

The final fusion occurs between the tip of the odontoid process and the rest of the process which usually has occurred by age 12 years. The atlas anterior bar and the

atlas arch unite around the same time as the axis vertebral body and odontoid process base (5–6 years).

The fusion patterns for the sacrum deviate from those of the presacral vertebrae. The first elements to unite are the costal elements of S1–S3 which unite with the sacral bodies between 2 and 6 years of age. At the same time, arch elements fuse with the costal elements. The arch elements only fuse with each other between 7 and 15 years. Fusion between the individual sacral vertebrae with each other commences on the posterior aspect, between the arches, followed by the union of the sacral vertebral bodies. This process starts around 12 years of age and is not finished before 25 years of age (Cardoso et al. 2014; Cunningham et al. 2016).

11.3.8 Secondary Ossification Centres Associated with Vertebral Body and Intervertebral Disc Growth

The annular epiphysis fusion pattern commences in the upper cervical region, continuing in a caudal direction. The cervical annular epiphyses also cover the uncinate processes. Studies of various skeletal material collections narrow the fusion age for cervical epiphyses to the period of 19–21 years of age. For the thoracic segment, a pattern of fusion starting at both ends has been described, with T5 and T6 often being the last ones to fuse. Thoracic annular epiphyses never closed before 14 years of age in females and 16 years of age in males. Complete union in any thoracic vertebra was earliest at the age 18 in females and almost 19 in males. Complete union in the whole of the thoracic spine was 25 in females and 24 in males.

The ring epiphyses of L5 appear first and close first; appearance and closing times have been reported as 14–23 years (Bogduk 2005; Dias 2007; Moore and Persaud 2008; Ríos and Cardoso 2009).

Sacroiliac joint secondary ossification centres also form, and they fuse late, at around age 16–21 years (Cardoso et al. 2014). The late fusion of individual sacral vertebrae, in combination with the late persistence of secondary ossification centres on the alar elements and the sacroiliac joint, allows for multidirectional adjustment of the sacral elements in relation to the pelvis and the femur. Due to this extended shape and size adaptation, it is possible to produce individually highly variable configurations of the sacral shape and position in relation to the pelvic bones. The secondary ossification centres of the presacral vertebral column in turn adjust the individually balanced upright position of the presacral spine.

11.3.9 Development of Segmental (Vertebral) Inclination

The previous section explored the increase of sagittal spinal curvature angles (kyphosis, lordosis) during postnatal ontogeny but not the different mechanisms that lead to the increase in their angles. Amongst them are the shape of the

intervertebral discs, the shape of the vertebral bodies, the inclination of neighbouring vertebrae and intervertebral discs in relation to each other (=segmental inclination) and the inclination of segments of the vertebral column (thoracic spine, lumbar spine) as well as the inclination of the spine as a whole (spinal tilt).

There are two main mechanisms forming the sagittal spinal curvatures. The first is the segmental tilt or inclination which describes the position of the vertebrae and intervertebral discs as functional units in relation to each other. The other is the shape of the vertebral bodies and intervertebral discs themselves. Looking closer at the lumbar lordosis, the main contributor for the establishment of the lumbar lordosis in early childhood is the segmental inclination and particularly the orientation of the intervertebral discs (Shefi et al. 2013). Around the age of 2–4 years, both the positions of the vertebrae and the intervertebral discs contribute equally to the formation of the (small) lordosis angle. However, both the position and the shape of the intervertebral disc become increasingly more important, and around the age of 17–20 years, the shape and position of the intervertebral discs account for 80–89% of the lordosis angle (Shefi et al. 2013). Up to the age of approximately 16 years of age, the lumbar vertebral inclination increases steadily but seems to contribute somewhat less to the lordosis angle from 17 to 20 years onwards (Shefi et al. 2013). Therefore, the early increase in lumbar lordosis relies on the development of segmental inclination which is gradually replaced by remodelling of the intervertebral disc shape and later in life (adult period) by remodelling of the vertebral bodies. This is supported by the fact that in general, vertebral inclination in adulthood shows little variation for the segments T6–T12 and L4 but a wide variation in T4, T5 and L1–L3 and L4 (Korovessis et al. 1998).

11.3.10 Development of Wedge Shape of the Intervertebral Discs and Vertebral Bodies

Studies of the adult lumbar spine indicate that both a posterior wedge shape of the adult lumbar vertebral bodies and the lumbar intervertebral discs contribute substantially to the curvature of the lumbar lordosis (Shefi et al. 2013). In childhood, however, the lumbar lordosis establishes predominantly due to changes in intervertebral disc shape. Different authors (Cil et al. 2005; Shefi et al. 2013) show that from 2 years onwards, mostly the intervertebral discs increase their dorsal wedge shape. The lower lumbar vertebrae follow the discs in acquiring a small amount of wedge shape, but the upper lumbar segments (e.g. L1, L2) hardly change at all. Whereas the difference in wedge shape and segmental angle (angle between neighbouring vertebrae/discs) was substantial especially when comparing the L5 segment with more cranially positioned lumbar segments, the vertebral body wedge shape between L3 and L5 was not significantly different between age groups (Shefi et al. 2013). It could be postulated that after the maturation of the vertebrae (reached around 18–25 years of age), the ongoing adult increase of the lordosis angle is due

to both intervertebral disc and vertebral body remodelling which will accentuate their posterior wedge shape over the course of adulthood (Shefi et al. 2013).

11.3.11 Growth Patterns of Vertebral Bodies

Vertebral body width and height growth occurs through periosteal ossification (Bogduk 2005). The increase in cranio-caudal vertebral body length on the other hand is a product of the proliferation and subsequent ossification of the cartilage covering the superior and inferior vertebral body surface (Bogduk 2005). This process is complex as it not only involves increase in vertebral body length but also the firm anchoring of the annulus fibrosus on the vertebral body rim and the adjustment of vertebral endplate width and height. The latter is important as it allows individual vertebrae and vertebral segments to adjust to position-specific biomechanical stresses and to variation of weight load occurring during adolescence and early adulthood.

Around the age of 3–4 years, the sagittal vertebral body profile undergoes a gradual shift from convexity to concavity. This seems to be associated with an increased length achievement in intervertebral disc length, particularly in the lumbar region. Anteroposterior and lateral expansion of the vertebral body seems to be established over the whole growth period and to be in response to the gradual adoption of the posterior or anterior wedge shape (see below) of the intervertebral discs (Taylor 1975).

With regard to the different vertebral body dimensions, comparative studies of ambulatory and non-ambulatory (cerebral palsy) children indicate that the increase in vertebral body length is genetically determined and independent of mechanical factors (Taylor 1975). In other words, vertebral bodies reach their full adult length despite the presence or absence of weight loads usually associated with bipedal locomotion.

The establishment of the adult vertebral body height and width (and intervertebral disc height and width) on the other hand is highly influenced by weight bearing in the erect posture and the acquisition of bipedal gait (Taylor 1975). Furthermore, vertebral body dimensions were also found to be sexually dimorph in both thoracic and lumbar vertebrae from the age of 8 years onwards. The body length to body width ratio was larger in females which indicates cranio-caudally taller, more slender vertebrae when compared to males. The earlier onset of the adolescent growth spurt in females "acts" on relatively narrower vertebral bodies when compared to males whose growth spurt usually initiates around the age of 13 years. Therefore, the difference in length to width ratio is achieved by increased increments in body length growth in females and increased increments in body width before the age of 13 years (Taylor and Twomey 1984). This might be one explanation as to why idiopathic scoliosis with adolescent onset is more common in females than males.

Geometric morphometric assessment of a total of 288 female and male human vertebrae (L1–L5), representing all age groups (infant, juvenile, subadult and adult),

reveals significant differences in both vertebral size and shape for adults. The shape variation between the sexes is significantly larger than the size variation. The most prominent shape variation observed is the greater opening of the female greater vertebral notch (Martelli and Schmid 2003).

Prediction would be that growth trajectories of the lumbar vertebral shape would follow with a pelvic and/or sacral trajectory and would only emerge to become significant around the adolescent growth spurt. A mix of body weight differences and variations in pelvic shape morphology are most likely responsible for the variation in lumbar vertebral size and shape.

11.3.12 Growth Patterns of Vertebral Discs

Overall, the increase in intervertebral disc length follows the same pattern as observed in the increase in vertebral body length with a rapid expansion during the first 2 years of age, followed by an extended period of steady increase with small increment rates. However, the pattern deviates from that of the vertebral bodies in that there is no marked increase in length gain increments during the adolescent growth spurt and discs reach their adult length around the age of 15–16 years.

There are differences in the pattern of disc length increase which depend on the spinal segment. Lumbar intervertebral discs and particularly the L4–L5 disc show increased increments of growth when compared to thoracic discs (Taylor 1975). This is especially the case between the ages of 2 and 7 years, where only the lumbar discs seem to substantially increase in length when compared either to cervical or thoracic discs (Taylor 1975).

The lumbar intervertebral disc shape undergoes other changes as well. The nucleus pulposus gradually migrates from a more anterior to a posterior position within the disc (cervical and lumbar vertebrae). Furthermore, after 7 years of age, the cervical and lumbar discs start to adopt a posterior wedge-shaped profile when viewed in the sagittal plane whereas thoracic vertebrae only just start to adopt an anterior (cranial portion of the thoracic spine) or posterior (caudal portion of the thoracic spine) wedge shape (Taylor 1975). The shift of the position of the nucleus pulposus of the lumbar intervertebral discs could be associated with the achievement of bipedal walking by the 2nd year of life.

Comparative studies of postnatal intervertebral disc profile in healthy children and children suffering from cerebral palsy but being able to walk vs. children suffering from cerebral palsy and not being able to walk indicate that the main factor contributing to the reshaping of the sagittal disc profile is weight bearing due to the development of bipedal gait. Only non-ambulant cerebral palsy patients lacked the reshaping of the discs into the characteristic posterior wedge-shaped profile of the lumbar intervertebral discs and additionally did not gain similar disc length either (Taylor 1975).

Around the age of 3–4 years, the sagittal vertebral body profile undergoes a gradual shift from convexity to concavity. This seems to be associated with an increased

length achievement in intervertebral disc length, particularly in the lumbar region. Anteroposterior expansion of the vertebral body on the other hand seems to be established over the whole growth period and to be in response to the gradual adoption of the posterior wedge shape of the lumbar intervertebral discs (Taylor 1975).

11.4 Postnatal Ontogeny of the Modern Ape Vertebral Column and Overview on the Postnatal Ontogeny of the Vertebral Column in Hominin Evolution

11.4.1 Introduction

In this last part, the focus is shifting from the modern human vertebral column development to that of our closest living relatives, the African and Asian great and lesser apes. This section explores the similarities and differences in the postnatal ontogeny of the modern hominoid vertebral column and uses this information, where possible, to look at what can be gleaned from the fossil record with regard to the development of the spine and how this might have shifted over time. Focus will be on comparing the duration of the vertebral column postnatal growth period and whether patterns of postnatal growth are different between humans, modern apes and fossil hominins.

11.4.2 The Modern Hominoid Pre- and Postnatal Ontogeny: Considerations of Varying Growth Periods

When comparing modern humans with other modern hominoids and fossil taxa, it is essential to take the interspecific variation in life history into consideration. All hominoids have an extended growth period (both pre- and postnatally) when compared to non-hominoid primates, e.g. Schultz (1940), Dean (2000) and Schwartz and Dean (2001). However, the modern human growth period extension stands out against all other taxa and seems to have emerged relatively late in human evolution (Dean et al. 2001; Smith et al. 2010; Rosas et al. 2017). The postnatal growth period of fossil hominoid taxa such as *Australopithecus* and early *Homo* resembles that of modern great apes the most (Dean et al. 2001). Furthermore, differences in growth period length are also observed between the modern great and lesser apes (gibbons), with the latter having less extended growth periods than the African and Asian great apes (Dirks et al. 2013). Table 11.2 summarises equivalent dental development stages and years of postnatal life for modern apes and humans which is used as a framework for comparison on the postnatal development of the vertebral column in this section.

Schultz reported that the prenatal periods of chimpanzee and modern humans are extended by 1.4 and 1.6 times, respectively, when compared to other catarrhine primates. However, the postnatal period is 1.5 times longer in chimpanzees and 2.9 times longer in humans. Although humans extend their prenatal developmental period compared to other catarrhine primates, they increase their postnatal period even more (Schultz 1940). Detailed studies on dental development and daily increments in tooth development confirm these earlier reports (Holly Smith et al. 1994; Dean 2000; Dean et al. 2001; Schwartz and Dean 2001; Dean and Wood 2003). Chimpanzees do have an extended postnatal growth period when compared to other catarrhine primates, but compared to modern humans, their growth period accounts for half of that. In other words, the human growth period seems to be extended when compared to great and lesser apes, and postnatal developmental processes take longer to complete.

11.4.3 Modern Ape Prenatal Vertebral Growth Period and the Establishment of Primary Ossification Centres

Information on prenatal vertebral development in hominoid taxa other than modern humans is scarce. The richest source of information comes from Schultz (1940, 1941, 1944). In general terms, species-specific variations increase throughout the prenatal period and become more accentuated to the end of the period (Schultz 1926). At time of birth, chimpanzee newborns are proportionately smaller than either non-hominoid primates such as macaques or the hominoid human newborns. This has been attributed to a species-specific slowing of prenatal growth after the 7th month when chimpanzee foetuses gain weight less quickly than human ones.

Since most primary ossification centres are established during the first 20 weeks of the prenatal period, it would be expected that they develop at similar times in modern apes. The earliest chimpanzee foetuses examined at 18 weeks old or older already had primary ossification centres in all arch elements and centra (Schultz 1940). Some secondary ossification centres of the sacral alar elements were also already present. Further information comes from the study of orangutan (*Pongo pygmaeus*) foetuses, 27 weeks old or older. In all specimens, all primary ossification centres were present. Additionally, the centres of the S1 and S2 sacral alar processes were visible at birth (Schultz 1941). Gibbon (*Hylobates*, various species) foetuses of unknown age but where the oldest ones were "*close to term*" (i.e. near 30 weeks old) (Schultz 1944) had all primary ossification centres present. Further foetal material studies will be necessary to resolve that matter in more detail and establish more precise patterns of primary ossification centre development.

11.4.4 Postnatal Development of the Modern Hominoid Vertebral Column: The Newborn Modern Hominoid Spine

At birth, and with the exception of the atlas, axis and the sacrum, all great and lesser ape vertebrae consist of three separate elements. The newborn ape vertebral column also has a C-shaped appearance, with the thoracic kyphosis already present to some degree (Fig. 11.2b). In great ape and human foetuses and at birth, the spine has not yet much migrated into the centre of the thorax and abdomen. However, this changes rapidly during postnatal growth, with larger growth in humans than apes (Schultz 1950). A small promontorial angle between the last lumbar and first sacral vertebra is observed in all ape species at birth as well.

11.4.5 Modern Hominoid Vertebral Column Length and Trunk Height

All hominoids (including humans) differ from catarrhine primates in that they have relatively longer cervical and sacral regions, a somewhat elongated thoracic region and markedly shortened lumbar and caudal regions (Schultz 1938). Throughout postnatal ontogeny, the cervical and thoracic regions incur relatively lesser growth increments, whereas the lumbar region increases more.

Amongst modern hominoids, humans achieve the smallest postnatal trunk growth, and gibbons achieve also less than great apes. This is linked to the relatively large human newborn size, particularly compared with the below hominoid average size of African ape newborns (Schultz 1973). The closest measure of postnatal vertebral column growth comes in the shape of observations of the postnatal growth of trunk height which encompasses the thoracic, lumbar and sacral segments of the spine. Chimpanzees reach about 50% of their adult trunk height at about 3 years of age (end of their infant period) (Schultz 1940). By the end of the early juvenile period, at around 5.5 years and thus halfway through the chimpanzee postnatal growth period of approximately 11 years, 75% of adult size has been achieved. Adult trunk height is established by age 8–9 years (subadult) (Schultz 1940).

11.4.6 Sagittal Curvature of the Modern Ape Vertebral Column

In contrast to the enormous sagittal curvature development observed in modern humans, the modern hominoid spine shows much more modest curve acquisition (Fig. 11.2). The cervical lordosis develops similarly in great apes and humans as its development is linked to the acquisition of being able to carry the head

independently. A similar relationship between curvature development and the development of the occipital condyles of the skull is present as well.

Due to the shorter postnatal development period of great apes compared to modern humans, the establishment of this curve falls within the first 3 months of life. As indicated before in modern humans, the great ape occipital condyles also undergo extended growth during that period, and this is likely to adjust to facial growth and development of head carriage (Ashton and Zuckerman 1952; Schultz 1955).

The thoracolumbar spine of all modern apes establishes some curvature as well. The thoracic kyphosis – already present at birth – is related to thorax anatomy and the fact that all modern hominoids have a wider, shallower thorax than cercopithecoids. The thoracic central position of the vertebrae is linked to this hominoid characteristic trunk shape.

The adult lumbar segment shows a very slight lumbar lordosis which establishes postnatally in all apes (Schultz 1961). The great ape lumbar spine is flanked by the elongated wings of the ilia of the pelvis, which have a restricting influence on the lumbar vertebral column. Due to the rather low flexibility of the great ape lumbar spine, the degree of lordosis varies little. Likewise, the establishment of the lumbosacral angle between the last lumbar vertebra and the sacrum is observed in all modern hominoids (Schultz 1961; Abitbol 1987). Nevertheless, the human lumbosacral angle is present at an earlier developmental stage (prenatal) and is larger at birth and continues to become larger throughout the postnatal ontogeny when compared to all modern apes (Schultz 1961). The acquisition of bipedal upright walking (or lack thereof) seems to have a large influence on the formation of the angle (Abitbol 1987, 1989).

11.4.7 Vertebral Element Fusion

In chimpanzees, orangutans and gibbons, the two arch elements fuse during the early infant period, i.e. during the first 6 months in great apes and very shortly after birth and all the way down to S2 in gibbons (Schultz 1940, 1941, 1944). The pattern of arch fusion seems very similar to that observed in modern humans.

Vertebral arch and vertebral body fusions start low, in the lumbosacral region, and then trail up in cranial direction along the thoracic and cervical spine. Chimpanzee studies (Schultz 1940) were not conclusive if there is a second early location of arch and body fusion starting in the cervical spine as is observed in modern humans. However, in both orangutans and gibbons, a pattern of fusion similar to modern humans, with the lumbar region uniting first, followed by the sacral and cervical regions was observed. The thoracic region is last (Schultz 1944). A comparison of arch union and arch and vertebral body fusion between humans and modern apes is shown in Fig. 11.3 and 11.4. In the following, a more detailed account of the sequence of these developmental events is given.

In chimpanzees, fused vertebral bodies and arches are observed in the lumbar and sacral region around the age of 2–2.5 years (late infant period). At this point in

time, the arches and vertebral bodies of the thoracic and cervical vertebrae appear still unfused. By the age of approximately 3–3.5 years, the thoracic vertebrae have fused, and by 5–6 years of age (early juvenile phase), all vertebrae, including the atypical cervical vertebrae atlas and axis, have finished the process which coincides with the approximate halfway mark of the postnatal growth period (Schultz 1940, 1944).

In orangutans, the arch/vertebral body fusion starts slightly later at 3–3.5 years (early juvenile period), and the process finishes later than in chimpanzees as well (Schultz 1941). Gibbon vertebral arches and bodies are separate during the first year of life (infant period) but start uniting during the early juvenile period (1–2 years of life) and up to halfway through the late juvenile phase (up to 3 years).

Like in modern humans, the atypical cervical vertebrae atlas and axis follow a different pattern from other cervical vertebrae as well. In chimpanzees, the base of odontoid process starts to unite with the axial vertebral body around 3–3.5 years (early juvenile period), and the process is usually finalised around 6 years of age (end of early juvenile). This developmental episode again takes place later in orangutans, where it starts around 5 years of age (late in early juvenile period) and is usually not finished until the end of the late juvenile period (8 years). The chimpanzee ventral bar of the atlas is visible but separate from the rest of the atlas from 3 years of age (infant period) but does not fuse until the end of the early juvenile period (6 years). Orangutans start this process in the early juvenile phase (older than 3 years), and the full fusion is usually not achieved until the end of the late juvenile phase (up to 8 years). In gibbons, these processes take place during the late juvenile period, between the ages of 2–3 years.

The costal elements of the sacrum unite with the transverse processes of the sacral vertebrae during the early infant period in chimpanzees (before 3 years of age). In orangutans, this process is again delayed into the early juvenile period (3–4 years). In gibbons, this process takes place even later and is usually observed around 2 years of age, corresponding with the late early juvenile period. Finally, the chimpanzee and gibbon sacral vertebrae do not unite with each other until early adulthood (older than 11 years and 8 years, respectively) and can remain partially unfused until much older (Schultz 1940, 1944). In the orangutan, the sacral vertebral fusion shows great variability, and they can stay unfused until early adulthood. However, they mostly fuse during the late juvenile period (6–8 years) (Schultz 1941).

11.4.8 Secondary Ossification Centres of the Modern Hominoid Vertebral Column

Similar to modern humans, the modern ape epiphyseal plates of the vertebral bodies are ring-shaped and not present at birth. In chimpanzees and orangutans, they appear around 5–6 years of age (early juvenile period) and in gibbons at around 4 years

(late juvenile period). In all three ape taxa, the plates remain unfused until at least the subadult phase (9–11 years and 4–8 years, respectively), but Schultz noticed that they were often still unfused in early adulthood. In all three taxa, the last plates to fuse were the distal thoracic ones and in the case of gibbons often the proximal lumbar ones as well (Schultz 1940, 1941, 1944).

11.4.9 Growth Trajectories of Individual Modern Hominoid Lumbar Vertebrae

The growth trajectories based on the five last presacral vertebrae (Th12/Th13–L3/L4) of modern great apes show sexual dimorphism in vertebral size in all species, but the smallest size differences were found in chimpanzees. Growth trajectories of gorilla males and females show that lumbar vertebral size and shape are linearly scaled. Males reach their larger vertebral size by extending the general gorilla vertebral growth trajectory whilst simultaneously increasing growth increments at an age of about 4 years or older (i.e. during early juvenile period). Furthermore, 50% of the total increase in lumbar vertebral size was achieved after the infant period only but before the end of the late juvenile phase (between 3 and 8 years). Sexual dimorphism in vertebral size and shape of gorillas should be considered the result of ontogenetic scaling by extending the general gorilla growth trajectory.

Chimpanzee females and males have different lumbar vertebral sizes, but show no sexual dimorphism in vertebral shape. This is also expressed in the postnatal ontogeny of the chimpanzee lumbar vertebral size and shape where no diversion in the growth trajectories of females and males is observed, particularly not at the juvenile stages as seen in gorillas. Male chimpanzees only slightly increase their growth rates when they reach the subadult stage (i.e. from 8 years of age). Fifty per cent of vertebral size is reached during the juvenile phase 3–6 years.

11.4.10 Summary of Modern Ape Vertebral Ontogeny

The overall patterns of postnatal growth of the vertebral column differ little between humans and modern apes – the same vertebral column segments (cervical, thoracic and lumbar) show similar length increase, with humans and gibbons having less expansive lumbar spines than great apes. However, humans achieve 50% of vertebral column growth towards the end of their early infant period, around 2 years of age whereas chimpanzees and orangutans reach half of their trunk size and vertebral size (at least lumbar ones) at the very end of their infant or early juvenile periods (3–5 years). The union of the vertebral arch elements is similar between humans and modern apes in that it is the first event of postnatal vertebral element ossification and that the process is finished by the end of the infant period in each of the taxa.

The fusion of vertebral arches and bodies follows a similar pattern in all humans and modern apes, starting at the lumbosacral region. However, the onset and end of this process vary in that in humans, chimpanzees and gibbons the onset usually occurs during the infant period. In orangutans, the onset is delayed until the early juvenile period. Process end is observed by the end of the late infant period in humans (around 4–5 years) and gibbons (before 1 year of age) whereas it is extended into the juvenile period in the great apes. For the atypical cervical vertebrae axis and atlas, fusions appear later in gibbons (late juvenile period) than great apes (early juvenile period), and humans have the earliest fusions during the late infant period (5–6 years). The epiphyseal plates of the vertebral bodies appear during similar growth periods in both modern humans and great apes (late juvenile period).

The appearance of the ape cervical lordosis and lumbar lordosis and the expansion of the thoracic kyphosis are similar to what is observed in modern humans. However, the degree of curve development is not as extensive as in humans in all curves. This might link to large spinous processes in the cervical spine linked to extensive neck muscles that prevent a massive cervical lordosis development. On top of that, the thoracic kyphosis is never as extensive in great apes as it is in modern humans and therefore does not need to be balanced with a large increase in the lordosis angle.

Some great ape taxa show larger degrees of sexual size dimorphism in vertebral size which is established through the extension of their growth trajectory, combined with increased growth increments. If ape vertebrae are sexually shape dimorph, the shape difference links to differences in body weight/vertebral size. In humans, the vertebral size dimorphism is modest, but the shape dimorphism outweighs that of all apes. The human vertebral shape differences are not exclusively linked to sexual dimorphism in body weight. It is therefore likely that the human vertebral shape dimorphism is linked to pelvic and sacral shape dimorphism.

11.4.11 Fossil Hominin Postnatal Ontogeny of the Vertebral Column

With the similarities and differences in the modern human and ape vertebral column development explored, it is of interest to now trace some of these differences in the fossil record.

An early window into examining the postnatal ontogeny of the hominoid vertebral column is provided by the East African *Australopithecus afarensis* specimen Dikika 1–1 from Ethiopia (Alemseged et al. 2006). The fossil dates to around 3.31 to 3.35 million years. Australopithecine postnatal growth patterns are best described using modern great ape models (Dean et al. 2001). Based on Dikika's dental developmental and tooth eruption status, its age at death has been estimated to be around 3 years of age, corresponding with a late infant or very early juvenile phase as seen in modern great apes (Alemseged et al. 2006). The specimen preserves the full

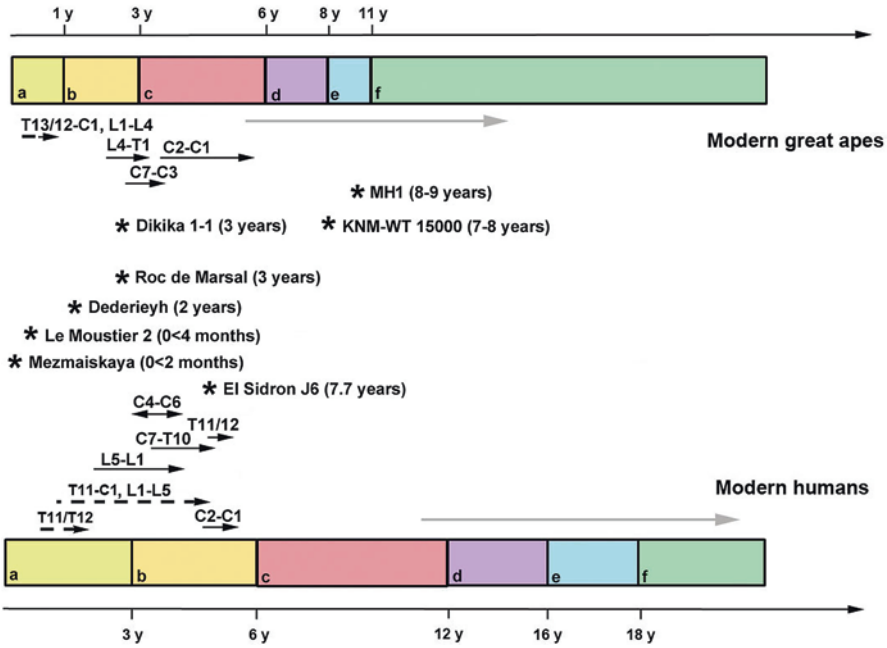

Fig. 11.5 Comparison of postnatal vertebral development stages of modern and fossil hominoids. Postnatal growth periods based on Table 11.2: (*a*) early infant, (*b*) late infant, (*c*) early juvenile, (*d*) late juvenile, (*e*) subadult, (*f*) adult. Dashed arrows, arch elements uniting; black arrows, arch and vertebral body fusion; grey arrows, appearance of epiphyseal growth plates. Note discrepancy between age at death of El Sidrón J6 and its younger vertebral maturation compared to modern humans. KNM-WT 15000 age at death best fits with assumption of a great ape-like vertebral maturation pattern

cervical and thoracic segment of the vertebral column but no lumbar vertebrae (Ward et al. 2017). The arch halves on the preserved thoracic elements have united, but the fusion between the vertebral arches and bodies is not complete. This state of fusion would be in line with the equivalent state in a 3-year-old modern African great ape where the fusion of arches and bodies starts around 2–2.5 years (Fig. 11.5).

Another not fully matured individual with associated vertebral material is the South African *Australopithecus sediba* specimen MH1, dated to around 2.5–1.5 million years (Dirks et al. 2010). This specimen is estimated to have been about 9–11 years of age if using a modern great ape model, which is considered more appropriate in view of the general reconstructed life history reported for *Australopithecus* (Dean et al. 2001; Cameron et al. 2017), this specimen is estimated to have been about 9–11 years of age at death. At this age, MH1 can be considered a very late juvenile or a subadult. The associated vertebral material has completely fused arches and vertebral bodies (Williams et al. 2013), but the first lumbar element does not have a fused epiphyseal plate. Based on the great ape model, the plate might have been formed around the age of 5–6 years. Since fusion of the plate with the vertebral body could not be expected until later in the subadult

or early adult phase, it most likely was lost. Non-fused epiphyseal plates at this stage are also in line with a more modern ape-like postnatal growth pattern.

The most complete early *Homo* skeleton, the *Homo erectus* individual KNM-WT 15000 from Kenya, presents a rich source of vertebral material in the form of the seventh cervical vertebra, most of the thoracic, the complete lumbar segment and most of the sacrum. Recent re-evaluation and allocation of small bone fragments collected during the original excavation seasons to previously more fragmentary vertebral material have helped clear up the identity of some of the vertebrae, and the specimen is now considered to have 12 thoracic, 5 lumbar and 5 sacral vertebrae as would be observed in most modern humans (Haeusler et al. 2011). The specimen is dated to about 1.53 million years (Brown et al. 1985).

The vertebrae have fully fused vertebral bodies and arch elements. The vertebral body surfaces are strongly grooved and indicate the presence but not fusion of epiphyseal endplates. The secondary ossification centres at the end of the processes (transverse and spinous) are also not fused, and this is the case for all vertebrae present (Walker and Leakey 1993). In modern humans, this stage of spinal maturation would be consistent with a late juvenile/early subadult stage older than 14 years due to the timing of the appearance of the secondary ossification centres and the fusion of the primary ones. However, based on detailed analyses of tooth formation in this specimen, its age at death can be estimated to about 7–8 years (Dean et al. 2001), indicating a growth period shorter than in modern humans but somewhat extended when compared to great apes. The tooth development and the more advanced vertebral maturation indicate that more of the skeletal maturity was achieved at a younger age in *Homo erectus* than in modern humans.

For Neanderthals, the immature fossil vertebral material is more abundant. Two very young Neanderthal specimens, Mezmaiskaya 1, Russia, a potentially newborn or no older than 2 months (Golovanova et al. 1999), and Le Moustier 2, France, no older than 4 months (Maureille 2002), preserve substantial portions of their vertebral columns. In the case of the latter specimen, almost all of the vertebral column is present. In both, all arch elements remain unfused, and the axis of Le Moustier 2 has a separate vertebral body and an odontoid process base element (Maureille 2002; Weaver et al. 2016).

The Neanderthal infant from Dederiyeh, Syria, was approximately 2 years old and also has an almost complete vertebral column and sacrum (Akazawa et al. 1996). All vertebrae except the fifth lumbar have united arch elements. All vertebral bodies and arches are still separate, which is within the remit of modern humans where the fusion of body and arch elements starts around 2 years of age (in the lumbar region) (Kondo et al. 2000). The arch elements of all vertebrae except the last lumbar and the atlas are fused in the somewhat older (3–3.5 years of age) Neanderthal child from Roc de Marsal, France (Madre-Dupouy 1999; Skinner 1997; Sandgathe et al. 2011). The right half of the atlas is preserved, and the developmental status of the arch element would correspond well with that of a 3–3.5-year-old modern human. The Roc de Marsal child's vertebral arches and vertebral bodies are not yet fused, which can be the case in a 3-year-old modern human child. Comparing these Neanderthal individuals with modern humans reveals hardly any

differences in the maturation patterns of the vertebrae until this stage of the postnatal growth period (i.e. early infant period).

Recent studies of the life history of Neanderthals based on a new juvenile specimen aged 7.7 years (Rosas et al. 2017) from El-Sidrón, Spain, however, indicate that at a point past the first 3 years of postnatal age, the spinal growth patterns of modern humans and Neanderthals start to drift apart. Whilst other parameters of postnatal growth seem to match that of modern humans well, i.e. dental development as well as various skeletal maturation patterns of the limbs (Rosas et al. 2017), the maturation patterns for the cerebrum and vertebral column deviate. In the latter, the pattern of fusions of vertebral bodies and arch elements matches a much younger modern human developmental stage of 4–5 years as the distal thoracic elements (T10–T12) still have unfused arches and vertebral bodies. Since all other investigated processes matched between humans and Neanderthals, it seems that Neanderthals slowed down the maturation process of the vertebral column past the infant period.

11.5 Discussion

This chapter set out to present an overview over the pre- and postnatal ontogeny of the modern human vertebral column and compare these to modern apes and fossil hominins.

All hominoids share the common mammalian process of vertebral formation and vertebral morphology differentiation prenatally. Differences in the length of the prenatal developmental period and a variation in prenatal growth processes do lead to differences in the appearance and presence of primary ossification centres in the vertebrae of different hominoid species.

Postnatally, the modern human vertebral column undergoes a complex process of developing and adjusting the length of the overall vertebral column, with changes in the spinal tilt and with different functional segments (cervical, thoracic, lumbar, sacral) reaching their adult configuration regarding length and shape at different stages of postnatal ontogeny.

The most striking developmental process of the modern human vertebral column is the accentuation of the primary sagittal spinal curvature, the thoracic kyphosis and the establishment of secondary lordotic sagittal curvatures in the cervical and lumbar regions. The establishment of the curvatures is linked to a multitude of factors, such as the acquirement of bipedal walking, lung development, head carriage and face development. Most importantly, the development of the pelvic configuration will have a high impact on the adjustment of the vertebral column curvatures.

The vertebrae themselves and the intervertebral discs follow similar patterns of growth. However, the remodelling of the intervertebral discs plays an important role earlier in the postnatal ontogeny whereas the remodelling of the vertebrae themselves catches up with the intervertebral discs towards the end of the adolescent period.

The patterns of postnatal development of the vertebral column are similar for all hominoids, but variations are observed in relation to species differences in growth period duration.

The most conserved hominoid vertebral growth pattern is that for establishing adult vertebral column length. However, the role of the intervertebral discs of great and lesser apes in this process is not yet investigated.

The ape vertebral column develops weak degrees of secondary sagittal curvatures, but the degree of these curvatures is minimal compared to modern humans and applies to the primary thoracic kyphosis curvature as well.

The patterns of growth for individual vertebrae are quite similar for all hominoids, but the ape vertebrae have a somewhat accelerated pattern of vertebral arch and vertebral arch and body element fusion. Perhaps the adjustments of individual vertebrae towards the establishment of the adult vertebral configuration are of a smaller magnitude in the apes and thus do not require the vertebral elements to be kept separate for an extended period of time.

When looking at the fossil material, it appears that the shift from a more great ape-like pattern of postnatal ontogeny as seen in *Australopithecus* happens late in the hominin evolution. *Homo ergaster* seems to have slowed down the fusion of vertebral elements compared to apes and australopithecines, but it is still faster than what is observed in modern humans and Neanderthals.

Interestingly, recent data from Neanderthal fossils indicates further diversity in those patterns in late hominin evolution, with a slowed down vertebral element fusion later in the postnatal ontogeny. The reasons for this are currently unknown, but it would be of great interest to further study the influence variations in body size, modes of locomotion and locomotor behaviour and variations in thorax and pelvic morphology might have on the postnatal ontogeny of the vertebral column.

Furthermore, the growth patterns and growth increments of intervertebral discs of all apes would be of great interest to further studies as the intervertebral discs are one of the vertebral structures which vary most between humans and great apes and which have not been studied in great detail.

Acknowledgements I thank Ella Been, Asier Gómez-Olivencia and Patricia Kramer for their invitation to contribute to this volume. Further thanks to Nicole Torres-Tamayo and Markus Bastir, Museo Nacional de Ciencias Naturales, Madrid; Takeshi Nishimura and the Digital Morphology Museum at the Primate Research Institute, Kyoto University; Christophe Zollikofer, Anthropologisches Institut und Museum der Universität Zürich; and S. Blau and VIFM, Monash University Melbourne for access to comparative modern human and chimpanzee illustrative CT scan data. And finally, thanks to Christopher Dean and Markus Bastir for the enjoyable and fruitful scientific discussions and the constructive remarks and criticisms.

References

Abitbol MM (1987) Evolution of the lumbosacral angle. Am J Phys Anthropol 72:361–372

Abitbol MM (1989) Sacral curvature and supine posture. Am J Phys Anthropol 80:379–389

Afonso ND, Catala M (2003) Neurosurgical embryology. Part 7: development of the spinal cord, the spine and the posterior fossa. Neurochirurgie 49:503–510

Akazawa T, Muhesen S, Dodo Y, Kondo O, Mizoguchi Y, Abe Y, Nishiaki Y, Ohta S, Oguchi T, Haydal J (1996) Neanderthal infant burial from the Dederiyeh Cave in Syria. Paléorient 21:77–86

Alemseged Z, Spoor F, Kimbel WH, Bobe R, Geraads D, Reed D, Wynn JG (2006) A juvenile early hominin skeleton from Dikika, Ethiopia. Nature 443:296–301

Aoyama H, Asamoto K (2000) The developmental fate of the rostral/caudal half of a somite for vertebra and rib formation: experimental confirmation of the resegmentation theory using chick-quail chimeras. Mech Dev 99:71–82

Ashton EH, Zuckerman S (1952) Age changes in the position of the occipital condyles in the chimpanzee and gorilla. Am J Phys Anthropol 10:277–288

Bastir M, Higuero A, Ríos L, García-Martínez D (2014) Three-dimensional analysis of sexual dimorphism in human thoracic vertebrae: implications for the respiratory system and spine morphology. Am J Phys Anthropol 155:513–521

Been E, Bailey JF (2019) The association between spinal posture and spinal biomechanics in modern humans: implications for extinct hominins. In: Been E, Gómez-Olivencia A, Kramer PA (eds) Spinal evolution: morphology, function, and pathology of the spine in hominoid evolution. Springer, New York, pp 283–300

Been E, Shefi S, Soudack M (2017) Cervical lordosis: the effect of age and gender. Spine J 17:880–888

Bernhardt RR, Görlinger S, Roos M, Schachner M (1998) Anterior-posterior subdivision of the somite in embryonic zebrafish: implications for motor axon guidance. Dev Dyn 213:334–347

Bogduk N (2005) Clinical anatomy of the lumbar spine and the sacrum. Elsevier, Edinburgh

Brown F, Harris J, Leakey R, Walker A (1985) Early *Homo erectus* skeleton from West Lake Turkana, Kenya. Nature 316:788–807

Burke AC, Nelson CE, Morgan BA, Tabin C (1995) Hox genes and the evolution of vertebrate axial morphology. Development 121:333–346

Byrd SE, Comiskey EM (2007) Postnatal maturation and radiology of the growing spine. Neurosurg Clin N Am 18:431–461

Cameron N, Bogin B, Bolter D, Berger LR (2017) The postcranial skeletal maturation of *Australopithecus sediba*. Am J Phys Anthropol 163:633–640

Cardoso HFV, Pereira V, Ríos L (2014) Chronology of fusion of the primary and secondary ossification centers in the human sacrum and age estimation in child and adolescent skeletons. Am J Phys Anthropol 153:214–225

Christ B, Huang RJ, Wilting J (2000) The development of the avian vertebral column. Anat Embryol 202:179–194

Cil A, Yazici M, Uzumcugil A, Kandemir U, Alanay A, Alanay Y, Acaroglu RE, Surat A (2005) The evolution of sagittal segmental alignment of the spine during childhood. Spine 30:93–100

Clément J-L, Geoffray A, Yagoubi F, Chau E, Solla F, Oborocianu I, Rampal V (2013) Relationship between thoracic hypokyphosis, lumbar lordosis and sagittal pelvic parameters in adolescent idiopathic scoliosis. Eur Spine J 22:2414–2420

Cunningham C, Scheuer L, Black S (2016) Developmental juvenile osteology. Elsevier, London

De la Cruz CC, Der-Avakian A, Spyropoulos DD, Tieu DD, Carpenter EM (1999) Targeted disruption of Hoxd9 and Hoxd10 alters locomotor behavior, vertebral identity and peripheral nervous system development. Dev Biol 216:595–610

Dean C (2000) Progress in understanding hominoid dental development. J Anat 197:77–101

Dean C, Leakey MG, Reid D, Schrenk F, Schwartz GT, Stringer C, Walker A (2001) Growth processes in teeth distinguish modern humans from *Homo erectus* and earlier hominins. Nature 414:628–631

Dean MC, Wood BA (1982) Basicranial anatomy of Pliopleistocene hominoids from East and South Africa. Am J Phys Anthropol 59:157–174

Dean C, Wood B (2003) A digital radiographic atlas of great apes skull and dentition. ADS Solutions, Milan

Dias MS (2007) Normal and abnormal development of the spine. Neurosurg Clin N Am 18:415–429

Dickson RA, Deacon P (1987) Spinal growth. J Bone Joint Surg Br 69:690–692
Dimeglio A, Canavese F (2012) The growing spine: how spinal deformities influence normal spine and thoracic cage growth. Eur Spine J 21:64–70
Dirks W, Barros AP, Dean C (2013) A tooth atlas for the developing dentition of *Hylobates lar* based on radiography and histology. Am J Phys Anthropol 150:113–114
Dirks P, Kibii JM, Kuhn BF, Steininger C, Churchill SE, Kramers JD, Pickering R, Farber DL, Meriaux AS, Herries AIR, King GCP, Berger LR (2010) Geological setting and age of *Australopithecus sediba* from Southern Africa. Science 328:205–208
Fromental-Ramain C, Warot X, Lakkaraju S, Favier B, Haack H, Birling C, Dietrich A, Dolle P, Chambon P (1996) Specific and redundant functions of the paralogous Hoxa-9 and Hoxd-9 genes in forelimb and axial skeleton patterning. Development 122:461–472
Giglio CA, Volpon JB (2007) Development and evaluation of thoracic kyphosis and lumbar lordosis during growth. J Child Orthop 1:187–193
Gilbert SF (2003) Developmental biology. Sinauer Associates, Inc., Sunderland
Golovanova LV, Hoffecker JF, Kharitonov VM, Romanova GP (1999) Mezmaiskaya cave: a Neanderthal occupation in the Northern Caucasus. Curr Anthropol 40:77–86
Haeusler M, Martelli SA, Boeni T (2002) Vertebrae numbers of the early hominid lumbar spine. J Hum Evol 43:621–643
Haeusler M, Schiess R, Boeni T (2011) New vertebral and rib material point to modern bauplan of the Nariokotome *Homo erectus* skeleton. J Hum Evol 61:575–582
Hellsing E, Reigo T, McWilliam J, Spangfort E (1987) Cervical and lumbar lordosis and thoracic kyphosis in 8, 11 and 15-year-old children. Eur J Orthod 9:129–138
Holly Smith B, Crummett TL, Brandt KL (1994) Ages of eruption of primate teeth: a compendium for aging individuals and comparing life history. Am J Phys Anthropol 37:177–231
Huang R, Zhi Q, Neubuser A, Muller TS, Brandsaberi B, Christ B, Wilting J (1996) Function of somite and somitocoele cells in the formation of the vertebral motion segment in avian embryos. Acta Anat (Basel) 155(4):231–241
Janssen M-MA, Drevelle X, Humbert L, Skalli W, Castelein RM (2009) Differences in male and female Spino-pelvic alignment in asymptomatic young adults a three-dimensional analysis using upright low-dose digital Biplanar X-rays. Spine 34:E826–E832
Johnson KT, Al-Holou WN, Anderson RCE, Wilson TJ, Karnati T, Ibrahim M, Garton HJL, Maher CO (2016) Morphometric analysis of the developing pediatric cervical spine. J Neurosurg Pediatr 18:377–389
Kapandji IA (1992) Rumpf und Wirbelsäule. Ferdinand Enke Verlag, Stuttgart
Kaplan KM, Spivak JM, Bendo JA (2005) Embryology of the spine and associated congenital abnormalities. Spine J 5:564–576
Karol LA, Johnston C, Mladenov K, Schochet P, Walters P, Brownie RH (2008) Pulmonary function following early thoracic fusion in non-neuromuscular scoliosis. J Bone Joint Surg Am 90A:1272–1281
Kessel M, Gruss P (1990) Murin developmental control genes. Science 249:347–379
Kessel M, Gruss P (1991) Homeotic transformations of murine vertebrae and concomitant alternations of Hox codes induced by retinoic acid. Cell 67:89–104
Kimbel WH, Rak Y (2010) The cranial base of *Australopithecus afarensis*: new insight from the female skull. Philos Trans R Soc Lond B Biol Sci 365:3365–3376
Kimura S, Steinbach GC, Watenpaugh DE, Hargens AR (2001) Lumbar spine disc height and curvature responses to an axial load generated by a compression device compatible with magnetic resonance imaging. Spine 26:2596–2600
Kondo O, Dodo Y, Akazawa T, Muhesen S (2000) Estimation of stature from the skeletal reconstruction of an immature Neandertal from Dederiyeh Cave, Syria. J Hum Evol 38:457–473
Korovessis PG, Stamatakis MV, Baikousis AG (1998) Reciprocal angulation of vertebral bodies in the sagittal plane in an asymptomatic Greek population. Spine 23:700–705
Lee CS, Noh H, Lee DH, Hwang CJ, Kim H, Cho SK (2012) Analysis of sagittal spinal alignment in 181 asymptomatic children. J Spinal Disord Tech 25:E259–E263

Mac-Thiong J-M, Labelle H, Berthonnaud E, Betz R, Roussouly P (2007) Sagittal spinopelvic balance in normal children and adolescents. Eur Spine J 16:227–234
Madre-Dupouy M (1999) L'enfant du Roc de Marsal. Étude analytique et comparative. Éditions du CNRS, Paris
Martelli SA, Schmid P (2003) Functional morphology of the lumbar spine in hominoids. Cour Forschungsinst Senck 243:61–69
Maureille B (2002) A lost Neanderthal neonate found. Nature 419:33–34
Moore KL, Persaud TVN (2008) The developing human clinically orientated embryology. Saunders Elsevier, Philadelphia
Neaux D, Bienvenu T, Guy F, Daver G, Sansalone G, Ledogar JA, Rae T, Wroe S, Brunet M (2017) Relationship between foramen magnum position and locomotion in extant and extinct hominoids. J Hum Evol 113:1–9
Okpala F (2014) Measurement of lumbosacral angle in normal radiographs: a retrospective study in Southeast Nigeria. Ann Med Health Sci Res 4:757–762
Pilbeam D (2004) The anthropoid postcranial axial skeleton: comments on development, variation and evolution. J Exp Zool B Mol Dev Evol 203B:241–267
Poussa MS, Heliövaara MM, Seitsamo JT, Könönen MH, Hurmerinta KA, Nissinen MJ (2005) Development of spinal posture in a cohort of children from the age of 11 to 22 years. Eur Spine J 14:738–742
Richardson MK, Allen SP, Wright GM, Raynaud A, Hanken J (1998) Somite number and vertebrate evolution. Development 125:151–160
Ríos L, Cardoso FV (2009) Age estimation from stages of union of the vertebral epiphyses of the ribs. Am J Phys Anthropol 140:265–274
Rosas A, Ríos L, Estalrrich A, Liversidge H, García-Tabernero A, Huguet R, Cardoso H, Bastir M, Lalueza-Fox C, De la Rasilla M, Dean C (2017) The growth pattern of Neandertals, reconstructed from a juvenile skeleton from El Sidrón (Spain). Science 357:1282–1287
Rowe N (1996) The pictorial guide to the living primates. In: East Hampton. Ponginas Press, New York
Sandgathe DM, Dibble HL, Goldberg P, McPherron SP (2011) The Roc de Marsal Neandertal child: A reassessment of its status as a deliberate burial. J Hum Evol 61:243–253
Schlösser TPC, Shah SA, Reichard SJ, Rogers K, Vincken KL, Castelein REM (2014) Differences in early sagittal plane alignment between thoracic and lumbar adolescent idiopathic scoliosis. Spine J 14:282–290
Schlösser TPC, Vincken KL, Rogers K, Castelein RM, Shah SA (2015) Natural sagittal spinopelvic alignment in boys and girls before, at and after the adolescent growth spurt. Eur Spine J 24:1158–1167
Schultz AH (1926) Fetal growth of man and other primates. Q Rev Biol 1:456–521
Schultz AH (1938) The relative length of the regions of the spinal column in old world primates. Am J Phys Anthropol 24:1–22
Schultz AH (1940) Growth and development of the chimpanzee. Contrib Embryol 170:1–63
Schultz AH (1941) Growth and development of the orang-utan. Contrib Embryol 182:57–110
Schultz AH (1944) Age changes and variability in gibbons. Am J Phys Anthropol 2:2–124
Schultz AH (1950) The specializations of man and his place among the catarrhine primates. Cold Spring Harb Symp Quant Biol 15:37–53
Schultz AH (1953) The relative thickness of the long bones and the vertebrae in primates. Am J Phys Anthropol 11:277–312
Schultz AH (1955) The position of the occipital condyles and of the face relative to the skull base in primates. Am J Phys Anthropol 13:97–120
Schultz AH (1961) Primatologia. Handbuch der Primatenkunde. S. Karger, Basel
Schultz AH (1973) Age changes, variability and generic differences in body proportions of recent hominoids. Folia Primatol 19:338–359
Schwartz GT, Dean C (2001) Ontogeny of canine dimorphism in extant hominoids. Am J Phys Anthropol 115:269–283

Shefi S, Soudack M, Konen E, Been E (2013) Development of the lumbar lordotic curvature in children from age 2 to 20 years. Spine 38:E602–E608
Skinner M (1997) Age at death of Gibraltar 2. J Hum Evol 32:469–470
Smith TM, Tafforeau P, Reid DJ, Pouech J, Lazzari V, Zemeno JP, Guatelli-Steinberg D, Olejniczak AJ, Hoffman A, Radovcic J, Makaremi M, Toussaint M, Stringer C, Hublin J-J (2010) Dental evidence for ontogenetic differences between modern humans and Neanderthals. Proc Natl Acad Sci USA 107:20923–20928
Stagnara P, De Mauroy J, Dran G, Gonon GP, Constanzo G, Diment J, Pasquet A (1982) Reciprocal angulation of vertebral bodies in a sagittal plane: approach to references for the evaluation of kyphosis and lordosis. Spine 7:335–342
Tanner JM, Whitehouse RH, Takaishi M (1966) Standards from birth to maturity for height, weight, height velocity, and weight velocity: British children 1965, part I. Arch Dis Child 41:454–471
Taylor JR (1975) Growth of human intervertebral discs and vertebral bodies. J Anat 120:49–68
Taylor JR, Twomey LT (1984) Sexual dimorphism in human vertebral body shape. J Anat 138:281–286
Torres-Tamayo N, García-Martínez D, Zlolniski SL, Torres-Sánchez I, García-Río F, Bastir M (2018) 3D analysis of sexual dimorphism in size, shape and breathing kinematics of human lungs. J Anat 232:227–237
Voutsinas SA, MacEwen GD (1986) Sagittal profiles of the spine. Clin Orthop Relat Res 210:235–242
Walker A, Leakey R (1993) The postcranial bones. In: Walker A, Leakey R (eds) The Nariokotome *Homo erectus* skeleton. Springer Verlag, Berlin, pp 95–161
Ward CV, Nalley TK, Spoor F, Tafforeau P, Alemseged Z (2017) Thoracic vertebral count and thoracolumbar transition in *Australopithecus afarensis*. Proc Natl Acad Sci U S A 114:6000–6004
Ward L, Pang ASW, Evans SE, Stern CD (2018) The role of the notochord in amniote vertebral column segmentation. Dev Biol 439:3–18
Weaver TD, Coqueugniot H, Golovanova LV, Doronichev VB, Maureille B, Hublin J-J (2016) Neonatal postcrania from Mezmaiskaya, Russia, and Le Moustier, France, and the development of Neandertal body form. Proc Natl Acad Sci U S A 113:6472–6477
Wehner R, Gehring W (2007) Zoologie. Georg Thieme Verlag, Stuttgart
Widhe T (2001) Spine: posture, mobility and pain. A longitudinal study from childhood to adolescence. Eur Spine J 10:118–123
Williams SA, Middleton ER, Villamil CI, Shattuck MR (2016) Vertebral numbers and human evolution. Am J Phys Anthropol 159:19–36
Williams SA, Ostrofsky KR, Frater N, Churchill SE, Schmid P, Berger LR (2013) The vertebral column of *Australopithecus sediba*. Science 340:1–5
Williams SA, Gómez-Olivencia A, Pilbeam D (2019) Numbers of vertebrae in hominoid evolution. In: Been E, Gómez-Olivencia A, Kramer PA (eds) Spinal evolution: morphology, function, and pathology of the spine in hominoid evolution. Springer, New York, pp 97–124
Willner S, Johnson B (1983) Thoracic kyphosis and lumbar lordosis during the growth period in children. Acta Paediatr Scand 72:873–878
Yong Q, Zhen L, Zezhang Z, Bangping Q, Feng Z, Tao W, Jun J, Xu S, Xusheng Q, Weiwei M, Weijun W (2012) Comparison of sagittal spinopelvic alignment in Chinese adolescents with and without idiopathic thoracic scoliosis. Spine 37:714–720

Chapter 12
The Association Between Spinal Posture and Spinal Biomechanics in Modern Humans: Implications for Extinct Hominins

Ella Been and Jeannie F. Bailey

12.1 Introduction

The human spine supports the body's weight, facilitates movement and flexibility, and protects the vulnerable spinal cord from injury (Izzo et al. 2013). Along with that, the spinal column possesses shock absorption abilities—it attenuates shocks and vibrations that occur in daily life activities (Castillo and Lieberman 2018).

Posture is a static position that serves as the base for movement and function. In healthy human adults, spinal posture is close to straight in the coronal plane (from a posterior view) and possesses four curvatures in the sagittal plane (cervical and lumbar lordosis, thoracic and sacral kyphosis) (Kapandji 1974). However, skeletal evidence reveals considerable variation in spinal curvatures within modern human populations and among fossil hominins (Been et al. 2012, 2014, 2017; Been and Kalichman 2014), suggesting an adaptive function for variations in spinal curvature. These postural differences might imply differences in spinal ROM, spinal stability, muscle force, kinematics, and shock attenuation between modern humans with different spinal postures and between hominin groups.

The aim of this review is to establish a connection between spinal posture, function, and biomechanics (ROM, stability, muscle force, movement pattern, and shock attenuation) in modern humans and to explore its implications for extinct hominins.

E. Been (✉)
Department of Sports Therapy, Faculty of Health Professions, Ono Academic College, Kiryat Ono, Israel

Department of Anatomy and Anthropology, Sackler Faculty of Medicine, Tel Aviv University, Tel Aviv, Israel

J. F. Bailey
Department of Orthopaedic Surgery, University of California, San Francisco, CA, USA

E. Been et al. (eds.), *Spinal Evolution*,
https://doi.org/10.1007/978-3-030-19349-2_12

12.2 Posture and Spinal Stability/Instability

The American Academy of Orthopedic Surgeons defined spinal stability as, "the capacity of the vertebrae to remain cohesive and to preserve the normal displacements in all physiological body movements" (Kirkaldy-Willis 1985; Castillo and Lieberman 2018). Spinal stability is the basic requirement for normal function; it protects nerve structures and prevents the early mechanical deterioration of spinal components. It is essential for the transfer of power forces between the upper and lower limbs and the active generation of forces in the trunk. Bones, discs, and ligaments contribute to spinal stability by playing a structural role and by acting as transducers through their mechanoreceptors (Izzo et al. 2013). Muscles are vital to spinal stability, as stronger muscles tend to increase the stiffness of the spine and prevent abnormal movement or buckling of the spinal column (Wilke et al. 1995; Meakin et al. 2013).

In the anthropological literature, spinal stability often refers to the amount of motion in the trunk/spine. A spine with limited motion would be considered as a stable spine whereas a spine with increased motion would be considered as an unstable spine. This is different from the orthopedic approach that defines instability as a loss of stiffness leading to abnormal and increased movement in the motion segments (Pope and Panjabi 1985). Damage to any spinal structure gives rise to some degree of instability that might lead to malfunction, pain, and pathology. For the purpose of this review, we will address instability as loss of stiffness leading to increased movement in the motion segments (two adjacent vertebrae, disc, facet joints, and all adjoining ligaments between them).

It has been hypothesized that straighter lumbar spines (i.e., low degrees of lumbar lordosis) offer greater stability whereas more curved lumbar postures allow the lower spine to act like a "shock absorber" during locomotion (Kapandji 1974; Adams and Hutton 1985; Rak 1993; Kobayashi et al. 2008; Been et al. 2012, 2017; Gómez-Olivencia et al. 2017).

Castillo and Lieberman (2018) suggest that lumbar lordosis is higher among athletes for whom running and dynamic impacts are integral part of their activity, such as runners and soccer players, implying greater instability of the lumbar spine. On the other hand, they suggest that athletes who do not experience high levels of impact-related loading, such as swimmers and body builders, tend to have much straighter lumbar spines possibly for greater stability.

Bailey (2016) examined spinal posture and stability in males and females. The research examined the degree of lumbar lordosis, spinal ROM, and the amount of translation of the lumbar vertebrae during flexion and extension. The research showed that lumbar instability, as well as lumbar lordosis, is greater in females than in males. In addition, females show the greatest degree of vertebral translation at L4-L5 level (indicating more instability) during spinal motion. Bailey speculated that greater lumbar lordosis in females is actually an adaptation to aid in bearing a pregnancy load, and that degenerative spondylolisthesis, spinal pathology associated with greater instability, is the orthopedic trade-off (see also Whitcome et al. 2007).

To summarize, all of the evidence we found suggest that higher lumbar lordosis is associated with lower spinal stability while a straighter spine (smaller lordosis) is associated with increased stability.

12.3 Spinal Posture and Range of Motion (ROM)

ROM is the amount of movement in a specific direction—expressed in degrees—which a joint can achieve. Spinal ROM is influenced by vertebral morphology, length and flexibility of spinal ligaments, intervertebral disc morphology, and facet joint capsule. The basic spinal movements include flexion–extension in the sagittal plane, side flexion in the coronal plane, and rotation in the horizontal plane (Kapandji 1974; Izzo et al. 2013). Most of the studies that explored interaction between spinal ROM and posture only examined sagittal plane motion (flexion and extension) (Schenkman et al. 1996; Miyakoshi et al. 2005; Miyazaki et al. 2008; Ro et al. 2010; Cho et al. 2011; Gong et al. 2012; Gong 2015; Moustafa et al. 2017). We did not find any research that explored the interaction between spinal posture and coronal/horizontal plane movements (side flexion and rotation).

12.3.1 Cervical Lordosis and Cervical ROM

The cervical spine withstands substantial compressive axial load, which is approximately twice the weight of the head because of muscle co-activation forces functioning to balance the head in the neutral position (Panjabi et al. 1993; Moroney et al. 1988; Patwardhan et al. 2000). The compressive force increases during flexion and extension and other routine movements. Cervical lordosis is considered to decrease the internal compressive load and is essential for appropriate spinal coupling motion (Miyazaki et al. 2008).

A few studies have shown that improved lordosis was associated with significant improved motions of the cervical spine (Miyazaki et al. 2008; Ro et al. 2010; Gong et al. 2012; Gong 2015; Moustafa et al. 2017). Miyazaki et al. (2008) found that when normal lordotic alignment progressed into hypolordotic alignment and straight alignment, all levels of the cervical spine tended to have decreased ROM in terms of translational motion and angular variation. When alignment shifted from normal lordosis to hyperlordosis, translational motion, angular variation, and the contribution percentage to the total angular variation at the mid-cervical levels increased. Gong et al. (2012) studied the cervical spines of normal young adults and found that as cervical lordosis increased, extension and the full range of flexion-extension of the cervical spine increased. Similar results were found in patients with herniated discs (Ro et al. 2010) and in patients with cervical spondylotic radiculopathy (Moustafa et al. 2017). This finding provides objective evidence that cervical flexion–extension is partially dependent on the posture and sagittal curve orientation (Gong et al. 2012; Gong 2015).

12.3.2 Thoracic Kyphosis and ROM

Concerning the thoracic spine, we found only one study that explored the interaction between thoracic curvature and ROM. Miyakoshi et al. (2005) found no correlation between thoracic kyphosis and spinal ROM (combined thoracic and lumbar ROM).

12.3.3 Lumbar Lordosis and Lumbar ROM

Only a few researchers explored the relationship between the degree of lumbar lordosis and the amount of spinal motion. Some authors explored the total ROM of the lumbar spine while others explored the motion at a segmental level, or divided the motion to forward flexion and backward extension (Schenkman et al. 1996; Cho et al. 2011; Bailey 2016; du Rose and Breen 2016; Castillo et al. 2017).

Schenkman et al. (1996) found no interaction between lumbar axial mobility and the amount of lumbar lordosis. On the other hand, Cho et al. (2011) examined the interaction between the degree of lumbar lordosis and spinal ROM (flexion–extension); they found weak positive correlation ($r = 0.37$) between spinal extension and the degree of lumbar lordosis, but did not find interaction between forward flexion and the degree of lordosis.

Du Rose and Breen (2016) described a complex relationship between the degree of lordosis and ROM. They found that interactions between lumbar lordosis and ROM were different between the lumbar segments. Lordosis was positively associated with L2–3 range and negatively with L4–L5 range, implying that higher lumbar lordosis is associated with higher overall ROM in the L2–3 segment and lower overall range in L4–5 segment. They argue that the degree of lordosis may allow a more even sharing of motion throughout the lumbar spine, offering a degree of protection to the L4–5 segment during bending, and that lordosis itself has an important role in spinal biomechanical behavior. Castillo et al. (2017) examined the correlation between the degree of lumbar lordosis and the angle of difference between maximum lumbar flexion and maximal extension. They found moderate correlation ($r = 0.5$) between the degree of lordosis and the amount of lumbar ROM in the sagittal plane (angle of difference between maximal flexion and maximal extension). Bailey (2016) found that lumbar intervertebral motion in the sagittal plane differed by sex with males having a greater range of flexion and females having a greater range of extension. The study suggested that these differences might indirectly relate to sex differences in lumbar lordosis as males have smaller lumbar lordosis than females. Bailey argued that one potential explanation to the differences in spinal posture and ROM between males and females is the greater joint laxity in the stabilizing ligaments of the lumbar spine of females.

Based on this data, it is hard to determine the nature of the interaction between lumbar lordosis and spinal ROM. Although it seems that there is evidence for some form of interaction between the two, the nature of this interaction should be further explored.

12.4 Spinal Posture and Muscle Strength

Strength is the most familiar characteristic of muscle performance. However, the term strength has many different interpretations. The basic activity of a muscle is to shorten, thus producing a tensile force. The force also produces a moment, or a tendency to rotate, when the force is exerted at some distance from the point of rotation. The ability to generate a tensile force and the ability to create a moment are both used to describe a muscle's strength (Oatis 2004).

The primary factors influencing the muscle's strength are muscle size, muscle moment arm, fiber length, contraction velocity, and level of fiber recruitment. Assessment of muscle strength in vivo is typically performed by determining the muscle's ability to produce a moment (Oatis 2004).

Many researchers explored the association between spinal posture and muscle strength, some by measuring muscle strength in living subjects, and others by using biomechanical models of the spine. Most of the researchers explored the strength of the flexors and extensors of the spine in relation to posture and did not relate to muscles that rotate or side flex the spine.

12.4.1 Muscle Strength and Cervical Lordosis

Both Mayoux-Benhamou et al. (1994) and Olson et al. (2006) found that hyperlordotic cervical spine is associated with weak deep cervical flexors (longus colli, longus capitis, and rectus capitis muscles) compared to the strength of these muscles in average lordotic cervical spines. Mayoux-Benhamou (1994) demonstrated smaller cross-sectional area (CSA) in longus colli muscle of subjects with hyperlordotic cervical spine. Alpayci et al. (2016) found that the loss of cervical lordosis, that is, hypolordosis, is associated with the weakness of neck extensors. They also found that the values of the extension-flexion ratio were lower in the hypolordotic group compared with the controls ($p = 0.004$), implying reduction in extensors' strength in relation to flexors' strength.

All of the above provides a simple picture: in modern humans, cervical hyperlordosis is associated with weak neck flexors and hypolordosis associate with weak neck extensors.

12.4.2 Muscle Strength and Thoracic Kyphosis

The results regarding spinal muscle strength and thoracic kyphosis are contradicting. Hongo et al. (2012) found no correlation between thoracic kyphosis angle and extensor muscle strength. Briggs et al. (2007) found that an increase in thoracic kyphosis is associated with significantly higher multi-segmental spinal loads and trunk muscle forces in an upright stance. On the other hand, Sinaki et al. (1996),

Mika et al. (2005), and Granito et al. (2012) found that hyperkyphosis is associated with weak thoracic extensors and hypokyphosis is associated with strong thoracic extensors. Based on this contradicting evidence, it is hard to determine the presence of association or lack of association between thoracic kyphosis and muscle strength.

12.4.3 Muscle Strength and Lumbar Lordosis

Many researchers examined the relationship between the lumbar lordosis angle and abdominal and spinal muscle strength. Some researchers found that none of the isometric maximum torques were related to lordotic angle (Walker et al. 1987; Heino et al. 1990; Kendall et al. 2005). On the other hand, Hongo (2012) found that back extensor strength was significantly associated with lumbar lordosis in Japanese postmenopausal females but not in American females. Bailey et al. (2018) found that a decrease in multifidus cross-sectional area following spaceflight is associated with decreases in lumbar lordosis and increased spinal stiffness (decreased intersegmental ROM).

Kim et al. (2006) tried a different approach. They examined the relationship between trunk muscle strength (ratio of abdominal vs. back muscles) and lumbar lordosis and found that the ratio of extensor torque to flexor torque was significantly related to the lordotic angle: Relatively strong spinal extensors and weak spinal flexors were associated with high lumbar lordosis and vice versa. The researchers concluded that an imbalance in trunk muscle strength can significantly influence the lordotic curvature of the lumbar spine. Hsu et al. (2015) found similar results. They examined the ratio between the CSA of rectus abdominis (spinal flexor) to that of erector spinae (spinal extensor). Their results indicate relatively large rectus abdominis in subjects with small lumbar lordosis and relatively large erector spinae in subjects with large lumbar lordosis. We can conclude that while individual muscle group strength is not necessarily associated with the degree of lordosis, the ratio between lumbar flexors and extensors is associated with lumbar lordosis.

12.5 Posture and Shock Attenuation (SA)

During locomotion, each step generates a shock wave that travels through the body toward the head. Ground reaction force (GRF) impact peaks can be substantial with magnitudes between 0.6 and 1.0 times the body weight during walking and 1.0 to 3.0 times the body weight during running (Nigg et al. 1995; Whittle and Levine 1999). Attenuation of these large, rapid impact peaks is crucial because the resulting impulse can disrupt the vestibulo–ocular reflex and potentially lead to injury and other pathology (Pozzo et al. 1990, 1991; Whittle 1999; Davis et al. 2016). Both the lower limbs and the spine play a major role in SA. Impact-related shocks can be attenuated passively via soft tissues, especially by the intervertebral discs and spinal

ligaments, or actively, through the eccentric construction of muscles or modification of gait kinematics (Derrick et al. 1998; Whittle 1999; Addison and Lieberman 2015). For many years, researchers claimed that the amount of spinal curvature is associated with its ability to absorb the shock wave that travels throw the body (Kapandji 1974; Adams and Hutton 1985; Rak 1993; Kobayashi et al. 2008; Been et al. 2012, 2017; Gómez-Olivencia et al. 2017), but there was no actual proof.

Castillo and Lieberman (2018) explored the SA in the human lumbar spine during walking and running. Their major findings indicate that there is a strong association between lumbar lordosis and lumbar SA during running (but not walking), which explains approximately 30% of the variation in resultant SA during running. Their results suggest that for every 1% increase in lumbar lordosis there is a 10% increase in lumbar SA.

They also found that resultant SA within the lumbar spine during running (−0.8 ± 3.1 dB) was much less intense than levels of resultant SA within the tibia and sacrum (−4.0 ± 3.1 dB) (Giandolini et al. 2016). They explained this difference by the fact that the majority of passive and active mechanisms for SA are associated with the lower limb. Therefore, the magnitude of shock is already mostly attenuated by the time it reaches the vertebral column (Derrick et al. 1998; Whittle 1999; Addison and Lieberman 2015).

After examining the relationship between dynamic changes in lordosis and SA, Castillo and Lieberman (2018) found support for the idea that the lumbar spine acts like a viscoelastic system to attenuate impact-related shocks. However, motions of the lumbar spine revealed that less dynamically compliant lumbar spines (i.e., smaller amplitudes of lordosis angular displacement) are associated with lower levels of SA during running. Their findings support the hypothesis that lumbar lordosis plays an important role in attenuating impact shocks transmitted through the human spine during high-impact, dynamic activities such as running.

12.6 Motion Pattern and Spinal Posture

Ultimately, differences in spinal stability, ROM, strength, and SA should have an impact on motion pattern and function. So how does the difference in spinal curvature influence motion pattern and function?

12.6.1 Posture and Gait

Many researchers have shown a positive correlation between the degree of lumbar lordosis and walking velocity (Grasso et al. 2000; Sarwahi et al. 2002; Hirose et al. 2004; Jang et al. 2009; Fox 2013; Schmid et al. 2017). Specifically, it has been shown that hypolordotic lumbar spine leads to slow walking speed and short steps (Fox 2013), while a hyperlordotic spine in older individuals leads to high walking

velocity (Schmid et al. 2017). Fox (2013) examined the gait of males and females with normal lumbar lordosis and an actively induced posterior pelvic tilt and reduced lordosis. The kinematic results of her study suggest that experimentally-induced hypolordotic gait is associated with certain gait deviations that make locomotion less efficient. These manipulations affect female efficiency more strongly due to a reduction in their stride length. Males and females also exhibited a differing pattern of thigh and knee flexion during posteriorly tilted walking: Females displayed more thigh flexion, whereas males displayed more knee flexion.

Assi et al. (2016) and Bakouny et al. (2017) explored gait kinematics between three groups of subjects: the first group with low pelvic incidence, sacral slope, and lumbar lordosis, the second group with average pelvic incidence, sacral slope, and lumbar lordosis and the third group with high pelvic incidence, sacral slope, and lumbar lordosis. There was no difference in thoracic kyphosis between the three groups. Gait analysis revealed that subjects from the first group had the most retroverted pelvis during the gait cycle, the highest hip extension during stance phase and the highest ROM of ankle plantar-dorsiflexion during the gait cycle. Subjects from the second and third groups (average or high pelvic incidence, sacral slope and lumbar lordosis) had similar gait patterns with decreased pelvic retroversion during the gait cycle, decreased hip extension during the stance phase, and decreased ankle plantar-dorsiflexion during the gait cycle compared to subjects from the first group. They concluded that sagittal spino-pelvic morphotypes seem to affect gait kinematics even in asymptomatic subjects. They have shown that different sagittal morphotypes affect gait not only proximally (pelvis and hip) but also more distally (ankle) (Assi et al. 2016; Bakouny et al. 2016, 2017). Despite the kinematic differences between the three groups, they found that asymptomatic subjects with different types of sagittal alignment have similar spatio-temporal characteristics of gait (walking speed, cadence, and step length). They suggest that kinematic corridors of normality should be specific of sagittal alignment profiles.

Altogether, there is evidence to suggest significant differences in both gait kinematics and speed between humans with lumbar hypolordosis and those with hyperlordosis.

12.6.2 Posture and Lifting Kinematics

Pavlova et al. (2018) examined the interaction between variation in lifting kinematics and the degree of lumbar lordosis. Their results indicate an interaction between lumbar curvature and lifting kinematics. They found that when no instruction was given, individuals with more lordotic lumbar spines preferred to stoop down (more hip and lumbar flexion, less knee flexion) to pick up the box from the floor, while those with straighter spines preferred to squat (more knee flexion, less hip and lumbar flexion) (Fig. 12.1). They suggested that these natural movement preferences are maintained when instructions are given, especially in individuals with hyperlordotic spines who prefer to lift by stooping. In changing between lifting styles, individuals adjusted their knee flexion while maintaining their preferred lumbar flexion range.

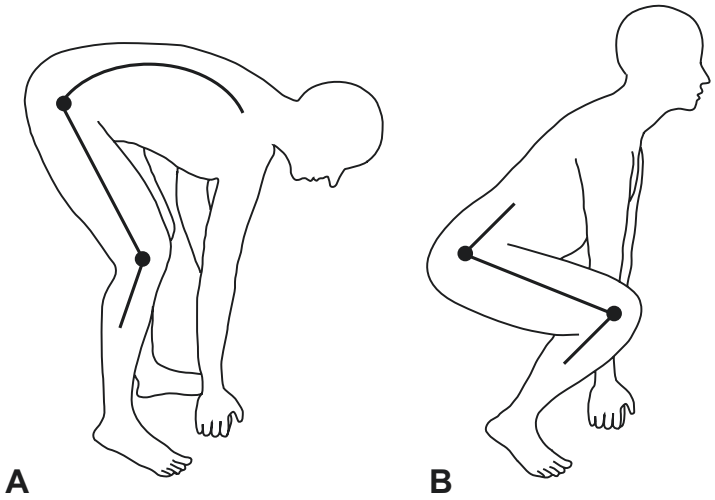

Fig. 12.1 Lifting kinematics: (**a**) stoop down (more lumbar flexion, less knee flexion) to pick up the box from the floor. (**b**) squat (more knee flexion, less lumbar flexion)

Flattening of the lumbar lordosis is suggested to cause considerable increase in spinal loads and the stoop technique is generally believed to result in greater peak lumbar loads (Pavlova et al. 2018). Consequently, it might be thought that curvier individuals, who tend to stoop, are at a greater risk of overload and injury. However, lumbar vertebrae are able to withstand very high loads (Hutton and Dhanendran 1979; Adams and Hutton 1982; Crisco et al. 1992), especially in pure compression. The intervertebral disc is at greater risk when compressive forces are combined with bending or twisting (Schmidt et al. 2007; Vergroesen et al. 2015). These results are comparable with those of du Rose and Breen (2016) who found that a greater degree of lordosis was related to greater peak intervertebral flexion at individual segmental levels. Together these findings suggest that those with straighter spines chose to squat as a means to reduce loading on the spine (du Rose and Breen 2016; Pavlova et al. 2018) and those with curvier spines chose to stoop as their initial spinal loads are smaller. Pavlova et al. (2018) emphasized the need for further studies, ideally using weight-bearing imaging to explore the preference for a stooped posture and the tendency toward greater intervertebral flexion in lordotic individuals, and whether this is a more efficient and safer movement strategy, especially during manual lifting.

12.6.3 Posture and Overhead Activities

Crawford and Jull (1993) explored the relationships between the range of bilateral arm elevation, thoracic extension motion, and thoracic posture in 60 normal females. They found that a large kyphosis was associated with reduced arm elevation in older

subjects. They also found that bilateral arm elevation induced an average of 15° and 13° of thoracic extension in the younger and the older groups, respectively. This represented half of the available extension range in the young subjects, but nearly 70% of available range in the older subjects. A strong relationship was found between the range of arm elevation and range of thoracic extension used in this movement in younger subjects.

Lewis et al. (2005) found similar results, they demonstrated that reducing the thoracic kyphosis could contribute to improving arm elevation (shoulder flexion/abduction) and, therefore, improving overhead activities such as throwing.

The mechanism underlying the interaction between thoracic kyphosis and overhead activities includes greater thoracic kyphosis (Kebaetse et al. 1999; Finley and Lee 2003) and a more anterior shoulder position–shoulder protraction (Wang et al. 1999; Borstad and Ludewig 2005) that have been demonstrated to be associated with altered scapular position, kinematics, and muscle activity (Thigpen et al. 2010). More precisely, an increase in thoracic kyphosis was positively associated with decreased scapular upward rotation, which is a major component of shoulder flexion/abduction (Kebaetse et al. 1999; Finley and Lee 2003).

12.7 Implications on Extinct Hominins

Been et al. (2017) identified three basic spinopelvic alignments in hominins (Fig. 12.2). First, the sinusoidal alignment with moderate to high spinal curvatures and pelvic incidence found in *H. erectus* and *H. sapiens*. Second, the straight alignment with small spinal curvatures and small pelvic incidence found in Neanderthal lineage hominins (NLH). Third, the compound alignment found in *Australopithecus* with moderate pelvic incidence and lumbar lordosis and a nearly straight cervical spine.

If we can indeed speculate from the modern human condition to extinct hominins based on spinal posture, then there are some interesting implications to draw.

H. erectus and early *H. sapiens* with moderate to high spinal curvatures, similar to the posture of modern humans, probably had similar biomechanical characteristics as modern humans. This is supported by the morphological similarity between the *H. erectus* (Meyer 2005; Haeusler et al. 2011; Schiess and Haeusler 2013) and *Early H. sapiens* spine (McCowan and Keith 1939; Been et al. 2012) and that of modern humans. Their spine might have been characterized by good SA capabilities relevant to fast walking/running. The relatively high spinal curvatures may imply a more mobile and less stable spine compared to other hominins, yet similar to modern humans. Their ROM and muscle force may imply lifting and throwing capabilities that are within the range of modern humans. However, differences in the orientation of the C7 spinous process, more horizontal in *H. erectus* (Carretero et al. 1999; Arlegi et al. 2017) may imply slight differences in the neck biomechanics.

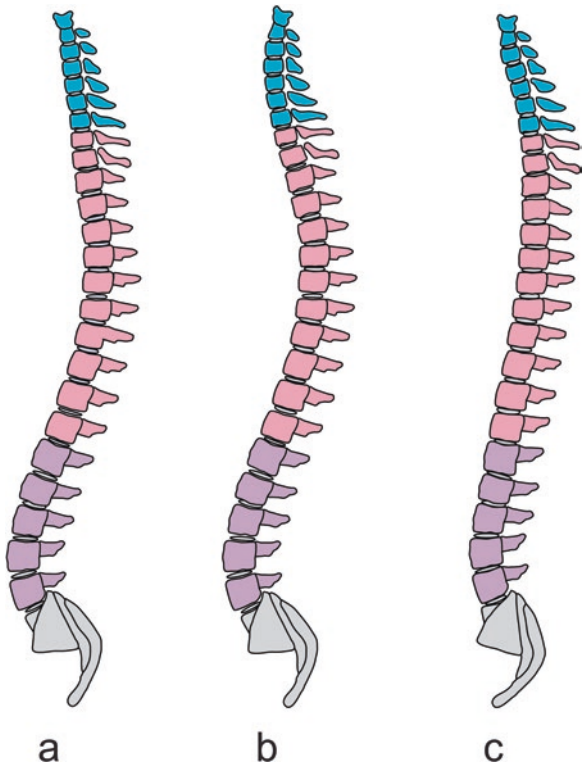

Fig. 12.2 Schematic configuration of spinal curvatures in hominins. The compound alignment with moderate pelvic incidence and lumbar lordosis, and a nearly straight cervical spine (**a**). The sinusoidal alignment with moderate to high spinal curvatures and pelvic incidence (center, **b**). The straight alignment with small spinal curvatures and small pelvic incidence (**c**). Blue, cervical vertebrae; Pink, thoracic vertebrae; Purple, lumbar vertebrae; Grey, sacrum

One must also remember that within each of these species, there might have been inter-personal biomechanical differences based on different spinal posture.

NLH with small spinal curvatures might have had somewhat different biomechanics. Based on this review, it seems that the relatively straighter spine of NLH might have been more stable and less mobile than that of modern humans, the early *H. sapiens* and *H. erectus*. Castillo and Lieberman (2018) have already speculated that the less lordotic lumbar spines of NLH may have been better adapted to stiffness and stability at the expense of reduced capacity for SA during dynamic activities such as running.

The ROM of the cervical spine in the sagittal plane (flexion-extension) of NLH might have been reduced compared to modern humans, but we cannot draw any definitive conclusions regarding the ROM in the thoracic and lumbar spines based on current literature.

In terms of muscle strength, the hypolordotic cervical and lumbar spines of NLH may imply a different ratio between spinal flexors and spinal extensors compared to modern humans. The cervical flexors might have been relatively stronger than the cervical extensors compared to modern humans and the lumbar flexors might have been stronger than lumbar extensors as well.

When it comes to motion pattern, there is evidence to suggest that NLH had a slower gait than modern humans do. Their gait pattern might have included a retroverted pelvis during the gait cycle, high hip extension during stance phase, and a high ROM of ankle plantar-dorsiflexion (Assi et al. 2016; Bakouny et al. 2016, 2017). This review does not take into consideration the differences in the length and orientation of the lumbar transverse processes in the Neanderthal spine, nor the differences in the pelvic anatomy in this region (Rak 1993; Been et al. 2010; Gómez-Olivencia et al. 2017). The presence of these differences also likely affects the gait pattern.

NLH might have also preferred to squat (more knee flexion, less hip and lumbar flexion) rather than to stoop down (more hip and lumbar flexion, less knee flexion) when lifting an object from the floor. Excessive squatting in Neanderthals has been suggested for the first time by the end of the nineteenth century, based on tibial morphology and later reaffirmed based on femoral morphology (Charles 1894; Trinkaus 1975). Our results provide support for this interpretation from an unexpected body part—the vertebral column. The straighter spine also suggests that NLH had better overhead function and most likely better throwing abilities than modern humans, which contradicts the results of Rhodes and Churchill (2009).

Some of these characteristics have been previously reported—slow gait, stable spine with reduced SA, and better throwing capabilities (Been et al. 2012, 2017; Gómez-Olivencia et al. 2017; Castillo and Lieberman 2018), while other findings are fairly recent (high hip extension during stance, increased ankle motion, and different lifting pattern) and should be explored in depth in future studies.

Australopithecus is characterized by a compound spinal posture with a combination of moderate lumbar lordosis and nearly straight cervical lordosis, deduced from the orientation of the Foramen Magnum (Been et al. 2017). The amount of thoracic kyphosis for this configuration is undetermined and can be anywhere from hyper thoracic kyphosis, as suggested by A.L. 288-1 (Cook et al. 1983) or hypokyphosis as suggested by Sts14 (Been et al. 2017).

Therefore, based on their moderate lumbar lordosis, *Australopithecus* probably had somewhat similar biomechanical characteristics to modern humans in the lumbar area, meaning that their stability, ROM shock attenuation, and movement pattern might have been within the range of modern humans. However, differences in the length and orientation of the transverse processes and the relative size of the vertebral bodies in relation to the articular processes may imply slight differences in the lumbar biomechanics (Sanders 1998; Meyer et al. 2015). On the other hand, the nearly straight cervical spine of *Australopithecus* may suggest a small cervical ROM. The limited ROM of the cervical spine is supported by the relatively long and horizontally oriented spinous processes of the cervical spine in *Australopithecus*, which mechanically limits flexion/extension movements (Arlegi et al. 2017). Our results regarding the cervical spine of *Australopithecus* support Arlegi et al. (2017) but contradict those of Meyer (2016). Meyer (2016) speculated that the cervical spine of *Australopithecus* KSD-VP-1/1 showed a human-like kinematic signal with a highly mobile neck and a head carriage consistent with habitual upright posture and bipedalism. Additional fossils and more studies are needed in order to resolve these discrepancies.

12.8 Conclusions

In this review, we found that spinal posture has vast biomechanical implications on spinal stability, ROM, muscle force, SA, and motion kinematics. We have applied these associations to infer the biomechanics of extinct hominins based on their posture.

Based on posture, we propose that the early *H. sapiens* and *H. erectus* with sinusoidal spine would have had spinal biomechanics within the range known to modern humans. NLH with their small spinal curvatures would have had a stable spine with limited ROM and reduced SA compared to modern humans. We further suggest that NLH might have had stronger cervical and lumbar flexors compared to extensors. Functionally, NLH might have also enjoyed better overhead activities such as throwing and different lifting patterns. NLH hominins might have also preferred squatting than stooping, had a slower gait velocity and an increased ankle motion during walking compared to modern humans.

The compound spine of *Australopithecus* with its human-like lumbar lordosis and nearly straight cervical spine suggests human-like biomechanics of the lumbar area, yet completely different biomechanics at the cervical area. Based on its posture, the cervical spine of *Australopithecus* had a smaller ROM than that of modern humans in the sagittal plane, and strong neck flexors in relation to neck extensors.

Exploring the biomechanical implications of posture is only one way to infer spinal biomechanics of extinct hominins. Future studies should try to incorporate knowledge based on bone density, trabecular orientation, and bone morphology along with posture in order to provide a wider view of extinct hominin biomechanics.

References

Adams M, Hutton W (1982) Prolapsed intervertebral disc: a hyperflexion injury. Spine 7(3):184–191

Adams M, Hutton W (1985) The effect of posture on the lumbar spine. J Bone Joint Surg 67(4):625–629

Addison BJ, Lieberman DE (2015) Tradeoffs between impact loading rate, vertical impulse and effective mass for walkers and heel strike runners wearing footwear of varying stiffness. J Biomech 48(7):1318–1324

Alpayci M, Şenköy E, Delen V, Şah V, Yazmalar L, Erden M, Toprak M, Kaplan Ş (2016) Decreased neck muscle strength in patients with the loss of cervical lordosis. Clin Biomech 33:98–102

Arlegi M, Gómez-Olivencia A, Albessard L, Martínez I, Balzeau A, Arsuaga JL, Been E (2017) The role of allometry and posture in the evolution of the hominin subaxial cervical spine. J Hum Evol 104:80–99

Assi A, Bakouny Z, Massaad A, Lafage V, Saghbini E, Kreichati G, Skalli W, Ghanem I (2016) How the type of sagittal alignment defined by Roussouly determines the gait of the asymptomatic adult subject. Revue de Chirurgie Orthopédique et Traumatologique 102(7):S179–S180

Bailey JF (2016) The effects of postural loading, sacral orientation, and age on sex differences in lumbar functional morphology and health. University of Washington, Seattle, WA

Bailey JF, Miller SL, Khieu K, O'Neill CW, Healey RM, Coughlin DG, Sayson JV, Chang DG, Hargens AR, Lotz JC (2018) From the international space station to the clinic: how prolonged unloading may disrupt lumbar spine stability. Spine J 18(1):7–14

Bakouny Z, Assi A, Massaad A, Saghbini E, Lafage V, Kreichati G, Skalli W, Ghanem I (2016) Roussouly's sagittal spino-pelvic morphotypes as determinants of gait in asymptomatic adult subjects. Gait Posture 49:57

Bakouny Z, Assi A, Massaad A, Saghbini E, Lafage V, Skalli W, Ghanem I, Kreichati G (2017) Roussouly's sagittal spino-pelvic morphotypes as determinants of gait in asymptomatic adult subjects. Gait Posture 54:27–33

Been E, Gómez-Olivencia A, Kramer PA (2012) Lumbar lordosis of extinct hominins. Am J Phys Anthropol 147(1):64–77

Been E, Gómez-Olivencia A, Kramer PA (2014) Brief communication: lumbar lordosis in extinct hominins: implications of the pelvic incidence. Am J Phys Anthropol 154(2):307–314

Been E, Gómez-Olivencia A, Shefi S, Soudack M, Bastir M, Barash A (2017) Evolution of spino-pelvic alignment in hominins. Anat Rec 300(5):900–911

Been E, Kalichman L (2014) Lumbar lordosis. Spine J 14(1):87–97

Been E, Peleg S, Marom A, Barash A (2010) Morphology and function of the lumbar spine of the Kebara 2 Neandertal. Am J Phys Anthropol 142(4):549–557

Borstad JD, Ludewig PM (2005) The effect of long versus short pectoralis minor resting length on scapular kinematics in healthy individuals. J Orthop Sports Phys Ther 35(4):227–238

Briggs AM, Van Dieën JH, Wrigley TV, Greig AM, Phillips B, Lo SK, Bennell KL (2007) Thoracic kyphosis affects spinal loads and trunk muscle force. Phys Ther 87(5):595–607

Carretero JM, Lorenzo C, Arsuaga JL (1999) Axial and appendicular skeleton of Homo antecessor. J Hum Evol 37(3–4):459–499

Castillo ER, Hsu C, Mair RW, Lieberman DE (2017) Testing biomechanical models of human lumbar lordosis variability. Am J Phys Anthropol 163(1):110–121

Castillo ER, Lieberman DE (2018) Shock attenuation in the human lumbar spine during walking and running. J Exp Biol 221:jeb177949

Charles RH (1894) Morphological peculiarities in the Panjabi, and their bearing on the question of the transmission of acquired characters. J Anat Physiol 28(Pt 3):271

Cho M, Lee Y, Kim CS, Gong W (2011) Correlations among sacral angle, lumbar lordosis, lumbar ROM, static and dynamic lumbar stability in college students. J Phys Ther Sci 23(5):793–795

Cook DC, Buikstra JE, DeRousseau CJ, Johanson DC (1983) Vertebral pathology in the Afar australopithecines. Am J Phys Anthropol 60(1):83–101

Crawford HJ, Jull GA (1993) The influence of thoracic posture and movement on range of arm elevation. Physiother Theory Pract 9(3):143–148

Crisco J, Panjabi M, Yamamoto I, Oxland T (1992) Euler stability of the human ligamentous lumbar spine. Part II: experiment. Clin Biomech 7(1):27–32

Davis IS, Bowser BJ, Mullineaux DR (2016) Greater vertical impact loading in female runners with medically diagnosed injuries: a prospective investigation. Br J Sports Med 50(14):887–892

Derrick TR, Hamill J, Caldwell GE (1998) Energy absorption of impacts during running at various stride lengths. Med Sci Sports Exerc 30(1):128–135

du Rose A, Breen A (2016) Relationships between lumbar inter-vertebral motion and lordosis in healthy adult males: a cross sectional cohort study. BMC Musculoskelet Disord 17(1):121

Finley MA, Lee RY (2003) Effect of sitting posture on 3-dimensional scapular kinematics measured by skin-mounted electromagnetic tracking sensors. Arch Phys Med Rehabil 84(4):563–568

Fox M (2013) Neandertal lumbopelvic anatomy and the biomechanical effects of a reduced lumbar lordosis. University of Cincinnati, Cincinnati, OH

Giandolini M, Horvais N, Rossi J, Millet GY, Samozino P, Morin JB (2016) Foot strike pattern differently affects the axial and transverse components of shock acceleration and attenuation in downhill trail running. J Biomech 49(9):1765–1771

Gómez-Olivencia A, Arlegi M, Barash A, Stock JT, Been E (2017) The Neandertal vertebral column 2: the lumbar spine. J Hum Evol 106:84–101

Gong W (2015) The effects of cervical joint manipulation, based on passive motion analysis, on cervical lordosis, forward head posture, and cervical ROM in university students with abnormal posture of the cervical spine. J Phys Ther Sci 27(5):1609–1611
Gong W, Kim C, Lee Y (2012) Correlations between cervical lordosis, forward head posture, cervical ROM and the strength and endurance of the deep neck flexor muscles in college students. J Phys Ther Sci 24(3):275–277
Granito RN, Aveiro MC, Renno ACM, Oishi J, Driusso P (2012) Comparison of thoracic kyphosis degree, trunk muscle strength and joint position sense among healthy and osteoporotic elderly women: a cross-sectional preliminary study. Arch Gerontol Geriatr 54(2):e199–e202
Grasso R, Zago M, Lacquaniti F (2000) Interactions between posture and locomotion: motor patterns in humans walking with bent posture versus erect posture. J Neurophysiol 83(1):288–300
Haeusler M, Schiess R, Boeni T (2011) New vertebral and rib material point to modern bauplan of the Nariokotome Homo erectus skeleton. J Hum Evol 61(5):575–582
Heino JG, Godges JJ, Carter CL (1990) Relationship between hip extension range of motion and postural alignment. J Orthop Sports Phys Ther 12(6):243–247
Hirose D, Ishida K, Nagano Y, Takahashi T, Yamamoto H (2004) Posture of the trunk in the sagittal plane is associated with gait in community-dwelling elderly population. Clin Biomech 19(1):57–63
Hongo M, Miyakoshi N, Shimada Y, Sinaki M (2012) Association of spinal curve deformity and back extensor strength in elderly women with osteoporosis in Japan and the United States. Osteoporos Int 23(3):1029–1034
Hsu C, Castillo E, Lieberman D (2015) The relationship between trunk muscle strength and flexibility, intervertebral disc wedging, and human lumbar lordosis. The Harvard Undergraduate Research Journal 8:35–41
Hutton W, Dhanendran M (1979) A study of the distribution of load under the normal foot during walking. Int Orthop 3(2):153–157
Izzo R, Guarnieri G, Guglielmi G, Muto M (2013) Biomechanics of the spine. Part I: spinal stability. Eur J Radiol 82(1):118–126
Jang SY, Kong MH, Hymanson HJ, Jin TK, Song KY, Wang JC (2009) Radiographic parameters of segmental instability in lumbar spine using kinetic MRI. J Korean Neurosurg Soc 45(1):24–31
Kapandji IA (1974) The physiology of the joints. Churchill Livingstone, Edinburg Scotland
Kebaetse M, McClure P, Pratt NA (1999) Thoracic position effect on shoulder range of motion, strength, and three-dimensional scapular kinematics. Arch Phys Med Rehabil 80(8):945–950
Kendall FP, McCreary EK, Provance PG, Rodgers M, Romani WA (2005) Muscles: testing and function, with posture and pain. Lippincott Williams & Wilkins, Philadelphia
Kim HJ, Chung S, Kim S, Shin H, Lee J, Kim S, Song MY (2006) Influences of trunk muscles on lumbar lordosis and sacral angle. Eur Spine J 15(4):409–414
Kirkaldy-Willis W (1985) Presidential symposium on instability of the lumbar spine: introduction. Spine 10(3):254
Kobayashi T, Takeda N, Atsuta Y, Matsuno T (2008) Flattening of sagittal spinal curvature as a predictor of vertebral fracture. Osteoporos Int 19(1):65–69
Lewis JS, Green A, Wright C (2005) Subacromial impingement syndrome: the role of posture and muscle imbalance. J Shoulder Elb Surg 14(4):385–392
Mayoux-Benhamou M, Revel M, Vallee C, Roudier R, Barbet J, Bargy F (1994) Longus colli has a postural function on cervical curvature. Surg Radiol Anat 16(4):367–371
McCowan T, Keith A (1939) The stone age of Mount Carmel. Oxford University Press, Oxford
Meakin JR, Fulford J, Seymour R, Welsman JR, Knapp KM (2013) The relationship between sagittal curvature and extensor muscle volume in the lumbar spine. J Anat 222(6):608–614
Meyer MR (2005) Functional biology of the Homo erectus axial skeleton from Dmanisi, Georgia. University of Pennsylvania, Philadelphia, PA
Meyer MR (2016) The cervical vertebrae of KSD-VP-1/1. The postcranial anatomy of Australopithecus afarensis. Springer, New York, pp 63–111
Meyer MR, Williams SA, Smith MP, Sawyer GJ (2015) Lucy's back: reassessment of fossils associated with the AL 288-1 vertebral column. J Hum Evol 85:174–180

Mika A, Unnithan VB, Mika P (2005) Differences in thoracic kyphosis and in back muscle strength in women with bone loss due to osteoporosis. Spine 30(2):241–246

Miyakoshi N, Hongo M, Maekawa S, Ishikawa Y, Shimada Y, Okada K, Itoi E (2005) Factors related to spinal mobility in patients with postmenopausal osteoporosis. Osteoporos Int 16(12):1871–1874

Miyazaki M, Hymanson HJ, Morishita Y, He W, Zhang H, Wu G, Kong MH, Tsumura H, Wang JC (2008) Kinematic analysis of the relationship between sagittal alignment and disc degeneration in the cervical spine. Spine 33(23):E870–E876

Moroney SP, Schultz AB, Miller JA (1988) Analysis and measurement of neck loads. J Orthop Res 6(5):713–720

Moustafa IM, Diab AAM, Hegazy FA, Harrison DE (2017) Does rehabilitation of cervical lordosis influence sagittal cervical spine flexion extension kinematics in cervical spondylotic radiculopathy subjects? J Back Musculoskelet Rehabil 30(4):937–941

Nigg BM, Cole GK, Bruggemann GP (1995) Impact forces during heel toe running. J Appl Biomech 11(4):407–432

Oatis C (2004) Biomechanics of skeletal muscle. Kinesiology: the mechanics and pathomechanics of human movement, 2nd edn. Lippincott Williams & Wilkins, New York, pp 44–66

Olson LE, Millar AL, Dunker J, Hicks J, Glanz D (2006) Reliability of a clinical test for deep cervical flexor endurance. J Manip Physiol Ther 29(2):134–138

Panjabi MM, Oda T, Crisco JJ III, Dvorak J, Grob D (1993) Posture affects motion coupling patterns of the upper cervical spine. J Orthop Res 11(4):525–536

Patwardhan AG, Havey RM, Ghanayem AJ, Diener H, Meade KP, Dunlap B, Hodges SD (2000) Load-carrying capacity of the human cervical spine in compression is increased under a follower load. Spine 25(12):1548–1554

Pavlova AV, Meakin JR, Cooper K, Barr RJ, Aspden RM (2018) Variation in lifting kinematics related to individual intrinsic lumbar curvature: an investigation in healthy adults. BMJ Open Sport Exerc Med 4(1):e000374

Pope MH, Panjabi M (1985) Biomechanical definitions of spinal instability. Spine 10(3):255–256

Pozzo T, Berthoz A, Lefort L (1990) Head stabilization during various locomotor tasks in humans. I. Normal subjects. Exp Brain Res 82(1):97–106

Pozzo T, Berthoz A, Vitte E, Lefort L (1991) Head stabilization during locomotion. Perturbations induced by vestibular disorders. Acta Otolaryngol Suppl 481:322–327

Rak Y (1993) Morphological variation in Homo neanderthalensis and *Homo sapiens* in the Levant. In: Species, species concepts and primate evolution. Springer, New York, NY, pp 523–536

Rhodes JA, Churchill SE (2009) Throwing in the middle and upper Paleolithic: inferences from an analysis of humeral retroversion. J Hum Evol 56(1):1–10

Ro H, Gong W, Ma S (2010) Correlations between and absolute rotation angle, anterior weight bearing, range of flexion and extension motion in cervical herniated nucleus pulposus. J Phys Ther Sci 22(4):447–450

Sanders WJ (1998) Comparative morphometric study of the australopithecine vertebral series Stw-H8/H41. J Hum Evol 34(3):249–302

Sarwahi V, Boachie-Adjei O, Backus SI, Taira G (2002) Characterization of gait function in patients with postsurgical sagittal (flatback) deformity: a prospective study of 21 patients. Spine 27(21):2328–2337

Schenkman M, Shipp KM, Chandler J, Studenski SA, Kuchibhatla M (1996) Relationships between mobility of axial structures and physical performance. Phys Ther 76(3):276–285

Schiess R, Haeusler M (2013) No skeletal dysplasia in the nariokotome boy KNM-WT 15000 (Homo erectus)—a reassessment of congenital pathologies of the vertebral column. Am J Phys Anthropol 150(3):365–374

Schmid S, Bruhin B, Ignasiak D, Romkes J, Taylor WR, Ferguson SJ, Brunner R, Lorenzetti S (2017) Spinal kinematics during gait in healthy individuals across different age groups. Hum Mov Sci 54:73–81

Schmidt H, Kettler A, Rohlmann A, Claes L, Wilke H-J (2007) The risk of disc prolapses with complex loading in different degrees of disc degeneration–a finite element analysis. Clin Biomech 22(9):988–998

Sinaki M, Itoi E, Rogers JW, Bergstralh EJ, Wahner HW (1996) Correlation of Back extensor strength with thoracic kyphosis and lumbar lordosis in estrogen-deficient Women1. Am J Phys Med Rehabil 75(5):370–374

Thigpen CA, Padua DA, Michener LA, Guskiewicz K, Giuliani C, Keener JD, Stergiou N (2010) Head and shoulder posture affect scapular mechanics and muscle activity in overhead tasks. J Electromyogr Kinesiol 20(4):701–709

Trinkaus E (1975) Squatting among the Neandertals: a problem in the behavioral interpretation of skeletal morphology. J Archaeol Sci 2(4):327–351

Vergroesen P-P, Kingma I, Emanuel KS, Hoogendoorn RJ, Welting TJ, van Royen BJ, van Dieën JH, Smit TH (2015) Mechanics and biology in intervertebral disc degeneration: a vicious circle. Osteoarthr Cartil 23(7):1057–1070

Walker ML, Rothstein JM, Finucane SD, Lamb RL (1987) Relationships between lumbar lordosis, pelvic tilt, and abdominal muscle performance. Phys Ther 67(4):512–516

Wang C-H, McClure P, Pratt NE, Nobilini R (1999) Stretching and strengthening exercises: their effect on three-dimensional scapular kinematics. Arch Phys Med Rehabil 80(8):923–929

Whitcome KK, Shapiro LJ, Lieberman DE (2007) Fetal load and the evolution of lumbar lordosis in bipedal hominins. Nature 450(7172):1075

Whittle MW (1999) Generation and attenuation of transient impulsive forces beneath the foot: a review. Gait Posture 10(3):264–275

Whittle MW, Levine D (1999) Three-dimensional relationships between the movements of the pelvis and lumbar spine during normal gait. Hum Mov Sci 18(5):681–692

Wilke H-J, Wolf S, Claes LE, Arand M, Wiesend A (1995) Stability increase of the lumbar spine with different muscle groups. A biomechanical in vitro study. Spine 20(2):192–198

Chapter 13
Spinal Posture and Pathology in Modern Humans

Ella Been, Azaria Simonovich, and Leonid Kalichman

13.1 Introduction

The habitual posture of humans and their mode of locomotion are unique among extant hominoids. Humans are the only living hominoid that combines erect posture and bipedal locomotion (Lovejoy 2005; Been et al. 2017). The evolution of erect posture required the development of pronounced spinal curvatures, as opposed to the nearly straight spines found in quadrupedal non-human hominoids (Schultz 1961; Lovejoy 2005; Been et al. 2010). This change included among others an increased inclination of the sacrum in relation to the pelvis, increased dorsal wedging of the lumbar vertebral bodies, decrease in length in the spinous processes of the cervical vertebrae, and changes in the position and orientation of the foramen magnum (Tardieu et al. 2013; Been et al. 2014, 2017; Arlegi et al. 2017). This configuration is regarded by scholars as the best solution between contradicting factors—that is, locomotion, obstetric, breathing, etc.

For many years, scholars have believed that erect posture with increased spinal curvatures is one of the leading reasons for the high prevalence of back pain and spinal pathology in humans (Merbs 1996; Lovejoy 2005). If this notion is true, we will expect to see a higher prevalence of spinal pathology and back pain in humans

E. Been (✉)
Department of Sports Therapy, Faculty of Health Professions, Ono Academic College, Kiryat Ono, Israel

Department of Anatomy and Anthropology, Sackler Faculty of Medicine, Tel Aviv University, Tel Aviv, Israel

A. Simonovich
Faculty of Health Sciences, Ben-Gurion University of the Negev, Beer Sheva, Israel

L. Kalichman
Department of Physical Therapy, Recanati School for Community Health Professions, Faculty of Health Sciences, Ben-Gurion University of the Negev, Beer Sheva, Israel

E. Been et al. (eds.), *Spinal Evolution*,
https://doi.org/10.1007/978-3-030-19349-2_13

with more pronounced spinal curvatures compared with humans with less pronounced curvatures. Also, Plomp et al. (2015) suggested that spines that are "less well adapted for bipedalism" (by which they mean less spinal curvature) suffer more from spinal pathology.

While researchers and clinicians in the past have looked at each spinal curvature (e.g. lumbar or cervical lordosis) as an individual characteristic, in recent years scholars approach the complexity of erect posture not only by looking at a single character, but also by analyzing the interaction between the major spinal and pelvic variables that compose erect posture (Boulay et al. 2006; Barrey et al. 2007; Lafage et al. 2008, 2016; Schlösser et al. 2014).

Variables most commonly used for assessing sagittal spinal alignment include the following (Figs. 13.1 and 13.2):

Sacral slope: The angle between the horizontal plane and the orientation of the sacral plateau (endplate)—a positional parameter (Marty et al. 2002).

Pelvic incidence: The relative position of the sacral plate in relation to the femoral heads. It is evaluated as an angle between a line drawn perpendicular to the superior sacral endplate at its midpoint (the center of the sagittal diameter)

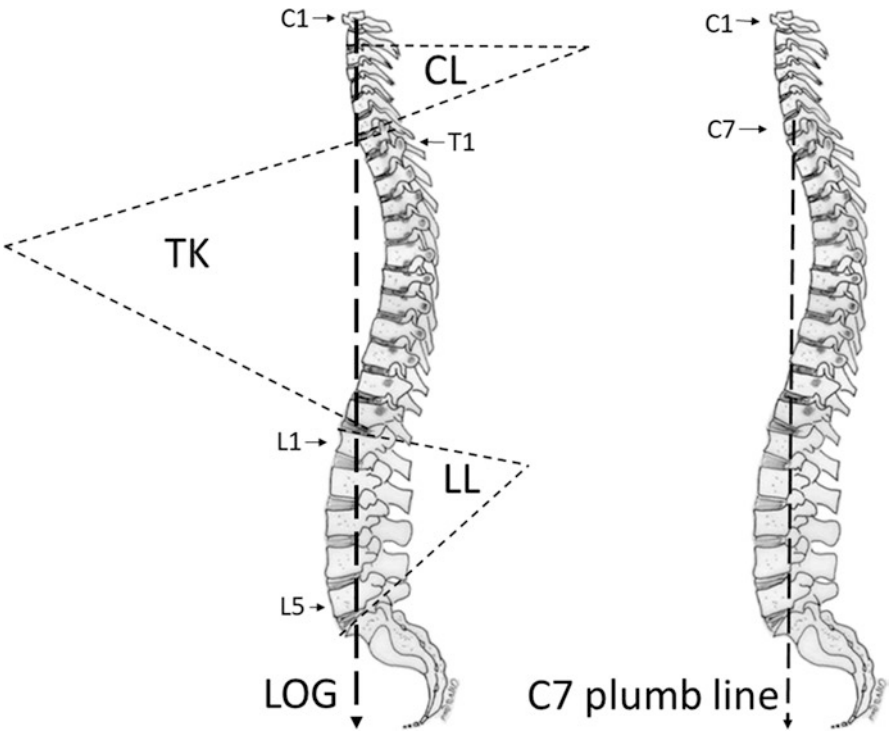

Fig. 13.1 Spinal variables most commonly used for assessing sagittal spinal alignment. *LL* lumbar lordosis, *TK* thoracic kyphosis, *CL* cervical lordosis, *LOG* line of gravity

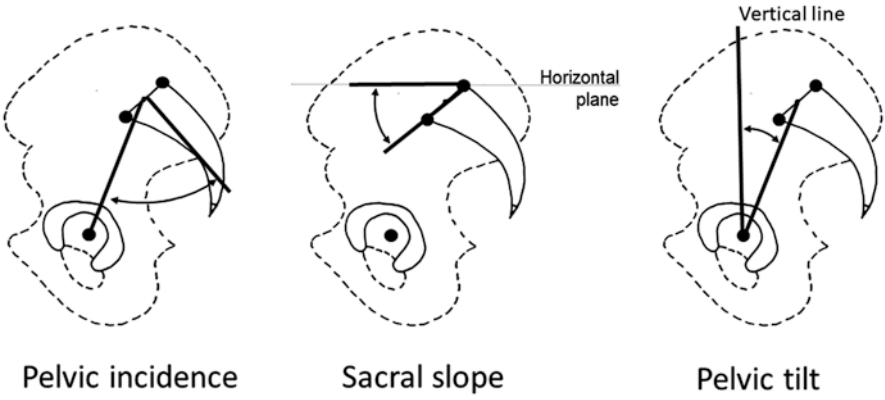

Fig. 13.2 Pelvic variables most commonly used for assessing sagittal spinopelvic alignment

and the line connecting this point to the center of the hip joint—a non-positional parameter (Legaye and Duval-Beaupere 2008; Tardieu et al. 2017).

Pelvic tilt: The angle between the vertical line and the line joining the middle of the sacral plate to the center of the bicoxo-femoral axis—a positional parameter (Marty et al. 2002).

Lumbar lordosis: A Cobb angle between the line parallel to the superior endplate of the first lumbar vertebra (L1) to the line parallel to the superior endplate of the first sacral vertebra (S1)—a positional parameter (Been and Kalichman 2014).

Thoracic kyphosis: A Cobb angle between the line parallel to the superior endplate of the first thoracic vertebra (T1) to the line parallel to the inferior endplate of the last thoracic vertebra (T12)—a positional parameter (Vrtovec et al. 2009).

Cervical lordosis: A Cobb angle between the line parallel to the inferior endplate of the second cervical vertebra (C2) to the line parallel to the inferior endplate of the last cervical vertebra (C7)—a positional parameter (Oe et al. 2017).

Line of gravity: A vertical line passing through the center of gravity. It is calculated by using a force plate. The sagittal vertical axis (SVA) is the horizontal distance between the line of gravity and the spine in selected areas (Lafage et al. 2008)—a positional parameter (Diebo et al. 2015).

C7 plumb line: A vertical line through C7—a positional parameter (Diebo et al. 2015).

Sagittal spinal posture is achieved by the interaction between pelvic orientation, sacral position, spinal curvatures, and the position of the line of gravity in relation to the spine, hip joint, and feet. The ability to maintain an upright posture and horizontal eye gaze is fundamental to normal activities of daily living (Klineberg et al. 2013). The ability to maintain this balance requires intercorrelation between pelvic/sacral orientation and spinal curvatures. For example, on the one hand, a horizontal sacral endplate (small sacral slope) is found with smaller curvatures (i.e., less lumbar lordosis, thoracic kyphosis, and cervical lordosis). On the other hand, a tilted (vertical) sacral endplate is found with large curvatures (i.e., more lumbar lordosis, thoracic kyphosis, and cervical lordosis). This chain of balancing curves also

correlates with the ventro-dorsal position of the spine relative to the line of gravity. Small sacral slope and spinal curvature correlate with a ventral position of the sacrum and lumbar spine and a ventral position of the line of gravity. Large sacral slope and pronounced spinal curvatures correlate with a dorsal position of the sacrum and of the lumbar spine relative to the pelvis, and a more dorsal position of the line of gravity (Schwab et al. 2006; Ames et al. 2012; Klineberg et al. 2013).

Ongoing debate regarding the interaction between sagittal spinal posture and spinal pathology, pain, and quality of life exists. While researchers agree that some pathologies such as isthmic spondylolisthesis and Scheuermann's disease are directly related to spinopelvic posture (Lowe 1990; Merbs 1996; Been et al. 2011), there is conflicting evidence regarding the relevance of sagittal spinopelvic posture to other pathologies, pain, or quality of life.

The purpose of this paper is to explore the interaction between sagittal spinal posture, spinal pathologies, back pain, and health-related quality of life. We propose that individuals in a neutral zone of moderate curvatures will experience less spinal pathology and pain and a better quality of life than do those outside this zone. If individuals with smaller or larger spinal curvatures suffer from a higher prevalence of spinal pathologies and pain, it will support the notion that humans "pay a price" for bipedalism. If the extremes of spinal curvature are not related to a higher prevalence of back pain and spinal pathologies, then they most probably result from other factors not related to the acquisition of erect posture and bipedalism.

13.2 Sagittal Spinal Posture and Spinal Pathologies

13.2.1 Disc Degeneration and Disc Herniation

Disc degeneration includes four degenerative features: loss of disc height, changes in disc signal intensity (seen in MRI), disc bulge or disc herniation, and anterior osteophytes (Stone et al. 2014) (Fig. 13.3).

Most researchers agree that degenerative disc disease correlates with small pelvic incidence, small sacral slope, and small lumbar lordosis (Table 13.1) (Barrey et al. 2007; Yang et al. 2013; Stone et al. 2014). Barrey et al. (2007) explored the sagittal spinal posture of 57 patients with disc herniation and degenerative disc disease. When compared to the non-pathological population, the patients demonstrated significant deviation of spinopelvic alignment: anterior translation of the C7 plumb line, loss of lumbar lordosis, and smaller sacral slope after matching for pelvic incidence. These results indicate an imbalance between pelvic incidence and lumbar curvature as a result of increased posterior pelvic tilt (Barrey et al. 2007).

Yang et al. (2013) found similar results for disc degeneration and posture. They performed a comparative study of the spinopelvic sagittal alignment in patients with lumbar disc degeneration or herniation and in the normal population. They found that the pelvic incidence, sacral slope, and lumbar lordosis in patients with disc disease were significantly lower than those in the normal population. They also

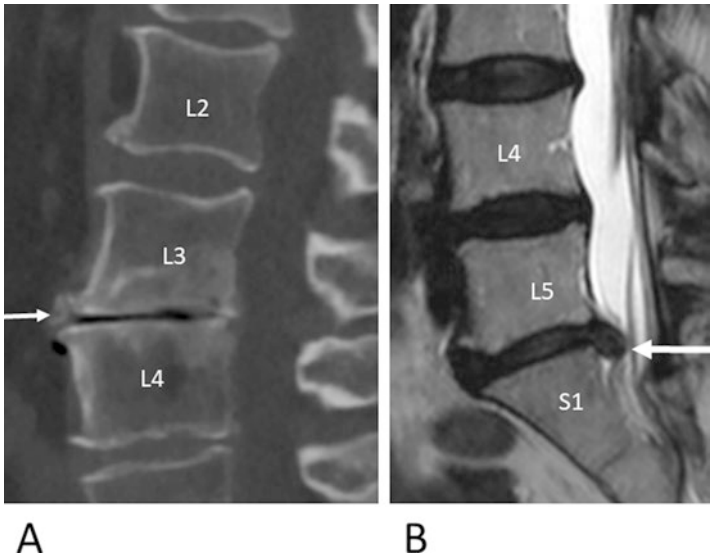

Fig. 13.3 A mid-sagittal CT scan (**a**) and MR image (**b**) of the lumbar spine showing the features of disc degeneration: loss of disc height and anterior osteophytes (**a**, white arrow) and disc herniation (**b**, white arrow). Note the difference in disc height between L2–L3 (healthy disc) and L3–L4 (degenerated disc) in (**a**). L2–L5, second to fifth lumbar vertebra; S1, first sacral vertebra

found that the C7 plumb line was significantly more ventral in patients with disc disease than in the normal population. At the same time, there were no differences in the pelvic tilt and thoracic kyphosis between the two groups.

The causal relationship between degenerative disc disease, disc herniation, and posture is not clear yet. Yang et al. (2013) suggested that small pelvic incidence might play a predisposing role in the pathogenesis of lumbar disc degeneration and that the secondary structural compensations would lead to a straighter spine after disc degenerative change. Stone et al. (2014) on the other hand suggested that lumbar lordosis is lost as discs degenerate.

Biomechanical research might explain the predisposing role of small pelvic incidence and lumbar lordosis on the development of disc degeneration. Ergun (2010) showed that biomechanical loads on intervertebral discs increase in parallel to the decrease in lumbar lordosis and sacral slope and that these changes contribute to the development of disc degeneration. When acting on a functional spinal unit, an axial force is distributed between the intervertebral disc in front and the facet joints behind. In a case of small lumbar lordosis, the axial force acts mainly on the discs (Roussouly and Pinheiro-Franco 2011), as evidenced by a finite element study of the cervical spine (Wei et al. 2013) that demonstrated increased loads on the intervertebral discs due to a decrease in lordosis angle.

In conclusion, disc degeneration and herniation correlate with small lumbar lordosis and sacral slope and small/normal pelvic incidence. Two possible mechanisms

Table 13.1 Sagittal spinal parameters (in degrees; mean ± standard deviation) in the healthy population and in patients with degenerative disc disease, disc herniation, degenerative spondylolisthesis, and isthmic spondylolisthesis

Research	Population	*n*	Sacral slope	Pelvic incidence	Lumbar lordosis	Thoracic kyphosis
Barrey et al. (2007)	Healthy adults	154	40 ± 8	52 ± 11	61 ± 10	47 ± 10
	Patients with disc herniation	25	35 ± 10	50 ± 11	49 ± 12	40 ± 11
	Patients with degenerative disc disease	32	35 ± 10	52 ± 12	49 ± 12	39 ± 10
	Patients with degenerative spondylolisthesis	28	40 ± 9	60 ± 11	59 ± 12	44 ± 10
Yang et al. (2013)	Healthy adults	80	38 ± 7	49 ± 9	53 ± 10	36 ± 7
	Patients with degenerative disc disease or herniation	80	28 ± 9	40 ± 10	40 ± 13	33 ± 10
Ferrero et al. (2015)	Healthy adults	709	40 ± 8	53 ± 10	57 ± 11	48 ± 12
	Patients with degenerative spondylolisthesis	654	36 ± 9	59 ± 11	53 ± 13	48 ± 15
Labelle et al. (2004)	Healthy population, age 10–40 years	160	40 ± 4	52 ± 5	43 ± 5	48 ± 5
	Patients with isthmic spondylolisthesis, age 10–40 years	214	50 ± 6	72 ± 8	66 ± 9	39 ± 6
Marty et al. (2002)	Healthy adults	44	41 ± 9	51 ± 10	60 ± 10	–
	Patients with isthmic spondylolisthesis	39	50 ± 12	64 ± 16	65 ± 13	–
Vialle et al. (2007)	Healthy adults	300	42 ± 8	55 ± 11	43 ± 11	41 ± 10
	Patients with isthmic spondylolisthesis	244	47 ± 13	73 ± 11	70 ± 17	23 ± 21
Schwab et al. (2006)	Healthy adults, 21–40 years	25	39 ± 9	52 ± 10	60 ± 14	38 ± 12
	Healthy adults, 41–60 years	24	40 ± 7	53 ± 8	60 ± 8	37 ± 9
	Healthy adults, >60 years	22	46 ± 9	51 ± 9	57 ± 11	44 ± 12

were suggested: a mechanical model showing that both small pelvic incidence and lumbar lordosis are the cause of disc degeneration and a compensatory mechanism suggesting that the decreased lumbar lordosis and sacral slope compensate for the disc pathology. Additional prospective studies are needed in order to resolve the causal relationship between disc degeneration, disc herniation and posture.

13.2.2 Facet Joint Osteoarthritis

Facet joint osteoarthritis includes the following degenerative features: joint space narrowing, osteophytes, hypertrophy of the articular process, subarticular sclerosis, subchondral cysts, and vacuum phenomenon (Kalichman et al. 2008).

Jentzsch et al. (2013), in a large CT-based study (620 cases), showed that individuals with high pelvic incidence and high lumbar lordosis exhibited higher grades of facet joint osteoarthritis. Weinberg et al. (2017) studied a large collection of human spines (n = 576) and also found a higher prevalence of facet arthritis in spines with high pelvic incidence, but they also demonstrated higher prevalence in spines with low pelvic incidence. Spines with average pelvic incidence showed the lowest prevalence of facet joint degeneration.

Roussouly and Pinheiro-Franco (2011) and Weinberg et al. (2017) suggested that increased pelvic incidence and lumbar lordosis lead to increased contact and shear force and, consecutively, to osteoarthritis of the lumbar facet joints. While the relationship between increased pelvic incidence and facet joint osteoarthritis has been elucidated, the relationship between facet joint arthritis and decreased pelvic incidence remains to be understood. Weinberg et al. (2017) suggested that the interaction between the hip, pelvis, and spine may be impaired with a decreased pelvic incidence, which can contribute to the development of facet joint arthritis, but more research is needed in order to determine the interaction and potential causal relationship between facet joint arthritis and posture.

13.2.3 Spinal Canal Stenosis

Suzuki et al. (2010) demonstrated that patients with lumbar spinal canal stenosis accompanied by intermittent claudication have forward-bending posture during standing and walking. Patients with more severe or advanced symptoms showed larger forward bending with increased posterior pelvic tilt, decreased lumbar lordosis, and ventral position of the line of gravity. Suzuki et al. (2010) argued that casual relationships, in this case, are not clear, but it is possible that a less lordotic posture is the position that a person takes due to the pain associated with spinal stenosis. An MRI study of the lumbar spinal canal during loading (Hansson et al. 2009) found that the *ligamentum flavum*, not the disc, dominates the load induced narrowing of the lumbar spinal canal. Less lordotic posture, transfers the load from the posterior part of the spine (and therefore from *ligamentum flavum*), thereby decreasing lumbar spinal canal narrowing.

13.2.4 Degenerative Spondylolisthesis

Degenerative spondylolisthesis is the anterior slippage of a vertebra in relation to its neighboring vertebra, in the absence of spondylolysis (Fig. 13.4a). Osteoarthritic remodeling of the facet joints, leading to a more sagittal orientation, allows the forward slippage (Merbs 1996).

Researchers agree that patients with degenerative spondylolisthesis show a significantly larger pelvic incidence than the healthy subjects (Barrey et al. 2007;

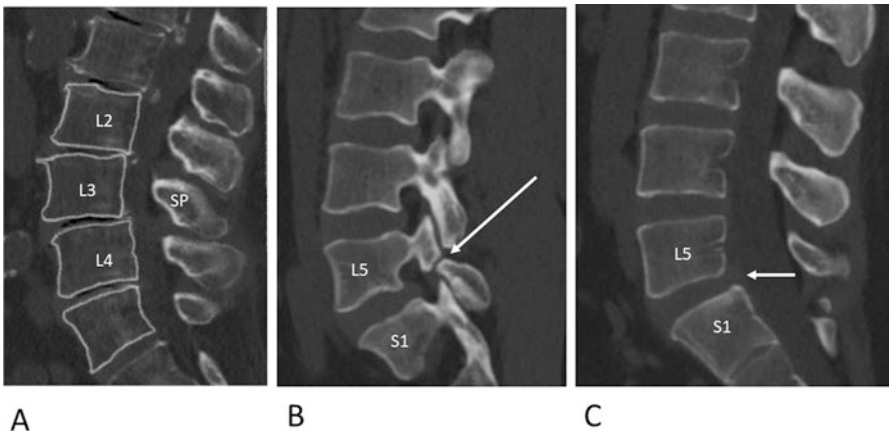

Fig. 13.4 CT scan of the lumbar spine showing degenerative spondylolisthesis (**a**), spondylolysis (**b**), and isthmic spondylolisthesis (**c**). (**a**) a midsagittal image showing the anterior slippage of L3 in relation to adjunct vertebrae. Note that the spinous process (SP) of L3 is also positioned more ventral. (**b**) a parasagittal image showing a fracture of the left isthmus of L5 (white arrow). (**c**) a midsagittal image showing the ventral slippage of the L5 vertebral body due to isthmic spondylolysis. Note that the spinous process did not move more ventral

Ferrero et al. 2015), but the evidence regarding lumbar lordosis is somewhat contradictory (Table 13.1).

Ferrero et al. (2015), in a large cohort study of 654 patients with degenerative spondylolisthesis and 709 asymptomatic volunteers, showed that large pelvic incidence of the patients coexisted with decreased lumbar lordosis, which occurred mainly in the lumbosacral area. Barrey et al. (2007) found that the large pelvic incidence in the degenerative spondylolisthesis group coexisted with average sacral slope and lumbar lordosis indicating an unbalanced spine. Among 4151 participants in the Copenhagen Osteoarthritis Study, 2.7% of males and 8.4% of females suffered from degenerative spondylolisthesis (Jacobsen et al. 2007). Women with degenerative spondylolisthesis had larger lumbar lordosis then the normal population, but males with degenerative spondylolisthesis had similar lordosis angles to the normal population. In a CT-based study, Been et al. (2011) and Kalichman et al. (2011) found similar lumbar lordosis angle between asymptomatic population and patients with degenerative spondylolisthesis. Individuals with degenerative spondylolisthesis have more lordotic vertebral bodies and less lordotic intervertebral discs compared with the asymptomatic population. The authors suggested that the small intervertebral disc wedging of the degenerative spondylolisthesis group might be a predisposing factor to the development of degenerative spondylolisthesis or a compensatory mechanism to the ventral slippage of the vertebra.

We propose a 3-stage cascade of events that explains the pathomechanism of degenerative spondylolisthesis:

1. *Remodeling*. Barrey et al. (2007) showed that the shape of the pelvis is a main predisposing factor for degenerative spondylolisthesis. The large pelvic incidence

and lordosis generate significant force on facet joints and probably excessive mechanical stresses on posterior facets, accelerating arthrosis changes.
2. *Slippage*. The arthritis of the facet joints associated with a marked inclination of the vertebral endplate of L5 represents a significant predisposing factor for slippage and the vertebra starts to slide anteriorly (Merbs 1996; Barrey et al. 2007).
3. *Compensation*. The slippage leads to spinal stenosis and pain (Kalichman et al. 2009a, b). Patients with degenerative spondylolisthesis, therefore, adopt forward bending posture in order to increase the volume of the spinal canal and compensate for the narrowing of the spinal canal due to the stenosis. They do so by reducing pelvic tilt, sacral slope, and lumbar lordosis.

This proposed pathomechanism differs from Ferrero et al. (2015), who suggested that decreased lordosis is one of the accelerating factors for lumbar degeneration and leads to anterior malalignment and degenerative spondylolisthesis. Nonetheless, Ferrero et al. (2015) argued that their pathomechanism may not be the only one, because some of the patients in their cohort with degenerative spondylolisthesis had low pelvic incidence.

13.2.5 Spondylolysis and Isthmic Spondylolisthesis

Spondylolysis and spondylolisthesis are conditions of the spine, almost exclusively of the lower spine, that have intrigued anthropologists for at least a century (Merbs 1996). Spondylolysis refers to any separation that divides a hemi-arch, completely or incompletely, regardless of etiology (Fig. 13.4b). Spondylolisthesis is the anterior slippage of one vertebra relative to the vertebra below, while isthmic spondylolisthesis refers to the anterior slippage of a vertebra due to a defect in the pars interarticularis (spondylolysis) (Fig. 13.4c). Although the two conditions may be related—spondylolysis can allow spondylolisthesis to take place—either condition frequently occurs without the other (Merbs 1996).

There is a consensus among researchers that patients suffering from spondylolysis and, especially those with isthmic spondylolisthesis, have high pelvic incidence (60°–80°), high sacral slope (45°–63°), and large lumbar lordosis (57°–75°) (Swärd et al. 1989; Hanson et al. 2002; Marty et al. 2002; Huang et al. 2003; Labelle et al. 2004; Vialle et al. 2007; Peleg et al. 2009; Been et al. 2011) (Table 13.1). Increased pelvic incidence and sacral slope create increased shear forces at the lumbosacral junction. These forces contribute to the anterior slippage of the lumbar vertebrae with pars inter articularis non/malunion (Swärd et al. 1989; Marty et al. 2002). Despite the biomechanical importance of the pelvic incidence to the development of isthmic spondylolisthesis, Huang et al. (2003) found that the degree of pelvic incidence does not predict the degree of anterior slippage of the affected vertebra.

13.2.6 Baastrup Disease

First described in 1933 by Christian Baastrup, a Danish radiologist, Baastrup disease, also known as kissing spine disease and lumbar interspinous bursitis, is caused by contact between adjacent spinous processes of the lumbar spine as a result of degenerative changes (Alonso et al. 2017) (Fig. 13.5). This contact leads to the enlargement, flattening, and reactive sclerosis of opposed interspinous surfaces. Baastrup disease is most common at L4–5 and associated with older age, vertebral canal stenosis, bulging discs, and spondylolisthesis (Maes et al. 2008). The spinous processes of the lumbar spine are thick and broad and have a caudal and dorsal orientation. Due to this orientation, an increase in lordosis or active hyperextension can lead to spinous process proximity (Alonso et al. 2017). Intervertebral disc degeneration with loss of height may lead to closer proximity between adjacent spinous processes. Subsequently, this may lead to spinous process proximity during extension of the spine and the development of reactive sclerosis and degenerative changes.

Although increased lumbar lordosis is believed to be one of the contributing factors to the development of Baastrup disease, Maes et al. (2008), who studied MRI of the spines of 44 patients with Baastrup disease and 495 controls, did not find any association between the degree of lumbar lordosis and the presence Baastrup disease.

13.2.7 Scheuermann's Disease

Scheuermann's disease is a juvenile osteochondrosis of the spine. It is a disease of the growth cartilage endplate, probably due to repetitive strain on the growth cartilage weakened by a genetic predisposition. The radiographic and osteologic aspects

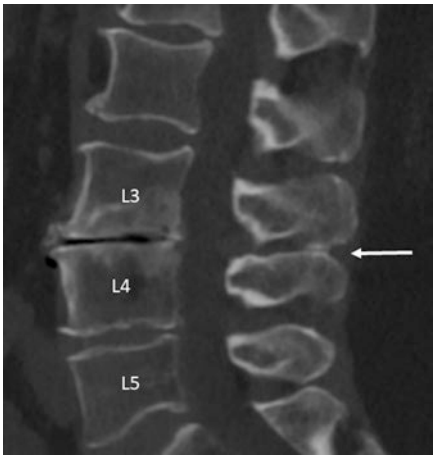

Fig. 13.5 A midsagittal CT scan of the lumbar spine showing Baastrup disease between the third and fourth spinous process (white arrow), due to loss of disc height

are related to the vertebral endplate lesions and include vertebral wedging, irregularity of the vertebral endplate, and Schmorl's node (intraosseous disc herniation) (Palazzo et al. 2014; Peleg et al. 2016).

Scheuermann's disease is identified as a structural kyphosis deformity (Lowe and Line 2007). Classically, the presence of three consecutive hyperkyphotic vertebrae confirms the diagnosis of Scheuermann's kyphosis. The deformity commonly involved the thoracic or thoracolumbar spine resulting in two different curve patterns, the thoracic pattern (thoracic kyphosis) and the thoracolumbar pattern (thoracolumbar kyphosis). Loder (2001), Jansen et al. (2006), and Jiang et al. (2014) found that Scheuermann's thoracic hyperkyphosis is commonly associated with lumbar and cervical hyperlordosis (Fig. 13.6). The hyperlordotic cervical and lumbar spines have been recognized as compensation to create a balanced posture and a forward visual gaze (Loder 2001).

Jiang et al. (2014) examined the posture of patients with Scheuermann's thoracic kyphosis or Scheuermann's thoracolumbar kyphosis and normal adolescents. The researchers found that patients with Scheuermann's kyphosis (thoracic and thoracolumbar) had significantly lower pelvic incidence and pelvic tilt than normal controls (32° vs. 45°, $p < 0.001$ for pelvic incidence; 0.2° vs. 11.9°,

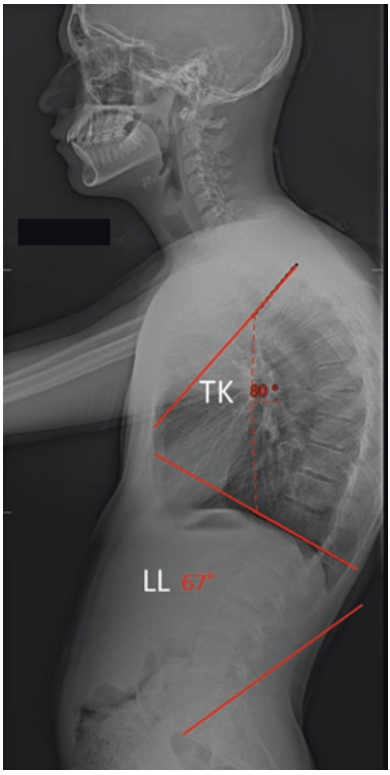

Fig. 13.6 A lateral standing radiograph showing Scheuermann's thoracic hyperkyphosis. Note the excessive thoracic kyphosis (TK) between T3 and T12, and the associated excessive lumbar lordosis (LL) between T12 and S1

$p < 0.001$ for pelvic tilt). Patients with Scheuermann's thoracic kyphosis had increased thoracic kyphosis and lumbar lordosis compare to age equivalent comparative group (46° vs. 21°, $p < 0.001$ for thoracic kyphosis; 56° vs. 48°, $p = 0.008$ for lumbar lordosis). Patients with Scheuermann's thoracolumbar kyphosis had similar (non-significant) thoracic kyphosis and lumbar lordosis to the control group (25° vs. 28° for thoracic kyphosis; 47° vs. 48° for lumbar lordosis). Jiang et al. (2014) concluded that patients with different curvature patterns (e.g., thoracic kyphosis, thoracolumbar kyphosis) could have distinct compensatory mechanisms to maintain the sagittal balance.

As pelvic incidence is determined at a young age (Bailey et al. 2016; Tardieu et al. 2013), small pelvic incidence might be one of the contributing factors for the development of Scheuermann's disease. On the other hand, the onset of Scheuermann's disease is during adolescence, its presence might alter the development of the pelvis and the orientation of the sacrum within the pelvis (Jiang et al. 2014). Prospective studies with a large cohort are needed to reveal the interaction between pelvic morphology and the development of Scheuermann's disease.

13.2.8 Osteoporosis

Osteoporosis is a skeletal disorder characterized by compromised bone strength predisposing the individual to an increased risk of fracture (Cosman et al. 2014). Between 16% and 50% of women will suffer an osteoporosis-related fracture in their lifetime. Spinal osteoporotic compression fractures mostly occur in the lower thoracic and thoracolumbar junction regions and result in a spinal kyphotic deformity. If not effectively treated, spinal kyphotic deformity becomes progressively aggravated in the late phase and gradually affects many vertebrae. Vertebral fractures, which are the most common osteoporotic fractures, lead to decreased quality of life (Miyakoshi et al. 2017; Zhang et al. 2017). Itoi (1991) studied lateral radiographs of 100 osteoporotic patients taken in a standing position. He found that thoracic kyphosis, a primary deformity of the osteoporotic spine, appeared compensated by the lumbar spine, sacroiliac joint, hip joint, and knee joint, respectively. Low-back pain was highly associated with decreased lumbar lordosis and increased sacropelvic angle, suggesting that the sacroiliac joint was one of the causes of low-back pain in osteoporotic population.

Both Zhang et al. (2017) and Miyakoshi et al. (2017) studied the posture of patients with osteoporosis but their results are contradictory. Miyakoshi et al. (2017) studied the spines of 236 female patients with postmenopausal osteoporosis and 93 healthy volunteers. They found that both thoracic kyphosis and lumbar lordosis were significantly larger in the osteoporosis group (34° and 47°, respectively) than in the volunteer group (27° and 15°, respectively, $p < 0.01$).

Zhang et al. (2017) studied the posture of 60 patients with osteoporotic fractures and compared it with a healthy elderly population. They found that the average thoracic kyphosis angle in the osteoporotic group (40° ± 4°) was significantly higher than in the control group (28° ± 2°) ($p < 0.05$). They also found that the average lumbar lordosis angle (L1–L5) in the osteoporotic group (10° ± 1°) was significantly lower than the control group (40° ± 3°). It is possible that the difference between the lumbar lordosis in these studies results from the fact that Miyakoshi et al. (2017) studied females with osteoporosis while Zhang et al. (2017) studied patients with osteoporotic fractures and the fractures might have altered the lordosis angle.

13.3 Sagittal Spinal Posture, Low Back Pain (LBP), and Health-Related Quality of Life

Chaléat Valayer et al. (2011) explored the differences in sagittal spinopelvic alignment between adults with chronic low back pain (LBP) and asymptomatic population. They found that sagittal spinopelvic alignment differed between the two populations. In particular, there were a larger proportion of chronic LBP patients with low sacral slope, low lumbar lordosis, and small pelvic incidence, suggesting the relationship between this specific pattern and the presence of chronic LBP. Similar results were obtained by Sadler et al. (2017) in a meta-analysis.

Araújo et al. (2014) analyzed the relation of suboptimal sagittal standing posture with back pain and health-related quality of life, in adult males and females. Their results are somewhat puzzling. The sagittal standing posture of males was not consistently associated with quality of life measures, but males with low lumbar lordosis had lower scores on health-related quality of life (a physical component of the SF-36 questionnaire—a 36-item, patient-reported survey of patient health). The sagittal standing posture of females showed that increased pelvic incidence and sacral slope correlated with severe back pain. On the other hand, small lumbar lordosis in females was most strongly associated with decreased physical health-related quality of life. They concluded that monitoring sagittal postural parameters has limited usefulness as a screening tool for causes of unspecific musculoskeletal symptoms in the general adult population.

Smith et al. (2008) explored spinal posture and back pain in adolescents. They found that more neutral thoraco-lumbo-pelvic postures are associated with less back pain.

In summary, these studies indicate that more neutral postures (i.e., moderate curvatures) associate with higher quality of life and less pain. The extreme postures with high or with low curvatures associated with lower quality of life and a higher incidence of back pain.

13.4 Discussion

We explored the relationship between sagittal spinal posture and spinal pathologies, back pain, and health-related quality of life, in order to reveal the influence of erect posture on the prevalence of back pain and spinal pathologies in humans. Table 13.2 summarizes the postures that characterize the major spinal pathologies.

Our findings indicate that interaction between spinal posture and spinal pathology exists. This interaction is not a simple one-way relationship between posture and pathology, but rather a more complex one as is demonstrated in Table 13.2. For example, some spinal pathologies associate with low pelvic incidence and low lumbar lordosis (disc degeneration and herniation), while other pathologies associate with high pelvic incidence and high lumbar lordosis (isthmic spondylolisthesis). Still, other pathologies associate with either high or low pelvic incidence (facet joint osteoarthritis) or with a combination of high pelvic incidence and low lumbar lordosis (degenerative spondylolisthesis). Even when we consider back pain, the picture is complex. Both low and high pelvic incidence and lumbar lordosis associate

Table 13.2 Association between spinal pathology, health-related quality of life and posture

	Pelvic incidence			Lumbar lordosis			Thoracic kyphosis		
	Low	Average	High	Low	Average	High	Low	Average	High
Disc herniation and degeneration	√	–	–	√	√	–	–	–	–
Facet joint osteoarthritis	√	–	√	–	–	√	–	–	–
Spinal stenosis	–	–	–	√	–	–	–	–	–
Degenerative spondylolisthesis	–	–	√	√	√	–	–	–	–
Isthmic spondylolisthesis	–	–	√	–	–	√	–	–	–
Baastrup disease	–	–	–	–	√	√	–	–	–
Scheuermann's thoracic hyperkyphosis	√	–	–	–	–	√	–	–	√
Scheuermann's thoracolumbar hyperkyphosis	√	–	–	–	√	–	–	√	–
Osteoporosis	–	–	–	–	–	√	–	–	√
Osteoporotic fractures	–	–	–	√	–	–	–	–	√
Severe back pain	–	–	√	–	–	√	–	–	–
Chronic back pain	√	–	–	√	–	–	–	–	–
Low health-related quality of life	√	–	–	√	√	–	–	–	–

√, an association exists

The results of this table are summarized from: Merbs (1996), Hanson et al. (2002), Marty et al. (2002), Huang et al. (2003); Labelle et al. (2004); Jacobsen et al. (2007); Vialle et al. (2007); Maes et al. (2008); Ergun (2010); Suzuki et al. (2010); Chaléat-Valayer et al. (2011); Yang et al. (2013); Araújo et al. (2014); Palazzo et al. (2014); Ferrero et al. (2015); Alonso et al. (2017); Jentzsch et al. (2017); Zhang et al. (2017); Weinberg et al. (2017); Oe et al. (2017); Miyakoshi et al. (2017)

with low back pain. As of today, it is not known whether sagittal posture is predominantly determined by genetic factors or is it the result of lifestyle and activity. It is therefore hard to determine if we can prevent the development of spinal pathology and pain by keeping posture within the neutral zone.

13.4.1 Causal Relationship Between Posture and Spinal Pathology

One of the most important questions regarding spinal pathology and posture is which comes first: the pathology or the posture? In positional dynamic variables like pelvic tilt, lumbar lordosis or thoracic kyphosis, it is very hard to determine which the cause is and which the result is. But in a non-positional parameter (pelvic incidence), that is determined at a young age (Tardieu et al. 2013; Bailey et al. 2016), the cause and the result can be more accurately discerned.

Small pelvic incidence with a more horizontal sacral end plate is a risk factor for the development of degenerative disc disease, disc herniation, facet joint arthritis, and Scheuermann's disease (both thoracic and thoracolumbar types). A high pelvic incidence with a vertical sacral end plate is a risk factor for the development of degenerative and isthmic spondylolisthesis, and facet joint osteoarthritis.

13.4.2 What is the Best Posture?

The important clinical question is: which alignment is associated with less pathology and pain and with a better quality of life? In this review of the literature, subjects with one of the two extreme postures (flattened and accentuated spinal curvatures) are more prone to exhibit pathology and pain compared to those with moderate curvatures. In addition, subjects with an unbalanced pelvis and spine, that is, one where the orientation between the sacrum, the vertebral curvatures, and the line of gravity is incongruent, are also prone to experience spinal pathology, pain, and reduced quality of life. These findings argue for a "neutral zone" of moderate curvatures with congruency between adjacent spinal elements.

One way to address describing a neutral spine configuration is to create cut-off values for spinal characteristics. Schwab et al. (2012) and Diebo et al. (2015) incorporated sagittal parameters into an adult spine deformity classification system and determined cutoff values for the most clinically relevant parameters in the sagittal profile (C2-C7 SVA, pelvic incidence minus lumbar lordosis (PI-LL), and pelvic tilt). They recommended SVA <40 mm, PI-LL within 10° and pelvic tilt < 20° as the targets for good sagittal alignment (Diebo et al. 2015).

Another approach to view this complex interaction is the "cone of economy," a concept of optimal posture and standing balance (Dubousset 1994). The "cone of

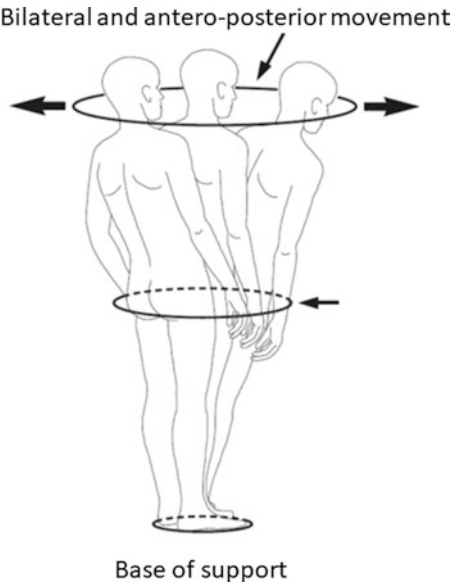

Fig. 13.7 The cone of economy, demonstrating the range of mobility that the body can achieve with minimal energy expenditure (after Dubousset 1994)

economy" (Fig. 13.7) defines the range of mobility that the body can achieve with minimal energy expenditure without external support. As long as the trunk is within the "cone of economy," balance is maintained between pelvic and spinal elements and the line of gravity passes close to the femoral heads and the feet. As the trunk of a standing individual nears the periphery of the "cone," increasing effort is required to maintain balance. If the trunk extends beyond the cone an individual will fall unless supported.

We suggest the concept of a "neutral zone" as an extension of these ideas. The spine is in the "neutral zone" as long as it has moderate curvatures that are in alignment with each other and the line of gravity passes close to the femoral heads. As long as the spine is within its "neutral zone," the risk of developing spinal pathology is low. Any deviation from the neutral zone, that is, flattened or accentuated curvatures, small or large pelvic incidence, or imbalance between the curvatures, increases the chances of spinal pathology.

13.4.3 Evolutionary Aspect

Our findings indicate that in modern humans both low and high spinal curvatures associate with spinal pathology. We have also demonstrated that spinal curvature and, especially, pelvic incidence are important contributors to the development of spinal pathologies. Importantly, both the presence of accentuated human morphology (large pelvic incidence and spinal curvatures) and the "less well adapted for bipedalism" (Plomp et al. 2015) human morphology (small spinal curvatures and

small pelvic incidence) are prone to develop spinal pathology, and pain, suggesting that upright posture is a delicate balance.

High pelvic incidence is a risk factor for the development of spondylolisthesis (isthmic and degenerative). This finding supports the notion that there are clinically relevant aspects with unique spinal pathology for erect posture and bipedalism (Merbs 1996; Lovejoy 2005). Further, individuals with smaller spinal curvatures and small pelvic incidence also experience a higher prevalence of disc degeneration and herniation, Scheuermann's disease, chronic back pain, and low quality of life. This suggests that these individuals also bear the consequences of erect posture and bipedalism by developing spinal pathologies, back pain, and low quality of life. This is in agreement with Sparrey et al. (2014) that showed that disc degeneration is strongly influenced by genetics with limited effects of loading or environment.

Evolution, mechanics, and biology, all point to the need for a stable spine to maintain erect posture and to perform normal daily activities (Sparrey et al. 2014). The evolutionary aspect of spinal pathology does not compensate for the influence of other factors (e.g., lifestyle, biomechanics) on the development of spinal pathology.

More studies that compare spinal pathologies between bipedal humans and quadrupedal non-human hominoids are needed to better clarify the evolutionary aspect of erect posture and spinal pathology. In addition, longitudinal studies that will follow the development of spinal pathologies and posture are needed in order to develop tools for early identification of patients at risk for postural deformities and spinal pathologies.

In summary, spinal posture closely correlates with spinal pathology, but its causal relationship is not fully understood. Individuals with well-aligned spine—within the neutral zone (moderate spinal curvatures and line of gravity close to the acetabulum)—tend to have a better quality of life, less back pain, and less spinal pathology. Individuals with spine outside the neutral zone—either with high or low spinal curvatures—are at risk of developing spinal pathologies. All of this indicates that there are clinically relevant aspects with unique spinal pathology as a result of the adoption of erect posture and bipedalism by humans.

References

Alonso F, Bryant E, Iwanaga J, Chapman JR, Oskouian RJ, Tubbs RS (2017) Baastrup's disease: a comprehensive review of the extant literature. World Neurosurg 101:331–334

Ames CP, Smith JS, Scheer JK, Bess S, Bederman SS, Deviren V, Lafage V, Schwab F, Shaffrey CI (2012) Impact of spinopelvic alignment on decision making in deformity surgery in adults. J Neurosurg 16(6):547–564

Araújo F, Lucas R, Alegrete N, Azevedo A, Barros H (2014) Sagittal standing posture, back pain, and quality of life among adults from the general population. Spine 39(13):E782–E794

Arlegi M, Gómez-Olivencia A, Albessard L, Martínez I, Balzeau A, Arsuaga JL, Been E (2017) The role of allometry and posture in the evolution of the hominin subaxial cervical spine. J Hum Evol 104:80–99

Bailey JF, Shefi S, Soudack M, Kramer PA, Been E (2016) Pelvic incidence in children and adolescents predicts mature lumbar lordosis. FASEB J 30(Suppl 1):1046.17

Barrey C, Jund J, Noseda O, Roussouly P (2007) Sagittal balance of the pelvis-spine complex and lumbar degenerative diseases. A comparative study about 85 cases. Eur Spine J 16(9):1459–1467

Been E, Barash A, Marom A, Kramer PA (2010) Vertebral bodies or discs: which contributes more to human-like lumbar lordosis? Clin Orthop Relat R 468(7):1822–1829

Been E, Gómez-Olivencia A, Shefi S, Soudack M, Bastir M, Barash A (2017) Evolution of spinopelvic alignment in hominins. Anat Rec 300(5):900–911

Been E, Kalichman L (2014) Lumbar lordosis. Spine J 14(1):87–97

Been E, Li L, Hunter DJ, Kalichman L (2011) Geometry of the vertebral bodies and the intervertebral discs in lumbar segments adjacent to spondylolysis and spondylolisthesis: pilot study. Eur Spine J 20(7):1159–1165

Been E, Shefi S, Zilka LR, Soudack M (2014) Foramen magnum orientation and its association with cervical lordosis: a model for reconstructing cervical curvature in archeological and extinct hominin specimens. Adv Anthropol 4(03):133

Boulay C, Tardieu C, Hecquet J, Benaim C, Mouilleseaux B, Marty C, Prat-Pradal D, Legaye J, Duval-Beaupère G, Pélissier J (2006) Sagittal alignment of spine and pelvis regulated by pelvic incidence: standard values and prediction of lordosis. Eur Spine J 15:415–422

Chaléat-Valayer E, Mac-Thiong J-M, Paquet J, Berthonnaud E, Siani F, Roussouly P (2011) Sagittal spino-pelvic alignment in chronic low back pain. Eur Spine J 20(S5):634–640

Cosman F, de Beur SJ, LeBoff MS, Lewiecki EM, Tanner B, Randall S, Lindsay R (2014) Clinician's guide to prevention and treatment of osteoporosis. Osteoporos Int 25(10):2359–2381

Diebo BG, Varghese JJ, Lafage R, Schwab FJ, Lafage V (2015) Sagittal alignment of the spine: what do you need to know? Clin Neurol Neurosurg 139:295–301

Dubousset J (1994) Three-dimensional analysis of the scoliotic deformity. In: Weinstein S (ed) The pediatric spine: principles and practice. Raven Press, New York, pp 479–496

Ergun T (2010) The relation between sagittal morphology of the lumbosacral spine and the degree of lumbar intervertebral disc degeneration. Acta Orthop Traumatol Turc 44(4):293–299

Ferrero E, Ould-Slimane M, Gille O, Guigui P (2015) Sagittal spinopelvic alignment in 654 degenerative spondylolisthesis. Eur Spine J 24(6):1219–1227

Hanson DS, Bridwell KH, Rhee JM, Lenke LG (2002) Correlation of pelvic incidence with low- and high-grade isthmic spondylolisthesis. Spine 27(18):2026–2029

Hansson T, Suzuki N, Hebelka H, Gaulitz A (2009) The narrowing of the lumbar spinal canal during loaded MRI: the effects of the disc and ligamentum flavum. Eur Spine J 18(5):679–686

Huang RP, Bohlman HH, Thompson GH, Poe-Kochert C (2003) Predictive value of pelvic incidence in progression of spondylolisthesis. Spine 28(20):2381–2385

Itoi E (1991) Roentgenographic analysis of posture in spinal osteoporotics. Spine 16(7):750–756

Jacobsen S, Sonne-Holm S, Rovsing H, Monrad H, Gebuhr P (2007) Degenerative lumbar spondylolisthesis: an epidemiological perspective – the Copenhagen osteoarthritis study. Spine 32(1):120–125

Jansen RC, van Rhijn LW, van Ooij A (2006) Predictable correction of the unfused lumbar lordosis after thoracic correction and fusion in Scheuermann kyphosis. Spine 31(11):1227–1231

Jentzsch T, Geiger J, Bouaicha S, Slankamenac K, Nguyen-Kim TDL, Werner CML (2013) Increased pelvic incidence may lead to arthritis and sagittal orientation of the facet joints at the lower lumbar spine. BMC Med Imaging 13:34

Jiang L, Qiu Y, Xu LL, Liu Z, Wang Z, Sha SF, Zhu ZZ (2014) Sagittal spinopelvic alignment in adolescents associated with Scheuermann's kyphosis: a comparison with normal population. Eur Spine J 23(7):1420–1426

Kalichman L, Cole R, Kim DH, Li L, Suri P, Guermazi A, Hunter DJ (2009a) Spinal stenosis prevalence and association with symptoms: the Framingham study. Spine J 9(7):545–550

Kalichman L, Kim DH, Li L, Guermazi A, Berkin V, Hunter DJ (2009b) Spondylolysis and spondylolisthesis prevalence and association with low Back pain in the adult community-based population. Spine 34(2):199–205

Kalichman L, Li L, Hunter DJ, Been E (2011) Association between computed tomography-evaluated lumbar lordosis and features of spinal degeneration, evaluated in supine position. Spine J 11(4):308–315

Kalichman L, Li L, Kim DH, Guermazi A, Berkin V, O'Donnell CJ, Hoffmann U, Cole R, Hunter DJ (2008) Facet joint osteoarthritis and low back pain in the community-based population. Spine 33(23):2560–2565

Klineberg E, Schwab F, Smith JS, Gupta MC, Lafage V, Bess S (2013) Sagittal spinal pelvic alignment. Neurosurg Clin N Am 24(2):157–162

Labelle H, Roussouly P, Berthonnaud E, Transfeldt E, O'Brien M, Chopin D, Hresko T, Dimnet J (2004) Spondylolisthesis, pelvic incidence, and spinopelvic balance – a correlation study. Spine 29(18):2049–2054

Lafage R, Schwab F, Challier V, Henry JK, Gum J, Smith J, Hostin R, Shaffrey C, Kim HJ, Ames C, Scheer J, Klineberg E, Bess S, Burton D, Lafage V (2016) Defining spino-pelvic alignment thresholds. Spine 41(1):62–68

Lafage V, Schwab F, Skalli W, Hawkinson N, Gagey PM, Ondra S, Farcy JP (2008) Standing balance and sagittal plane spinal deformity – analysis of spinopelvic and gravity line parameters. Spine 33(14):1572–1578

Legaye J, Duval-Beaupere G (2008) Gravitational forces and sagittal shape of the spine. Int Orthop 32(6):809–816

Loder RT (2001) The sagittal profile of the cervical and lumbosacral spine in Scheuermann thoracic kyphosis. J Spinal Disord 14(3):226–231

Lovejoy CO (2005) The natural history of human gait and posture. Gait Posture 21(1):95–112

Lowe TG (1990) Current concepts review – Scheuermann disease. J Bone Joint Surg Am 72a(6):940–945

Lowe TG, Line BG (2007) Evidence based medicine – analysis of Scheuermann kyphosis. Spine 32(19):S115–S119

Maes R, Morrison WB, Parker L, Schweitzer ME, Carrino JA (2008) Lumbar interspinous bursitis (Baastrup disease) in a symptomatic population. Spine 33(7):E211–E215

Marty C, Boisaubert B, Descamps H, Montigny J, Hecquet J, Legaye J, Duval-Beaupère G (2002) The sagittal anatomy of the sacrum among young adults, infants, and spondylolisthesis patients. Eur Spine J 11(2):119–125

Merbs CF (1996) Spondylolysis spondylolisthesis: a cost of being an erect biped or a clever adaptation? Yearb Phys Anthropol 39:201–228

Miyakoshi N, Kudo D, Hongo M, Kasukawa Y, Ishikawa Y, Shimada Y (2017) Comparison of spinal alignment, muscular strength, and quality of life between women with postmenopausal osteoporosis and healthy volunteers. Osteoporos Int 28(11):3153–3160

Oe S, Togawa D, Yoshida G, Hasegawa T, Yamato Y, Kobayashi S, Yasuda T, Banno T, Mihara Y, Matsuyama Y (2017) Difference in spinal sagittal alignment and health-related quality of life between males and females with cervical deformity. Asian Spine J 11(6):959

Palazzo C, Sailhan F, Revel M (2014) Scheuermann's disease: an update. Joint Bone Spine 81(3):209–214

Peleg S, Dar G, Steinberg N, Masharawi Y, Been E, Abbas J, Hershkovitz I (2009) Sacral orientation and spondylolysis. Spine 34(25):E906–E910

Peleg S, Dar G, Steinberg N, Masharawi Y, Hershkovitz I (2016) Sacral orientation and Scheuermann's kyphosis. Springerplus 5(1):141

Plomp KA, Vietharsdottir US, Weston DA, Dobney K, Collard M (2015) The ancestral shape hypothesis: an evolutionary explanation for the occurrence of intervertebral disc herniation in humans. BMC Evol Biol 15:68

Roussouly P, Pinheiro-Franco JL (2011) Biomechanical analysis of the spino-pelvic organization and adaptation in pathology. Eur Spine J 20(S5):609–618

Sadler SG, Spink MJ, Ho A, De Jonge XJ, Chuter VH (2017) Restriction in lateral bending range of motion, lumbar lordosis, and hamstring flexibility predicts the development of low back pain: a systematic review of prospective cohort studies. BMC Musculoskelet Disord 18:179

Schlösser TP, Janssen MM, Vrtovec T, Pernuš F, Öner FC, Viergever MA, Vincken KL, Castelein RM (2014) Evolution of the ischio-iliac lordosis during natural growth and its relation with the pelvic incidence. Eur Spine J 23(7):1433–1441

Schultz AH (1961) Vertebral column and thorax. Primatologia 4:1–66

Schwab F, Lafage V, Boyce R, Skalli W, Farcy JP (2006) Gravity line analysis in adult volunteers – age-related correlation with spinal parameters, pelvic parameters, and foot position. Spine 31(25):E959–E967

Schwab F, Lafage V, Shaffrey CI, Smith JS, Moal B, Ames CP, Fu KMG, Mummaneni PV, Burton DC, Gupta M, Deviren V, Mundis G, Hart R, Bess S (2012) The Schwab-SRS adult spinal deformity classification: assessment and clinical correlations based on a prospective operative and non-operative cohort. Neurosurgery 71(2):E556–E556

Smith A, O'Sullivan P, Straker LM (2008) Classification of sagittal thoraco-lumbo-pelvic alignment of the adolescent spine in standing and its relationship to low back pain. Spine 33(19):2101–2107

Sparrey CJ, Bailey JF, Safaee M, Clark AJ, Lafage V, Schwab F, Smith JS, Ames CP (2014) Etiology of lumbar lordosis and its pathophysiology: a review of the evolution of lumbar lordosis, and the mechanics and biology of lumbar degeneration. Neurosurg Focus 36(5):E1

Stone MA, Osei-Bordom D-C, Inman RD, Sammon C, Wolber LE, Williams FMK (2014) Heritability of spinal curvature and its relationship to disc degeneration and bone mineral density in female adult twins. Eur Spine J 24(11):2387–2394

Suzuki H, Endo K, Kobayashi H, Tanaka H, Yamamoto K (2010) Total sagittal spinal alignment in patients with Lumbar Canal stenosis accompanied by intermittent claudication. Spine 35(9):E344–E346

Swärd L, Hellström M, Jacobsson B, Peterson L (1989) Spondylolysis and the Sacro-horizontal angle in athletes. Acta Radiol 30(4):359–364

Tardieu C, Bonneau N, Hecquet J, Boulay C, Marty C, Legaye J, Duval-Beaupere G (2013) How is sagittal balance acquired during bipedal gait acquisition? Comparison of neonatal and adult pelves in three dimensions. Evolutionary implications. J Hum Evol 65(2):209–222

Tardieu C, Hasegawa K, Haeusler M (2017) How did the pelvis and vertebral column become a functional unit during the transition from occasional to permanent bipedalism? Anat Rec 300(5):912–931

Vialle R, Ilharreborde B, Dauzac C, Lenoir T, Rillardon L, Guigui P (2007) Is there a sagittal imbalance of the spine in isthmic spondylolisthesis? A correlation study. Eur Spine J 16(10):1641–1649

Vrtovec T, Pernus F, Likar B (2009) A review of methods for quantitative evaluation of axial vertebral rotation. Eur Spine J 18(8):1079–1090

Wei W, Liao S, Shi S, Fei J, Wang Y, Chen C (2013) Straightened cervical lordosis causes stress concentration: a finite element model study. Australas Phys Eng Sci Med 36(1):27–33

Weinberg DS, Liu RW, Xie KK, Morris WZ, Gebhart JJ, Gordon ZL (2017) Increased and decreased pelvic incidence, sagittal facet joint orientations are associated with lumbar spine osteoarthritis in a large cadaveric collection. Int Orthop 41(8):1593–1600

Yang X, Kong Q, Song Y, Liu L, Zeng J, Xing R (2013) The characteristics of spinopelvic sagittal alignment in patients with lumbar disc degenerative diseases. Eur Spine J 23(3):569–575

Zhang YL, Shi LT, Tang PF, Sun ZJ, Wang YH (2017) Correlation analysis of osteoporotic vertebral compression fractures and spinal sagittal imbalance. Orthopade 46(3):249–255

Chapter 14
Cervical Posture, Pain, and Pathology: Developmental, Evolutionary and Occupational Perspective

David Ezra, Ella Been, Deborah Alperovitch-Najenson, and Leonid Kalichman

14.1 Introduction

The cervical column acts as a bridge between the torso and the head, playing a crucial role in maintaining head position, gaze, and visual field (Nalley and Grider-Potter 2015). In humans, the cervical spine is the most mobile component of the spinal column (Gay 1993) and its curvature (lordosis) supports the head above the shoulders. Cervical lordosis is a commonly used term for the inward (ventral) curvature of the cervical spine, which shape is maintained through the wedged shape of the cervical vertebrae, the intervertebral discs, and the balance between the forces of gravity and neck muscle activity (Clement 1985; Gay 1993). Various factors may affect the cervical lordosis, e.g. the shape of vertebral bodies (Chen et al. 2013), the shape and integrity of the intervertebral discs (Markuske 1979), the spinous process length (Refshauge et al. 1994), the shape of the other spinal curves (Visscher and Naeije 1998), head position (Cuccia et al. 2008), and age (Yukawa et al. 2012). Muscular activity also contributes to the shape and magnitude of the cervical lordosis. Yoon et al. (2018) discovered a significant relationship between the weakness of the cervical extensor muscles and the loss of cervical lordosis. Restoring the balance between the flexor and extensor muscles is essential for maintaining the

D. Ezra
School of Nursing Science, Tel Aviv Jaffo Academic College, Tel Aviv-Yafo, Israel

E. Been (✉)
Department of Sports Therapy, Faculty of Health Professions, Ono Academic College, Kiryat Ono, Israel

Department of Anatomy and Anthropology, Sackler Faculty of Medicine, Tel Aviv University, Tel Aviv, Israel

D. Alperovitch-Najenson · L. Kalichman
Department of Physical Therapy, Recanati School for Community Health Professions, Faculty of Health Sciences, Ben-Gurion University of the Negev, Beer Sheva, Israel

E. Been et al. (eds.), *Spinal Evolution*,
https://doi.org/10.1007/978-3-030-19349-2_14

physiological cervical lordotic curvature. Moreover, spinal degeneration, pathology, and neck and head pain have been found associated with cervical alignment (Helliwell et al. 1994; Gok et al. 2008; Okada et al. 2009; Bayerl et al. 2013; Grosso et al. 2013; Mohanty et al. 2015; Ezra et al. 2017). However, there is considerable variability in the cervical spine curvature among individuals (Gay 1993) generating several unresolved questions: What is a normal cervical curvature? How does the morphology of cervical vertebrae and intervertebral discs influence cervical curvature? Is the cervical curvature associated with cervical spine degeneration (disc narrowing, facet joints, osteoarthritis, etc.)? Why is cervical curvature associated with neck pain? Is modern lifestyle associated with cervical pain and pathology? Endeavoring to answer these questions, we examined the major morphological aspects of the cervical curvature and its association with the development of cervical pathology in modern humans, archaeological populations, and extinct hominins.

14.2 Evaluation of Cervical Alignment

Cervical curvature is generally defined by the cervical lordosis (measured in angles) and by the ventrodorsal position of the head or the upper spine in relation to the last cervical vertebra (C7) (measured in millimeters). The principal methods for evaluating the cervical lordosis are the centroid, posterior tangent, and the Cobb methods (Fig. 14.1) (Cobb 1948; Gore et al. 1986; Owens 1990; Harrison et al. 1996; Ohara et al. 2006). The Cobb method remains the clinical mainstay of cervical lordosis measurement due to its ease of use, as well as its intra- and inter-observer reliability (Polly et al. 1996; Prasarn et al. 2012). Cobb angle can be measured in different ways, the most common of which are: C0–C7, between the foramen magnum and the inferior endplate C7; C1–C7, between a line parallel to C1 and a line parallel to the inferior endplate C7; and C2–C7, between a line parallel to C2 and a line parallel to the inferior endplate C7 (Fig. 14.1). The ventrodorsal position of the upper cervical spine in relation to C7 is usually determined by the Sagittal Vertical Axis method (C2–C7 SVA) (Fig. 14.2), which measures the horizontal distance between a plumb line from the center of the C2 vertebral body and the posterior superior corner of C7 (Scheer et al. 2013; Oe et al. 2017).

Cervical alignment is divided into five types (Table 14.1, Fig. 14.3) (Borden et al. 1960; Juhl et al. 1962):

1. The lordotic type (Fig. 14.3a): An inward ventral curvature from the upper to the lower cervical spine. In normal (i.e., no known pathology) adults, this curvature has been observed in 60–91% of individuals (Borden et al. 1960; Juhl et al. 1962).
2. The straight type (Fig. 14.3b): A straightened cervical spine (neither lordotic nor kyphotic curvatures). In normal adults, this form appears in 7–19% of individuals.
3. The kyphotic type (Fig. 14.3c): The normal inward lordotic curve reverses into a kyphotic curve. In normal adults, this form appears in 2–14% of individuals.

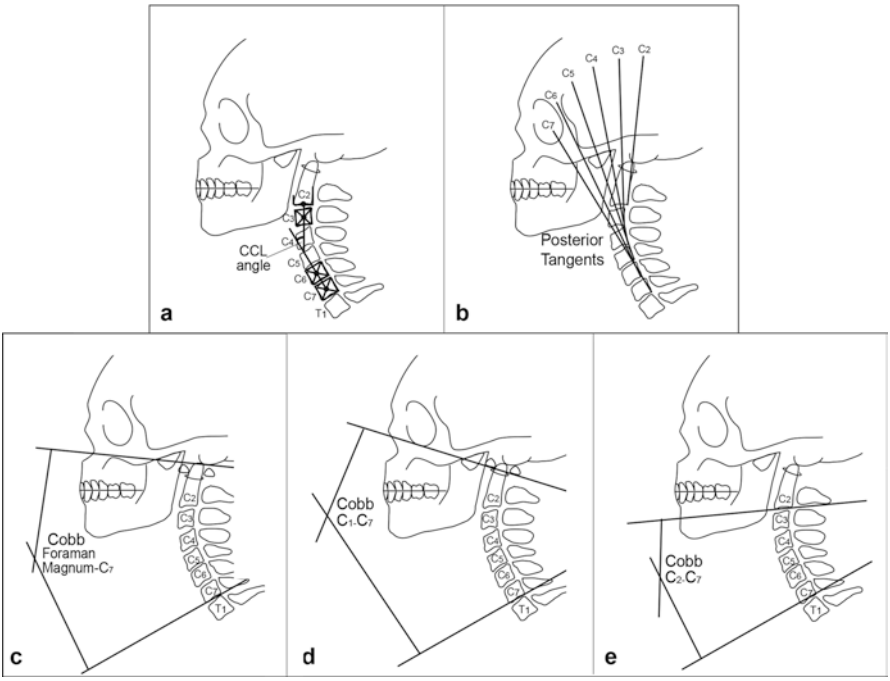

Fig. 14.1 Angular methods for evaluating the cervical lordosis. (**a**) Centroid method; (**b**) Posterior tangent method; (**c**) Cobb angle measured between the foramen magnum and the lower end plate of the C7 vertebra; (**d**) the Cobb angle measured between a line drawn through the midpoints of the anterior and posterior tubercles of the atlas (C1) and the lower end plate of the C7 vertebra; (**e**) the Cobb angle measured between the lower part of the C2 and the lower end plate of the C7 vertebra

4. The S-shape type (Fig. 14.3d1, d2): This form has a kyphotic upper curve and a lordotic lower cervical shape (Fig. 14.3d1) or a lordotic upper curve and a kyphotic lower cervical shape (Fig. 14.3d2). In normal adults, this form appears in 7–9% of individuals (Juhl et al. 1962; Gore et al. 1986).

14.3 Ontogenetic Development of Cervical Alignment

The cervical spine of the human fetus is usually described to be in a flexed position as part of the primary kyphotic curve. In utero, a slight flattening occurs in the lumbosacral region, and yet, in these studies, a secondary cervical curvature in fetuses is not mentioned (O'Rahilly et al. 1980; Moore et al. 2013). Nonetheless, in a study of 195 radiographs of human fetuses obtained from hysterotomies (gestational age 8–23 weeks), well-defined cervical lordosis was found in 83% of the fetuses (Bagnall et al. 1977). The authors concluded that the cervical curvature exists early in utero, but subsequently decreases as a result of an increase in head weight and

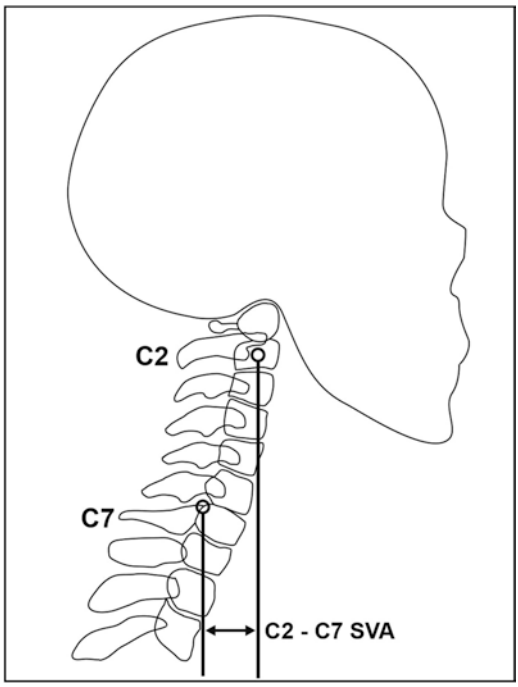

Fig. 14.2 C2–C7 SVA. The horizontal distance (arrow) between a plumb line from the center of the C2 vertebral body and a plumb line from the posterior superior corner of the C7

Table 14.1 Prevalence of cervical alignments measured on standing x-rays

Study	Subjects *n*	Lordotic shape *n* (%)	Straight shape *n* (%)	Kyphotic shape *n* (%)	Sigmoid shape *n* (%)
Borden et al. (1960)	180	164 (91.1)	13 (7.2)	3 (1.6)	0
Juhl et al. (1962)	116	70 (60.3)	22 (18.9)	16 (13.7)	8 (6.8)
Gore et al. (1986)	200				18 (9.0)
Tahara et al. (2008)	40-young	17 (42.5)	6 (15.0)	2 (5.0)	1 (2.5)
	28-old	11 (39.2)	12 (42.8)	16 (57.1)	1 (3.5)
Beltsios et al. (2013)	100	36 (36.0)	34 (34.0)	4 (4.0)	26 (26.0)
Grob et al. (2007)	53-no pain 50-with pain	48 (90.5) 48 (96.0)	4 (7.5) 2 (4.0)	1 (1.8) 0	0 0
Yukawa et al. (2012)	1230			164 (13.3)	
Yu et al. (2015)	120-asymptomatomatic 121-cervical spondylosis	33 (38.3) 44 (36.4)	55 (45.8) 53 (43.8)	26 (21.8) 13 (10.7)	5 (4.2) 11 (9.1)
Been et al. (2017b)	28-girls 48-boys 60-adult females 61-adult males	19 (68) 35 (72.7) 28 (47.2) 33 (54.6)	8 (28) 10 (20.5) 25 (41.5) 26 (41.8)	0 0 0 0	1(4.1) 3 (6.8) 7 (11.3) 2 (3.6)

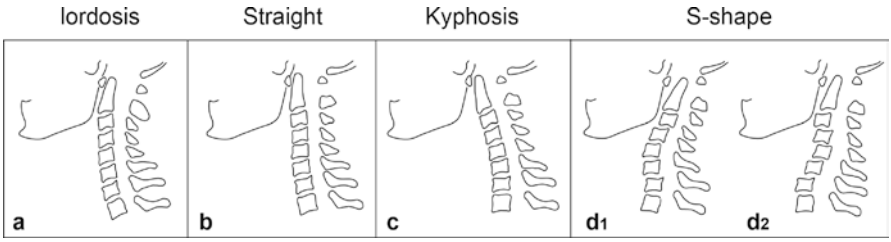

Fig. 14.3 Four types of cervical alignment. (**a**) Lordotic; (**b**) Straight; (**c**) Kyphotic; (**d**) S-shaped

uterine constraints. Cervical lordosis becomes more distinct at 3–4 months after birth, as the infant begins to raise his/her head and then again when the baby adopts the sitting position (Kasai et al. 1996).

Kasai et al. (1996) described the morphological changes during growth. The authors defined three periods of cervical curvature modifications. *The first period* encompasses birth to 2 years of age. During this stage, cervical lordosis becomes more distinct and the lordotic angle of the inferior cervical spine (C3–C7) increases to 20°. *During the second period* (2–9 years of age), the inferior cervical spine angle (C3–C7) gradually decreases due to the influence of an asymmetrical anteroposterior growth of the vertebral bodies and decrease of the facet joint angles. By 9 years old, the lordosis decreases to 9.5°. *During the third period* (10–18 years of age), the inferior cervical spine angle increases again to 16°. Simultaneously, the facet angles tend to stabilize and the anterosuperior aspect of the vertebral bodies ossifies.

The differences in the morphology of the cervical lordosis between children and adults have been observed not only in the extent of the lordosis but also in its internal architecture. The intervertebral discs of children are more lordotic than in adults and the vertebral bodies of children are more kyphotic (Been et al. 2017b). Cervical alignment type also differs between children and adults. Children (6–19 years old) have a higher prevalence of lordotic type than adults and a lower prevalence of the straight or sigmoid type. The kyphotic type has not been observed in the pediatric population (Been et al. 2017b).

Studies reporting cervical alignment in the elderly are contradictory. Some authors report a noticeable increase in the cervical lordosis with age (Gore et al. 1986; Marchiori and Henderson 1996; Okada et al. 2009; Yukawa et al. 2012). Yukawa et al. (2012) reported that, due to the aging process, the cervical lordosis measured between C2 and C7 increased from 8° in the third decade to 20° in the eighth decade. Other studies have reported a decrease in the lordosis angle or even the development of a kyphotic cervical curve as part of the aging process (Braaf and Rosner 1975; Boyle et al. 2002; Nagasawa et al. 1993).

In conclusion, cervical lordosis begins to develop in fetuses. The major increase of the lordosis angle occurs during the first 2 years of life, but continues to change in a non-linear way through skeletal maturation and into old age. Current knowledge regarding the ontogenetic development of cervical alignment is incomplete and additional studies are needed to fill in this gap and identify the factors that determine cervical alignment development.

14.4 Normal Parameters of Cervical Alignment in the Adult Population

A wide range of normal cervical alignment has been described in the literature (Table 14.2; Scheer et al. 2013). The differences in the extent of the cervical lordosis are partially the result of the high mobility of the neck, different methods used to measure the lordosis (Cobb/posterior tangent/centroid), and the diverse anatomical landmarks used (C0–C7/C1–C7/C2–C7/C3–C7).

We present, herein, cervical alignment measurements in asymptomatic individuals (Table 14.2). In the adult population, the mean total cervical lordosis (C0–C7) measured by the Cobb angle in standing individuals, is approximately 40° (Hardacker et al. 1997; Been et al. 2017b) and the mean lower cervical lordosis C2–C7 Cobb (Fig. 14.1) is between 15.2° and 17.3° (Harrison et al. 2000; Protopsaltis et al. 2015). At the segmental level, the occiput-C1 angle is usually kyphotic (Scheer et al. 2013). The angle between C1 and C2 constitutes approximately 75–80% of standing cervical lordosis (Hardacker et al. 1997; Jackson and McManus 1994), whereas only 6° (15%) of lordosis occurs at the lowest three cervical segments (C3–C7) (Hardacker et al. 1997).

14.5 Sex Differences in Cervical Lordosis

Been et al. (2017b) found that total cervical lordosis (C0–C7) and cervical lordosis (C1–C7) of males and females were similar, but the internal architecture of the lordosis revealed several significant differences between sexes. Females exhibited a higher (by 5°) upper cervical lordosis (C0–C3; C1–C3) than males, while males exhibited a higher lower cervical lordosis (C3–C7) than females (by 6°). Both males and females had kyphotic vertebral body wedging, but males had more lordotic intervertebral disc wedging (6°) than females. These results are in agreement with Yukawa et al. (2012), who found greater lower cervical lordosis (C2–C7) in males compared with females between the third and eighth decades of life. Been et al. (2017b) also found that some of the differences between sexes were present in children. Girls exhibited a higher upper cervical lordosis (C0–C3; C1–C3) than boys, while boys had already exhibited a tendency toward a higher lower cervical lordosis (C3–C7), similar to adult males and females. In contrast, there was no difference in the wedging of the intervertebral discs between boys and girls, which is in agreement with Abelin-Genevois et al. (2014), who found similar differences in upper and lower cervical lordosis angles between boys and girls. This, however, contradicts the results of Kasai et al. (1996) who found no difference in the lower cervical lordosis between boys and girls.

Table 14.2 Descriptive statistics (mean and standard deviation in brackets) of the angular measurements on the cervical spine in asymptomatic individuals[a]

Study	Method	Modality	*n*	Age	FM-C7	C1–C2	C1–C3	C1–C7	C3–C7	C2–C6	C2–C7	C1–C6
Hardacker et al. (1997)	Cobb	X-ray	100	20–70	40.0 (9.7)	32.2 (7.0)		41.8			9.6	37.2
Harrison et al. (2000)	Cobb	X-ray	30					53.5 (12.7)			17.2 (14.7)	
Harrison et al. (2000)	Posterior tangent	X-ray	30								25.7 (13.4)	
Yukawa et al. (2012)	Cobb	X-ray	1230	30–80							13.9 (12.3)	
Sub Jun et al. (2014)	Cobb	X-ray CT	50	24–80							17.3 (9.3) 11.35 (9.3)	
Le Huec et al. (2015)	Cobb	X-ray	106	18–80		29.2 (7.2)		34.0 (12.2)			4.9 (12.8)	
Gore et al. (1986)	Posterior tangent		53	45–90							23.0 (12.0)	
Shilton et al. (2015)	Posterior tangent	Fluoroscopic	30	40.5 (12.7)						4.4 (14.0)		
Núñez-Pereira et al. (2015)	Cobb	X-ray	34			20.8 (7.3)					15.8 (13.2)	
Been et al. (2017b)	Cobb	X-ray	121	20–50	38.0 (10.6)		33.7 (7.7)		11.8 (10.4)			
Been et al. (2017b)	Cobb	X-ray	76	6–19	39.6 (10.0)		35.8 (8.7)		14.9 (11.3)			

[a]All radiographs were taken while standing, fluoroscopic evaluation while sitting, and CT in supine positions. *FM* foramen magnum

14.6 Morphological Aspects Associated with Cervical Lordosis

Cervicothoracic junction. The cervicothoracic junction typically involves the C7 and T1 vertebrae, the C7–T1 disc, and associated ligaments (Wang and Chou 2007). It also includes the thoracic inlet, a fixed bony circle composed of the T1 vertebral body, the first ribs on both sides, and the upper part of the sternum (Fig. 14.4, Scheer et al. 2013). The thoracic inlet alignment is correlated with craniocervical sagittal balance. The thoracic inlet angle and the T1 slope could be employed as parameters to predict the physiological alignment of the cervical spine (Lee et al. 2012). Lee et al. (2012) demonstrated that the T1 slope is the most important thoracic variable determining cervical lordosis and cervical spine sagittal balance. Although both spinopelvic balance and thoracic inlet alignment significantly influence the cervical spine's sagittal balance via the T1 slope, the thoracic inlet angle exhibited a stronger effect than the thoracic kyphosis. An individual with a large T1 slope requires a large cervical lordosis to preserve the physiologic sagittal balance of the cervical spine, or in other words, to keep the head above the spine.

Craniofacial morphology. Craniofacial morphology influences cervical lordosis during the life cycle. Huggare and Houghton (1996) reported a correlation between the sagittal length of atlas (C1) between the anterior and the posterior tubercles, mandibular length, and mandibular ramus height, signifying a close association of the growth mechanism in the two regions. Festa et al. (2003), based on lateral skull radiographs, evaluated the association between the cervical lordosis angle and mandibular length. They observed a negative correlation between cervical lordosis and mandibular length, indicating that a straighter cervical lordosis correlates with a

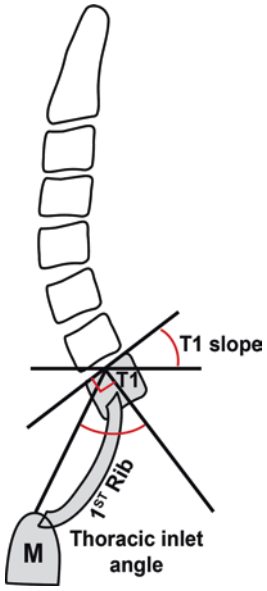

Fig. 14.4 T1 slope and thoracic inlet angle. T1 slope is the angle between a line parallel to the superior endplate of T1 and a horizontal line. Thoracic inlet angle is the angle between a line connecting the center of the T1 endplate and the top center of the manubrium (M), with a perpendicular line descending from the center of T1 endplate

long mandible, while more curved cervical spines with higher lordosis angle correlate with short mandibles. Sonnesen et al. (2007) also found an interaction between mandibular morphology and cervical lordosis. Been et al. (2014) measured the orientation of the foramen magnum and its association with cervical lordosis demonstrating that the orientation of the foramen magnum positively correlated with the cervical lordosis angle. Accentuated lordosis angles correlated with the anterior orientation of the foramen magnum, whereas straight lordosis angles correlated with the more posterior orientation of the foramen magnum. Zhu et al. (2018) reported similar results of a positive correlation between the orientation of the foramen magnum and cervical lordosis.

14.7 Cervical Spine Pathology and Pain

Cervical pain and discomfort are one of the major causes of lost work in the western world, accounting for a large proportion of health care expenditures (Martin et al. 2008). It has been found that in the general population, the 1-year prevalence of neck pain can be as high as 40% (Ariëns et al. 2001). The cervical spine is primarily responsible for the location of the head on top of the body, as well as the level of the horizontal gaze. Any deviations from the normal alignment of the head mass results in an increase in cantilever loads, which subsequently induces an increase in muscular energy expenditure and uneven load transmission. The natural biomechanics of the spine rely on a lordotic curve to distribute most of the load posteriorly. Thus, deviations from this form might lead to the development of cervical pathology (Pal and Sherk 1988; Scheer et al. 2013).

Although cervical pain is multifactorial, long hours of sitting, maintaining the head in a forward position, and cervical sagittal imbalance, contribute to the development of cervical pain and pathology (Ariëns et al. 2001; Smith et al. 2013). Cervical pathology greatly influences neighboring areas, leading to headaches, shoulder and arm pain, and temporomandibular malfunction (Scheer et al. 2013). While there is some evidence to suggest that cervical posture impacts the development of cervical pathology, this relationship, if it exists, is as yet not fully understood (Ames et al. 2012).

14.8 Cervical Myelopathy

Cervical myelopathy refers to cervical spinal cord compression. Any space-occupying lesion within the cervical spine with the potential to compress the spinal cord can cause cervical myelopathy. Worldwide, cervical spondylotic myelopathy, an often progressive, degenerative disease, is the leading cause of acquired spinal cord dysfunction (Smith et al. 2013). The degenerative changes associated with cervical spondylotic myelopathy include cervical disc degeneration, disc

herniation, loss of disc height, and posterior osteophytes. These changes can also result in the loss of normal segmental and regional sagittal alignment, including kyphosis and sagittal imbalance, and may ensue from primary cervical disease or changes in the subjacent spinal regions, including thoracic kyphosis and loss of lumbar lordosis. Compensatory cervical hyperlordosis, with subsequent dorsal ligamentous buckling and cord impingement, may result from global sagittal imbalance. Furthermore, segmental kyphosis may contribute to spinal cord dysfunction through multiple mechanisms, including direct compression, repeated flexion/extension injury and vascular compromise (Smith et al. 2008, 2013).

In a large research study, Machino et al. (2016) analyzed radiographic data from 1016 patients with cervical spondylotic myelopathy and 1230 asymptomatic subjects and found that patients with cervical spondylotic myelopathy showed significantly smaller lordotic angles (Cobb angle between C2 and C7) compared with the asymptomatic subjects. They also observed that the range of motion (ROM) of patients with cervical spondylotic myelopathy was significantly less than the ROM in asymptomatic subjects. Smith et al. (2013) examined 56 patients after cervical spondylotic myelopathy surgery and found a positive correlation between sagittal cervical balance (C2–C7 SVA) and myelopathy severity. As C2 is more anterior in relation to C7, the severity of cervical myelopathy increased.

Progressive cervical kyphosis is known to associate with myelopathy (Scheer et al. 2013; Uchida et al. 2009). Cervical kyphosis leads to spinal cord pressure against the vertebral bodies and increased longitudinal cord tension due to the cord being tethered by the dentate ligaments and cervical nerve roots. As the kyphotic curve becomes further pronounced over time, the spinal cord becomes compressed and flattened. The anterior and posterior margins of the cord compress while the lateral margins expand. Tethering of the cord can produce increased intramedullary pressure and can lead to neuronal loss and demyelination of the cord (Albert and Vacarro 1998; Scheer et al. 2013).

14.9 Cervical Alignment and Health-Related Quality of Life

In a large cohort study, Oe et al. (2017) evaluated spinal sagittal alignment and health-related quality of life in 656 Japanese aged >50 years. The participants were divided into four groups based on gender and presence or absence of cervical deformity. Participants with cervical deformity had C2–C7 SVA >40 mm; participants without cervical deformity had C2–C7 SVA <40 mm. The authors found that the mechanism underlying spinal sagittal deformity was different in males than in females. Females with a cervical deformity had already suffered from malalignment of the pelvis and thoracic spine compared with the females without a cervical deformity. On the other hand, there was no significant difference in pelvic and thoracic parameters between the males with cervical deformity and those without cervical deformity. Oe et al. (2017) concluded that spinal deformity originates from lumbopelvic lesions in females and from cervical lesions in males. Moreover, a cervical

deformity was significantly associated with health-related quality of life in males (a higher cervical deformity indicated a lower quality of life), but not in females. Ling et al. (2018) determined that the most clinically relevant parameters to cervical sagittal balance are: C7 or T1 slope <40° and C2–C7 SVA < 40 mm.

Smith et al. (2013) reported negative correlations between C2–C7 SVA and the health-related quality of life score and found a better quality of life for patients with small C2–C7 SVA (C2 plumb line is close to C7 in the sagittal plane). Cervical lordosis (Cobb angle between C2 and C7) did not influence the health-related quality of life scores. Protopsaltis et al. (2015) examined the relationship between cervical and thoracolumbar alignment parameters with health-related quality of life scores among patients with an operative and non-operative adult thoracolumbar deformity, finding that patients with operative deformity had significantly worse baseline health-related quality of life scores and higher C2–C7 SVA. For all patients, baseline C2–C7 SVA and cervical lordosis (Cobb angle between C2 and C7) significantly correlated with baseline health-related quality of life scores. They concluded that there is a direct effect of cervical alignment on health measures and that improvements in regional cervical alignment postoperatively, positively correlated with an improved quality of life.

14.10 Occupational Ergonomic Risk Factors for Neck Pain

Workers in various professions, such as office personnel (Nejati et al. 2015; Jun et al. 2017), ultrasonographers (Claes et al. 2015; Simonsen et al. 2017), dental hygienists (Hayes et al. 2016), and professional drivers (Alperovitch-Najenson et al. 2010; Bovenzi 2015), experience neck pain. Forward head posture, weekly computer use for 6–9 or more hours, sustained sitting, dissatisfaction with the computer workstation, inappropriate placement of computer devices such as the monitor, keyboard, and mouse, and how close to the body the keyboard is positioned have been linked to the prevalence and incidence of neck pain in office workers (Smith et al. 2009; Tornqvist et al. 2009; Nejati et al. 2015; Darivemula et al. 2016; Jun et al. 2017). Other occupations were found to have different ergonomic risk factors. An uncomfortable steering wheel and seat and back support were found associated with a higher prevalence of neck pain in professional urban bus drivers (Alperovitch-Najenson et al. 2010). Driving with a bent or twisted trunk was associated with neck pain (Bovenzi 2015). Sonographers, whose screen is on their left side, had significantly more neck pain (Claes et al. 2015). In the general population, a combination of sustained/repeated arm abduction with high physical exertion was the strongest risk factor for neck pain in women. Prolonged forward head flexion was associated with a higher incidence of neck pain in men (Petit et al. 2018). Only a few explanations of the ergonomic causes of neck pain have been found in the literature. When working with one's hands and fingers, the muscles in the proximal areas such as the neck and shoulders must act as stabilizers. This static contraction of the muscles is expressed more strongly when neck

rotation or forward head bending occurs, e.g. when a computer screen is placed to the side of the worker. Continuous rotation of the neck throughout the working day might also cause neck pain (Claes et al. 2015). Drivers also maintain static awkward body postures for prolonged periods of time and, thus, cause mechanical stress on the spine and surrounding soft structures, which ultimately cause neck pain (Alperovitch-Najenson et al. 2010). It is important to note that adjustable equipment was found associated with a lower prevalence of pain (Simonsen et al. 2017). Ergonomic adjustment of the surrounding furniture and equipment to the anthropometry of the worker is warranted.

14.11 Evolutionary Perspective

In a study of 26 extant primate taxa, Nalley and Grider-Potter (2015) found that species with more pronograde (i.e., more perpendicular to the line of gravity) heads and necks exhibited cervical vertebral morphologies that indicate increased mechanical advantage for deep nuchal musculature and an emphasis on lordosis curve formation. Apes, however, lack the pronounced cervical lordosis seen in humans. Modern humans have a well-defined cervical lordosis that helps situate the head above the thorax in erect posture, whereas the head of quadrupedal apes is situated anterior to the thorax, with a small cervical lordosis (Schultz 1961; Filler 2007; Arlegi et al. 2017). Extinct hominins show a variety of cervical postures: australopithecines have nearly straight cervical lordosis (C0–C7 Cobb angle of 6.5–12°), well below the normal values for modern humans (C0–C7 Cobb angle of 38.68 ± 10.6°); Neandertals have moderate cervical lordosis (C0–C7 Cobb angle of 21.5–28°); and *Homo erectus* has cervical lordosis within the range of modern humans (C0–C7 Cobb angle of 28–43°) (Been et al. 2017a).

Cervical pathology in extinct and extant species can be observed on the vertebrae in the form of osteophytes, flat and enlarged facet joints, Schmorl's nodes, vertebral asymmetry, and other osteological changes. Very few scholars have explored cervical spine pathology in great apes. Jurmain (2000) found a low prevalence of cervical spine pathology in a cohort of wild great apes, while Lowenstine et al. (2016) found a high prevalence of cervical spine degeneration in captive aging great apes. Another anecdotal report (Lovell 1990) describes a cervical scoliosis deformity in a 55–60-year-old wild male gorilla. The contradictory results of these studies might result from age differences (young in the wild group and old in the captive group) or from differences in the habitat and activity between the ape groups.

Complete or nearly complete cervical spines are rarely found in the fossil record. Nevertheless, evidence for cervical pathology, i.e., osteophytes or facet joint osteoarthritis, is apparent. The earliest evidence is in the 3.58 Ma old KSD-VP-1/1 specimen (*Australopithecus afarensis*), which shows small to moderate osteophytes on the vertebral bodies of C4, C5, and C6 (Meyer 2016; Haeusler 2019).

Gómez-Olivencia et al. (2007) described the degenerative joint disease in the atlas and axis (C1–C2) of two different individuals from Sima de Los Huesos (SH) dated to c. 430 kya (Arsuaga et al. 2014). Degenerative changes, probably due to old age, are apparent in the cervical vertebrae of the 50 kya Neandertal individual from La Chapelle-aux-Saints 1, including osteophytes in the lower cervical spine and facet joint osteoarthritis (Trinkaus 1985; Gómez-Olivencia 2013b; Haeusler 2019). Similar degenerative changes were found in the cervical vertebrae of the Neandertals from Krapina (Gómez-Olivencia et al. 2013). Degenerative changes were also observed in the cervical spine (C1–C7) of the La Ferrassie 1 (LF1) Neandertal (Gómez-Olivencia 2013a; Gómez-Olivencia et al. 2018).

Many scholars have described cervical pathology in human populations during the Neolithic and Bronze Age (e.g. Lovell 1994; Gerszten et al. 2001; Pearson et al. 2005; Papathanasiou 2005; Köhler et al. 2014). The leading causes of cervical pathologies include age-related degenerative changes, traumatic changes due to falling or violence, congenital changes, and infectious diseases—the most common of which was tuberculosis. In at least one prehistoric human population, cervical spondylosis was determined to be the result of an occupational disease resulting from transporting heavy loads on the neck (Gerszten et al. 2001).

The current data regarding pathological changes in the cervical spines of hominoids is sparse and sometimes inconsistent. Therefore, it is hard to establish an explicit pattern of pathological changes or conclusions with regard to the impact of erect posture and bipedalism on the development and prevalence of cervical spine pathology. Future research exploring cervical pathology in captive/wild monkeys and apes could provide more information regarding some of these queries. A thorough research study regarding cervical pathology in all known cervical vertebrae of extinct hominins and in pre- and post-agricultural societies could help enlighten scholars as to the nature and prevalence of cervical pathology throughout human evolution, which might enhance our understanding of the effect of erect posture, bipedalism, and function on cervical pathology.

14.12 Conclusions

There are three major approaches to evaluate cervical alignment in modern humans. The first and most popular is the angular measurements, i.e., the Cobb angle or the posterior tangent methods. The second approach is to measure the ventrodorsal position of the upper cervical spine in relation to the lower cervical spine as in C2–C7 SVA. The third approach is to evaluate the cervical spine by its overall posture and dividing it into five categories: lordotic, straight, kyphotic, and two S shape configurations. Cervical alignment, whether described by angular measurements, dorsoventral position, or by cervical postural categories, is correlated with cervical pathology and with health-related quality of life. In the adult population, individuals with lordotic cervical spines [a Cobb angle (between C0 and C7) of

~40° ± 10 and SVA C2–C7 < 40 mm] have less pathology and a better quality of life. Individuals with a straight/kyphotic/S-shape cervical spine, a small Cobb angle, and SVA C2–C7 >40 mm exhibit greater cervical pathology, pain, and a lower quality of life. These findings suggest that individuals with cervical pathology might benefit from an improvement in cervical lordosis. Future studies should explore whether and how the correction of cervical alignment can reduce cervical pathology and pain.

Many factors influence the extent of cervical lordosis and its internal architecture, including age, sex, and morphology of the thorax, head, pelvis, and spine. Age has a strong influence on the extent of cervical lordosis and on the cervical postural category (lordotic, straight, kyphotic, and sigmoid). Young individuals are characterized by a lordotic cervical spine, but the degree of lordosis is age-related and develops in a non-linear way. Age also impacts the internal architecture of cervical lordosis, i.e., the intervertebral discs of younger individuals are more lordotic than the adult discs and the vertebral bodies of children are more kyphotic than the bodies of adults.

Sex is another factor influencing cervical lordosis. Although the total lordosis of males and females is similar, females exhibit greater upper cervical lordosis (C1–C3), whereas males have greater lower cervical lordosis (C3–C7). Males also have more lordotic intervertebral discs than females. Similar differences between the sexes are already apparent in young individuals. Many morphological features correlate with cervical lordosis. The most important features are those of the cervicothoracic junction –C7 or T1 slope; the craniofacial features, including mandibular morphology and the orientation of the foramen magnum; and the pelvic and lumbar posture. The interaction between these features is occasionally straightforward, i.e., the positive correlation between the T1 slope and the extent of cervical lordosis; however, occasionally, these correlations are harder to explain, i.e., the correlation between facial features and the extent of lordosis.

It is evident today that certain workers have neck pain more than others and that the prevalence of the neck pain might be greater than back pain. Neck pain appears generally in those who sit for long periods of time, i.e., mostly office workers. Forward head posture and sustained sitting associated with computer use are typical risk factors expressed by prolonged static trunk and neck postures that together with excessive stabilizing muscles cause neck pain. It is vital to develop adjustable furniture and equipment adapted to the worker's anthropometry.

The evolution of cervical lordosis in hominins is far from resolved. We do not know whether erect posture and accentuated cervical lordosis angles are possible contributions to the high prevalence of neck pain and dysfunction, or if they are mostly influenced by lifestyle and function. Future studies should explore the prevalence and nature of cervical pathology in extinct and extant hominoids and in pre- and post-agricultural societies. This might shed light on the different contributing factors to cervical pain, pathology, evolutionary components, and postural and/or functional mechanisms.

References

Abelin-Genevois K, Idjerouidene A, Roussouly P, Vital JM, Garin C (2014) Cervical spine alignment in the pediatric population: a radiographic normative study of 150 asymptomatic patients. Eur Spine J 23(7):1442–1448

Albert TJ, Vacarro A (1998) Postlaminectomy kyphosis. Spine 23(24):2738–2745

Alperovitch-Najenson D, Katz-Leurer M, Santo Y, Golman D, Kalichman L (2010) Upper body quadrant pain in bus drivers. Arch Environ Occup Health 65(4):218–223

Ames CP, Smith JS, Scheer JK, Bess S, Bederman SS, Deviren V, Lafage V, Schwab F, Shaffrey CI (2012) Impact of spinopelvic alignment on decision making in deformity surgery in adults: a review. J Neurosurg Spine 16(6):547–564

Ariëns GA, Bongers PM, Hoogendoorn WE, Houtman IL, van der Wal G, van Mechelen W (2001) High quantitative job demands and low coworker support as risk factors for neck pain: results of a prospective cohort study. Spine 26(17):1896–1901

Arlegi M, Gómez-Olivencia A, Albessard L, Martínez I, Balzeau A, Arsuaga JL, Been E (2017) The role of allometry and posture in the evolution of the hominin subaxial cervical spine. J Hum Evol 104:80–99

Arsuaga JL, Martínez I, Arnold LJ, Aranburu A, Gracia-Téllez A, Sharp WD, Quam RM, Falguères C, Pantoja-Pérez A, Bischoff J, Poza-Rey E, Parés JM, Carretero JM, Demuro M, Lorenzo C, Sala N, Martinón-Torres M, García N, Alcázar De Velasco A, Cuenca-Bescós G, Gómez-Olivencia A, Moreno D, Pablos A, Shen C-C, Rodríguez L, Ortega AI, García R, Bonmatí A, Bermúdez De Castro JM, Carbonell E (2014) Neandertal roots: cranial and chronological evidence from Sima de los Huesos. Science 344:1358–1363

Bagnall KM, Harris PF, Jones PR (1977) A radiographic study of the human fetal spine. 2. The sequence of development of ossification centres in the vertebral column. J Anat 124(Pt 3):791

Bayerl S, Wiendieck K, Koeppen D, Topalovic M, Übelacker A, Kroppenstedt S, Cabraja M (2013) Single-and multi-level anterior decompression and fusion for cervical spondylotic myelopathy - A long-term follow-up with a minimum of 5 years. Clin Neurol Neurosurg 115(10):1966–1971

Been E, Gómez-Olivencia A, Shefi S, Soudack M, Bastir M, Barash A (2017a) Evolution of spinopelvic alignment in hominins. Anat Rec 300(5):900–911

Been E, Shefi S, Soudack M (2017b) Cervical lordosis: the effect of age and gender. Spine J 17(6):880–888

Been E, Shefi S, Zilka LR, Soudack M (2014) Foramen magnum orientation and its association with cervical lordosis: a model for reconstructing cervical curvature in archeological and extinct hominin specimens. Adv Anthropol 4(03):133

Beltsios M, Savvidou O, Mitsiokapa EA, Mavrogenis AF, Kaspiris A, Efstathopoulos N, Papagelopoulos PJ (2013) Sagittal alignment of the cervical spine after neck injury. Eur J Orthop Surg Traumatol 23(1):47–51

Borden AB, Rechtman AM, Gershon-Cohen J (1960) The normal cervical lordosis. Radiology 74(5):806–809

Bovenzi M (2015) A prospective cohort study of neck and shoulder pain in professional drivers. Ergonomics 58(7):1103–1116

Boyle JJ, Milne N, Singer KP (2002) Influence of age on cervicothoracic spinal curvature: an ex vivo radiographic survey. Clin Biomech 17(5):361–367

Braaf MM, Rosner S (1975) Trauma of cervical spine as cause of chronic headache. J Trauma Acute Care Surg 15(5):441–446

Chen H, Zhong J, Tan J, Wu D, Jiang D (2013) Sagittal geometry of the middle and lower cervical endplates. Eur Spine J 22(7):1570–1575

Claes F, Berger J, Stassijns G (2015) Arm and neck pain in ultra-sonographers. Hum Factors 57(2):238–245

Clement CD (1985) Gray's anatomy, 13th edn. Lea & Febiger, Philadelphia, p 128

Cobb JR (1948) Outline for the study of scoliosis. Instructional Course Lectures AAOS 5:261–275

Cuccia AM, Lotti M, Caradonna D (2008) Oral breathing and head posture. Angle Orthod 78(1):77–82

Darivemula SB, Goswami K, Gupta SK, Salve H, Singh U, Goswami AK (2016) Work-related neck pain among desk job workers of tertiary care hospital in New Delhi, India: burden and determinants. Indian journal of community medicine: official publication of Indian Association of Preventive & social. Medicine 41(1):50

Ezra D, Masharawi Y, Salame K, Slon V, Alperovitch-Najenson D, Hershkovitz I (2017) Demographic aspects in cervical vertebral bodies' size and shape (C3–C7): a skeletal study. Spine J 17(1):135–142

Festa F, Tecco S, Dolci M, Ciufolo F, Meo SD, Filippi MR, Ferritto AL, D'Attillio M (2003) Relationship between cervical lordosis and facial morphology in Caucasian women with a skeletal class II malocclusion: a cross-sectional study. Cranio 21(2):121–129

Filler AG (2007) Emergence and optimization of upright posture among hominiform hominoids and the evolutionary pathophysiology of back pain. Neurosurg Focus 23(1):E4

Friedman MJ (2006) The evolution of hominid bipedalism. Honors Projects. 16. https://digitalcommons.iwu.edu/socanth_honproj/16

Gay RE (1993) The curve of the cervical spine: variations and significance. J Manip Physiol Ther 16(9):591–594

Gerszten PC, Gerszten E, Allison MJ (2001) Diseases of the spine in south American mummies. Neurosurgery 48(1):208–213

Gok B, Sciubba DM, McLoughlin GS, McGirt M, Ayhan S, Wolinsky JP, Bydon A, Gokaslan ZL, Witham TF (2008) Surgical treatment of cervical spondylotic myelopathy with anterior compression: a review of 67 cases. J Neurosurg Spine 9(2):152–157

Gómez-Olivencia A (2013a) The presacral spine of the La Ferrassie 1 Neandertal: a revised inventory. Bulletins et Mémoires de la Societé d'Anthropologie de Paris 25:19–38

Gómez-Olivencia A (2013b) Back to the old man's back: reassessment of the anatomical determination of the vertebrae of the Neandertal individual of La Chapelle-aux-saints. Annales de Paléontologie 99:43–65

Gómez-Olivencia A, Been E, Arsuaga JL, Stock JT (2013) The Neandertal vertebral column 1: the cervical spine. J Hum Evol 64(6):608–630

Gómez-Olivencia A, Carretero JM, Arsuaga JL, Rodríguez-García L, García-González R, Martínez I (2007) Metric and morphological study of the upper cervical spine from the Sima de Los Huesos site (sierra de Atapuerca, Burgos, Spain). J Hum Evol 53(1):6–25

Gómez-Olivencia A, Quam R, Sala N, Bardey M, Ohman JC, Balzeau A (2018) La Ferrassie 1: new perspectives on a "classic" Neandertal. J Hum Evol 117:13–32

Gore DR, Sepic SB, Gardner GM (1986) Roentgenographic findings of the cervical spine in asymptomatic people. Spine 11(6):521–524

Grave B, Brown T, Townsend G (1999) Comparison of cervicovertebral dimensions in Australian aborigines and Caucasians. Eur J Orthod 21(2):127–135

Grob D, Frauenfelder H, Mannion AF (2007) The association between cervical spine curvature and neck pain. Eur Spine J 16(5):669–678

Grosso MJ, Hwang R, Mroz T, Benzel E, Steinmetz MP (2013) Relationship between degree of focal kyphosis correction and neurological outcomes for patients undergoing cervical deformity correction surgery. J Neurosurg Spine 18(6):537–544

Haeusler M (2019) Spinal pathologies in fossil hominins. In: Been E, Gómez-Olivencia A, Kramer PA (eds) Spinal evolution: morphology, function, and pathology of the spine in hominoid evolution. Springer, New York, pp 213–246

Hardacker JW, Shuford RF, Capicotto PN, Pryor PW (1997) Radiographic standing cervical segmental alignment in adult volunteers without neck symptoms. Spine 22(13):1472–1479

Harrison DE, Harrison DD, Cailliet R, Troyanovich SJ, Janik TJ, Holland B (2000) Cobb method or Harrison posterior tangent method: which to choose for lateral cervical radiographic analysis. Spine 25(16):2072–2078

Harrison DD, Janik TJ, Troyanovich SJ, Holland B (1996) Comparisons of lordotic cervical spine curvatures to a theoretical ideal model of the static sagittal cervical spine. Spine 21(6):667–675

Hayes MJ, Osmotherly PG, Taylor JA, Smith DR, Ho A (2016) The effect of loupes on neck pain and disability among dental hygienists. Work 53(4):755–762
Helliwell PS, Evans PF, Wright V (1994) The straight cervical spine: does it indicate muscle spasm? J Bone Joint Surg 76(1):103–106
Huggare J, Houghton P (1996) Associations between atlantoaxial and craniomandibular anatomy. Growth Dev Aging 60(1):21–30
Jackson RP, McManus AC (1994) Radiographic analysis of sagittal plane alignment and balance in standing volunteers and patients with low back pain matched for age, sex, and size. A prospective controlled clinical study. Spine 19(14):1611–1618
Juhl JH, Miller SM, Roberts GW (1962) Roentgenographic variations in the normal cervical spine. Radiology 78(4):591–597
Jun HS, Chang IB, Song JH, Kim TH, Park MS, Kim SW, Oh JK (2014) Is it possible to evaluate the parameters of cervical sagittal alignment on cervical computed tomographic scans? Spine 39(10):E630–E636
Jun D, Zoe M, Johnston V, O'Leary S (2017) Physical risk factors for developing non-specific neck pain in office workers: a systematic review and meta-analysis. Int Arch Occup Environ Health 90(5):373–410
Jurmain RD (2000) Degenerative joint disease in African great apes: an evolutionary perspective. J Hum Evol 39:185–203
Kasai T, Ikata T, Katoh S, Miyake R, Tsubo M (1996) Growth of the cervical spine with special reference to its lordosis and mobility. Spine 21(18):2067–2073
Köhler K, Pálfi G, Molnár E, Zalai-Gaál I, Osztás A, Bánffy E, Kirinó K, Kiss KK, Mende BG (2014) A late Neolithic case of Pott's disease from Hungary. Int J Osteoarchaeol 24(6):697–703
Le Huec JC, Demezon H, Aunoble S (2015) Sagittal parameters of global cervical balance using EOS imaging: normative values from a prospective cohort of asymptomatic volunteers. Eur Spine J 24(1):63–71
Lee SH, Kim KT, Seo EM, Suk KS, Kwack YH, Son ES (2012) The influence of thoracic inlet alignment on the craniocervical sagittal balance in asymptomatic adults. J Spinal Disord Tech 25(2):E41–E47
Ling FP, Chevillotte T, Thompson W, Bouthors C, Le Huec JC (2018) Which parameters are relevant in sagittal balance analysis of the cervical spine? A literature review. Eur Spine J 27:1–8
Lovell NC (1990) Skeletal and dental pathology of free-ranging mountain gorillas. Am J Phys Anthropol 81(3):399–412
Lovell NC (1994) Spinal arthritis and physical stress at bronze age Harappa. Am J Phys Anthropol 93(2):149–164
Lowenstine LJ, McManamon R, Terio KA (2016) Comparative pathology of aging great apes: bonobos, chimpanzees, gorillas, and orangutans. Vet Pathol 53(2):250–276
Machino M, Yukawa Y, Imagama S, Ito K, Katayama Y, Matsumoto T, Inoue T, Ouchida J, Tomita K, Ishiguro N, Kato F (2016) Age-related and degenerative changes in the osseous anatomy, alignment, and range of motion of the cervical spine: a comparative study of radiographic data from 1016 patients with cervical spondylotic myelopathy and 1230 asymptomatic subjects. Spine 41(6):476–482
Marchiori DM, Henderson CN (1996) A cross-sectional study correlating cervical radiographic degenerative findings to pain and disability. Spine 21(23):2747–2751
Markuske H (1979) Relationships between the height of intervertebral discs and the degree of lordosis of the cervical spine in children. A roentgenometric study. Anat Anz 145(3):286–292
Martin BI, Deyo RA, Mirza SK, Turner JA, Comstock BA, Hollingworth W, Sullivan SD (2008) Expenditures and health status among adults with back and neck problems. JAMA 299(6):656–664
Meyer MR (2016) The cervical vertebrae of KSD-VP-1/1. In: Haile-Selassie Y, Su D (eds) The postcranial anatomy of *Australopithecus afarensis*: new insights from KSD-VP-1/1. Springer, New York, pp 63–111
Mohanty C, Massicotte EM, Fehlings MG, Shamji MF (2015) Association of preoperative cervical spine alignment with spinal cord magnetic resonance imaging hyperintensity and myelopathy severity: analysis of a series of 124 cases. Spine 40(1):1–16

Moore KL, Dalley AF, Agur AM (2013) Clinically oriented anatomy. Lippincott Williams & Wilkins, Baltimore, MD

Nagasawa A, Sakakibara T, Takahashi A (1993) Roentgenographic findings of the cervical spine in tension-type headache. Headache 33(2):90–95

Nalley TK, Grider-Potter N (2015) Functional morphology of the primate head and neck. Am J Phys Anthropol 156(4):531–542

Nejati P, Lotfian S, Moezy A, Nejati M (2015) The study of correlation between forward head posture and neck pain in Iranian office workers. Int J Occup Med Environ Health 28(2):295

Núñez-Pereira S, Hitzl W, Bullmann V, Meier O, Koller H (2015) Sagittal balance of the cervical spine: an analysis of occipitocervical and spinopelvic interdependence, with C-7 slope as a marker of cervical and spinopelvic alignment. J Neurosurg Spine 23(1):16–23

O'Rahilly R, Muller F, Meyer DB (1980) The human vertebral column at the end of the embryonic period proper. 1. The column as a whole. J Anat 131(Pt 3):565

Oe S, Togawa D, Yoshida G, Hasegawa T, Yamato Y, Kobayashi S, Yasuda T, Banno T, Mihara Y, Matsuyama Y (2017) Difference in spinal sagittal alignment and health-related quality of life between males and females with cervical deformity. Asian Spine J 11(6):959–967

Ohara A, Miyamoto K, Naganawa T, Matsumoto K, Shimizu K (2006) Reliabilities of and correlations among five standard methods of assessing the sagittal alignment of the cervical spine. Spine 31(22):2585–2591

Okada M, Minamide A, Endo T, Yoshida M, Kawakami M, Ando M, Hashizume H, Nakagawa Y, Maio K (2009) A prospective randomized study of clinical outcomes in patients with cervical compressive myelopathy treated with open-door or French-door laminoplasty. Spine 34(11):1119–1126

Owens E (1990) Cervical curvature assessment using digitized radio-graphic analysis. Chiropractic Res J 4:47–62

Pal GP, Sherk HH (1988) The vertical stability of the cervical spine. Spine 13(5):447–449

Papathanasiou A (2005) Health status of the Neolithic population of Alepotrypa cave, Greece. Am J Phys Anthropol 126(4):377–390

Pearson MP, Chamberlain A, Craig O, Marshall P, Mulville J, Smith H, Chenery C, Collins M, Cook G, Craig G, Evans JA, Hiller J, Montgomery J, Schwenninger JL, Taylor G, Wess T (2005) Evidence for mummification in bronze age Britain. Antiquity 79(305):529–546

Petit A, Bodin J, Delarue A, D'Escatha A, Fouquet N, Roquelaure Y (2018) Risk factors for episodic neck pain in workers: a 5-year prospective study of a general working population. Int Arch Occup Environ Health 91(3):251–261

Polly DW Jr, Kilkelly FX, McHale KA, Asplund LM, Mulligan M, Chang AS (1996) Measurement of lumbar lordosis: evaluation of intraobserver, interobserver, and technique variability. Spine 21(13):1530–1535

Prasarn ML, Baria D, Milne E, Latta L, Sukovich W (2012) Adjacent-level biomechanics after single versus multilevel cervical spine fusion. J Neurosurg Spine 16(2):172–177

Protopsaltis TS, Scheer JK, Terran JS, Smith JS, Hamilton DK, Kim HJ, Mundis GM Jr, Hart RA, McCarthy IM, Klineberg E, Lafage V (2015) How the neck affects the back: changes in regional cervical sagittal alignment correlate to HRQOL improvement in adult thoracolumbar deformity patients at 2-year follow-up. J Neurosurg Spine 23(2):153–158

Refshauge KM, Goodsell M, Lee M (1994) The relationship between surface contour and vertebral body measures of upper spine curvature. Spine 19(19):2180–2185

Scheer JK, Tang JA, Smith JS, Acosta FL Jr, Protopsaltis TS, Blonde B, Bess S, Shaffrey CI, Deviren V, Lafage V, Schwab F (2013) Cervical spine alignment, sagittal deformity, and clinical implications: a review. J Neurosurg Spine 19(2):141–159

Schultz AH (1961) Vertebral column and thorax. In: Hofer H, Schultz AH, Stark D (eds) Primatologia, vol 4. Karger, Basel, pp 1–46

Shilton M, Branney J, Vries BP, Breen AC (2015) Does cervical lordosis change after spinal manipulation for non-specific neck pain? A prospective cohort study. Chiropr Man Therap 23(1):33

Simonsen JG, Axmon A, Nordander C, Arvidsson I (2017) Neck and upper extremity pain in sonographers–associations with occupational factors. Appl Ergon 58:245–253

Smith JS, Lafage V, Ryan DJ, Shaffrey CI, Schwab FJ, Patel AA, Brodke DS, Arnold PM, Riew KD, Traynelis VC, Radcliff K (2013) Association of myelopathy scores with cervical sagittal balance and normalized spinal cord volume: analysis of 56 preoperative cases from the AOSpine North America myelopathy study. Spine 38(22S):S161–S170

Smith L, Louw Q, Crous L, Grimmer-Somers K (2009) Prevalence of neck pain and headaches: impact of computer use and other associative actors. Cephalalgia 29(2):250–257

Smith A, O'Sullivan P, Straker L (2008) Classification of sagittal thoraco-lumbo-pelvic alignment of the adolescent spine in standing and its relationship to low back pain. Spine 33(19):2101–2107

Sonnesen L, Pedersen CE, Kjær I (2007) Cervical column morphology related to head posture, cranial base angle, and condylar malformation. Eur J Orthod 29(4):398–403

Tahara R, Motegi E, Nomura M, Tsuchiya Y, Shino T, Inoue E, Sueishi K, Matsuda I (2008) Curvature of cervical vertebra in 8020 achievers observed by lateral cephalogram. Bull Tokyo Dent Coll 49(1):15–21

Tornqvist EW, Hagberg M, Hagman M, Risberg EH, Toomingas A (2009) The influence of working conditions and individual factors on the incidence of neck and upper limb symptoms among professional computer users. Int Arch Occup Environ Health 82(6):689–702

Trinkaus E (1985) Pathology and the posture of the La Chapelle-aux-saints Neandertal. Am J Phys Anthropol 67(1):19–41

Uchida K, Nakajima H, Sato R, Yayama T, Mwaka ES, Kobayashi S, Baba H (2009) Cervical spondylotic myelopathy associated with kyphosis or sagittal sigmoid alignment: outcome after anterior or posterior decompression. J Neurosurg Spine 11(5):521–528

Visscher CM, Naeije M (1998) The relationship between posture and curvature of the cervical spine. J Manip Physiol Ther 21(6):388–391

Wang VY, Chou D (2007) The cervicothoracic junction. Neurosurg Clin N Am 18(2):365–371

Yoon SY, Moon HI, Lee SC, Eun NL, Kim YW (2018) Association between cervical lordotic curvature and cervical muscle cross-sectional area in patients with loss of cervical lordosis. Clin Anat 31(5):716–723

Yu M, Zhao WK, Li M, Wang SB, Sun Y, Jiang L, Wei F, Liu XG, Zeng L, Liu ZJ (2015) Analysis of cervical and global spine alignment under Roussouly sagittal classification in Chinese cervical spondylotic patients and asymptomatic subjects. Eur Spine J 24(6):1265–1273

Yukawa Y, Kato F, Suda K, Yamagata M, Ueta T (2012) Age-related changes in osseous anatomy, alignment, and range of motion of the cervical spine. Part I: Radiographic data from over 1,200 asymptomatic subjects. European Spine Journal 21(8):1492–1498.

Zhu W, Sha S, Liu Z, Li Y, Xu L, Zhang W, Qiu Y, Zhu Z (2018) Influence of the occipital orientation on Cervical Sagittal Alignment: a prospective radiographic study on 335 normal subjects. Sci Rep 8(1):15336

Chapter 15
How to Build a 3D Model of a Fossil Hominin Vertebral Spine Based on Osseous Material

Ella Been, Tatiana Waintraub, Asier Gómez-Olivencia, Leonid Kalichman, Patricia Ann Kramer, Sara Shefi, Michalle Soudack, and Alon Barash

15.1 Introduction

Reconstructing the spine of fossil hominins and individuals from archaeological sites can provide important information to advance the understanding of their paleobiology and pathology (Trinkaus 1985; Bonmatí et al. 2010; Been et al. 2017a) because spinal posture has important biomechanical, locomotor, and pathological implications (Vialle et al. 2005; Been and Kalichman 2014; Castillo and Lieberman 2017). Etymologically, "reconstruction" means to construct or to assemble again. Reconstruction of the spinal column based on osteological material requires (1) the presence of complete or nearly complete vertebrae; (2) proper alignment of consecutive vertebrae; (3) overcoming the absence of the soft tissues; and (4) determining the spinal curvatures that were present when the individual was alive and reconstructing the spine accordingly.

E. Been (✉)
Department of Sports Therapy, Faculty of Health Professions, Ono Academic College, Kiryat Ono, Israel

Department of Anatomy and Anthropology, Sackler Faculty of Medicine, Tel Aviv University, Tel Aviv, Israel

T. Waintraub
Department of Anatomy and Anthropology, Sackler Faculty of Medicine, Tel Aviv University, Tel Aviv, Israel

A. Gómez-Olivencia
Departamento de Estratigrafía y Paleontología, Facultad de Ciencia y Tecnología, Universidad del País Vasco/Euskal Herriko Unibertsitatea (UPV/EHU), Leioa, Spain

IKERBASQUE. Basque Foundation for Science, Bilbao, Spain

Centro Mixto UCM-ISCIII de Evolución y Comportamiento Humanos, Madrid, Spain

L. Kalichman
Department of Physical Therapy, Recanati School for Community Health Professions, Faculty of Health Sciences at the Ben-Gurion University of the Negev, Beer-Sheva, Israel

E. Been et al. (eds.), *Spinal Evolution*,
https://doi.org/10.1007/978-3-030-19349-2_15

Due to these difficulties, few attempts to reconstruct the complete spine of an extinct hominin have been accomplished. For example, until recently the only reconstruction of the spine of Neandertals was a plaster reconstruction of a complete Neandertal skeleton by Sawyer and Maley (2005), based on the vertebrae of Kebara 2 (thoracic and lumbar vertebrae, sacrum) and La Ferrassie 1 (cervical vertebrae). This reconstruction is missing the unique features of the Neandertal vertebral spine, such as the hypolordotic lumbar (Been et al. 2012, 2014a; Gómez-Olivencia et al. 2017) and cervical spines (Been et al. 2017c). Recently, Been et al. (2017a) published a 3D reconstruction of the thoracic, lumbar, and sacral spine of Kebara 2, but this reconstruction lacks the cervical spine.

The spinal column can be reconstructed either by using casts of the original bones (Sawyer and Maley 2005) or by using 3D models of the original bones (Been et al. 2017a) and both methods enable new insights regarding spinal alignment of the reconstructed individual. First, knowing the length of the spine makes stature estimation more accurate. Second, the interaction between spinal curvatures can be easily observed. Third, spinal balance can be obtained by measuring the position of C2/C7/T4 plumb lines in relation to different vertebral levels. This information is important in order to establish posture and equilibrium of the reconstructed individual (Been et al. 2017a).

Spinal reconstruction is the first step in achieving a reconstruction of the thorax (Gómez-Olivencia et al. 2018) and the pelvis in order to provide information regarding the pelvic/thorax ratio. This ratio has implications for the reconstruction of the breathing mechanism and of locomotion. Adding muscles, discs, and ligaments to the geometric model generated by the reconstructed spinal column enables a biomechanical simulation of spinal and pelvic motion in different activities. Spinal reconstruction is the basis for estimating body bauplan—the structural body plan that characterizes a group of organisms and, especially, a major taxon.

Researchers face many difficulties in reconstructing the spine and spinal posture of an individual based on osseous material alone. These difficulties are due to the absence of soft tissues, especially the absence of the intervertebral discs (Been et al. 2017a). In the presence of a complete set of vertebrae (C1–L5), the major questions a researcher should ask when attempting a reconstruction of a spine are as follows:

P. A. Kramer
Departments of Anthropology and Orthopaedics and Sports Medicine, University of Washington, Seattle, WA, USA

S. Shefi
Department of Sports Therapy, Faculty of Health Professions, Ono Academic College, Kiryat Ono, Israel

M. Soudack
Sackler School of Medicine, Tel Aviv University, Tel Aviv, Israel

Department of Diagnostic Imaging, Sheba Medical Center, Tel Hashomer, Israel

A. Barash
The Azrieli Faculty of Medicine, Bar Ilan University, Safed, Israel

(1) How far apart should consecutive vertebrae be from each other, or in other words, what size and shape disc should be placed between consecutive vertebrae; and (2) What degree of curvature should be present in the three major spinal curvatures, i.e., cervical and lumbar lordosis and thoracic kyphosis?

The size and shape of the intervertebral discs in modern humans in relatively well known (Goh et al. 1999; Kunkel et al. 2011; Been et al. 2017c; Zhang et al. 2018), but only limited data on the size and shape of the intervertebral discs in hominoids are available (Been et al. 2010a).

Spinal curvature is intimately linked to posture: different postures—whether in standing, sitting, or supine position—result from differences in spinal curvatures (Chevillotte et al. 2018). The habitual posture for humans is upright standing; consequently, this posture is the most relevant for describing and evaluating spinal curvatures. For many years, researchers have defined the spinal curvatures of extinct hominins as human-like or not (Trinkaus 1985; Sanders 1998; Haeusler et al. 2002; Williams et al. 2013). This definition is vague due to the high variability of spinal curvature in modern humans. For example, the range of normal lumbar lordosis of modern humans is 30–80° (Been and Kalichman 2014) while the normal cervical lordosis is between 20 and 60° (Hardacker et al. 1997; Been et al. 2017c). Consequently, describing the spine of a fossil hominin as human-like provides little information about its curvature.

No widely accepted definitions of hyper- or hypolumbar lordosis exist. Most researchers agree, however, that the range of standing lordosis is between 30 and 80°, with the average lumbar lordosis (L1–S1) between 50 and 60° and the standard deviations of 10° (Schwab et al. 2006; Damasceno et al. 2006; Barrey et al. 2007; Been et al. 2010b; Yang et al. 2013; Le Huec and Hasegawa 2016). Based on these values, we can divide the range of 30–80 of lordosis into three major parts, normal, hyper-, and hypolordosis. Normal lordosis is between 35°/40° and 70°/75°, hyperlordosis is above 70°/75°, and hypolordosis is below 35°/40°. Each of these lordotic curvature ranges has associated biomechanical/pathological characteristics and concurrent functional advantages and disadvantages. The biomechanical and pathological aspects related to different postures are discussed in other chapters in this volume (i.e., Been et al. 2019; Been and Bailey 2019).

Despite the variability in observed curvatures in modern humans, proper reconstruction of the spine and spinal curvatures can, however, provide a more accurate estimation of the posture of bioarcheological and paleoanthropological material. Reconstruction has the possibility of enhancing our understanding of the evolutionary pathway of erect posture, as well as the functional, biomechanical, and pathological aspects of the specimens (Sawyer and Maley 2005; Been et al. 2017a; Gómez-Olivencia et al. 2017).

Until recently, few studies offered reliable methods for assessing spinal posture based solely on osteological material (e.g., Cleuvenot 1999), but this situation has been rectified. Peleg et al. (2007) demonstrated how to establish sacral orientation within the pelvic girdle. Been et al. (2007, 2012, 2014a) established methods for calculating the lordotic curvature of the lumbar spine, and Goh et al. (1999) offered a way to reconstruct thoracic kyphosis. Been et al. (2014b, 2017b)

established a method for calculating cervical lordosis based on the orientation of the foramen magnum compared to the Frankfurt horizontal plane. A new method for calculating thoracic kyphosis (T4–T12), based on vertebral wedging, will be presented here for the first time. In this volume, Bastir et al. (2019) present a new approach for the reconstruction of the thoracic and lumbar spine based on geometric morphometric.

All of the reconstruction methods are based on extant taxa because only they have both osseous and soft tissue available to examine. That raises the following questions: what is the appropriate reference taxon for a reconstruction? For hominins, should the reconstruction be based on modern humans alone, because only humans are bipeds, or should we base the reconstruction on both bipedal humans and on quadrupedal nonhuman hominoids? Should we use the same reference taxa and reconstruction methods for Pliocene, lower, Middle, and Late Pleistocene hominins?

The aim of this chapter is to provide a comprehensive methodological approach for the 3D virtual reconstruction of the spine of fossil hominins, from the sacrum through the cervical spine, based solely on osseous material. We propose a method based on two steps: first, we align the consecutive vertebrae, starting inferiorly, taking into consideration the available information on disc size and shape. Second, based on regression equations, we estimate the orientation of the sacrum and the degree of the different spinal curvatures (lumbar lordosis, thoracic kyphosis, and cervical lordosis) and adjust the model appropriately. These estimates of curvature are based on measurements of the isolated vertebrae. We have applied this methodology to reconstruct the complete spine of the Kebara 2 Neandertal. In this chapter, we first recapitulate our previous work on reconstructing the intervertebral discs and summarize the current information on intervertebral disc size and shape in modern humans and in other primates. Then, we discuss the different methods for the reconstruction of spinal curvatures based on skeletal material and examine their advantages and disadvantages.

The virtual 3D reconstruction of a fossil hominin spine can be done using various software packages that handle 3D virtual objects (e.g., Amira, Avizo, Meshlab). Data can be derived from either CT or surface scans of the fossil materials. In this particular case, we have derived 3D objects from medical CT scans of the Kebara 2 individual and the virtual reconstruction was done using Amira (Thermo Fisher Scientific, Berlin).

15.2 Intervertebral Disc Reconstruction

In order to conduct a full spinal reconstruction based on osseous material and to align properly two consecutive vertebrae, the absence of intervertebral discs must be overcome. Two major questions concern the discs: what is the disc height and what is the disc shape (specifically, is it wedged and if so, how and to what degree)?

15.2.1 Disc Height

Although average disc height for modern humans can be obtained from several sources (Goh et al. 1999; Kunkel et al. 2011; Zhang et al. 2018), the disc height of extinct hominins will remain an approximation. To overcome this problem, we relied on the facet joints to limit the possible thickness and shape of the disc. In upright standing, the inferior articular facet of one vertebra and the superior articular facet of the following vertebra are congruent (Simon et al. 2012). Adjusting the superior vertebrae on top of the inferior one, based on facet congruency on the right and the left sides, allows us to position the vertebrae and determine the relative position of the vertebral bodies and hence the height of the disc between the vertebral bodies.

15.2.2 Disc Wedging

When viewed laterally, intervertebral discs, like vertebrae, are not rectangular. Most intervertebral discs, including the cervical discs, the lower thoracic discs, and the lumbar discs (Table 15.1), exhibit lordotic wedging, meaning that the ventral height of the disc is greater than the dorsal height. The discs in the middle thorax are either rectangular (i.e., not wedged) or have a slightly kyphotic wedging (Table 15.1). Little is known about the wedging of the intervertebral discs of nonhuman extant hominoids or other primates. In the lumbar spine, both the genus *Macaca* and great apes have lordotic intervertebral discs similar to modern humans (Table 15.1). Unfortunately, the wedging of the intervertebral discs of nonhuman primates in the thoracic or cervical spines remains undefined. Additionally, it should be kept in mind (1) that the total number of pre-sacral vertebrae and the number of thoracic and lumbar vertebrae differs among primate species (Pilbeam 2004; Williams et al. 2016, 2019) and (2) that postures among this mammal order differ with substantial biomechanical and anatomical consequences, even between closely related species, such as modern humans, chimpanzees, and gorillas.

For the reconstruction of disc wedging of *H. sapiens*, the values presented in Table 15.1 can be used. For the reconstruction of disc wedging in extinct hominins, several features should be taken into account: curvatures of the spine (lumbar lordosis, thoracic kyphosis, or cervical lordosis), facet joint congruency, and disc wedging of modern humans and/or extant hominoids. When reconstructing a lumbar spine, we recommend applying lordotic wedging to each of the five lumbar discs as both humans, nonhuman hominoids, and *Macaca* have lordotic discs in the lumbar spine. For the reconstruction of the thoracic and cervical spines, we recommend adjusting the vertebrae based on facet joint congruency and total calculated curvature because no reference for disc wedging in nonhuman hominoids is currently available.

Table 15.1 Intervertebral disc wedging (in°) of extant hominoids and *Macaca*

Disc level	*Homo sapiens*			*Pan*	*Pongo*	Hylobatids	*Macaca*
Cervical spine (Been et al. 2017c)							
	Male (n = 53) Mean (SD)	Female (n = 48) Mean (SD)	All (n = 101) Mean (SD)				
C2–3	4.4 (3.2)	3.7 (4.7)	4.0 (4.0)				
C3–4	4.6 (3.9)	3.5 (4.4)	4.1 (4.1)				
C4–5	4.4 (3.5)	2.7 (3.9)	3.6 (3.8)				
C5–6	4.7 (4.1)	4.0 (2.9)	4.3 (3.6)				
C6–7	4.7 (3.6)	3.9 (2.8)	4.3 (3.3)				
Thoracic spine, current study[a]							
	Male n = 17 Mean (SD)	Female n = 30 Mean (SD)	All n = 50 Mean (SD)				
T3–4	−0.9 (1.8)	−1.6 (1.5)	−1.3 (1.6)				
T4–5	−1.0 (2.4)	−0.8 (1.6)	−0.9 (1.9)				
T5–6	−0.4 (1.9)	−0.5 (1.9)	−0.4 (1.9)				
T6–7	−0.4 (1.9)	0.0 (2.2)	−0.2 (2.1)				
T7–8	0.2 (1.9)	0.5 (2.0)	0.3 (2.0)				
T8–9	0.9 (2.0)	1.0 (2.0)	1.0 (2.0)				
T9–10	1.0 (1.8)	1.0 (1.9)	1.0 (1.9)				
T10–11	1.0 (2.6)	1.3 (2.0)	1.2 (2.3)				
T11–12	3.3 (2.7)	2.6 (2.6)	2.9 (2.6)				
T12–L1			3.5 Vialle et al. (2005)				
Lumbar spine (Been et al. 2010a)							
	Male n = 53 Mean (SD)	Female n = 47 Mean (SD)	All n = 100 Mean (SD)	n = 1	n = 1	n = 1	n = 56 Mean (SD)
L1–2	6.5 (3.0)	5.4 (3.7)	6.0 (3.3)	2	12	4	5.3 (4.1)
L2–3	7.0 (2.9)	7.6 (2.7)	7.3 (2.8)	9	5	3	6.2 (4.5)
L3–4	9.1 (3.1)	8.9 (3.4)	9.0 (3.2)	6	6	4	7.8 (4.8)
L4–5	11.4 (3.7)	11.1 (3.7)	11.3 (3.7)	13	7	9	9.2 (4.4)
L5–S1	11.7 (3.7)	12.0 (4.9)	11.8 (4.3)	11	3	8	11.2 (6.3)
Lumbar spine (Bailey et al. 2014)							
	Male N = 73 Mean (SE)	Female N = 121 Mean (SE)					
L1–2	5.5 (0.3)	5.3 (0.4)					
L2–3	6.8 (0.3)	6.8 (0.3)					
L3–4	8.1 (0.3)	8.1 (0.3)					
L4–5	11.4 (0.4)	10.9 (0.5)					
L5–S1	15.1 (0.6)	15.1 (0.8)					

SD standard deviation, *SE* standard error. Positive values indicate lordotic wedging. Negative values indicate kyphotic wedging. T test between disc wedging of males to that of females revealed no difference ($p > 0.05$) between the sexes at all spinal levels

[a]These results are based on the thoracic radiographs of 50 standing adult humans

In order to reconstruct the intervertebral disc height of Kebara 2, we used the disc heights of modern humans (Goh et al. 1999; Kunkel et al. 2011; Zhang et al. 2018). Beginning from the sacrum, we aligned each vertebra in the sagittal, coronal, and horizontal planes to the vertebra immediately inferior to it. Each vertebra was positioned such that the articular processes of the inferior and superior facets of the adjacent vertebrae were parallel to each other and the distance between them was 1–2 mm, which is similar to the value seen in modern humans (Simon et al. 2012). The full reconstruction of the Kebara 2 spine, from the sacrum to the first cervical vertebra is shown in Fig. 15.2a–c.

15.3 Estimation of Sacral Orientation and Spinal Curvatures

15.3.1 Estimation of the Sacral Orientation

Two complementary approaches to describe and reconstruct the orientation of the sacrum in relation to the pelvis exist: pelvic incidence (PI) and sacral anatomical angle (SAA) (Peleg et al. 2007).

Pelvic Incidence (PI)

PI measures the orientation of the sacral superior surface in relation to the hip joint (Fig. 15.1a) (Duval-Beaupère et al. 1992; Legaye et al. 2007; Peleg et al. 2007; Been et al. 2014a) and is defined as the angle between a line drawn perpendicular to the superior surface of the first sacral vertebra (S1) at its midpoint (the center of the sagittal diameter) and the line connecting this point to an axis that connects the center of the acetabula (Legaye et al. 2007; Legaye and Duval-Beaupère 2008)

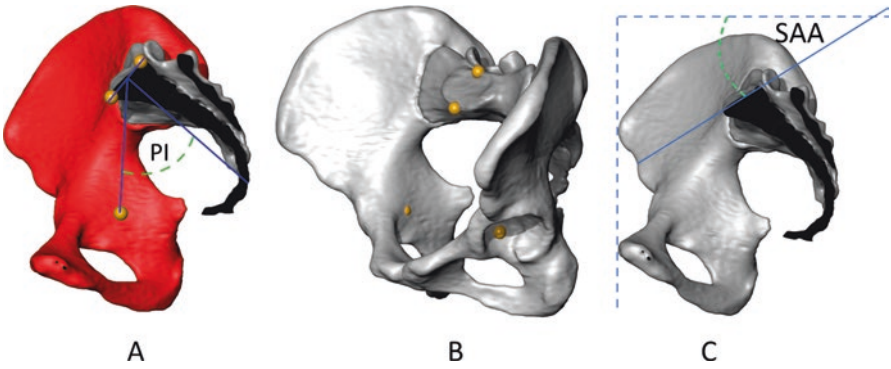

Fig. 15.1 Pelvic incidence (PI) and sacral anatomical angle (SAA). (**a**) Measurement of pelvic incidence; (**b**) the four points used to calculate PI using a Micro-scribe or a 3D pelvic model; (**c**) SAA, similar to sacral slope in an erect posture

(Fig. 15.1a). In functional terms, PI measures the orientation of the S1 superior surface to the axis of rotation of the body on the hind limbs.

PI can only be measured on articulated pelves, using either a radiological or a digital approach. In the radiological approach, PI is measured on plain lateral pelvic radiographs. Lines are drawn on the radiograph and measurements are conducted following the method of Legaye et al. (1998) (Fig. 15.1a). In the digital approach, four anatomical landmarks are used, including two on the superior surface of the first sacral vertebra (at the ventral and dorsal edge of the vertebral endplate in the midsagittal plane) and two at the centers of the acetabula (Fig. 15.1b). The XYZ coordinates of each landmark are recorded using a 3D Micro-scribe directly from the bone or on a 3D pelvis reconstruction after the pelvis has been scanned. PI is calculated based on these four points as described by Peleg et al. (2007).

Sacral Anatomical Angle (SAA)

SAA measures the orientation of the sacral superior surface to the plane connecting the superior part of the pubic symphysis and the left and right anterior superior iliac spines (Peleg et al. 2007). This measurement is similar to sacral slope in living modern humans. This angle measures the orientation of the sacral endplate when the pelvis is held in anatomical position. The SAA can be measured in three ways: (1) on plain lateral pelvic radiographs, (2) by using the device and methods described by Peleg et al. (Peleg et al. 2007) (angle γ), and (3) directly on a 3D pelvic reconstruction (Fig. 1C). All three methods provide similar results (Peleg et al. 2007).

We measured the reconstructed pelvis of Kebara 2 that was made by Yoel Rak. Both the PI (36°) and the SAA (19°) of Kebara 2 indicate an orientation of the sacral superior surface that is 20–22° less vertical (i.e., more horizontal) than that of the average modern human (Been et al. 2017a). The sacral superior surface of modern humans is aligned at an angle of 39–41° to the horizontal plane (Boulay et al. 2006; Legaye et al. 2007; Peleg et al. 2007; Mac-Thiong et al. 2010), but the alignment of the Kebara 2 sacral superior surface is 20° less vertical, at 21° to the horizontal plane (Fig. 15.2).

15.3.2 Estimation of Lumbar Lordosis

Lumbar lordosis, the ventral curvature of the lumbar spine, is defined here as the angle between the superior surface of the sacrum and the superior surface of the first lumbar vertebra (L1–S1) (Fig. 15.3). Lumbar lordosis results from the wedging of the lumbar vertebral bodies and the morphology of the intervertebral discs (Korovessis et al. 1998; Kimura et al. 2001; Vialle et al. 2005; Been et al. 2010b). Both equally influence the lordosis of the lumbar spine (Been et al. 2010b). Consequently, the major challenge in reconstructing the lumbar spine of Kebara 2 (and any other fossil hominin) is deciding how to overcome the absence of the

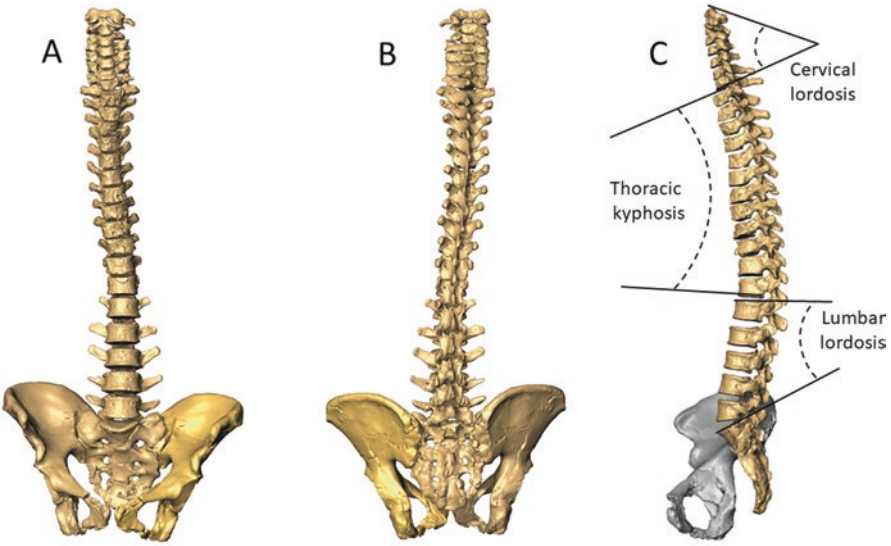

Fig. 15.2 A full reconstruction of the spine of the Kebara 2 Neandertal, from the first cervical vertebra to the last sacral vertebra. The pelvis of Kebara 2 is added for illustrative purposes but was not used in the reconstruction. (**a**) Anterior view; (**b**) posterior view; (**c**) lateral view with the three spinal curvatures

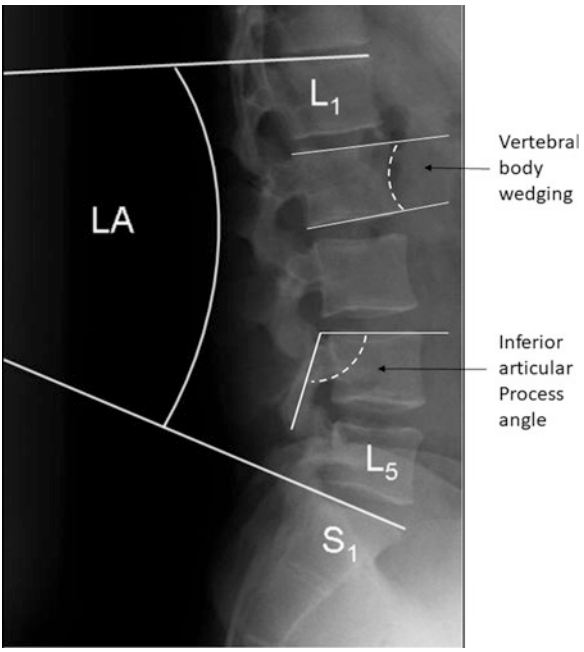

Fig. 15.3 Radiograph (lateral) of the lumbar spine of an adult human. LA, lumbar lordosis angle. *L1* first lumbar vertebra, *L5* fifth lumbar vertebra, *S1* first sacral vertebra

intervertebral discs. The methods to reconstruct lumbar lordosis based on osseous material all rely on the correlation between either the morphology of the pelvis or that of the lumbar vertebrae and the lumbar lordosis.

The first method, the inferior articular process angle (IAPA), is based on the correlation between the degree of lordosis and the orientation of the inferior articular processes of the lumbar vertebrae L1–L5 (Been et al. 2007, 2012). In this method, the orientation of the inferior articular process (IAPA), in relation to the superior surface, of each of the lumbar vertebrae is measured on a lateral spinal radiograph (Fig. 15.3). Lordosis is then calculated (using a regression formula) from the sum of the angles from L1 to L5 (Σ IAPA). If the reconstruction is for *H. sapiens*, then the formula based exclusively on modern humans should be used (Table 15.2). If the reconstruction is for an extinct hominin, then both formulae (i.e., the one based on modern humans and the other one based on extant hominoids) could be appropriate, depending on the species, so both should be considered. If substantial difference between the results of the formulae exist, then the average should be calculated and judgment should be used in the spine reconstruction. The IAPA method is more predictive and has a lower root mean square error compared to the other methods (Table 15.2). Its shortcoming, however, lies in the difficulty of measuring the inferior articular process angle. Also, this method has a higher predictive ability when all five vertebrae are available. If the IAPA is obtained from three or four

Table 15.2 The different methods for the calculation of lumbar lordosis (LA) and results of the application of these formulae to Kebara 2

Measurement	Sample	Formula (based on standard major axis technique)	R^2	Root mean square error (RMSE)	Kebara 2	Ref.
IAPA	Modern humans	LA = 0.565 × ΣIAPA (L1–L5) − 237	0.62	6.8°	26	Been et al. (2007)
	Modern humans and non-human hominoids	LA = 0.528 × ΣIAPA (L1–L5) − 220.5	0.95	4.0°	25	Been et al. (2012)
LLPI	Modern humans and non-human hominoids	LA = 0.999 × PI − 5.2	0.89	6.7°	29	Been et al. (2014a)
	Modern humans	LA = 0.718 × PI + 11.7	0.48	8.5°	36	Been et al. (2014a)
LVBW	Modern humans	LA = 0.511 × ΣB (L1–L5) + 48.3	0.22	9.6°	40.6	Been et al. (2007)
					Average LA: 31.3	

All of the formulae are based on regressions that are statistically significant $p < 0.05$
"Sample" refers to which sample was used to derive the regression equation shown in the column called "Formula". The column "Kebara 2" provides the value used in the reconstruction. *Ref* reference

lumbar vertebrae, then its predictive ability is reduced. This method should not be used based only on one or two lumbar vertebrae, because its predictive ability is minimal (Been et al. 2012). Thus, in order to calculate accurate lordosis estimations, fossil specimens which preserve a minimum of three lumbar vertebrae are necessary, a situation that is not often the case due to the general fragility of the vertebrae compared to other anatomical regions, such as mandibles or long bones.

The second method, lumbar lordosis based on PI (LLPI), depends on the correlation between PI and the degree of lordosis (Table 15.2; Been et al. 2013, 2014a). This is a simple method to use, providing that the pelvis is complete. Here again, formulae based on a sample of modern humans and based on extant hominoids exist (Table 15.2). The application of each formula depends on the taxonomical status of the specimen to be reconstructed. The shortcoming of this method is that its predictive ability is lower than the first method (IAPA) and its root mean square error is higher.

The third method estimates lordosis based on vertebral body wedging (LVBW) of L1–L5 (Been et al. 2007, 2012) (Fig. 15.3). In this method, the vertebral body wedging of the five lumbar vertebrae is measured and the sum of the wedging of the five vertebrae (ΣB) is used to predict the lordosis angle (Table 15.2). This method has the lowest predictive ability and the highest root mean square error and, therefore, should be used only if the other two methods cannot be used.

As with all reconstructions, the more consistency within the methods of prediction of lordosis, the more confidence one should have in the reconstruction. For the reconstruction of Kebara 2, we used the average of the methods. Figure 15.2 shows the reconstruction of the lumbar lordosis of Kebara 2, after Been et al. (2017a). The calculated lordosis for Kebara 2 (31.3°) is at the lower range of modern humans, indicating hypolordotic lumbar curvature. Neandertals, as a group, demonstrate a significantly lower degree of lordosis than do modern humans (Been et al. 2012, 2014a; Gómez-Olivencia et al. 2017).

15.3.3 Estimation of Thoracic Kyphosis

Thoracic kyphosis is the dorsal curvature of the thoracic spine, defined here as the angle between the inferior surface of the 12th thoracic vertebra (T12) and the superior surface of the first thoracic vertebra (T1) (Fig. 15.4). Similar to lumbar lordosis, thoracic kyphosis is the result of the wedging of the thoracic vertebral bodies and the morphology of the intervertebral discs. Thoracic kyphosis has been suggested, however, to be dependent on vertebral body morphology to a greater extent than to intervertebral disc morphology, different from the co-dependence of osseous and soft tissue shape in lumbar lordosis (Goh et al. 1999).

The two methods for calculating the thoracic kyphosis of osseous material are based on vertebral body morphology. The first method of assessing thoracic kyphosis is based on vertebral body height difference (TVBHD) (Goh et al. 1999). In this method, the anterior (ventral) and the posterior (dorsal) vertebral body

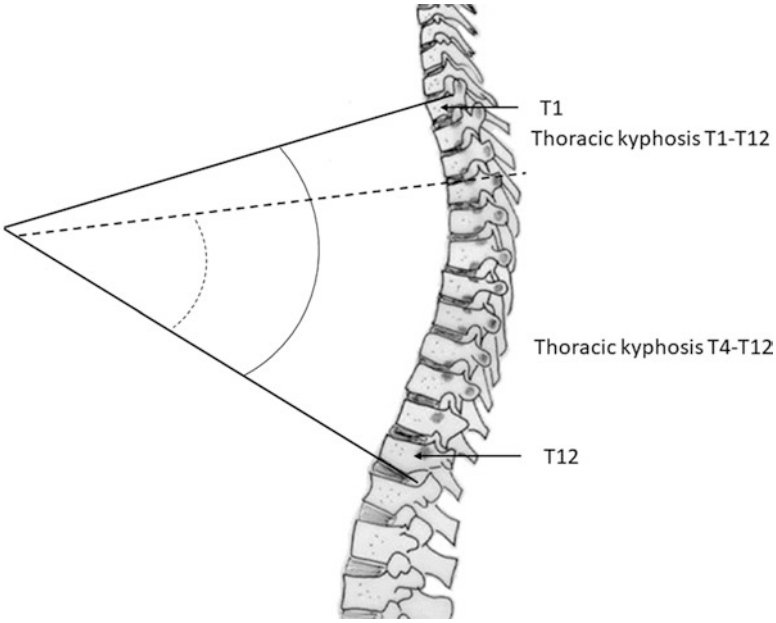

Fig. 15.4 An illustration of a thoracic kyphosis of an adult human. T1, first thoracic vertebra; T12, 12th thoracic vertebra. Note the difference between the T1–T12 kyphosis and the T4–T12 kyphosis

cranio-caudal dimensions (heights) of the twelve thoracic vertebrae are measured. Then, the sum of the anterior heights is divided by the sum of the posterior heights (A–P ratio). This ratio is used to calculate the thoracic kyphosis (Table 15.3). This method is easy to use provided that the bodies of T1–T12 are complete. The shortcoming of this method is that it only takes into account vertebral cranio-caudal heights; it does not consider the antero-posterior length of the vertebral bodies, which also contributes to the curvature of the vertebral column. Given the same absolute difference between the ventral and dorsal heights, antero-posteriorly longer vertebrae will show a lower degree of wedging.

The second method, which is based on the thoracic vertebral body wedging (TVBW), uses the vertebral body wedging for the reconstruction of thoracic kyphosis, similar to LVBW. This method was developed recently and is presented here for the first time. Fifty radiographs of standing adult humans without spinal or thoracic pathology were measured. On each radiograph, the vertebral body wedging of T4–T12 as well as the T4–T12 Cobb angle were measured (Fig. 15.4, T4–T12 kyphosis). We could not measure the angles between T1 and T3 due to the scapulae. Each measurement was taken three times and the final angle is the average of the three measurements. Then, the sum of vertebral wedging (ΣB T4–T12) was calculated and used to develop a formula for calculating thoracic kyphosis based on osseous material (Table 15.3). This method is simple to use, provided that the thoracic vertebral bodies are complete. If some of the vertebral bodies are missing or too damaged to use, then a specific formula should be developed based on the available number of

Table 15.3 The different methods for the calculation of thoracic kyphosis (TK) and results of the application of these formulae to Kebara 2

TK based on	Method	Sample	Formula (based on standard major axis technique)	R^2	Root mean square error (RMSE)	TK modern humans	Kebara 2
T1–T12	TVBHD Goh et al. (1999)	Modern humans, females	TK = 428.756 − 411.87 × (A-P ratio)	0.47			
		Modern humans, males	TK = 297.114 − 272.31 × (A-P ratio)	0.39		50	44
T4–T12	TVBW (ΣB T4–T12) Present study	Modern humans	TK = 0.55 × (ΣB T4–T12) + 14.6	0.40	7.9		
T4–T8+ T11-12	TVBW (ΣB T4–T8+ T11–12) Present study	Modern humans	TK = 0.69 × (ΣB T4–T8, T11, T12) + 13.3	0.38	8.1	33.5 ± 10	36.8

All of the formulae are based on regressions that are statistically significant $p < 0.05$
"Sample" refers to which sample was used to derive the regression equation shown in the column called "Formula". The column "Kebara 2" provides the value used in the reconstruction

complete vertebral bodies. The advantage of this method is that it explicitly takes into account vertebral body wedging and not simply the anterior–posterior ratio. This method is based on radiographs of standing subjects whose upright posture is appropriate for the posture that we wish to reconstruct in the fossil hominins. The disadvantage of this method is that it can only be used to calculate thoracic kyphosis between T4 and T12 and not the full thoracic kyphosis between T1 and T12.

Both methods, TVBHD (Goh et al. 1999) and the newly described TVBW method, are based on thoracic vertebrae of modern humans. These methods are reliable, therefore, for the reconstruction of thoracic kyphosis of osseous material that belongs to *H. sapiens* and caution is warranted when applied to extinct hominins. Additional formulae derived from samples which include extant hominoids are required to better understand potential diversity in hominoid thoracic kyphosis, which could inform regarding the validity of the reconstruction of thoracic kyphosis in extinct hominins. In the meantime, the current methods can be cautiously used for reconstruction of thoracic kyphosis of extinct hominins, particularly hominins that are assigned to genus *Homo*. Of importance to note, the predictive ability of both methods for thoracic kyphosis ($r^2 = 0.38$–0.47) is less than that of some of the methods for calculating lumbar lordosis.

Based on the ratio between the ventral and dorsal vertebral body heights (Goh et al. 1999), the calculated thoracic kyphosis (T1–T12) for Kebara 2 is 44°, which falls within the range of modern humans and close, but below, the human average value (50°).

Vertebral body wedging for Kebara 2 cannot be accurately measured on three thoracic vertebrae: T2, T9, and T10. We developed a specific formula, therefore, for calculating the T4–T12 kyphosis for Kebara 2 based on vertebral wedging of T4–T8 + T11–T12 from the data used to calculate the general formula. The calculated

T4–T12 kyphosis of Kebara 2 (36.8°) is within the range for modern humans and is close to, but slightly above, the human average (33.5° ± 10) (Table 15.3). We presume that the very kyphotic wedging of the lower thoracic vertebrae (T11–T12) of Kebara 2 (Been et al. 2017a) has more influence on the T4–T12 kyphosis than on the T1–T12 kyphosis, hence the differences in relation to modern humans. In any case, this result would be consistent with the other method and underlines that Kebara 2 had a thoracic kyphosis similar to modern humans, a surprising finding given the lower values of lumbar lordosis. Figure 15.2 shows the reconstruction of the thoracic kyphosis of Kebara 2, after Been et al. (2017a). Currently, Kebara 2 is the only Neandertal for which it has been possible to estimate thoracic kyphosis.

15.3.4 Estimation of Cervical Lordosis

Cervical lordosis is the ventral curvature of the cervical spine. It is defined here as the angle between a line parallel to the foramen magnum and a line parallel to the inferior surface of the last cervical vertebra (C7) (Fig. 15.5). To the best of our knowledge, only one method for calculating cervical lordosis based on osseous material exists. This method depends on the correlation between the position of the foramen magnum in relation to the Frankfurt horizontal plane and cervical lordosis (Been et al. 2014b).

The first step in applying this method is to measure the orientation of the foramen magnum in relation to the Frankfurt horizontal plane (FM-HP) (Fig. 15.5; after Been et al. 2014b, 2017b). Based on this measurement, the cervical lordosis is calculated using the regression formula shown in Table 15.4 (Been et al. 2014b). In order to use this method, a relatively complete skull, where both the foramen magnum (between the basion and the opisthion), the porion, and the orbita are intact. This method is based on modern humans only and, therefore, should be applied with some caution when estimating the cervical lordosis of extinct hominins.

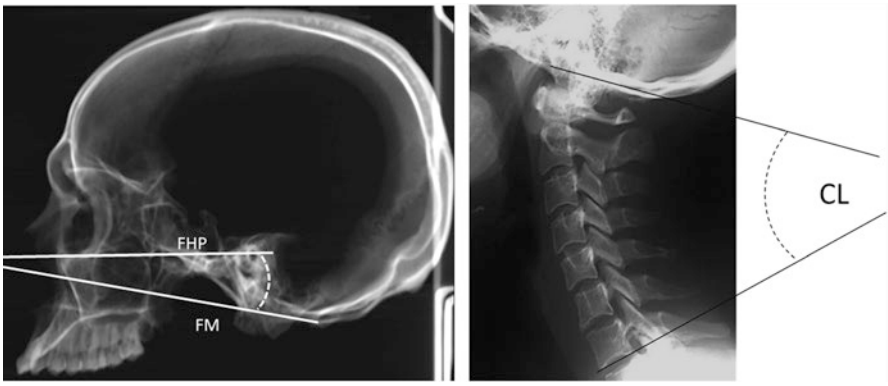

Fig. 15.5 Radiograph of the cervical lordosis angle (CL) of an adult human and foramen magnum (FM) orientation in relation to the Frankfurt horizontal plane (FHP)

Table 15.4 A method for the calculation of the cervical lordosis (CL), and results of application of this formula to Neandertal specimens (Been et al. 2017b)

Measurement	Sample	Formula (based on standard major axis technique)	R^2	Root mean square error (RMSE)	Modern humans	Neandertals (average)
FM-HP	Modern humans	CL = 26.92 + 1.03 × (FM-HP)	0.51	6.92	40 ± 10	25.8 ± 3.7

The formula is based on regression that is statistically significant $p < 0.05$

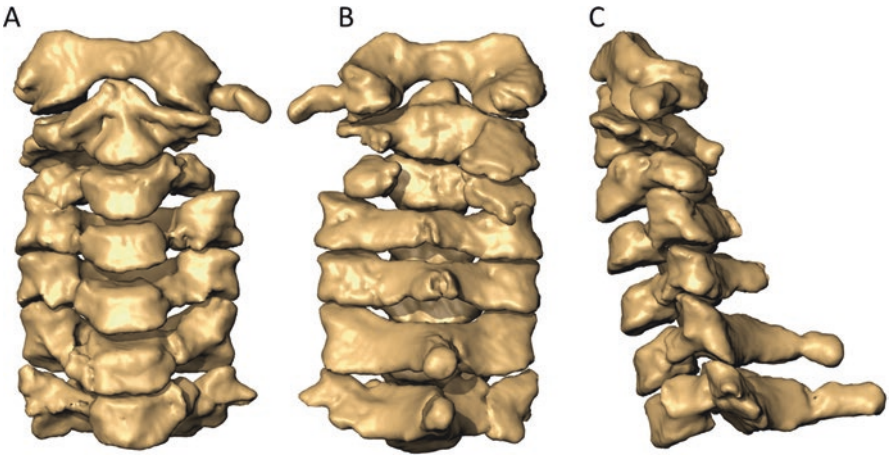

Fig. 15.6 The reconstructed cervical spine (C1–C7) of Kebara 2. (**a**) Anterior view; (**b**) posterior view; (**c**) left lateral view

We have tried to develop other methods for calculating the cervical lordosis based on cervical vertebrae morphology (for example, based on vertebral body wedging) with no success. The morphology of the vertebral body of the cervical vertebrae is more complex than that of the thoracic and lumbar regions. The development of additional methods for reconstructing cervical lordosis based on osseous material, can potentially complement the existing foramen magnum-based method, and should be a research priority.

Kebara 2 preserves (although in an incomplete state) all seven cervical vertebrae, but no skull. We cannot, therefore, directly calculate Kebara 2's cervical lordosis. For the estimation of the cervical lordosis of Kebara 2, we used the average cervical lordosis estimated for Neandertal specimens that preserve the skull (25.8° ± 2.6) (Been et al. 2017b).

The complete alignment of the cervical lordosis of Kebara 2 is presented here for the first time (Fig. 15.6a–c). We faced numerous challenges when positioning the cervical vertebrae into anatomical position (i.e., aligning them one above the other). The major problem is that both T1 and C3–C7 are partially reconstructed (Arensburg 1991) due to the presence of taphonomic distortion. This affects the congruency between adjacent vertebrae, especially between T1–C7 and C3–C4.

In order to align C7 to T1 and C3 to C4, we had to choose between two options: either to align the vertebrae based on the shape of the vertebral bodies or based on the articular facets. The current reconstructed shape of the vertebrae does not allow us to align both regions (vertebral body and facets) simultaneously. In both locations, we used the vertebral body to align the vertebrae because the vertebral body is more complete than the facets for each vertebra and because the bodies are an integral contributor to the shape of the kyphosis. Unlike the problems described above, the alignment of C6–C4 and of C1–C2 is straightforward and is based on the congruency between vertebral bodies and right and left facet joints. Future study should consider the taphonomic problems present in this specimen (Gómez-Olivencia et al. 2009), given these alignment issues, in order to establish a better alignment of the cervical vertebrae of Kebara 2.

15.4 Reconstruction of the Kebara 2 Neandertal

The Kebara 2 reconstruction has allowed us to gain new insights regarding the stature of this individual. Our estimation of stature is 170 cm (Been et al. 2017a), which is consistent with the estimations obtained using the maximum length of the humerus and radius (but slightly below than that obtained using the ulnar maximum length) (Carretero et al. 2012). The reconstruction also allowed us to measure spinal balance for Kebara 2. The position of the T4 plumb line of Kebara 2 is more ventral than its position in healthy modern humans (Been et al. 2017a), but this ventral position is not surprising given that it is similar to the position of the plumb line of adult humans with small PI and horizontal sacral endplate (Barrey et al. 2007). The implications of this difference for sagittal balance and locomotion remain to be explored.

15.5 Summary and Conclusions

The spinal column can be reconstructed either by using casts of the original bones (Sawyer and Maley 2005) or by using 3D models of the original bones (Been et al. 2017a) and both methods enable new insights regarding spinal alignment of the reconstructed individual. Using geometric morphometrics also provides new and promising approaches for the 3D reconstruction of the spinal column (Bastir et al. 2019). In this chapter, we provided ways to overcome the major problems in the reconstruction of spinal column: how to align the vertebrae in the absence of the intervertebral disc space and how much curvature should be applied to cervical, thoracic, and lumbar areas.

Spinal reconstruction is the basis for a full-body reconstruction and for determining the bauplan—the generalized structural body plan. A full spinal reconstruction enables us to determine head position in relation to the rest of the body, to perform full thorax reconstruction to examine the breathing mechanism in extinct hominins

(Bastir et al. 2017; Gómez-Olivencia et al. 2017), to investigate the pelvic/thorax ratio, and to explore locomotion in extinct hominins.

In our view, description of the spinal curvatures from a quantitative, orthopedic approach, i.e., describing spinal curvatures using specific angular variables rather than the vague dichotomy of "human-like" or "non-human-like" spinal curvatures, is critical to further understanding of spinal evolution. More methods for the reconstruction of spinal curvature based on osseous material need to be developed, especially for thoracic kyphosis and cervical lordosis. We also need a more in-depth knowledge of the spinal curvatures of extant primates and their variation in order to better understand the osseous and soft tissue components of their spines that will also provide information regarding spinal evolution.

Acknowledgements We thank M. Haeusler and M. Bastir for their useful comments in a previous version of this paper. AGO receives support from the Spanish Ministerio de Ciencia y Tecnología (Project: CGL-2015-65387-C3-2-P, MINECO/FEDER), by the Spanish Ministerio deCiencia, Innovación y Universidades (project PGC2018-093925-BC33) and from the Research Group IT1418-19 from the Eusko Jaurlaritza-Gobierno Vasco.

References

Arensburg B (1991) The vertebral column, thoracic cage and hyoid bone. In: Bar-Yosef O, Vandermeersch B (eds) Le squelette moustérien de Kébara 2. Éditions du CNRS, Paris, pp 113–147

Bailey J, Been E, Kramer P (2014) Higher lumbar lordosis among women: a study examining lumbar angle and dorsoventral wedging of vertebral bodies and discs in standing and supine radiographs. FASEB J 28:1

Barrey C, Jund J, Noseda O, Roussouly P (2007) Sagittal balance of the pelvis-spine complex and lumbar degenerative diseases. A comparative study about 85 cases. Eur Spine J 16(9):1459–1467

Bastir M, García-Martínez D, Torres-Tamayo N, Sanchis-Gimeno JA, O'Higgins P, Utrilla C, Torres Sánchez I, García Río F (2017) In vivo 3D analysis of thoracic kinematics: changes in size and shape during breathing and their implications for respiratory function in recent humans and fossil hominins. Anat Rec 300(2):255–264

Bastir M, Torres-Tamayo N, Palancar CA, Zlolniski SL, García-Martínez D, Riesco-López A, Vidal D, Blanco-Pérez E, Barash A, Nalla S, Martelli S, Sanchis-Gimeno JA, Schlager S (2019) Geometric morphometric studies in the human spine. In: Been E, Gómez-Olivencia A, Kramer PA (eds) Spinal evolution: morphology, function, and pathology of the spine in hominoid evolution. Springer, New York, pp 360–386

Been E, Bailey JF (2019) The association between spinal posture and spinal biomechanics in modern humans: implications for extinct hominins. In: Been E, Gómez-Olivencia A, Kramer PA (eds) Spinal evolution: morphology, function, and pathology of the spine in hominoid evolution. Springer, New York, pp 283–300

Been E, Barash A, Marom A, Kramer PA (2010a) Vertebral bodies or discs: which contributes more to human-like lumbar lordosis? Clin Orthop Relat Res 468(7):1822–1829

Been E, Barash A, Pessah H, Peleg S (2010b) A new look at the geometry of the lumbar spine. Spine 35(20):E1014–E1017

Been E, Gó mez-Olivencia A, Kramer PA (2012) Lumbar lordosis of extinct hominins. Am J Phys Anthropol 147(1):64–77

Been E, Gómez-Olivencia A, Kramer PA (2014a) Brief communication: lumbar lordosis in extinct hominins: implications of the pelvic incidence. Am J Phys Anthropol 154(2):307–314

Been E, Shefi S, Soudack M, Zilka LR, Barash A, Rak Y (2014b) Cervical lordosis and the orientation of the foramen magnum, implications to human evolution. Am J Phys Anthropol 153:75

Been E, Gómez-Olivencia A, Kramer P, Barash A (2017a) 3D reconstruction of spinal posture of the Kebara 2 Neanderthal. In: Marom A, Hovers E (eds) Human paleontology and prehistory contributions in honor of Yoel Rak. Springer, Cham, pp 239–251

Been E, Gómez-Olivencia A, Shefi S, Soudack M, Bastir M, Barash A (2017b) Evolution of spino-pelvic alignment in hominins. Anat Rec 300(5):900–911

Been E, Shefi S, Soudack M (2017c) Cervical lordosis: the effect of age and gender. Spine J 17(6):880–888

Been E, Kalichman L (2014) Lumbar lordosis. Spine J 14(1):87–97

Been E, Pessah H, Been L, Tawil A, Peleg S (2007) New method for predicting the lumbar lordosis angle in skeletal material. Anat Rec (Hoboken) 290(12):1568–1573

Been E, Pessah H, Peleg S, Kramer PA (2013) Sacral orientation in hominin evolution. Adv Anthropol 03(03):133–141

Been E, Simonovich A, Kalichman L (2019) Spinal posture and pathology in modern humans. In: Been E, Gómez-Olivencia A, Kramer PA (eds) Spinal evolution: morphology, function, and pathology of the spine in hominoid evolution. Springer, New York, pp 301–320

Bonmatí A, Gómez-Olivencia A, Arsuaga JL, Carretero JM, Gracia A, Martínez I, Lorenzo C, Bermúdez de Castro JM, Carbonell E (2010) Middle Pleistocene lower back and pelvis from an aged human individual from the Sima de los Huesos site, Spain. Proc Natl Acad Sci U S A 107(43):18386–18391

Boulay C, Tardieu C, Hecquet J, Benaim C, Mouilleseaux B, Marty C, Prat-Pradal D, Legaye J, Duval-Beaupère G, Pelissier J (2006) Sagittal alignment of spine and pelvis regulated by pelvic incidence: standard values and prediction of lordosis. Eur Spine J 15(4):415–422

Carretero JM, Rodríguez L, Garcia-Gonzalez R, Arsuaga JL, Gómez-Olivencia A, Lorenzo C, Bonmatí A, Gracia A, Martínez I, Quam R (2012) Stature estimation from complete long bones in the middle Pleistocene humans from the Sima de los Huesos, sierra de Atapuerca (Spain). J Hum Evol 62(2):242–255

Castillo ER, Lieberman DE (2017) Lordosis variability and shock attenuation in the hominin lumbar spine. Am J Phys Anthropol 162:139–140

Chevillotte T, Coudert P, Cawley D, Bouloussa H, Mazas S, Boissière L, Gille O (2018) Influence of posture on relationships between pelvic parameters and lumbar lordosis: comparison of the standing, seated, and supine positions. A preliminary study. Orthop Traumatol Surg Res 104(5):565–568

Cleuvenot E (1999) Courbures sagittales de la colonne vertébrale déterminées par la morphologie des vertèbres. Développement d'une nouvelle méthodologie et application chez *Homo sapiens*. PhD thesis. Université Bordeaux I

Damasceno LHF, Catarin SRG, Campos AD, Defino HLA (2006) Lumbar lordosis: a study of angle values and of vertebral bodies and intervertebral discs role. Acta Ortopédica Brasileira 14(4):193–198

Duval-Beaupère G, Schmidt C, Cosson PH (1992) A Barycentremetric study of the sagittal shape of spine and pelvis: the conditions required for an economic standing position. Ann Biomed Eng 20(4):451–462

Goh S, Price RI, Leedman PJ, Singer KP (1999) The relative influence of vertebral body and intervertebral disc shape on thoracic kyphosis. Clin Biomech (Bristol, Avon) 14(7):439–448

Gómez-Olivencia A, Arlegi M, Barash A, Stock JT, Been E (2017) The Neandertal vertebral column 2: the lumbar spine. J Hum Evol 106:84–101

Gómez-Olivencia A, Barash A, García-Martínez D, Arlegi M, Kramer P, Bastir M, Been E (2018) 3D virtual reconstruction of the Kebara 2 Neandertal thorax. Nat Commun 9(1):4387

Gómez-Olivencia A, Eaves-Johnson KL, Franciscus RG, Carretero JM, Arsuaga JL (2009) Kebara 2: new insights regarding the most complete Neandertal thorax. J Hum Evol 57(1):75–90

Haeusler M, Martelli SA, Boeni T (2002) Vertebrae numbers of the early hominid lumbar spine. J Hum Evol 43(5):621–643

Hardacker JW, Shuford RF, Capicotto PN, Pryor PW (1997) Radiographic standing cervical segmental alignment in adult volunteers without neck symptoms. Spine (Philadelphia PA 1976) 22(13):1472–1480

Kimura S, Steinbach GC, Watenpaugh DE, Hargens AR (2001) Lumbar spine disc height and curvature responses to an axial load generated by a compression device compatible with magnetic resonance imaging. Spine 26(23):2596–2600

Korovessis PG, Stamatakis MV, Baikousis AG (1998) Reciprocal angulation of vertebral bodies in the sagittal plane in an asymptomatic Greek population. Spine 23(6):700–704

Kunkel ME, Herkommer A, Reinehr M, Bockers TM, Wilke HJ (2011) Morphometric analysis of the relationships between intervertebral disc and vertebral body heights: an anatomical and radiographic study of the human thoracic spine. J Anat 219(3):375–387

Le Huec JC, Hasegawa K (2016) Normative values for the spine shape parameters using 3D standing analysis from a database of 268 asymptomatic Caucasian and Japanese subjects. Eur Spine J 25(11):3630–3637

Legaye J, Duval-Beaupère G (2008) Gravitational forces and sagittal shape of the spine. Int Orthop 32(6):809–816

Legaye J, Duval-Beaupère G, Hecquet J, Marty C (1998) Pelvic incidence: a fundamental pelvic parameter for three-dimensional regulation of spinal sagittal curves. Eur Spine J 7(2):99–103

Legaye J, Duval-Beaupère G, Tardieu C, Hecquet J (2007) The conditions required for an economic standing position in humans: key role of the pelvic parameter: the sacral incidence angle. Growth, evolution and plasticity of this parameter. J Morphol 268(12):1099–1099

Mac-Thiong JM, Roussouly P, Berthonnaud E, Guigui P (2010) Sagittal parameters of global spinal balance: normative values from a prospective cohort of seven hundred nine Caucasian asymptomatic adults. Spine 35(22):E1193–E1198

Peleg S, Dar G, Steinberg N, Peled N, Hershkovitz I, Masharawi Y (2007) Sacral orientation revisited. Spine 32(15):E397–E404

Pilbeam D (2004) The anthropoid postcranial axial skeleton: comments on development, variation, and evolution. J Exp Zool B Mol Dev Evol 302b(3):241–267

Sanders WJ (1998) Comparative morphometric study of the australopithecine vertebral series Stw-H8/H41. J Hum Evol 34(3):249–302

Sawyer GJ, Maley B (2005) Neanderthal reconstructed. Anat Rec 283(1):23–31

Schwab F, Lafage V, Boyce R, Skalli W, Farcy JP (2006) Gravity line analysis in adult volunteers – age-related correlation with spinal parameters, pelvic parameters, and foot position. Spine 31(25):E959–E967

Simon P, Orias AAE, Andersson GBJ, An HS, Inoue N (2012) In vivo topographic analysis of lumbar facet joint space width distribution in healthy and symptomatic subjects. Spine 37(12):1058–1064

Trinkaus E (1985) Pathology and the posture of the La-Chapelle-aux-saints Neandertal. Am J Phys Anthropol 67(1):19–41

Vialle R, Levassor N, Rillardon L, Templier A, Skalli W, Guigui P (2005) Radiographic analysis of the sagittal alignment and balance of the spine in asymptomatic subjects. J Bone Joint Surg Am 87(2):260–267

Williams SA, Gómez-Olivencia A, Pilbeam DR (2019) Numbers of vertebrae in hominoid evolution. In: Been E, Gómez-Olivencia A, Kramer PA (eds) Spinal evolution: morphology, function, and pathology of the spine in hominoid evolution. Springer, New York, pp 97–124

Williams SA, Middleton ER, Villamil CI, Shattuck MR (2016) Vertebral numbers and human evolution. Am J Phys Anthropol 159(Suppl 61):S19–S36

Williams SA, Ostrofsky KR, Frater N, Churchill SE, Schmid P, Berger LR (2013) The vertebral column of Australopithecus sediba. Science 340(6129):1232996

Yang X, Kong Q, Song Y, Liu L, Zeng J, Xing R (2013) The characteristics of spinopelvic sagittal alignment in patients with lumbar disc degenerative diseases. Eur Spine J 23(3):569–575

Zhang F, Zhang K, Tian HJ, Wu AM, Cheng XF, Zhou TJ, Zhao J (2018) Correlation between lumbar intervertebral disc height and lumbar spine sagittal alignment among asymptomatic Asian young adults. J Orthop Surg Res 13(1):34

Chapter 16
Geometric Morphometric Studies in the Human Spine

Markus Bastir, Nicole Torres-Tamayo, Carlos A. Palancar, Stephanie Lois-Zlolniski, Daniel García-Martínez, Alberto Riesco-López, Daniel Vidal, Esther Blanco-Pérez, Alon Barash, Shahed Nalla, Sandra Martelli, Juan Alberto Sanchis-Gimeno, and Stefan Schlager

16.1 Introduction

Geometric morphometrics (GM) is the statistical analysis of Cartesian landmark coordinates, which have biological meanings and homologous locations between biological structures (Bookstein 1991; Rohlf and Marcus 1993; O'Higgins 2000; Mitteroecker and Gunz 2009; Zelditch et al. 2012). This technique allows for the quantification of geometric features of anatomical structures in two (2D) or three dimensions (3D) and their spatial relationships. By using Procrustes superimposition or Generalized Procrustes superimposition (GPA) of the landmarks configurations (Gower 1975), GM allows for a quantitative separation of size and shape. Size is measured as centroid size (the summed squared distances between the centroid and each of the

M. Bastir (✉) · N. Torres-Tamayo · C. A. Palancar · S. Lois-Zlolniski · A. Riesco-López
Paleoanthropology Group, Museo Nacional de Ciencias Naturales, CSIC, Madrid, Spain
e-mail: mbastir@mncn.csic.es

D. García-Martínez
Paleoanthropology Group, Museo Nacional de Ciencias Naturales, CSIC, Madrid, Spain

Laboratoire PACEA—De la Préhistoire à l'Actuel: Culture, Environnement et Anthropologie, CNRS, Université de Bordeaux, Talence, France

D. Vidal
Grupo de Biología Evolutiva, Departamento de Física Matemática y de Fluidos, Facultad de Ciencias—UNED, Madrid, Spain

E. Blanco-Pérez
Radiología, Hospital Universitario de La Ribera, Valencia, Spain

Department of Anatomy and Human Embryology, GIAVAL Research Group, University of Valencia, Faculty of Medicine, Valencia, Spain

A. Barash
Faculty of Medicine, Bar-Ilan University, Ramat Gan, Israel

E. Been et al. (eds.), *Spinal Evolution*,
https://doi.org/10.1007/978-3-030-19349-2_16

landmarks of a given configuration). Shape contains all features of the landmark configurations that are invariant to scale, position and orientation (Bookstein 1991; Zelditch et al. 2012) and can be quantified through the Procrustes shape coordinates of landmark configurations after GPA. While centroid size is a variable with only one dimension, shape is intrinsically multidimensional (2D and 3D shape coordinates) and requires multivariate statistics for its analysis (Bookstein 1991, 1996). Thus, all landmark coordinates of each specimen are a single data point in a multivariate shape space and the distances between two data points in shape space are a linear approximation that corresponds directly to the square root of the sum of squared inter-landmark distances after GPA (Rohlf and Marcus 1993; Rohlf 1996). Therefore, any statistical analysis in GM can be directly visualized as thin-plate splines transformations of 2D or 3D landmark configurations that can directly be interpreted graphically (Bookstein 1991; O'Higgins 2000). This analytical power is not achieved by traditional morphometrics of distances or angles where any statistical analysis and graphic needs to be interpreted morphologically by the researcher.

In GM, the thin-plate splines transformations can also be applied to virtual 3D meshes, which is ideal for virtual morphological modelling, that can be seen as computer-based, GM-driven manipulations of virtual 3D meshes (Ponce de León and Zollikofer 2001; Gunz et al. 2005; Weber and Bookstein 2011; Weber 2015). Virtual morphological modelling has proven particularly useful in palaeoanthropology for its potential for reconstructing incomplete fossils (Gunz et al. 2009). Because of all these characteristics, GM has become one of the standard toolkits in both physical anthropology and human palaeontology during the last two decades.

The aim of this chapter is to overview the methodological aspects in GM applied to the pre-sacral spine in a palaeoanthropological context, and to review geometric morphometric studies of the cervical, thoracic and lumbar spine. We will also provide some examples of methods in order to give a glimpse on their potential future applications on the reconstruction of the hominin spine.

S. Nalla
Department of Anatomy and Human Embryology, GIAVAL Research Group, University of Valencia, Faculty of Medicine, Valencia, Spain

Department of Human Anatomy and Physiology, Faculty of Health Sciences, University of Johannesburg, Johannesburg, South Africa

Evolutionary Studies Institute (ESI), University of the Witwatersrand (Wits), Johannesburg, South Africa

S. Martelli
Department of Cell and Developmental Biology, University College London, London, UK

J. A. Sanchis-Gimeno
Department of Anatomy and Human Embryology, GIAVAL Research Group, University of Valencia, Faculty of Medicine, Valencia, Spain

S. Schlager
Anthropologie, Medizinische Fakultät der Albert Ludwigs- Universität Freiburg, Freiburg, Germany

16.1.1 Geometric Morphometric Methods of the Spine: Challenges in the Data Acquisition of Serial Structures

So far, not many GM studies have been performed on human/hominin spines/vertebrae. This scarcity is likely related to the metameric nature of the spine, which is composed of serial homological structures (vertebrae) that pose challenges both to the acquisition of GM data as well as to its analysis. But also, the fragility of the vertebrae usually prevents the spine from well-preservation in the fossil record which results in complications for GM analyses.

At a practical level, the acquisition of a representative sample by digitizing landmarks on a set of serial structures (such as vertebrae or ribs) requires considerably more effort than measuring non-serial data (crania, mandibles, individual bones). While in the latter case the specimen itself is representative of the individual organism, metameric data requires *n*-times the number of individual organisms, with *n* being the number of vertebrae composing their spines (or regions of it). Thus, representing properly the spine of a fossil hominin requires seven cervical, 12 thoracic or 5 lumbar vertebrae to be measured and compared with a sufficiently sized reference sample. Virtual 3D data sets of vertebrae or spines are usually achieved by time-consuming surface or computed tomography (CT) scanning, and similarly, landmarks and semilandmarks collection is also a time-consuming process. This is particularly true for studies that quantify curves or surfaces using 3D semilandmarks (Gunz et al. 2005; Gunz and Mitteroecker 2013). Unlike landmarks, which can be both physically and virtually collected, semilandmarks require a virtual environment for their post-processing, i.e. the resliding along curves or surfaces, which is necessary for establishing their geometrical homology (Gunz and Mitteroecker 2013). All these technical difficulties complicate geometric morphometric analyses of vertebrae and spines; in fact, GM studies addressing entire series of vertebrae often cover fewer individuals than GM studies of non-serial structures.

Despite all these technical challenges, 3D geometric morphometrics offers advantages for spine morphometrics compared to other techniques. This is because the articulation between the different elements of the spine is based on complex interactions in which curves and surfaces play an important role, particularly in a functional sense (lordosis, kyphosis) (Plomp et al. 2012, 2015a, b; Ríos et al. 2017; Meyer et al. 2018). Only 3D geometric morphometrics of sliding semilandmarks can rigorously quantify these spatial relationships, allowing us to analyse individual elements of the spine to morpho-functionally understand the complex interactions between them. This is also useful for reconstructing both missing fragments and serial elements. Therefore, the following sections aim to show how GM has been used for the study of form and function of individual vertebral levels, as well as of different anatomical parts of the spine.

16.1.2 Geometric Morphometric Methods of the Spine: Challenges in the Statistical Analysis of Serial Data

Not only the acquisition but also the analysis of serial data requires special considerations. Serial anatomical structures are similar to other kinds of seriality such as time series at different scales (evolutionary, ontogenetic or functional [e.g. movement] scales). This is comparable to measuring the same structure under different conditions, as in experiments. Therefore, the observations (data points) are not independent, neither biologically nor statistically, and thus require consideration such as an adjustment of degrees of freedom in parametric statistics similar to a repeated measurement protocol (Sokal and Rohlf 1998).

One key challenge is the question of how to summarize serial vertebral shapes and their cumulative effects on the shape of the spine, composed by these vertebrae, in GM analyses. In other words, how could we represent the relation between many *parts* (vertebrae) and the *whole* (spine)? And how could we compare many parts that compose many 'wholes' (many spines)? In ordination methods such as principal components analysis (PCA), serial data can be represented by trajectories. Shape trajectories describe the dynamics of shape changes with respect to a given factor, such as numerical seriality. Comparisons of trajectories offer great potential for answering questions about similarity or difference of complex systems, for example, developmental or functional systems (Cobb and O'Higgins 2004; Bastir et al. 2006; Waldock et al. 2016). In many studies, the question of similarity or difference has been assessed by quantifying the angle between these trajectories; as for a developmental study for example, if the trajectories were parallel, the differentiation between them must have occurred prenatally; if there is an angle between the trajectories, this implies also postnatal contributions to intergroup differences (Cobb and O'Higgins 2002, 2004; Bastir et al. 2007; Klingenberg and Marugán-Lobón 2013). However, this requires trajectories to be modelled as straight lines.

But in many data sets such as vertebrae, the comparisons of trajectories are complicated due to their non-linear structure (shape). For quantitative comparison of trajectories, the superimposition of the entire trajectory shapes has been suggested (Adams and Cerney 2007; Adams and Collyer 2009). Similarity of trajectories is then expressed as proximity of their representation in a trajectory-shape space. However, while trajectory shape itself can be indeed compared, it should be noted that these trajectories make sense in the original relation to their PC axes. These axes usually represent variables of shape relative to a serial (biological) process. Hence, it needs to be discussed whether it makes sense to rescale, or rotate trajectories for a common registration and so de-couple the trajectory from its driving variables.

Trajectories of the serial shapes of vertebrae can describe the characteristics of the spine as a morpho-functional system. This is because the spine curvatures (lordosis of the cervical and lumbar spine and thoracic kyphosis) are the result of the combination and relationships between the different elements of the spine (e.g. vertebral morphologies, intervertebral discs, ligaments, muscles, etc.). Analysing

sets of serial structures can reveal anatomical information about the conceptual relation between the parts and the whole. For example, different patterns of lumbar lordosis show up as differently curved trajectories in the comparison of human and chimpanzee spines (Solanas et al. 2015).

However, these non-linear distributions of shapes in shape space can also be potentially problematic in the analysis of the spine. When serial structures are analysed by GM and ordination methods in multidimensional space, their trajectories often take a 'U', or arch shape (Sarris and Chamero 2009; Sarris 2013). Such distributions are called a 'horseshoe' phenomenon (Kendall 1970; Diaconis et al. 2008), and it has been suggested by some to be an artefact of the multivariate analysis with respect to a specific structure of data matrix, particularly in ecology (Williamson 1978). But horseshoe-like trajectories in serial structures can also indicate that similar factors of shape variation affect structures both at the beginning and end of the serial structure. They are frequently found in geometric morphometric studies of spines as spatial series but could also be detected in temporal series (ontogeny, movement) (Adams and Cerney 2007; Bastir and Rosas 2009; Sarris and Chamero 2009; Bastir et al. 2014; Chamero et al. 2014). Horseshoes are often a combination of unidirectional variation along the first axis and unimodal variation along the second (Sarris 2013). The graphic appearance is due to a single, dominant gradient describing the samples of the serial structures driving the variance along the first PC (Sarris 2013). The arrangements of vertebrae along such a trajectory correspond to their numerical (serial) position within the vertebral column.

In the case of vertebral columns, a horseshoe phenomenon would mean that cranial and caudal vertebrae share similar features of serial shape variation and change. However, it should be noted that a horseshoe effect implies that shape differences between adjacent structures are more precisely estimated than differences between structures more distant to each other (Sarris 2013). This requires caution in visual interpretation of the analysis.

Bookstein (2017a) recently proposed an important argument: there might not be an a priori reason to assume any biological factor being reflected by principal components, particularly in the context of classification. This is because PCA is a statistical method designed for finding uncorrelated (latent) variables, which successively maximize the variance. This, however, may not be the case for the biological variable one is searching for. Consequently, PCA should not be used to look for them in the first place and alternatives to PCA are being proposed (Bookstein 2017a). In the case of serial vertebral shapes, it can be argued that developmental factors (*HOX* genes) (McIntyre et al. 2007) generating spine metamerism do provide a major morphogenetic process that contributes to maximize variation along a seriality vector.

Despite all these technical challenges, 3D geometric morphometrics offer clear advantages for spine morphometrics compared to other techniques. This is because the articulation between the different elements of the spine is based on complex interactions in which curves and surfaces play an important role, particularly in a functional sense (lordosis, kyphosis) (Plomp et al. 2012, 2015b; Ríos et al. 2017; Meyer et al. 2018; Lois Zlolniski et al. 2019). In this sense, only 3D geometric morphometrics of sliding semilandmarks can rigorously quantify these

spatial relationships, allowing us to analyse individual elements of the spine to morpho-functionally understand the complex interactions between them. This is also useful for reconstructing both missing fragments and serial elements. Therefore, the following sections aim to show how GM has been used for the study of form and function of individual vertebral levels as well as of different anatomical parts of the spine.

In this chapter, we aim to provide an overview of the use of geometric morphometrics to the study of the spine, with special emphasis on the studies performed by our group. We have divided these studies by anatomical regions (cervical, thoracic, lumbar). We finish this chapter by discussing the advantages and disadvantages of the GM methods.

16.2 The Cervical Spine

16.2.1 GM Study of the Functional Anatomy and Variation of the Cervical Spine

GM techniques have been used to study several factors of variation, such as ontogeny, sexual dimorphism, pathologies and evolution of head posture. Chatzigianni and Halazonetis (2009) studied ontogeny and sexual dimorphism applying GM on 98 radiographs of sub-adult patients using 187 landmarks (34 true landmarks and 153 sliding semilandmarks) on the first four cervical vertebrae, with the aim of assessing the potential predictive power of vertebral 3D shape on skeletal maturation. They concluded that although cervical shape was highly correlated to skeletal age, it was not a good age predictor. Chatzigianni and Halazonetis (2009) also observed that cervical vertebrae are larger in male sub-adults than in females of the same age. These sex-related differences in isolated cervical vertebrae could be also reflected in the shape and curvature of the whole cervical spine.

A clinical application of GM to the cervical vertebrae was carried out by Ríos et al. (2017). These authors found that congenital unfused posterior arches of atlas vertebrae lead to substantial modifications of both superior and inferior articular facets. Such modifications include a more transverse or horizontal orientation compared to the more superomedially oriented surfaces in control (healthy) vertebrae, resulting in flattened atlanto-occipital and atlanto-axial joints. Also, these authors reported that in this pathological condition, the transverse processes of the atlas are displaced more anteriorly relative to the lateral masses. The neural canal also presented differences in shape at the level of the anterior tubercle, elongation and transverse diameters. Identification of such 3D shape differences are useful, as they could affect the biomechanics of the cranio-cervical junction leading to functional defects and injuries.

Manfreda et al. (2006) addressed the morpho-functional relationship between the atlas and locomotion patterns in different primate species. These authors

identified features related to the species-specific locomotion patterns in addition to different allometric scaling patterns. They further proposed that the morphology of the non-human primate atlas does not allow for bipedal locomotion, suggesting that the human atlas morphology is a unique adaptation. In the same line, Nalley and Grider-Potter (2017) reported a correlation between posture and upper cervical column (C1 and C2) in primates, as a more horizontal neck was linked to craniocaudally longer pedicle and lamina lengths, more caudally inclined superior facet and more dorsally inclined dens of the axis.

Arlegi et al. (2017) used 3D GM to explore possible relationships between vertebral shape and the movement of the head, upper limbs and trunk by comparing African apes, modern humans and fossil hominin vertebrae. They found that shape differences are related to size (allometry), locomotion and head posture, with the spinous processes longer and less angled relative to the vertebral bodies in African apes than in humans, confirming previous findings (Schultz 1942). In addition, they analysed the spatial orientation of the superior articular facet and found that australopiths had more *Homo*-like upper sub-axial cervical vertebrae and more primitive lower cervical vertebrae. They hypothesized that those changes, perhaps related to postural adaptations derived from bipedalism, did not affect the entire subaxial cervical spine at the same time. This is in line with Arlegi et al. (2018), who reported differences in the degree of similarity of C3 and C7 between *H. sapiens* and australopiths, the latter preserving a chimpanzee-like C7 but a human-like C3.

Meyer et al. (2018) analysed the curved morphology of the uncinate processes of subaxial cervical vertebrae in early hominins and extant primates using semilandmarks along standardized photographs of vertebrae. These authors showed that variations in the morphology of the uncinate process can be related to head posture in terms of its stability, mobility and locomotion, inferring a different morphology among australopith species. This variation in the uncinated process has been interpreted in terms of possible ecological differences, *A. sediba* being more similar to the arboreal taxa and *A. afarensis* more similar to humans. This work evinces the importance of analysing bone curves and not only linear measurements or relative lengths.

16.2.2 A Geometric Morphometric Reconstruction of the First Cervical Vertebra (C1) from La Chapelle-aux-Saints 1

The atlas (C1), which is key in connecting anatomically the cranium with the postcranium, is a badly preserved bone in the fossil record because of its fragility. The atlas of *La Chapelle-aux-Saints* 1 Neandertal (France, 56–47 ky) is broken into different fragments (Fig. 16.1a): left and right lateral masses, which are fairly complete, a right transverse process and the anterior tubercle of the anterior arch (Gómez-Olivencia 2013). Here we describe the 3D GM reconstruction of *La Chapelle-aux-Saints* 1 (LC1) C1 based on the combination of allometric variation,

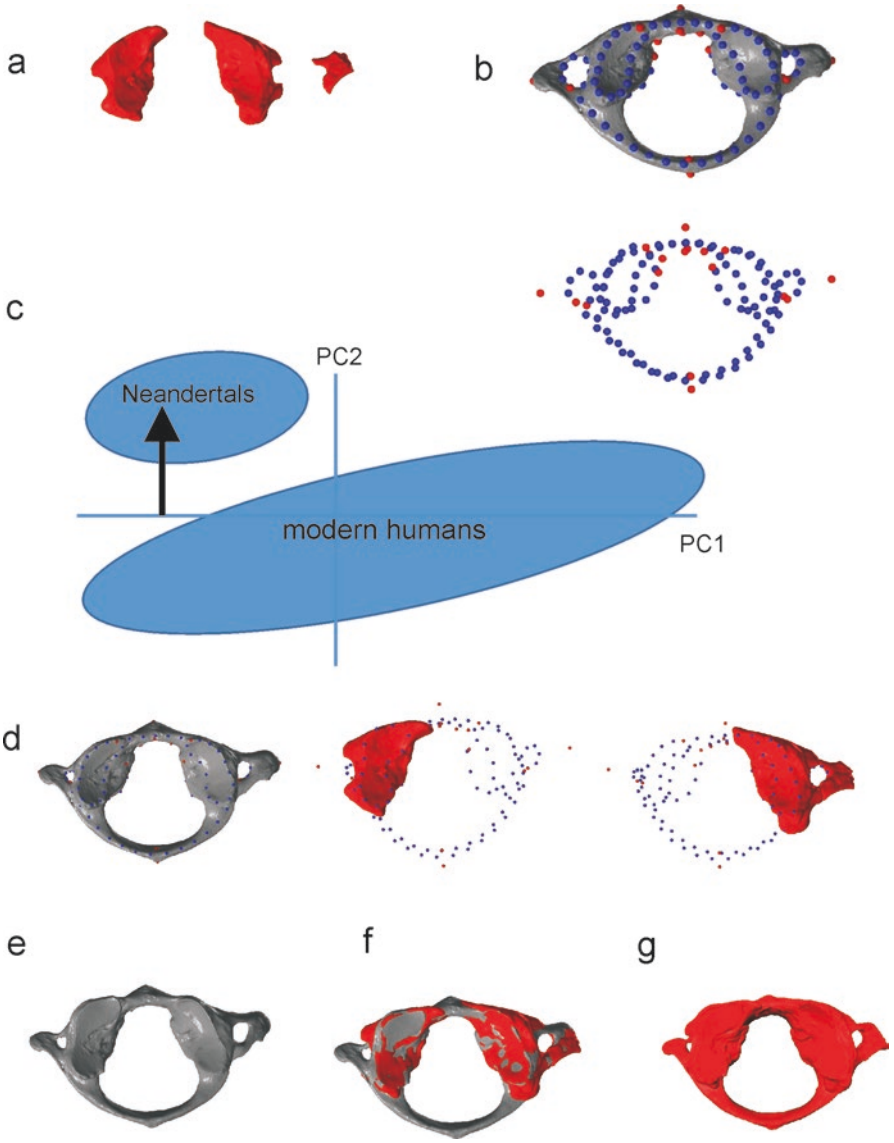

Fig. 16.1 (**a**) Surface models of the original atlas of La Chapelle-aux-Saints 1; (**b**) modern human atlas and the landmarks and curve semilandmarks; (**c**) schematic representation of the Procrustes form space of the modern humans and Neandertal sample. The arrow indicates the position in this form space where the atlas of La Chapelle-aux-Saints 1 is expected (allometric PC1 shape score −0.14; Neandertal means PC2 shape score 0.08). (**d**) Left image: shape corresponding to this location in form space (indicated by the arrowhead). Middle image: landmarks at left LC1 condyle with TPS estimated remaining landmarks; Right: landmarks at right LC1 condyle with TPS estimated remaining landmarks; shape deformed to the landmarks obtained previously by the fossils; (**e**, **f**) original fossils (red) in their corresponding position base on the GM reconstruction; (**g**) fused single 3D mesh for virtual manipulation and 3D printing

species-specific differences and semilandmarks in close vicinity of missing anatomical structures (Gunz et al. 2009; Palancar et al. 2018). In this reconstruction, we aimed to fully consider the size and 3D shape of the original fragments of the fossil and to generate a virtual 3D model that best-possibly fits with the morphology of the original parts. The reconstructed atlas could then be the subject of comparative anatomical studies.

The reconstruction process consisted of different consecutive and interrelated steps. First, the determination of allometric and non-allometric species-specific features of Neandertal atlas morphology; second, the prediction of the full LC1 atlas centroid size (CS); third, the prediction of a 3D LC1 Neandertal model that corresponds in allometric shape to the size predicted for LC1; and fourth, the virtual insertion of the original parts of LC1 into the previously reconstructed 3D model.

In step 1, the shape of 27 atlas of different hominin species (*H. sapiens*, $n = 21$; *H. neanderthalensis*, $n = 5$: Kebara 2, La Ferrassie 1, SD-1605, SD-1643, Krapina 98; *H. antecessor*, $n = 1$: ATD6-90) was quantified using a total of 119 landmarks and curve semilandmarks (Fig. 16.1b, see protocol of landmark digitization in Ríos et al. 2017). Once the sample was measured, we carried out a PCA in form space of Procrustes coordinates (Mitteroecker et al. 2004) (Fig. 16.1c). As form space includes the log-transformed CS as first variable within the shape data (PC1, 47.4% of total variation), a size gradient can be visualized along this PC, with larger atlases plotting towards negative PC1 scores and smaller ones towards positive PC1 scores; PC2 (11.4% variation) separated Neandertals in positive values from modern humans in negative values. This preliminary exploration gave us an idea of the main factors of variation influencing the atlas morphology in our sample.

Step 2 aimed at predicting the hypothetic size of the full atlas from LC1. To do so, we performed a statistical correlation using our modern comparative sample between the full size of the atlas (unknown in LC1) and the sizes of the left lateral masses (preserved in LC1). Therefore, we extracted the 26 landmarks of the left lateral mass in order to correlate its centroid size with the CS of the entire vertebra ($r^2 = 0.73$; p-value = 0.001). Thereby, we obtained an estimated CS for the entire LC1 atlas (234.92) from the CS of its left lateral mass (56.37).

Step 3 aimed at generating an overall estimate of the LC1 atlas shape. Since the first two PCs account for shape variation under the effect of size (PC1) and species-specific factors (PC2), they combine the necessary morphological information to carry out our fossil reconstruction in terms of size and shape. We used PC1 and PC2 of the PCA in form space of Procrustes coordinates (Fig 16.1c). First, we calculated a regression between the CS of the whole atlas sample and the PC1 scores ($r^2 = 0.98$; p-value < 0.001). Based on this linear regression model B, we predicted the PC1 score (as a proxy for atlas morphology in PC1) from the previously estimated CS for the entire LC1 atlas. The shape associated to the resulting PC1 score was then warped along PC2 axis to match it with the previously calculated arithmetic mean of the Neandertal subsample PC2 scores (Fig. 16.1c). As a result, we obtained the hypothetical shape of a Neandertal mean atlas, rescaled allometrically to the estimated CS for the entire LC1 atlas (predicted previously during step 2; Fig. 16.1d, left).

Our next goal (step 4) was to fit the original landmarks of the LC1 lateral masses into the rescaled Neandertal shape via thin plate spine surface warps (according to Gunz et al. 2009). For that, we carried out a GPA to superimpose the rescaled Neandertal atlas and the landmarks of the original lateral masses ($n = 26$) plus their estimated missing landmarks ($n = 93$) via TPS-estimation method (Gunz et al. 2009) (Fig. 16.1d). After this superimposition, we removed the Procrustes shape coordinates of the consensus lateral masses, which were replaced by the Procrustes shape coordinates of the original left and right lateral masses. This gave rise to the shape coordinates of the LC1 atlas (Fig. 16.1e), with its lateral masses corresponding to the original fossil and the rest of the structure to the C1 of the allometrically rescaled Neandertal.

In the final step, we rescaled these shape coordinates to the CS of LC1 and translated the virtual 3D meshes of the original left and right lateral masses, using their landmarks, into their corresponding positions within the full model (Fig. 16.1f). After fusing the meshes of these three surfaces, we obtained the reconstruction of a single hypothetical virtual 3D model of the *La Chapelle-aux-Saints 1* atlas (Fig. 16.1g). This reconstruction's overall size corresponds statistically to the size estimated from its lateral masses. The 3D shape of the lateral masses represents the exact geometry of the original LC1 fossils (Fig. 16.1a), and the non-preserved parts correspond to the statistical estimates of an allometrically rescaled and 'Neandertalized' atlas 3D shape. Its size and shape can thus be used for further comparative analyses. This method is an example that shows how virtual morphological modelling on the one hand and quantitative 3D GM 'engineering' on the other hand can be combined for a quantitative reconstruction of an incomplete fossil bone. Future work could apply this procedure to other incomplete fossils increasing the number of atlases available for future studies.

16.3 The Thoracic Spine

16.3.1 GM Studies of the Functional Anatomy and Variation in the Thoracic Spine

Geometric morphometrics have been used so far for the study of thoracic spine pathologies, sexual dimorphism and the evolutionary anatomy in Neandertals and *H. erectus*. Plomp et al. (2012) measured equidistant landmarks of the vertebral body, the pedicles and the neural canal. They demonstrated a correlation between the morphology of the posterior margin of the vertebral body and the pedicles and the presence of Schmorl's nodes (i.e. depressions on vertebrae due to herniation of the nucleus pulposus of the intervertebral disc into the vertebral body) in the lower thoracic spine. Variation of the 2D shape at the posterior margin of the vertebral bodies illustrated that the affected thoracic vertebrae were more circular and less 'heart-shaped' than in the healthy sample (Plomp et al. 2012). This trend was clearer

at T12 level than at T11 or T10. Another study has used geometric morphometrics in clinical data in relation to idiopathic scoliosis. Schlösser et al. (2016) measured curves along transverse cross sections of vertebrae of the thoraco-lumbar spine. They showed that anterior overgrowth is confined to primary and compensatory curves and not a generalized growth disturbance as it was traditionally assumed (Schlösser et al. 2016). These clinical applications show how the shape of curves and their position relative to other structures provide new information which helps improve hypotheses on aetiology and pathogenesis of the spine.

Sexual dimorphism of thoracic vertebrae has been addressed by our own research group (Bastir et al. 2014). True 3D landmarks were measured with a Microscribe digitizer on dry bones of thoracic spines (T1 to T10) of 11 males and 11 females to test the hypothesis of different transverse process orientation in males and female trunks. Analysis of serial trajectories in males and females revealed that in all vertebrae the transverse processes increased their dorsal orientation in a craniocaudal sequence, with a greater dorsal transverse processes orientation in the caudal part of the thoracic spine in males than in females (Bastir et al. 2014). These features were related to their difference in thorax morphology, since males show relatively wider caudal areas of the thorax than females (García-Martínez et al. 2016), possibly in relation to overall functional differences in body shape, energetics and its associated implications for the respiratory apparatus (Bastir and Rosas 2011; Torres-Tamayo et al. 2018).

A similar phenomenon was found in an evolutionary anatomical context, where it was shown that the 3D morphology of the thoracic vertebrae in Neandertals was significantly different from that of modern humans (Bastir et al. 2017). The larger and more dorsally oriented transverse processes of the thoracic vertebrae of Neandertals (Bastir et al. 2017; Been et al. 2017a) related to a more invaginated spine into the thorax (García-Martínez et al. 2018a; Gómez-Olivencia et al. 2018).

Importantly, a most recent study of *H. erectus* vertebrae demonstrated that this morphological pattern is also present in the sub-adult thoracic vertebrae of KNM-WT 15000 (Bastir et al. 2018). This could imply that similarities in lower thoracic spine morphology in Neandertals and *H. erectus* are a primitive feature in *Homo*. However, such hypotheses need to be tested also on entire spines, which requires reconstructing them from isolated vertebrae.

16.3.2 Reconstructing 'Wholes' by 'Parts': A Geometric Morphometric Validation of Reconstruction Methods in the Thoracic Spine

Thoracic vertebrae are well preserved in several fossil hominins (e.g. Sts 14, StW-431, A.L. 288-1, MH1, MH2, KNM-WT 15000, Kebara 2, etc.). However, despite a good state of preservation, one of the challenges when reconstructing vertebral columns is the choice and validation of a criterion that allows for a faithful

articulation and assemblage of the isolated fossil vertebrae. Sawyer and Maley (2005) reconstructed physically and, more recently, Been et al. (2017a) virtually, the Kebara 2 thoracic spine. Been et al. (2017a) first calculated the thoracic kyphosis based on the relationship between (a) the ratio of the summed anterior vertebral heights and the summed posterior heights of the thoracic spine, and (b) the thoracic kyphosis. Once this value was obtained, contiguity and maximal overlap of the zygapophyseal facets was searched as a guiding reference for the reassembling of the thoracic spine. This led to a thoracic spine reconstruction of Kebara 2 that was less kyphotic than the mean of their modern human reference data, although it was within the human range.

Mallison (2010) presented a different standardized method for the reconstruction of the spine: the Osteological Neutral Pose (ONP) method, which aimed for a maximal and parallel overlap between the inferior and superior endplates of the adjacent vertebrae. The ONP method was developed for standardized thoracic spine reconstructions, but not necessarily for a rigorous reconstruction of the functional anatomy of the original spine. So far, the ONP method has been only applied to the reconstruction of quadrupedal animals (sauropodomorphs). Its potential usefulness for reflecting the specific spinal curvatures in bipedal humans has yet to be tested, and the well-known wedging shape of the vertebral bodies justifies such an approach.

Because the morphology of the thoracic spine affects the shape of the thorax (Jellema et al. 1993; Bastir et al. 2013; Latimer et al. 2016), quantified information about the uncertainty of reconstructions is desirable. Therefore, in the following, we describe a geometric morphometrics method for validation of different kinds of spine reconstructions following what we have called ‘zygapophyseal facet method’ (ZAM; contiguity and maximal overlap of the zygapophyseal facets), and ONP (Riesco López et al. 2018).

First, segmentation of CT scans of articulated spines to isolate the 3D meshes of the individual vertebrae of these spines was performed. Our CT data came from one European and one African subject who were chosen to work with some morphological variation in the data. Once the isolated virtual vertebrae were obtained, a reassembly was carried out of the individual vertebrae to the spines according to the ZAM and ONP methods (Mallison 2010; Been et al. 2017a).

Method 1 (ZAM) was based on a virtual reconstruction using the articular facets of the thoracic vertebrae as a reference. Method 2 (ONP) was a virtual reconstruction method following the criteria suggested by Mallison (2010) and was performed twice: the first time in a caudal direction, starting from the first thoracic vertebra, and the second time in a cranial direction, starting from the T12 vertebra. Method 3 (physical ZAM) used 3D printed models of isolated vertebrae to carry out a physical assemblage similar to Sawyer and Maley (2005). Thermoplastic glue was used for the adhesion of fitted vertebrae, simulating both intervertebral synovial joints (between articular facets) and cartilaginous joints (intervertebral discs). The final, physically assembled spine was surface scanned for landmark digitization. Finally, a 3D GM comparison of the reconstructed ($n = 8$) and the original ($n = 2$) thoracic

spines was carried out to compare the methods and to identify possible biases in the corresponding reconstructions.

A total of 108 points (9 landmarks × 12 vertebrae) were measured on each spine, and GPA, PCA and Procrustes distance matrix were performed to analyse the data. Riesco López et al. (2018) showed that the original spine (Fig. 16.2a) was slightly closer in overall shape (Procrustes distance = 1.25) to the spine reconstructed by the ZAM (Fig. 16.2b) method than to the reconstructions obtained by the ONP (PD = 1.34) method (Fig. 16.2c). The PCA of this preliminary data set also revealed that both ONP and facet-guided methods underestimated the original thoracic spine kyphosis: all reconstructions were slightly less kyphotic than their originals (Fig. 16.2). However, these findings are based on a small data set and need to be investigated in more detail in a larger sample.

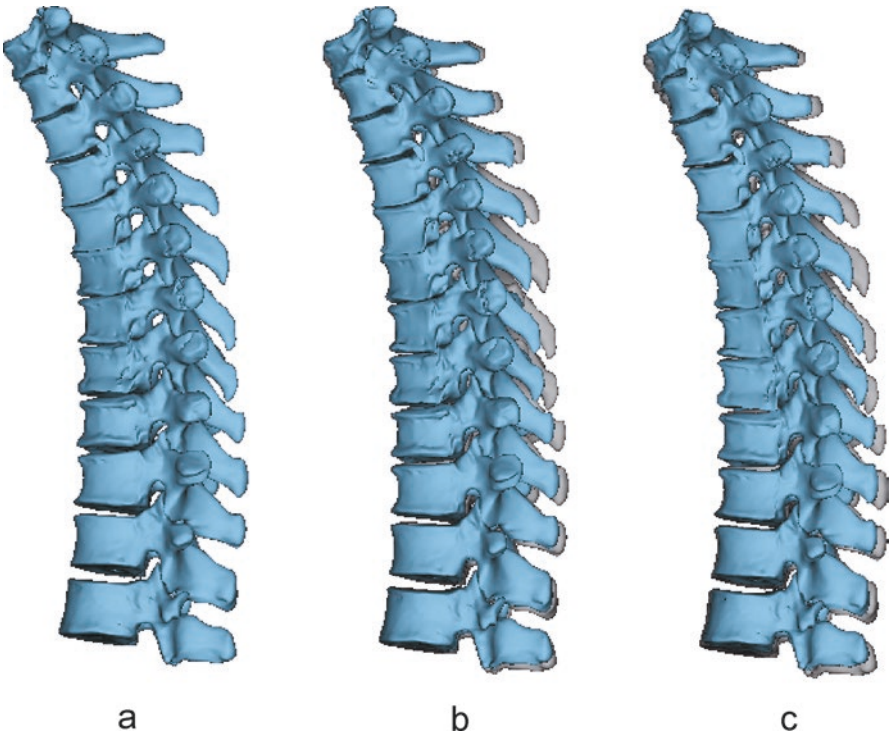

Fig. 16.2 Mean shapes of thoracic spines reconstructed by different methods fitting their isolated and adjacent vertebrae. (**a**) Mean shape of the original spines; (**b**) mean shape of the spine assemblage following the zygapophyseal methods (ZAM) compared to the original (in grey); (**c**) mean shape of the spine assemblage following osteological neutral pose (ONP) method compared to the original (in grey). Note the slight but systemic underestimation of thoracic kyphosis as a reconstruction artefact produced by ZAM and by ONP compared with the original biological form

16.4 The Lumbar Spine

The morphology of the lumbar spine is one of the key factors of the evolution of bipedal posture in hominins (Lovejoy 2005). Its distinctive sagittal convex curvature (lordosis) is directly related to maintaining an upright posture during bipedal gait (Shefi et al. 2013). This has both clinical and evolutionary implications and is the major framework in which GM work has been applied to the study of lumbar spine variation so far.

Martelli (2005) used 3D geometric morphometrics to assess the size and shape variation of the lumbar spine within and among extant and fossil hominoids. She collected $n = 62$ landmarks to cover the 3D morphology of the last five consecutive pre-sacral vertebrae and applied this protocol to the study of fossil lumbar vertebrae of *A. afarensis*, *A. africanus* and *H. ergaster* within a comparative context of extant great apes. She found that extant hominoids (except *Pan*) showed different degrees of sexual dimorphism in the size and shape of the lumbar vertebrae. Also, she encountered shape differences between taxa that can be discussed in the light of functional implications. This background allowed for characterization of the vertebral morphology of fossil lumbar vertebrae, concluding that *A. afarensis* and *A. africanus* lumbar vertebrae are more similar in shape to those of modern humans and less to those of great apes, and that *H. ergaster* lumbar vertebrae morphology falls within the range of modern humans. Therefore, she concluded that there are intra-specific patterns of scaling and of sexual dimorphism in the lumbar vertebrae that appear to vary according to functionality between apes and humans.

More recently, the data set of Martelli (2005) was extended by García-Martínez et al. (2015) for the study of the preserved fossil lumbar vertebrae of Kebara 2, Shanidar 3 and *La Chapelle-aux-Saints 1*, reporting the first 3D geometric morphometric analyses on the Neandertal lumbar vertebrae. Preliminary results indicated differences between the vertebral wedging of the upper and the lower lumbar spine in Neandertals: they showed posterior wedging at L1–L3 similar to modern human males but an increased vertebral height at L4 and L5 compared to modern males (but see Gómez-Olivencia et al. 2017 for different results). Their findings also show variation in modern humans related to sexual dimorphism, with males showing larger vertebral bodies than females.

Sexual dimorphism and population variation were part of a 3D GM study by Lois Zlolniski et al. (2017). In two different populations, they tested the hypothesis of a greater lumbar lordosis in females, proposed by Whitcome et al. (2007) as an adaptation for a better body stability during pregnancy. This hypothesis was rejected because their findings on sexual dimorphism showed up by differences in robustness possibly related to body size, rather than by differences on the degree of lordotic curvature. Variation in lumbar spine curvature was, however, associated to geographic factors: their European sample was more lordotic than the South African one (Lois Zlolniski et al. 2017, 2019). 3D GM further indicated that a similar angle of lordosis can be produced by different 3D morphometric patterns of curvature, possibly also in relation to the shape of the intervertebral discs.

In a clinical context, Plomp et al. (2015a, b) developed a 2D landmark protocol to characterize the thoracic [mentioned previously, (Plomp et al. 2012) and lumbar vertebral morphology of patients affected by Schmorl's nodes. By means of sliding semilandmarks measured in photographs of isolated lumbar vertebrae, they described the affected vertebrae as showing a relative decrease of the neural foramen size relative to the vertebral body, larger and rounder vertebral bodies as well as relative shorter and wider pedicles. Plomp et al. (2015a, b) hypothesized that shorter pedicles cannot support wider vertebral bodies and this could spark the development of Schmorl's nodes. Roundness is a difficult feature to describe by traditional morphometrics and so GM contributed to a finding of great clinical importance, shedding light on the aetiology of the Schmorl's nodes. In a more recent study, Plomp et al. (2018) applied 3D geometric morphometrics to isolated lumbar vertebrae of extant Hominoids and found features associated to bipedalism in *H. sapiens* that are discussed in the light of biomechanical implications.

The aforementioned palaeoanthropological studies make evident that the assessment, reconstruction and understanding of the lumbar lordosis are among the most important problems in the lumbar spine (Been et al. 2010, 2012, 2017b). Therefore, in the following, we present a method for the reconstruction of this functionally important part of the human spine.

16.4.1 Using 3D GM and Partial Least Squares Analysis (PLS) for Predicting Lumbar Lordosis

Lois Zlolniski et al. (2017) measured 390 landmarks and surface semilandmarks on the vertebral bodies and discs of lumbar spines in anatomical connection. They demonstrated a high and significant morphological covariation between the size and shape of individual lumbar vertebrae and the entire lumbar spine. Specifically, they found that L4 and L5 vertebral bodies show the highest percentage of covariation with the whole lumbar spine form. This covariation can be exploited for quantitative prediction of missing data in a way previously demonstrated by Archer et al. (2018) in an archaeological context.

Here we use 3D GM for a virtual reconstruction and validation of a complete lumbar spine on the basis of individual lumbar vertebrae (L4 and L5). The estimation of missing data based on this approach can be assessed considering the covariation between two different anatomical regions that do not need to be adjacent. Specifically, one anatomical region can be estimated from another one, with the only condition that these structures are highly covariant. The strength of covariation can be quantified through a Two-Blocks Partial Least Squares analysis (2B-PLS) (Rohlf and Corti 2000; Bookstein et al. 2003). Unlike linear regression analysis, which allows for the quantification of the variation of an independent variable explained by one or more factors, the 2B-PLS analysis treats two blocks symmetrically (Rohlf and Corti 2000). This is important in terms of the results interpretation,

since the PLS prediction method is based on the covariation between the blocks, not on the dependence of one block on the other one.

Here we use the shape data of Lois Zlolniski et al. (2017) (L4 and L5) as predictors of the shape of a complete lumbar spine (vertebral bodies). Analyses were performed in the statistical platform R version 3.4.1 (R-Core Team 2017) and specifically using the R-package Morpho 2.5.1 (Schlager 2017).

To avoid asymmetries inherent to the digitization template, data were symmetrized by reflected relabelling (Mardia et al. 2000) and the symmetrized landmark configurations were subjected to an iterative sliding process to minimize the bending energy of each specimen with respect to the symmetrized sample mean (Gunz et al. 2005; Gunz and Mitteroecker 2013). A random specimen was removed from the human lumbar spine sample ($n = 31$) to serve as 'test' object for future fossils we might encounter, so 30 human lumbar spines and a 'test' lumbar spine were obtained.

Since we treated this specimen as a hypothetic fossil, we simulated that we only had its L4 and L5 vertebrae as 'predictors', while the morphology of the complete lumbar spine was supposedly unknown. Therefore, predictions and validations were carried out twice: one with L4 as predictor and the other one with L5. Although the strength of covariation between two structures is primarily dependent on the relationship between them, the alignment of all the specimens in the Procrustes superimposition is crucial because an alignment of the entire configuration to a common centroid can overestimate the covariation between the two blocks, while an alignment to separate centroids can underestimate this covariation. To cope with this issue, we aligned the 30 specimens only by the predictors—either by their L4 or by their L5 vertebrae separately—and let the rest of the vertebrae without alignment. This ensures that the analysis incorporates the variability under the constraint that all data are aligned correctly to the predictor: in 'real-world' cases, this is the only viable way, as the missing part obviously cannot be used for the alignment. Then, we carried out two different 2B-PLS analyses between the sets (blocks) of variables as illustrated in Fig. 16.3, and we predicted the lumbar spine shape from its L4 and L5 vertebrae based on the covariation yielded by the 2B-PLS analyses.

The lumbar spines predictions were cross-validated for the quantification of the prediction error (Fig. 16.4), following Archer et al. (2018). That is, we developed a separate 2B-PLS model for each of the 30 lumbar spines excluding the particular specimen for which the prediction is being sought. This leaving-one-out cross-validation allowed us to know the number of latent variables of the PLS analysis that are necessary to make the predictions, those that report the lowest error (RMSE, root mean square error). The first latent variable of the 2B-PLS analysis between L4 vertebra and the rest of the lumbar spine accounted for 92.72% of the covariance and the PLS scores of the two blocks fit to a linear model ($R^2 = 0.71$; $p < 0.05$). The lumbar spine prediction from L4 was cross-validated and the first 18 latent variables were selected to perform the prediction, since they reflected the lowest prediction RMSE as indicated by the cross-validation analysis (Fig. 16.4a). The first latent variable of the 2B-PLS analysis between L5 vertebra and the rest of

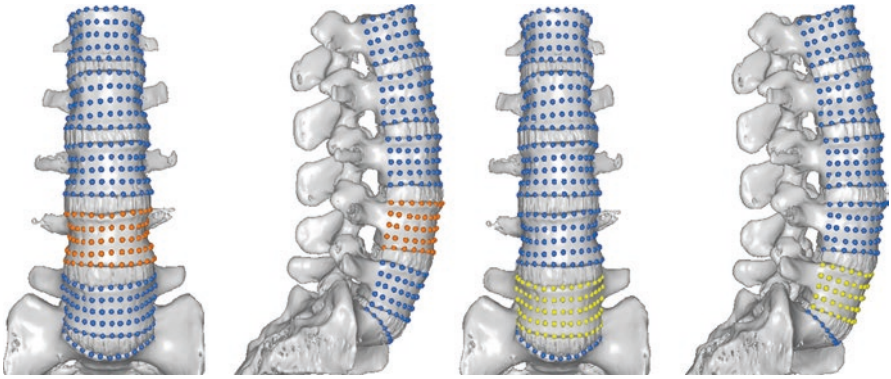

Fig. 16.3 Sets of coordinates (blocks) used in the Two-blocks Partial Least Squares analyses in frontal view and right lateral view. (**a**) Block 1 (blue, 390 landmarks), block 2 (orange, 75 landmarks); (**b**) Block 1 (blue, 390 landmarks), block 2 (yellow, 75 landmarks)

the lumbar spine accounts for 89.85% of the covariance and the PLS scores of the two blocks fit a linear model ($R^2 = 0.56$; $p < 0.05$). The shape prediction from L5 vertebra was cross-validated, and it was performed using the first 15 latent variables (Fig. 16.4b).

After cross-validating the predictions from L4 to L5, we calculated the procrustes distance (Pd) between the original and the predicted specimens in full shape space. We expected to obtain a smaller Pd between the original and the predicted specimens than between the original specimen and any other from the rest of the sample as a reflection of the accuracy in the prediction. The Pd between the L4-predicted and the original lumbar spine was the lowest (Pd = 0.032) among all Pds between the original specimen and the rest of the specimens (mean = 0.062, standard deviation = 0.021). This is a reflection of the similarity of these two shapes (original and reconstructed lumbar spines) in full shape space, and it can be visually observed in detail in Fig. 16.5. The Pd between the predicted lumbar spine from L5 and the original specimen in full shape space (Pd = 0.043) is not the lowest. The shape differences between the original and the predicted specimen are shown in Fig. 16.5.

This difference is caused by the strength of covariation between the sets involved in the analysis, that is, the greater the strength of covariation, the more accurate the result will be. Because of this, the predicted lumbar spine from L4 ($R^2 = 0.71$; $p < 0.05$) is more similar to the original specimen than the predicted lumbar spine from L5 ($R^2 = 0.56$; $p < 0.05$). However, although covariation and prediction quality are related to the sample size and the number of landmarks, this method provides a useful tool for the virtual quantitative reconstruction of parts and wholes. It is based on the biological factors driving covariation and provides a repeatable and complementary method for other kind of reconstructions based on anatomical experience.

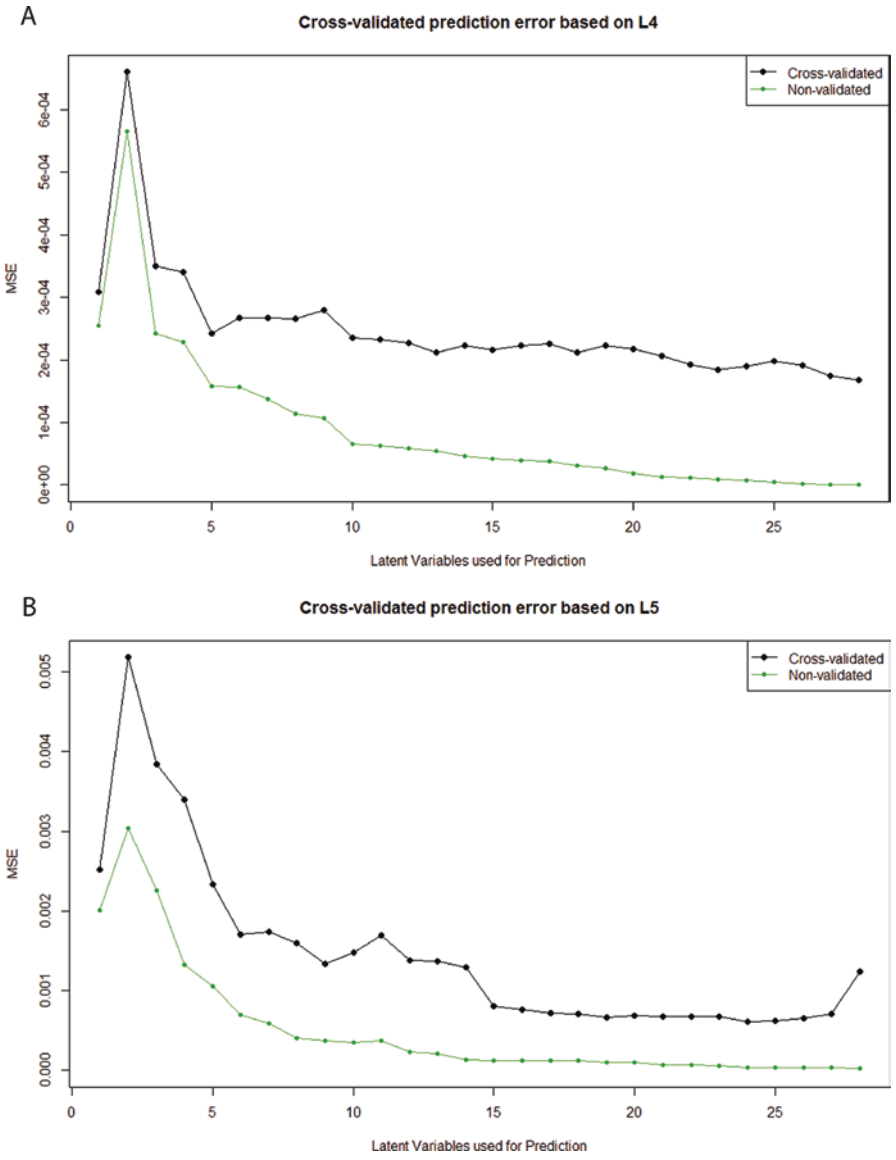

Fig. 16.4 Cross-validation: comparison between the cross-validated prediction of mean square error (MSE) (black) and non-validated prediction MSE (green) based on (**a**) L4 and (**b**) L5 vertebra

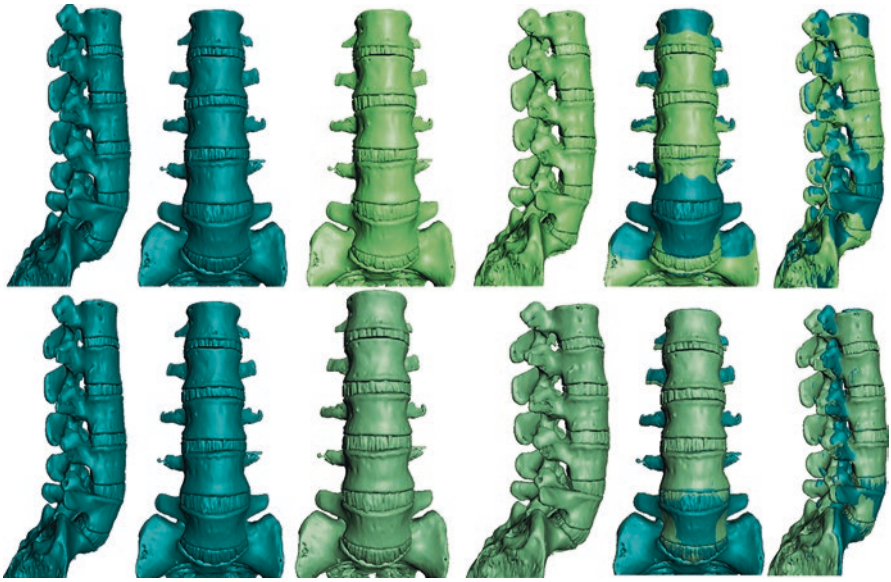

Fig. 16.5 Predicted and original lumbar spines (please note that the landmark acquisition was only performed on the vertebral bodies and thus the neural arc does not participate in the thin plate spline (TPS) warp, and therefore it may not be completely 'realistic' despite being quantitatively correct). Results of the predictions from L4 vertebra (upper row) and from L5 vertebra (lower row), showing the original lumbar spine in lateral and frontal view (left), the predicted lumbar spine (centre), and the original and the predicted lumbar spines superimposed together (right)

16.5 Discussion

In this book chapter, we aimed to review the most important aspects of using geometric morphometrics for the study of the hominin pre-sacral spine. Although GM has so far only rarely been applied to the spine, this review shows that GM is a powerful toolkit available for the measurement, analysis and reconstruction of vertebrae and spines. Therefore, many factors of intra- and interspecific variation need yet to be investigated. We furthermore provided some examples of 3D GM reconstructions of incomplete fossils and spines and proposed some methods for testing the validity of virtually assembled spines. This discussion aims to summarize the advantages and limitations of the presented methods applied to the study of the human and hominin spine.

16.5.1 What Can We Learn or Get from GM Studies of the Spine that We Cannot Learn or Get Using Traditional Approaches?

Traditional morphometrics represent the morphology of a given structure by abstract numbers (e.g. angles, distances) which become decontextualized from the anatomy of a structure during the process of measurement and analysis (Rohlf and Marcus 1993; Zelditch et al. 2012). For example, the meaning of a given length, distance or angle between two lines is very different biologically when these measurements describe horizontal, vertical or oblique structures. That means the spatial information of this distance is not part of the statistical analysis and, consequently, must be interpreted by the researcher and it cannot be reconstructed by the analysed data (Rohlf and Marcus 1993).

Conversely, in GM, there is a direct correspondence between the real 3D morphology of a structure, the measurement of its Cartesian coordinates of landmarks and its statistical analysis (Bookstein 1991; Rohlf and Marcus 1993; Rohlf 1996; Mitteroecker and Gunz 2009). Indeed, by using 3D semilandmarks the morphology of a vertebra is almost completely reflected by its landmark configuration (Manfreda et al. 2006; Palancar et al. 2018; Fig.16.1b). This, together with the isomorphic relation between statistical and configuration spaces (Rohlf 2000, 2003), provides the researcher with a GM toolkit capable to reflect graphically directly what has been analysed. No interpretation or data reconstruction is necessary because the statistical results *are* the 3D images, visualizations and scatterplots produced during the GM analysis (Mitteroecker and Gunz 2009).

These advantages can be directly extrapolated to the analysis of the spine, at the level of measurement, analysis and reconstructions. The possibility of measuring vertebral or spine shapes in terms of 3D landmarks and curve- and surface semilandmarks (Gunz and Mitteroecker 2013) lets the researcher to fully describe not only the morphology of the shape of the vertebral bodies, its processes and the curves of the neural canal, but also the spatial properties of all these structures relative to each other. All analyses of vertebral and spine landmark data will benefit from these general advantages of GM over the traditional methods mentioned above (Rohlf and Marcus 1993). But there are also some pitfalls.

16.5.2 When Can These Approaches Be Applied and When Do They Fail?

While a greater number of landmarks and semilandmarks will lead to a better correspondence between the real anatomy of the object (vertebra) and its geometric representation (landmark configuration), there are some situations when GM analyses can fail. These are related to the relationship between the number of landmarks

(variables) and the number of specimens (cases). This is because any kind of statistical analyses that involve the inversion of a covariance matrix, for example, multiple regression analysis, canonical variate analysis (CVA) and parametric multivariate tests (MANOVA, MANCOVA), require a data set that consists of many more specimens than landmarks (Mitteroecker and Bookstein 2011; Bookstein 2017b). In such cases, variable reduction by principal components or other factor analyses could be carried out before applying statistical methods which require the inversion of the covariance matrix. The calculation of principal component analyses and mean shapes is not affected by this problem (Mitteroecker and Bookstein 2011).

16.5.3 Applications of GM to Virtual Reconstructions of Vertebrae and Spines

In palaeoanthropology, a frequent problem is how to analyse and compare by GM fossils of fragmented anatomical structures with a reference sample consisting of complete (unbroken) structures. Because a GM study requires all specimens of the sample to provide the same number of homologous landmarks, there are only two possibilities: one can reduce the landmark set of the reference sample of the complete structures to equal those that are preserved in the broken fossil, but this may provide limited anatomical information. Alternatively, one can proceed to estimate the missing landmarks to equal those of the reference sample (Gunz et al. 2009; Gunz and Mitteroecker 2013). This, however, requires some hypotheses to be made by the researcher. Such hypotheses could include assumptions about interspecific similarity of covariation patterns among structures that could be tested in phylogenetically related extant species (Arlegi et al. 2018). For example, if covariation between two structures is similar in a chimpanzee and a human data set, this similarity could be assumed also in a given fossil hominin species. Ideally, different methods for missing landmark estimations are carried out revealing the possible bias of the reconstructions (Gunz et al. 2009; Neubauer et al. 2018).

The combination of 3D GM and virtual morphology enables the palaeoanthropologist to elaborate reconstructions that are both, quantitatively and morphologically valuable (Gunz et al. 2009; García-Martínez et al. 2018b; Palancar et al. 2018). On the one hand, GM-based virtual reconstructions are useful quantitatively because these estimated landmark coordinates have a reproducible and statistical basis that justifies their use in comparative morphometric analyses. On the other hand, GM-based virtual reconstructions are useful morphologically, because landmarks can be used to deform the 3D mesh of a complete structure to the geometry of landmarks that were previously statistically estimated. We have shown how GM can be used to combine the originally preserved fossil fragments with the reconstructed mesh (Fig. 16.1). These reconstruction methods reflect the direct link of GM between statistical shape and morphological configuration spaces of landmarks (Rohlf and Marcus 1993; Rohlf 1996).

Our review suggests that several notions of reconstruction could be distinguished: (1) reconstruction as the *estimation of missing landmark data* (either statistically, geometrically, or even manually (Gunz et al. 2009) resulting in a set of estimated landmarks); (2) the proper *reconstruction* of missing parts of an incomplete bone, resulting in the reconstruction of a complete structure in virtual morphology (Fig. 16.1); and (3) the reconstruction of a complex anatomical structure (e.g. a spine built by its multiple vertebrae) as *assembling* the individual anatomical elements. The result of this last kind of reconstruction is a complete metameric (or otherwise complex) structure (Figs. 16.2 and 16.3). Usually, and in the context of the spine, a GM reconstruction will make use of more than one notion of reconstruction. In fact, there is even a specific case, which is the estimation of missing elements in serial structures (García-Martínez et al. 2018b). The result of this kind of reconstruction is a set of coordinates of an entire bone.

However, whenever possible, the reconstructions should be validated. We provided here two examples: an empirical validation based on *reconstruction experiments* of the thoracic spine, as well as a statistical validation of the lumbar spine. We showed on preliminary data that some methods for assembly may lead to a potential underestimation of thoracic kyphosis (Fig. 16.2). This bias can be quantified by GM as a difference vector between the original and the reassembled spines. This vector could then be used for virtual morphological modelling to adjust assemblages of thoracic spines in fossils. Similar experiments should be applied to the lumbar and cervical spine. We also used a statistical validation such as applying a leave-one-out resampling methods. This has shown that the morphological integration (covariation) among lumbar vertebrae is an important factor that affects the biological accuracy of the spine reconstruction supporting previous suggestions (Gunz et al. 2009).

Finally, despite the stimulating potential and the attractiveness of 3D images of hominin fossils in GM analyses and virtual reconstructions, it should be noted that the anatomical and morphological experience of the palaeoanthropologist cannot be replaced by methods, and should always guide any virtual morphological manoeuvre whatever sophisticated. Only the combination of virtual, quantitative methods with experienced descriptive morphology and anatomy of real fossils will provide the best possible approximation to palaeoanthropological reality (Bastir 2018). With respect to reconstructions, it is here where traditional morphometric methods should come into play again. After the completion of the workflows reviewed above, the final outcome is a fossil, either a virtual or 3D printed one. By measuring linear distances or angles, we can back these fossils again into the broader context of other specimens, published independent on specific methods over the history of palaeoanthropology.

Acknowledgments We thank Ella Been, Patricia Kramer, Asier Gómez-Olivencia and Alon Barash for the invitation to participate in this volume. Antonio Rosas provided access to material from El Sidrón. Paul O'Higgins and the anonymous reviewers and the editors have provided useful thoughts. This work is funded by CGL2015-63648-P (MINECO, Spain).

References

Adams DC, Cerney MM (2007) Quantifying biomechanical motion using Procrustes motion analysis. J Biomech 40(2):437–444

Adams DC, Collyer ML (2009) A general framework for the analysis of phenotypic trajectories in evolutionary studies. Evolution 63(5):1143–1154

Archer W, Pop CM, Rezek Z, Schlager S, Lin SC, Weiss M, Dogandžić T, Desta D, McPherron SP (2018) A geometric morphometric relationship predicts stone flake shape and size variability. Archaeol Anthropol Sci 10:1991–2003

Arlegi M, Gómez-Olivencia A, Albessard L, Martínez I, Balzeau A, Arsuaga JL, Been E (2017) The role of allometry and posture in the evolution of the hominin subaxial cervical spine. J Hum Evol 104:80–99

Arlegi M, Gómez-Robles A, Gómez-Olivencia A (2018) Morphological integration in the gorilla, chimpanzee, and human neck. Am J Phys Anthropol 166(2):408–416

Bastir M (2018) Back to basics: morphological analysis in paleoanthropology. In: Schwartz J (ed) Rethinking human evolution. The MIT Press, Cambridge, pp 205–227

Bastir M, García Martínez D, Recheis W, Barash A, Coquerelle M, Rios L, Peña-Melián Á, García Río F, O'Higgins P (2013) Differential growth and development of the upper and lower human thorax. PLoS One 8(9):e75128

Bastir M, García Martínez D, Rios L, Higuero A, Barash A, Martelli S, García Tabernero A, Estalrrich A, Huguet R, de la Rasilla M, Rosas A (2017) Three-dimensional morphometrics of thoracic vertebrae in Neandertals and the fossil evidence from El Sidrón (Asturias, Northern Spain). J Hum Evol 108:47–61

Bastir M, García Martínez D, Spoor F, Williams SA (2018) Thoracic vertebral morphology of KNM-WT 15000. Proc Eur Soc Study Human Evol 7:11

Bastir M, Higuero A, Ríos L, García Martínez D (2014) Three-dimensional analysis of sexual dimorphism in human thoracic vertebrae: implications for the respiratory system and spine morphology. Am J Phys Anthropol 155(4):513–521

Bastir M, O'Higgins P, Rosas A (2007) Facial ontogeny in Neanderthals and modern humans. Proc R Soc B Biol Sci 274:1125–1132

Bastir M, Rosas A (2009) Mosaic evolution of the basicranium in *Homo* and its relation to modular development. Evol Biol 36:57–70

Bastir M, Rosas A (2011) Nasal form and function in Midpleistocene human facial evolution. A first approach. Am J Phys Anthropol 144(S52):83

Bastir M, Rosas A, O'Higgins P (2006) Craniofacial levels and the morphological maturation of the human skull. J Anat 209(5):637–654

Been E, Gómez-Olivencia A, Kramer PA (2012) Lumbar lordosis of extinct hominins. Am J Phys Anthropol 147(1):64–77

Been E, Gómez-Olivencia A, Kramer PA, Barash A (2017a) 3D reconstruction of the spinal posture in the Kebara 2 Neanderthal. In: Marom A, Hovers E (eds) Human paleontology and prehistory. Springer International Publishing, Cham, pp 239–251

Been E, Gómez-Olivencia A, Shefi S, Soudack M, Bastir M, Barash A (2017b) Evolution of spinopelvic alignment in hominins. Anat Rec 300(5):900–911

Been E, Peleg S, Marom A, Barash A (2010) Morphology and function of the lumbar spine of the Kebara 2 Neandertal. Am J Phys Anthropol 142(4):549–557

Bookstein FL (1991) Morphometric tools for landmark data. Cambridge University Press, Cambridge

Bookstein FL (1996) Combining the tools of geometric Morphometrics. In: Marcus LF (ed) Advances in Morphometrics. Plenum Press, New York, pp 131–151

Bookstein FL (2017a) A method of factor analysis for shape coordinates. Am J Phys Anthropol 164(2):221–245

Bookstein FL (2017b) A newly noticed formula enforces fundamental limits on geometric morphometric analyses. Evol Biol 44(4):522–541

Bookstein FL, Gunz P, Mitteroecker P, Prossinger H, Schaefer K, Seidler H (2003) Cranial integration in *Homo*: singular warps analysis of the midsagittal plane in ontogeny and evolution. J Hum Evol 44(2):167–187

Chamero B, Buscalioni AD, Marugán-Lobón J, Sarris I (2014) 3D geometry and quantitative variation of the cervico-thoracic region in crocodylia. Anat Rec 297(7):1278–1291

Chatzigianni A, Halazonetis DJ (2009) Geometric morphometric evaluation of cervical vertebrae shape and its relationship to skeletal maturation. Am J Orthod Dentofac Orthop 136(4):481.e481–481.e489

Cobb S, O'Higgins P (2002) The ontogeny of form in the African ape facial skeleton: a hierarchical approach to the interspecific comparison of ontogenetic trajectories. Am J Phys Anthropol 117(S34):55

Cobb S, O'Higgins P (2004) Hominins do not share a common postnatal facial ontogenetic shape trajectory. J Exp Zool B Mol Dev Evol 302B(3):302–321

Diaconis P, Goel S, Holmes S (2008) Horseshoes in multidimensional scaling and local kernel methods. Ann Appl Stat 2(3):777–807

García-Martínez D, Riesco A, Bastir M (2018b) Missing element estimation in sequential anatomical structures: the case of the human thoracic vertebrae and its potential application to the fossil record. In: Carme Rissech LL, Joordi Nadal, Josep Maria Fullola (eds) Geometric morphometrics Trends in biology, paleobiology and archaeology: Seminari d'Estudis i Recerques Preshistoriques, Universitat de Barcelona (SERP), Societat Catalana d'Arqueologia (SCA), p 93–97

García-Martínez D, Torres-Tamayo N, Torres-Sanchez I, García-Río F, Bastir M (2016) Morphological and functional implications of sexual dimorphism in the human skeletal thorax. Am J Phys Anthropol 161(3):467–477

García-Martínez D, Martelli S, Bastir M, O'Higgins P (2015) Neanderthal lumbar lordosis assessed by 3D geometric morphometrics of vertebral morphology, ESHE. PESHE, London, p 95

García-Martínez D, Torres-Tamayo N, Torres-Sánchez I, García-Río F, Rosas A, Bastir M (2018a) Ribcage measurements indicate greater lung capacity in Neanderthals and lower Pleistocene hominins compared to modern humans. Commun Biol 1(1):117

Gómez-Olivencia A (2013) Back to the old man's back: reassessment of the anatomical determination of the vertebrae of the Neandertal individual of La Chapelle-aux-saints. Annales de Paléontologie 99(1):43–65

Gómez-Olivencia A, Arlegi M, Barash A, Stock JT, Been E (2017) The Neandertal vertebral column 2: the lumbar spine. J Hum Evol 106:84–101

Gómez-Olivencia A, Barash A, García-Martínez D, Arlegi M, Kramer P, Bastir M, Been E (2018) 3D virtual reconstruction of the Kebara 2 Neandertal thorax. Nat Commun 9(1):4387

Gower JC (1975) Generalized procrustes analysis. Psychometrika 40(1):33–51

Gunz P, Mitteroecker P (2013) Semilandmarks: a method for quantifying curves and surfaces. Hystrix 24(1):103–109

Gunz P, Mitteroecker P, Bookstein FL (2005) Semilandmarks in three dimensions. In: Slice D (ed) Modern morphometrics in physical anthropology. Springer, New York, pp 73–98

Gunz P, Mitteroecker P, Neubauer S, Weber GW, Bookstein FL (2009) Principles for the virtual reconstruction of hominin crania. J Hum Evol 57(1):48–62

Jellema LM, Latimer B, Walker A (1993) The rib cage. In: Walker A, Leakey R (eds) The Nariokotome *Homo erectus* skeleton. Harvard University Press, Cambridge, MA, pp 294–325

Kendall DG (1970) A mathematical approach to seriation. Philos Trans R Soc Lond A Math Phys Eng Sci 269(1193):125–134

Klingenberg CP, Marugán-Lobón J (2013) Evolutionary covariation in geometric morphometric data: analyzing integration, modularity and allometry in a phylogenetic context. Syst Biol 62:591–610

Latimer B, Lovejoy CO, Spurlock L, Haile-Selassie Y (2016) The thoracic cage of KSD-VP-1/1. In: Haile-Selassie Y, Su DF (eds) The postcranial anatomy of Australopithecus afarensis: new insights from KSD-VP-1/1. Springer Science+Business Media, Dordrecht, pp 143–153

Lois Zlolniski S, García Martínez D, García Blanco E, Sanchis Gimeno JA, Barash A, Martelli S, Nalla S, Bastir M (2017) 3D geometric morphometrics of lumbar vertebral curvatures in *H. sapiens*. Am J Phys Anthropol 162(S64):265

Lois Zlolniski S, Torres-Tamayo N, García Martínez D, Blanco-Pérez E, Mata Escolano F, Barash A, Nalla S, Martelli S, Sanchis Gimeno JA, Bastir M (2019) 3D geometric morphometric analysis of variation in the human lumbar spine. Am J Phys Anthropol

Lovejoy CO (2005) The natural history of human gait and posture. Gait Posture 21(1):95–112

Mallison H (2010) The digital *Plateosaurus* II: an assessment of the range of motion of the limbs and vertebral column and of previous reconstructions using a digital skeletal mount. Acta Paleontologica Polonia 55(3):433–458

Manfreda E, Mitteroecker P, Bookstein FL, Schaefer K (2006) Functional morphology of the first cervical vertebra in humans and nonhuman primates. Anat Rec B New Anat 289B(5):184–194

Mardia KV, Bookstein FL, Moreton IJ (2000) Statistical assessment of bilateral symmetry of shapes. Biometrika 87(2):285–300

Martelli SA (2005) A comparative morphometric study of the hominoid lumbar spine. Ph.D. thesis, University of London

McIntyre DC, Rakshit S, Yallowitz AR, Loken L, Jeannotte L, Capecchi MR, Wellik DM (2007) Hox patterning of the vertebrate rib cage. Development 134(16):2981–2989

Meyer MR, Woodward C, Tims A, Bastir M (2018) Neck function in early hominins and suspensory primates: insights from the uncinate process. Am J Phys Anthropol 166(3):613–637

Mitteroecker P, Bookstein F (2011) Linear discrimination, ordination, and the visualization of selection gradients in modern morphometrics. Evol Biol 38(1):100–114

Mitteroecker P, Gunz P (2009) Advances in geometric morphometrics. Evol Biol 36(2):235–247

Mitteroecker P, Gunz P, Bernhard M, Schaefer K, Bookstein FL (2004) Comparison of cranial ontogenetic trajectories among great apes and humans. J Hum Evol 46(6):679–698

Nalley TK, Grider-Potter N (2017) Functional analyses of the primate upper cervical vertebral column. J Hum Evol 107:19–35

Neubauer S, Gunz P, Leakey L, Leakey M, Hublin J-J, Spoor F (2018) Reconstruction, endocranial form and taxonomic affinity of the early *Homo* calvaria KNM-ER 42700. J Hum Evol 121:25–39

O'Higgins P (2000) The study of morphological variation in the hominid fossil record: biology, landmarks and geometry. J Anat 197:103–120

Palancar CA, García-Martínez D, Barash A, Radovčić D, Rosas A, Bastir M (2018) Reconstruction of the atlas (C1) of the La Chapelle-aux-saints Neanderthal through geometric morphometric techniques. Proc Eur Soc Study Human Evol 7:152

Plomp KA, Roberts CA, Viðarsdóttir US (2012) Vertebral morphology influences the development of Schmorl's nodes in the lower thoracic vertebrae. Am J Phys Anthropol 149(4):572–582

Plomp KA, Roberts C, Viðarsdóttir US (2015a) Does the correlation between Schmorl's nodes and vertebral morphology extend into the lumbar spine? Am J Phys Anthropol 157(3):526–534

Plomp KA, Viðarsdóttir US, Weston DA, Dobney K, Collard M (2015b) The ancestral shape hypothesis: an evolutionary explanation for the occurrence of intervertebral disc herniation in humans. BMC Evol Biol 15:68

Plomp KA, Viðarsdóttir US, Weston DA, Dobney K, Collard M (2018) Adaptations for bipedalism in human vertebrae: a 3D geometric morphometric analysis. Proc Eur Soc Study Human Evol 7:152

Ponce de León M, Zollikofer C (2001) Neandertal cranial ontogeny and its implications for late hominid diversity. Nature 412:534–538

R Core Team (2017) R: a language and environment for statistical computing. R Foundation for Statistical Computing, Vienna

Riesco López A, García-Martínez D, Bastir M (2018) Reconstrucción del segmento torácico de la columna vertebral en Paleoantropología. In: Amayuelas E, Bilbao-Lasa P, Bonilla O, del Val M, Errandonea-Martin J, Garate-Olave I, García-Sagastibelza A, Intxauspe-Zubiaurre B, Martinez-Braceras N, Perales-Gogenola L, Ponsoda-Carreres M, Portillo H, Serrano H,

Silva-Casal R, Suárez-Bilbao A, Suarez-Hernando O (eds) Life finds a way. Encuentro de Jóvenes Investigadores en Paleontología, Gasteiz, pp 241–244
Ríos L, Palancar CA, Pastor F, Llidó S, Sanchís-Gimeno JA, Bastir M (2017) Shape change in the atlas with congenital midline non-union of its posterior arch: a morphometric geometric study. Spine J 17(10):1523–1528
Rohlf FJ (1996) Morphometric spaces, shape components and the effects of linear transformations. In: Marcus LF (ed) Advances in morphometrics. Plenum Press, New York, pp 117–128
Rohlf FJ (2000) On the use of shape spaces to compare morphometric methods. Hystrix 111:19–25
Rohlf FJ (2003) Bias and error in estimates of mean shape in geometric morphometrics. J Hum Evol 44(6):665–683
Rohlf FJ, Corti M (2000) The use of two-block partial least-squares to study covariation in shape. Syst Zool 49:740–753
Rohlf FJ, Marcus LF (1993) A revolution in morphometrics. Trends Ecol Evol 8(4):129–132
Sarris I (2013) Organización morfológica y variación del esqueleto axial de víboras. Doctoral dissertation, Universidad Autónoma de Madrid, Spain
Sarris I, Chamero B (2009) Serial homology and the horseshoe effect. Proceedings of the I Iberian Symposium on Geometric Morphometrics. p 111–112
Sawyer GJ, Maley B (2005) Neanderthal reconstructed. Anat Rec B New Anat 283B(1):23–31
Schlager S (2017) Morpho and Rvcg – shape analysis in R: R-packages for geometric morphometrics, shape analysis and surface manipulations. In: Zheng G, Li S, Székely G (eds) Statistical shape and deformation analysis: methods, implementation and applications. Elsevier Academic Press, San Diego, pp 217–256
Schlösser TPC, van Stralen M, Chu WCW, Lam T-P, Ng BKW, Vincken KL, Cheng JCY, Castelein RM (2016) Anterior overgrowth in primary curves, compensatory curves and junctional segments in adolescent idiopathic scoliosis. PLoS One 11(7):e0160267
Schultz AH (1942) Conditions for balancing the head in primates. Am J Phys Anthropol 29(4):483–497
Shefi S, Soudack M, Konen E, Been E (2013) Development of the lumbar lordotic curvature in children from age 2 to 20 years. Spine 38(10):E602–E608
Sokal RR, Rohlf FJ (1998) Biometry. W.H. Freeman and Company, New York
Solanas S, García-Martínez D, Bastir M (2015) Morfometría geométrica 3D de la columna vertebral de hominoideos y sus implicaciones para el entendimiento de la postura bípeda en *Australopithecus*. Proceedings of the 19th annual meeting of the Sociedad Española de Antropología Física SEAF. p 132
Torres-Tamayo N, García-Martínez D, Lois Zlolniski S, Torres-Sánchez I, García-Río F, Bastir M (2018) 3D analysis of sexual dimorphism in size, shape and breathing kinematics of human lungs. J Anat 232(2):227–237
Waldock C, Milne N, Rubenson J, Donnelly CJ (2016) The use of geometric morphometric techniques to identify sexual dimorphism in gait. J Appl Biomech 32(5):441–448
Weber GW (2015) Virtual anthropology. Am J Phys Anthropol 156:22–42
Weber GW, Bookstein FL (2011) Virtual anthropology: a guide to a new interdisciplinary field. Springer-Verlag, Vienna
Whitcome KK, Shapiro LJ, Lieberman DE (2007) Fetal load and the evolution of lumbar lordosis in bipedal hominins. Nature 450(7172):1075–1078
Williamson MH (1978) The ordination of incidence data. J Ecol 66(3):911–920
Zelditch ML, Swiderski DL, Sheets HD, Fink WL (2012) Geometric morphometrics for biologists: a primer. Elsevier Academic Press, San Diego

Chapter 17
Modeling the Spine Using Finite Element Models: Considerations and Cautions

Patricia Ann Kramer, Alexandra G. Hammerberg, and Adam D. Sylvester

17.1 Introduction

The preceding chapters of this volume describe in exquisite detail variation in spinal morphology among individuals, populations, and species. For most researchers interested in the evolution of the hominin spine, though, the central question is not "what is the shape?" but rather "what does the shape tell us about the function?" and, therefore, analyses of shape are usually only the first step in a research program. Traditional methods of interrogating function rely on the association of a function with a form that can be observed (e.g., wedging of lumbar vertebrae is associated with lumbar lordosis (e.g., Been et al. 2009; Pickering et al. 2019) which is associated with bipedalism in modern humans (e.g., Lovejoy 1988)). This association can then be extrapolated to infer function in forms whose function cannot be observed (e.g., fossil hominins (Been et al. 2010, 2012, 2014)).

But what happens when a form is seen in the fossil record that has no modern analogue? An example of this quandary is the recently detailed (Gómez-Olivencia et al. 2018; Been et al. 2016) lumbar spinal morphology in Neandertals (and their precursors). Neandertals have flat lumbar spines (relative to modern humans and to earlier hominins); what does that mean for their function, their form of bipedalism? A traditional method in engineering, finite element analysis (FEA) is becoming part of the toolkit of researchers interested in the fossil record (e.g., Püschel et al. 2018), and FEA offers the opportunity to explore connections between form and function from a theoretical perspective.

P. A. Kramer (✉) · A. G. Hammerberg
Department of Anthropology, University of Washington, Seattle, WA, USA
e-mail: pakramer@uw.edu

A. D. Sylvester
Center for Functional Anatomy and Evolution, Johns Hopkins University School of Medicine, Baltimore, MD, USA

E. Been et al. (eds.), *Spinal Evolution*,
https://doi.org/10.1007/978-3-030-19349-2_17

In mathematical terms, FEA is a method of evaluating the response of geometric constructs that are subjected to external conditions. Numerical integration techniques are used to solve boundary value problems defined by the governing partial differential equations. The essential aspects of the geometric construct are discretized into elements of finite, but small size, such that a numerical method solution exists for each element. The partial differential equation then reduces to the matrix algebra manipulation of these many finite elements (Dhatt et al. 2012).

Although these external conditions can require solutions that range from vibration analyses to those associated with fluid dynamics, most applications in biological anthropology and evolutionary biology involve the analysis of structural systems, i.e., ones where physical objects (such as bones or soft tissues) are exposed to applied loads (such as those originating from gravitational forces or generated by muscular action). Returning to the example of flat lumbar spines in Neandertals, a finite element model (FEM) of the lumbar spine of modern humans could be built and validated for important loading conditions, such as walking or carrying a burden. The modern human model could then be modified to the morphology of Neandertals to examine how Neandertal form changes such things as the deflection of the spine or the loads that are transferred to the pelvis.

This is but one example of a myriad of potential models or questions that could be examined with the FEA approach. For instance, representing bones and the soft tissue environment in a FEM allows for the examination of fine-grained details, such as a crest or ridge for muscular attachment or the impact of variations in geometry on muscle origins or insertions (e.g., differences between the orientation of the spinous process in *Homo sapiens* vs. Neandertals); for the calculation of three-dimensional effects, such as forces applied in secondary planes (e.g., compression and torsion in intervertebral disks); and for easier changes to such things as the shape of the bone or loading environment (e.g., loads associated with bipedalism vs. suspensory movements) than possible with manual calculations. The most common assumption for the solution of the problem in structural systems is static equilibrium, but dynamic problems can also be addressed. Common results from FEA include displacements, elemental stress and strain, and strain energy density.

The spine, with its intricate shapes and the complexity of the interactions of the multiple critical bony and soft tissue parts, is a structure that is well-suited to the time and effort required to recreate it virtually. This review focuses on the application of FEMs of the spine in static equilibrium to understand spinal morphology within and among extinct and extant primate species.

17.2 FEA as a Technique

FEA harnesses the ability of computers to perform calculations rapidly in order to approximate the action of the structure of interest (Dhatt et al. 2012), which in the case of this review is the spine. FEAs, as with all analyses, are predicated on the problems to be solved or questions to answered. Many questions can be asked of

any structure regardless of geometry or material composition, e.g., is it strong enough to withstand the forces applied to it or will it bend too much—or too little—to perform its function? The scope of the inquiry is important, too. Does the question involve the entire structure or only part of it? The nature of the question to be answered and the scale over which the analysis extends determine the FEM to be developed (Sylvester and Kramer 2018). In other words, the FEM should replicate those aspects that are of most importance and considerable effort should be devoted to this consideration before any model is conceived or attempted.

Three basic inputs are needed for any structural FEM: geometry, material properties, and boundary conditions. Each of these inputs will be discussed in detail below. The resultant of FEA is typically element strain that can be manipulated to calculate element stress and model strain energy, as well as other parameters. The choice of resultant parameter is dictated by an assessment of which one(s) can be used to answer the initial question of interest.

The material of the physical object is represented by geometric shapes (elements) that are small enough such that their actions relative to the whole object can be represented mathematically (Dhatt et al. 2012). Each element is of finite size, but that size is deemed by the developer to be sufficiently small such that the sum of the actions of each element relative to those contiguous with it represents the whole (Sack and Urrutia 1999). The choice of element size is, therefore, critical. In FEM development, models, or regions within models, can be described by the researcher as "fine" or "coarse" grid, but that assessment is based on how detailed the answer needs to be. For instance, a question concerning overall spinal motion might allow for a model with larger elements to represent the vertebra than one focused on understanding the effect of trabecular density on fracture. No global "right" size finite element exists and the effect of element size needs to be evaluated at multiple stages in the FEM development process from an assessment of element quality in the initial FEM development to evaluation of the displacements and other results.

In linear static solutions, the action of each finite element is governed by the equations of solid mechanics. The solution to these equations for each element is relatively simple, but in order to represent the whole object, the number of elements can exceed hundreds of thousands, if not millions. These governing equations of each interaction between the finite elements need to be solved simultaneously, resulting in a computationally immense problem. For questions that involve understanding how an object, such as a bone, reacts to the application of a force, from such things as muscular action or contact, this mathematical problem can be solved by representing the equations in matrix form (the stiffness matrix) and then decomposing that matrix.

Of importance to note: linear static analyses assume that small displacement theory is appropriate, i.e., that the stiffness matrices of the initial and deformed structure are effectively the same (Carrera et al. 2014). As the name implies, displacement of the structure or its parts is considered to be small, where "small" means that the angle of displacement is approximately equal to its cosine (Fig. 17.1). The level of approximation that is acceptable should, as with all model parameters,

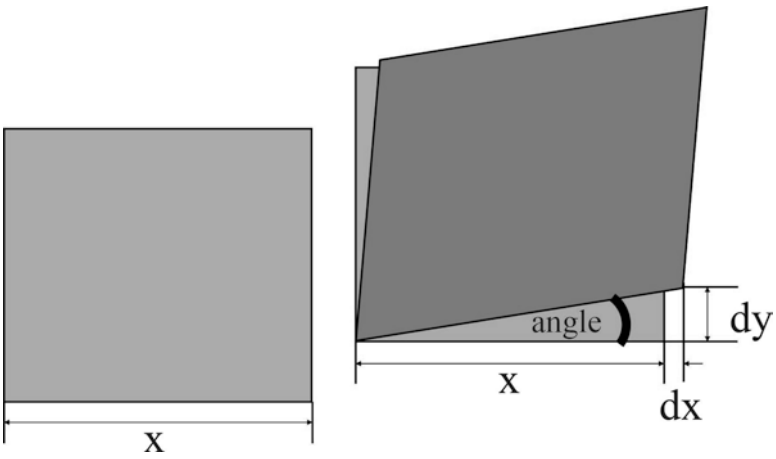

Fig. 17.1 Small displacement theory. The initial shape of the finite element (light gray square) displaces and changes into the final shape of the finite element (dark gray, overlaid on initial shape). The displacement is small when the cosine of the angle approaches 1

be carefully considered by the researcher. For instance, the cosine of 1° is 0.9999 (0.01% difference between the angle and its cosine), while the cosine of 10° is 0.9848 (1.5% difference). If this assumption is violated, i.e., if the structure is not rigid, then other, more complex analysis methods are required. The spine presents opportunities to use static analysis, such as an examination of the effect of burdens or center of mass variation on vertebral body stress or strain, but regions of the spine (e.g., the intervertebral disks) can experience comparatively large displacements where linear static analyses may not fully capture the complexity of the system. Nonetheless, linear static analysis is attempted before more complicated ones.

FEMs can be organized into regions or components to aid in handling the millions of elements in typical models. In some cases, the structure to be modeled can be aggregated into a single component, but in many cases, multiple components may be desirable. For instance, bone (e.g., the vertebral body) should be in a separate component from soft tissues (such as ligaments or the vertebral disks), which should also be separated. Depending on the question of interest, cortical bone can be in a component separate from trabecular bone. Modern finite element software provides many labor-saving short cuts (such as automatic property assignment), but most of these short cuts depend heavily on component assignment.

17.3 Inputs to FEA

Geometry. Obtaining the geometry of the physical system to be modeled is the first step in FEM development. For the spine, this usually means obtaining 3D images of the area of interest. Surface, CT, or microCT scans of bone can be acquired and

manipulated as necessary, while soft tissue morphology can be obtained via MRI or ultrasound. The goal of the manipulation is to obtain geometry that represents the physical system to the level of detail required. For some questions or components, 2D (e.g., plate and shell) elements may suffice; in which case, surface scans may provide the required geometric information. More manipulation of CT, microCT, MR or ultrasound scans is necessary for questions that require 3D modeling. In those cases, the internal structure may need to be segmented from adjacent structures to produce distinct volumes that can be imported individually into FEM software. Fortunately, obtaining accurate spinal bony geometry is relatively straightforward with current scanning technology. Soft tissue, if necessary to the question of interest, can also be scanned in extant species, but that of extinct species requires reconstruction. Parts of the model that have different constitutive properties (e.g., cortical bone vs. intervertebral disk) should be segmented into distinct portions, because creation of the elements is easier if the material properties do not vary within a component. After the geometry is complete, it is imported into the FEA software.

Once the geometry representing the individual components has been imported into the FEA software, the geometry is used to create the finite elements themselves. These elements can be 1D (e.g., a rod), 2D (e.g., a plate), or 3D (e.g., a tetrahedron). The choice of elements influences the behavior of the FEM and the availability of results. For instance, rod elements only have stiffness in their long axis (i.e., axial tension or compression), so they cannot transfer loads or constrain motion in the other two axes, nor will their element results contain shears or moments. Element size depends on the resolution needed (as indicated above), on the geometric constraints, and on the available computational power (Fig. 17.2). Optimizing a model for element size and number is both practical and necessary. Because each element represents material acting at the element's center, larger elements provide less sensitivity to localized phenomena. Too few elements and the model lacks sensitivity to geometric subtleties, but too many create a model that is computationally time-intensive with little scientific value added for the time investment. As a practical example of this balance, the cortical shell of the vertebral centrum is thin—therefore requiring small element size—but the interior trabecular bone could be effectively represented with larger elements (for discussion of the balance between modeling inner trabecular and cortical shell finite element geometry, see Sylvester and Kramer 2018). The obvious solution—transitioning from small to larger elements—should only be done with the understanding that element size effects how elements interact with each other because elements are only connected at discrete locations. Unequal element size should be avoided in those areas of the model critical to the analysis.

Generally, element behavior is influenced by the shape of the element; 2D and 3D elements which are closer to having equal length sides, symmetrical, and planar behave more consistently during the stiffness matrix decomposition. Element quality describes how well individual elements are expected to behave and consists of many factors. For instance, aspect ratio describes the slenderness of elements, while skew describes symmetricity where a corner angle value that is equal to 360° divided

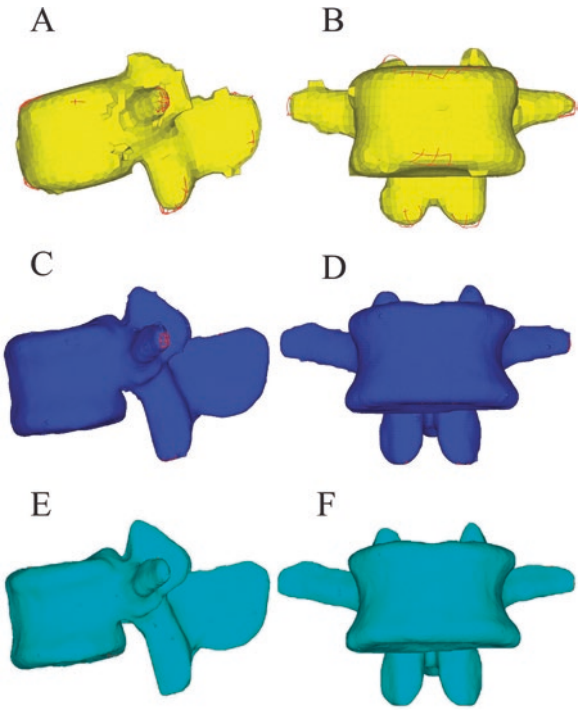

Fig. 17.2 Element size. (**a**) Lateral and (**b**) front view 3 mm element target size in yellow; (**c**) lateral and (**d**) front view of 1 mm target size in dark blue; and (**e**) lateral and (**f**) front view of 0.5 mm target size in light blue. The target size of the finite elements is provided to guide mesh autogeneration and is a compromise between the number of elements (e.g., smaller target size of elements requires more elements) and, hence, the time required to perform the FEA and the fidelity of the model to the original shape. More elements allow the original shape to be represented more faithfully, but more elements take longer to create, validate, and evaluate. In all views, the red lines indicate the outline of the original geometry file (in this case, in iges format), which is the virtual representation of the original shape. The 3 mm version has numerous locations where the FEM does not match the original scan, while the 0.5 mm version the discrepancies are limited to the left transverse process. In all versions, small areas of irregularities that are present are due to the original scan. These irregularities could have been eliminated when the scans were processed to create the geometry file

by the number sides of the element is preferred. Each of these element quality factors has a recommended range. Individual element quality should be assessed for all of the factors, and elements that exceed the recommended range for a factor should be corrected. Most FEA software has semi-automated methods for improving mesh quality, but some manual manipulation may also be required (Fig. 17.3). Adequate mesh quality is a critical aspect to any FEM and should be reported (Bern and Plassmann 1999).

Once all the components are meshed, they must be connected to other components with which they interface. These interfaces can be straightforward, such as the continuous connection between trabecular and cortical bone. Others are more

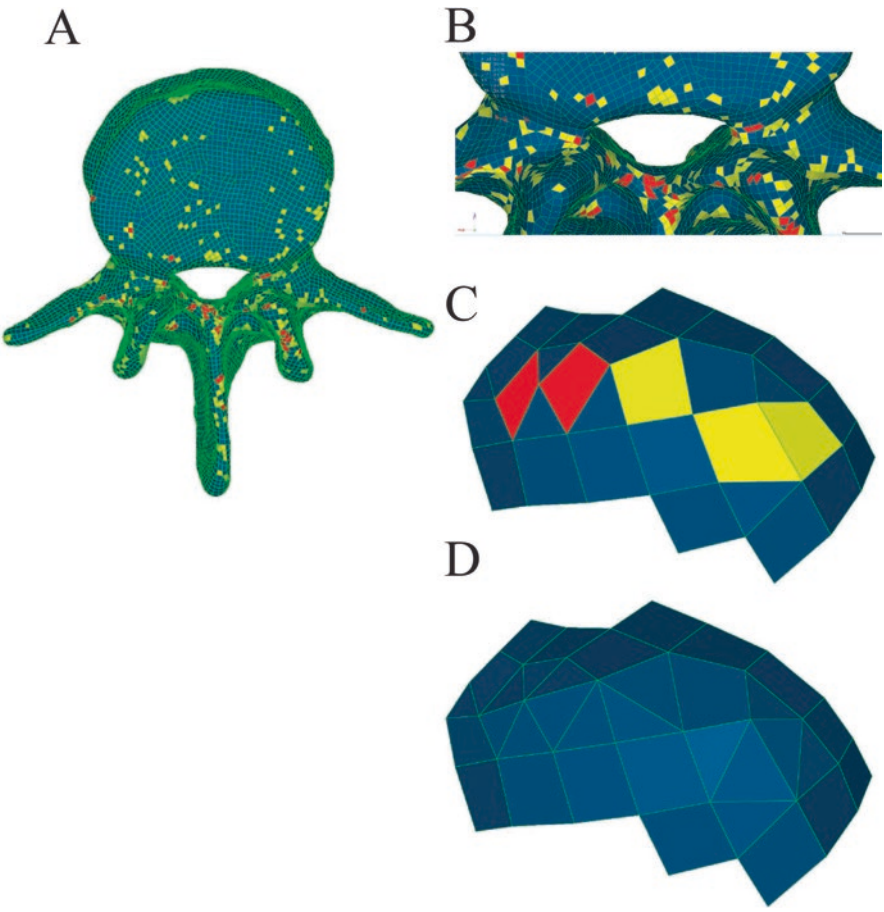

Fig. 17.3 Element quality. (**a**) inferior view (**b**) area of inferior view close-up; localized patch of elements with failed element quality (**c**) before and (**d**) after modification. Surface elements that passed the element quality check are shown in dark blue and outlined in green. Those elements shaded yellow have poor element quality, while those shaded red have failed at least one test of quality

complicated such as articular surfaces, which are "connected" when they are in contact and the applied forces would cause the surfaces to experience compression, but have no connection when separated or when forces would be tensile. In any case, these connections can be imagined to act like internal versions of boundary conditions, which are described below.

Materials. Selecting material properties for the skeletal elements under evaluation is a critical step in modeling in FEA. In static analyses, a minimum two of the three primary material properties (i.e., Young's Modulus (E), Shear Modulus (G), and Poisson's ratio (μ); discussed in more detail later on in this chapter) are required. These material parameters are determined from standardized structural tests and

have been extensively documented (e.g., Currey 2013). For many structural materials, including bone, tendons, and ligaments, Poisson's ratio is 0.3 (Martin et al. 2015). Young's and Shear moduli vary among materials over orders of magnitude, so choosing appropriate values is vital. Homogeneous materials, such as metals, which are used in many engineering applications, exhibit similar properties at most scales. Bone, however, is a laminate and, as a result, the appropriate properties depend on the scale of inquiry. (For a detailed discussion of the material complexities of bone, the authors recommend the work of Currey, his research team, and his many collaborators, e.g., Zioupos et al. (2008).) Accurately modeling a 1 mm^3 cube of trabecular bone from a vertebral body will require different assigned properties than modeling the entire centrum, or more especially the entire spine.

Bone's material complexity at almost every length scale from molecular to macro stymies a superficial approach to material property selection. Nonetheless, all bone is essentially composed of the same foundational modules that develop different material properties depending on form, function, size, and position in the body. A region of trabecular bone reacts differently to forces than does one of cortical bone, even though both are dependent on their physical density and internal structure in the region of interest. In addition, bone continually adjusts its density and alignment to strain patterns (e.g., Wolff 1986; Frost 1983, 2003) and is, therefore, constantly in flux. Creating an FEM that accurately reflects the complex directionality of the overall bone structure in conjunction with the continuous remodeling, adaptation, and non-catastrophic fracture repair in vivo has been theoretically attempted (e.g., Taylor and Tilmans 2004) but remains difficult. Fortunately, if the question of interest is more concerned with the behavior of the spine or vertebrae than with the details of bone physiology, material properties can be realistically estimated.

For static analyses using FEMs of the whole spine, researchers commonly simplify the material properties and assign a generalized Young's Modulus and Poisson's Ratio for regions of cortical and trabecular bone (Dreischarf et al. 2014 and references therein). In models of localized spinal structures, more fine-grained values for Young's Modulus can also be used. Typically, these variable moduli are computed from the grayscale values of the CT scans that were used to create the FEM geometry. The grayscale value of each voxel from a CT scan provides information regarding the degree of mineralization of the bone in that voxel. Lighter grayscale values are more mineralized regions. A calibration curve, which is developed from a known standard, allows researchers to convert from grayscale to a hydroxyapatite density value. Young's Modulus specific to that bony region is, then, estimated from the hydroxyapatite density (Cann and Genant 1980).

If the question of interest is more focused, then more precise estimations of the material properties can be used. For instance, microCT and nanoCT scanning technology has begun to allow researchers to move away from using the homogeneous hydroxyapatite approximation (e.g., Wagner et al. 2011) to more accurately model bone material properties to the scale of material variation within individual trabeculae. Ultrasounds can also provide density data by tracking the time it takes for the sound wave to travel through the substrate but are limited to a single direction per scan. Consequently, the substrate must be scanned multiple times from different

directions to accurately represent the anisotropy of the material. These fine-grained approaches are time intensive and sensitive to error and so should only be attempted if the question of interest requires this level of material specificity.

As cortical bone is the rigid shell encapsulating the porous trabecular interior, the thickness of the cortical envelope is a critical component of the structure to consider. While there are differences across extant primate species in the distribution of cortical and trabecular bone of the vertebral bodies (Cotter et al. 2011), when a CT scan is not available, an averaged distribution or an assumed cortical thickness may be acceptable if the problem involves such things as overall spine behavior. Similarly, fossilized primate specimens may be completely mineralized, making it impossible to distinguish the boundary between cortical shell and trabecular lattice. Generalized properties can, however, be used. In these cases, determining the sensitivity of the results to the assumptions regarding Young's Modulus is a crucial step.

Boundary conditions are the external influences on the structure, including constraints and applied loads.

Constraints (also called supports) are points where features outside the model restrain the movement of the model in one or more of the six degrees of freedom that a point can have in cartesian coordinates: translations in the x-, y-, and z-directions and rotations about the x-, y-, and z-axes. Joint articular surfaces and ligamentous attachments are typically modeled as constraints. Care should be exercised to make sure that the constraint added to the model reflects the capability of the physical structure. For instance, ligaments are capable of exerting a constraint that requires the ligament to develop an axial load, but that load must be tensile, not compressive (Fig. 17.4). Likewise, articular surfaces provide restraint from movement perpendicular to the surface but only in compression (i.e., when the surfaces move closer to each other). Most constraints are modeled as single point constraints (SPCs), i.e., the node acts independently of others, but more complex arrangements where multiple nodes need to act together (multipoint constraints, MPCs) are also possible to construct. As with its geometric modeling, the spine is complex to constrain with multiple ligamentous and articular structures present in every segment. For instance, if the question of interest is understanding the shape of vertebral centra, does the FEM need to include the constraint provided by the ligamentum flava, interspinous ligaments, supraspinous ligaments, etc., and if so, how? Consequently, great care needs to be taken to understand the effect of constraints on adjacent structures.

Applied loads, such as forces, pressures, and moments, are introduced to the structure that the FEM represents from agents that exist outside the model. For instance, if the FEM is of a single bone, one set of articular surfaces are typically constrained while another set is loaded (Fig. 17.5). Muscles and ligaments can also introduce forces to the FEM. The development of muscular and ligamentous forces is not a trivial task and is outside the scope of this review. Of note, however, is that evaluating the sensitivity of the results to the applied forces is a task well-suited to a FEA because multiple load cases, i.e., particular combinations of applied loads are easily processed.

Modeling the spinal column produces a potentially challenging loading scenario because the orientation of the boundary conditions can change with applied load

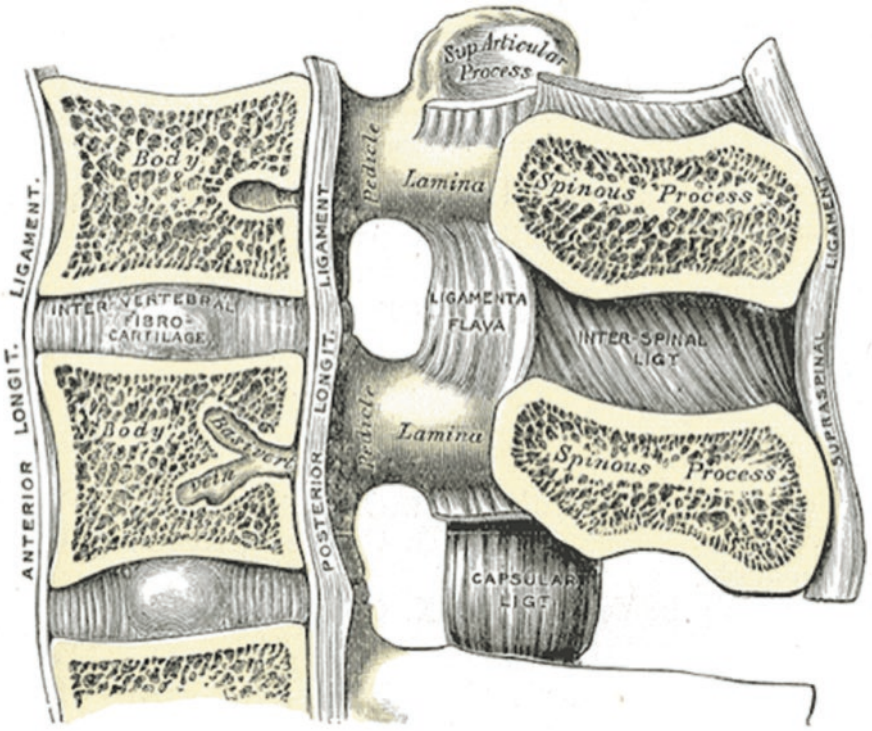

Fig. 17.4 Intervertebral ligaments. (from Henry Gray (1918) *Anatomy of the Human Body* Gray's Anatomy, Plate 301.)

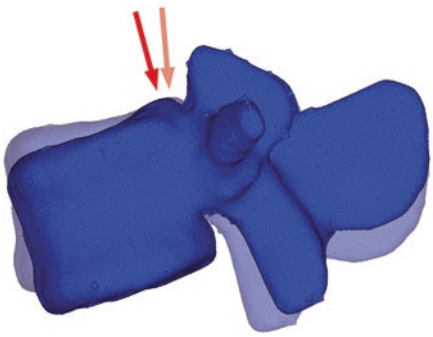

Fig. 17.5 Boundary conditions for a single vertebra. Lateral view of a lumbar vertebra in anatomical position (blue) and in flexion (gray). The orientation of the applied load from the vertebra immediately cranial the one of interest in anatomical position (pink arrow) is more vertically oriented than after movement (red arrow) because the load "follows" the movement

and this change can be sufficiently large to be of importance. Even if the stiffness is believed to be unaffected by the relatively large displacements in, for instance, spine flexion and extension, the orientation of the boundary conditions may be affected. Forces that change direction as the spine orientation changes (called "follower" loads because they follow the changes in the spine's curvature; e.g., Rohlmann 2001; Rohlmann et al. 2009) are, for example, necessary to simulate in biomechanical testing of cadaver spines. FEMs modeling similar scenarios also need to account for spine curvature in developing appropriate boundary conditions.

17.4 Results of FEA

How do you know that the answer is reasonable? As with all numerical techniques, the responsibility for understanding the validity and meaning of the results lies with the investigator. FEA is not a hypothesis in and of itself; it is a data collection and analysis tool, albeit a technically complex one, to investigate well-conceived hypotheses. The investigator needs to predict the outcome and then understand the meaning of the resultant data. Even though the element results can appear overwhelming, several types of information are relatively straightforward to report and evaluate.

The first of these results are *deflections*. Linear static solutions are based on small deflection theory, so the results can be interrogated to determine maximum displacements of the overall FEM. Validation of the FEM displacements to those obtained via empirical testing should occur. If the FEM exhibits unexpectedly large deflections, the model constraints may be inadequate. Further, localized displacements can be assessed to make sure that elements that lie adjacent to each exhibit similar displacements (i.e., strain compatibility). Discontinuous strains in continuous material typically indicate that the elements are not connected correctly. Another important way to determine if the results from a model are reasonable is to evaluate the forces of the constraints. Constraints represent physical structures and the constraint forces must align to the capability of the component for which the constraint is a proxy. Beyond testing model assumptions, displacements can also be used as primary results. For instance, questions about changes in shape (such as how much do the lumbar disks compress in running?) can be answered with displacement data.

Strain is a measure of the deformation of a structure, while stress is a distribution of applied forces in a cross section. In linear elastic materials, the ratio of stress and strain is called Young's Modulus (E), which is a fundamental material property that is described above. Both stress and strain can be used to assess whether or not a component is structurally adequate to withstand the forces applied to it. Typically, this assessment is made through the use of material properties that document empirically the maximum allowable values. Here "maximum allowable" could mean the maximum sustainable strain or stress before the region fails (e.g., a break in a bone) or before the material exceeds its elastic (or yield) limit, after which removal of the load does not result in a return to the original shape (e.g., a "stretched" ligament). Both failure and yield limits are pertinent, and because bone and soft tissue behave

differently under load (i.e., bone is generally more brittle than soft tissues are), the determination of which limit to use will depend on the question of interest.

Of importance to note here is that the most "efficiently" designed structure from a biological perspective is the one in which all regions are near to their limits (whatever those limits might be), but do not exceed these allowable limits during the useful life of the structure under applied loads that are reasonable. In other words, structures with "hot spots" are inefficient because while some material in the same component is close to failure ("hot"), some areas are not being strained to their capacity and, therefore, this underutilized material is redundant. From an evolutionary adaptation perspective, selection should favor living tissues that are the size that they need to be for their function but no larger and that adjust this balance depending on the environment (such as the forces from daily activities). Consequently, failure analyses are only one way to use stress and strain to analyze a structure.

Strain energy is the energy required, or work done, to deform a volume or, alternatively, the energy stored in a deformed volume: $U = \text{VEstrain}^2$, where V is the volume. Strain energy provides a compact parameter that relates stress, strain, and volume, effectively weighting the interaction of each. Higher strain energy can accrue from more deformation (i.e., higher strains and hence stresses), higher stiffness (i.e., Young's Modulus), or more material volume. Strain energy is determined from elemental parameters (strains, E, and volumes) and then is summed over all elements in the model or component. It is related to the efficiency of the structure; if the volume and stiffness are held constant, then applied loads that produce more strain energy could mean a greater number of elements experiencing higher strains. Unfortunately, it could also mean high strains in some areas and low strains in others (i.e., strain "hot spots"). Strain energy is also a measure of the capacity of a component to store energy. Components with high strain energy but that do not exceed their allowable strains have higher energy storage capability. Some ligaments store energy through displacement (e.g., the Achilles tendon). Finally, it can be used as a metric for assessing the sensitivity of a model component to such choices as element size. When strain energy converges between models with varying element size, further reductions in element size may be unnecessary, saving computational resources.

As with any computational model, until it is corroborated by experimentation (e.g., Xu et al. 2016), the results of an FEA are simply a tentative answer to a hypothesis and should be approached as such.

17.5 An Example of the Application of FEA to the Spine: Reduced Lumbar Lordosis in Neandertals Compared to Earlier Hominins and Modern Humans

As discussed at the beginning of this chapter, the recently documented thoracic shape of Kebara 2—with its reduced lumbar lordosis and spinal invagination along the spine's length compared to earlier hominins and to *H. sapiens* (Gómez-Olivencia et al. 2018; Been et al. 2016)—provides the context for an example of how FEM

might be used to allow insight into the implications of the Neandertal form. While many questions could be asked, the effect of the differences on spinal deflection is an obvious initial concern—curved columns displace more under compressive loads than do straight ones. This ability of the modern human spine to "give" under dynamic loading has been associated with the dissipation of the high forces generated by impact loading, such as running (e.g., Castillo and Lieberman 2018). This shock attenuation is hypothesized to reduce the deleterious effects to the spine of the transient, high forces that occur during each foot strike in running.

If more lumbar lordosis allows more shock attenuation, then what does reduced lumbar lordosis imply for Neandertals? FEA would be an ideal technique to evaluate this question. Using the steps described above, a model of the human spine—vertebrae, disks, and other soft tissues—could be built and validated for boundary constraints that reflect running conditions. The model could then be modified to represent the shape of the Neandertal spine and the difference in the compliance behavior of the spinal forms could be determined. Other central questions regarding the effects of the observed differences between Neandertal and modern human form are also amenable to FEA, including determining the difference in load distribution between the anterior (vertebral body) and posterior (facet) elements of the spine and how changes in thoracic shape impact breathing dynamics, to name but two more. Further, this model could also be modified to represent earlier hominin forms.

17.6 Conclusion

As with all analysis techniques, the results will only be as good as the assumptions used to create the model, so great care and a strong grounding in the first principles of the theory are required to implement an FEA. Of particular importance with the spine is the question of interest. The approach to understand "how do osteophytes form?" will be substantively different from "how does the lumbar curve change when loaded?". The interface of vertebra and soft tissues (such as the intervertebral disks and ligaments) make modeling the spine challenging. Nonetheless, the spine is a 3D structure whose substantial complexity in its morphology and boundary conditions make it worth the effort required to create an FEM to analyze it.

References

Been E, Barash A, Marom A, Aizenberg I, Kramer PA (2010) A new model for calculating the lumbar lordosis angle in early hominids and in the spine of the Neanderthal from Kebara. Anat Rec 293(7):1140–1145

Been E, Barash A, Marom A, Kramer PA (2009) Vertebral bodies or discs: which contributes more to human-like lumbar lordosis? Clin Orthop Relat Res 468:1822–1829

Been E, Gómez-Olivencia A, Kramer PA (2012) Lumbar lordosis of extinct hominins. Am J Phys Anthropol 147:64–77

Been E, Gómez-Olivencia A, Kramer PA (2014) Lumbar lordosis in extinct hominins: implications of the pelvic incidence. Am J Phys Anthropol 154:307–314
Been E, Gómez-Olivencia A, Kramer PA, Barash A (2016) 3D reconstruction of spinal posture of the Kebara 2 Neandertal. In: Marom A, Hovers E (eds) Human prehistory and paleontology: contributions in honor of Yoel Rak, Vertebrate paleobiology and paleoanthropology series. New York, Springer, New York, pp 239–252
Bern M, Plassmann P (1999) Mesh generation. In: Sack J-R, Urrutia J (eds) Handbook of computational geometry. Elsevier, Amsterdam, pp 291–332
Cann CE, Genant HK (1980) Precise measurement of vertebral mineral content using computed tomography. J Comput Assist Tomogr 4:493–500
Carrera E, Cinefra M, Zappino E, Petrolo M (2014) Finite element analysis of structures through unified formulation. John Wiley & Sons, Chichester
Castillo ER, Lieberman DE (2018) Shock attenuation in the human lumbar spine during walking and running. J Exp Biol 221:1–11
Cotter MM, Loomis DA, Simpson SW, Latimer B, Hernandez CJ (2011) Human evolution and osteoporosis-related spinal fractures. PLoS One 6:e26658
Currey JD (2013) Bones. Princeton University Press, Princeton, NJ
Dhatt G, Touzot G, Lefrançois E (2012) Finite element method. John Wiley & Sons, Inc., Hoboken, NJ
Dreischarf M, Zander T, Shirazi-Adl A, Puttlitz CM, Adam CJ, Chen CS, Goel VK, Kiapour A, Kim YH, Labus KM, Little JP, Park WM, Wang YH, Wilke HJ, Rohlmann A, Schmidt H (2014) Comparison of eight published static finite element models of the intact lumbar spine: predictive power of models improves when combined together. J Biomech 47:1757–1766
Frost HM (1983) Determinant of bone architecture. Clin Orthop Relat Res 175:1–7
Frost HM (2003) Bone's mechanostat: a 2003 update. The anatomical record: advances in integrative anatomy and evolutionary biology, vol 275, pp 1081–1101
Gómez-Olivencia A, Barash A, García-Martinez D, Arlegi M, Kramer P, Bastir M, Been A (2018) 3D virtual reconstruction of the Kebara 2 Neandertal thorax. Nat Commun 9:4387
Gray H (1918) Anatomy of the human body. Lea and Febiger, Philadelphia, PA
Lovejoy CO (1988) Evolution of human walking. Sci Am 259(5):118–125
Martin RB, Burr DB, Sharkey NA, Fyhrie DP (2015) Skeletal tissue mechanics. Springer-Verlag, New York, NY
Pickering TR, Heaton JL, Clarke RJ, Stratford D (2019) Hominin vertebrae and upper limb bone fossils from Sterkfontein Caves, South Africa (1998–2003 excavations). Am J Phys Anthropol,. Epub ahead of print 168:459
Püschel TA, Marcé-Noqué J, Gladman JT, Bobe R, Sellers WI (2018) Inferring locomotor behaviours in Miocene new world monkeys using finite element analysis, geometric morphometrics and machine-learning techniques applied to talar morphology. J R Soc Interface 15:1–16
Rohlmann A (2001) Influence of a follower load on intradiscal pressure and intersegmental rotation of the lumbar spine. Spine 16:E557–E561
Rohlmann A, Zander T, Rao M, Bergmann G (2009) Applying a follower load delivers realistic results for simulating standing. J Biomech 42:1520–1526
Sack JR, Urrutia J (1999) Handbook of computational geometry. Elsevier, Amsterdam
Sylvester AD, Kramer PA (2018) Young's modulus and load complexity: modeling their effects on proximal femur strain. Anat Rec 74:747–714
Taylor D, Tilmans A (2004) Stress intensity variations in bone microcracks during the repair process. J Theor Biol 229:169–177
Wagner DW, Lindsey DP, Beaupré GS (2011) Deriving tissue density and elastic modulus from microCT bone scans. Bone 49:931–938
Wolff J (1986) The law of bone remodelling. Springer, Berlin
Xu M, Yang J, Lieberman IH, Haddas R (2016) Lumbar spine finite element model for healthy subjects: development and validation. Comput Methods Biomech Biomed Engin 20:1–15
Zioupos P, Hansen U, Currey JD (2008) Microcracking damage and the fracture process in relation to strain rate in human cortical bone tensile failure. J Biomech 41:2932–2939

Index

E. Been et al. (eds.), *Spinal Evolution*,
https://doi.org/10.1007/978-3-030-19349-2